frontiers | Research Topics

Molecular mechanism of neuroimmune modulation and synaptic plasticity in acute and chronic pain

Edited by
Linlin Zhang, Xin Zhang, Zilong Wang and Yize Li

Published in
Frontiers in Molecular Neuroscience

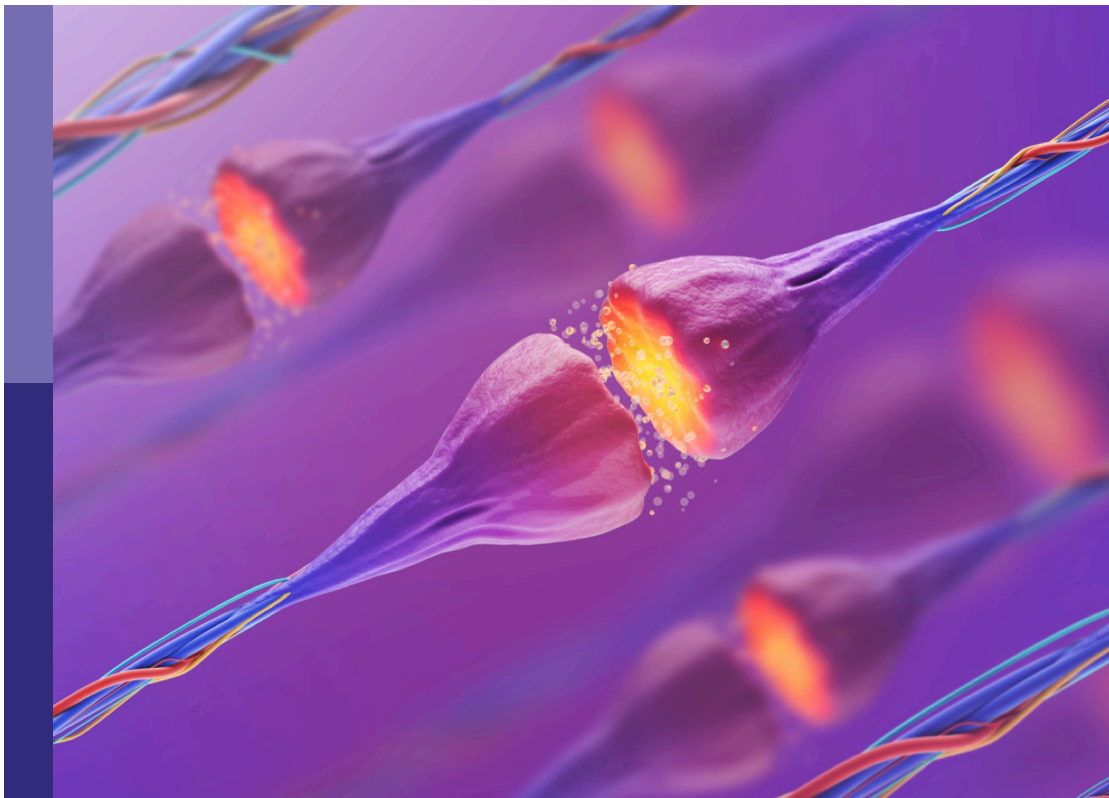

ISSN 1664-8714
ISBN 978-2-8325-2797-9
DOI 10.3389/978-2-8325-2797-9

About Frontiers

Frontiers is more than just an open access publisher of scholarly articles: it is a pioneering approach to the world of academia, radically improving the way scholarly research is managed. The grand vision of Frontiers is a world where all people have an equal opportunity to seek, share and generate knowledge. Frontiers provides immediate and permanent online open access to all its publications, but this alone is not enough to realize our grand goals.

Frontiers journal series

The Frontiers journal series is a multi-tier and interdisciplinary set of open-access, online journals, promising a paradigm shift from the current review, selection and dissemination processes in academic publishing. All Frontiers journals are driven by researchers for researchers; therefore, they constitute a service to the scholarly community. At the same time, the *Frontiers journal series* operates on a revolutionary invention, the tiered publishing system, initially addressing specific communities of scholars, and gradually climbing up to broader public understanding, thus serving the interests of the lay society, too.

Dedication to quality

Each Frontiers article is a landmark of the highest quality, thanks to genuinely collaborative interactions between authors and review editors, who include some of the world's best academicians. Research must be certified by peers before entering a stream of knowledge that may eventually reach the public - and shape society; therefore, Frontiers only applies the most rigorous and unbiased reviews. Frontiers revolutionizes research publishing by freely delivering the most outstanding research, evaluated with no bias from both the academic and social point of view. By applying the most advanced information technologies, Frontiers is catapulting scholarly publishing into a new generation.

What are Frontiers Research Topics?

Frontiers Research Topics are very popular trademarks of the *Frontiers journals series*: they are collections of at least ten articles, all centered on a particular subject. With their unique mix of varied contributions from Original Research to Review Articles, Frontiers Research Topics unify the most influential researchers, the latest key findings and historical advances in a hot research area.

Find out more on how to host your own Frontiers Research Topic or contribute to one as an author by contacting the Frontiers editorial office: frontiersin.org/about/contact

Molecular mechanism of neuroimmune modulation and synaptic plasticity in acute and chronic pain

Topic editors

Linlin Zhang — Tianjin Medical University General Hospital, China
Xin Zhang — Duke University, United States
Zilong Wang — Southern University of Science and Technology, China
Yize L — Tianjin Medical University General Hospital, China

Citation

Zhang, L., Zhang, X., Wang, Z., Li, Y., eds. (2023). *Molecular mechanism of neuroimmune modulation and synaptic plasticity in acute and chronic pain*. Lausanne: Frontiers Media SA. doi: 10.3389/978-2-8325-2797-9

Table of contents

frontiers | Frontiers in Molecular Neuroscience

TYPE Editorial
PUBLISHED 09 June 2023
DOI 10.3389/fnmol.2023.1224792

OPEN ACCESS

EDITED AND REVIEWED BY
Robert John Vandenberg,
The University of Sydney, Australia

*CORRESPONDENCE
Linlin Zhang
✉ linlinzhang@tmu.edu.cn
Yize Li
✉ liyizelisa@126.com

†These authors have contributed equally to this work

RECEIVED 18 May 2023
ACCEPTED 26 May 2023
PUBLISHED 09 June 2023

CITATION
Zhang L, Zhang X, Wang Z and Li Y (2023) Editorial: Molecular mechanism of neuroimmune modulation and synaptic plasticity in acute and chronic pain. *Front. Mol. Neurosci.* 16:1224792. doi: 10.3389/fnmol.2023.1224792

Editorial: Molecular mechanism of neuroimmune modulation and synaptic plasticity in acute and chronic pain

Linlin Zhang[1,2*†], Xin Zhang[3,4†], Zilong Wang[5] and Yize Li[1,2*]

[1]Department of Anesthesiology, Tianjin Medical University General Hospital, Tianjin, China, [2]Tianjin Research Institute of Anesthesiology, Tianjin, China, [3]Center for Translational Pain Medicine, Department of Anesthesiology, Duke University Medical Center, Durham, NC, United States, [4]Department of Anesthesiology, The Affiliated Wuxi People's Hospital of Nanjing Medical University, Wuxi, Jiangsu, China, [5]SUSTech Center for Pain Medicine, School of Medicine, Southern University of Science and Technology, Shenzhen, China

KEYWORDS

pain, dorsal root ganglion, neuroinflammation, astrocyte, microglia, synaptic plasticity, sleep deprivation

Editorial on the Research Topic
Molecular mechanism of neuroimmune modulation and synaptic plasticity in acute and chronic pain

As editors of this Research Topic, it was our pleasure to collect a wide range of fascinating articles and reviews to further our understanding of novel pain-associated molecules and their signaling pathways, which can be used as therapeutic targets for acute and chronic pain treatment. In this editorial we recapitulate the major findings and perspectives detailed within each of the accepted articles.

In the past decades, we have witnessed exciting discoveries that the interaction between neurons and glial cells contributes to peripheral and central sensitization of nociceptive circuitry, which governs multiple nociceptive perception and excitatory synaptic transmission. However, the specific molecular and cellular mechanisms underlying neuroimmune modulation, synaptic plasticity, and pain behaviors remain elusive and attract considerable interests. Cheng et al. summarized the latest findings that astrocyte activation and the alternations in the molecular cascades (such as intracellular kinases, channels, receptors, and transcription factors) and mechanisms involved in the spinal dorsal horn and supraspinal structures are dominant steps for the initiation and persistence of neuropathic pain. Li X. et al. reported that 147 differentially expressed mRNAs (136 upregulated and 11 downregulated) in the medial prefrontal cortex (mPFC) of rats with bone cancer pain using high-throughput sequencing of the transcriptome. Among them, MHCII in the mPFC may be a key biomarker for microglia activation and neuroinflammation to facilitate antigen processing and further evoke bone cancer pain. Toll like receptor 9 (TLR9) is an important sensor for danger-associated molecular patterns (DAMPs) and an indispensable effector of non-sterile/sterile inflammation among all TLRs. Chen Y. et al. found the robust increase of TLR9 mRNA and decrease of paw withdrawal mechanical threshold in CFA-treated mice. Both TLR9 antagonism and neuronal TLR9 downregulation in the spinal cord elevated paw withdrawal mechanical threshold after complete Freund's adjuvant (CFA) injection, demonstrating the involvement of neuronal TLR9 in the spinal cord in CFA-induced inflammatory pain. Great attentions have been recently paid to emphasizing and criticallydiscussing the cGAS-STING cascades, which is required for the elimination of pathogens and damaged host cells during innate and tumor immunity, as well as inflammatory

diseases. Wu et al. summarizes the advances made in identifying the mechanisms underlying the involvement of cGAS-STING cascades in primary sensory neurons and glia cells in the regulation of chronic pain with different etiologies, such as low back pain, bone cancer pain, fractures-associated postoperative pain, chemotherapy-induced neuropathy and nerve injuries-induced neuropathic pain, but it continues to be incomprehensible about our understanding of its diverse functions on chronic pain.

The activation of excitatory pain-related proteins and receptors is a cardinal feature of nociceptive synaptic plasticity and sensory neuronal excitability. TMEM100, a two-transmembrane protein, was recently identified as an effector to disinhibition of TRPA1 activity in sensory neurons. Wang P. et al. reported that TMEM100 co-expressed with TRPA1 and TRPV1 in trigeminal ganglion neurons-innervating the temporomandibular joint and masseter muscle and their up-regulation of co-expressions was detected following temporomandibular disorder pain induced by the inflammation of temporomandibular joint or the trauma of masseter muscles. Furthermore, specific deficiency of TMEM100 in trigeminal ganglion neurons or local treatment with TMEM100 inhibitor into the temporomandibular joint or masseter muscles reduced temporomandibular disorder pain and TRPA1 activation in trigeminal ganglion neurons. Collectively, these intriguing findings demonstrate that TMEM100 in trigeminal ganglion neurons causes temporomandibular disorder pain via modulating the activity of TRPA1 within the TRPA1-TRPV1 complex. A study by Li W. et al. observed several dorsal root ganglion (DRG) neurons innervating the ST36 acupoint and ipsilateral hind paw plantar using retrograde tracing, chemogenetic, morphological, and behavioral experiments. Suppressing these shared neurons attenuated CFA-induced inflammatory pain in mice, and elevated the mechanical pain threshold of ST36 acupoint in the CFA model. Moreover, most of the shared DRG neurons express TRPV1, a marker of nociceptive neurons. These results indicate that the shared nociceptive DRG neurons participate in ST36 acupoint sensitization in CFA-induced chronic pain. Huang et al. review the recent pathogenesis of synapses dysfunction by Shank3 regulation in Autism spectrum disorder (ASD)-related nociceptive paresthesia. Also, Li Z. et al. review recent literature focusing on menthol-related drugs for pathologic pain management in clinical trials, especially in neuropathic pain, cancer pain, musculoskeletal pain, as well as postoperative pain, with the purpose to search the novel therapeutic candidates for pain resolution in clinics.

To achieve molecular and neurobiological insights into the peripheral sensory neurons in chemotherapy-induced neuropathic pain, Mao et al. utilized transcriptomic analysis to profile mRNA and non-coding RNA expression in the DRGs of mice receiving paclitaxel treatment. They detected 372 differentially expressed genes in the DRGs of paclitaxel-treated mice. Among them, there were 8 mRNAs, 3 long non-coding RNAs (lncRNAs), 16 circular RNAs (circRNAs), and 345 microRNAs (miRNAs). More interestingly, they compared the expression levels of differentially expressed miRNAs and mRNA in the DRGs of mice with paclitaxel-induced neuropathic pain against those evaluated in other models of neuropathic pain induced by other chemotherapeutic agents, nerve trauma, or diabetes. There are dozens of shared differentially expressed miRNAs between paclitaxel and diabetes, but only a few shared miRNAs between paclitaxel and nerve trauma. Simultaneously, there is no shared differentially expressed mRNA between paclitaxel and nerve trauma. These identify that differentially expressed genes in DRGs vary greatly among neuropathic pain with different etiologies. Guo et al. discovered that *Rmst* (rhabdomyosarcoma 2-associated transcript) as a lncRNA was specifically expressed *Atf3*$^{+}$ injured DRG neurons and considerably increased following peripheral nerve trauma. Disrupting the expression of *Rmst* in injured DRGs ameliorated nerve trauma-caused allodynia and blocked *Dnmt3a* (DNA methyltransferase 3 alpha) expression, revealing the pivotal roles of *Rmst* for neuropathic pain development.

Patients with pain often experience insomnia, depression, anxiety and cognitive impairments, which is known to be associated with worsening pain and a serious threat to their quality of life. One study by Chen S. et al. reported that one night of sleep deprivation is sufficient to increase nociceptive sensitivity and cause oxidative insult in rats and humans. One night of recovery sleep restored basal nociceptive sensitivity in rats and improved the sleep deprivation-induced increase in pain intensity in volunteers, but with a slight protection against oxidative damage. Yet, it remains largely unclear whether sleep deprivation-induced hyperalgesia is associated with oxidative stress. Another study by Abdul et al. showed that ventral tegmental area glutamatergic neurons with projections to nucleus accumbens are important in chronic constrictive injury (CCI)-induced neuropathic pain and CFA-induced inflammatory pain and pain-induced anxiety and depression, providing a promising mechanism for developing novel therapeutic methods. Also, Shen et al. gave an overview on the structural functions implicated in the nociceptive circuitry and advanced emotional cortex circuitry. They further emphasize the current insights into sex dimorphism in neuromodulation of pain and related mental disorders via endogenous dopamine, 5-hydroxytryptamine, GABAergic inhibition, norepinephrine, and peptide pathways like oxytocin, as well as their receptors, which is critical for improving individualized medical care.

Author contributions

All authors listed have made a substantial, direct, and intellectual contribution to the work and approved it for publication.

Funding

This work was supported by research grants of National Natural Science Foundation of China to LZ (Grant Nos. 82171205 and 81801107).

Conflict of interest

The authors declare that the research was conducted in the absence of any commercial or financial relationships that could be construed as a potential conflict of interest.

Publisher's note

frontiers | Frontiers in Molecular Neuroscience

TYPE Original Research
PUBLISHED 15 July 2022
DOI 10.3389/fnmol.2022.960460

OPEN ACCESS

EDITED BY
Yize Li,
Tianjin Medical University General Hospital, China

REVIEWED BY
Kai Mo,
Southern Medical University, China
Shaogen Wu,
Cedars Sinai Medical Center, United States
Lingli Liang,
Xi'an Jiaotong University, China

*CORRESPONDENCE
Jun Zhang
30119030@nankai.edu.cn

†These authors have contributed equally to this work

SPECIALTY SECTION
This article was submitted to Pain Mechanisms and Modulators, a section of the journal Frontiers in Molecular Neuroscience

RECEIVED 03 June 2022
ACCEPTED 27 June 2022
PUBLISHED 15 July 2022

CITATION
Yang X, Yuan C, Wang H, Wang Y, Liu M, Li Z and Zhang J (2022) Changes in serum angiogenic factors among patients with acute pain and subacute pain.
Front. Mol. Neurosci. 15:960460.
doi: 10.3389/fnmol.2022.960460

Changes in serum angiogenic factors among patients with acute pain and subacute pain

Xuewei Yang[1†], Chunmei Yuan[1†], Huanling Wang[1], Yunxia Wang[1], Mei Liu[1], Zongjin Li[2] and Jun Zhang[1,2*]

[1]Department of Anesthesiology and Pain Medical Center, Tianjin Union Medical Center, Nankai University, Tianjin, China, [2]School of Medicine, Nankai University, Tianjin, China

Screening serum biomarkers for acute and subacute pain is important for precise pain management. This study aimed to examine serum levels of angiogenic factors in patients with acute and subacute pain as potential biomarkers. Serum samples were collected from 12 healthy controls, 20 patients with postherpetic neuralgia (PHN), 4 with low back pain (LBP), and 1 with trigeminal neuralgia (TN). Pain intensity in these patients was evaluated using the visual analog scale (VAS). The serum concentrations of 11 angiogenic biomarkers were examined by Milliplex Map Human Angiogenesis Magnetic Bead Panel 2. The pain assessment from VAS showed that all patients showed moderate and severe pain. Among 11 angiogenic factors, osteopontin (OPN), thrombospondin-2 (TSP-2), soluble platelet endothelial cell adhesion molecule-1 (sPECAM-1), soluble urokinase-type plasminogen activator receptor (suPAR), and soluble epidermal growth factor receptors (sErbB2) were up-regulated and soluble interleukin-6 receptor α (sIL-6Rα) were down-regulated in patients with pain compared to the healthy participants (all *P*-values were < 0.005). Moreover, a linear regression model showed that the serum OPN concentration was correlated with pain intensity in patients with PHN ($P = 0.03$). There was no significant difference between the serum concentration of soluble epidermal growth factor receptors, sErbB3, soluble AXL, tenascin, and soluble neuropilin-1 in patients with acute and subacute pain and that of healthy controls. The results of this study provided new valuable insights into our understanding of angiogenic factors that may contribute to as mechanistic biomarkers of pain, and reveal the pathophysiological mechanism of pain.

Clinical Trial Registration: www.chictr.org.cn, identifier ChiCTR2200061775.

KEYWORDS

angiogenic factors, acute pain, postherpetic neuralgia, low back pain, trigeminal neuralgia, TSP-2

Introduction

Pain may be conceived as a disease in conditions, such as fibromyalgia or non-specific low back pain (LBP) (Reckziegel et al., 2019; Treede et al., 2019). More popularly, pain is a leading complaint in some diseases such as postherpetic neuralgia (PHN), trigeminal neuralgia (TN), peripheral nerve injury, painful polyneuropathy, etc.

(Scholz et al., 2019; Treede et al., 2019). The cost of acute or subacute pain due to direct medical treatment and productivity lost represents a heavy economic burden. Moreover, therapeutic management of pain is challenging, and complete relief is uncommon, owing to efficacy limitations of current treatments (Scholz et al., 2019). It is also intricately related to opiate addiction and has a significant impact on disability and overdose deaths. To combat these massive societal burdens, more effort is required to develop novel tools and therapies for combating chronic pain and reducing reliance on opiates for managing chronic pain (Reckziegel et al., 2019). This effort has emphasized the urgent need to develop validated biomarkers, with the assumption that such biomarkers would, in turn, facilitate mechanically driven development of novel therapies (Reckziegel et al., 2019). The current study aim to identify new biomarkers for acute and subacute pain by examining blood samples of patients with pain, and to identify clues for pain pathogenesis.

Angiogenesis, which is the formation of new blood vessels from the endothelium of the existing vasculature, is a fundamental process that occurs in physiological and pathophysiological conditions (Sajib et al., 2018). Insufficient or excessive blood vessel growth underlies many diseases, including cardiovascular and cerebrovascular diseases, osteoarthritis and cancer (Lawton et al., 2015; Viallard and Larrivée, 2017; Sajib et al., 2018). Normal angiogenesis and angiogenic signaling in pathological conditions are mediated by soluble growth factors, membrane-bound receptors, and cell-cell and cell-matrix interactions (Sajib et al., 2018). These factors may also play a role in pain pathogenesis by enhancing inflammation and inappropriate sensory innervation of local tissues (Mapp and Walsh, 2012). Angiogenesis-related signaling factors such as interleukin-1β (IL-1β), IL-6, tumor necrosis factor-α, and cyclooxygenase 2 are known to contribute to pain hypersensitivity by inducing the production of prostaglandins and other proalgesic agents, which activate nociceptors (Mafu et al., 2018). Moreover, previous studies have shown that angiogenesis contributes to pain in osteoarthritis patients and shoulder pain of breast cancer survivors (Mapp and Walsh, 2012; Mafu et al., 2018). All of the above studies shed light on the role of angiogenesis in pain pathogenesis.

We examined the serum levels of 11 angiogenic factors in patients with PHN, LBP, or TN using the Millipore Milliplex Map Human Angiogenesis Magnetic Bead Panel 2 assay and evaluated the correlations of these factors with pain intensity in PHN patients. These 11 angiogenic factors included osteopontin (OPN), thrombospondin-2 (TSP-2), soluble platelet endothelial cell adhesion molecule-1 (sPECAM-1), soluble urokinase-type plasminogen activator receptor (suPAR), soluble epidermal growth factor receptors (sEGFR/sHER1/sErbB1), soluble human epidermal growth factor receptor 2 (sEGFR2/sErbB2s/HER2), sErbB3 (sEGFR3/sHER3), soluble interleukin-6 receptor α (sIL-6Rα), soluble AXL (sAXL), tenascin C (TN-C), and soluble neuropilin-1 (sNRP-1). We will observe the expression levels of their homologous genes in the dorsal root ganglion (DRG), spinal cord, and the key parts of the sensory nervous system using a mouse neuropathic pain model in the next step.

Methods

Patients

All the participants were recruited from the Tianjin Union Medical Centre, Tianjin, China. There were 20 patients with PHN, 4 with LBP, and 1 with TN. All the patients were diagnosed by clinically qualified doctors. Twelve age-matched healthy participants without pain-related diseases or conditions were enrolled from the physical examination center of the Tianjin Union Medical Centre. Baseline characteristics (age and sex) of the participants are listed in **Table 1**. All the patients were notified of no analgesic medication 24 h before the study visit. Ethical approval for this research was approved by the ethical committee of Tianjin Union Medical Centre (approval number: 2016-B08).

Pain assessment

All the patients and healthy participants completed a visual analog scale (VAS) questionnaire for pain. The participants were asked to rate their current pain intensity on a VAS, ranging between "0–10." A VAS of "0" represents "no pain"; "1–3" represents mild tolerable pain; "4–6" represents moderate tolerable pain and sleep was disturbed. A VAS pain score from of "7–10" represents intense intolerable pain and both sleep and diet were disturbed.

Serum preparation

Blood samples from the participants were collected into 10 mL sterile tubes containing no additives. The samples were immediately centrifuged at 1,000 × g for 10 min and sediment-free serum samples were obtained, aliquoted, and frozen at −80°C until further analysis.

TABLE 1 Baseline characteristics of healthy controls and patients with PHN, LBP, or TN.

	HC	PHN	LBP	TN
Total, n	12	20	4	1
Gender (M/F)	6M/6F	11M/9F	3M/1F	1F
Mean age in years, range	66.7 (50–82)	74.8 (60–85)	76.5 (73–81)	64

HC, healthy controls; PHN, postherpetic neuralgia; LBP, low back pain; TN, trigeminal neuralgia; M, male; F, female.

Milliplex map assay for angiogenic factors

Serum concentrations of the 11 angiogenic factors (OPN, TSP-2, sPECAM-1, suPAR, sHER2, sIL-6Rα, sEGFR, sHER3, sAXL, TN-C, and sNRP-1) were measured by commercially available Milliplex Map Human Angiogenesis Magnetic Bead Panel 2 assay (EMD Millipore, Darmstadt, Germany). The serum samples were diluted to 1:5 before use. All procedures were carried out according to manufacturer's the instructions and all the samples were tested along with the quality controls and standard samples provided in the kit. After all steps were completed, the 96-well plate was placed onto Luminex® 200™ and analyzed using the Bio-Plex Manager software. The equipment settings were provided in the instruction book. Results were expressed in nanogram per milliliter (ng/mL) for the serum levels.

Statistical analysis

Serum levels of the angiogenic factors were evaluated using absolute concentration values. Data are reported as mean ± standard error of the mean (SEM). Comparisons of each angiogenic factor between the patients with pain and healthy controls was performed using the Student's *t*-test.

Correlations between the concentration of the angiogenic factors and pain intensity or duration in patients with PHN were determined using linear regression analysis. The F-test was used to determine statistical significance, with $P < 0.05$ considered as significant. Spearman's order correlation was performed to examine the correlation and calculate the correlation coefficients.

All analyses were performed using Statistical Package for the Social Sciences (SPSS; Chicago, IL, United States). Statistical significance was set at $P < 0.05$.

Results

Descriptive characteristics

Descriptive characteristics of the patients are shown in Table 1. Male and female patients were enrolled randomly in each group (Table 1). All the patients were aged > 55 years. Pain duration varied among the patients (Table 2). According to the classification of acute, subacute and chronic pain, most patients with PHN were classified as having acute pain with a duration less than 3 months. There was only one patient with subacute pain and two with chronic pain in the PHN patients. There was one LBP patient with acute pain and three LBP patients with subacute pain. One patient with TN was classified as having subacute pain. All the patients experienced medium to severe pain (Figure 1). The mean VAS was 8.7 in the PHN patients and 6.3 in the LBP patients, respectively. The mean VAS score of the TN patient was 10.

TABLE 2 Classification of patients with pain as acute, subacute, and chronic pain.

		Numbers
PHN	Acute pain (0–3 m)	15
	Subacute pain (3–6 m)	2
	Chronic pain (>6 m)	2
LBP	Acute pain (0–3 m)	1
	Subacute pain (3–6 m)	3
	Chronic pain (>6 m)	0
TN	Acute pain (0–3 m)	0
	Subacute pain (3–6 m)	1
	Chronic pain (>6 m)	0

PHN, postherpetic neuralgia; LBP, low back pain; TN, trigeminal neuralgia.

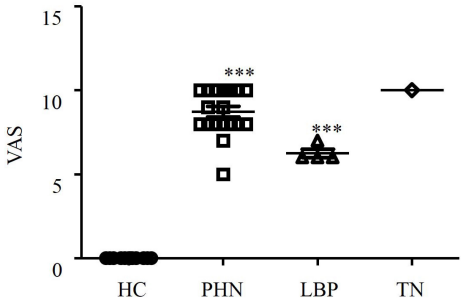

FIGURE 1
Comparison of visual analog scale (VAS) in healthy controls and patients with postherpetic neuralgia (PHN), low back pain (LBP), or trigeminal neuralgia (TN). ***$P < 0.001$.

Levels of serum angiogenic factors in the postherpetic neuralgia and low back pain patients

The mean ± S.E.M. levels of the serum angiogenic factors are shown in Table 3. Serum OPN, TSP-2, sPECAM-1, suPAR, and sErbB2 levels were significantly higher in patients with PHN (Figures 2A–E), while the serum sIL-6Rα levels were lower in the PHN patients than in the healthy controls (Figure 2F). Similarly, in patients with LBP, serum levels of TSP-2, sPECAM-1, sHER2, and suPAR were significantly increased, while serum sIL-6Rα levels were significantly decreased compared to those in the healthy control group (Figures 2B–F). However, the serum OPN level in patients with LBP didn't differ from those in the healthy controls (Figure 2A). The serum concentrations of OPN, TSP-2, sPECAM-1, sErbB2, and suPAR in TN patients

TABLE 3 Serum levels of angiogenic factors in healthy controls and patients with PHN, LBP, or TN.

	HC ($N = 12$)	PHN ($N = 20$)		LBP ($N = 4$)		TN ($N = 1$)
	$\overline{X} \pm SEM$	$\overline{X} \pm SEM$	P	$\overline{X} \pm SEM$	P	X
OPN (ng/mL)	6.94 ± 1.02	12.45 ± 1.31	0.007**	10.14 ± 1.63	0.16	1.00
TSP-2 (ng/mL)	4.37 ± 0.94	16.02 ± 2.02	0.0007***	22.32 ± 6.24	0.002**	21.82
sPECAM-1 (ng/mL)	4.85 ± 0.20	8.54 ± 0.41	0.0000***	8.52 ± 0.73	0.0000***	8.12
suPAR (ng/mL)	6.22 ± 0.44	13.81 ± 1.31	0.0002***	14.62 ± 3.19	0.001**	18.33
sHer2 (ng/mL)	5.48 ± 0.22	7.25 ± 0.36	0.002**	7.54 ± 0.69	0.004**	8.04
sIL-6Ra (ng/mL)	37.2 ± 2.03	27.73 ± 1.91	0.004**	25.74 ± 0.42	0.009**	31.20
sEGFR (ng/mL)	1.65 ± 0.18	1.28 ± 0.13	0.13	1.21 ± 0.35	0.28	1.34
sHer3 (ng/mL)	5.34 ± 0.78	5.09 ± 0.36	0.76	4.09 ± 0.58	0.42	2.65
sAxl (ng/mL)	2.38 ± 0.26	2.87 ± 0.21	0.16	1.67 ± 0.18	0.17	2.68
TN-C (ng/mL)	4.81 ± 0.37	5.92 ± 0.41	0.08	5.94 ± 1.47	0.34	6.54
sNRP-1 (ng/mL)	343.25 ± 46.38	304.39 ± 31.54	0.49	290.53 ± 41.74	0.57	713.12

**$P < 0.01$; ***$P < 0.001$.

HC, healthy controls; PHN, postherpetic neuralgia; LBP, low back pain; TN, trigeminal neuralgia; OPN, osteopontin; TSP-2, thrombospondin-2; sPECAM-1, soluble platelet endothelial cell adhesion molecule-1; suPAR, soluble urokinase-type plasminogen activator receptor; sHER2, soluble human epidermal growth factor receptor 2; sIL-6Rα, soluble interleukin-6 receptor α; sEGFR, soluble epidermal growth factor receptors; sHER3, soluble human epidermal growth factor receptor 3; sAXL, soluble AXL; TN-C, tenascin C; sNRP-1, soluble neuropilin-1.

were higher than those in the healthy controls (Figures 2A–E), while serum sIL-6Rα in the TN patient was lower than the mean value of the healthy controls (Figure 2F). The other five angiogenic factors, including sEGFR, sErbB3, sAXL, TN-C, and sNRP-1 didn't show any significant differences in patients with pain compared to the healthy controls (Figures 2G–K).

Associations between angiogenic factors and visual analog scale in the postherpetic neuralgia patients

The altered angiogenic factors including OPN, TSP-2, sPECAM-1, sHER2, suPAR, and sIL-6Rα in the PHN patients were further analyzed according to pain intensity and duration (Figure 3). We found that only serum OPN level was significantly correlated with VAS scores in the patients with PHN ($P = 0.03$, Figure 3A). The correlation coefficient between serum OPN level and VAS scores in patients with PHN was 0.49. Other factors were not significantly correlated with VAS in the PHN patients although higher levels of TSP-2, sPECAM-1 sErbB2, suPAR and a lower level of sIL-6Rα were found in the serum of PHN patients (Figures 3B–F). None of these angiogenic factors were significantly correlated with pain duration (Figures 4A–F).

Discussion

The objective of this study was to compare the levels of angiogenic factors in the sera of patients with pain and healthy controls. We found that higher levels of OPN, TSP-2, sPECAM-1, sErbB2, and suPAR and lower levels of sIL-6Rα were up-regulated and sIL-6Rα were down-regulated in those patients with pain compared to the healthy participants. Moreover, serum OPN levels were correlated with pain intensity in patients with PHN. These angiogenic factors may be involved in the pathogenesis of pain, and their soluble part in the blood can serve as biochemical indicators of acute or subacute pain.

Function of osteopontin in health and disease

The biological functions of OPN are diverse as it can be beneficial for wound healing, bone homeostasis, and extracellular matrix function, and deleterious in cardiovascular diseases, cancer, diabetes, and kidney stone diseases (Icer and Gezmen-Karadag, 2018; Lamort et al., 2019). Circulating OPN has also been indicated in some pain conditions as elevated plasma OPN levels have been found in patients with pain and unstable angina or multiple sclerosis (Soejima et al., 2006; Agah et al., 2018). A statistically significant correlation between OPN in synovial fluid and pain has been found in symptomatic patients with primary knee osteoarthritis and in patients who underwent anterior cruciate ligament reconstruction surgery (Yamaga et al., 2012; Calvet et al., 2018). Osteopontin has been reported to upregulate the expression of IL-6 and IL-8 cytokines in chondrocytes isolated from human osteoarthritis knee cartilage (Yang et al., 2014). Moreover, OPN in the peripheral DRG may contribute to the mechanisms of neuropathic pain. In the DRG, 25% of neurons were immunoreactive for OPN. These neurons were

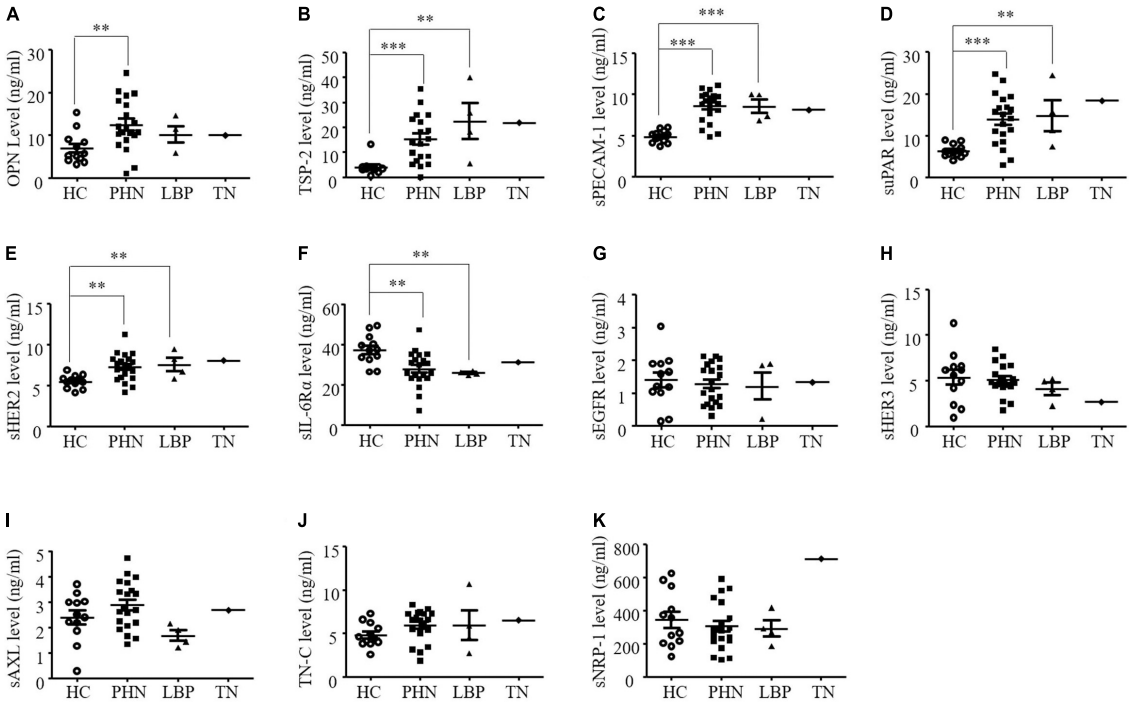

FIGURE 2

(A-K) Comparison of serum angiogenic factors in healthy controls (HC) and patients with postherpetic neuralgia (PHN), low back pain (LBP), or trigeminal neuralgia (TN). $^{**}P < 0.01$; $^{***}P < 0.001$. OPN, osteopontin; TSP-2, thrombospondin-2; sPECAM-1, soluble platelet endothelial cell adhesion molecule-1; suPAR, soluble urokinase-type plasminogen activator receptor; sErbB2, soluble human epidermal growth factor receptor 2; sIL-6Rα, soluble interleukin-6 receptor α; sEGFR, soluble epidermal growth factor receptors; sErbB3, soluble human epidermal; sAXL, soluble AXL; TN-C, tenascin C; sNRP-1, solubleneuropilin-1.

mostly large and exhibited parvalbumin-immunoreactivity, but not calcitonin gene-related peptide immunoreactivity (Ichikawa et al., 2000). Nerve injury induced an increase in OPN in DRG sensory neurons, and OPN knockout reversed mechanical hypersensitivity in mice with neuropathic pain (Ichikawa et al., 2000; Marsh et al., 2007). In the present study, we found an increased OPN levels in the sera of patients with PHN, which was positively associated with pain intensity in the PHN patients. This strongly supports that OPN exerts a role in pain pathogenesis, which may serve as a potential target for pain management.

Function of PECAM-1 in health and disease

Platelet endothelial cell adhesion molecule-1, also called CD31, is a 130-kDa protein belonging to the Ig superfamily; it has distinct variants and therefore different isoforms which allow diversity of PECAM-1 functions, including inflammation, angiogenesis and vascular development (Kalinowska and Losy, 2006). Splicing of exon 9, which encodes the transmembrane domain, results in the formation sPECAM-1, a soluble form of PECAM-1 (Goldberger et al., 1994) may result in PECAM-1 inhibition (Kalinowska and Losy, 2006). Thus, PECAM-1 is also involved in pain. For example, the sevenfold higher density of PECAM-1-positive capillaries in the cell body-rich area of mouse DRG than in the cell fiber-rich area of the DRG or the sciatic nerve facilitated many potentially neurotoxic agents by preferentially accumulating and injuring cells within the DRG, thereby inducing peripheral sensory neuropathy (Jimenez-Andrade et al., 2008). Moreover, PECAM-1 may also contribute to spinal mechanisms of pain because peripheral nerve injury induces an increase in PECAM-1 immunoreactivity in related spinal cord (Rutkowski et al., 2002; Sweitzer et al., 2002). In the blood circulation, PECAM-1 may mediate the analgesic effect of endomorphin on inflammatory pain by recruiting immunocytes containing β-endorphin to sites of painful inflammation (Sweitzer et al., 2002). The above studies have suggested various roles of PECAM-1 in multilevel pain transmission and various pain conditions. Herein, we found an increase in serum sPECAM-1 levels in patients with pain. Soluble PECAM-1, which may originate from endothelial cells, along with PECAM-1, may result in altered immune cell-endothelial cell interactions and thus, affect pain behaviors under pain conditions (Goldberger et al., 1994; Onore et al., 2012).

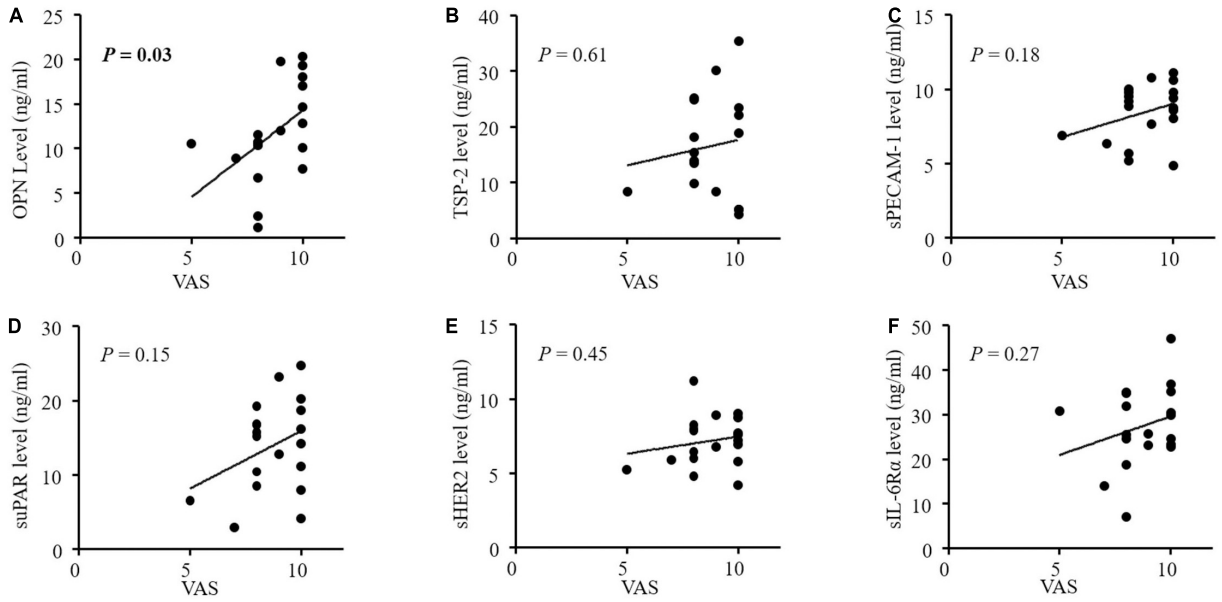

FIGURE 3
(A-F) Correlations between concentrations of angiogenic factors and pain intensity by VAS in patients with postherpetic neuralgia (PHN). Only serum OPN levels were significantly correlated with VAS in PHN patients (P = 0.03). OPN, osteopontin; TSP-2, thrombospondin-2; sPECAM-1, soluble platelet endothelial cell adhesion molecule-1; suPAR, soluble urokinase-type plasminogen activator receptor; s ErbB2, soluble human epidermal growth factor receptor 2; sIL-6Rα, soluble interleukin-6 receptor α; VAS, visual analog scale.

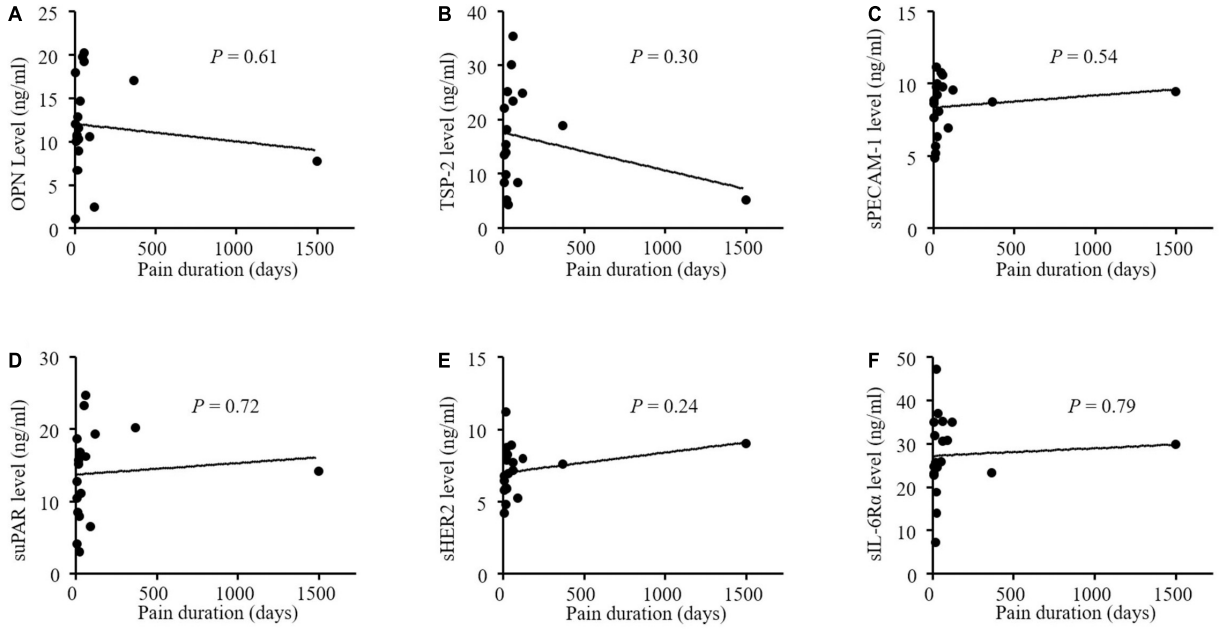

FIGURE 4
(A-F) No correlations between concentrations of angiogenic factors and pain duration in patients with postherpetic neuralgia (PHN). OPN indicates osteopontin; TSP-2, thrombospondin-2; sPECAM-1, soluble platelet endothelial cell adhesion molecule-1; suPAR, soluble urokinase-type plasminogen activator receptor; s ErbB2, soluble human epidermal growth factor receptor 2; sIL-6Rα, soluble interleukin-6 receptor α; VAS, visual analog scale.

Function of ErbB2 in health and disease

ErbB2 is a member of the EGFR family of receptor tyrosine kinases, which comprises ErbB1/EGFR/HER1, ErbB2/HER2, ErbB3/HER3, and ErbB4/HER4 (Moasser, 2007; Ho et al., 2017). ErbB2 is thought to be an oncogene and has become a target for a number of targeted anti-cancer drugs (Moasser, 2007; Al-Dasooqi et al., 2009). Soluble ErbB2, generated from ErbB2 proteolytic cleavage, includes only the extracellular domain of ErbB2 (Perrier et al., 2018). Soluble HER2 has been detected in the blood of cancer patients, and anticancer strategies targeting it are being developed (Dokala and Thakur, 2017; Perrier et al., 2018). In the present study, we found an increase in sErbB2 but not in sErbB1 or sErbB3 in patients with pain. Clinical and experimental studies have shown that EGFR/ErbB1 inhibitors can relieve neuropathic and breast cancer-related pain (Kaufman et al., 2010; Kersten and Cameron, 2012; Kersten et al., 2013, 2015, 2019; Martin et al., 2017; Wang et al., 2019). Moreover, EGFR/ErbB1 has been implicated in peripheral mechanisms of neuropathic pain (Martin et al., 2017; Wang et al., 2019). Therefore, ErbB2 signaling may be involved in the pathogenesis of pain. However, further studies are required to support this hypothesis.

Function of IL-6 in health and disease

Interleukin-6 is a key cytokine in many inflammatory and autoimmune diseases and IL-6, as well as IL-6 signaling, have been implicated in pain pathogenesis (Kawasaki et al., 2008; Assier et al., 2010; Boettger et al., 2010; Rendina et al., 2018). The IL-6 receptor is a heterodimer composed of an α chain (IL-6Rα) and a transmembrane chain gp130. Interleukin-6 can also induce cell signaling via sIL-6Rα which is generated by proteolysis of the transmembrane form of IL-6Rα, or by alternative splicing of the messenger RNAs for the α chain. Soluble IL-6Rα allows cells that do not express IL-6Rα to respond to IL-6 (Assier et al., 2010). Increased sIL-6R levels have been found in the sera of Paget disease patients with LBP, suggesting an enhanced transmission of IL-6 signaling in the specialized neural system linked to irregular perception in these patients (Rendina et al., 2018). In DRGs, IL-6 and IL-6R mRNA are expressed in DRG neurons and satellite glial cells, and are significantly elevated in response to peripheral nerve injury (Brázda et al., 2013). Moreover, IL-6, as well as sIL-6Rα, induced long-lasting robust sensitization of joint nociceptors to mechanical stimuli in an experimental arthritis model (Boettger et al., 2010). Spinal injection of sIL-6Rα produces heat hyperalgesia and sIL-6Rα and IL-6 enhance spinal central sensitization (Kawasaki et al., 2008). All these studies provide strong evidence of the close correlation between IL-6 signaling and pathological pain development. Currently, we observed decreased levels of sIL-6Rα in the sera of patients with pain. As a high level of sIL-6Rα is indicative of inflammation and increased nociception, sIL-6Rα levels in these patients with acute or subacute pain conflicts with our expectation. A study on a monoclonal antibody (tocilizumab) to transmembrane and sIL-6Rα showed that tocilizumab was effective in patients with rheumatoid arthritis although tocilizumab increased serum levels of IL-6 and sIL-6Rα. It has been suggested that sIL-6Rα is taken up by immune complexes which might increase the half-life of IL-6Rα and sIL-6Rα (Nishimoto et al., 2008). Therefore, an unidentified complex may be responsible for the decrease in sIL-6Rα levels in the blood of patients with pain observed in the current study.

Function of uPAR in health and disease

Urokinase-type plasminogen activator receptor is a glycosyl-phosphatidylinositol-anchored membrane glycoprotein belonging to the plasminogen activator system (Irigoyen et al., 1999; Thunø et al., 2009). Soluble uPAR, a free soluble receptor, is cleaved from uPAR. Soluble uPAR levels can be determined in the blood and have been used as biomarkers for chronic inflammatory conditions (Thunø et al., 2009). Elevated serum suPAR levels have been found in patients with chest pain osteoarthritis and migraine with attacks and aura (Tang et al., 2010; Lyngbæk et al., 2013; Yılmaz et al., 2017). Similarly, we postulate that suPAR and its related plasminogen activator system may be involved in the pathogenesis of pain. Urokinase-type plasminogen activator receptor mRNA was found in small and large DRG neurons (Hayden and Seeds, 1996; Siconolfi and Seeds, 2001). Sciatic nerve crush leads to elevated expression of uPAR, tissue-type plasminogen activator (tPA), and urokinase plasminogen activator (uPA) in DRG neurons (Siconolfi and Seeds, 2001). In the future, it will be important to determine the underlying mechanisms for the release of suPAR into circulation under acute or subacute pain conditions and to investigate the role of the plasminogen activator system in acute pain or subacute pain development.

Function of TSP-2 in health and disease

Thrombospondin-2, a matricellular glycoprotein of the thrombospondin family, regulates multiple biological functions, including proliferation, angiogenesis, cell adhesion, and extracellular matrix modeling (Bornstein et al., 2000; Adams and Lawler, 2011). High TSP-2 levels in human sera and tissues have been reported in various patients (Neuschwander-Tetri et al., 2006; Farrow et al., 2009; Naumnik et al., 2015; Liu et al., 2018). Herein, we demonstrated a high serum TSP-2 level in patients with pain. Although the exact mechanisms linking serum TSP-2 and pain conditions are not well-understood, it has been found that TSP-4, another member of

the thrombospondin family, contributes to spinal centralization by regulating the calcium channel Cavα2δ-1 in the spinal dorsal horn (Park et al., 2016). Therefore, investigation of TSP-2 expression and the local effects of TSP-2 in the pain pathway may provide clues on how TSP-2 is involved in pain pathogenesis.

We found significant changes in OPN, TSP-2, sPECAM-1, sErbB2, suPAR, and sIL-6Rα levels in the serum of patients with pain. Moreover, the serum OPN concentration may indicate pain severity. The results from this study provide new valuable insights into our understanding of angiogenic factors that may contribute to mechanistic biomarkers of pain to reveal the pathophysiological mechanisms of acute and subacute pain.

Summary

The present study showed significant changes in OPN, TSP-2, sPECAM-1, sErbB2, suPAR, and sIL-6Rα levels in the serum of patients with pain, especially with PHN. Moreover, the serum OPN concentration may indicate pain severity. Based on our findings, we hypothesized that elevated levels of circulating angiogenic factors contribute to the development of pain pathogenesis. Further studies should focus on their local effects and functions in the pain pathway, such as in the dorsal root ganglion and spinal cord, to determine their contribution to pain pathogenesis. To date, the expression of genes encoding these altered angiogenic factors has been found to be increased in the injured DRG in an experimental neuropathic pain model based on RNA-sequencing analysis (Wu et al., 2016). However, it needs to be noted that the correlation of circulating angiogenic factors and their local expression is not always consistent. For example, investigation of EGFR and AXL in DRG sensory neurons showed that they are involved in the peripheral mechanism of neuropathic pain although we didn't observe a significant change in sEGFR and sAXL in the sera of patients with pain (Martin et al., 2017; Wang et al., 2019). Therefore, serum indices unquestionably enlighten some ideas on pain pathogenesis, but further experimental animal studies need to be performed to explore precise mechanisms.

Study limitations

A limitation of our study was the study group selection. Healthy controls were chosen from among age-matched elderly individuals who may have various other diseases, which may have affected serum angiogenic factor concentrations. Another limitation of this study was the inadequate number of patients, especially those with LBP and TN. We recruited only one patient with TN; therefore, the data could not be statistically analyzed. Further large-scale studies are required to define the role of these markers in patients with pain.

Data availability statement

The raw data supporting the conclusions of this article will be made available by the authors, without undue reservation.

Ethics statement

The studies involving human participants were reviewed and approved by the Ethical Committee of Tianjin Union Medical Center. The patients/participants provided their written informed consent to participate in this study.

Author contributions

XY and JZ: conceptualization. HW and YW: methodology. HW and ML: formal analysis. XY and CY: writing—original draft preparation. JZ and ZL: writing—review and editing. CY: visualization. XY: supervision. JZ and XY: project administration and funding acquisition. All authors have read and agreed to the published version of the manuscript.

Funding

This work was supported by the Applied Basic Research Joint Project of Tianjin (Item No. 21JCYBJC00030) and Tianjin Health Research Project (No. ZC20035).

Acknowledgments

We are grateful to the study participants for their continued participation.

Conflict of interest

The authors declare that the research was conducted in the absence of any commercial or financial relationships that could be construed as a potential conflict of interest.

Publisher's note

References

Adams, J. C., and Lawler, J. (2011). The thrombospondins. *Cold Spring Harb. Perspect. Biol.* 3:a009712. doi: 10.1101/cshperspect.a009712

Agah, E., Zardoui, A., Saghazadeh, A., Ahmadi, M., Tafakhori, A., and Rezaei, N. (2018). Osteopontin (OPN) as a CSF and blood biomarker for multiple sclerosis: a systematic review and meta-analysis. *PLoS One* 13:e0190252. doi: 10.1371/journal.pone.0190252

Al-Dasooqi, N., Gibson, R., Bowen, J., and Keefe, D. (2009). HER2 targeted therapies for cancer and the gastrointestinal tract. *Curr. Drug Targets* 10, 537–542. doi: 10.2174/138945009788488440

Assier, E., Boissier, M. C., and Dayer, J. M. (2010). Interleukin-6: from identification of the cytokine to development of targeted treatments. *Joint Bone Spine* 77, 532–536. doi: 10.1016/j.jbspin.2010.07.007

Boettger, M. K., Leuchtweis, J., Kümmel, D., Gajda, M., Bräuer, R., and Schaible, H. G. (2010). Differential effects of locally and systemically administered soluble glycoprotein 130 on pain and inflammation in experimental arthritis. *Arthritis Res. Ther.* 12:R140. doi: 10.1186/ar3079

Bornstein, P., Armstrong, L. C., Hankenson, K. D., Kyriakides, T. R., and Yang, Z. (2000). Thrombospondin 2, a matricellular protein with diverse functions. *Matrix Biol.* 19, 557–568. doi: 10.1016/s0945-053x(00)00104-9

Brázda, V., Klusáková, I., Hradilová Svíženská, I., and Dubový, P. (2013). Dynamic response to peripheral nerve injury detected by in situ hybridization of IL-6 and its receptor mRNAs in the dorsal root ganglia is not strictly correlated with signs of neuropathic pain. *Mol. Pain* 9:42. doi: 10.1186/1744-8069-9-42

Calvet, J., Orellana, C., Albiñana Giménez, N., Berenguer-Llergo, A., Caixàs, A., García-Manrique, M., et al. (2018). Differential involvement of synovial adipokines in pain and physical function in female patients with knee osteoarthritis. Cross-sectional Study *Osteoarthr. Cartil.* 26, 276–284. doi: 10.1016/j.joca.2017.11.010

Dokala, A., and Thakur, S. S. (2017). Extracellular region of epidermal growth factor receptor: a potential target for anti-EGFR drug discovery. *Oncogene* 36, 2337–2344. doi: 10.1038/onc.2016.393

Farrow, B., Berger, D. H., and Rowley, D. (2009). Tumor-derived pancreatic stellate cells promote pancreatic cancer cell invasion through release of thrombospondin-2. *J. Surg. Res.* 156, 155–160. doi: 10.1016/j.jss.2009.03.040

Goldberger, A., Middleton, K. A., Oliver, J. A., Paddock, C., Yan, H. C., DeLisser, H. M., et al. (1994). Biosynthesis and processing of the cell adhesion molecule PECAM-1 includes production of a soluble form. *J. Biol. Chem.* 269, 17183–17191.

Hayden, S. M., and Seeds, N. W. (1996). Modulated expression of plasminogen activator system components in cultured cells from dissociated mouse dorsal root ganglia. *J. Neurosci.* 16, 2307–2317. doi: 10.1523/jneurosci.16-07-02307.1996

Ho, J., Moyes, D. L., Tavassoli, M., and Naglik, J. R. (2017). The Role of ErbB receptors in infection. *Trends Microbiol.* 25, 942–952. doi: 10.1016/j.tim.2017.04.009

Icer, M. A., and Gezmen-Karadag, M. (2018). The multiple functions and mechanisms of osteopontin. *Clin. Biochem.* 59, 17–24. doi: 10.1016/j.clinbiochem.2018.07.003

Ichikawa, H., Itota, T., Nishitani, Y., Torii, Y., Inoue, K., and Sugimoto, T. (2000). Osteopontin-immunoreactive primary sensory neurons in the rat spinal and trigeminal nervous systems. *Brain Res.* 863, 276–281. doi: 10.1016/s0006-8993(00)02126-0

Irigoyen, J. P., Muñoz-Cánoves, P., Montero, L., Koziczak, M., and Nagamine, Y. (1999). The plasminogen activator system: biology and regulation. *Cell Mol. Life Sci.* 56, 104–132. doi: 10.1007/pl00000615

Jimenez-Andrade, J. M., Herrera, M. B., Ghilardi, J. R., Vardanyan, M., Melemedjian, O. K., and Mantyh, P. W. (2008). Vascularization of the dorsal root ganglia and peripheral nerve of the mouse: implications for chemical-induced peripheral sensory neuropathies. *Mol. Pain* 4:10. doi: 10.1186/1744-8069-4-10

Kalinowska, A., and Losy, J. (2006). PECAM-1, a key player in neuroinflammation. *Eur. J. Neurol.* 13, 1284–1290. doi: 10.1111/j.1468-1331.2006.01640.x

Kaufman, B., Wu, Y., Amonkar, M. M., Sherrill, B., Bachelot, T., Salazar, V., et al. (2010). Impact of lapatinib monotherapy on QOL and pain symptoms in patients with HER2+ relapsed or refractory inflammatory breast cancer. *Curr. Med. Res. Opin.* 26, 1065–1073. doi: 10.1185/03007991003680323

Kawasaki, Y., Zhang, L., Cheng, J. K., and Ji, R. R. (2008). Cytokine mechanisms of central sensitization: distinct and overlapping role of interleukin-1beta, interleukin-6, and tumor necrosis factor-alpha in regulating synaptic and neuronal activity in the superficial spinal cord. *J. Neurosci.* 28, 5189–5194. doi: 10.1523/jneurosci.3338-07.2008

Kersten, C., and Cameron, M. G. (2012). Cetuximab alleviates neuropathic pain despite tumour progression. *BMJ Case Rep.* 2012, bcr1220115374. doi: 10.1136/bcr.12.2011.5374

Kersten, C., Cameron, M. G., Bailey, A. G., Fallon, M. T., Laird, B. J., Paterson, V., et al. (2019). Relief of neuropathic pain through epidermal growth factor receptor inhibition: a randomized proof-of-concept trial. *Pain Med.* 20, 2495–2505. doi: 10.1093/pm/pnz101

Kersten, C., Cameron, M. G., Laird, B., and Mjåland, S. (2015). Epidermal growth factor receptor-inhibition (EGFR-I) in the treatment of neuropathic pain. *Br. J. Anaesth.* 115, 761–767. doi: 10.1093/bja/aev326

Kersten, C., Cameron, M. G., and Mjåland, S. (2013). Erratum to "Epithelial growth factor receptor (EGFR)-inhibition for relief of neuropathic pain-A case series" [Scand. J. Pain 4 (2013) 3-7]. *Scand. J. Pain* 4:125. doi: 10.1016/j.sjpain.2013.02.001

Lamort, A. S., Giopanou, I., Psallidas, I., and Stathopoulos, G. T. (2019). Osteopontin as a link between inflammation and cancer: the thorax in the spotlight. *Cells* 8:815. doi: 10.3390/cells8080815

Lawton, M. T., Rutledge, W. C., Kim, H., Stapf, C., Whitehead, K. J., Li, D. Y., et al. (2015). Brain arteriovenous malformations. *Nat. Rev. Dis. Primers* 1:15008. doi: 10.1038/nrdp.2015.8

Liu, J. F., Lee, C. W., Tsai, M. H., Tang, C. H., Chen, P. C., Lin, L. W., et al. (2018). Thrombospondin 2 promotes tumor metastasis by inducing matrix metalloproteinase-13 production in lung cancer cells. *Biochem. Pharmacol.* 155, 537–546. doi: 10.1016/j.bcp.2018.07.024

Lyngbæk, S., Andersson, C., Marott, J. L., Møller, D. V., Christiansen, M., Iversen, K. K., et al. (2013). Soluble urokinase plasminogen activator receptor for risk prediction in patients admitted with acute chest pain. *Clin. Chem.* 59, 1621–1629. doi: 10.1373/clinchem.2013.203778

Mafu, T. S., September, A. V., and Shamley, D. (2018). The potential role of angiogenesis in the development of shoulder pain, shoulder dysfunction, and lymphedema after breast cancer treatment. *Cancer Manag. Res.* 10, 81–90. doi: 10.2147/cmar.S151714

Mapp, P. I., and Walsh, D. A. (2012). Mechanisms and targets of angiogenesis and nerve growth in osteoarthritis. *Nat. Rev. Rheumatol.* 8, 390–398. doi: 10.1038/nrrheum.2012.80

Marsh, B. C., Kerr, N. C., Isles, N., Denhardt, D. T., and Wynick, D. (2007). Osteopontin expression and function within the dorsal root ganglion. *Neuroreport* 18, 153–157. doi: 10.1097/WNR.0b013e328010d4fa

Martin, L. J., Smith, S. B., Khoutorsky, A., Magnussen, C. A., Samoshkin, A., Sorge, R. E., et al. (2017). Epiregulin and EGFR interactions are involved in pain processing. *J. Clin. Invest.* 127, 3353–3366. doi: 10.1172/jci87406

Moasser, M. M. (2007). The oncogene HER2: its signaling and transforming functions and its role in human cancer pathogenesis. *Oncogene* 26, 6469–6487. doi: 10.1038/sj.onc.1210477

Naumnik, W., Ossolińska, M., Płońska, I., Chyczewska, E., and Nikliński, J. (2015). Circulating thrombospondin-2 and FGF-2 in Patients with advanced non-small cell lung cancer: correlation with survival. *Adv. Exp. Med. Biol.* 833, 9–14. doi: 10.1007/5584_2014_78

Neuschwander-Tetri, B. A., Talkad, V., and Otis Stephen, F. (2006). Induced thrombospondin expression in the mouse pancreas during pancreatic injury. *Int. J. Biochem. Cell Biol.* 38, 102–109. doi: 10.1016/j.biocel.2005.08.008

Nishimoto, N., Terao, K., Mima, T., Nakahara, H., Takagi, N., and Kakehi, T. (2008). Mechanisms and pathologic significances in increase in serum interleukin-6 (IL-6) and soluble IL-6 receptor after administration of an anti-IL-6 receptor antibody, tocilizumab, in patients with rheumatoid arthritis and Castleman disease. *Blood* 112, 3959–3964. doi: 10.1182/blood-2008-05-155846

Onore, C. E., Nordahl, C. W., Young, G. S., Van de Water, J. A., Rogers, S. J., and Ashwood, P. (2012). Levels of soluble platelet endothelial cell adhesion molecule-1 and P-selectin are decreased in children with autism spectrum disorder. *Biol. Psychiatry* 72, 1020–1025. doi: 10.1016/j.biopsych.2012.05.004

Park, J., Yu, Y. P., Zhou, C. Y., Li, K. W., Wang, D., Chang, E., et al. (2016). Central mechanisms mediating thrombospondin-4-induced pain states. *J Biol Chem* 291, 13335–13348. doi: 10.1074/jbc.M116.723478

Perrier, A., Gligorov, J., Lefèvre, G., and Boissan, M. (2018). The extracellular domain of Her2 in serum as a biomarker of breast cancer. *Lab Invest* 98, 696–707. doi: 10.1038/s41374-018-0033-8

Reckziegel, D., Vachon-Presseau, E., Petre, B., Schnitzer, T. J., Baliki, M. N., and Apkarian, A. V. (2019). Deconstructing biomarkers for chronic pain: context- and

hypothesis-dependent biomarker types in relation to chronic pain. *Pain 160 Suppl* 1(Suppl. 1), S37–S48. doi: 10.1097/j.pain.0000000000001529

Rendina, D., De Filippo, G., Postiglione, L., Covelli, B., Ricciardone, M., Guillaume, S., et al. (2018). Interleukin-6 trans-signaling and pathological low back pain in patients with Paget disease of bone. *Pain* 159, 1664–1673. doi: 10.1097/j.pain.0000000000001260

Rutkowski, M. D., Winkelstein, B. A., Hickey, W. F., Pahl, J. L., and DeLeo, J. A. (2002). Lumbar nerve root injury induces central nervous system neuroimmune activation and neuroinflammation in the rat: relationship to painful radiculopathy. *Spine* 27, 1604–1613. doi: 10.1097/00007632-200208010-00003

Sajib, S., Zahra, F. T., Lionakis, M. S., German, N. A., and Mikelis, C. M. (2018). Mechanisms of angiogenesis in microbe-regulated inflammatory and neoplastic conditions. *Angiogenesis* 21, 1–14. doi: 10.1007/s10456-017-9583-4

Scholz, J., Finnerup, N. B., Attal, N., Aziz, Q., Baron, R., Bennett, M. I., et al. (2019). The IASP classification of chronic pain for ICD-11: chronic neuropathic pain. *Pain* 160, 53–59. doi: 10.1097/j.pain.0000000000001365

Siconolfi, L. B., and Seeds, N. W. (2001). Induction of the plasminogen activator system accompanies peripheral nerve regeneration after sciatic nerve crush. *J. Neurosci.* 21, 4336–4347. doi: 10.1523/jneurosci.21-12-04336.2001

Soejima, H., Irie, A., Fukunaga, T., Sugamura, K., Kojima, S., Sakamoto, T., et al. (2006). Elevated plasma osteopontin levels were associated with osteopontin expression of CD4+ T cells in patients with unstable angina. *Circ. J.* 70, 851–856. doi: 10.1253/circj.70.851

Sweitzer, S. M., White, K. A., Dutta, C., and DeLeo, J. A. (2002). The differential role of spinal MHC class II and cellular adhesion molecules in peripheral inflammatory versus neuropathic pain in rodents. *J. Neuroimmunol.* 125, 82–93. doi: 10.1016/s0165-5728(02)00036-x

Tang, Y. L., Zhu, G. Q., Hu, L., Zheng, M., Zhang, J. Y., Shi, Z. D., et al. (2010). Effects of intra-articular administration of sodium hyaluronate on plasminogen activator system in temporomandibular joints with osteoarthritis. *Oral Surg. Oral Med. Oral Pathol. Oral Radiol. Endod.* 109, 541–547. doi: 10.1016/j.tripleo.2009.11.007

Thunø, M., Macho, B., and Eugen-Olsen, J. (2009). suPAR: the molecular crystal ball. *Dis. Markers* 27, 157–172. doi: 10.3233/dma-2009-0657

Treede, R. D., Rief, W., Barke, A., Aziz, Q., Bennett, M. I., Benoliel, R., et al. (2019). Chronic pain as a symptom or a disease: the IASP classification of chronic pain for the international classification of diseases (ICD-11). *Pain* 160, 19–27. doi: 10.1097/j.pain.0000000000001384

Viallard, C., and Larrivée, B. (2017). Tumor angiogenesis and vascular normalization: alternative therapeutic targets. *Angiogenesis* 20, 409–426. doi: 10.1007/s10456-017-9562-9

Wang, S., Liu, S., Xu, L., Zhu, X., Liu, W., Tian, L., et al. (2019). The upregulation of EGFR in the dorsal root ganglion contributes to chronic compression of dorsal root ganglions-induced neuropathic pain in rats. *Mol. Pain* 15:1744806919857297. doi: 10.1177/1744806919857297

Wu, S., Marie Lutz, B., Miao, X., Liang, L., Mo, K., Chang, Y. J., et al. (2016). Dorsal root ganglion transcriptome analysis following peripheral nerve injury in mice. *Mol. Pain* 12:1744806916629048. doi: 10.1177/1744806916629048

Yamaga, M., Tsuji, K., Miyatake, K., Yamada, J., Abula, K., Ju, Y. J., et al. (2012). Osteopontin level in synovial fluid is associated with the severity of joint pain and cartilage degradation after anterior cruciate ligament rupture. *PLoS One* 7:e49014. doi: 10.1371/journal.pone.0049014

Yang, Y., Gao, S. G., Zhang, F. J., Luo, W., Xue, J. X., and Lei, G. H. (2014). Effects of osteopontin on the expression of IL-6 and IL-8 inflammatory factors in human knee osteoarthritis chondrocytes. *Eur. Rev. Med. Pharmacol. Sci.* 18, 3580–3586.

Yılmaz, N., Yılmaz, M., Sirin, B., Yılmaztekin, S., and Kutlu, G. (2017). The relationship between levels of plasma-soluble urokinase plasminogen activator receptor (suPAR) and presence of migraine attack and aura. *J. Recept. Signal Transduct. Res.* 37, 447–452. doi: 10.1080/10799893.2017.1328440

frontiers | Frontiers in Molecular Neuroscience

TYPE Review
PUBLISHED 28 July 2022
DOI 10.3389/fnmol.2022.953765

OPEN ACCESS

EDITED BY
Yize Li,
Tianjin Medical University General Hospital, China

REVIEWED BY
Dong Yang,
Huazhong University of Science and Technology, China
Zhixiang Cheng,
Nanjing Medical University, China
Jian Cui,
Army Medical University, China

*CORRESPONDENCE
Lingjie Xia
xialingjiesy@126.com
Yanqing Liu
lyqttyy@126.com

SPECIALTY SECTION
This article was submitted to Pain Mechanisms and Modulators, a section of the journal Frontiers in Molecular Neuroscience

RECEIVED 26 May 2022
ACCEPTED 27 June 2022
PUBLISHED 28 July 2022

CITATION
Fan X, Fu Z, Ma K, Tao W, Huang B, Guo G, Huang D, Liu G, Song W, Song T, Xiao L, Xia L and Liu Y (2022) Chinese expert consensus on minimally invasive interventional treatment of trigeminal neuralgia. *Front. Mol. Neurosci.* 15:953765. doi: 10.3389/fnmol.2022.953765

Chinese expert consensus on minimally invasive interventional treatment of trigeminal neuralgia

Xiaochong Fan[1], Zhijian Fu[2], Ke Ma[3], Wei Tao[4], Bing Huang[5], Gang Guo[6], Dong Huang[7], Guangzhao Liu[8], Wenge Song[2], Tao Song[9], Lizu Xiao[10], Lingjie Xia[11]* and Yanqing Liu[12]*

[1]Department of Pain Medicine, The First Affiliated Hospital of Zhengzhou University, Zhengzhou, China, [2]Department of Pain Medicine, Shandong Provincial Hospital Affliated to Shandong First Medical University, Jinan, China, [3]Department of Pain Medicine, Xinhua Hospital Affiliated to Shanghai Jiao Tong University School of Medicine, Shanghai, China, [4]Department of Functional Neurosurgery, Shenzhen University General Hospital, Shenzhen, China, [5]Department of Pain Medicine, The Affliated Hospital of Jiaxing University, Jiaxing, China, [6]Department of Interventional Medicine, Lanzhou University First Hospital, Lanzhou, China, [7]Department of Pain Medicine, The Third Xiangya Hospital of Central South University, Changsha, China, [8]Department of Pain Medicine, The Second Hospital of Hebei Medical University, Shijiazhuang, China, [9]Department of Pain Medicine, The First Hospital of China Medical University, Shenyang, China, [10]Department of Pain Medicine, The Union Shenzhen Hospital of Huazhong Science and Technology University, Shenzhen, China, [11]Department of Pain Medicine, Henan Provincial People's Hospital, Zhengzhou, China, [12]Department of Pain Medicine, Beijing Tiantan Hospital, Capital Medical University, Beijing, China

Background and purpose: Trigeminal neuralgia is a common condition that is associated with severe pain, which seriously affects the quality of life of patients. When the efficacy of drugs is not satisfactory or adverse drug reactions cannot be tolerated, minimally invasive interventional therapy has become an important treatment because of its simple operation, low risk, high repeatability and low cost. In recent years, minimally invasive interventional treatments, such as radiofrequency thermocoagulation (RF) of the trigeminal nerve and percutaneous microcompression (PMC), have been widely used in the clinic to relieve severe pain in many patients, however, some related problems remain to be addressed. The Pain Association of the Chinese Medical Association organizes and compiles the consensus of Chinese experts to standardize the development of minimally invasive interventional treatment of trigeminal neuralgia to provide a basis for its clinical promotion and application.

Materials and methods: The Pain Association of the Chinese Medical Association organizes the Chinese experts to compile a consensus. With reference to the evidence-based medicine (OCEBM) system and the actual situation of the profession, the Consensus Development Committee adopts the nominal group method to adjust the recommended level.

Results: Precise imaging positioning and guidance are the keys to ensuring the efficacy and safety of the procedures. RF and PMC are the most widely

performed and effective treatments among minimally invasive interventional treatments for trigeminal neuralgia.

Conclusions: The pain degree of trigeminal neuralgia is severe, and a variety of minimally invasive intervention methods can effectively improve symptoms. Radiofrequency and percutaneous microcompression may be the first choice for minimally invasive interventional therapy.

KEYWORDS

trigeminal neuralgia, radiofrequency thermocoagulation, percutaneous microcompression, neuropathic pain, headache

Overview

Trigeminal neuralgia is a common condition that is associated with severe pain, which seriously affects the quality of life of patients. When the efficacy of drugs is not satisfactory or adverse drug reactions cannot be tolerated, minimally invasive interventional therapy has become an important treatment because of its simple operation, low risk, high repeatability and low cost. In recent years, minimally invasive interventional treatments, such as RF of the trigeminal nerve and PMC, have been widely used in the clinic to relieve severe pain in many patients, however, some related problems remain to be addressed.

In order to standardize the development of minimally invasive interventional treatment for trigeminal neuralgia and provide a basis for its clinical promotion and application, The pain Association of Chinese Medical Association organized Chinese experts to compile a consensus with reference to evidence-based medicine (OCEBM) system and the actual situation of the profession, using the nominal grouping method to adjust the recommendation level (**Table 1**).

Definition

Trigeminal neuralgia is a typical neuropathic pain. ICD-11(International Classification of Diseases11) defines trigeminal neuralgia as "a unilateral disease characterized by transient electrical shock-like pain, with sudden onset and resolution, and the location of the pain is limited to one or more innervation areas of the trigeminal nerve" (Jones et al., 2019; Scholz et al., 2019a).

Epidemiology

Approximately 12–29/100,000 people suffer from trigeminal neuralgia every year (Tai and Nayar, 2019). The incidence among women (5.9/100,000) is slightly higher than that among men (3.4/100,000) (Obermann and Katsarava, 2009). Trigeminal neuralgia can appear for the first time at any age, but more than 90% of cases have an onset age after 40, and the peak age is between 50 and 60 years old (MacDonald et al., 2000).The right side of the face is more affected than the left side (Cruccu et al., 2020).

Pathogenesis

Trigeminal neuralgia is mainly divided into primary and secondary neuralgia. Primary neuralgia is divided into classic and idiopathic trigeminal neuralgia. The mechanism of primary trigeminal neuralgia is unknown. The main hypothesis of classic trigeminal neuralgia is that the trigeminal nerve root is compressed by abnormal blood vessels, which causes morphological changes in the trigeminal nerve. This may be related to ectopic impulses caused by demyelination and remyelination of the trigeminal nerve after compression (Cruccu et al., 2016; Tai and Nayar, 2019).Secondary trigeminal neuralgia is caused by identifiable diseases, such as trauma, tumors, viruses, and infections.

Diagnosis and treatment

Clinical manifestations

Trigeminal neuralgia is characterized mostly by a chronic course of illness that gradually worsens, and there may be a period of symptomatic relief. The pain is located in the distribution area of one or more branches of the unilateral trigeminal nerve. The nature of the pain is mostly that of an electric shock or knife cut that is. characterized by a paroxysmal onset and sudden cessation. The duration is usually several seconds to several minutes, and there is no pain in the intermittent period. Chewing, brushing, and touching can trigger pain. On physical examination, the "trigger point" can be elicited in the area of pain; trigger

Abbreviations: RF, radiofrequency thermocoagulation; PMC, Percutaneous microcompression.

TABLE 1 Oxford University Center for Evidence-Based Medicine (OCEBM) evidence level and recommendation level standard.

Level of evidence	Definition
1a	Systematic review of randomized controlled trials (homogeneity)
1b	Individual randomized controlled trials (narrow confidence interval)
1c	When all patients died before the measure was introduced, but some patients now survive on it.
2a	Systematic review of cohort studies (homogeneity)
2b	Individual cohort studies (including low-quality randomized controlled trials; e g., follow-up rate < 80%)
2c	A study of the outcome; an ecological study
3a	Systematic review of case–control studies (homogeneity)
3b	Individual case-control study
4	Case series (and poor-quality cohort studies and case–control studies)
5	Lack of clear and strictly evaluated expert advice, or derived from physiology, laboratory research, or "first principles"
Level of recommended	**Definition**
A	Evidence of consistent level 1
B	Consistent level 2 or 3 evidence, or extrapolation based on level 1 evidence. ("extrapolation" means that data are applied to situations with potentially clinically important differences rather than the original research)
C	Level 4 evidence, or extrapolation based on level 2 or 3 evidence
D	Level 5 evidence, either inconsistent or inadequate research (any level)

OCEBM, Oxford University Center for Evidence-Based Medicine.

points are mostly located beside the nose, upper and lower lips, and gums.

Imaging examination

Head CT or MRI can determine whether there is secondary trigeminal neuralgia caused by intracranial lesions, such as cerebellopontine angle-occupying lesions (1b evidence level, A level recommendation) (Chun-Cheng et al., 2009). Three-dimensional time-of-flight magnetic resonance angiography (3D-TOFMRA) can help clarify the anatomical relationship between the trigeminal nerve root and surrounding blood vessels(2b evidence level, B level recommendation) (Cha et al., 2011). Although it cannot be used as a diagnostic basis for primary trigeminal neuralgia, it can help guide the formulation of treatment plans (Bendtsen et al., 2020).

Diagnosis and differential diagnosis

The diagnosis of primary trigeminal neuralgia is mainly based on clinical manifestations. You can refer to the following diagnostic criteria for trigeminal neuralgia in ICHD-3 of the International Headache Association:

(1) Recurrent unilateral pain occurs in one or more branches of the trigeminal nerve, does not involve the trigeminal nerve outside the distribution area, and fully meets the criteria of (2) and (3).

(2) Pain meets all of the following characteristics:

① It lasts from a few tenths of a second to 2 min;

② Severe pain;

③ The nature of the pain is lightning, electric shock, acupuncture or sharp pain.

(3) Harmless stimuli on the affected side can induce pain.

(4) Other ICHD-3 diagnoses cannot provide a better explanation for the pain.

The differential diagnosis includes glossopharyngeal neuralgia, sphenopalatine neuralgia, cluster headache, atypical facial pain, and temporomandibular joint pain.

Treatment

If the effect is not satisfactory or an adverse drug reaction cannot be tolerated, the choices for the treatment of trigeminal neuralgia include minimally invasive intervention, surgery, and gamma knife treatment.

(1) Drug treatment: Carbamazepine is the first-line choice, followed by oxcarbazepine. To avoid the risk of serious adverse reactions, it is recommended that drug genetic tests be performed before taking the drug when possible. If the patient cannot tolerate the side effects of the above drugs, other drugs can be used, such as pregabalin, gabapentin, phenytoin and sodium valproate. If the pain is persistent, a combination of medications can be used.

(2) Minimally invasive interventional treatment: Therapies include image-guided trigeminal nerve branch block or RF therapy, trigeminal nerve semilunar ganglion RF, chemical

damage, or PMC. A minimally invasive interventional treatment technique is easy to perform, causes less trauma, is less costly and reliable. The main complications are hypoesthesia, keratitis, and masticatory muscle disorders.

(3) Surgical treatment: Surgeries include trigeminal nerve MVD, selective trigeminal nerve sensory roototomy, and peripheral neurotomy. MVD may be a non-destructive but highly traumatic surgical method for trigeminal neuralgia, with high immediate satisfaction of patients, a low incidence of postoperative complications such as facial numbness and weakness in mastication, and a complete pain relief rate of more than 90% after surgery, and 71% after 10 years (Sarsam et al., 2010). However, patients need to bear the risk of craniotomy, and high treatment costs, and frail elderly patients with more comorbidities have a higher risk. Surgical risks mainly include loss of facial sensation, hearing loss, cerebrospinal fluid leakage, and cerebellar hematoma.

(4) Gamma knife treatment: Gamma knife treatment for trigeminal neuralgia is widely used in the clinic, but there are few randomized controlled trials in clinical studies. Gamma knife treatment often does not relieve pain immediately and can take 1–2 months. At 3, 5, 7, and 10 years after treatment, the probabilities of remaining pain-free without the use of drugs were 77.9%, 73.8%, 68%, and 51.5%, respectively; the incidence of facial sensory disturbances was 20.8% (Régis et al., 2016).

(5) Other treatments include acupuncture, traditional Chinese medicine, and botulinum toxin injection.

Minimally invasive interventional therapy

Radiofrequency treatment

The common method of percutaneous RF involves puncture through the foramen ovale to reach the semilunar ganglion and temperature control to thermally coagulate the trigeminal nerve (Rabb and Cheema, 2015).

Sweet (1974) first reported that RF was used to treat primary trigeminal neuralgia. After years of improvement and development, this technique has many advantages, such as good curative effects, less trauma, low risk, and repeatable treatment (2a evidence level, B level recommendation) (Yan et al., 2021). RF, is indicated for patients with contraindications to surgery, especially elderly patients with underlying diseases. According to reports, during the 20-year follow-up, 41% of patients underwent a single operation, 100% of multiple operations resulted in pain relief, and there were no deaths (Kanpolat et al., 1999). Mathews (Mathews and Scrivani, 2000) reported the results of a study of 258 cases with an average follow-up of 38 months. Among them, the rate of excellent pain relief in the early follow-up was 87%. At the end of the long-term follow-up, 83% of patients had good pain relief.

The most commonly used puncture approach of RF for trigeminal neuralgia is the Hartel approach, which refers to the precise positioning of the foramen ovale and puncture path through X-ray or CT and selective puncturing into the corresponding trigeminal ganglion. Combined with electrophysiological stimulation for precise positioning tests, selective thermocoagulation damages the corresponding area of the trigeminal nerve semilunar ganglion to achieve analgesia (Fang et al., 2014). In addition to the commonly used semilunar radiofrequency, radiofrequency for the peripheral branch of the extracranial trigeminal nerve can also be selected to relieve the pain. The puncture sites include the supraorbital foramen, infraorbital foramen, mental foramen, circular foramen, and foramen ovale. In particular, RF for precise positioning of the circular hole under image guidance provides a good treatment option for patients with pain involving only the second branch of the trigeminal nerve (V2). When multiple branches are painful, multitarget radiofrequency treatment can be used (Wan et al., 2018).

(1) Indications

① Patients with poor drug-protection treatment for primary trigeminal neuralgia or those who are unable to tolerate adverse drug reactions;

② Patients with severe systemic diseases who cannot tolerate surgery or who refuse surgery;

③ Patients with secondary trigeminal neuralgia who still have pain after treatment of the primary disease or who refuse treatment of the primary disease;

④ Patients who relapse after various operations (Huang et al., 2019; Abdel-Rahman et al., 2020).

(2) Contraindications (Emril and Ho, 2010)

① Patients with infection at the puncture site;

② Patients with coagulation dysfunction;

③ Patients with severely unstable heart and cerebrovascular diseases;

④ Patients with severe mental illness.

(3) Operating routine

① Preoperative preparation

Tests such as routine blood tests, coagulation studies, biochemical examinations, and electrocardiograms should be performed to assess the patient's body condition, along with head CT or MRI examination. The patients and their families should be fully informed of the treatment methods, expected results and possible complications before surgery.

② Methods of anesthesia

Sedative and analgesic drugs are recommended during local anesthesia to reduce the pain of puncture; thus, the patient can obtain analgesia and maintain sufficient cognition to achieve sensory positioning during puncture. After the positioning is successful, intravenous general anesthesia can be implemented.

③ Operative process

The patient is placed in a supine position, with a thin pillow under the shoulders, after which the head is tilted posteriorly. Routinely sterilized drapes are used. According to the Hartel approach, the puncture needle point is determined, usually at the intersection of the perpendicular line of the outer edge of the affected orbit and the interlabial line region. The foramen ovale is punctured under image guidance (C-arm, DSA or CT). In the axial view, the first branch of the trigeminal nerve semilunar ganglion radiofrequency target is located above the medial edge of the foramen ovale, the second branch is located at the medial edge of the foramen ovale, and the third branch is located in the center of the foramen ovale. In the lateral view, the second branch of the semilunar ganglion of the trigeminal nerve is approximately, located at the slope line, the first branch is located deeper, and the third branch is loacted shallow relative to the slope line. After the puncture is in place, the RF electrode is connected, and the impedance at 300∼500 Ω is observed. A sensory test with 0.1∼0.3 V high-frequency current stimulation is performed, and the corresponding nerve innervation area will experience numbness and pain symptoms. When the movement test begins at 0.1∼0.3 V, the third innervation area will appear on the masseter. For convulsions, the needle tip position can be adjusted appropriately according to the patient's response during the stimulation process to make the stimulation area consistent with the branch area to be treated. After the electrophysiological test is completed, radiofrequency thermocoagulation is performed. The recommended temperature for the treatment of the second and third branches is 60∼75°C. The first branch should be treated with caution. The time of treatment is based on the decrease in sensation of the target nerve distribution area on the affected side, usually 2∼3 min. The higher the temperature is, the longer the time, the greater the extent of nerve destruction, and the lower the recurrence rate. However, this treatment can induce a higher probability of adverse complications, such as keratitis or ulcer perforation, excessive numbness of the corresponding innervation area of the trigeminal nerve, and masseter muscle weakness after the operation (Xie et al., 2020). Therefore, during the treatment process, the patient's treatment benefits and risks should be weighed, and as low a temperature as possible should be selected while still being effective. In addition, pulsed radiofrequency therapy is available (Elawamy et al., 2017; Telischak et al., 2018; Abdel-Rahman et al., 2020; Xie et al., 2020).

(4) Postoperative test and effect

Generally, immediate pain relief can be obtained, and the original pain area has decreased sensation after the operation.

(5) Matters needing attention

① Special attention should be given to changes in the operation center rate and blood pressure (Meng et al., 2008; Schaller et al., 2008).

② Accurate display of the foramen ovale and precise puncture guarantee the success of interventional therapy (Guo et al., 2016; Weßling and Duda, 2019).

③ The RF temperature should be strictly controlled to avoid excessive temperature-induced damage to the target nerve and adjacent branches, which can cause postoperative facial numbness, masseter muscle weakness and other complications (Yao et al., 2016). If the corneal reflex is delayed after surgery, medical care should be implemented to avoid keratitis, ulcers, and perforations (Tang et al., 2015).

Percutaneous microcompression

PMC of the meniscus ganglion refers to the treatment of trigeminal neuralgia by placing a balloon into Meckel's cavity and injecting a contrast agent into the balloon to mechanically compress the meniscus. Mullan and Lichtor (1983) first used this technique to treat trigeminal neuralgia in 1978 and published his research paper in 1983 (Mullan and Lichtor, 1983). At present, the treatment mechanism of PMC is not clear. In recent years, because this technology is safe and effective, it has been widely used in the treatment of primary trigeminal neuralgia (1a evidence level, A level recommendation) (Wu et al., 2022). Grewal et al. (2018) conducted a median follow-up of 31.1 months for 222 patients with refractory trigeminal neuralgia who were treated using PMC, and all patients had remission within 12 months after PMC. It has been reported that the 5-year effective rate after surgery is 80%, and the 10-year effective rate is 70% (Lichtor and Mullan, 1990). Fan et al. conducted a 12 months follow-up of study of 121 patients with recurrent trigeminal neuralgia treated using PMC. It has been reported that 101 (83.5%) patients remained pain-free, while 5 patients (4.1%) experienced recurrence. There were significant improvements in anxiety, depression, and sleep status postoperatively compared with the preoperatively status (Fan et al., 2021).

(1) Indications

In recent years, clinical practices have shown that PMC has a wide range of indications, especially for patients with pain involving the first branch of the trigeminal nerve. Because PMC

selectively acts on large and medium myelinated nerve fibers, it can reduce the impairment of nerves (small, myelinated fibers) innervating the corneal reflex (Cheng et al., 1982).

The indications include the following

① Patients with primary trigeminal neuralgia involving single or multiple branches, especially within the first branch;

② Patients who have undergone strict and regular drug treatment with poor outcomes and those cannot tolerate adverse reactions;

③ Imaging data suggesting that microvascular decompression will be relatively difficult or risky in patients who do not undergo craniotomy;

④ Patients who relapse after other surgery (Fan et al., 2021);

⑤ Patients with secondary trigeminal neuralgia who still have pain after treatment of the primary disease or who refuse treatment of the primary disease (Liu, 2018).

(2)Contraindications

① Patients with severe systemic diseases who cannot tolerate surgery;

② Patients with uncorrected coagulation dysfunction;

③ Severe systemic infection or infection at the puncture site.

(3) Operating routine

① Preoperative preparation

Before surgery, routine blood tests, routine blood coagulation tests, biochemical examinations, electrocardiograms, head CT or MRI examinations, etc., should be performed to assess the whole body and local nerve condition. Patients provided full informed consent which covers the treatment methods, expected results and possible complications before surgery.

② Anesthesia method

General anesthesia: The advantage of general anesthesia is that the patient is unconscious and out of pain during the operation, but the disadvantage is that some patients with systemic diseases cannot tolerate it, and the incidence of trigeminal nerve-cardiac reflex is relatively high (Tibano et al., 2010; Agarwal et al., 2015).

General anesthesia-assisted trigeminal ganglion block: the advantages of general anesthesia can be retained, and the incidence of the trigeminal nerve-cardiac reflex is lower than that of general anesthesia alone (Tibano et al., 2010).

Trigeminal ganglion block anesthesia: The puncture point and puncture direction are the same as those under general anesthesia. The local anesthetic needle is used for local anesthesia at the puncture point and needle channel. Under the guidance of imaging, the puncture needle enters through the foramen ovale to reach the ganglion, and 0.3∼0.5 ml of the local anesthetics is injected for the ganglion block. This method is suitable for patients who cannot tolerate general anesthesia, and the incidence of the trigeminal nerve-cardiac reflex is low (Ren et al., 2020). The disadvantage is that when some patients are awake and experience anxiety, but they can administered.

③ Operative process

After the image guide reaches the ideal position, non-ionic contrast agent is injected, with a dose of usually no more than 1 ml, and the pressure is adjusted to the balloon such that resistance is experienced. The position is adjusted until the balloon shows a "pear shape." The balloon compression time is usually 60–180 s (Tibano et al., 2010; Bergenheim et al., 2013; de Cordoba et al., 2015; Grewal et al., 2018), and it can be extended appropriately for elderly or relapsed patients. After the compression is completed, the contrast medium in the balloon is withdrawn, and the balloon catheter and puncture needle are removed. The puncture point is compressed for 5 min to stop the bleeding and then is covered with sterile gauze.

(4) Postoperative test and effect

The ideal balloon filling shape should be a "pear shape." The affected side will have decreased sensation after surgery, and pain relief can generally be achieved. If the balloon shape is not ideal, the puncture position and direction should be adjusted (Asplund et al., 2010).

TABLE 2 Comparison of minimally invasive interventional treatments of characteristics for trigeminal neuralgia.

Characteristics	Radiofrequency treatment	Percutaneous microcompression	Chemical damage
Anesthesia	Local anesthesia	General anesthesia/Local anesthesia	Local anesthesia
Operation difficulty	Low	Low	Low
Long-term curative effect	Medium	High	Medium
Recurrence rate	Low	Low	Medium
Degree of safety	High	High	Low
Complications	Medium	Low	Medium
Expenses	Low	Medium	Low

(5) Matters needing attention

① Preoperative MRI thin-slice scans can be used to estimate the volume of Meckel's cavity. The volume of the contrast medium injected during the operation should be greater than the estimated volume of Meckel's cavity, but it must be subject to obvious resistance when the contrast medium is injected.

② During balloon compression, a trigeminal nerve-cardiac reflex may occur. It is necessary to closely monitor changes in heart rate and blood pressure and address changes in a timely manner.

③ During the operation, advancing the puncture needle too deeply and allowing it to deviate to the inside should be avoided (Spaziante et al., 1988). Damage to the internal carotid artery, cavernous sinus or other cranial nerves should be avoided.

④ The incidence of postoperative perioral herpes is 14.7%, and preventive antiviral therapy may reduce its incidence (Berra et al., 2019).

⑤ After PMC, the sensations in the oral cavity on the operative side are decreased. Overheated or sharp foods should be avoided to prevent damage to the oral mucosa.

Other interventional treatments

In addition to the abovementioned mechanical compression or physical damage methods, minimally invasive treatment of primary trigeminal neuralgia employs chemical injections into the semilunar ganglia, trigeminal nerve pool or peripheral branches for chemical damage. Chemical drugs include absolute ethanol, glycerin, botulinum toxin A and doxorubicin. Among them, the effect of glycerol on the semilunar ganglion and trigeminal nerve pool is supported by domestic and foreign literature (2b evidence level, B level recommendation) (Chen et al., 2010; Asplund et al., 2016; Staudt et al., 2020). Anhydrous alcohol can be used for the semilunar ganglion and peripheral division (2b evidence level, B level recommendation) (Han and Kim, 2010; Han et al., 2017), and botulinum toxin A (1a evidence level, A level recommendation) (Morra et al., 2016; Steinberg, 2018; Yang et al., 2018) and doxorubicin are only used in the peripheral branches (Wang et al., 2011; Zheng et al., 2018); these drugs have a damaging effect on the surrounding tissues, and their range of action is not easy to control, which may cause serious injuries. At present, with the popularization and application of technologies such as radio frequency and microballoon compression, the use of chemical damage has become increasingly less common (Udupi et al., 2012; Asplund et al., 2016; Noorani et al., 2016, 2019), and it is only used at the grassroots level or on specific occasions. It is recommended that chemical damage in the peripheral branches of the trigeminal nerve be used as a supplementary treatment for other therapies. It should be used with caution in the intracranial semilunar ganglion. When used in peripheral branches, attention should be given to signs of local tissue damage, such as swelling.

In summary, among these minimally invasive interventional treatments for trigeminal neuralgia, RF and PMC are the most widely performed and effective treatments. The comparison of the characteristics of minimally invasive interventional treatment for trigeminal neuralgia is shown in **Table 2**. Precise imaging positioning and guidance are the key to ensuring the efficacy and safety of the procedures. X-ray has the advantages of being convenient, fast and involving low radiation, and it is easy to determine the shape of the balloon in the lateral view. 3D CT involves the use of a large amount of radiation, but it can help to analyze the size and shape of the foramen ovale and simulate the puncture path, and it is easier to observe the path of the RF needle and puncture needle, thus, it is suitable for beginners. Many clinicians have accumulated much experience in puncture procedures, but there are still many controversies about the key criteria of radiofrequency temperature, time, microballoon volume, compression time, and related factors. Further basic and clinical studies are needed to provide more accurate evidence to guide clinical applications.

Author contributions

All authors made significant contributions to the content of the article, drafted or critically revised the article, and ultimately approved the version to be published.

Funding

National Key Research and Development Program of China (2020YFC2008400) and National Natural Science Foundation of China (82001182).

Acknowledgments

The authors thank Zhongyuan Lu, Huan Ren, and Huilian Bu for their search and verification of the literature.

Conflict of interest

The authors declare that the research was conducted in the absence of any commercial or financial relationships that could be construed as a potential conflict of interest.

Publisher's note

References

Abdel-Rahman, K. A., Elawamy, A. M., Mostafa, M. F., Hasan, W. S., Herdan, R., Osman, N. M., et al. (2020). Combined pulsed and thermal radiofrequency versus thermal radiofrequency alone in the treatment of recurrent trigeminal neuralgia after microvascular decompression: a double blinded comparative study. *Eur. J. Pain (United Kingdom)* 24, 338–345. doi: 10.1002/ejp.1489

Agarwal, A., Dhama, V., Manik, Y. K., Upadhyaya, M. K., Singh, C. S., and Rastogi, V. (2015). Percutaneous balloon compression of gasserian ganglion for the treatment of trigeminal neuralgia: an experience from India. *Middle East J. Anesthesiol.* 23, 105–110.

Asplund, P., Blomstedt, P., and Tommy Bergenheim, A. (2016). Percutaneous balloon compression vs percutaneous retrogasserian glycerol rhizotomy for the primary treatment of trigeminal neuralgia. *Neurosurgery* 78, 421–428. doi: 10.1227/NEU.0000000000001059

Asplund, P., Linderoth, B., and Bergenheim, A. T. (2010). The predictive power of balloon shape and change of sensory functions on outcome of percutaneous balloon compression for trigeminal neuralgia: clinical article. *J. Neurosurg.* 113, 498–507. doi: 10.3171/2010.2.JNS091466

Bendtsen, L., Zakrzewska, J. M., Heinskou, T. B., Hodaie, M., Leal, P. R. L., Nurmikko, T., et al. (2020). Advances in diagnosis, classification, pathophysiology, and management of trigeminal neuralgia. *Lancet Neurol.* 19, 478–496. doi: 10.1016/S1474-4422(20)30233-7

Bergenheim, A. T., Asplund, P., and Linderoth, B. (2013). Percutaneous retrogasserian balloon compression for trigeminal neuralgia: review of critical technical details and outcomes. *World Neurosurg.* 79, 359–368. doi: 10.1016/j.wneu.2012.03.014

Berra, L. V., Armocida, D., Pesce, A., di Rita, A., and Santoro, A. (2019). Herpes simplex reactivation after surgical treatment of trigeminal neuralgia: a retrospective cohort study. *World Neurosurg.* 127, e16–e21. doi: 10.1016/j.wneu.2019.01.226

Cha, J., Kim, S. T., Kim, H. J., Choi, J. W., Kim, H. J., Jeon, P., et al. (2011). Trigeminal neuralgia: assessment with T2 VISTA and FLAIR VISTA fusion imaging. *Eur. Radiol.* 21, 2633–2639. doi: 10.1007/s00330-011-2216-1

Chen, L. Z., Xu, M. H., and Zou, Y. W. (2010). Treatment of trigeminal neuralgia with percutaneous glycerol injection into Meckel's cavity: experience in 4012 patients. *Cell Biochem. Biophys.* 58, 85–89. doi: 10.1007/s12013-010-9094-z

Cheng, J. S., Lim, D. A., Chang, E. F., and Barbaro, N. M. (1982). A review of percutaneous treatments for trigeminal neuralgia. *Neurosurgery* 10, 25–33. doi: 10.1227/NEU.00000000000001687

Chun-Cheng, Q., Qing-Shi, Z., Ji-Qing, Z., and Zhi-Gang, W. (2009). A single-blinded pilot study assessing neurovascular contact by using high-resolution MR imaging in patients with trigeminal neuralgia. *Eur. J. Radiol.* 69, 459–463. doi: 10.1016/j.ejrad.2007.10.010

Cruccu, G., di Stefano, G., and Truini, A. (2020). Trigeminal neuralgia. *N. Engl. J. Med.* 383, 754–762. doi: 10.1056/NEJMra1914484

Cruccu, G., Finnerup, N. B., Jensen, T. S., Scholz, J., Sindou, M., Svensson, P., et al. (2016). Trigeminal neuralgia: new classification and diagnostic grading for practice and research. *Neurology* 87, 220–228. doi: 10.1212/WNL.0000000000002840

de Cordoba, J. L., Garcia Bach, M., Isach, N., and Piles, S. (2015). Percutaneous balloon compression for trigeminal neuralgia: imaging and technical aspects. *Reg. Anesth. Pain Med.* 40, 616–622. doi: 10.1097/AAP.0000000000000292

Elawamy, A., Abdalla, E. E., and Shehata, G. A. (2017). Effects of pulsed versus conventional versus combined radiofrequency for the treatment of trigeminal neuralgia: a prospective study. *Pain Phys.* 20, E873–E881.

Emril, D. R., and Ho, K. Y. (2010). Treatment of trigeminal neuralgia: role of radiofrequency ablation. *J. Pain Res.* 3, 249–254. doi: 10.2147/JPR.S14455

Fang, L., Ying, S., Tao, W., Lan, M., Xiaotong, Y., and Nan, J. (2014). 3D CT-guided pulsed radiofrequency treatment for trigeminal neuralgia. *Pain Pract.* 14, 16–21. doi: 10.1111/papr.12041

Fan, X., Xu, F., Ren, H., Lu, Z., Bu, H., Ma, L., et al. (2021). The analysis of percutaneous balloon compression on efficacy and negative emotion in the treatment of recurrent trigeminal neuralgia after surgical procedures. *Pain Phys.* 24, e1255–e1262.

Grewal, S. S., Kerezoudis, P., Garcia, O., Quinones-Hinojosa, A., Reimer, R., and Wharen, R. E. (2018). Results of percutaneous balloon compression in trigeminal pain syndromes. *World Neurosurg.* 114, e892–e899. doi: 10.1016/j.wneu.2018.03.111

Guo, Z., Wu, B., Du, C., Cheng, M., and Tian, Y. (2016). Stereotactic approach combined with 3D CT reconstruction for difficult-to-access foramen ovale on radiofrequency thermocoagulation of the gasserian ganglion for trigeminal neuralgia. *Pain Med. (United States)* 17, 1704–1716. doi: 10.1093/pm/pnv108

Han, K. R., Chae, Y. J., Lee, J. D., and Kim, C. (2017). Trigeminal nerve block with alcohol for medically intractable classic trigeminal neuralgia: long-term clinical effectiveness on pain. *Int. J. Med. Sci.* 14, 29–36. doi: 10.7150/ijms.16964

Han, K. R., and Kim, C. (2010). The long-term outcome of mandibular nerve block with alcohol for the treatment of trigeminal neuralgia. *Anesth. Anal.* 111, 550–553. doi: 10.1213/ANE.0b013e3181e4204c

Huang, B., Xie, K., Chen, Y., Wu, J., and Yao, M. (2019). Bipolar radiofrequency ablation of mandibular branch for refractory V3 trigeminal neuralgia. *J. Pain Res.* 12, 1465–1474. doi: 10.2147/JPR.S197967

Jones, M. R., Urits, I., Ehrhardt, K. P., Cefalu, J. N., Kendrick, J. B., Park, D. J., et al. (2019). A comprehensive review of trigeminal neuralgia. *Curr. Pain Head. Rep.* 23:74. doi: 10.1007/s11916-019-0810-0

Kanpolat, Y., Savas, A., Bekar, A., and Berk, C. (1999). Percutaneous controlled radiofrequency trigeminal rhizotomy for the treatment of idiopathic trigeminal neuralgia: a 25-year experience with 1,600 patients. *Neurosurgery* 45, 532–534. doi: 10.1097/00006123-199909000-00209

Lichtor, T., and Mullan, J. F. (1990). A 10-year follow-up review of percutaneous microcompression of the trigeminal ganglion. *J. Neurosurg.* 72, 49–54. doi: 10.3171/jns.1990.72.1.0049

Liu, Q. (2018). Interpretation of "Chinese expert consensus on diagnosis and treatment of trigeminalneuralgia. *Chin. J. Contemp. Neurol. Neurosurg.* 18, 643–646. doi: 10.3969/j.issn.1672-6731.2018.09.003

MacDonald, B. K., Cockerell, O. C., Sander, J. W. A. S., and Shorvon, S. D. (2000). The incidence and lifetime prevalence of neurological disorders in a prospective community-based study in the UK. *Brain* 123, 665–676. doi: 10.1093/brain/123.4.665

Mathews, E. S., and Scrivani, S. J. (2000). Percutaneous stereotactic radiofrequency thermal rhizotomy for the treatment of trigeminal neuralgia. *Mt. Sinai J. Med.* 67, 288–299.

Meng, Q., Zhang, W., Yang, Y., Zhou, M., and Li, X. (2008). Cardiovascular responses during percutaneous radiofrequency thermocoagulation therapy in primary trigeminal neuralgia. *J. Neurosurg. Anesthesiol.* 20:270. doi: 10.1097/ANA.0b013e3181628305

Morra, M. E., Elgebaly, A., Elmaraezy, A., Khalil, A. M., Altibi, A. M. A., Vu, T. L. H., et al. (2016). Therapeutic efficacy and safety of botulinum toxin a therapy in trigeminal neuralgia: a systematic review and meta-analysis of randomized controlled trials. *J. Head. Pain* 17:63. doi: 10.1186/s10194-016-0651-8

Mullan, S., and Lichtor, T. (1983). Percutaneous microcompression of the trigeminal ganglion for trigeminal neuralgia. *J. Neurosurg.* 59, 745–748. doi: 10.3171/jns.1983.59.6.1007

Noorani, I., Lodge, A., Vajramani, G., and Sparrow, O. (2016). Comparing percutaneous treatments of trigeminal neuralgia: 19 years of experience in a single centre. *Stereotact. Funct. Neurosurg.* 94, 75–85. doi: 10.1159/000445077

Noorani, I., Lodge, A., Vajramani, G., and Sparrow, O. (2019). The effectiveness of percutaneous balloon compression, thermocoagulation, and glycerol rhizolysis for trigeminal neuralgia in multiple sclerosis. *Clin. Neurosurg.* 85, E684–E692. doi: 10.1093/neuros/nyz103

Obermann, M., and Katsarava, Z. (2009). Update on trigeminal neuralgia. *Exp. Rev. Neurother.* 9, 323–329. doi: 10.1586/14737175.9.3.323

Rabb, C., and Cheema, A. (2015). "Trigeminal neuralgia: viewpoint—surgery," in *Principles and Practice of Stereotactic Radiosurgery*, eds L. Chin and W. Regine (New York, NY: Springer), 659–664. doi: 10.1007/978-1-4614-8363-2_53

Régis, J., Tuleasca, C., Resseguier, N., Carron, R., Donnet, A., Yomo, S., et al. (2016). The very long-term outcome of radiosurgery for classical trigeminal neuralgia. *Stereotact. Funct. Neurosurg.* 94, 24–32. doi: 10.1159/000443529

Ren, Y., Han, W., du, Y., Cong, H., and Liu, G. (2020). Efficacy and safety of CT-guided percutaneous microballoon compression in the treatment of patients with primary trigeminal neuralgia under conscious trigeminal ganglion local block. *Chine. J. Painol.* 1, 30–35. doi: 10.3760/cma.j.issn.2096-8019.2020.01.009

Sarsam, Z., Garcia-Fiana, M., Nurmikko, T. J., Varma, T. R. K., and Eldridge, P. (2010). The long-term outcome of microvascular decompression for trigeminal neuralgia. *Br. J. Neurosurg.* 24, 1077–1083. doi: 10.3109/02688690903370289

Schaller, B., Sandu, N., Fili, A., and Buchfelder, M. (2008). Cardiovascular responses during percutaneous radiofrequency thermocoagulation therapy in primary trigeminal neuralgia: an explanation of the trigeminocardiac reflex? *J. Neurosurg. Anesthesiol.* 20:270. doi: 10.1097/ANA.0b013e3181817b50

Scholz, J., Finnerup, N. B., Attal, N., Aziz, Q., Baron, R., Bennett, M. I., et al. (2019a). The IASP classification of chronic pain for ICD-11: chronic neuropathic pain. *Pain* 160, 53–59. doi: 10.1097/j.pain.0000000000001365

Spaziante, R., Cappabianca, P., Peca, C., and de Divitiis, E. (1988). Subarachnoid hemorrhage and "normal pressure hydrocephalus": fatal complication of percutaneous microcompression of the gasserian ganglion: case report. *Neurosurgery* 22, 148–151. doi: 10.1227/00006123-198801000-00028

Staudt, M. D., Joswig, H., Pickett, G. E., MacDougall, K. W., and Parrent, A. G. (2020). Percutaneous glycerol rhizotomy for trigeminal neuralgia in patients with multiple sclerosis: a long-term retrospective cohort study. *J. Neurosurg.* 132, 1405–1413. doi: 10.3171/2019.1.JNS183093

Steinberg, D. I. (2018). Review: in trigeminal neuralgia, carbamazepine, botulinum toxin type A, or lidocaine improve response rate vs placebo. *Ann. Intern. Med.* 169:43. doi: 10.7326/ACPJC-2018-169-8-043

Tai, A. X., and Nayar, V. V. (2019). Update on trigeminal neuralgia. *Curr. Treat. Opt. Neurol.* 21:42. doi: 10.1007/s11940-019-0583-0

Telischak, N. A., Heit, J. J., Campos, L. W., Choudhri, O. A., Do, H. M., and Qian, X. (2018). Fluoroscopic C-arm and CT-guided selective radiofrequency ablation for trigeminal and glossopharyngeal facial pain syndromes. *Pain Med. (United States)* 19, 130–141. doi: 10.1093/pm/pnx088

Tibano, A. T., de Siqueira, S. R. D. T., da Nóbrega, J. C. M., and Teixeira, M. J. (2010). Cardiovascular response during trigeminal ganglion compression for trigeminal neuralgia according to the use of local anesthetics. *Acta Neurochir.* 152, 1347–1351. doi: 10.1007/s00701-010-0664-z

Udupi, B. P., Chouhan, R. S., Dash, H. H., Bithal, P. K., and Prabhakar, H. (2012). Comparative evaluation of percutaneous retrogasserian glycerol rhizolysis and radiofrequency thermocoagulation techniques in the management of trigeminal neuralgia. *Neurosurgery* 70, 407–412. doi: 10.1227/neu.0b013e318233a85f

Wan, Q., Zhang, D., Cao, X., Zhang, Y., Zhu, M., and Zuo, W. (2018). CT-guided selective percutaneous radiofrequency thermocoagulation via the foramen rotundum for isolated maxillary nerve idiopathic trigeminal neuralgia. *J. Neurosurg.* 128, 211–214. doi: 10.3171/2016.9.JNS152520

Wang, H., Zheng, B., Shi, K., Liu, J., Ma, W., Liu, Q., et al. (2011). The effect of adriamycin interventional therapy for patients with trigeminal neuralgia of ophthalmic branch guided by X ray and nerve stimulator. *Chine. J. Pain Med.* 5, 286–290. doi: 10.3969/j.issn.1006-9852.2011.05.009

Weßling, H., and Duda, S. (2019). ioCT-guided percutaneous radiofrequency ablation for trigeminal neuralgia: how I do it. *Acta Neurochir.* 161, 935–938. doi: 10.1007/s00701-019-03859-8

Wu, J., Xiao, Y., Chen, B., Zhang, R., Dai, M., and Zhang, Y. (2022). Efficacy and safety of microvascular decompression versus percutaneous balloon compression in the treatment of trigeminal neuralgia: a systematic review and meta-analysis. *Ann. Palliat. Med.* 11, 1391–1400. doi: 10.21037/apm-21-3901

Xie, K., Liu, S., Huang, B., and Yao, M. (2020). Effects of supraorbital foramen variations on the treatment efficacy of radiofrequency therapy for V1 trigeminal neuralgia: a retrospective study. *Pain Res. Manage.* 2020:8142489. doi: 10.1155/2020/8142489

Yan, C., Zhang, Q., Liu, C., Yang, J., Bian, H., Zhu, J., et al. (2021). Efficacy and safety of radiofrequency in the treatment of trigeminal neuralgia: a systematic review and meta-analysis. *Acta Neurol. Belg.* doi: 10.1007/s13760-021-01654-w

Yang, F., Lin, Q., Dong, L., Gao, X., and Zhang, S. (2018). Efficacy of 8 different drug treatments for patients with trigeminal neuralgia: a network meta-analysis. *Clin. J. Pain* 34, 685–690. doi: 10.1097/AJP.0000000000000577

Yao, P., Hong, T., Wang, Z. B., Ma, J. M., Zhu, Y. Q., Li, H. X., et al. (2016). Treatment of bilateral idiopathic trigeminal neuralgia by radiofrequency thermocoagulation at different temperatures. *Medicine (United States)* 95:E4274. doi: 10.1097/MD.0000000000004274

Tang, Y. Z., Wu, B. S., Yang, L. Q., Yue, J. N., He, L. L., Li, N., et al. (2015). The long-term effective rate of different branches of idiopathic trigeminal neuralgia after single radiofrequency thermocoagulation. *Medicine (United States)* 94:e1994. doi: 10.1097/MD.0000000000001994

Zheng, B., Song, L., and Liu, H. (2018). Gasserian ganglion injected with adriamycin successfully relieves intractable trigeminal nerve postherpetic neuralgia for an elderly patient: a case report. *Medicine (United States)* 97:e12388. doi: 10.1097/MD.0000000000012388

frontiers | Frontiers in Molecular Neuroscience

TYPE Review
PUBLISHED 01 August 2022
DOI 10.3389/fnmol.2022.963206

OPEN ACCESS

EDITED BY
Xin Zhang,
Duke University, United States

REVIEWED BY
Xiaqing Ma,
Medical School of Nantong University, China
Shunmei Lu,
Wuxi People's Hospital Affiliated to Nanjing Medical University, China

*CORRESPONDENCE
Xingji You
yoyo1976@shu.edu.cn

†These authors have contributed equally to this work

SPECIALTY SECTION
This article was submitted to Pain Mechanisms and Modulators, a section of the journal Frontiers in Molecular Neuroscience

RECEIVED 07 June 2022
ACCEPTED 11 July 2022
PUBLISHED 01 August 2022

CITATION
Wu J, Li X, Zhang X, Wang W and You X (2022) What role of the cGAS-STING pathway plays in chronic pain? *Front. Mol. Neurosci.* 15:963206. doi: 10.3389/fnmol.2022.963206

What role of the cGAS-STING pathway plays in chronic pain?

Jingxiang Wu[1†], Xin Li[1,2†], Xiaoxuan Zhang[1,2†], Wei Wang[1] and Xingji You[2*]

[1]Department of Anesthesiology, Shanghai Chest Hospital, Shanghai Jiao Tong University, Shanghai, China, [2]School of Medicine, Shanghai University, Shanghai, China

Chronic pain interferes with daily functioning and is frequently accompanied by depression. Currently, traditional clinic treatments do not produce satisfactory analgesic effects and frequently result in various adverse effects. Pathogen recognition receptors (PRRs) serve as innate cellular sensors of danger signals, sense invading microorganisms, and initiate innate and adaptive immune responses. Among them, cGAS-STING alerts on the presence of both exogenous and endogenous DNA in the cytoplasm, and this pathway has been closely linked to multiple diseases, including auto-inflammation, virus infection, and cancer. An increasing numbers of evidence suggest that cGAS-STING pathway involves in the chronic pain process; however, its role remains controversial. In this narrative review, we summarize the recent findings on the involvement of the cGAS-STING pathway in chronic pain, as well as several possible mechanisms underlying its activation. As a new area of research, this review is unique in considering the cGAS-STING pathway in sensory neurons and glial cells as a part of a broader understanding of pain, including potential mechanisms of inflammation, immunity, apoptosis, and autophagy. It will provide new insight into the treatment of pain in the future.

KEYWORDS

cGAS-STING pathway, chronic pain, inflammation, autophagy, immunity, apoptosis

Introduction

Chronic pain is classified as neuropathic and inflammatory pain that affects many patients worldwide. In contrast to short-lasting acute pain, chronic pain can be caused by various conditions. Once developed, it may seriously affect the patient's quality of life and cause numerous syndromes. Mechanisms of chronic pain are complex; peripheral nerve lesions or chemical mediators may evoke receptors (nociceptors) sensitive to noxious stimuli in nerve fibers. The spinal cord then processes somatosensory information, further contributing to central sensitization (Descalzi et al., 2015). Typical treatment measures for chronic pain currently include opioid analgesics, non-steroidal anti-inflammatory drugs, and surgical intervention; however, they all have limited long-term benefits and certain risks. For instance, long-term use of opioids in patients will increase the risk of addiction and produce opioid-induced hyperalgesia (Brush, 2012). Meanwhile, surgical intervention may induce postoperative disability, and the recurrence rates are high (Tarnanen et al., 2012). How to alleviate chronic pain and improve patients'

prognosis remains a global health problem to be solved. Thus, novel therapeutic targets are urgent and worth developing.

Recently, special attention has been paid to emphasizing and critically discussing the cGAS-STING pathway, which is a dominant pathway that responds to cytosolic DNA in the context of tumor immunity, cellular senescence, and inflammatory diseases (Ablasser and Chen, 2019). Concerning the roles of the cGAS-STING pathway in chronic pain, it has been reported that activating the cGAS-STING may have various effects. Some studies indicated that STING releases proinflammatory cytokines, which may cause neuroinflammation to aggravate chronic pain (Wang et al., 2019; Tian et al., 2020; Sun et al., 2021). In contrast, another study showed that type 1 interferons over-activated by cGAS-STING pathway might exert an antinociceptive effect in sensory neurons (Donnelly et al., 2021). Today, cGAS-STING pathway in host immunity is more understood, and the therapeutic approaches targeting this pathway show promise for future clinical pain applications. Given the limitations of the current research, we review recent literature focusing on several chronic pain models such as low back pain, bone cancer pain, and spared nerve injury, demonstrating that cGAS-STING pathway is central to the progression and maintenance of chronic pain (Figure 1), but our understanding of its diverse functions on chronic pain still remains incomprehensible.

Overview of cGAS-STING signaling

Innate immunity is the first line of defense against foreign substances and pathogens, and recognizing DNA is one of the most fundamental aspects of host defense. Pathogen recognition receptors (PRRs) serve as innate cellular sensors of danger signals, detect invading microorganisms, and initiate innate and adaptive immune responses (Thompson et al., 2011). PRRs comprised of toll-like receptors (TLRs), retinoic acid-inducible gene I-like receptors (RLRs), nucleotide oligomerization domain-like receptors (NLRs, also called NACHT, LRR, and PYD domain proteins), and cytosolic DNA sensors (Thompson et al., 2011). In 2008, several research teams discovered a new protein named "stimulator of interferon genes" (STING), which is the major type of innate immune receptor in the endoplasmic reticulum (ER) (Ishikawa and Barber, 2008). Bacteria-derived cyclic di-guanylate monophosphate (c-dGMP) or cyclic di-adenosine monophosphate (c-dAMP) were confirmed to be ligands for STING (Burdette et al., 2011).

First, cGAS is activated upon dsDNA recognition, undergoes an allosteric structural change, and subsequently catalyzes the synthesis of cyclic dinucleotide GMP-AMP (cGAMP) (Wan et al., 2020). Second, cGAMP interacts with and activates STING, which is a multi-structure transmembrane protein mainly located in the endoplasmic reticulum (ER). Subsequently, STING translocates from ER to ER-Golgi intermediate compartment (ERGIC) and afterward to the Golgi. Third, the c-terminal tail of the STING recruits TBK1 through a conserved PLPLRT/SD amino acid-binding motif and promotes the autophosphorylation of TBK1 in Golgi. After TBK1 phosphorylation, the complex of STING and TBK1 may further recruit IRF3 to phosphorylate it (Couillin and Riteau, 2021). IRF3 phosphorylation aimed to promote its dimerization, nuclear translocation, and target gene induction of type 1 interferons. Additionally, IRF3 activity is essential for inducing numerous target genes, including genes encoding inflammasome (such as NLRP3) and proinflammatory cytokines (Li et al., 2019). Another major signaling module in the STING pathway is that TBK1 may promote NF-κB activation by triggering nuclear translocation of NF-κB (Yum et al., 2021).

The activators of the cGAS-STING pathway in chronic pain

In vivo, host detection of pathogen-derived nucleic acids by pathogen recognition receptors (PRRs) is involved in context-dependent recognition of intrinsic dsDNA and extrinsic dsDNA (Thompson et al., 2011). Notably, emerging studies paid attention to PRRs as molecules involved in the pathogenesis of neuropathic pain (Kato et al., 2016). Therefore, it is reasonable to believe that the potential release of extrinsic and intrinsic dsDNA may activate the cGAS-STING pathway in chronic pain.

Activated by extrinsic DsDNA

Extrinsic dsDNA, from pathogens such as viruses, bacteria, and parasites, can be internalized into the cytosol in several ways to activate the cGAS-STING pathway (Diamond et al., 2018). The patrol nuclease degrades the dsDNA entering the cell in the lysosome or cytoplasm. In cells with abundant dsDNA or a lack of nuclease, internalized DNA may remain in the cytoplasm and be converted into cGAMP to activate STING (Ablasser et al., 2013). Currently, the evidence indicates that SARS-CoV-2, the etiologic agent of COVID-19, can damage and alter the nervous system, causing headaches and myalgia (Abboud et al., 2020). Another report has suggested that the pain may be related to the increase of type 1 interferons, which is the downstream of STING in young patients (Papa et al., 2021). Simultaneously, an animal experiment has also proved that viral infection induces pain by directly affecting nociceptors in dorsal root ganglion with type 1 interferons (Barragán-Iglesias et al., 2020). The above studies suggest that extrinsic dsDNA-like viruses and bacteria may cause pain *via* activating the cGAS-STING pathway.

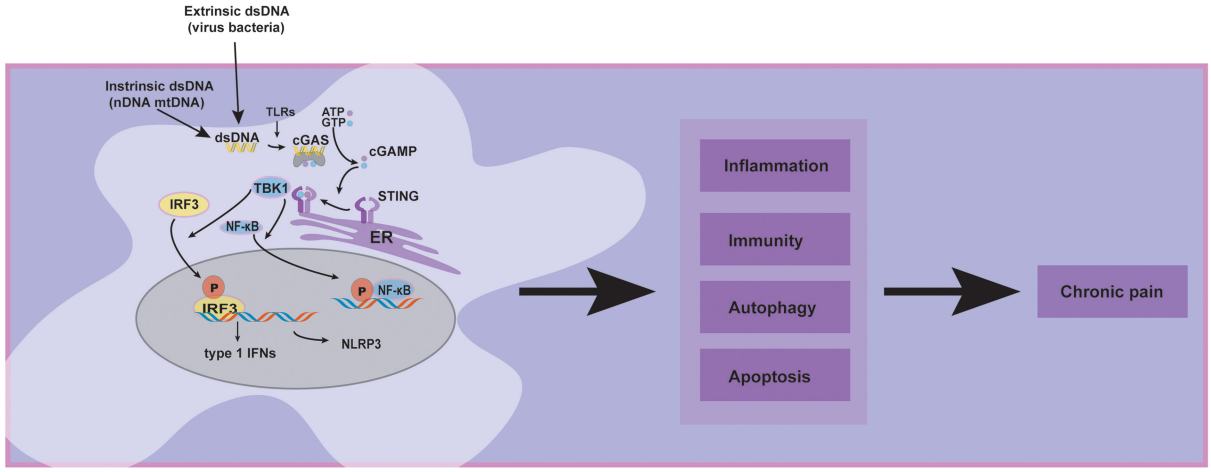

FIGURE 1
The diversity of cGAS-STING pathway activation in chronic pain and its related pathways.

The intrinsic self-dsDNA may activate cGAS-STING in chronic pain

Furthermore, extrinsic dsDNA and intrinsic dsDNA can activate cGAS-STING pathway and induce chronic pain. For example, self-dsDNA was increased and mediated the activation of cGAS-STING pathway in the spinal cord, contributing to the spared nerve injury (SNI)-induced neuropathic pain (Sun et al., 2021). The intrinsic self-dsDNA is composed of nDNA and mtDNA, which can be segregated inaccurately and released into the cytosol, triggering the STING pathway (Bhattacharya et al., 2017). Additionally, in the peripheral neuropathy pain model, DNA damage and the nuclear DNA released are associated with pain production (Canta et al., 2015), suggesting that STING may be activated in that pain model. Another intrinsic dsDNA was mtDNA, which is a component of mitochondria that belongs to the only non-nuclear genome. Compared with nDNA, mtDNA is more unstable and vulnerable to the effects of oxidative stress due to its proximity to mitochondrial reactive oxygen species (mtROS) and a lack of repair machinery. mtDNA stress may contribute to the cGAS-STING pathway activation and type 1 interferon responses in various pathological states, including infectious diseases, cancer, neurodegeneration, and other mitochondria-related illnesses (Zhou et al., 2021). Importantly, it has been established that mtDNA depletion inhibited the cGAS-STING pathway and nuclear translocation of p65 and IRF3 (Zhou et al., 2021).

Additionally, mitochondrial dysfunction contributes to the etiology of pain, as indicated by microscopic analysis performed on peripheral nerve sensory axons: abundant vacuolated and swollen mitochondria were observed in the rats treated with paclitaxel to induce pain (Canta et al., 2015; Dai et al., 2020). The increase of mtDNA is associated with pain-like behavior (Trecarichi et al., 2022). Additionally, it has evidenced that mtDNA released and activated the cGAS-STING pathway in low back pain model (Ning et al., 2020). Altogether, this evidence above suggests that mtDNA or nuclear DNA released may activate the cGAS-STING pathway in the process of chronic pain.

Other PRRs, such as TLRs, may be involved in the activation of cGAS-STING of chronic pain

Several lines of evidence have shown that Toll-like receptors (TLRs) signaling enables the cGAS-STING pathway to induce a strong type 1 interferon response during HIV-1 infection (Siddiqui and Yamashita, 2021). Additionally, TLR4 has been considered essential for activating the cGAS-STING pathway in macrophages stimulated by LPS (Ning et al., 2020), although current studies have suggested that after nerve injury, TLRs are involved in Wallerian degeneration and the generation of neuropathic pain (Thakur et al., 2017). Particularly, TLR3 promotes neuropathic pain by regulating autophagy in rats with L5 spinal nerve ligation model (Chen and Lu, 2017), and knockdown of TLR3 in bone malignancy pain model mice can impair pain thoroughly (Zhang et al., 2020). Furthermore, TLR3 has also been proven to trigger type 1 interferon responses *via* Toll/IL-1 receptor domain containing adaptor inducing IFN-β (TRIF) signaling to regulate pain and itch (Szöllosi et al., 2019). It is suggested that TLRs may be involved in activating the

cGAS-STING pathway in chronic pain, although it remains to be examined.

The main downstream signaling pathways of cGAS-STING in chronic pain

Type 1 interferons

The cGAS-STING pathway, which controls immunity to cytosolic DNA, is a critical driver of aberrant type 1 interferon responses (Domizio et al., 2022). Furthermore, the latest research on COVID-19 has revealed that type 1 interferon response, which is activated by cGAS-STING pathway, induces microangiopathic changes and produces neuropathic pain in young patients (Papa et al., 2021). Simultaneously, according to a study of hepatitis C virus patients, IFN-α therapy causes significant somatic pain and promotes major depressive disorder as early as the second week of treatment (Lin et al., 2020), although early reports have demonstrated that IFN-α and IFN-β, two major family members of type 1 interferons, exert an antinociceptive action (Menzies et al., 1992). In addition, STING regulates the type 1 interferon signaling in dorsal root ganglion sensory neurons, which has been disclosed to control nociception in bone cancer pain models (Donnelly et al., 2021). Consistently, in chronic constriction injury-induced neuropathic pain, protein tyrosine phosphatase receptor type D (PTPRD) activates STING-type 1 interferon pathway in dorsal root ganglion and displays an analgesic effect (Sun et al., 2022). In the light of this, researchers have reviewed that IFN-α and IFN-β may rapidly suppress neuronal activity and synaptic transmission to potent analgesia *via* nongenomic regulation (Tan et al., 2021), while the discrepancy in antinociceptive against pronociceptive effects of type 1 interferons may ascribe to various conditions, and the exact role of STING/type 1 interferons in chronic pain requires further investigation.

NLRP3

STING predominantly inhabits the endoplasmic reticulum to regulate innate immune signaling processes and recruits NLRP3 to the ER to promote the inflammasome formation in the HSV-1 infection (Wang et al., 2020). Lipopolysaccharide (LPS) activates STING and afterward upregulates NLRP3 expression in acute lung injury (Ning et al., 2020). Simultaneously, an increasing body of evidence verified that NLRP3 inflammasome controls the processing of proinflammatory cytokine interleukin 1β (IL-1β) and is implicated in chronic pain (Pan et al., 2018; Chen et al., 2021). In another study of lower back pain, NLRP3 activation in nucleus pulposus cells was associated with cGAS and STING and participated in chronic pain (Tian et al., 2020). The inhibitor of NLRP3 inflammasome can effectively modify nitroglycerin-induced mechanical hyperalgesia (He et al., 2019). Therefore, NLRP3 has become an emerging therapeutic target for chronic pain, and it shows promise that STING may regulate NLRP3 to participate in chronic pain.

NF-κB

Nuclear factor-kappa B (NF-κB) is an important nuclear transcription factor in almost all cell types and participates in numerous biological processes, including inflammation, cell differentiation, immunity, cell growth and apoptosis, and tumorigenesis (Ghosh and Dass, 2016). STING activation can trigger nuclear factor κB (NF-κB) signaling to mediate immune defense against tumors and viral infections (Yum et al., 2021). Simultaneously, STING antagonist H-151 has been shown that suppresses STING/NF-κB-mediated inflammation to ameliorate psoriasis (Pan et al., 2021). Notably, the latest research in neuropathic pain has indicated that STING may activate the NF-κB and release the proinflammatory cytokines IL-6 in the spinal cord to aggravate chronic pain. However, injecting STING antagonist C-176 can provide an analgesic effect and reverse the increased expression of NF-κB (Sun et al., 2021). Additionally, NF-κB is a transcription factor for various cytokines, including CX3CL1, IL-1β, IL-6, and TNF-α, to induce peripheral and central sensitization in chronic pain (Sun et al., 2012; Liu et al., 2018; Xiang et al., 2019; Li Y. et al., 2020; Xu et al., 2021). Undoubtedly, NF-κB activation may contribute to chronic pain; therefore, as an important mediator of NF-κB, STING is supposed to play a significant role in chronic pain.

The potential mechanism of the cGAS-STING pathway in chronic pain

The extrinsic dsDNA (virus and bacteria), intrinsic dsDNA (nDNA and mtDNA), and other pathogen recognition receptors (PRRs) such as Toll-like receptors (TLRs) may contribute to chronic pain by activating the cGAS-STING pathway. Meanwhile, the downstream proteins of the cGAS-STING pathway, such as type 1 interferons, NLRP3, and NF-κB, have been established that participate in chronic pain. Furthermore, cluster analysis displayed that cGAS-STING activation could affect inflammation, immunity, apoptosis, autophagy, and other signaling pathways (Wu et al., 2020); these cellular processes may involve chronic pain. Based on the preceding evidence, we hypothesized that the cGAS-STING pathway might significantly affect chronic pain.

cGAS-STING may induce inflammation to contribute to chronic pain

Evidence accumulates that STING pathway is involved in inflammation (Chin, 2019); for instance, STING-mediated type 1 interferons regulates the elevation of proinflammatory cytokine profile with increased TNF-α, IL-6, and IL-1β in microglia of traumatic brain injury (Abdullah et al., 2018). Moreover, these studies have revealed that the cGAS-STING pathway was activated, and the inflammatory cytokines IL-6 and CXCL10 were released in mitochondrial dysfunction (Zhou et al., 2021). Additionally, in cerebral ischemic stroke, cGAS knockdown promotes microglial M2 polarization to alleviate inflammation (Jiang et al., 2021). Emerging evidence suggested that inflammation plays an essential role in chronic pain (Ji et al., 2016, 2018): The upregulation of inflammatory mediators (TNF-α, IL-6, and IL-1β) in the spinal cord has been evidenced that might be involved in the process of bone cancer pain. Inhibition of endoplasmic reticulum stress may decrease the inflammatory mediators and show an antinociception effect (Wei et al., 2016; Mao et al., 2020). Particularly, in inflammatory pain, magnetic resonance imaging (MRI) and histopathology have demonstrated that inflammation caused by cGAS, STING, and NLRP3 is associated with intervertebral disc degeneration in low back pain (Zhang et al., 2022). Moreover, STING can also participate in the inflammatory reaction process of neuropathic pain. In spinal cord injury mice, STING knockout may alleviate inflammatory response (Wang et al., 2019); in spared nerve injury rats, STING inhibitor C-176 administration provides an antinociceptive effect that is reversed by injecting recombinant IL-6 (Sun et al., 2021), which indicates that STING is an essential downstream factor for chronic pain by regulating IL-6 expression. Accordingly, it would not surprise that activation of the cGAS-STING pathway may induce inflammation to mediate inflammatory and neuropathic pain.

cGAS-STING may mediate immunity to participate in chronic pain

The cGAS-STING pathway has a significant role in the immune, and emerging studies provide solid evidence that cGAS-STING is mainly attributed to antigen-presenting cell (APC)-mediated activation of $CD8^+$ T cells (Flood et al., 2019) and spontaneous $CD8^+$ T cell priming against tumors was defective in mice lacking STING (Woo et al., 2014). Meanwhile, cGAS-STING-mediated DNA sensing has been reported that maintains $CD8^+$ T cell stemness and promotes anti-tumor T cell therapy (Li W. et al., 2020). Although the clinical research disclosed that STING agonist ADU-S100 might induce $CD8^+$ T cell immune response at a low dose, when administered at a high dose, the $CD8^+$ T cell death, and compromised anti-tumor immunity (Sivick et al., 2018), it is no doubt that STING mediates $CD8^+$ T cells.

A variety of inflammatory pain processes are believed to be mediated by T cells, including rheumatoid arthritis, intestinal inflammation, etc. (Basso et al., 2015; Swain et al., 2022). Recent studies have found that T cells are also involved in neuropathic pain: $CD8^+$ T cells and endogenous IL-10 are required to resolve chemotherapy-induced neuropathic pain (Krukowski et al., 2016); educating $CD8^+$ T cells can prevent and resolve chemotherapy-induced peripheral neuropathy in mice (Laumet et al., 2019; Singh et al., 2022). Intriguingly, in the bone cancer pain model which may involve both inflammatory pain and neuropathic pain, systemic administration of STING activator DMXAA attenuated the measures of spontaneous and ongoing pain; the analgesic effect may attribute to the increasing proportion of $CD8^+$ T cells in the bone marrow tumor microenvironment (Donnelly et al., 2021). Therefore, these findings suggest that the cGAS-STING pathway may involve chronic pain by mediating the immunity of $CD8^+$ T cells.

cGAS-STING may induce autophagy to contribute to chronic pain

Autophagy is a lysosomal degradation pathway that maintains tissue homeostasis by recycling damaged and aged cellular components, which plays a significant role in developing the nervous system, neuronal function, and survival (Liu X. et al., 2019). Emerging studies showed that innate immunity-related proteins control the progress of autophagy (Wild et al., 2011). Extracellular M. tuberculosis DNA induces autophagy by activating the cGAS-STING pathway, suggesting a link between STING and autophagy (Watson et al., 2012). Additionally, injecting the activator of IRF3, the downstream protein of the cGAS-STING pathway, can inhibit the fusion of the autophagosome with the lysosome to reduce autophagy flux (67), indicating that the activation of the STING pathway may impair the autophagy. In neuropathic pain, autophagy flux is impaired and mainly exists in astrocytes during the maintenance of the study by Li et al. (2021) and Liao et al. (2022); no matter the stage of neuropathic pain induction or maintenance, upregulation of autophagy can suppresses pain behavior (Li et al., 2021). Researchers suggest that upregulated autophagic activities may facilitate myelin clearance, promote nerve regeneration, and reduce pain. Furthermore, the cGAS-STING pathway has been reported to directly interact with microtubule-associated protein light chain 3 (LC3) and subsequent autophagy to regulate the innate immune responses (Liu D. et al., 2019). The expression of LC3 is upregulated in GABAergic interneurons of rat spinal dorsal horn after SNL, suggesting

that autophagic disruption following SNL might be involved in the induction and maintenance of neuropathic pain (Liu X. et al., 2019). Intrathecal injection of autophagy activator exerts an analgesic effect on neuropathic pain by activating LC3 in astrocytes (Yuan and Fei, 2021). It can be suggested that STING may interact with LC3 to aggravate chronic pain further. The role of autophagy in inflammatory pain has been studied relatively less, while a study by Liu found that CFA-induced inflammatory pain can be alleviated by restoring autophagic flux in the spinal cord (Liu et al., 2022). Autophagy may mediate both inflammatory and neuropathic pain, although there is no solid evidence to confirm this hypothesis, it is still appropriate to predict that STING may mediate autophagy flux and contribute to chronic pain.

cGAS-STING may induce apoptosis to contribute to chronic pain

Apoptosis is a form of programmed cell death and shrinkage when cells encounter stress or damage (Liao et al., 2022). There is evidence for this occurring that STING-dependent apoptosis directly through the interaction of IRF3 and BCL2-associated x, apoptosis regulator (Bax) (Sze et al., 2013), and in microglia and other immune cells, HSV-1 at a high viral load can trigger cGAS/STING-dependent apoptosis (Reinert et al., 2021). Additionally, STING-IRF3 contributes to lipopolysaccharide-induced cardiac apoptosis *via* activating NLRP3 (Li et al., 2019). Consequently, cGAS-STING pathway is essential for apoptosis regulation. Furthermore, apoptotic activity in the injured nerve, dorsal root ganglia, and spinal cord has changed during neuropathic pain formation (Liao et al., 2022). The number of cleaved caspase-3 in the spinal cord increased on days 8 and 14 after nerve injury (Fu et al., 2017). Meanwhile, increased spinal cell apoptosis may probably induce inflammatory pain (Baniasadi et al., 2020). Although there is no clear evidence demonstrating that inhibiting apoptotic activities could attenuate pain behavior, daily hyperbaric oxygen therapy has been proved to suppress pain behavior and reduce apoptotic activities of GABAergic neurons in the spinal dorsal horn of rats (Fu et al., 2017). The apoptosis level was increased in osteoarthritic, which develops slowly and worsens over time, accompanied by chronic pain (Aigner et al., 2001); recently, it has been evidenced that STING might induce apoptosis and senescence in chondrocytes *via* NF-κB pathway in osteoarthritic mice; STING knockdown may reduce the level of chondrocyte apoptosis and ameliorate the symptom (Guo et al., 2021). Simultaneously, epigallocatechin gallate also has been found that reduces the apoptotic rate *via* inhibiting the cGAS-STING pathway activation in nucleus pulposus cells of low back pain models (Tian et al., 2020). The process of apoptosis may contribute to the pathology of inflammatory or neuropathic pain. In view of cGAS-STING that can promote apoptosis in various diseases, it is proposed that cGAS-STING may induce apoptosis and promote chronic pain.

Concluding remarks and future perspectives

The cGAS-STING axis is initially recognized as the an essential mechanism for the host to defeat bacteria and virus invasions (Ding et al., 2020), as the crucial role in the neuro-immune, activation of immunostimulatory pathways is required for normal functioning, but the persistent engagement of these responses can prove detrimental.

It was found in the recent studies that the cGAS-STING may be an important mediator of chronic pain, and this review summarized and discussed the potential relationship. First, pathogens and damaged cells will release exogenous and endogenous DNA, which may activate the cGAS-STING pathway and then contribute to chronic pain. Additionally, TLRs were activated in chronic pain, which may be in concert with the cGAS-STING pathway. As such, it is unsurprising that the cGAS-STING pathway may be activated in chronic pain; however, the different types and mechanisms of DNA and TLRs should be further explored. Moreover, the activated STING further exerted its effect by promoting the expressions of type 1 interferons, NF-κB, and NLRP3. Intriguingly, the downstream has been shown to play a significant role in chronic pain. It can be conceived that the cGAS-STING pathway may mediate chronic pain by activating these downstream; however, more mechanisms are required for further research. Besides, STING may influence inflammation, immunity (such as $CD8^+$ T cells), autophagy, and apoptosis, which has been proved to be the essential cause of chronic pain. Particularly, these cellular processes may influence each other in chronic pain; for example, LC3-associated phagocytosis can assist remove apoptotic cells by macrophages and inhibit proinflammatory processes (Eid and Ito, 2022). The relevance of these branches of cGAS/STING pathway for their potential role in chronic pain is currently not well-understood. Further research may be required to provide a more comprehensive picture of STING in chronic pain and pain-related cellular signals.

What role cGAS-STING plays in chronic pain is still controversial. Agonists and inhibitors targeting cGAS-STING have been developed with potentials for the treatment of auto-inflammation, virus infection, and cancers (Ding et al., 2020). In chronic-refractory pain, STING-related adjuvant therapy appears to have translational potential, and the latest research has reported that a small molecule drug 7-BIA could alleviate neuropathic pain by upregulating STING and IFN-α in the DRG (Sun et al., 2022). There is a possibility of developing new drugs

that target the STING signal pathway to treat refractory cancer-induced bone pain or neuropathic pain in patients to avoid systemic effects.

STING enhances the production and secretion of type 1 interferons (IFN-α and IFN-ß). As we know, IFN-α and IFN-ß have already been successfully used for adjuvant therapy in malignancy, infection, and autoimmune disease. As well as trials of IFN-α, STING agonists more recently used for adjuvant anti-malignancy treatment were also tested (Lv et al., 2020; Verdegaal et al., 2020; Meric-Bernstam et al., 2022). It is therefore possible to determine whether low-dose IFN-α and STING agonists reduced or induced pain by examining existing datasets and patients previously treated with this drug.

Additionally, STING's effect on nociceptors, which affect immune cells (Donnelly et al., 2021), might be an interesting target in basic science. If immune-mediated attenuation of STING's analgesic function occurs, then the analgesic effects of STING could be further enhanced by blocking (currently unknown) immune-mediated pro-analgesic effects. What is the mechanism by which immune cells modulate STING's analgesic effects? How the new STING analgesic signaling plays out in young/old subjects, and whether male/female sex differences exist? There are still questions to be answered.

Author contributions

JW, XL, and XZ searched the literature and participated in manuscript preparation. WW, JW, and XY made the critical revision of the manuscript. All authors have read and approved the final manuscript.

Funding

This work was supported by the National Natural Science Foundation of China (grant No. 82071233), Shanghai Sailing Program (grant No. 21YF1442900), and Nurture projects for basic research of Shanghai Chest Hospital (grant Nos. 2019YNJCM08, 2020YNJCQ13).

Conflict of interest

The authors declare that the research was conducted in the absence of any commercial or financial relationships that could be construed as a potential conflict of interest.

Publisher's note

All claims expressed in this article are solely those of the authors and do not necessarily represent those of their affiliated organizations, or those of the publisher, the editors and the reviewers. Any product that may be evaluated in this article, or claim that may be made by its manufacturer, is not guaranteed or endorsed by the publisher.

References

Abboud, H., Abboud, F. Z., Kharbouch, H., Arkha, Y., El Abbadi, N., and El Ouahabi, A. (2020). COVID-19 and SARS-CoV-2 infection: pathophysiology and clinical effects on the nervous system. *World Neurosurg.* 140, 49–53. doi: 10.1016/j.wneu.2020.05.193

Abdullah, A., Zhang, M., Frugier, T., Bedoui, S., Taylor, J. M., and Crack, P. J. (2018). STING-mediated type-I interferons contribute to the neuroinflammatory process and detrimental effects following traumatic brain injury. *J. Neuroinflamm.* 15, 323. doi: 10.1186/s12974-018-1354-7

Ablasser, A., Schmid-Burgk, J. L., Hemmerling, I., Horvath, G. L., Schmidt, T., Latz, E., et al. (2013). Cell intrinsic immunity spreads to bystander cells via the intercellular transfer of cGAMP. *Nature* 503, 530–534. doi: 10.1038/nature12640

Ablasser, A., and Chen, Z. J. (2019). cGAS in action: expanding roles in immunity and inflammation. *Science* 363, eaat8657. doi: 10.1126/science.aat8657

Aigner, T., Hemmel, M., Neureiter, D., Gebhard, P. M., Zeiler, G., Kirchner, T., et al. (2001). Apoptotic cell death is not a widespread phenomenon in normal aging and osteoarthritis human articular knee cartilage: a study of proliferation, programmed cell death (apoptosis), and viability of chondrocytes in normal and osteoarthritic human knee cartilage. *Arthrit. Rheum.* 44, 1304–1312. doi: 10.1002/1529-0131(200106)44:6<1304::AID-ART222>3.0.CO;2-T

Baniasadi, M., Manaheji, H., Maghsoudi, N., Danyali, S., Zakeri, Z., Maghsoudi, A., et al. (2020). Microglial-induced apoptosis is potentially responsible for hyperalgesia variations during CFA-induced inflammation. *Inflammopharmacology* 28, 475–485. doi: 10.1007/s10787-019-00623-3

Barragán-Iglesias, P., Franco-Enzástiga, Ú., Jeevakumar, V., Shiers, S., Wangzhou, A., Granados-Soto, V., et al. (2020). Type I interferons act directly on nociceptors to produce pain sensitization: implications for viral infection-induced pain. *J. Neurosci.* 40, 3517–3532. doi: 10.1523/JNEUROSCI.3055-19.2020

Basso, L., Bourreille, A., and Dietrich, G. (2015). Intestinal inflammation and pain management. *Curr. Opin. Pharmacol.* 25, 50–55. doi: 10.1016/j.coph.2015.11.004

Bhattacharya, S., Srinivasan, K., Abdisalaam, S., Su, F., Raj, P., Dozmorov, I., et al. (2017). RAD51 interconnects between DNA replication, DNA repair and immunity. *Nucleic Acids Res.* 45, 4590–4605. doi: 10.1093/nar/gkx126

Brush, D. E. (2012). Complications of long-term opioid therapy for management of chronic pain: the paradox of opioid-induced hyperalgesia. *J. Med. Toxicol.* 8, 387–392. doi: 10.1007/s13181-012-0260-0

Burdette, D. L., Monroe, K. M., Sotelo-Troha, K., Iwig, J. S., Eckert, B., Hyodo, M., et al. (2011). STING is a direct innate immune sensor of cyclic di-GMP. *Nature* 478, 515–518. doi: 10.1038/nature10429

Canta, A., Pozzi, E., and Carozzi, V. A. (2015). Mitochondrial dysfunction in chemotherapy-induced peripheral neuropathy (CIPN). *Toxics* 3, 198–223. doi: 10.3390/toxics3020198

Chen, R., Yin, C., Fang, J., and Liu, B. (2021). The NLRP3 inflammasome: an emerging therapeutic target for chronic pain. *J. Neuroinflamm.* 18, 84. doi: 10.1186/s12974-021-02131-0

Chen, W., and Lu, Z. (2017). Upregulated TLR3 promotes neuropathic pain by regulating autophagy in rat with L5 spinal nerve ligation model. *Neurochem. Res.* 42, 634–643. doi: 10.1007/s11064-016-2119-2

Chin, A. C. (2019). Neuroinflammation and the cGAS-STING pathway. *J. Neurophysiol.* 121, 1087–1091. doi: 10.1152/jn.00848.2018

Couillin, I., and Riteau, N. (2021). STING signaling and sterile inflammation. *Front. Immunol.* 12, 753789. doi: 10.3389/fimmu.2021.753789

Dai, C. Q., Guo, Y., and Chu, X. Y. (2020). Neuropathic pain: the dysfunction of Drp1, mitochondria, and ROS homeostasis. *Neurotox. Res.* 38, 553–563. doi: 10.1007/s12640-020-00257-2

Descalzi, G., Ikegami, D., Ushijima, T., Nestler, E. J., Zachariou, V., and Narita, M. (2015). Epigenetic mechanisms of chronic pain. *Trends Neurosci.* 38, 237–246. doi: 10.1016/j.tins.2015.02.001

Diamond, J. M., Vanpouille-Box, C., Spada, S., Rudqvist, N. P., Chapman, J. R., Ueberheide, B. M., et al. (2018). Exosomes shuttle TREX1-sensitive IFN-stimulatory dsDNA from irradiated cancer cells to DCs. *Cancer Immunol. Res.* 6, 910–920. doi: 10.1158/2326-6066.CIR-17-0581

Ding, C., Song, Z., Shen, A., Chen, T., and Zhang, A. (2020). Small molecules targeting the innate immune cGAS–STING–TBK1 signaling pathway. *Acta Pharm. Sin. B* 10, 2272–2298. doi: 10.1016/j.apsb.2020.03.001

Domizio, J. D., Gulen, M. F., Saidoune, F., Thacker, V. V., Yatim, A., Sharma, K., et al. (2022). The cGAS-STING pathway drives type I IFN immunopathology in COVID-19. *Nature* 603, 145–151. doi: 10.1038/s41586-022-04421-w

Donnelly, C. R., Jiang, C., Andriessen, A. S., Wang, K., Wang, Z., Ding, H., et al. (2021). STING controls nociception via type I interferon signalling in sensory neurons. *Nature* 591, 275–280. doi: 10.1038/s41586-020-03151-1

Eid, N., and Ito, Y. (2022). Oxoglaucine alleviates osteoarthritis by activation of autophagy via blockade of Ca(2+) influx and TRPV5/calmodulin/CAMK-II pathway. *Br. J. Pharmacol.* 179, 1282–1283. doi: 10.1111/bph.15706

Flood, B. A., Higgs, E. F., Li, S., Luke, J. J., and Gajewski, T. F. (2019). STING pathway agonism as a cancer therapeutic. *Immunol. Rev.* 290, 24–38. doi: 10.1111/imr.12765

Fu, H., Li, F., Thomas, S., and Yang, Z. (2017). Hyperbaric oxygenation alleviates chronic constriction injury (CCI)-induced neuropathic pain and inhibits GABAergic neuron apoptosis in the spinal cord. *Scand J. Pain* 17, 330–338. doi: 10.1016/j.sjpain.2017.08.014

Ghosh, S., and Dass, J. F. P. (2016). Study of pathway cross-talk interactions with NF-κB leading to its activation via ubiquitination or phosphorylation: a brief review. *Gene* 584, 97–109. doi: 10.1016/j.gene.2016.03.008

Guo, Q., Chen, X., Chen, J., Zheng, G., Xie, C., Wu, H., et al. (2021). STING promotes senescence, apoptosis, and extracellular matrix degradation in osteoarthritis via the NF-κB signaling pathway. *Cell Death Dis.* 12, 13. doi: 10.1038/s41419-020-03341-9

He, W., Long, T., Pan, Q., Zhang, S., Zhang, Y., Zhang, D., et al. (2019). Microglial NLRP3 inflammasome activation mediates IL-1β release and contributes to central sensitization in a recurrent nitroglycerin-induced migraine model. *J. Neuroinflamm.* 16, 78. doi: 10.1186/s12974-019-1459-7

Ishikawa, H., and Barber, G. N. (2008). STING is an endoplasmic reticulum adaptor that facilitates innate immune signalling. *Nature* 455, 674–678. doi: 10.1038/nature07317

Ji, R. R., Chamessian, A., and Zhang, Y. Q. (2016). Pain regulation by non-neuronal cells and inflammation. *Science* 354, 572–577. doi: 10.1126/science.aaf8924

Ji, R. R., Nackley, A., Huh, Y., Terrando, N., and Maixner, W. (2018). Neuroinflammation and central sensitization in chronic and widespread pain. *Anesthesiology* 129, 23. doi: 10.1097/ALN.0000000000002130

Jiang, G. L., Yang, X. L., Zhou, H. J., Long, J., Liu, B., Zhang, L. M., et al. (2021). cGAS knockdown promotes microglial M2 polarization to alleviate neuroinflammation by inhibiting cGAS-STING signaling pathway in cerebral ischemic stroke. *Brain Res. Bull.* 171, 183–195. doi: 10.1016/j.brainresbull.2021.03.010

Kato, J., Agalave, N. M., and Svensson, C. I. (2016). Pattern recognition receptors in chronic pain: mechanisms and therapeutic implications. *Eur. J. Pharmacol.* 788, 261–273. doi: 10.1016/j.ejphar.2016.06.039

Krukowski, K., Eijkelkamp, N., Laumet, G., Hack, C. E., Li, Y., Dougherty, P. M., et al. (2016). CD8+ T cells and endogenous IL-10 are required for resolution of chemotherapy-induced neuropathic pain. *J. Neurosci.* 36, 11074–11083. doi: 10.1523/JNEUROSCI.3708-15.2016

Laumet, G., Edralin, J. D., Dantzer, R., Heijnen, C. J., and Kavelaars, A. (2019). Cisplatin educates CD8+ T cells to prevent and resolve chemotherapy-induced peripheral neuropathy in mice. *Pain* 160, 1459–1468. doi: 10.1097/j.pain.0000000000001512

Li, J., Tian, M., Hua, T., Wang, H., Yang, M., Li, W., et al. (2021). Combination of autophagy and NFE2L2/NRF2 activation as a treatment approach for neuropathic pain. *Autophagy* 17, 4062–4082. doi: 10.1080/15548627.2021.1900498

Li, N., Zhou, H., Wu, H., Wu, Q., Duan, M., Deng, W., et al. (2019). STING-IRF3 contributes to lipopolysaccharide-induced cardiac dysfunction, inflammation, apoptosis and pyroptosis by activating NLRP3. *Redox Biol.* 24, 101215. doi: 10.1016/j.redox.2019.101215

Li, W., Lu, L., Lu, J., Wang, X., Yang, C., Jin, J., et al. (2020). cGAS-STING-mediated DNA sensing maintains CD8(+) T cell stemness and promotes antitumor T cell therapy. *Sci. Transl. Med.* 12, eaay9013. doi: 10.1126/scitranslmed.aay9013

Li, Y., Yang, Y., Guo, J., Guo, X., Feng, Z., and Zhao, X. (2020). Spinal NF-kB upregulation contributes to hyperalgesia in a rat model of advanced osteoarthritis. *Mol. Pain* 16, 1744806920905691. doi: 10.1177/1744806920905691

Liao, M. F., Lu, K. T., Hsu, J. L., Lee, C. H., Cheng, M. Y., and Ro, L. S. (2022). The role of autophagy and apoptosis in neuropathic pain formation. *Int. J. Mol. Sci.* 23, 2685. doi: 10.3390/ijms23052685

Lin, C. Y., Guu, T. W., Lai, H. C., Peng, C. Y., Chiang, J. Y., Chen, H. T., et al. (2020). Somatic pain associated with initiation of interferon-alpha (IFN-α) plus ribavirin (RBV) therapy in chronic HCV patients: a prospective study. *Brain Behav. Immun. Health* 2, 100035. doi: 10.1016/j.bbih.2019.100035

Liu, C., Zhang, F., Liu, H., and Wei, F. (2018). NF-kB mediated CX3CL1 activation in the dorsal root ganglion contributes to the maintenance of neuropathic pain induced in adult male Sprague Dawley rats1. *Acta Cir. Bras.* 33, 619–628. doi: 10.1590/s0102-865020180070000007

Liu, C., Zheng, X., Liu, L., Hu, Y., Zhu, Q., Zhang, J., et al. (2022). Caloric restriction alleviates CFA-induced inflammatory pain via elevating β-hydroxybutyric acid expression and restoring autophagic flux in the spinal cord. *Front. Neurosci.* 16, 828278. doi: 10.3389/fnins.2022.828278

Liu, D., Wu, H., Wang, C., Li, Y., Tian, H., Siraj, S., et al. (2019). STING directly activates autophagy to tune the innate immune response. *Cell Death Differ.* 26, 1735–1749. doi: 10.1038/s41418-018-0251-z

Liu, X., Zhu, M., Ju, Y., Li, A., and Sun, X. (2019). Autophagy dysfunction in neuropathic pain. *Neuropeptides* 75, 41–48. doi: 10.1016/j.npep.2019.03.005

Lv, M., Chen, M., Zhang, R., Zhang, W., Wang, C., Zhang, Y., et al. (2020). Manganese is critical for antitumor immune responses via cGAS-STING and improves the efficacy of clinical immunotherapy. *Cell Res.* 30, 966–979. doi: 10.1038/s41422-020-00395-4

Mao, Y., Wang, C., Tian, X., Huang, Y., Zhang, Y., Wu, H., et al. (2020). Endoplasmic reticulum stress contributes to nociception via neuroinflammation in a murine bone cancer pain model. *Anesthesiology* 132, 357–372. doi: 10.1097/ALN.0000000000003078

Menzies, R. A., Patel, R., Hall, N. R., O'Grady, M. P., and Rier, S. E. (1992). Human recombinant interferon alpha inhibits naloxone binding to rat brain membranes. *Life Sci.* 50, Pl227–232. doi: 10.1016/0024-3205(92)90555-4

Meric-Bernstam, F., Sweis, R. F., Hodi, F. S., Messersmith, W. A., Andtbacka, R. H. I., Ingham, M., et al. (2022). Phase I dose-escalation trial of MIW815 (ADU-S100), an intratumoral STING agonist, in patients with advanced/metastatic solid tumors or lymphomas. *Clin. Cancer Res.* 28, 677–688. doi: 10.1158/1078-0432.CCR-21-1963

Ning, L., Wei, W., Wenyang, J., Rui, X., and Qing, G. (2020). Cytosolic DNA-STING-NLRP3 axis is involved in murine acute lung injury induced by lipopolysaccharide. *Clin. Transl. Med.* 10, e228. doi: 10.1002/ctm2.228

Pan, Y., You, Y., Sun, L., Sui, Q., Liu, L., Yuan, H., et al. (2021). The STING antagonist H-151 ameliorates psoriasis via suppression of STING/NF-κB-mediated inflammation. *Br. J. Pharmacol.* 178, 4907–4922. doi: 10.1111/bph.15673

Pan, Z., Shan, Q., Gu, P., Wang, X. M., Tai, L. W., Sun, M., et al. (2018). miRNA-23a/CXCR4 regulates neuropathic pain via directly targeting TXNIP/NLRP3 inflammasome axis. *J. Neuroinflamm.* 15, 29. doi: 10.1186/s12974-018-1073-0

Papa, A., Salzano, A. M., Di Dato, M. T., Lo Bianco, G., Tedesco, M., Salzano, A., et al. (2021). COVID-19 related acro-ischemic neuropathic-like painful lesions in pediatric patients: a case series. *Anesth. Pain Med.* 11, e113760. doi: 10.5812/aapm.113760

Reinert, L. S., Rashidi, A. S., Tran, D. N., Katzilieris-Petras, G., Hvidt, A. K., Gohr, M., et al. (2021). Brain immune cells undergo cGAS/STING-dependent apoptosis during herpes simplex virus type 1 infection to limit type I IFN production. *J. Clin. Invest.* 131, e136824. doi: 10.1172/JCI136824

Siddiqui, M. A., and Yamashita, M. (2021). Toll-like receptor (TLR) signaling enables cyclic GMP-AMP synthase (cGAS) sensing of HIV-1 infection in macrophages. *MBio* 12, e0281721. doi: 10.1128/mBio.02817-21

Singh, S. K., Krukowski, K., Laumet, G. O., Weis, D., Alexander, J. F., Heijnen, C. J., et al. (2022). CD8+ T cell-derived IL-13 increases macrophage IL-10 to resolve neuropathic pain. *JCI Insight* 7, e154194. doi: 10.1172/jci.insight.154194

Sivick, K. E., Desbien, A. L., Glickman, L. H., Reiner, G. L., Corrales, L., Surh, N. H., et al. (2018). Magnitude of therapeutic STING activation determines CD8(+) T cell-mediated anti-tumor immunity. *Cell Rep.* 25, 3074–3085.e3075. doi: 10.1016/j.celrep.2018.11.047

Sun, C., Wu, G., Zhang, Z., Cao, R., and Cui, S. (2022). Protein tyrosine phosphatase receptor type D regulates neuropathic pain after nerve injury via the STING-IFN-I pathway. *Front. Mol. Neurosci.* 15, 859166. doi: 10.3389/fnmol.2022.859166

Sun, J., Zhou, Y. Q., Xu, B. Y., Li, J. Y., Zhang, L. Q., Li, D. Y., et al. (2021). STING/NF-κB/IL-6-mediated inflammation in microglia contributes to spared nerve injury (SNI)-induced pain initiation. *J. Neuroimmune Pharmacol.* doi: 10.1007/s11481-021-10031-6

Sun, T., Luo, J., Jia, M., Li, H., Li, K., and Fu, Z. (2012). Small interfering RNA-mediated knockdown of NF-κBp65 attenuates neuropathic pain following peripheral nerve injury in rats. *Eur. J. Pharmacol.* 682, 79–85. doi: 10.1016/j.ejphar.2012.02.017

Swain, N., Tripathy, A., Padhan, P., Raghav, S. K., and Gupta, B. (2022). Toll-like receptor-7 activation in CD8+ T cells modulates inflammatory mediators in patients with rheumatoid arthritis. *Rheumatol. Int.* 42, 1235–1245. doi: 10.1007/s00296-021-05050-8

Sze, A., Belgnaoui, S. M., Olagnier, D., Lin, R., Hiscott, J., and van Grevenynghe, J. (2013). Host restriction factor SAMHD1 limits human T cell leukemia virus type 1 infection of monocytes via STING-mediated apoptosis. *Cell Host Microbe* 14, 422–434. doi: 10.1016/j.chom.2013.09.009

Szöllosi, A. G., McDonald, I., Szabó, I. L., Meng, J., van den Bogaard, E., and Steinhoff, M. (2019). TLR3 in chronic human itch: a keratinocyte-associated mechanism of peripheral itch sensitization. *J. Invest. Dermatol.* 139, 2393–2396.e2396. doi: 10.1016/j.jid.2019.04.018

Tan, P. H., Ji, J., Yeh, C. C., and Ji, R. R. (2021). Interferons in pain and infections: emerging roles in neuro-immune and neuro-glial interactions. *Front. Immunol.* 12, 783725. doi: 10.3389/fimmu.2021.783725

Tarnanen, S., Neva, M. H., Dekker, J., Häkkinen, K., Vihtonen, K., Pekkanen, L., et al. (2012). Randomized controlled trial of postoperative exercise rehabilitation program after lumbar spine fusion: study protocol. *BMC Musculoskelet. Disord.* 13, 123. doi: 10.1186/1471-2474-13-123

Thakur, K. K., Saini, J., Mahajan, K., Singh, D., Jayswal, D. P., Mishra, S., et al. (2017). Therapeutic implications of toll-like receptors in peripheral neuropathic pain. *Pharmacol. Res.* 115, 224–232. doi: 10.1016/j.phrs.2016.11.019

Thompson, M. R., Kaminski, J. J., Kurt-Jones, E. A., and Fitzgerald, K. A. (2011). Pattern recognition receptors and the innate immune response to viral infection. *Viruses* 3, 920–940. doi: 10.3390/v3060920

Tian, Y., Bao, Z., Ji, Y., Mei, X., and Yang, H. (2020). Epigallocatechin-3-gallate protects H(2)O(2)-induced nucleus pulposus cell apoptosis and inflammation by inhibiting cGAS/Sting/NLRP3 activation. *Drug Des. Devel. Ther.* 14, 2113–2122. doi: 10.2147/DDDT.S251623

Trecarichi, A., Duggett, N. A., Granat, L., Lo, S., Malik, A. N., Zuliani-Álvarez, L., et al. (2022). Preclinical evidence for mitochondrial DNA as a potential blood biomarker for chemotherapy-induced peripheral neuropathy. *PLoS ONE* 17, e0262544. doi: 10.1371/journal.pone.0262544

Verdegaal, E., van der Kooij, M. K., Visser, M., van der Minne, C., de Bruin, L., Meij, P., et al. (2020). Low-dose interferon-alpha preconditioning and adoptive cell therapy in patients with metastatic melanoma refractory to standard (immune) therapies: a phase I/II study. *J. Immunother. Cancer* 8, e000166. doi: 10.1136/jitc-2019-000166

Wan, D., Jiang, W., and Hao, J. (2020). Research advances in how the cGAS-STING pathway controls the cellular inflammatory response. *Front. Immunol.* 11, 615. doi: 10.3389/fimmu.2020.00615

Wang, W., Hu, D., Wu, C., Feng, Y., Li, A., Liu, W., et al. (2020). STING promotes NLRP3 localization in ER and facilitates NLRP3 deubiquitination to activate the inflammasome upon HSV-1 infection. *PLoS Pathog.* 16, e1008335. doi: 10.1371/journal.ppat.1008335

Wang, Y. Y., Shen, D., Zhao, L. J., Zeng, N., and Hu, T. H. (2019). Sting is a critical regulator of spinal cord injury by regulating microglial inflammation via interacting with TBK1 in mice. *Biochem. Biophys. Res. Commun.* 517, 741–748. doi: 10.1016/j.bbrc.2019.07.125

Watson, R. O., Manzanillo, P. S., and Cox, J. S. (2012). Extracellular *M. tuberculosis* DNA targets bacteria for autophagy by activating the host DNA-sensing pathway. *Cell* 150, 803–815. doi: 10.1016/j.cell.2012.06.040

Wei, T., Guo, T.-Z., Li, W.-W., Kingery, W. S., and Clark, J. D. (2016). Acute versus chronic phase mechanisms in a rat model of CRPS. *J. Neuroinflammation* 13, 14. doi: 10.1186/s12974-015-0472-8

Wild, P., Farhan, H., McEwan, D. G., Wagner, S., Rogov, V. V., Brady, N. R., et al. (2011). Phosphorylation of the autophagy receptor optineurin restricts Salmonella growth. *Science* 333, 228–233. doi: 10.1126/science.1205405

Woo, S. R., Fuertes, M. B., Corrales, L., Spranger, S., Furdyna, M. J., Leung, M. Y., et al. (2014). STING-dependent cytosolic DNA sensing mediates innate immune recognition of immunogenic tumors. *Immunity* 41, 830–842. doi: 10.1016/j.immuni.2014.10.017

Wu, J., Dobbs, N., Yang, K., and Yan, N. (2020). Interferon-independent activities of mammalian STING mediate antiviral response and tumor immune evasion. *Immunity* 53, 115–126.e115. doi: 10.1016/j.immuni.2020.06.009

Xiang, H. C., Lin, L. X., Hu, X. F., Zhu, H., Li, H. P., Zhang, R. Y., et al. (2019). AMPK activation attenuates inflammatory pain through inhibiting NF-κB activation and IL-1β expression. *J. Neuroinflamm.* 16, 34. doi: 10.1186/s12974-019-1411-x

Xu, M., Fei, Y., He, Q., Fu, J., Zhu, J., Tao, J., et al. (2021). Electroacupuncture attenuates cancer-induced bone pain via NF-κB/CXCL12 signaling in midbrain periaqueductal gray. *ACS Chem. Neurosci.* 12, 3323–3334. doi: 10.1021/acschemneuro.1c00224

Yuan, J., and Fei, Y. (2021). Lidocaine activates autophagy of astrocytes and ameliorates chronic constriction injury-induced neuropathic pain. *J. Biochem.* 170, 25–31. doi: 10.1093/jb/mvaa136

Yum, S., Li, M., Fang, Y., and Chen, Z. J. (2021). TBK1 recruitment to STING activates both IRF3 and NF-κB that mediate immune defense against tumors and viral infections. *Proc. Natl. Acad. Sci. U. S. A.* 118, e2100225. doi: 10.1073/pnas.2100225118

Zhang, W., Li, G., Luo, R., Lei, J., Song, Y., Wang, B., et al. (2022). Cytosolic escape of mitochondrial DNA triggers cGAS-STING-NLRP3 axis-dependent nucleus pulposus cell pyroptosis. *Exp. Mol. Med.* 54, 129–142. doi: 10.1038/s12276-022-00729-9

Zhang, Z., Zhang, X., Zhang, Y., Li, J., Xing, Z., and Zhang, Y. (2020). Spinal circRNA-9119 suppresses nociception by mediating the miR-26a-TLR3 axis in a bone cancer pain mouse model. *J. Mol. Neurosci.* 70, 9–18. doi: 10.1007/s12031-019-01378-w

Zhou, L., Zhang, Y. F., Yang, F. H., Mao, H. Q., Chen, Z., and Zhang, L. (2021). Mitochondrial DNA leakage induces odontoblast inflammation via the cGAS-STING pathway. *Cell Commun. Signal.* 19, 58. doi: 10.1186/s12964-021-00738-7

frontiers | Frontiers in Molecular Neuroscience

TYPE Original Research
PUBLISHED 11 August 2022
DOI 10.3389/fnmol.2022.938280

OPEN ACCESS

EDITED BY
Yize Li,
Tianjin Medical University General Hospital, China

REVIEWED BY
Cheng-fu Wan,
China Medical University, China
Lizu Xiao,
Shenzhen Sixth Hospital of Guangdong Medical University, China
Tao Sun,
Shandong University, China
Mohammed Abu El-Hamd,
Sohag University, Egypt
Dong Yang,
Huazhong University of Science and Technology, China

*CORRESPONDENCE
Jingjing Yuan
yjingjing_99@163.com
Xiaochong Fan
fccfxc@zzu.edu.cn

†These authors have contributed equally to this work

SPECIALTY SECTION
This article was submitted to Pain Mechanisms and Modulators, a section of the journal Frontiers in Molecular Neuroscience

RECEIVED 07 May 2022
ACCEPTED 13 July 2022
PUBLISHED 11 August 2022

CITATION
Fan X, Ren H, Bu C, Lu Z, Wei Y, Xu F, Fu L, Ma L, Kong C, Wang T, Zhang Y, Liu Q, Huang W, Bu H and Yuan J (2022) Alterations in local activity and functional connectivity in patients with postherpetic neuralgia after short-term spinal cord stimulation. *Front. Mol. Neurosci.* 15:938280. doi: 10.3389/fnmol.2022.938280

Alterations in local activity and functional connectivity in patients with postherpetic neuralgia after short-term spinal cord stimulation

Xiaochong Fan [1*†], Huan Ren[1†], Chunxiao Bu[2†], Zhongyuan Lu[1], Yarui Wei[2], Fuxing Xu[1], Lijun Fu[1], Letian Ma[1], Cunlong Kong[1], Tao Wang[1], Yong Zhang[2], Qingying Liu[1], Wenqi Huang[3], Huilian Bu[1] and Jingjing Yuan [4*]

[1]Department of Pain Medicine, The First Affiliated Hospital of Zhengzhou University, Zhengzhou, China, [2]Department of Magnetic Resonance Imaging, The First Affiliated Hospital of Zhengzhou University, Zhengzhou, China, [3]Department of Anesthesiology, The First Affiliated Hospital Sun Yat-sen University, Guangzhou, China, [4]Department of Anesthesiology, Pain and Perioperative Medicine, The First Affiliated Hospital of Zhengzhou University, Zhengzhou, China

Introduction: The efficacy of short-term spinal cord stimulation (stSCS) as a treatment for neuropathic pain in patients with postherpetic neuralgia (PHN) has already been validated. However, the potential alterations in brain functionality that are induced by such treatment have yet to be completely elucidated.

Methods: This study use resting-state functional magnetic resonance imaging (rs-fMRI) to detect the changes in regional homogeneity (ReHo) and degree centrality (DC) related to stimulator-induced pain relief in patients with PHN. A total of 10 patients with PHN underwent an MRI protocol at baseline and after stSCS. Alterations in ReHo and DC were then compared between baseline and after stSCS. We investigated the relationship between clinical parameters and functional changes in the brain.

Results: Clinical parameters on pain, emotion, and sleep quality were correlated with ReHo and DC. ReHo and DC were significantly altered in the middle temporal gyrus, precuneus, superior frontal gyrus, supramarginal gyrus, inferior parietal lobule, rolandic operculum, middle occipital gyrus, superior parietal gyrus, and the precentral gyrus after stSCS. A significant correlation was detected between ReHo changes in the middle occipital gyrus, precuneus, inferior parietal gyrus, and changes in pain, emotion, and sleep quality. A significant negative correlation was detected between DC changes in the middle temporal gyrus, rolandic operculum, supramarginal gyrus, precuneus, inferior parietal gyrus, and changes in pain, emotion, and sleep quality.

Conclusion: This study found that stSCS is able to induce ReHo and DC changes in patients with PHN, thus suggesting that stSCS can change brain function to alleviate pain, sleep, and emotional disorder.

KEYWORDS

spinal cord stimulation, pain, postherpetic neuralgia, functional magnetic resonance imaging, mechanisms of action, emotion

Introduction

Herpes zoster (HZ) results from the reactivation of varicella-zoster virus and manifests as a vesicular, painful, dermatomal rash (Johnson and Rice, 2014). The annual incidence of HZ is 3.4 cases per 1,000 persons (Insinga et al., 2005). Postherpetic neuralgia (PHN) is the most frequent complication of HZ. After the age of 50 years, 20% of patients with HZ will develop PHN (Brisson et al., 2001). PHN results in lasting physical discomfort, mental suffering. PHN reduces the quality of life and increases the financial burden.

Pain is a multidimensional experience that covers diverse and integrated brain functions. Local brain chemistry, construction, and function reorganized in patients with neuropathic pain (Li et al., 2020). Due to the complicated pathogenesis of PHN, we incompletely understand about how this condition affects the function of the brain. A study has revealed abnormal local brain activity in patients with PHN (Dai et al., 2020).

The treatment is based on the control of symptoms (Johnson and Rice, 2014). In addition to medicinal therapy (Moore et al., 2014), other forms of interventional therapies have been shown to effectively alleviate pain, such as nerve block (Kuo et al., 2016), pulsed radiofrequency (PRF) (Han et al., 2020), and spinal cord stimulation (SCS). The oral medications have systemic and cognitive adverse effects. Although nerve block is effective, its duration is transient (Kuo et al., 2016). The short-term SCS (stSCS) which based on the electric stimulation, is an effective clinical treatment. The stSCS is more effective than PRF for patients with PHN (Wan and Song, 2021).

Since the day that SCS was introduced, researchers have been investigating the mechanism of action. Supraspinal structures may play a role in the pain alleviating effects of SCS (Meyerson and Linderoth, 2006). However, potential functional brain alterations associated with the application of SCS as a treatment for PHN remain unclear. Functional magnetic resonance imaging (fMRI) is a powerful non-invasive modality that can map the areas of the brain involved in pain perception and modulation (Tracey, 2011). Spontaneous local and long-range brain activity can be quantitatively measured by regional homogeneity (ReHo) (Zuo et al., 2013) and degree centrality (DC), respectively.

The first proposed that ReHo could be a methodology to characterize functional homogeneity of resting-state fMRI (rs-fMRI) signals by Zang et al. (2004). ReHo reflects the local coherence of local spontaneous neuronal activity. Degree centrality (DC) shows the number of direct connections with the rest of brain (Wu et al., 2020). A brain regional node with high centrality is potentially a hub for information transition. Previous research has not considered the alteration in ReHo during SCS treatment. With regard to functional connectivity, the study reported that connection strength changed in patients treated with SCS for neuropathic pain (De Groote et al., 2020). Based on the available information, we speculate that ReHo and DC may be altered when stSCS is utilized to treat PHN. Additionally, we explore the potential key mechanism for rational use of stSCS to treat PHN.

To address this gap of knowledge about the mechanisms responsible for the action of stSCS therapy on patients with PHN, we studied the alterations in ReHo and DC by rs-fMRI in patients with PHN who were treated with stSCS. Then, we investigated whether there is an association between clinical data and functional brain mapping changes in patients with PHN who were treated with stSCS.

Materials and methods

Participants

We recruited nineteen right-handed patients diagnosed with PHN, whose pain cannot be alleviated only by conventional medications, so they receive the therapeutic procedure of stSCS, from the First Affiliated Hospital of Zhengzhou University between January 2021 and October 2021. All participants provided written informed consent prior to participating in this study. A total of nine patients withdrew their consent; therefore, our final analysis featured 10 patients.

This study was approved by the Medical Ethics Committee of the First Affiliated Hospital of Zhengzhou University, Zhengzhou, China (reference no.: 2020-KY-0299-001). The trial registration number is ChiCTR2000040239 (http://www.chictr.org.cn/listbycreater.aspx). The date of trial is November 2020.

Study protocol

In this exploratory and prospective cohort study, patients were included before stSCS implantation and followed up for 14 days after receiving SCS. During this period, four additional individual appointments took place (Figure 1). The first (V1) and third (V3) visits were short appointments of 30 min and were scheduled 1 day before the neuroimaging visits (V2, V4). All patients were asked to complete pain numerical rating scale (NRS) scores, the short-form McGill pain questionnaire version-2 (SF-MPQ-2), the Pittsburgh sleep quality index (PSQI), and the hospital anxiety and depression scale (HADS), during visits V1 and V3. The SF-MPQ-2 contains four subscale scores (continuous pain, intermittent pain, predominantly neuropathic pain, and affective descriptors)

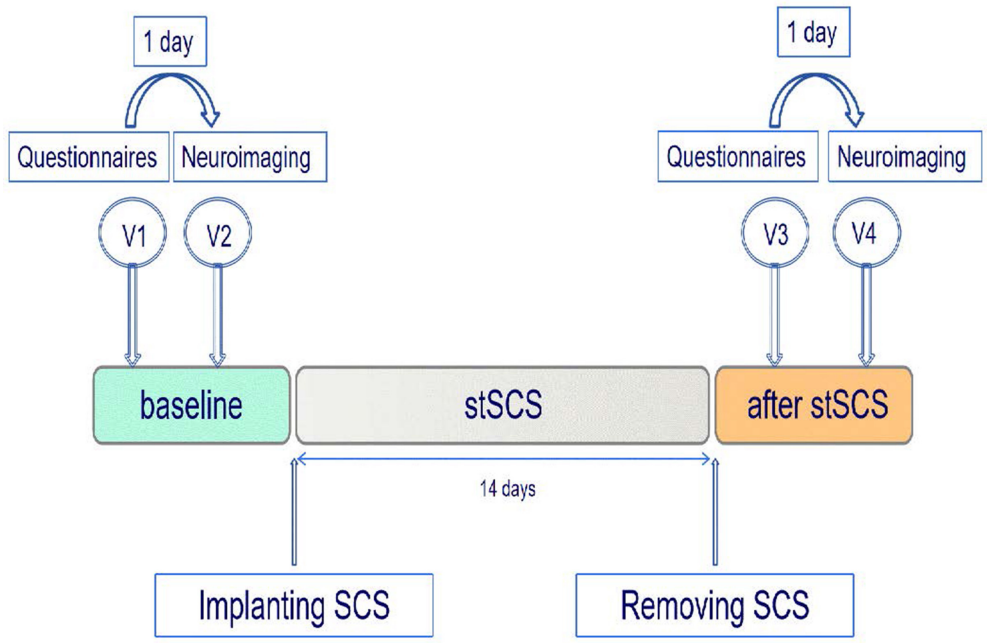

FIGURE 1
Study protocol. Patients with PHN were enrolled prior to the implantation of the SCS and were followed up after the removal of the stSCS. Each patient underwent a neuroimaging protocol prior to SCS and 14 days after SCS. SCS, spinal cord stimulation; stSCS, short-time spinal cord stimulation; V, visit.

that were all recorded. All patients underwent a neuroimaging fMRI-protocol, during V2 (baseline) and V4 (14 days after SCS). We lost the questionnaires from one patient. Between the second and third visits, patients underwent stSCS implantation. All patients received SCS at the cervicothoracic level for PHN. The test electrode (Model 3873, US) was connected to an extension multi-lead cable (Model 355531, Medtronic, US). To program the implantable electrode, an external cable was inserted into the neurostimulator (Model 37022, Medtronic, US). The stimulation parameters were as follows: pulse width was 210–480 μs, frequency was 30–60 Hz, voltage ranged from 0 V to 10.5 V. The electrode was implanted for 14 days. Spinal electrical stimulation results in efficacy about 2 weeks. Moreover, the time of SCS more than 2 weeks will increase the risk of infection. The stimulation parameters were adjusted one time a day to ensure effectiveness. The patient had the liberty to change the amplitude with steps of 0.1 mV to provide adequate pain relief.

MRI data acquisition

All MRI images were obtained by a 3.0T scanner (MAGNETOM PRISMA, SIEMENS, Germany) at the First Affiliated Hospital of Zhengzhou University. All subjects were requested to keep their eyes closed, and foam padding and earplugs were used to control the head movements of the participants and reduce scanning noise. At the end of scanning, patients were asked if they had fallen asleep during scanning; all patients reported that they had been awake. Resting-state functional images were collected using an echo-planar imaging sequence (repetition time = 1,000 ms, echo time = 30 ms, flip angle = 70°). A total of fifty-two transverse slices (field of view = 220 mm^2 × 220 mm^2, slice thickness = 2.2 mm) that aligned along the AC-PC line were acquired with a total scan time of 412 s.

Imaging processing

The rs-fMRI data were preprocessed by the Data Processing Assistant for rs-fMRI Analysis Toolkit (DPARSF, http://rest.restfmri.net/forum/DPARSF) (Song et al., 2011) and by SPM8 software (Wellcome Department, University College of London, UK) based on MATLAB R2012a (MathWorks, USA). DPARSF was also used for the following steps: the first 10 volumes were deleted and then underwent slice-timing, realignment, spatial normalization to the Montreal Neurological Institute (MNI) space, and resampling with a 3 mm^3 × 3 mm^3 × 3 mm^3 resolution. Participants with a head motion >2.5 mm of translation or >2.5° of rotation in any direction were excluded from further processing. The linear trend of the

fMRI data was also removed. Band-pass filtering (0.01–0.08 Hz) was conducted to discard high-frequency physiological noise and a frequency drift lower than 0.01 Hz (Greicius et al., 2003).

Preprocessed ReHo data were analyzed as previously described (Cao et al., 2017a). First, an individual ReHo map was generated by calculating the Kendall's coefficient of concordance (KCC) of the time series of a given voxel with those of its neighbors (26 voxels) in a voxel-wise way (Li et al., 2012). Afterward, the individual ReHo maps were divided by their own global mean KCC within the whole-brain mask. Then, spatial smoothing was performed on the standardized individual ReHo map with a Gaussian kernel of 4 mm full width at half maximum (FWHM). Preprocessed data were used for DC calculations; Pearson's correlation analysis of time series was executed between each voxel and every other voxel in the entire brain. Correlation coefficients where $r > 0.25$ were summed for each voxel; then, the binary DC was obtained for each gray matter voxel (Zuo and Xing, 2014). Subsequently, spatial smoothing was performed with a 4-mm FWHM Gaussian kernel. The weighted DC of each voxel was further divided by the global mean DC for standardization. Z scores were then calculated in a voxel-wise way by subtracting the mean ReHo or DC values from each voxel's value; this was then divided by the standard deviation of the ReHo or DC values, respectively. In this way, the Z score represents a voxel's ReHo or DC value in relation to all voxels in the whole brain. Therefore, a positive Z score represents higher synchronicity (ReHo) or activity (DC) in a particular individual's brain. Similarly, a negative Z score represents lower synchronicity or activity.

Statistical analysis

Statistical analyses were performed using SPSS software (version 21.0). Wilcoxon signed rank tests were calculated to analyze the differences in clinical outcomes between the two visits. The significance level was set at 0.05. Paired *t*-tests were conducted with SPM8 in a whole-brain voxel-wise manner for ReHo and DC comparisons between two time points. All of the results were corrected by Gaussian random field (GRF). The significance levels of the voxel and cluster were $p < 0.005$ and $p < 0.05$, respectively. Correlations between the relative change in score on the questionnaires and the relative significant change in ReHo and DC values were calculated with non-parametric Spearman correlation tests. Relative differences between baseline and treatment were calculated as (baseline-treatment)/baseline. Only clinical outcomes with a significant effect between both visits were used for correlation analysis. Multiple comparisons were corrected for correlation analysis using the Bonferroni method ($p < 0.05/120 = 0.0004$).

TABLE 1 Individual patient's characteristics for all patients ($N = 10$).

Patient	Sex	Age (y)	Pain side	Pain duration (month)	Time of SCS (day)
1	M	39	Right	6	14
2	M	77	Left	1	14
3	F	79	Left	3	14
4	F	62	Left	6	14
5	M	60	Right	7	14
6	F	70	Right	2	14
7	F	68	Left	4	14
8	F	87	Right	1.5	14
9	M	70	Left	1	14
10	M	83	Left	1	14

F, female; M, male; SCS, spinal cord stimulation.

Results

Patient's characteristics

A total of 10 patients with PHN (five women and five men), and a median age of 70 years (Q1–Q3: 61.5–80) were included in this study (Table 1). Then, one patient has diabetes mellitus and five patients suffer from hypertension.

Clinical results

There was a significant decrease in the total scores for the NRS score ($Z = -2.694$, $p = 0.007$), PSQI ($Z = -2.675$, $p = 0.007$), SF-MPQ-2($Z = -2.668$, $p = 0.008$), and HADS ($Z = -2.668$, $p = 0.008$) when compared between the baseline and after stSCS treatment (Figure 2).

SF-MPQ-2

When considering the continuous pain, intermittent pain, neuropathic pain, and affective descriptors for SF-MPQ-2, we identified a significant decrease in scores between baseline and after stSCS: ($Z = -2.371$, $p = 0.018$), ($Z = -2.207$, $p = 0.027$), ($Z = -2.527$, $p = 0.012$), and ($Z = -2.524$, $p = 0.012$), respectively. When comparing the baseline with the status after stSCS, the median scores for the four dimensions of the SF-MPQ-2 were 12 (Q1–Q3: 1.5–17.5) to 2 (Q1–Q3:0–4.5), 10 (Q1–Q3: 0–15.5) to 0 (Q1–Q3:0–7), 22 (Q1–Q3: 15–23.5) to 0 (Q1–Q3:0–4), and 9 (Q1–Q3: 4.5–15.5) to 2 (Q1–Q3: 0–4), as shown in Figure 2.

Sleep quality

A significant reduction in PSQI score was identified between baseline and after stSCS ($Z = -2.675$, $p = 0.007$). At baseline, the

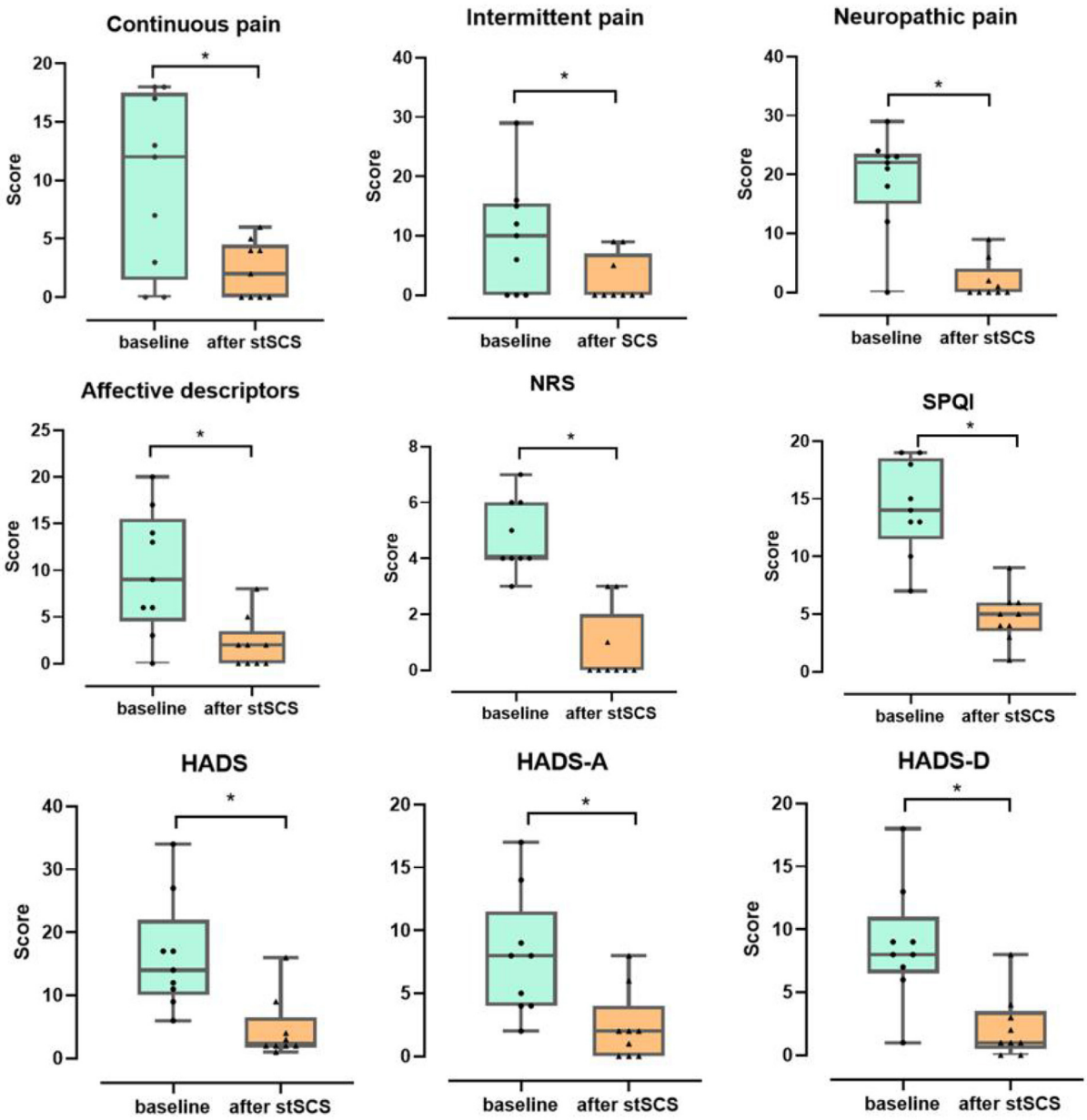

FIGURE 2
Boxplots for the clinical outcomes for all patients at baseline (in green) and after stSCS (in orange). The beginning four boxplots represent the four subscale scores of the SF-MPQ-2 (continuous pain, intermittent pain, predominantly neuropathic pain, and affective descriptors). The last two boxplots represent the two subscale scores for the HADS (HADS-A and HADS-D). NRS, numeric rating scale; PSQI, Pittsburgh sleep quality index; SCS, spinal cord stimulation. *$p < 0.05$.

median PSQI score was 14 (Q1–Q3: 11.5–18.5) and after stSCS was 5 (Q1–Q3:3.5–6), as shown in Figure 2.

HADS

A significant decrease in HADS score was identified between baseline and after stSCS ($Z = -2.668$, $p = 0.008$). At baseline, the median HADS score was 14 (Q1–Q3:10–22) and after stSCS was 2 (Q1–Q3:2–6.5). For the anxiety and depression dimensions of the HADS, we identified a significant reduction in HADS-A and HADS-D scores between baseline and after stSCS: ($Z = -2.677$, $p = 0.007$) and ($Z = -2.673$, $p = 0.008$), respectively. When comparing the baseline with after stSCS, the median scores for the two dimensions of HADS were 8 (Q1–Q3: 4–11.5) to 2 (Q1–Q3: 0–4) and 8 (Q1–Q3: 6.5–11) to 1 (Q1–Q3: 0.5–3.5), as shown in Figure 2.

TABLE 2 Clusters of different ReHo values between baseline and after stSCS.

Regions Regions	Peak MNI coordinate			Peak *T*-value	Cluster size (voxels)
	x	y	z		
Baseline < after stSCS					
Temporal_Mid_L	−54	−63	9	8.184	61
Frontal_Sup_R	18	63	6	7.2821	39
Precuneus	−3	−60	39	8.7368	49
SupraMarginal-L	−48	−45	33	9.8058	81
Parietal_Inf_L	−36	−60	48	7.6008	46
Parietal_Sup_R	24	−51	60	6.6291	81
Baseline > after stSCS					
Rolandic_Oper_R	39	−30	18	−6.5298	45
Occipital_Mid_R	27	−72	30	−6.5043	60

ReHo, regional homogeneity.

NRS

A significant reduction in NRS score was identified between baseline and after stSCS ($Z = -2.694$, $p = 0.007$). At baseline, the median NRS score for PHN was 4 (Q1–Q3: 4–6) and after stSCS was 0 (Q1–Q3:0–2), as shown in Figure 2.

fMRI results

Comparison of ReHo between baseline and after stSCS

As shown in Table 2 and Figure 3, compared with baseline, there was a significantly increased ReHo in the vast region of the left middle temporal gyrus, right superior frontal gyrus (SFG), precuneus, left supramarginal gyrus, left inferior parietal lobule (IPL), and right superior parietal gyrus. We also observed the decreased ReHo in the right rolandic operculum and the right middle occipital gyrus after stSCS treatment.

Correlation between ReHo and clinical results

As mentioned earlier, the NRS, PSQI scores, SF-MPQ-2, and HADS were statistically significant after stSCS therapy and were then correlated with ReHo alterations. A significant positive correlation was found between ReHo changes in the right middle occipital gyrus and changes in intermittent pain ($r = 0.725$, $p = 0.027$). A significant negative correlation was identified between ReHo changes in the left precuneus and changes in intermittent pain ($r = -0.673$, $p = 0.047$) and PSQI ($r = -0.736$, $p = 0.024$) and left inferior parietal and affective descriptors ($r = -0.746$, $p = 0.021$) and HADS-A ($r = -0.782$, $p = 0.013$). However, this level of significance was abolished after Bonferroni correction ($p < 0.05/120 = 0.0004$).

Comparison of DC between baseline and after stSCS

As shown in Table 3 and Figure 4, there was a significantly increased DC in the vast region of the left middle temporal gyrus, right rolandic operculum, left supramarginal gyrus, right supramarginal gyrus, right precentral gyrus (PCG), left precuneus, and left inferior parietal after stSCS.

Correlation between DC and clinical results

The NRS, PSQI scores, SF-MPQ-2, and HADS were statistically significant after stSCS and were then correlated with DC alterations. A significant negative correlation was identified between DC changes in the left middle temporal gyrus ($r = -0.690$, $p = 0.040$), right rolandic operculum ($r = -0.742$, $p = 0.022$), right supramarginal gyrus ($r = -0.845$, $p = 0.004$) and changes in intermittent pain, left precuneus and PSQI ($r = -0.778$, $p = 0.014$), right rolandic operculum and HADS ($r = -0.753$, $p = 0.019$) and HADS-D ($r = -0.678$, $p = 0.045$), left inferior parietal ($r = -0.686$, $p = 0.041$) and HADS-D. However, this level of significance did not remain after Bonferroni correction ($p < 0.05/120 = 0.0004$).

Discussion

In our study, we investigated the changes in ReHo and DC values related to stimulator-induced pain relief in patients with PHN. ReHo and DC analysis validated the improvement in symptoms to some extent at the level of regional brain function. We also observed correlation between the change in brain function and clinical questionnaires. Our results indicate that stSCS therapy can change local activity and functional connectivity to alleviate pain, sleep, and emotional disorder.

In this study, we identified several functional brain mapping alterations related to pain following the treatment of PHN with stSCS therapy. Patients with PHN show significantly reduced ReHo levels in the temporal lobe (Cao et al., 2017b). We observed increased DC and ReHo values in the middle temporal gyrus after stSCS. The middle temporal gyrus is associated with language and semantic memory processing, visual perception, multimodal sensory integration, and pain inhibition (Kucyi et al., 2013). We also identified a significant correlation between DC and ReHo changes in the middle temporal gyrus, the right middle occipital gyrus and changes in intermittent pain. The middle occipital gyrus is related to pain and may take part in the descending pain-inhibitory mechanisms (Reis et al., 2010). The occipital lobe has been shown to be associated with sensitivity to fearful stimuli, emotion processing, levels of trait anxiety, and the sensory processing (Collignon et al., 2011). It is possible that stSCS treatment may act on these regions of brain to alleviate pain.

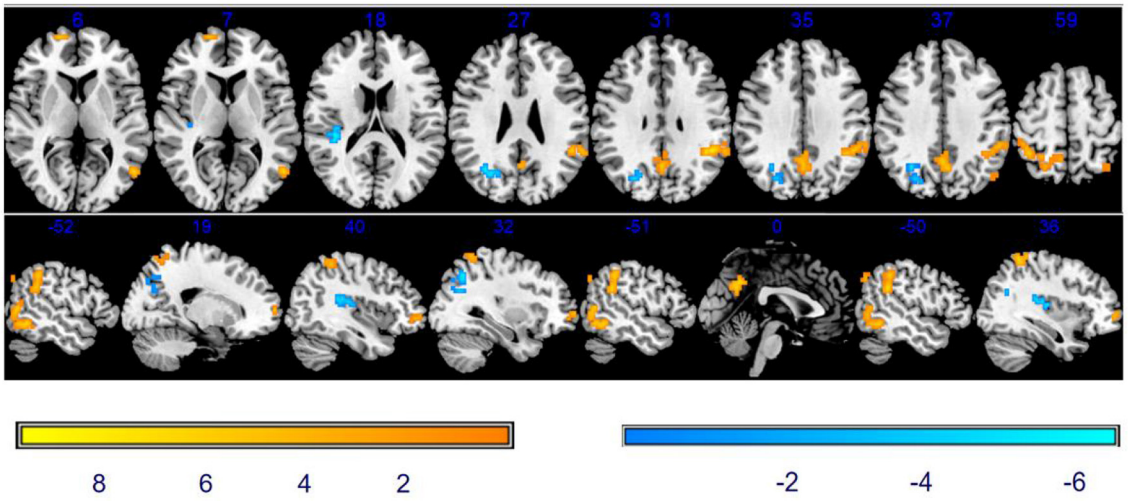

FIGURE 3
Significant differences in ReHo between baseline and after stSCS in axial and sagittal slices. The warm colors indicate a higher ReHo value whereas the cooler colors indicate a lower ReHo value at baseline and after stSCS ($p < 0.05$). Brain images are displayed in radiology convention (the left of the figure represents the right side of the patient's brain and *vice versa*).

TABLE 3 Clusters of different DC values between baseline and after stSCS.

Regions	Peak MNI coordinate			Peak *T*-value	Cluster size (voxels)
	x	y	z		
Baseline < after stSCS					
Temporal_Mid_L	−54	−63	12	13.5598	22
Rolandic_Oper_R	54	3	12	6.5985	20
Supramarginal_L	−42	−45	30	9.6256	62
Supramarginal_R	69	−72	24	5.8351	24
Precentral_R	57	3	27	6.238	17
Precuneus_L	0	−63	27	7.2906	42
Parietal_Inf_L	−60	−42	39	7.2755	21

DC, degree centrality.

We found that the precuneus was related to pain intensity and sleep quality. We observed increased DC and ReHo values in the left precuneus after stSCS when compared to baseline. There was also a significant correlation between ReHo and DC changes in the left precuneus and changes in intermittent pain and PSQI. The precuneus gathers information for somatosensory sensation and is therefore responsible for the recognition of pain sensation (Nagamachi et al., 2006). The precuneus plays a significant role in sleep. Altena et al. reported that reduced gray matter volume was found in the precuneus in patients with insomnia (Altena et al., 2010). One of the reasons for sleep improvement may be related to the changes in the precuneus. The precuneus in a wide range of highly integrated tasks, including visuospatial imagery, episodic memory retrieval, self-processing operations, aspects of consciousness, pain perception, and endogenous pain modulation (Greicius et al., 2009). Groote et al. (2020) suggested the role of the precuneus as a monitoring tool for the effect of SCS. We found an increase in ReHo and DC values in the left precuneus after stSCS; these data may confirm the important role of the precuneus in the alleviation of pain. Depression severity was previously correlated with functional connectivity in the left middle temporal cortex and precuneus (Lassalle-Lagadec et al., 2012). The precuneus is the main hub of the brain and represents a core region of the default-mode network (DMN). The DMN is the resting-state network of the brain and consists of the posterior cingulate cortex, medial frontal, precuneus, posterior parietal cortex, and lateral temporal cortex (Raichle et al., 2001). The DMN is not only responsible for emotional processing, self-introspection, awareness, and the extraction of scenario memory, but also correlative pain suppression (Argaman et al., 2020), functional connectivity hubs, and brain networks (Tomasi and Volkow, 2011). The resting-state DMN is abnormal in patients with chronic painful conditions, thus implicating the impact of such chronic conditions on areas beyond pain perception.

Several brain regions related to emotion were changed after stSCS therapy. The parietal lobe is associated with emotion, sensory, and cognitive function (Lai, 2019). Anxiety is associated with reduced cerebral blood flow in the parietal lobe (Fredrikson et al., 1997). The severity of anxiety is inversely correlated with metabolism in the temporal and parietal regions in patients with mood disorder (Osuch et al., 2000). Improvements in the

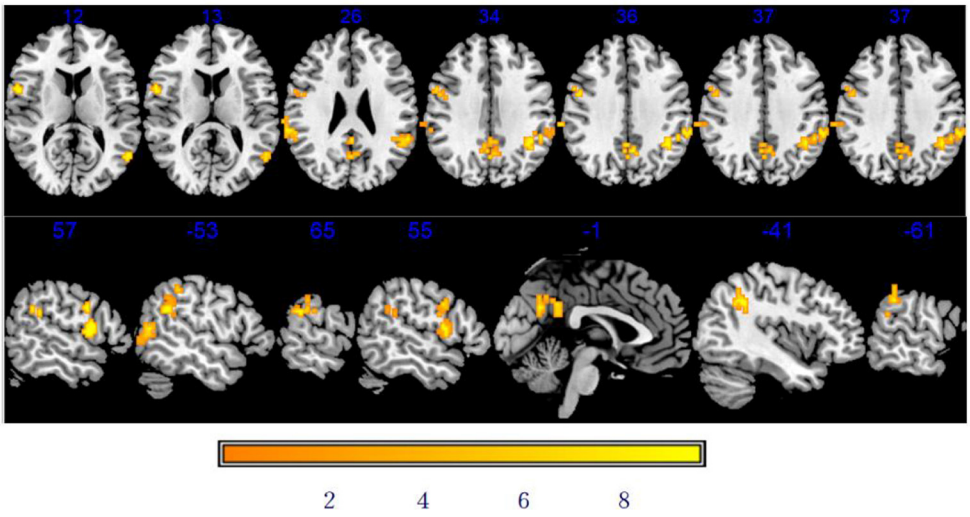

FIGURE 4
Significant differences in DC between baseline and after stSCS in axial and sagittal slices. The warm colors indicate higher DC values at baseline and after stSCS ($p < 0.05$). Brain images are presented in radiology convention (the left of the figure represents the right side of the patient's brain and *vice versa*).

severity of panic symptoms have also been negatively correlated with the changes in ReHo values in the right superior parietal lobe (Lai and Wu, 2013). Patients with PHN show significantly reduced ReHo values in the right parietal lobe (Cao et al., 2017b). We also observed an increased ReHo value in the superior parietal gyrus after stSCS. It is possible that the superior parietal lobe plays an important role in improving emotions following treatment with stSCS. Moreover, increases in DC and ReHo values in the inferior parietal lobule (IPL), which includes the angular gyrus and the supramarginal gyrus, were observed after stSCS. A significant correlation was identified between DC and ReHo changes in the IPL and changes in the HADS-D and HADS-A. We also identified a significant correlation between DC changes in the left supramarginal gyrus and changes in intermittent pain. It is possible that the IPL may be engaged in attention control, self-awareness, and the regulation of negative affection (Zhuang et al., 2017). The IPL participates in emotional expression and is related to happiness (Schmidt et al., 2020). The angular gyrus is both a node of the DMN and a subregion of the inferior parietal lobule (Gray et al., 2020). The supramarginal gyrus processes external/perceptual information, whereas the angular gyrus processes internal/conceptual information (Rubinstein et al., 2021). The IPL plays a role in episodic memory encoding (Rubinstein et al., 2021). It is possible that stSCS may influence ILP to alleviate pain and emotional function. With regard to emotion, we also found that the ReHo value increased and the DC value decreased in the rolandic operculum after stSCS. There was a significant correlation between DC changes in the rolandic operculum and changes in the HADS, HADS-D, and intermittent pain. One of the reasons why SCS therapy led to an improvement in emotions may be related to the changes in rolandic operculum. Previous studies have reported that the rolandic operculum is associated with psychology and also emotional responses to music (Zhang et al., 2020). Lesions in the right rolandic operculum are known to contribute to worse psychological conditions (high apathy, depression, anxiety, and perceived stress) (Sutoko et al., 2020). The rolandic operculum and IPL may also play the important roles in alleviating the comorbidity of emotion disorder and pain.

The motor function of several brain regions was found to undergo the changes after stSCS therapy. The ReHo value for the superior frontal gyrus was found to increase following stSCS. The human SFG into the anteromedial (SFGam), dorsolateral (SFGdl), and posterior (SFGp) subregions is based on the diffusion tensor tractography (Li et al., 2013). The SFGam is a node of the DMN and is involved in self-referential processing and cognitive control (Northoff et al., 2006). The SFGdl plays a role in the execution of cognitive manipulation (Li et al., 2013). The SFGp is connected with sensorimotor areas (Yu et al., 2011). Regions in the right SFG are implicated in a variety of tasks, including motor movement, working memory, sensorimotor, and cognitive control (Briggs et al., 2020). The concurrent involvement in motor nerves could induce the symptoms of segmental zoster paresis, a condition that is manifested by localized asymmetric myasthenia; the range of this condition generally follows the distribution of myomeres with skin rashes (Meng et al., 2021). SCS has also been shown to alleviate motor deficit (Megía García et al., 2020). The stSCS may exert an effect on the SFGp to alleviate pain and motor function.

In this study, the PCG is also involved in motion function in that the DC value of the PCG was increased. The PCG features the whole primary motor area (M1); a very small part of this is located by the most caudal edge of the premotor cortex. The M1 has recently been shown to be a crucial node in the processing of cognitive information related to motor function (e.g., spatial transformations, serial order coding, stimulus-response incompatibility, motor skill learning and memory, and motor imagery) (Georgopoulos, 2000). Changes in the SGF and PCG may represent central mechanisms by which SCS can alleviate motor function although this requires further investigation.

Since several patients withdrew from their consent, the most evident limitation of this study is the relatively small sample size; this may have had an influence on statistical power. Since the patients had a strong desire to accept stSCS therapy to alleviate pain, unfortunately, there is no other treatment control group. Future research should investigate the correlation between motor function and neural activity changes.

Conclusion

Collectively, this study dynamically and visually investigated the local activity and functional connectivity of brain regions in patients with PHN when treated by stSCS therapy. We demonstrated that after stSCS treatment, patients with PHN exhibit the alterations in ReHo and DC in several brain regions; these regions are related to sensory, motor, memory, sleep, and emotional processes. Moreover, we also observed significant correlations between alterations within these regions and pain intensity, sleep quality, and emotional disorder. This suggests that stSCS therapy may alleviate pain, sleep, and emotional disorder *via* mechanisms in specific brain segments. Our results provide further insights into the mechanisms of stSCS therapy that may activate neurophysiological pathway in the brain.

Data availability statement

The original contributions presented in the study are included in the article/supplementary material, further inquiries can be directed to the corresponding author/s.

Ethics statement

The studies involving human participants were reviewed and approved by the Medical Ethics Committee of the First Affiliated Hospital of Zhengzhou University, Zhengzhou, China (Reference: 2020-KY-0299-001). The patients/participants provided their written informed consent to participate in this study. Written informed consent was obtained from the individual(s) and/or minor(s)' legal guardian/next of kin for the publication of any potentially identifiable images or data included in this article.

Author contributions

XF helped to conceive, design, and examine the manuscript. HR helped to collect, assemble, analyze the data, and write the manuscript. CB helped to collect, assemble, and analyze the data. ZL and LF helped to collect and assemble the data. YW helped to assemble and analyze the data. FX helped to collect and assemble the data and write the manuscript. LM, CK, and TW helped to analyze and interpret the data. YZ helped to analyze the data. QL and WH helped to interpret the data. HB helped to conceive and design. JY helped to design and examine the manuscript. All authors contributed to the article and approved the submitted version.

Funding

This study was supported by the National Key Research and Development Program of China (grant no. 2020YFC2008400) and the National Natural Science Foundation of China (82001182).

Acknowledgments

The authors would like to thank Professor Peng Yonggang of the University of Florida for revising the manuscript.

Conflict of interest

The authors declare that the research was conducted in the absence of any commercial or financial relationships that could be construed as a potential conflict of interest.

Publisher's note

References

Altena, E., Vrenken, H., Van Der Werf, Y. D., van den Heuvel, O. A., and Van Someren, E. J. (2010). Reduced orbitofrontal and parietal gray matter in chronic insomnia: a voxel-based morphometric study. *Biol. Psychiatry*. 67, 182–185. doi: 10.1016/j.biopsych.2009.08.003

Argaman, Y., Kisler, L. B., Granovsky, Y., Coghill, R. C., Sprecher, E., Manor, D., et al. (2020). The endogenous analgesia signature in the resting brain of healthy adults and migraineurs. *J. Pain*. 21, 905–918. doi: 10.1016/j.jpain.2019.12.006

Briggs, R. G., Khan, A. B., Chakraborty, A. R., Abraham, C. J., Anderson, C. D., Karas, P. J., et al. (2020). Anatomy and White matter connections of the superior frontal gyrus. *Clin. Anat*. 33, 823–832. doi: 10.1002/ca.23523

Brisson, M., Edmunds, W. J., Law, B., Gay, N. J., Walld, R., Brownell, M., et al. (2001). Epidemiology of varicella zoster virus infection in Canada and the United Kingdom. *Epidemiol. Infect*. 127, 305–314. doi: 10.1017/S0950268801005921

Cao, S., Li, Y., Deng, W., Qin, B., Zhang, Y., Xie, P., et al. (2017a). Local brain activity differences between herpes zoster and postherpetic neuralgia patients: a resting -state functional MRI study. *Pain Physician* 20, E687–E99.

Cao, S., Song, G., Zhang, Y., Xie, P., Tu, Y., Li, Y., et al. (2017b). Abnormal local brain activity beyond the pain matrix in postherpetic neuralgia patients: a resting-st ate functional MRI study. *Pain Physician* 20, E303–E14. doi: 10.36076/ppj.2017.E314

Collignon, O., Vandewalle, G., Voss, P., Albouy, G., Charbonneau, G., Lassonde, M., et al. (2011). Functional specialization for auditory-spatial processing in the occipital cortex of congenitally bli nd humans. *Proc. Natl. Acad. Sci. U. S. A*. 108, 4435–4440. doi: 10.1073/pnas.1013928108

Dai, H., Jiang, C., Wu, G., Huang, R., Jin, X., Zhang, Z., et al. (2020). A combined DTI and resting state functional MRI study in patients with postherpetic neuralgia. *Jpn. J. Radiol*. 38, 440–450. doi: 10.1007/s11604-020-00926-4

De Groote, S., Goudman, L., Peeters, R., Linderoth, B., Vanschuerbeek, P., Sunaert, S., et al. (2020). Magnetic resonance imaging exploration of the human brain during 10 kHz spinal cord stimulation for f ailed back surgery syndrome: a resting state functional magnetic resonance imaging study. *Neuromodulation* 23, 46–55. doi: 10.1111/ner.12954

Fredrikson, M., Fischer, H., and Wik, G. (1997). Cerebral blood flow during anxiety provocation. *J. Clin. Psychiatry*. 58(Suppl. 16), 16–21.

Georgopoulos, A. P. (2000). Neural aspects of cognitive motor control. *Curr. Opin. Neurobiol*. 10, 238–241. doi: 10.1016/S0959-4388(00)00072-6

Gray, O., Fry, L., and Montaldi, D. (2020). Information content best characterises the hemispheric selectivity of the inferior parietal lobe: a m eta-analysis. *Sci. Rep*. 10, 15112. doi: 10.1038/s41598-020-72228-8

Greicius, M. D., Krasnow, B., Reiss, A. L., and Menon, V. (2003). Functional connectivity in the resting brain: a network analysis of the default mode hypothesis. *Proc. Natl. Acad. Sci. U. S. A*. 100, 253–258. doi: 10.1073/pnas.0135058100

Greicius, M. D., Supekar, K., Menon, V., and Dougherty, R. F. (2009). Resting-state functional connectivity reflects structural connectivity in the default mode network. *Cereb. Cortex* 19, 72–78. doi: 10.1093/cercor/bhn059

Groote, S. D., Goudman, L., Schuerbeek, P. V., Peeters, R., Sunaert, S., Linderoth, B., et al. (2020). Effects of spinal cord stimulation on voxel-based brain morphometry in patients with failed back surgery syndrome. *Clin. Neurophysiol*. 131, 2578–2587. doi: 10.1016/j.clinph.2020.07.024

Han, Z., Hong, T., Ding, Y., Wang, S., and Yao, P. (2020). CT-guided pulsed radiofrequency at different voltages in the treatment of postherpetic neuralgia. *Front. Neurosci*. 14, 579486. doi: 10.3389/fnins.2020.579486

Insinga, R. P., Itzler, R. F., Pellissier, J. M., Saddier, P., and Nikas, A. A. (2005). The incidence of herpes zoster in a United States administrative database. *J. Gen. Intern. Med*. 20, 748–753. doi: 10.1111/j.1525-1497.2005.0150.x

Johnson, R. W., and Rice, A. S. (2014). Clinical practice. Postherpetic neuralgia. *N Engl J Med*. 371, 1526–1533. doi: 10.1056/NEJMcp1403062

Kucyi, A., Salomons, T. V., and Davis, K. D. (2013). Mind wandering away from pain dynamically engages antinociceptive and default mode brain networks. *Proc. Natl. Acad. Sci. U. S. A*. 110, 18692–18697. doi: 10.1073/pnas.1312902110

Kuo, Y. C., Hsieh, L. F., and Chiou, H. J. (2016). Ultrasound-guided musculocutaneous nerve block in postherpetic neuralgia. *Am. J. Phys. Med. Rehabil*. 95, e1–e6. doi: 10.1097/PHM.0000000000000387

Lai, C. H. (2019). Fear network model in panic disorder: the past and the future. *Psychiatry Investig*. 16, 16–26. doi: 10.30773/pi.2018.05.04.2

Lai, C. H., and Wu, Y. T. (2013). Changes in regional homogeneity of parieto-temporal regions in panic disorder patients who achieved r emission with antidepressant treatment. *J. Affect. Disord*. 151, 709–714. doi: 10.1016/j.jad.2013.08.006

Lassalle-Lagadec, S., Sibon, I., Dilharreguy, B., Renou, P., Fleury, O., Allard, M., et al. (2012). Subacute default mode network dysfunction in the prediction of post-stroke depression severity. *Radiology* 264, 218–224. doi: 10.1148/radiol.12111718

Li, H., Li, X., Feng, Y., Gao, F., Kong, Y., Hu, L., et al. (2020). Deficits in ascending and descending pain modulation pathways in patients with postherpetic neuralgia. *Neuroimage* 221, 117186. doi: 10.1016/j.neuroimage.2020.117186

Li, W., Qin, W., Liu, H., Fan, L., Wang, J., Jiang, T., et al. (2013). Subregions of the human superior frontal gyrus and their connections. *Neuroimage* 78, 46–58. doi: 10.1016/j.neuroimage.2013.04.011

Li, Z., Kadivar, A., Pluta, J., Dunlop, J., and Wang, Z. (2012). Test-retest stability analysis of resting brain activity revealed by blood oxygen level-dependent fun ctional MRI. *J. Magn. Reson. Imaging* 36, 344–354. doi: 10.1002/jmri.23670

Megía García, A., Serrano-Muñoz, D., Taylor, J., Avendaño-Coy, J., and Gómez-Soriano, J. (2020). Transcutaneous spinal cord stimulation and motor rehabilitation in spinal cord injury: a systematic review. *Neurorehabil. Neural Repair*. 34, 3–12. doi: 10.1177/1545968319893298

Meng, Y., Zhuang, L., Jiang, W., Zheng, B., and Yu, B. (2021). Segmental zoster paresis: a literature review. *Pain Physician* 24, 253–261. doi: 10.36076/ppj.2021/24/253

Meyerson, B. A., and Linderoth, B. (2006). Mode of action of spinal cord stimulation in neuropathic pain. *J. Pain Symptom Manage*. 31, S6–12. doi: 10.1016/j.jpainsymman.2005.12.009

Moore, R. A., Wiffen, P. J., Derry, S., Toelle, T., and Rice, A. S. (2014). Gabapentin for chronic neuropathic pain and fibromyalgia in adults. *Cochrane Database Syst. Rev*. 2014, Cd007938. doi: 10.1002/14651858.CD007938.pub3

Nagamachi, S., Fujita, S., Nishii, R., Futami, S., Wakamatsu, H., Yano, T., et al. (2006). Alteration of regional cerebral blood flow in patients with chronic pain–evaluation before and after epidural spinal cord stimulation. *Ann. Nucl. Med*. 20, 303–310. doi: 10.1007/BF02984647

Northoff, G., Heinzel, A., de Greck, M., Bermpohl, F., Dobrowolny, H., Panksepp, J., et al. (2006). Self-referential processing in our brain–a meta-analysis of imaging studies on the self. *Neuroimage* 31, 440–457. doi: 10.1016/j.neuroimage.2005.12.002

Osuch, E. A., Ketter, T. A., Kimbrell, T. A., George, M. S., Benson, B. E., Willis, M. W., et al. (2000). Regional cerebral metabolism associated with anxiety symptoms in affective disorder patients. *Biol. Psychiatry* 48, 1020–1023. doi: 10.1016/S0006-3223(00)00920-3

Raichle, M. E., MacLeod, A. M., Snyder, A. Z., Powers, W. J., Gusnard, D. A., Shulman, G. L., et al. (2001). A default mode of brain function. *Proc. Natl. Acad. Sci. U. S. A*. 98, 676–682. doi: 10.1073/pnas.98.2.676

Reis, G. M., Dias, Q. M., Silveira, J. W., Del Vecchio, F., Garcia-Cairasco, N., Prado, W. A., et al. (2010). Antinociceptive effect of stimulating the occipital or retrosplenial cortex in rats. *J. Pain* 11, 1015–1026. doi: 10.1016/j.jpain.2010.01.269

Rubinstein, D. Y., Camarillo-Rodriguez, L., Serruya, M. D., Herweg, N. A., Waldman, Z. J., Wanda, P. A., et al. (2021). Contribution of left supramarginal and angular gyri to episodic memory encoding: an intracranial EEG study. *Neuroimage* 225, 117514. doi: 10.1016/j.neuroimage.2020.117514

Schmidt, S. N. L., Sojer, C. A., Hass, J., Kirsch, P., and Mier, D. (2020). fMRI adaptation reveals: the human mirror neuron system discriminates emotional valence. *Cortex* 128, 270–280. doi: 10.1016/j.cortex.2020.03.026

Song, X. W., Dong, Z. Y., Long, X. Y., Li, S. F., Zuo, X. N., Zhu, C. Z., et al. (2011). REST: a toolkit for resting-state functional magnetic resonance imaging data processing. *PLoS ONE* 6, e25031. doi: 10.1371/journal.pone.0025031

Sutoko, S., Atsumori, H., Obata, A., Funane, T., Kandori, A., Shimonaga, K., et al. (2020). Lesions in the right Rolandic operculum are associated with self-rating affective and apathetic depre ssive symptoms for post-stroke patients. *Sci. Rep*. 10, 20264. doi: 10.1038/s41598-020-77136-5

Tomasi, D., and Volkow, N. D. (2011). Association between functional connectivity hubs and brain networks. *Cereb. Cortex* 21, 2003–2013. doi: 10.1093/cercor/bhq268

Tracey, I. (2011). Can neuroimaging studies identify pain endophenotypes in humans? *Nat. Rev. Neurol.* 7, 173–181. doi: 10.1038/nrneurol.2011.4

Wan, C. F., and Song, T. (2021). Efficacy of pulsed radiofrequency or short-term spinal cord stimulation for acute/subacute zoster-rel ated pain: a randomized, double-blinded, controlled trial. *Pain Physician* 24, 215–222. doi: 10.36076/ppj.2021/24/215

Wu, K., Liu, M., He, L., and Tan, Y. (2020). Abnormal degree centrality in delayed encephalopathy after carbon monoxide poisoning: a resting-state fMRI study. *Neuroradiology* 62, 609–616. doi: 10.1007/s00234-020-02369-0

Yu, C., Zhou, Y., Liu, Y., Jiang, T., Dong, H., Zhang, Y., et al. (2011). Functional segregation of the human cingulate cortex is confirmed by functional connectivity based ne uroanatomical parcellation. *Neuroimage* 54, 2571–2581. doi: 10.1016/j.neuroimage.2010.11.018

Zang, Y., Jiang, T., Lu, Y., He, Y., and Tian, L. (2004). Regional homogeneity approach to fMRI data analysis. *Neuroimage* 22, 394–400. doi: 10.1016/j.neuroimage.2003.12.030

Zhang, Y. N., Huang, Y. R., Liu, J. L., Zhang, F. Q., Zhang, B. Y., Wu, J. C., et al. (2020). Aberrant resting-state cerebral blood flow and its connectivity in primary dysmenorrhea on arterial s pin labeling MRI. *Magn. Reson. Imaging* 73, 84–90. doi: 10.1016/j.mri.2020.07.012

Zhuang, K., Bi, M., Li, Y., Xia, Y., Guo, X., Chen, Q., et al. (2017). A distinction between two instruments measuring dispositional mindfulness and the correlations betwee n those measurements and the neuroanatomical structure. *Sci. Rep.* 7, 6252. doi: 10.1038/s41598-017-06599-w

Zuo, X. N., and Xing, X. X. (2014). Test-retest reliabilities of resting-state FMRI measurements in human brain functional connectomics: a systems neuroscience perspective. *Neurosci. Biobehav. Rev.* 45, 100–118. doi: 10.1016/j.neubiorev.2014.05.009

Zuo, X. N., Xu, T., Jiang, L., Yang, Z., Cao, X. Y., He, Y., et al. (2013). Toward reliable characterization of functional homogeneity in the human brain: preprocessing, scan du ration, imaging resolution and computational space. *Neuroimage* 65, 374–386. doi: 10.1016/j.neuroimage.2012.10.017

frontiers | Frontiers in Molecular Neuroscience

TYPE Original Research
PUBLISHED 18 August 2022
DOI 10.3389/fnmol.2022.937468

OPEN ACCESS

EDITED BY
Robert John Vandenberg,
The University of Sydney, Australia

REVIEWED BY
Shaogen Wu,
Cedars Sinai Medical Center,
United States
Xiyao Gu,
Shanghai Jiao Tong University, China
Zhiqiang Pan,
Xuzhou Medical University, China

*CORRESPONDENCE
Jingjing Yuan
yjingjing_99@163.com
Zhongyu Wang
wzy781217@163.com

†These authors have contributed equally to this work

SPECIALTY SECTION
This article was submitted to Pain Mechanisms and Modulators, a section of the journal Frontiers in Molecular Neuroscience

RECEIVED 06 May 2022
ACCEPTED 11 July 2022
PUBLISHED 18 August 2022

CITATION
Chen S, Xie Y, Li Y, Fan X, Xing F, Mao Y, Xing N, Wang J, Yang J, Wang Z and Yuan J (2022) Sleep deprivation and recovery sleep affect healthy male resident's pain sensitivity and oxidative stress markers: The medial prefrontal cortex may play a role in sleep deprivation model.
Front. Mol. Neurosci. 15:937468.
doi: 10.3389/fnmol.2022.937468

Sleep deprivation and recovery sleep affect healthy male resident's pain sensitivity and oxidative stress markers: The medial prefrontal cortex may play a role in sleep deprivation model

Shuhan Chen[1,2†], Yanle Xie[1,2†], Yize Li[3†], Xiaochong Fan[1,2], Fei Xing[1,2], Yuanyuan Mao[1,2], Na Xing[1,2], Jingping Wang[4], Jianjun Yang[1,2], Zhongyu Wang[1,2*] and Jingjing Yuan[1,2*]

[1]Department of Anesthesiology, Pain and Perioperative Medicine, The First Affiliated Hospital of Zhengzhou University, Zhengzhou, China, [2]Henan Province International Joint Laboratory of Pain, Cognition and Emotion, Zhengzhou, China, [3]Department of Anesthesiology, Tianjin Research Institute of Anesthesiology, Tianjin Medical University General Hospital, Tianjin, China, [4]Massachusetts General Hospital Department of Anesthesia, Critical Care and Pain Medicine, Harvard Medical School, Boston, MA, United States

Sleep is essential for the body's repair and recovery, including supplementation with antioxidants to maintain the balance of the body's redox state. Changes in sleep patterns have been reported to alter this repair function, leading to changes in disease susceptibility or behavior. Here, we recruited healthy male physicians and measured the extent of the effect of overnight sleep deprivation (SD) and recovery sleep (RS) on nociceptive thresholds and systemic (plasma-derived) redox metabolism, namely, the major antioxidants glutathione (GSH), catalase (CAT), malondialdehyde (MDA), and superoxide dismutase (SOD). Twenty subjects underwent morning measurements before and after overnight total SD and RS. We found that one night of SD can lead to increased nociceptive hypersensitivity and the pain scores of the Numerical Rating Scale (NRS) and that one night of RS can reverse this change. Pre- and post-SD biochemical assays showed an increase in MDA levels and CAT activity and a decrease in GSH levels and SOD activity after overnight SD. Biochemical assays before and after RS showed a partial recovery of MDA levels and a basic recovery of CAT activity to baseline levels. An animal study showed that SD can cause a significant decrease in the paw withdrawal threshold and paw withdrawal latency in rats, and after 4 days of unrestricted sleep, pain thresholds can be restored to normal. We performed proteomics in the rat medial prefrontal cortex (mPFC) and showed that 37 proteins were significantly altered after 6 days of SD. Current findings

showed that SD causes nociceptive hyperalgesia and oxidative stress, and RS can restore pain thresholds and repair oxidative stress damage in the body. However, one night of RS is not enough for repairing oxidative stress damage in the human body.

KEYWORDS

sleep deprivation, pain, oxidative stress, recovery sleep, night shift

Introduction

Chronic pain is a major health problem worldwide (Cohen et al., 2021). sleep might be relevant for predicting both the onset and the resolution of pain (Aili et al., 2015). The deprivation or the disturbance of sleep enhances pain sensitivity (Lautenbacher et al., 2006). Previous studies suggest that sleep deprivation (SD), or sleep loss, results in augmented pain response in healthy subjects (Roehrs et al., 2006; Azevedo et al., 2011). Experimental studies highlight the profound impact of sleep disruptions on pain, suggesting that SD leads to hyperalgesic pain changes, while chronic pains are often accompanied by sleep disturbances (McBeth et al., 2015; Sivertsen et al., 2015). In chronic pain, the activity of the medial prefrontal cortex (mPFC), a brain region critical for executive function and working memory, is severely impaired. The major extracortical sources of excitatory input to the mPFC come from the thalamus, the hippocampus, and the amygdala, which enables the mPFC to integrate multiple streams of information required for the cognitive control of pain, namely, sensory information, context, and emotional salience (Jefferson et al., 2021). One study found that one night of total SD impaired descending pain pathways and sensitized peripheral pathways to cold and pressure pain (Staffe et al., 2019). Chronic SD may alter the habituation and sensitization of pain, thereby increasing susceptibility to pain (Simpson et al., 2018). At the same time, some studies showed that undisturbed sleep and recovery sleep (RS) may in turn help the pain system return to normal overnight. The question of whether RS helps to reset occurring pain changes has gained special interest. Roehrs et al. (2012) have demonstrated that, in healthy sleep-deprived subjects, improved sleep quality/quantity leads to decreased pain sensitivity thereafter.

Night shift work has a critical effect on sleep, and it is inevitable for anesthesiologists to work on the night shift. Many anesthesiologists even work through the night when they are on the night shift. Extended shift durations and interrupted sleep are integral parts of an anesthesiologist's professional life (Tucker and Byrne, 2014). Despite recommendations in the United States and in Europe to limit work hours, the amount worked can still not only lead to acute and chronic SD but may also present a potential hazard for doctors' health. Anesthesiologists experience disruptions in their circadian rhythms as a result of working through the night. Sleep disruption or SD is thought to increase oxidative stress, defined as an imbalance in the normal balance between reactive oxygen species formation and antioxidant defense mechanisms. Anesthesiologists switching between night shifts and day shifts, or taking shifts off, are at risk of circadian rhythm disruptions. Circadian rhythms provide the regulation of protein expression in response to oxidative stress (Wilking et al., 2013). Chronic oxidative stress caused by sleep disruption can lead to chronic systemic low-grade inflammation (Besedovsky et al., 2019) and long-term disruption of circadian rhythms (Morris et al., 2018).

Many studies have shown a close link between the mPFC and sleep. Up to 12 circadian core clock genes are altered by SD in mice mPFC (Guo et al., 2019). Acute paradoxical deprivation leads to microglia activation and inflammatory responses in the prefrontal cortex of mice (Liu et al., 2022), which can also cause oxidative stress and lead to a decrease in glutathione (GSH) levels (Kanazawa et al., 2016). SD selectively enhances the expression and activity of prefrontal cortical 5-α reductase in rats, thereby affecting their mental status (Frau et al., 2017). Also, several pieces of clinical evidence showed that the morphology of the mPFC is altered in humans after SD (Mullin et al., 2013; Elvsåshagen et al., 2017; Feng et al., 2018).

Given the above evidence, we believe that oxidative stress and pain threshold sensitivity may be increased after one night of SD, which may be ameliorated by one night of RS. Therefore, the purpose of this study was to evaluate (1) the effect of SD and RS on the pain sensitivity of participants and animals, (2) the extent of overnight total SD and one night of RS on systemic redox of participants, and (3) changes and effects of mPFC in rats during SD.

Materials and methods

Participants

The study was approved by the ethics committee of the First Affiliated Hospital of Zhengzhou University (2021-KY-1149-004). The trial was registered at the Chinese Clinical Trial

Registry (ChiCTR2200058546). Anesthesia residents of the First Affiliated Hospital of Zhengzhou University, years 18 to 44, were invited to participate in the study. The recruited subjects were all anesthesiologists working in the First Affiliated Hospital of Zhengzhou University. We recruited 24 male volunteers within the hospital department, four of whom were excluded due to ineligibility, so, a total of 20 participants were selected for the study. The mean age of male participants was 26 ± 2 years (range 18∼44 years). Participants were screened to ensure good health, including the documentation of habitual nightly sleep duration between 7 and 9 h; the absence of sleep disorders based on questionnaires; the absence of any psychiatric disorders or chronic health disorders (e.g., hypertension, chronic pain disorders); the absence of any acute health problems (e.g., broken arm, cold, or flu); the absence of regular medication use; the absence of dietary supplements use, namely, vitamins and cod liver oil; and body mass index (BMI) <27.5 kg/m^2. Baseline demographic measures were collected. Participants were not allowed to consume alcohol, chocolate, or caffeine for 72 h before and during the study. Strenuous exercise and napping were prohibited.

In the pilot trial, subjects' pressure pain thresholds (PPTs) were measured at baseline, after SD, and after RS. The PPTs at the three timespoints were 265, 160, and 250 mg, respectively, with a standard deviation of 80. While setting α to 0.05 (bilateral), β to 0.10, and the number of groups k to 3, the minimum sample size of 13 cases was calculated. Twenty-four patients were recruited to ensure complete data collection, considering the trial's dropout rate, exclusion rate, and compliance.

Procedure

The study was conducted in the First Affiliated Hospital of Zhengzhou University. **Figure 1** depicts the participants' schedules and study protocols. Participants were not divided into groups and were self-controlled. Intensive 24-h recordings for 3 days were obtained (baseline night, SD night, and RS night). These intensive recording periods included major signs check, blood sampling, Epworth sleepiness scale (ESS), and pain evaluation.

During SD, the participants were permitted to engage in non-stressful activities (e. g., talking, board games, etc.) or were only allowed to drink water and were forbidden to take food or drink or do strenuous exercise. During the SD evening, the participants were not allowed to sleep after 8 p.m. overnight. Participants were continuously monitored by researchers and smart watches throughout the night (Huawei Watch Fit 6, FRA-B19, Huawei Technologies Co., Ltd.).

Blood sample collection

To measure the levels of malondialdehyde (MDA), catalase (CAT), GSH, and superoxide dismutase (SOD), 3 mL of blood was taken through venipuncture and collected into ethylenediaminetetraacetic acid (EDTA) coated tubes. The tubes were immediately centrifuged for 10 min at 1,500 × *g* at 4°C after collection. The plasma was then apportioned into 0.5 mL aliquots and stored at −20°C until analyses were conducted.

Pressure pain thresholds of the volunteers

Pressure pain thresholds of participants were evaluated by using von Frey filaments. A von Frey hair weighing 60 to 300 g was used. The filaments were presented in the increasing order of strength, perpendicular to the surface of the back of the subject's hand, with enough force to cause it to bend slightly. Until the subjects reported a pain response and stopped, the weight of the filaments was then recorded as the subject's pain threshold. Pain sensitivity were assessed on the Numerical Rating Scale (NRS) every morning after each night. Taking circadian rhythm into account, these recordings were assessed by 20 anesthesiologists between 7:30 and 8:00 a.m. for 3 days. The research environment was tightly controlled. The investigators conducting the tests were blinded to the group.

Animals

This study was approved by the Ethics Committee of Zhengzhou University and was performed in accordance with the Guide for the Care and Use of Laboratory Animals from the National Institutes of Health, United States. Adult male Sprague-Dawley rats [total n = 26; SPF (Beijing) biotechnology co., Ltd.], weighing 220∼250 g on arrival, were initially housed in pairs in an animal colony room under a 12-h light/dark cycle (lights on at 7:00 a.m.) at 23 ± 1°C, with food and water available *ad libitum*. All rats were allowed 2 weeks to acclimate to the surroundings before the beginning of the experiments.

Animal treatment

Rats were divided into the control group (sham, n = 8) and the SD group (SDR, n = 8). Rats were subjected to 6 h of SD from 9 a.m. to 3 p.m. per day for 6 days. An SD rat model was established using a modified multiplatform water environment method (Gao et al., 2019) and was provided food and drinking water. Control rats were allowed to sleep in cages without restriction. After 6 days of SD, the rats in both groups slept unrestrictedly, which was called RS.

Paw withdrawal threshold in rats

Mechanical allodynia was evaluated by determining PWT by using the up and down method with von Frey filaments. The rats were placed on a barbed wire platform and allowed to acclimate for 30 min before the test. A von Frey hair weighing 2.0 to 26.0 g was used. Then, the filaments were presented, in ascending order of strength, perpendicular to the plantar surface with sufficient force to cause slight bending against the paw. Paw withdrawal, flinching, or paw licking was considered a positive response. After a response, the filament of the next lower force

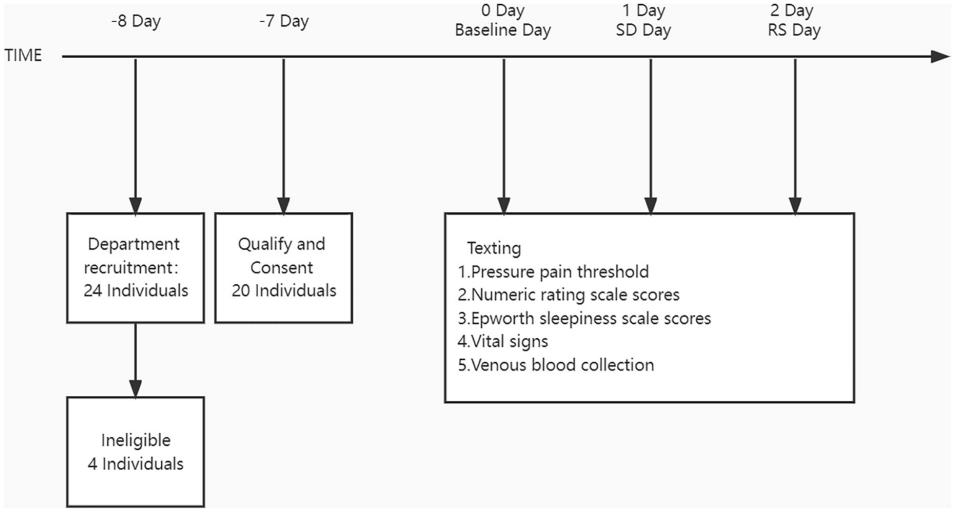

FIGURE 1
Study protocols.

was applied. In the absence of a response, the filament of the next greater force was applied. The tactile stimulus producing a 50% likelihood of withdrawal was determined using the "up-down" method. The investigators performing the behavioral tests were blinded to the group.

Paw withdrawal latency in rats

The Model 336 Analgesia Meter (IITC Inc. Life Science Instruments, Woodland Hills, CA, United States) was used to measure PWL to noxious heat. The rats were placed on an elevated glass plate and allowed to acclimatize for 30 min before the test. A radiant thermal stimulator was focused on the plantar surface of the hind paw through the glass plate. The nociceptive endpoint of the radiant heat test was characteristic movements like lifting or licking the hind paw, and the time to the endpoint was considered PWL. To avoid tissue damage, 20 s was used as a cutoff time. Each animal had five trials with a 10-min interval per side. The investigators conducting the behavioral tests were blinded to the group.

Biochemical analysis of oxidative stress

As described in the study protocol, plasma samples were collected upon completing all tests. The following parameters were measured: (1) MDA concentration, (2) GSH concentration, (3) SOD activity, and (4) CAT activity.

The MDA concentration in the plasma was determined using a commercially available kit (Nanjing Jiancheng Bioengineering Institute, Nanjing, China) based on thiobarbituric acid (TBA) reactivity. The test principle is that MDA in the degradation product of lipid peroxide can be combined with thiobarbituric acid to form a red product with a maximum absorption peak at 532 nm.

The GSH concentration in the plasma was determined by the microplate method using a commercially available kit (Nanjing Jiancheng Bioengineering Institute, Nanjing, China). Reduced GSH can react with 5,5-Dithio-bis-(2-nitrobenzoic acid) (DTNB) to produce a yellow compound, and the content of reduced GSH can be determined by colorimetric quantification at 405 nm.

The SOD activity in the plasma was determined using a commercial kit (Nanjing Jiancheng Bioengineering Institute, Nanjing, China) based on the hydroxylamine method. When SOD is contained in the tested sample, it has a specific inhibitory effect on superoxide anion free radical, reducing the formation of nitrite, and the absorbance value of the determination tube is lower than that of the care. SOD activity in the tested sample can be calculated by formula calculation.

The CAT activity in plasma was determined by an ammonium molybdate assay using a commercial kit (Nanjing Jiancheng Bioengineering Institute, Nanjing, China). The decomposition of H_2O_2 by CAT can be stopped rapidly by adding ammonium molybdate, and the remaining H_2O_2 reacts with ammonium molybdate to form a yellowish complex. The activity of CAT can be calculated by measuring its change at 405 nm.

Proteomic detection and analysis

Protein extraction and sample preparation

Rats were anesthetized with chloral hydrate and mPFC was removed on ice. We performed five biological replicates for each group of rats. The removed tissue was rapidly frozen in liquid nitrogen and then stored at −80°C. RIPA lysate was mixed with PMSF (Beijing Solarbio Science & Technology Co., Ltd)

to remove the frozen tissue, and 1,000 μL of the lysate was added to the mix and sonicated in an ice bath for 5 min until the tissue fully dissolved. The mixed solution was centrifuged at 14,000 × g for 15 min at 4°C to obtain the sample lysate. Then, the lysate was subjected to bicinchoninic acid (BCA) quantification, acetone precipitation, protein re-solubilization, protein reduction, protein alkylation, proteolysis, sodium deoxycholate (SDC) removal, peptide desalting, and nano ultra-performance liquid chromatography (UPLC) separation to obtain the final sample preparation solution.

Label-free quantitative and liquid chromatography-mass spectrometry/mass spectrometry analysis

The sample preparation solution was analyzed by liquid chromatography-mass spectrometry/mass spectrometry (LC-MS/MS). The Q Exactive (Thermo Fisher Scientific, Inc., Shanghai, China) was used to perform LC-MS/MS on the samples to be tested, and each sample was detected for 120 min to obtain the detection data.

Database search

For the obtained data, raw files were processed using MaxQuant (2.0.1.0). The protein database was obtained from the UNIPROT database (uniprot-proteome-rat-2021.2).

Protein sequences and their reverse decoy sequences were used for both MaxQuant search libraries. The quantification type was LFQ containing match between run; trypsin was set as a specific endonuclease with a maximum of 2 missed cut sites, oxidation (M) and acetyl (protein N-term) were set as variable modifications, and carbamidomethyl (C) was fixed modification with maximum variable modifications of 5. Peptide and protein level FDR was 0.01. FDR was 0.01 for both peptide and protein levels, and unique peptides without variable modifications were used for quantification. LFQ is used to analyze the mass spectrum data generated during the large-scale identification of proteins by using liquid mass spectrometry technology to compare the signal intensity of corresponding peptides in different samples so as to carry out the relative quantification of proteins corresponding to peptides.

Bioinformatics annotation

The normalized quantitative results were then statistically analyzed to obtain the corresponding differentially expressed proteins. Subsequent gene ontology (GO), Kyoto encyclopedia of genes and genomes (KEGG) pathway, protein interaction analysis, and demonstration were performed. Molecular functions, cellular components, and biological processes of GO were analyzed. The KEGG online service tools were used to annotate the protein descriptions. Pathways were classified according to the KEGG website, and further cluster analysis was performed to explore potential connections and differences between specific functions.

Statistics

For the biochemical indicators and nociceptive test data of the subjects at three-time points, the one-way ANOVA was used for the data that met the normal distribution, and the Kruskal–Wallis test was used to compare the difference of the medians for the data that did not meet the normal distribution. For the pairwise comparisons among three groups, the continuous data satisfied the normal distribution and the homogeneity of variance test used LSD, and the non-parametric test for the pairwise comparisons used the Kruskal–Wallis *H*-test. Behavioral data of rats before and after SD were analyzed by a two-way ANOVA, and Sidak's multiple comparisons test was used for pairwise comparison of time points. All reported *p*-values are two-tailed with an *a priori* significance level of $P < 0.05$. All statistical analyses of participants were performed using SPSS 24 (SPSS Statistics, IBM, Armonk, NY, United States). Data analysis of rats and graphing software using Prism GraphPad Prism 8 were performed using GraphPad Software Inc.

Results

A total of 20 volunteers, mainly unmarried (n = 15 or 75%) men with a BMI of 24.2 kg m^{-2} (standard deviation = 3.8), were recruited for this study. The mean age of the study participants was 26 years (standard deviation = 2) and the mean work experience was 2 (1 to 3) years. Participants' major signs before and after SD and RS are shown in **Table 1**. We also recorded ESS scores at these three-time points (**Figure 2**). One night of SD could significantly increase the degree of drowsiness of participants during the day and significantly decrease the degree of drowsiness after experiencing unrestricted RS.

Sleep deprivation led to nociceptive hypersensitivity

Among participants, we measured nociceptive mechanical pain thresholds and NRS subjective pain scores at baseline, after one night of SD, and after one night of RS (**Figure 3**). We found that participants' nociceptive pain thresholds dropped significantly after one night of SD and that one night of RS reversed this hyperalgesia. The NRS scores increased significantly after one night of SD and recovered with one night of RS.

We examined nociceptive thresholds after SD in rats. In the evoked nociceptive tests, compared with the sham group, the SDR group showed significant reductions in both PWT and PWL at 6 days after SD. Our experiments showed a partial recovery of thermal nociceptive sensitization in rats after 2 days of RS and a trend toward the recovery of mechanical

TABLE 1 Participants' vital signs.

	Baseline (n = 20)	SD (n = 20)	RS (n = 20)	F	Overall significance (P-value)
Heart rate (times per minute)	82 (76 to 87)	81 (70 to 90)	82 (78 to 87)		0.939
SpO_2 (%)	100 (99 to 100)	100 (99 to 100)	99 (99 to 100)		0.454
Mean artery Pressure (mmHg)	93.6 ± 7.6	94.5 ± 7.9	93.1 ± 7.7	0.998	0.857

nociceptive sensitization without statistical significance. On the fourth day of RS, mechanical nociceptive sensitization and thermal nociceptive sensitization in the SDR group rats returned to baseline (Figure 4).

Biochemical measures

Plasma-derived biochemical measures before and after SD are shown in Figure 5. Relative to baseline (mean = 2.8, standard deviation = 1.0 nmol/mL), the MDA levels were significantly increased following one night of SD (mean = 5.0, standard deviation = 1.0 nmol/mL, $P \leq 0.0001$). The MDA levels partially recovered after RS (mean = 3.9, standard deviation = 1.0 nmol/mL), increasing from baseline ($P = 0.001$), and decreasing from one night of SD ($P = 0.001$). After SD, CAT (12.5 [8.0 to 21.3] U/mL) levels were also significantly increased relative to baseline (5.3 [3.1 to 9.5] U/mL, $P = 0.001$). CAT levels after RS (8.1 [5.5 to 10.9] U/mL) were almost restored to the baseline level ($P = 0.844$) and decreased significantly compared with SD ($P = 0.038$). On the contrary, SD resulted in reduced GSH (mean = 51.0, standard deviation = 10.3 μmol/L) levels that were reduced relative to baseline (mean = 78.4, standard deviation = 11.0 μmol/L, $P \leq 0.0001$). The level of GSH (mean = 53.9, standard deviation = 15.0 μmol/L) after sleep recovery increased slightly compared with SD, which was not statistically significant ($P = 0.470$), and decreased significantly compared with baseline ($P \leq 0.0001$). In parallel to this result, SOD levels were also lower after SD (mean = 115.2, standard deviation = 33.1 U/mL) compared with baseline (mean = 174.0, standard deviation = 22.6 U/mL, $P \leq 0.0001$). There was no significant recovery of the SOD level after RS compared to SD ($P = 0.095$). Compared with baseline, the SOD (mean = 130.4, standard deviation = 28.2 U/mL) levels decreased significantly after RS ($P < 0.0001$).

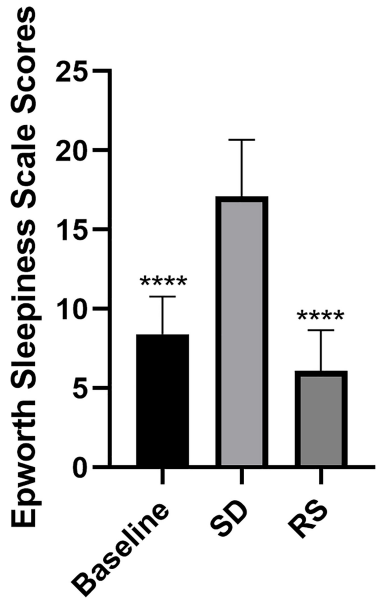

FIGURE 2
Epworth sleepiness scale scores. Subjects were scored on the Epworth sleepiness scale at three time points. Sleep deprivation significantly increased subjects' daytime sleepiness compared to baseline, and this was significantly reduced after recovery sleep. ****$P < 0.0001$ compared to SD.

Proteomics of medial prefrontal cortex in rats with sleep deprivation

We removed mPFC from the rats after SD for proteomic, and the following results were determined.

Medial prefrontal cortex changes in rats treated with sleep deprivation

In order to identify mPFC proteins' abundances in SD, we searched the raw data in LC-MS/MS databases and got a core set of 260 quantified proteins. Based on the differences in the protein ratios of 260 proteins between the different study groups, we identified 37 potentially differentially expressed proteins associated with SD. Of these 37 proteins, 24 proteins were increased in the SDR group compared to the sham group, while 13 proteins were decreased in the SDR group, and the expression of these proteins differed between experimental groups. Differentially expressed proteins are displayed in the volcano diagram in Figure 6.

Functional analysis of the differential proteins associated with sleep deprivation

We then compared differentially expressed proteins between the study groups through an enrichment analysis of gene ontology biological processes and identified key biological processes and potential pathways that may distinguish the SDR group from the sham group. The cellular processes represented

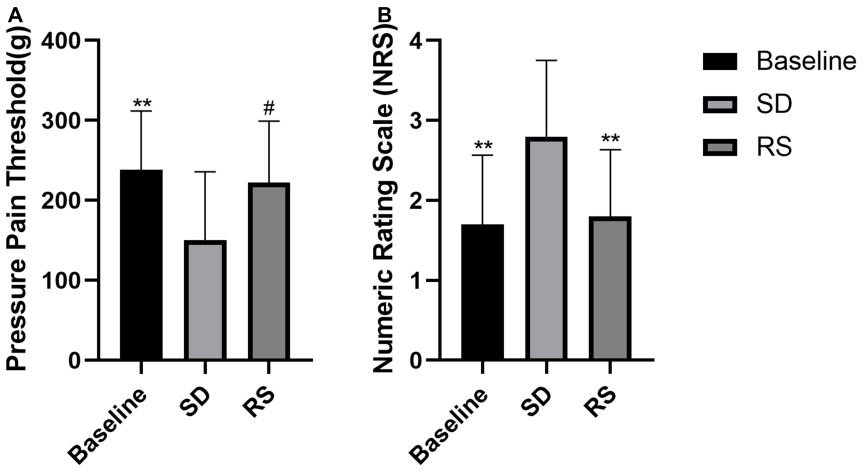

FIGURE 3
Pressure pain threshold **(A)** and NRS subjective pain scores **(B)**. Subjects' changes in pressure pain threshold and subjective NRS scores. Sleep deprivation (SD) significantly increased perceived pain compared to baseline, and this nociceptive hyperalgesia was significantly reduced after recovery sleep (RS). $^{\#}P < 0.05$ compared to SD. $^{**}P < 0.01$ compared to SD.

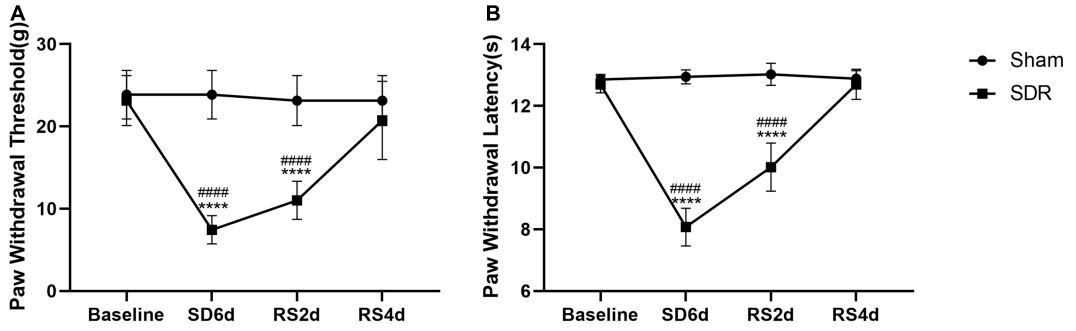

FIGURE 4
Paw withdrawal threshold **(A)** and paw withdrawal latency **(B)** in rats. Rats 1–8 in the Sham group and 1–8 in the SDR group. The PWT and PWL of rats decreased significantly after 6 days of SD, and the PWL recovered after 2 days of RS compared to 6 days of SD, and both PWT and PWL returned to baseline levels after 4 days of RS. $^{****}P < 0.0001$ compared to the sham group. $^{\#\#\#\#}P < 0.0001$ compared with baseline and RS4d in the SDR group.

by the mPFC proteome mainly include guanine transport, glial cell migration, collagen biosynthetic process, erythrocyte aggregation and regulation, post-synaptic signal transduction, and post-synapse to the nucleus signaling pathway. The enrichment analysis of GO cellular components (**Figure 7**) showed that these proteins were mainly localized in the dendritic spine, the neuron spine, the respiratory chain complex II, and the lipid droplet. These active factors participated in starch and sucrose metabolism, amino sugar and nucleotide sugar metabolism, and the biosynthesis of cofactors, as described in KEGG pathway mapping (**Figure 8**). GO enrichment analysis showed that tryptophan 5-monooxygenase activity induced changes in molecular function during SD. As a redox substrate, tryptophan 5-monooxygenase is an important enzyme in the synthesis of 5-hydroxytryptamine and is also involved in the synthesis of melatonin. Melatonin is secreted by the brain's pineal gland, and its secretion has a distinct circadian rhythm regulation and antioxidant effects (Zhang and Zhang, 2014).

Network analysis identifies sleep deprivation-related specific protein network in medial prefrontal cortex

To explore the relationship between differentially expressed proteins associated with SD, we performed a gene network analysis of differentially expressed proteins in mPFC to identify specific proteins associated with SD, as seen in **Figure 9**. We analyzed the significantly different proteins expressed in mPFC of rats in the SDR group and the sham group, in an attempt to explore their connection to biological processes or molecular functions. Among them, METTL7A was significantly downregulated in neuropathic pain rats (Gong et al., 2021) and showed a decreasing trend in our SD rats. Bi-allelic

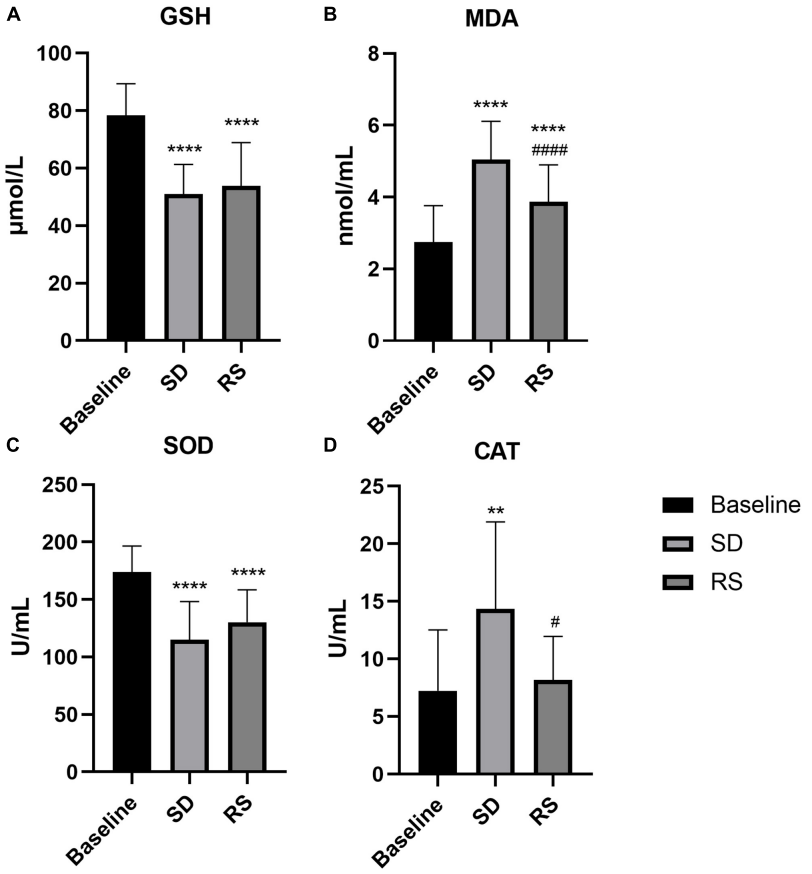

FIGURE 5
Plasma GSH **(A)**, MDA **(B)**, SOD **(C)**, and CAT **(D)** levels or activity measurements before and after SD and RS. $^{**}P < 0.01$ compared to Baseline, $^{****}P < 0.0001$ compared to Baseline, $^{\#}P < 0.05$ compared to SD, $^{\#\#\#\#}P < 0.0001$ compared to SD.

PGM2L1 mutations are associated with a neurodevelopmental disorder (Morava et al., 2021). Galectin-1 (ALGAS1) is highly expressed at the sites of infection and inflammation and plays a role in regulating cell differentiation, proliferation, and apoptosis (Méndez-Huergo et al., 2017). Furthermore, pro-inflammatory cytokines in ALGAS1$^{-/-}$ mice were significantly downregulated in the liver tissue (Baek et al., 2021), consistent with our finding that ALGAS1 is significantly upregulated in SD rats. MacroD1 modulates mitochondrial function and DNA damage (Agnew et al., 2018) and can further exacerbate the inflammatory response induced by lipopolysaccharide stimulation (Zang et al., 2018).

Discussion

Night shifts are very common among clinicians, and anesthesiologists inevitably work night shifts, and they often stay up late on duty in SD. Sleep plays a critical role in regulating cognitive performance and productivity. This is especially true for anesthesiologists and intensivists who often work in shifts (Ariès and Lamblin, 2020). Studies demonstrated that, in residents, acute SD impaired medical management of life-threatening situations occurring during high fidelity simulated anesthesia cases (Arzalier-Daret et al., 2018). Cognitive deficits emerge and accumulate to significant levels when sleep duration falls below 7 h per night, while fatigue also affects work performance and professional alertness (Saadat et al., 2017). Fatigue in anesthesiologists would have more serious implications that extend beyond individual health and affect patient management, safety, and the quality of healthcare. Saadat et al. (2016) previously reported a significant worsening of mood, the cognitive status, and total mood disturbance after night calls by anesthesiologists compared to normal working hours. While SD has many effects on physicians' health, this study evaluated the effects of SD on pain thresholds and the redox state of the organism in young male physicians. Studies showed that predictors of pain sensitivity differ by gender (Al'absi et al., 2022), that women experience greater anxiety than men when sleep deprived (Goldstein-Piekarski et al., 2018), and that women are more susceptible to pain in the clinic (Fillingim et al., 2009). Effects of total SD on descending pain

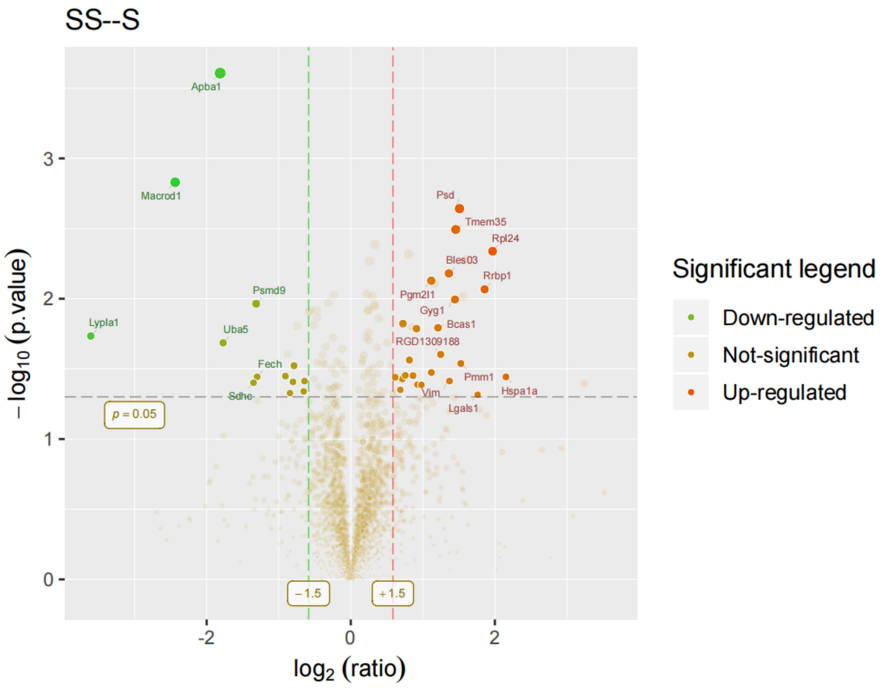

FIGURE 6
Volcano diagram: Rats 9–14 in the sham group and 9–13 in the SDR group. Differentially expressed proteins were displayed in the volcano diagram. *Y*-axis: -log10 (*p*-value); *X*-axis: log2 (ratio). The dots that lie beyond the two vertical boundaries and above the horizontal boundaries represent proteins that differ significantly. Clear spots in salient regions mean that these proteins do not meet the other conditions.

inhibition are sex-specific (Eichhorn et al., 2018). Considering the possible influence of gender on the experimental results and the fact that women's physical conditions are susceptible to menstrual cycles, we selected healthy male residents for the trial. Age was significantly associated with daily sleep duration and subjective sleepiness (Bonnefond et al., 2006), and a previous study demonstrated that somatosensory thresholds for non-injurious stimuli increase with age whereas pressure pain thresholds decrease (Lautenbacher et al., 2005). To reduce the effect of age on the trial results, we included physicians aged 18∼44 years.

In two country samples of community-dwelling older adults in Singapore and Japan, sleep deficiency increased the risk of any new pain onset and pain increased the risk of newly presenting sleep deficiency (Chen et al., 2019). A related clinical study showed that, in healthy adults with mild sleepiness, extended bedtime led to increased sleep duration and decreased drowsiness, resulting in reduced pain sensitivity (Roehrs et al., 2012). To prevent this variation from influencing the results of our experiment, we chose to measure pain thresholds and NRS pain scores at 8:00 a.m. each day. As previously described, we found that one night of SD can lead to significantly higher nociceptive hyperalgesia and NRS pain scores compared to baseline. This was similarly demonstrated in rat experiments, where nociceptive tests on rats SD for 6 days showed that both PWT and PWL were significantly lower in the SDR group compared to the sham group, and this reduction recovered after 4 days of RS. Our study demonstrated that SD leads to increased pain sensitivity in both healthy subjects and animals. Prostaglandin 2 (PGE2), a key mediator of inflammation and pain, has been shown to be a potential mediator in SD-induced changes in pain sensation, and the increase in spontaneous pain caused by total SD is significantly associated with an increase in PGE2 metabolites (Haack et al., 2009). Activation of inflammation-related pathways leads to the production of ROS and RNS, and the generated ROS can lead to the activation of pro-inflammatory cytokines such as IL-1β and TNF-α to induce inflammatory responses, thereby participating in the underlying pathogenic mechanisms of various diseases (Atrooz and Salim, 2020). In this study, it may be related to hyperalgesia in subjects and animals.

The current study showed that SD leads to alterations in the redox state of the body. A recent meta-analysis showed that sleep disturbance is associated with an increase in markers of systemic inflammation (Irwin et al., 2016). Systemic inflammation resulted in a lower pain threshold (de Goeij et al., 2013). It has been shown that SD leads to increased oxidative DNA damage and dying cells in rats and that 2 days of RS restores the balance between DNA damage and repair, leading to normal or below normal oxidative damage (Everson et al., 2014). Sleep is known to replenish redox metabolites in the body, and altered sleep patterns may limit

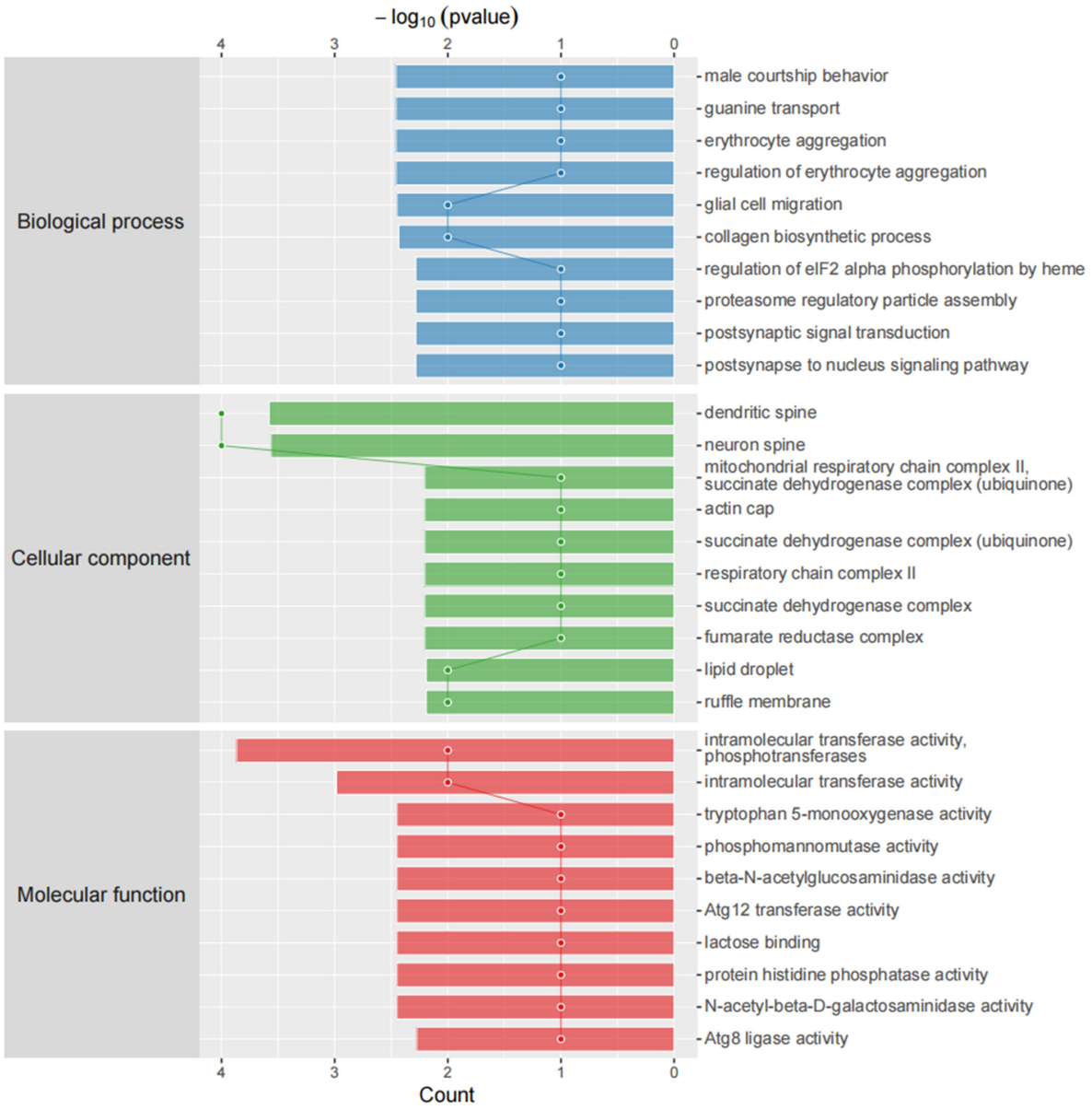

FIGURE 7
Gene ontology (GO) cellular components. Top axis is -log10 (*p*-values) and bottom axis is gene count. The ontology covers three domains: biological process, cellular component, and molecular function.

this ability. As expected, in the present study, we found that plasma antioxidant GSH levels and SOD activity decreased with increased oxidative damage, while CAT activity and the MDA levels increased with increased oxidative damage. Thus, we found that antioxidants and redox metabolites in the organism are altered under the influence of SD. The alteration caused by SD is important, especially because previous studies showed that this change is an important factor in neurological diseases (Durmer and Dinges, 2005; Goel et al., 2009; Lowe et al., 2017). It follows that we should not ignore the damage that SD can cause to our body.

The hyperalgesic effect of SD seems reversible by napping (Faraut et al., 2015) as well as by the effective treatment of sleep disorders (Khalid et al., 2011). Roehrs et al. (2012) showed that extended sleep reduces pain sensitivity. Low vigilance following SD might lead to higher pain sensitivity and prevent adequate pain coping, whereas the restoration of vigilance following RS might be accompanied by a normalization of pain perception (Stroemel-Scheder et al., 2020). Several research have shown that RS (i.e., improved quality or quantity of sleep) has the potential to restore normal nociceptive sensitivity after SD-induced nociceptive hypersensitivity (Roehrs et al., 2012;

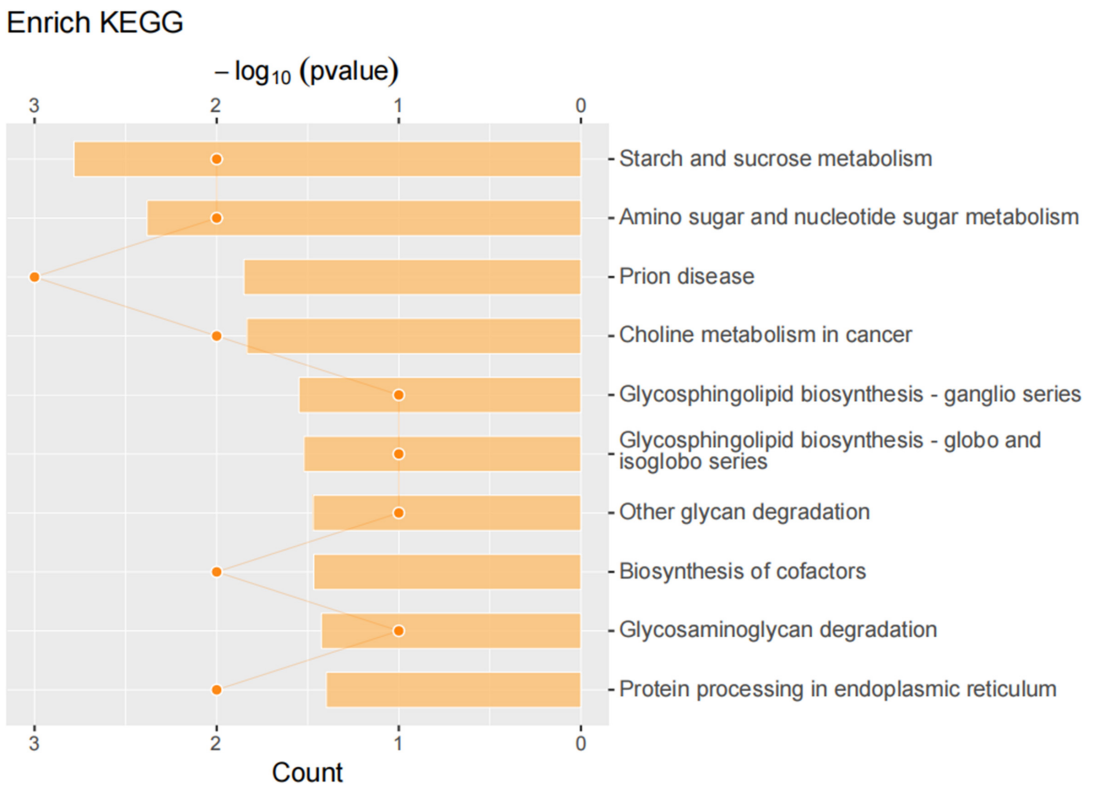

FIGURE 8
Kyoto Encyclopedia of Genes and Genomes (KEGG) pathway analysis of differentially expressed proteins. KEGG pathway annotation was performed on the selected differentially expressed proteins to analyze and determine the most important metabolic and signal transduction pathways involved in the differentially expressed proteins.

Karmann et al., 2014; Vitiello et al., 2014; Smith et al., 2015). Consistent with the above, our study demonstrated that one night of restorative sleep not only reduces nociceptive hyperalgesia induced by SD but also substantially restores subjects' subjective pain NRS scores to their pre-SD levels.

Studies related to the effect of RS on altered nociception after SD have been reported, but little has been mentioned about whether RS can improve the altered oxidative stress state of an organization induced by SD. We found that, after one night of RS, MDA levels and CAT vitality could be partially restored, with MDA levels still elevated compared to baseline but significantly lower than after one night of SD and CAT vitality largely restored to baseline levels. Unfortunately, GSH levels and SOD activity were not improved after RS. This shows that even just one night of SD can have a profound effect on redox metabolites. Chronic sleep restriction or acute total SD results in persistent and distinct biological, physiological, and/or neurological changes that are not significantly reversed with chronic, long-duration RS (Yamazaki et al., 2021). A recent study showed that induced sleep deficiency causes the deterioration of body functions and that 1 week of recovery is not enough for full recovery (Ochab et al., 2021). Thus, one night of RS can only partially ameliorate the oxidative damage caused by SD.

Numerous studies were conducted to elucidate the mechanisms of neuropathic pain, and oxidative stress is considered to be one of the important causative factors in damaging peripheral sensory neurons (Areti et al., 2014). Shim et al. (2019) found that the chemotherapeutic drug-induced mechanical hypersensitivity was fractionally mediated by sustained oxidative stress. Indeed, antioxidants can reduce chemotherapy-induced neuropathic pain that has developed in animal models, suggesting that reducing oxidative stress is a promising pain therapy (Kim et al., 2010, 2016; Fidanboylu et al., 2011). We found that SD can cause the body to suffer from oxidative stress and lead to mechanical hypersensitivity. Many studies showed that oxidative stress can cause pain, but whether this mechanical hypersensitivity response is directly mediated by oxidative stress needs further experimental verification. One night of RS can significantly improve mechanical hypersensitivity and only slightly improve oxidative stress damage to the body. It is known that sleep can replenish antioxidants in the body and thus improve the oxidative stress status of the organism. In the present study, the oxidative stress status of the body did not improve well after RS, which may

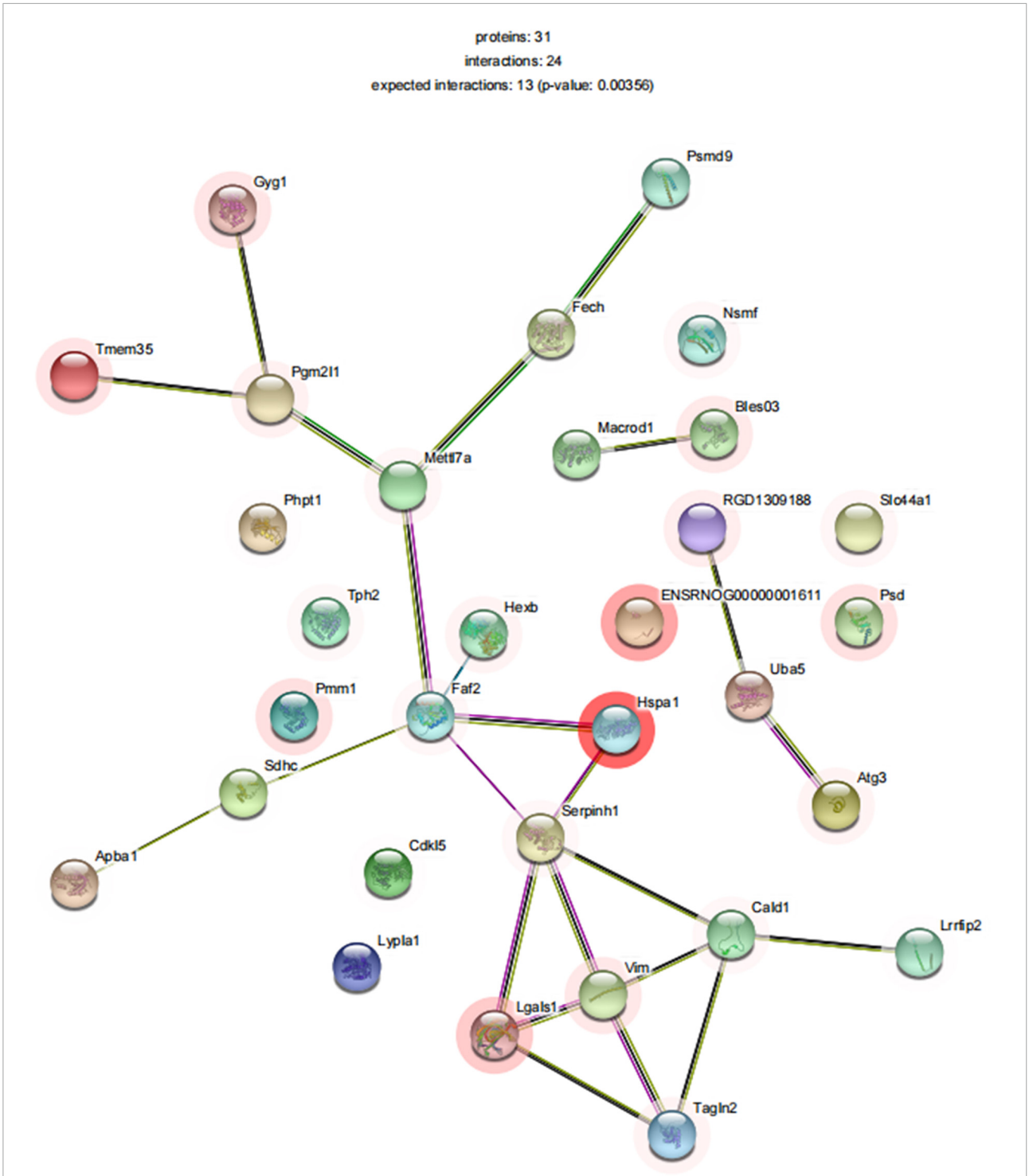

FIGURE 9
STRINGdb protein–protein network enrichment analysis. The protein–protein interaction network of significant proteins is shown. STRING database integrates various information from curated databases that were experimentally determined; gene neighborhood, gene fusions, and gene co-occurrence; text mining, co-expression, and protein homology.

be due to insufficient sleep time or the fact that one night of RS could not compensate for the lack of sleep caused by one night of SD.

We performed proteomic assays in mPFC of sham and SDR rats; overall, we quantified 3,790 proteins using the LFQ proteomics approach, with 2,956 quantifiable proteins. In total,

37 of these proteins were significantly differentially expressed, of which 24 were upregulated and 13 were downregulated during SD. These differentially expressed proteins were mainly involved in biological processes such as starch and sucrose metabolism, amino and nucleotide sugar metabolism, and protein processing in the endoplasmic reticulum. For example, sleep fragmentation induces endoplasmic reticulum stress in the hypothalamus of mice (Hakim et al., 2015), and circadian rhythm dysregulation induced by chronic night work promotes endoplasmic reticulum stress activation, which directly affects the human metabolism (Ferraz-Bannitz et al., 2021).

We acknowledge several study limitations. We did not use electroencephalography (EEG) to monitor our subjects' sleep conditions during a whole night of SD, so we cannot be sure that they did not experience transient sleep during this time period. However, our subjects were continuously monitored and clinically engaged throughout the night of SD, so we are confident that the subjects did not experience transient sleep during SD. High-intensity and stressful night shift work might be different from simple SD, but we did not study it. Since anesthesiologists work during night shifts, we were unable to perform simple SD on the participating anesthesiologists, which was a limitation of this study. Our study only demonstrated that SD can cause nociceptive hypersensitivity and altered oxidative stress status in the body. Future studies are encouraged to investigate if this nociceptive hypersensitivity is mediated by oxidative stress in patients with sleep-deprived chronic pain.

In conclusion, this study showed that one night of SD can cause nociceptive hypersensitivity and increase oxidative stress damage in the body. One night of RS restored nociceptive hypersensitivity and improved the SD-induced increase in NRS pain scores, but it only slightly improved the markers of oxidative stress after SD. Whether SD-induced nociceptive hypersensitivity is mediated by oxidative stress remains uncertain and further studies are warranted.

Data availability statement

The original contributions presented in this study are publicly available. This data can be found here: http://www.medresman.org.cn/pub/cn/proj/projectshshow.aspx?proj=4386.

Ethics statement

The studies involving human participants were reviewed and approved by The First Affiliated Hospital of Zhengzhou University Research Ethics Committee; The First Affiliated Hospital of Zhengzhou University. The patients/participants provided their written informed consent to participate in this study. The animal study was reviewed and approved by The First Affiliated Hospital of Zhengzhou University Research Ethics Committee; The First Affiliated Hospital of Zhengzhou University.

Author contributions

SC and JYu helped with conceptualization, methodology, analysis, preparation of the manuscript, and review and editing of the manuscript. YX helped with the interpretation of data, methodology, resources, and analysis and was responsible for project administration. YL and XF helped with research design, supervision, interpretation of data, preparation of the manuscript, and approval of the final manuscript. FX helped with data collection and research supervision. YM helped with the conceptualization, methodology, and review and editing of the manuscript. NX and ZW helped with research supervision and review editing. JW helped with the interpretation of data, preparation of the manuscript, and review editing. JYa helped with research design, supervision, and review editing. All authors contributed to the article and approved the submitted version.

Funding

This work was supported by the Joint Construction Project of Henan Province Medical Science & Technology Research Plan (SBGJ202002066), the National Natural Science Foundation of China (Grant no. 82071243), the Tianjin Natural Science Foundation (20JCYBJC00460), and the Natural Science Foundation of Henan Province (212300410239).

Conflict of interest

The authors declare that the research was conducted in the absence of any commercial or financial relationships that could be construed as a potential conflict of interest.

Publisher's note

References

Agnew, T., Munnur, D., Crawford, K., Palazzo, L., Mikoè, A., Ahel, I., et al. (2018). MacroD1 is a promiscuous ADP-Ribosyl hydrolase localized to mitochondria. *Front. Microbiol.* 9:20. doi: 10.3389/fmicb.2018.0002

Aili, K., Nyman, T., Svartengren, M., and Hillert, L. (2015). Sleep as a predictive factor for the onset and resolution of multi-site pain: a 5-year prospective study. *Eur. J. Pain* 19, 341–349. doi: 10.1002/ejp.552

Al'absi, M., Petersen, K. L., and Wittmers, L. E. (2022). Adrenocortical and hemodynamic predictors of pain perception in men and women. *Pain* 96, 197–204.

Areti, A., Yerra, V. G., Naidu, V., and Kumar, A. (2014). Oxidative stress and nerve damage: role in chemotherapy induced peripheral neuropathy. *Redox Biol.* 2, 289–295.

Ariès, P., and Lamblin, A. (2020). Insufficient sleep among Anaesthesiologists and Intensive Care Physicians: It's time to wake up!. *Anaesth. Crit. Care Pain Med.* 39, 749–751. doi: 10.1016/j.accpm.2020.09.003

Arzalier-Daret, S., Buléon, C., Bocca, M. L., Denise, P., Gérard, J. L., and Hanouz, J. L. (2018). Effect of sleep deprivation after a night shift duty on simulated crisis management by residents in anaesthesia. A randomised crossover study. *Anaesth. Crit. Care Pain Med.* 37, 161–166. doi: 10.1016/j.accpm.2017.05.010

Atrooz, F., and Salim, S. (2020). Sleep deprivation, oxidative stress and inflammation. *Adv. Protein Chem. Struct. Biol.* 119, 309–336.

Azevedo, E., Manzano, G. M., Silva, A., Martins, R., Andersen, M. L., and Tufik, S. (2011). The effects of total and REM sleep deprivation on laser-evoked potential threshold and pain perception. *Pain* 152, 2052–2058. doi: 10.1016/j.pain.2011.04.032

Baek, J., Kim, D., Lee, J., and Kim, S., Chun, K. (2021). Galectin-1 accelerates high-fat diet-induced obesity by activation of peroxisome proliferator-activated receptor gamma (PPARγ) in mice. *Cell Death Dis.* 12:66. doi: 10.1038/s41419-020-03367-z

Besedovsky, L., Lange, T., and Haack, M. (2019). The sleep-immune crosstalk in health and disease. *Physiol. Rev.* 99, 1325–1380. doi: 10.1152/physrev.00010.2018

Bonnefond, A., Härmä, M., Hakola, T., Sallinen, M., Kandolin, I., and Virkkala, J. (2006). Interaction of age with shift-related sleep-wakefulness, sleepiness, performance, and social life. *Exp. Aging Res.* 32, 185–208. doi: 10.1080/03610730600553968

Chen, T. Y., Lee, S., Schade, M. M., Saito, Y., Chan, A., and Buxton, O. M. (2019). Longitudinal relationship between sleep deficiency and pain symptoms among community-dwelling older adults in Japan and Singapore. *Sleep* 42:zsy219. doi: 10.1093/sleep/zsy219

Cohen, S. P., Vase, L., and Hooten, W. M. (2021). Chronic pain: An update on burden, best practices, and new advances. *Lancet (London, England)*, 397, 2082–2097.

de Goeij, M., van Eijk, L. T., Vanelderen, P., Wilder-Smith, O. H., Vissers, K. C., van der Hoeven, J. G., et al. (2013). Systemic inflammation decreases pain threshold in humans in vivo. *PLoS One* 8:e84159. doi: 10.1371/journal.pone.0084159

Durmer, J., and Dinges, D. F. (2005). Neurocognitive consequences of sleep deprivation. *Semin. Neurol.* 25, 117–129.

Eichhorn, N., Treede, R. D., and Schuh-Hofer, S. (2018). The role of sex in sleep deprivation related changes of nociception and conditioned pain modulation. *Neuroscience* 387, 191–200. doi: 10.1016/j.neuroscience.2017.09.044

Elvsåshagen, T., Zak, N., Norbom, L., Pedersen, P., Quraishi, S., Bjørnerud, A., et al. (2017). Evidence for cortical structural plasticity in humans after a day of waking and sleep deprivation. *Neuroimage* 156, 214–223. doi: 10.1016/j.neuroimage.2017.05.027

Everson, C. A., Henchen, C. J., Szabo, A., and Hogg, N. (2014). Cell injury and repair resulting from sleep loss and sleep recovery in laboratory rats. *Sleep* 37, 1929–1940. doi: 10.5665/sleep.4244

Faraut, B., Léger, D., Medkour, T., Dubois, A., Bayon, V., Chennaoui, M., et al. (2015). Napping reverses increased pain sensitivity due to sleep restriction. *PLoS One* 10:e0117425. doi: 10.1371/journal.pone.0117425

Feng, P., Becker, B., Feng, T., and Zheng, Y. (2018). Alter spontaneous activity in amygdala and vmPFC during fear consolidation following 24?h sleep deprivation. *Neuroimage* 172, 461–469. doi: 10.1016/j.neuroimage.2018.01.057

Ferraz-Bannitz, R., Beraldo, R., Coelho, P., Moreira, A., Castro, M., and Foss-Freitas, M. (2021). Circadian misalignment induced by chronic night shift work promotes endoplasmic reticulum stress activation impacting directly on human metabolism. *Biology* 10:197. doi: 10.3390/biology10030197

Fidanboylu, M., Griffiths, L. A., and Flatters, S. J. (2011). Global inhibition of reactive oxygen species (ROS) inhibits paclitaxel-induced painful peripheral neuropathy. *PLoS One* 6:e25212. doi: 10.1371/journal.pone.0025212

Fillingim, R. B., King, C. D., Ribeiro-Dasilva, M. C., Rahim-Williams, B., Riley, J. L. (2009). Sex, gender, and pain: a review of recent clinical and experimental findings. *J. Pain* 10, 447–485. doi: 10.1016/j.jpain.2008.12.001

Frau, R., Bini, V., Soggiu, A., Scheggi, S., Pardu, A., Fanni, S., et al. (2017). The neurosteroidogenic enzyme 5α-reductase mediates psychotic-like complications of sleep deprivation. *Neuropsychopharmacology* 42, 2196–2205. doi: 10.1038/npp.2017.13

Gao, T., Wang, Z., Dong, Y., Cao, J., Lin, R., Wang, X., et al. (2019). Role of melatonin in sleep deprivation-induced intestinal barrier dysfunction in mice. *J. Pineal Res.* 67:e12574. doi: 10.1111/jpi.12574

Goel, N., Rao, H., Durmer, J., and Dinges, D. (2009). Neurocognitive consequences of sleep deprivation. *Semin. Neurol.* 29, 320–339.

Goldstein-Piekarski, A. N., Greer, S. M., Saletin, J. M., Harvey, A. G., Williams, L. M., and Walker, M. P. (2018). Sex, sleep deprivation, and the anxious brain. *J. Cogn. Neurosci.* 30, 565–578.

Gong, D., Yu, X., Jiang, M., and Li, C., Wang, Z. J. (2021). Differential proteomic analysis of the hippocampus in rats with neuropathic pain to investigate the use of electroacupuncture in relieving mechanical allodynia and cognitive decline. *Neural Plast.* 2021:5597163. doi: 10.1155/2021/5597163

Guo, X., Keenan, B., Sarantopoulou, D., Lim, D., Lian, J., and Grant, G., Pack, A. J. (2019). Age attenuates the transcriptional changes that occur with sleep in the medial prefrontal cortex. *Aging Cell* 18:e13021. doi: 10.1111/acel.13021

Haack, M., Lee, E., Cohen, D. A., Mullington, J. M. (2009). Activation of the prostaglandin system in response to sleep loss in healthy humans: potential mediator of increased spontaneous pain. *Pain* 145, 136–141. doi: 10.1016/j.pain.2009.05.029

Hakim, F., Wang, Y., Carreras, A., Hirotsu, C., Zhang, J., Peris, E., et al. (2015). Chronic sleep fragmentation during the sleep period induces hypothalamic endoplasmic reticulum stress and PTP1b-mediated leptin resistance in male mice. *Sleep* 38, 31–40. doi: 10.5665/sleep.4320

Irwin, M. R., Olmstead, R., and Carroll, J. E. (2016). Sleep disturbance, sleep duration, and inflammation: a systematic review and meta-analysis of cohort studies and experimental sleep deprivation. *Biol. Psychiatry* 80, 40–52. doi: 10.1016/j.biopsych.2015.05.014

Jefferson, T., Kelly, C. J., and Martina, M. (2021). Differential rearrangement of excitatory inputs to the medial prefrontal cortex in chronic pain models. *Front. Neural Circ.* 15:791043. doi: 10.3389/fncir.2021.791043

Kanazawa, L., Vecchia, D., Wendler, E., Hocayen, P., Dos Reis Lívero, F., Stipp, M., et al. (2016). Quercetin reduces manic-like behavior and brain oxidative stress induced by paradoxical sleep deprivation in mice. *Free Radic. Biol. Med.* 99, 79–86. doi: 10.1016/j.freeradbiomed.2016.07.027

Karmann, A. J., Kundermann, B., and Lautenbacher, S. (2014). [Sleep deprivation and pain: a review of the newest literature]. *Schmerz* 28, 141–146.

Khalid, I., Roehrs, T. A., Hudgel, D. W., and Roth, T. (2011). Continuous positive airway pressure in severe obstructive sleep apnea reduces pain sensitivity. *Sleep* 34, 1687–1691.

Kim, H. K., Hwang, S. H., and Abdi, S. (2016). Tempol ameliorates and prevents mechanical hyperalgesia in a rat model of chemotherapy-induced neuropathic pain. *Front. Pharmacol.* 7:532. doi: 10.3389/fphar.2016.00532

Kim, H. K., Zhang, Y. P., Gwak, Y. S., and Abdi, S. (2010). Phenyl N-tert-butylnitrone, a free radical scavenger, reduces mechanical allodynia in chemotherapy-induced neuropathic pain in rats. *Anesthesiology* 112, 432–439. doi: 10.1097/ALN.0b013e3181ca31bd

Lautenbacher, S., Kundermann, B., and Krieg, J. C. (2006). Sleep deprivation and pain perception. *Sleep Med. Rev.* 10, 357–369.

Lautenbacher, S., Kunz, M., Strate, P., Nielsen, J., and Arendt-Nielsen, L. (2005). Age effects on pain thresholds, temporal summation and spatial summation of heat and pressure pain. *Pain* 115, 410–418. doi: 10.1016/j.pain.2005.03.025

Liu, H., Huang, X., Li, Y., Xi, K., Han, Y., Mao, H., et al. (2022). TNF signaling pathway-mediated microglial activation in the PFC underlies acute paradoxical sleep deprivation-induced anxiety-like behaviors in mice. *Brain Behav. Immun.* 100, 254–266. doi: 10.1016/j.bbi.2021.12.006

Lowe, C., Safati, A., and Hall, P. (2017). The neurocognitive consequences of sleep restriction: A meta-analytic review. *Neurosci. Biobehav. Rev.* 80, 586–604. doi: 10.1016/j.neubiorev.2017.07.010

McBeth, J., Wilkie, R., Bedson, J., Chew-Graham, C., and Lacey, R. J. (2015). Sleep disturbance and chronic widespread pain. *Curr. Rheumatol. Rep.* 17:469.

Méndez-Huergo, S., Blidner, A., and Rabinovich, G. (2017). Galectins: emerging regulatory checkpoints linking tumor immunity and angiogenesis. *Curr. Opin. Immunol.* 45, 8–15. doi: 10.1016/j.coi.2016.12.003

Morava, E., Schatz, U., Torring, P., Abbott, M., Baumann, M., Brasch-Andersen, C., et al. (2021). Impaired glucose-1,6-biphosphate production due to bi-allelic PGM2L1 mutations is associated with a neurodevelopmental disorder. *Am. J. Hum. Genet.* 108, 1151–1160. doi: 10.1016/j.ajhg.2021.04.017

Morris, G., Stubbs, B., Köhler, C. A., Walder, K., Slyepchenko, A., Berk, M., et al. (2018). The putative role of oxidative stress and inflammation in the pathophysiology of sleep dysfunction across neuropsychiatric disorders: Focus on chronic fatigue syndrome, bipolar disorder and multiple sclerosis. *Sleep Med. Rev.* 41, 255–265. doi: 10.1016/j.smrv.2018.03.007

Mullin, B., Phillips, M., Siegle, G., Buysse, D., and Forbes, E., Franzen, P. J. (2013). Sleep deprivation amplifies striatal activation to monetary reward. *Psychol. Med.* 43, 2215–2225.

Ochab, J., Szwed, J., Oleś, K., Bereś, A., Chialvo, D., Domagalik, A., et al. (2021). Observing changes in human functioning during induced sleep deficiency and recovery periods. *PLoS One* 16:e0255771. doi: 10.1371/journal.pone.0255771

Roehrs, T. A., Harris, E., Randall, S., and Roth, T. (2012). Pain sensitivity and recovery from mild chronic sleep loss. *Sleep* 35, 1667–1672. doi: 10.5665/sleep.2240

Roehrs, T., Hyde, M., Blaisdell, B., Greenwald, M., and Roth, T. (2006). Sleep loss and REM sleep loss are hyperalgesic. *Sleep* 29, 145–151. doi: 10.1093/sleep/29.2.145

Saadat, H., Bissonnette, B., Tumin, D., Raman, V., Rice, J., Barry, N., et al. (2017). Effects of partial sleep deprivation on reaction time in anesthesiologists. *Paediatr. Anaesth.* 27, 358–362. doi: 10.1111/pan.13035

Saadat, H., Bissonnette, B., Tumin, D., Thung, A., Rice, J., Barry, N., et al. (2016). Time to talk about work-hour impact on anesthesiologists: The effects of sleep deprivation on Profile of Mood States and cognitive tasks. *Paediatr. Anaesth.* 26, 66–71. doi: 10.1111/pan.12809

Shim, H. S., Bae, C., Wang, J., Lee, K. H., Hankerd, K. M., Kim, H. K., et al. (2019). Peripheral and central oxidative stress in chemotherapy-induced neuropathic pain. *Mol. Pain* 15:17448069198 40098.

Simpson, N. S., Scott-Sutherland, J., Gautam, S., Sethna, N., and Haack, M. (2018). Chronic exposure to insufficient sleep alters processes of pain habituation and sensitization. *Pain* 159, 33–40. doi: 10.1097/j.pain.0000000000001053

Sivertsen, B., Lallukka, T., Petrie, K. J., Steingrímsdóttir, ÓA., Stubhaug, A., and Nielsen, C. S. (2015). Sleep and pain sensitivity in adults. *Pain* 156, 1433–1439.

Smith, M. T., Finan, P. H., Buenaver, L. F., Robinson, M., Haque, U., Quain, A., et al. (2015). Cognitive-behavioral therapy for insomnia in knee osteoarthritis: a randomized, double-blind, active placebo-controlled clinical trial. *Arthritis Rheumatol.* 67, 1221–1233. doi: 10.1002/art.39048

Staffe, A. T., Bech, M. W., Clemmensen, S. L. K., Nielsen, H. T., Larsen, D. B., and Petersen, K. K. (2019). Total sleep deprivation increases pain sensitivity, impairs conditioned pain modulation and facilitates temporal summation of pain in healthy participants. *PLoS One* 14:e0225849. doi: 10.1371/journal.pone.0225849

Stroemel-Scheder, C., Kundermann, B., and Lautenbacher, S. (2020). The effects of recovery sleep on pain perception: A systematic review. *Neurosci. Biobehav. Rev.* 113, 408–425. doi: 10.1016/j.neubiorev.2020.03.028

Tucker, P., and Byrne, A. (2014). The tiring anaesthetist. *Anaesthesia* 69, 6–9.

Vitiello, M. V., McCurry, S. M., Shortreed, S. M., Baker, L. D., Rybarczyk, B. D., Keefe, F. J., et al. (2014). Short-term improvement in insomnia symptoms predicts long-term improvements in sleep, pain, and fatigue in older adults with comorbid osteoarthritis and insomnia. *Pain* 155, 1547–1554. doi: 10.1016/j.pain.2014.04.032

Wilking, M., Ndiaye, M., Mukhtar, H., and Ahmad, N. (2013). Circadian rhythm connections to oxidative stress: implications for human health. *Antioxidants Redox Signal.* 19, 192–208.

Yamazaki, E., Antler, C., Lasek, C., and Goel, N. (2021). Residual, differential neurobehavioral deficits linger after multiple recovery nights following chronic sleep restriction or acute total sleep deprivation. *Sleep* 44:zsaa224.

Zang, L., Hong, Q., Yang, G., Gu, W., Wang, A., Dou, J., et al. (2018). MACROD1/LRP16 Enhances LPS-stimulated inflammatory responses by Up-regulating a Rac1-dependent pathway in adipocytes. *Cell Physiol. Biochem.* 51, 2591–2603. doi: 10.1159/000495931

Zhang, H. M., and Zhang, Y. (2014). Melatonin: a well-documented antioxidant with conditional pro-oxidant actions. *J. Pineal. Res.* 57, 131–146. doi: 10.1111/jpi.12162

frontiers | Frontiers in Molecular Neuroscience

TYPE Original Research
PUBLISHED 29 August 2022
DOI 10.3389/fnmol.2022.974007

OPEN ACCESS

EDITED BY
Xin Zhang,
Duke University, United States

REVIEWED BY
Yiling Qian,
Wuxi People's Hospital Affiliated to Nanjing Medical University, China
Seungtae Kim,
Pusan National University, South Korea
Qian Bai,
Second Affiliated Hospital of Zhengzhou University, China

*CORRESPONDENCE
Lize Xiong
mzkxlz@126.com
Xiao-Fei Gao
drgaoxiaofei@163.com

†These authors have contributed equally to this work

SPECIALTY SECTION
This article was submitted to Pain Mechanisms and Modulators, a section of the journal Frontiers in Molecular Neuroscience

RECEIVED 20 June 2022
ACCEPTED 26 July 2022
PUBLISHED 29 August 2022

CITATION
Li W, Liu J, Chen A, Dai D, Zhao T, Liu Q, Song J, Xiong L and Gao X-F (2022) Shared nociceptive dorsal root ganglion neurons participating in acupoint sensitization. *Front. Mol. Neurosci.* 15:974007. doi: 10.3389/fnmol.2022.974007

Shared nociceptive dorsal root ganglion neurons participating in acupoint sensitization

Wanrong Li[1,2,3,4†], Jia Liu[5†], Aiwen Chen[1,2,3,4], Danqing Dai[1,2,3,4], Tiantian Zhao[1,2,3,4], Qiong Liu[1,2,3,4], Jianren Song[1], Lize Xiong[1,2,3,4*] and Xiao-Fei Gao[1,2,3,4*]

[1]Translational Research Institute of Brain and Brain-Like Intelligence, Shanghai Fourth People's Hospital, School of Medicine, Tongji University, Shanghai, China, [2]Clinical Research Center for Anesthesiology and Perioperative Medicine, Tongji University, Shanghai, China, [3]Department of Anesthesiology and Perioperative Medicine, Shanghai Fourth People's Hospital, School of Medicine, Tongji University, Shanghai, China, [4]Shanghai Key Laboratory of Anesthesiology and Brain Functional Modulation, Shanghai, China, [5]Faculty of Anesthesiology, Changhai Hospital, Naval Medical University, Shanghai, China

When the body is under pathological stress (injury or disease), the status of associated acupoints changes, including decreased pain threshold. Such changes in acupoint from a "silent" to an "active" state are considered "acupoint sensitization," which has become an important indicator of acupoint selection. However, the mechanism of acupoint sensitization remains unclear. In this study, by retrograde tracing, morphological, chemogenetic, and behavioral methods, we found there are some dorsal root ganglion (DRG) neurons innervating the ST36 acupoint and ipsilateral hind paw (IHP) plantar simultaneously. Inhibition of these shared neurons induced analgesia in the complete Freund's adjuvant (CFA) pain model and obstruction of nociceptive sensation in normal mice, and elevated the mechanical pain threshold (MPT) of ST36 acupoint in the CFA model. Excitation of shared neurons induced pain and declined the MPT of ST36 acupoint. Furthermore, most of the shared DRG neurons express TRPV1, a marker of nociceptive neurons. These results indicate that the shared nociceptive DRG neurons participate in ST36 acupoint sensitization in CFA-induced chronic pain. This raised a neural mechanism of acupoint sensitization at the level of primary sensory transmission.

KEYWORDS

pain, dorsal root ganglion, acupoint sensitization, ST36 acupoint, nociceptive neuron, acupuncture

Introduction

Acupuncture and moxibustion are crucial components of traditional Chinese medicine (TCM). By applying physical stimulations, such as mechanical (acupuncture, pressing, etc.), thermal (moxibustion), or electrical (electroacupuncture, transcutaneous electrical nerve stimulation, etc.) stimuli, to certain specific points (acupoints) on the body surface, the relief of symptoms or treatment of diseases can be achieved. For

example, a meta-analysis indicated that acupuncture had a beneficial effect on knee osteoarthritis in reducing pain and improved patient function activities (Tian et al., 2022). In the treatment of diarrhea-predominant irritable bowel syndrome, moxibustion had a more positive influence on the symptoms as compared to western medicines, TCM prescription, or acupuncture (Dai et al., 2022). In terms of improving immune function, studies have found that acupuncture significantly increased the numbers of white blood cells in patients with breast cancer who were undergoing ameliorating leukopenia during chemotherapy (Shih et al., 2021). At the same time, in the treatment of different diseases, some acupoints are often stimulated to receive better curative effects than others, so these acupoints are more favored. Acupoints such as ST36 (Zusanli) and EX-LE5 (Xiyan) were usually used in the treatments of knee osteoarthritis (Ma et al., 2018; Tong et al., 2021; Tian et al., 2022; Wei et al., 2022). To relieve diarrhea-predominant irritable bowel syndrome, ST36 and ST37 (Shangjuxu) were chosen with the highest frequency during the moxibustion treatments (Wang et al., 2018; Bao et al., 2019; Dai et al., 2022). Acupoints like ST36, SP6 (Sanyinjiao), BL23 (Shenyu), etc. were frequently used to improve immune function (Shih et al., 2018, 2021; Li et al., 2021; Oh and Kim, 2021; Ramires et al., 2021; Zhu et al., 2022). Therefore, to obtain a good therapeutic effect in acupuncture or moxibustion treatment, the selection of appropriate acupoints plays a key role.

It has been reported that when the body is under pathological stress (injury or disease), the status of associated acupoints changes, including sensation threshold, receptive field, biophysical properties, and morphology (Ngai et al., 2011; Wong, 2014; He et al., 2015; Zhu, 2015; Jung et al., 2017; Qi et al., 2017; Fan et al., 2018; Tan et al., 2019; Ma, 2021). In particular, acupoints undergo sensory mutations that increase sensitivity to various stimuli (similar to "allodynia") (Zhu, 2019). Such changes in acupoint from a "silent" to an "active" state during pathological processes are considered "acupoint sensitization" (Tan et al., 2019). Selected sensitized acupoints for acupuncture treatment are in line with the account of "taking the tender point as acupoint" in *The Yellow Emperor's Classics of Internal Medicine (Huang Di Nei Jing)*. For example, a recent trial study showed that acupressure at sensitized acupoints effectively reduced the frequency of stable angina pectoris episodes (Huang et al., 2021). Acupoint sensitization has become an important indicator of acupoint selection. However, the mechanism of acupoint sensitization remains unclear.

The neural system plays important role in the therapeutic effect of acupoints (Lee et al., 2020; Liu et al., 2020, 2021; Song et al., 2021; Li et al., 2022). Pain and heat sensitization is an important manifestation of acupoint sensitization, which also indicates the criticality of the sensory nervous system. The cell bodies of the sensory nerves innervating the acupoints gather in the dorsal root ganglia (DRG). In our previous study, we found that most DRG neurons innervating ST36 acupoint are middle-sized neurons with a single spike firing pattern, which suggests that proprioceptive neurons have a greater possibility than small-size nociceptive neurons to mediate the acupuncture signals (Li et al., 2022). However, small-diameter neurons are generally considered to mediate pain, itch, and heat sensations (Gao X. F. et al., 2015; Li et al., 2016; Zhang Z. J. et al., 2018; Dong et al., 2020). Therefore, it still needs to be elucidated which type of DRG neurons participate in acupoint sensitization.

In this study, we employed morphological, chemogenetic, and behavioral methods and explored the anatomical distribution and functional types of DRG neurons that mediate acupoint sensitization. We found that there were some DRG neurons innervating ST36 acupoint and ipsilateral hind paw (IHP) plantar simultaneously. Excitation of these shared neurons induced pain in normal mice, while inhibition of them elevated the mechanical pain threshold (MPT) of ST36 acupoint in the complete Freund's adjuvant (CFA) model mice. TRPV1 channels, always expressed by nociceptive neurons, were also expressed by most of these shared neurons. These results indicate that the shared DRG neurons, most of which are nociceptive neurons, explain the neural mechanism of acupoint sensitization at the level of primary sensory transmission.

Materials and methods

Animals

Specific pathogen-free (SPF) grade C57BL/6J male mice (4–8 weeks old) were purchased from the Shanghai Tongji Biotechnology Co., Ltd. (Shanghai, China). All mice were kept in a room with controlled temperature (25 ± 1°C) and humidity (55 ± 5%), and 12 h (8:00 a.m. to 8:00 p.m.) light–dark cycle with free access to water and rodent chow. All mice were group-housed (4–6 per cage) to avoid social isolation stress. All experimental protocols were approved by the Ethics Committee of the Laboratory Animal Center of Tongji University (Approval Number: TJBH05621101) and performed following the Guide for the Care and Use of Laboratory Animals of Tongji University (Shanghai, China) and the International Guide for the Care and Use of Laboratory Animals.

Retrograde tracer injections

Retrograde tracer in this study included Fluoro-Gold (FG, Fluorochrome Inc., Englewood, CO, United States) and the lipophilic tracer, 1′-dioctadecyl-3,3,3′,3′-tetramethylindocarbocyanine perchlorate (DiI, D282; Invitrogen, Thermo Fisher Scientific, Waltham, MA, United States) (Chang et al., 2016). FG was dissolved in 0.9% saline to yield a 4% concentration (Szawka et al., 2013; Pattwell et al., 2016). DiI was dissolved in dimethyl sulfoxide

(DMSO, D2650; Sigma-Aldrich, St. Louis, MO, United States) as a stock solution, and freshly prepared in 0.9% saline.

During DiI stereotaxic injections, the mice were fixed in mouse pockets and held in the appropriate position of the stereotaxic apparatus. The left leg that needed to be injected was secured to the outer wall of the mouse pocket. The injection site was ST36 acupoint, so fur around ST36 acupoint needs to be shaved to expose the skin. ST36 acupoint is 2–3 mm below the small head of the fibula and lateral to the anterior tubercle of the tibia (Zhang K. et al., 2018; Lin et al., 2019). According to the location of the ST36 acupoint, the tip of the injection needle was first positioned on the skin surface of the small head of the fibula as the starting points (lateral 0 mm, longitudinal 0 mm, and depth 0 mm). Then, 5 μL of DiI (2 mg/mL) was injected unilaterally into ST36 acupoint (lateral 2.5 mm, longitudinal 0 mm, and depth 3 mm) at a flow rate of 1 μL/min by a monitored microsyringe. The needle stayed at ST36 acupoint for an extra 1 min before being withdrawn slowly. Ten days after DiI injection, 1.5 μL FG was injected into the plantar surface of the left hind paw of mice. Two weeks after DiI injection and 4 days after FG injection, lumbar 4 to lumbar 6 (L4–L6) DRGs were dissected for immunofluorescence. A total of 15 mice were used in this experiment.

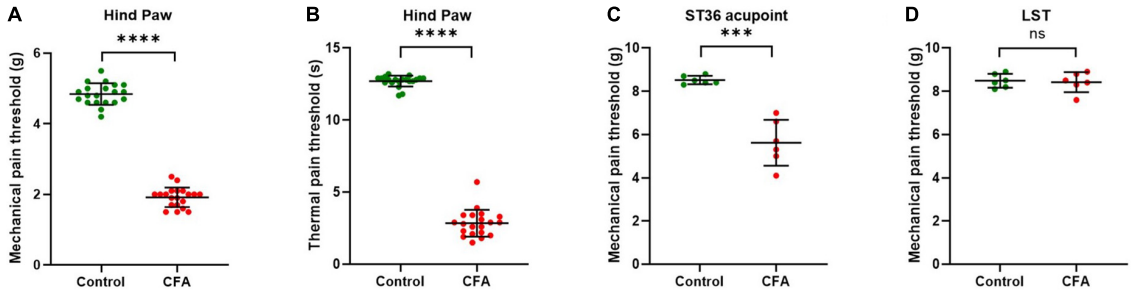

FIGURE 1
ST36 acupoints were sensitized in CFA model mice. **(A)** The mechanical pain threshold of the hind paw decreased in the CFA model. $n = 20$, $^{****}P < 0.0001$, paired t-test. **(B)** The thermal pain threshold of the hind paw decreased in the CFA model. $n = 20$, $^{****}P < 0.0001$, paired t-test. **(C)** The mechanical pain threshold of ST36 acupoints decreased in the CFA model. $n = 6$, $^{***}P = 0.0009$, paired t-test. **(D)** The mechanical pain threshold of LST did not change significantly in the CFA model. $n = 6$, $P = 0.7412$, paired t-test. LST, the position 5 mm lateral side of the ST36.

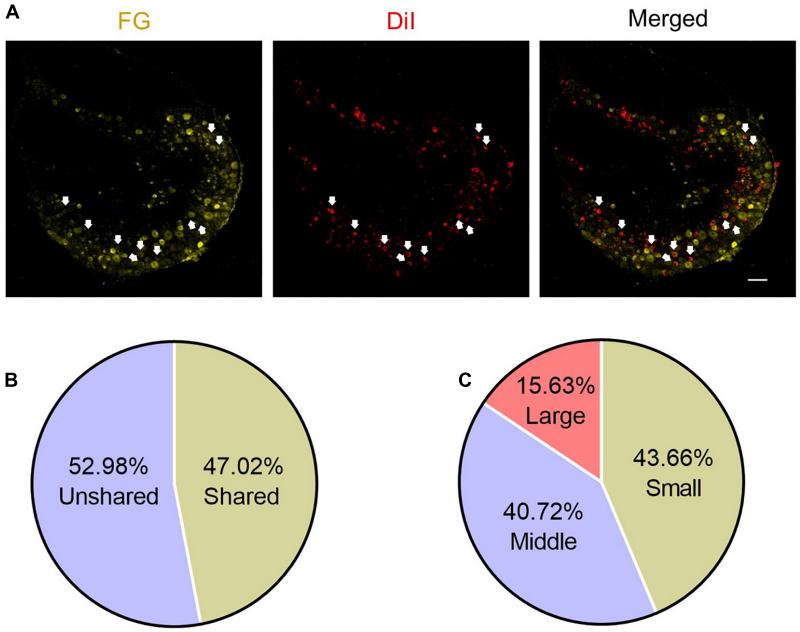

FIGURE 2
Some DRG neurons innervate both ST36 acupoint and ipsilateral hind paw plantar. **(A)** The representative pictures of shared DRG neurons. FG, Fluoro-Gold. The white arrows indicate double-labeled DRG neurons. Bar = 100 μm. **(B)** The percentage of shared neurons in all DRG neurons. **(C)** The percentages of neurons with different diameters in shared neurons.

Chemogenetic method

Viruses utilized in this study included AAVRetro-hSyn-DIO-hM4D(Gi)-mCherry (titer 1.060 × 10^{12} virus particles/mL), AAVRetro-hSyn-DIO-hM3D(Gq)-mCherry (titer 1.135 × 10^{12} virus particles/mL), AAVRetro-hSyn-DIO-mCherry (titer 1.163 × 10^{12} virus particles/mL), and AAVRetro-hSyn-Cre-EGFP (titer 1.285 × 10^{12} virus particles/mL), all of which were obtained from the Shanghai Genechem Technology Co., Ltd. Viruses were injected 3–4 weeks before behavioral tests.

ST36 acupoint stereotaxic injection was performed as previously described. Eight microliters of AAVRetro-hSyn-DIO-hM4D(Gi)-mCherry, AAVRetro-hSyn-DIO-hM3D(Gq)-mCherry or AAVRetro-hSyn-DIO-mCherry was injected into left ST36 acupoint (lateral 2.5 mm, longitudinal 0 mm, sand depth 3 mm) at a flow rate of 1.5 μL/min. And 8 μL of AAVRetro-hSyn-Cre-EGFP was injected into the plantar surface of the left hind paw of mice who were fixed in mouse pockets during the injection. During all injections, the needle was allowed to remain at the target site for an additional 10 min and then removed slowly to prevent efflux of the virus. All virus injections were completed on the same day. A total of 85 mice received virus injections.

For hM4Di silencing or hM3Dq activation, mice were injected clozapine-N-oxide (CNO, C0832, Sigma-Aldrich) intraperitoneal (i.p.) at 5 mg/kg, 30 min before the behavioral test (Stoodley et al., 2017; Liu et al., 2020). CNO was dissolved in DMSO at 10 mg/mL as a stock solution, kept at – 20°C until used, and freshly diluted with 0.9% saline to the corresponding working concentrations in a final volume of 300 μL before intraperitoneal administration. The final concentration of DMSO in working solutions did not exceed 0.1% (vol/vol). Saline was injected as vehicle control.

Complete Freund's adjuvant model

Fifty mice received CFA injections. CFA was purchased from Sigma-Aldrich (F5881), which contains 1 mg/mL of heat-killed and dried mycobacterium tuberculosis in 85% paraffin oil and 15% mannide monooleate. Unilateral inflammation pain was induced by injecting 20 μL CFA into the plantar surface of the left hind paw of mice who were fixed in mouse pockets during the injection (Wu et al., 2019). Once finished injection, the injection site was immediately pressed gently with cotton to prevent bleeding and drug leakage.

Behavioral tests

Behavioral tests were performed on 97 mice, of which 12 mice were measured before and 7 days after CFA injection to confirm the CFA model was built successfully. Three to four weeks after virus injection, mice were measured before or 4 days after CFA injection (Goldman et al., 2010). During the subsequent studies, mice were first injected with saline (vehicle-only i.p. injection), followed by behavioral testing 30 min later (CNO OFF state). And then, the mice were injected with CNO (i.p. injection), followed by behavioral testing another 30 min later (CNO ON state). The results of each test were paired for comparison as a vehicle control group (saline) and a treatment group (CNO). Throughout the study, all criteria for behavioral tests that followed were determined *a priori*. All behavioral testing was performed between 8 a.m. and 12 a.m. Before experiments, mice were randomly assigned to groups. Researchers involved in behavioral testing and data analysis were blinded to the group assignment. Mice were habituated to the test environment for 30 min daily for successive 3 days before the behavioral testing. And before the initiation of each test session, mice were allowed to acclimate to the testing apparatus for 30 min. Three trials were performed per mouse with an interval between measurements of at least 5 min, and the average of the 3 trials was taken as the result.

Behavioral data in **Figures 1A,B** ($n = 20$) were collected from the same batch of mice in **Figure 3B** ($n = 9$) and **Figure 5B** ($n = 11$). And behavioral data in **Figures 1C,D** ($n = 6$) were collected from the same batch of mice in **Figure 4A** ($n = 6$).

Mechanical pain sensitivity

Mechanical pain threshold (MPT) was assessed with the electronic Von Frey test (BIO-EVF4, Bioseb, Vitrolles, France) at three locations separately, ST36 acupoint, 5 mm lateral side of ST36 acupoint (LST), and plantar of the IHP. To measure the MPT of IHP, each mouse was placed in a suspended plastic cage (66 × 22 × 13 cm) with a wire grid floor (0.6 × 0.6 cm^2 spacing). And to measure the MPT of ST36 acupoint or LST, the mice were fixed in mouse pockets. The electronic von Frey apparatus, consisting of an elastic spring-type tip fitted in a hand-held force transducer, was applied perpendicularly to the skin surface of the three locations and the force applied was gradually increased until hind paw withdrawal. Finally, MPT (expressed in grams) was automatically recorded by the electronic Von Frey device and regarded as a pain parameter (Ferrier et al., 2013).

Thermal pain sensitivity

Thermal pain threshold (TPT) was evaluated with a thermal pain test apparatus (Hargreaves Apparatus, No. 37370, Ugo Basile, Comerio, Italy). Before testing, mice were individually kept in a transparent plastic test chamber (62 × 20 × 14 cm) fixed in the proper position on a suspended, specially constructed, and non-insulated transparent glass panel (86 × 35 cm). The intensity of the infrared radiant heat source (IR value) was adjusted and kept constant. And to prevent

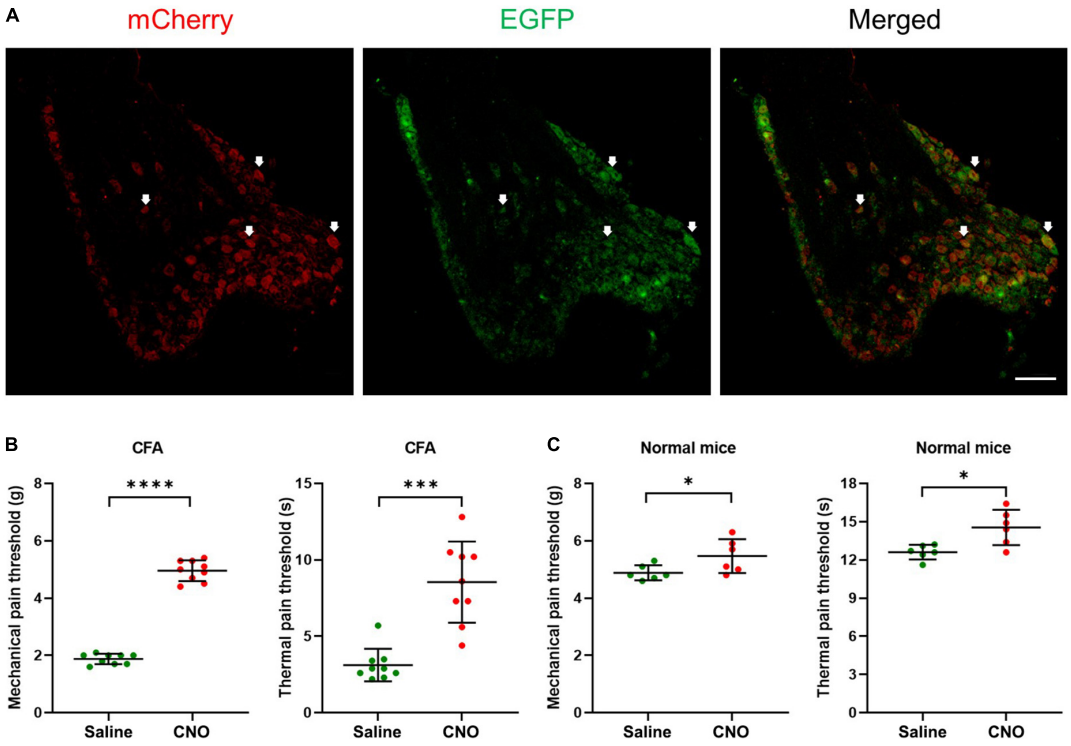

FIGURE 3
Inhibition of shared neurons induced analgesia in CFA mice. **(A)** The representative pictures of DRG neurons expressing hM4D(Gi) receptors. The white arrows indicate double-labeled DRG neurons. As the EGFP signals were from original EGFP proteins expressed by the AAVRetro-hSyn-Cre-EGFP virus, while the mCherry proteins were expressed in a cre-dependent manner and their signals were amplified by the mCherry antibodies, all mCherry signal positive neurons were shared neurons. Bar = 150 μm. **(B)** The mechanical pain thresholds and thermal pain thresholds of the ipsilateral hind paw plantar were elevated after CNO treatment in the CFA model. $n = 9$, paired t-test. For mechanical pain thresholds, $^{****}P < 0.0001$. For thermal pain thresholds, $^{***}P = 0.0004$. **(C)** The mechanical pain thresholds and thermal pain thresholds of the ipsilateral hind paw plantar were increased a little after CNO treatment in normal mice. $n = 6$, paired t-test. For mechanical pain thresholds, $^{*}P = 0.0472$. For thermal pain thresholds, $^{*}P = 0.0122$.

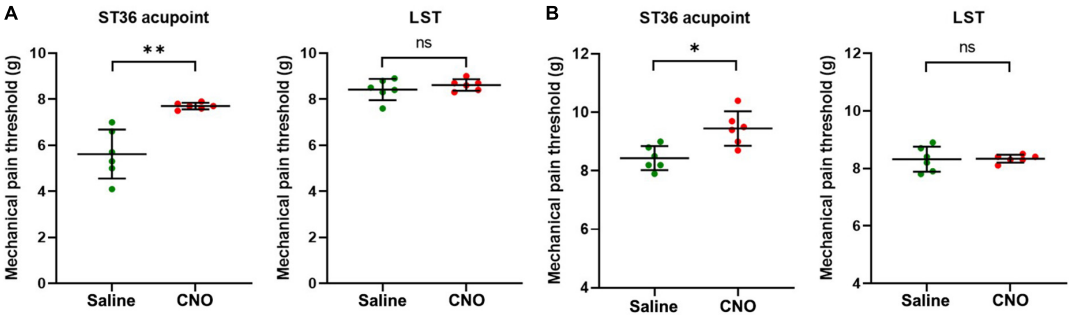

FIGURE 4
Inhibition of shared neurons elevated the mechanical pain threshold of ST36 acupoint. **(A)** The CNO treatment increased the mechanical pain thresholds of the ipsilateral ST36 acupoint but not the LST in the CFA model. $n = 6$, paired t-test. For ST36 acupoint, $^{**}P = 0.0032$. For LST, $P = 0.3632$. LST, the position 5 mm lateral side of the ST36. **(B)** The CNO treatment increased the mechanical pain thresholds of the ipsilateral ST36 acupoint but not the LST in the normal mice. $n = 6$, paired t-test. For ST36 acupoint, $^{*}P = 0.0284$. For LST, $P = 0.9343$.

possible tissue damage, the basal TPT was adjusted to 10–12 s and a cutoff of 20 s (Mao-Ying et al., 2012; Feng et al., 2019). In this study, a movable stimulus of infrared radiant heat (IR = 23) was placed under the glass floor directly beneath the middle plantar surface of the left hind paw. When the withdrawal response occurred, the IR source switched off, and the reaction time counter stopped. The TPT was automatically detected and recorded (in seconds) with an accuracy of 0.1 s.

Immunofluorescence staining

DRGs (L4-L6) were harvested from 15 mice perfused with ice-cold PBS and 4% paraformaldehyde (PFA). DRGs were fixed at 4°C in 4% PFA for at least 2 h, incubated in 30% sucrose overnight at 4°C, and embedded in optimal cutting temperature compound (OCT, 4583, Tissue-Tek, SAKURA, Torrance, CA, United States). Coronal sections (30 μm thick) were cut with a cryomicrotome (CM 1950, Leica Microsystems, Nussloch, Germany), and adhered to slides. For staining, sections were washed in PBS three times (3 min for each wash), blocked in PBS containing 5% normal goat serum for 2 h at room temperature, and incubated with primary antibodies overnight at 4°C. Primary antibodies utilized in this study included rabbit polyclonal anti-transient receptor potential vanilloid 1 (TRPV1) antibody (1:400 dilution, ab6166, Abcam, Cambridge, United Kingdom), and rabbit monoclonal anti-Parvalbumin (PV) Antibody (1:200 dilution, MA5-35259, Thermo Fisher Scientific). After three washes with PBS for 3 min each time, the sections were incubated with goat polyclonal secondary antibody to rabbit IgG-H&L (Alexa Fluor® 488, 1:500 dilution, ab150077, Abcam) for 2 h at room temperature. Finally, sections were washed in PBS three times (3 min for each wash) and sealed with an appropriate amount of antifading mounting reagent (S2100, Solarbio, Shanghai, China). The images were captured by confocal laser-scanning microscopy using an Olympus FluoView FV3000 self-contained confocal laser scanning microscope system (Olympus, Tokyo, Japan). The data of immunofluorescent staining presented in the **Figures 2A**, **3A**, **7A,D** are representative images of at least five mice (Rezende et al., 2017; Lavian and Korngreen, 2019).

Statistics

The statistical analysis was performed using the Graphpad Prism 8 software (GraphPad, San Diego, CA, United States). All data are presented as mean ± standard deviation (SD) and checked for normality before analysis. For comparison of parameters between two groups (**Figures 1**, **3B,C**, **4–6**), the variance similarity was determined by the *F*-test. And significance was determined by paired *t*-test. For all tests, differences of $P < 0.05$ were considered to be statistically significant. Statistical analysis of individual experiments is also described in figure legends.

Results

The mechanical pain threshold of ST36 acupoint was decreased in complete Freund's adjuvant-treated mice

The acupoint being more sensitive to external mechanical stimuli is one of the characteristics of acupoint sensitization. After the CFA model was confirmed to be built successfully (**Supplementary Figure 1**), we checked the pain threshold of hind paw plantar in the CFA-treated mice. After 4 days of CFA injection into the hind paw plantar, the MPTs of the hind paws were decreased from 4.8 ± 0.3 g to 1.9 ± 0.3 g (**Figure 1A**), and the TPTs were reduced from 12.7 ± 0.4 s to 2.8 ± 0.9 s (**Figure 1B**). These indicate that we achieved a stable CFA pain model. Then we evaluated the MPTs of ipsilateral ST36 acupoints in these CFA model mice by the von Frey method. CFA treatment significantly reduced the MPTs from 8.4 ± 0.4 g to 5.6 ± 1.1 g (**Figure 1C**), while the thresholds of the position 5 mm lateral side of the ST36 (LST) did not change much, from 8.3 ± 0.4 g to 8.4 ± 0.5 g (**Figure 1D**). These data suggested that ST36 acupoint was sensitized in the CFA-induced inflammatory pain state.

Dorsal root ganglion neurons shared by ST36 acupoint and ipsilateral hind paw plantar

Since the sensory afferents of the calf and foot are the component of the sciatic nerve, and our previous study also showed that the somata of the nerve terminals innervating the ST36 acupoint were distributed in the L4–L6 DRG (Li et al., 2022), we hypothesized that there may be DRG neurons innervating both the plantar and ipsilateral ST36 acupoint in naïve mice. We retro-labeled DRG neurons innervating ST36 acupoint and ipsilateral plantar by injecting DiI or FG dyes at these two sites, respectively (**Figure 2A**). Since we are more concerned about how many neurons related to ST36 acupoint belong to shared neurons, we used the number of DiI-positive neurons as the denominator and the number of double-labeled neurons as the numerator when calculating the percentage, that is $(DiI^+ FG^+)/DiI^+ \times 100\%$. After statistical analysis, we found that about 47.02% (1,056/2,246) of DRG neurons were double-labeled by DiI and FG, which indicated that these neurons were shared by ST36 acupoint and IHP plantar (**Figure 2B**). Of these shared neurons, 43.66% (461/1,056) were small-diameter neurons, 40.72% (430/1,056) were middle-size neurons, and only 15.63% (165/1,056) were large-diameter neurons (**Figure 2C**).

Inhibition of shared neurons induced analgesia

To understand the potential function of shared DRG neurons, we injected the AAVRetro-hSyn-Cre-EGFP virus into hind paw plantar and AAVRetro-hSyn-DIO-hM4D(Gi)-mCherry virus into ipsilateral ST36 acupoint at the same time to induce the expression of Gi-coupled human M4 muscarinic DREADD receptors in the shared DRG neurons. By immunofluorescence method, mCherry signals were detected in many DRG neurons (**Figure 3A**), which indicated that

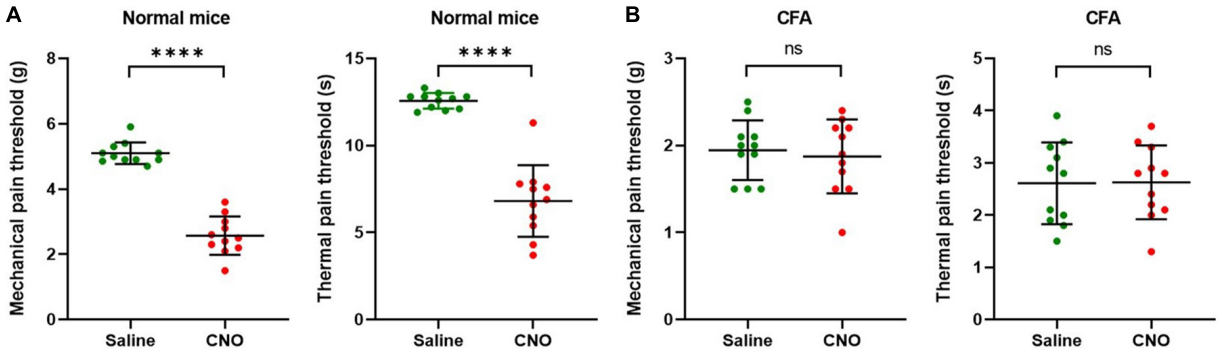

FIGURE 5
Activation of shared neurons induced pain. **(A)** The mechanical pain thresholds and thermal pain thresholds of the ipsilateral hind paw plantar were decreased after CNO treatment in normal mice. $n = 11$, paired t-test. For mechanical pain thresholds, ****$P < 0.0001$. For thermal pain thresholds, ****$P < 0.0001$. **(B)** The mechanical pain thresholds and thermal pain thresholds of the ipsilateral hind paw plantar did not change significantly after CNO treatment in the CFA model. $n = 11$, paired t-test. For mechanical pain thresholds, $P = 0.7334$. For thermal pain thresholds, $P = 0.9560$.

two viruses infected DRG terminals at two separate positions were retrogradely transported to the same soma, and expressed mCherry in a cre-dependent manner. Then CNO was injected intraperitoneally to specifically inhibit shared DRG neurons. We compared the MPTs and the TPTs after CNO treatment with those before CNO treatment and found that, in the CFA model, both thresholds were elevated significantly (MPTs from 1.9 ± 0.2 g to 5.0 ± 0.4 g, TPTs from 3.1 ± 1.1 s to 8.5 ± 2.7 s) (**Figure 3B**). Even in normal mice, the thresholds were also increased a little (MPTs from 4.9 ± 0.3 g to 5.5 ± 0.6 g, TPTs from 12.6 ± 0.6 s to 14.5 ± 1.4 s) (**Figure 3C**). These data suggest that selectively inhibition of shared DRG neurons induced analgesic effect in the CFA pain model and obstruction of nociceptive sensation in normal mice. We also performed the same studies as shown in **Figure 3**, except that the AAVRetro-hSyn-DIO-hM4D(Gi)-mCherry virus was replaced by the AAVRetro-hSyn-DIO-mCherry virus, which means that only the mCherry proteins, but not M4 muscarinic DREADD receptors, were expressed in shared DRG neurons. The data showed that CNO did not change the pain thresholds of plantar both in the CFA model and in normal mice (**Supplementary Figures 2A,B**), which indicates that the change of pain thresholds was dependent on the expression of M4 muscarinic DREADD receptors in the shared DRG neurons, in other words, the inhibition of shared DRG neurons.

Inhibition of shared neurons elevated the mechanical pain threshold of ST36 acupoint

As the shared DRG neurons innervate both hind paw plantar and ST36 acupoint, they may be involved in the sensation of both locations. We hypothesize that inhibition of these neurons might also block the pain sensation of the ipsilateral ST36 acupoint as they did of the hind paw. In the CFA model, the MPTs of ST36 elevated from 5.0 ± 1.1 g to 7.7 ± 0.1 g by CNO treatment, while those of the LST position did not change much, from 8.4 ± 0.5 g to 8.6 ± 0.2 g (**Figure 4A**). In normal mice, the thresholds of LST also did not change by CNO, from 8.3 ± 0.4 g to 8.3 ± 0.1 g, but those of the ST36 still increased a little, from 8.4 ± 0.4 g to 9.4 ± 0.6 g (**Figure 4B**). The changing trend of MPTs at the ST36 acupoint was quite like those at the ipsilateral plantar.

Excitation of shared neurons induced pain

The results of inhibition of shared DRG neurons indicate that these neurons are necessary conditions for, or at least involved in, transmitting nociceptive pain information from paw plantar or ST36 acupoint to the spinal cord. Then, we performed similar chemogenetic experiments to activate the shared DRG neurons specifically and evaluated the pain thresholds of the hind paw. The AAVRetro-hSyn-Cre-EGFP virus and AAVRetro-hSyn-DIO-hM3D(Gq)-mCherry virus were injected into hind paw plantar and ipsilateral ST36 acupoint separately at the same time. The CNO was injected intraperitoneally to specifically excite shared DRG neurons. The MPTs and the TPTs after CNO treatment were compared with those before CNO treatment. In normal mice, both thresholds declined significantly (MPTs from 5.1 ± 0.3 g to 2.6 ± 0.6 g, TPTs from 12.6 ± 0.5 s to 6.8 ± 2.1 s) (**Figure 5A**). These data suggest that selective activation of shared DRG neurons was sufficient to induce pain. But in the CFA model, the thresholds were not changed much (MPTs from 1.9 ± 0.3 g to 1.9 ± 0.4 g, TPTs from 2.6 ± 0.8 s to 2.6 ± 0.7 s) (**Figure 5B**).

Excitation of shared neurons declined the mechanical pain threshold of ST36 acupoint

Furthermore, we examined the change in the MPT of ST36 acupoint when shared DRG neurons were activated by CNO. In normal mice, the MPTs of ST36 declined from 8.2 ± 0.2 g to 6.6 ± 0.3 g by CNO treatment, while those of the LST position did not change much, from 8.3 ± 0.2 g to 8.4 ± 0.2 g (**Figure 6A**). In the CFA model, the thresholds of LST also did not change by CNO, from 8.6 ± 0.4 g to 8.6 ± 0.1 g, while those of the ST36 still decreased a little, from 6.1 ± 0.7 g to 5.4 ± 0.5 g (**Figure 6B**). The changing trend of the MPTs at ST36 acupoint was also quite like those at the ipsilateral plantar.

We also performed the same studies as in **Figure 6**, except that the AAVRetro-hSyn-DIO-hM3D(Gq)-mCherry virus was replaced by the AAVRetro-hSyn-DIO-mCherry virus, which means that only the mCherry proteins, but not M3 muscarinic DREADD receptors, were expressed in shared DRG neurons. The data showed that CNO did not change the pain thresholds of ST36 acupoint or LST both in normal mice and in the CFA model (**Supplementary Figures 3A,B**), which indicates that the change of pain thresholds of ST36 acupoint in normal mice was dependent on the expression of M3 muscarinic DREADD receptors in the shared DRG neurons, in other words, the activation of shared DRG neurons.

Most of the shared dorsal root ganglion neurons were nociceptive neurons

Based on the cell-size ratio of shared DRG neurons, most neurons were small to middle size. And the results of chemogenetic experiments strongly suggest that they are necessary and sufficient for the transmission of pain signaling. Thus, we stained the DRG slices with TRPV1 or PV antibodies to verify the expression properties of these neurons. About 62.93% (382/607) of shared DRG neurons were $TRPV1^+$ neurons (**Figures 7A,B**), of which about 83.51% neurons were small (149/382) or middle (170/382) size neurons (**Figure 7C**). About 36.97% (166/449) of shared DRG neurons were PV^+ neurons (**Figures 7D,E**). The 69.88% of PV^+ neurons were large (51/166) or middle (65/166) size neurons (**Figure 7F**). These results went along that most of the shared DRG neurons were nociceptive neurons.

Discussion

The mechanical and TPTs of the sensitized acupoints decreased, which is very similar to that of the specific areas of the body surface in visceral pain, such as the preferred pain on the body surface in angina pectoris (Foreman et al., 2015; Gebhart and Bielefeldt, 2016). The myofascial trigger point is quite a sensitized acupoint in knee-joint pain (Dorsher, 2008; Qin et al., 2020). In our study, we also found sensitization of ST36 acupoints in the CFA pain model. These results suggest that sensitization of the corresponding acupoints is a common phenomenon in both visceral pain and superficial pain. A similar neural mechanism may be shared by these two pain states.

Since the change of the pain thresholds of the plantar and ST36 acupoint showed the same trend (**Figure 1**), we hypothesized that there might be the same group of neurons to sense pain in these two places. Compared to the hypothesis that CFA leads to the emergence of new anatomical structures, the explanation that the existence of shared neurons under physiological conditions is simpler. Based on the principle of simplification, we first examined the existence of shared neurons in naïve mice. Fortunately, we did find neurons that were co-labeled with both dyes (**Figure 2A**). Furthermore, excitation of

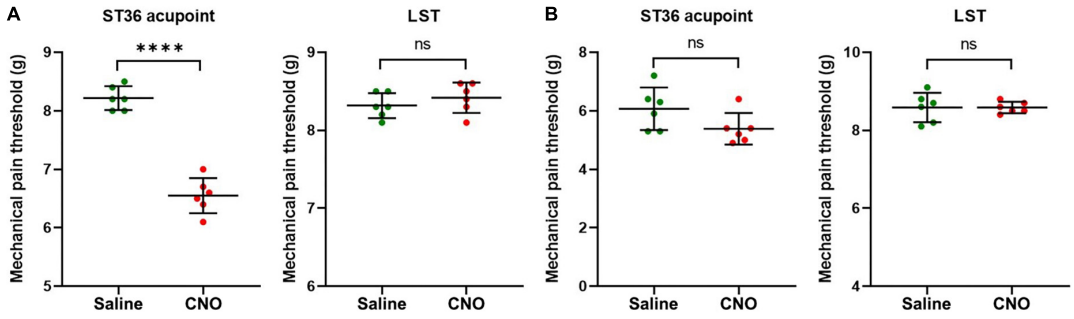

FIGURE 6
Activation of shared neurons declined the mechanical pain threshold of ST36 acupoint. **(A)** The CNO treatment decreased the mechanical pain thresholds of the ipsilateral ST36 acupoint but not the LST in the normal mice. $n = 6$, paired t-test. For ST36 acupoint, $^{****}P < 0.0001$. For LST, $P = 0.4466$. LST, the position 5 mm lateral side of the ST36. **(B)** The CNO treatment did not significantly change the mechanical pain thresholds of the ipsilateral ST36 acupoint and the LST in the CFA model. $n = 6$, paired t-test. For ST36 acupoint, $P = 0.1849$. For LST, $P > 0.9999$.

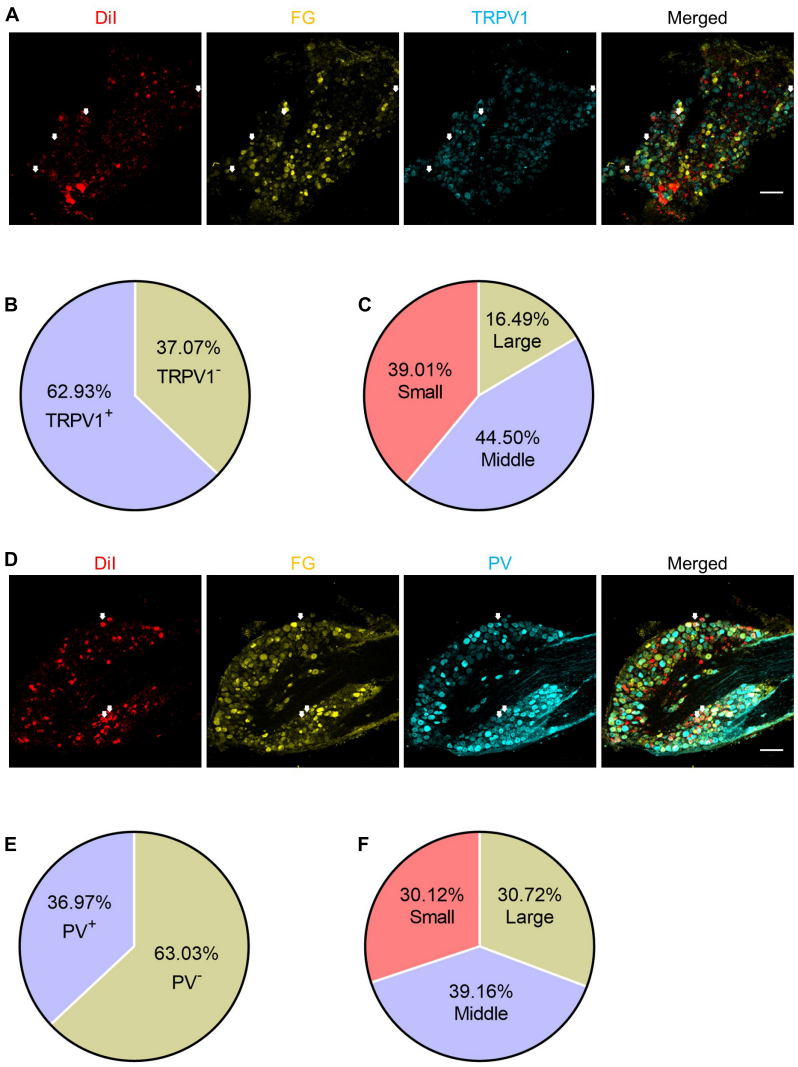

FIGURE 7
The expression patterns of TRPV1 and PV in the shared DRG neurons. **(A)** The representative pictures of expression of TRPV1 in shared DRG neurons. FG, Fluoro-Gold. The white arrows indicate triple-labeled DRG neurons. Bar = 150 μm. **(B)** The percentage of TRPV1 positive neurons in shared neurons. **(C)** The percentages of TRPV1 positive shared neurons with different diameters. **(D)** The representative pictures of expression of PV in shared DRG neurons. The white arrows indicate triple-labeled DRG neurons. Bar = 150 μm. **(E)** The percentage of PV positive neurons in shared neurons. **(F)** The percentages of PV positive shared neurons with different diameters.

shared neurons declined the MPT of ST36 acupoint (Figure 6A), which mimics that the MPT of ST36 acupoint was decreased in CFA-treated mice (Figure 1C). Of course, we cannot exclude the possibility that CFA may also influence the terminal distribution of DRG neurons, but we believe our findings are also an important explanation for acupoint sensitization.

By chemogenetic methods, we specifically inhibited shared DRG neurons and found that the MPTs and the TPTs increased significantly in the CFA pain model (Figure 3B), which suggested the shared DRG neurons are necessary conditions for pain sensation of plantar. On the other hand, both thresholds declined significantly in normal mice when the shared DRG neurons were activated selectively (Figure 5A), which suggested that these neurons are also sufficient conditions for the pain sensation of plantar. The same trends of pain thresholds of ST36 acupoint were also detected when the shared DRG neurons were selectively modulated by CNO (Figures 4A,B, 5A,B). Thus, the shared DRG neurons are both necessary and sufficient conditions for pain transmitting of plantar and ST36 acupoint. In normal mice, inhibition of shared DRG neurons did not elevate the MPTs and TPTs dramatically (Figure 3C). This may be because in the saline control group, the pain induced by the von Frey stimulation itself was very weak and the shared DRG neurons were still relatively quiet. Therefore, selective inhibition of shared neurons by CNO could only raise the pain thresholds relatively limited. On the contrary, in the CFA model, the shared

DRG neurons had been activated much in the saline control group. Selective activation of shared neurons by CNO could not further decrease the pain thresholds anymore (**Figure 5B**).

Recently, some DRG neurons have been reported to innervate both the skin and the distal colon simultaneously (Fang et al., 2020). *In vivo* extracellular electrophysiological recordings of those DRG neurons revealed that they robustly respond to both expansions of the distal colon and the mechanical, nociceptive, warm, or cold stimulation of the cutaneous receptive field (Fang et al., 2020). These results indicate that DRG neurons shared by both the skin and the distal colon participate in the transmission or modulation of multiple sensation signals. In this study, we also found some DRG neurons shared by ST36 acupoint and IHP plantar. The similar neuroanatomy again strongly suggests that the two groups of shared neurons may underlie the common mechanistic basis of the referred skin pain (the acupoint sensitization) in the visceral pain and superficial pain. Therefore, by morphological, chemogenetic, and behavioral methods, we further confirmed that the shared neurons we found were nociceptive and highly correlated with the decrease in pain threshold of ST36 acupoint. Our behavioral results are consistent with their extracellular electrophysiological findings, both indicating that shared neurons are involved in pain transmission.

Our previous study also found that the excitability of C-type DRG neurons innervating the sensitized ST35 (Dubi) acupoint was increased in the knee osteoarthritis rat model (Zhang et al., 2019). Based on the above findings, we believe that the increased excitability of shared nociceptive neurons that innervate both lesions and acupoints is one of the neural mechanisms leading to the acupoints sensitization, at least at the level of primary afferent neurons. In this study, the inflammatory substances induced by CFA in the hind paw plantar continue to stimulate the terminals of shared neurons, resulting in increased neuronal excitability, which makes it easier to transmit signals of mechanical stimuli from ST36 acupoint upward (**Figure 8A**; Prato et al., 2017; Zhang et al., 2019).

Many works of literature have reported that the efficacy of acupuncture is related to the C-type fibers innervating acupoints or DRG neurons expressing TRPV1 (Wang et al., 1996; Tjen et al., 2005; Qin et al., 2014; Gao X. et al., 2015; Chen et al., 2018; Guo et al., 2018; Liu et al., 2018; Li et al., 2019; Du et al., 2021; Fang et al., 2021; Song et al., 2021). However, the TRPV1-expressing shared DRG neurons in this study are unlikely to be involved in the analgesia produced by acupuncture at the ST36 acupoint. Because these neurons facilitate pain sensation of the hind paw. It is logically contradictory if the same neuron mediates both pain and analgesia at the same time. Or there may be some complex signal modulation mechanisms in the DRG or spinal cord to decide what kind of signal to pass up, but these still need further experiments to prove. In addition, there is also a lot of literature claiming that type A fibers are also involved in the analgesia of acupuncture (Katz et al., 1989;

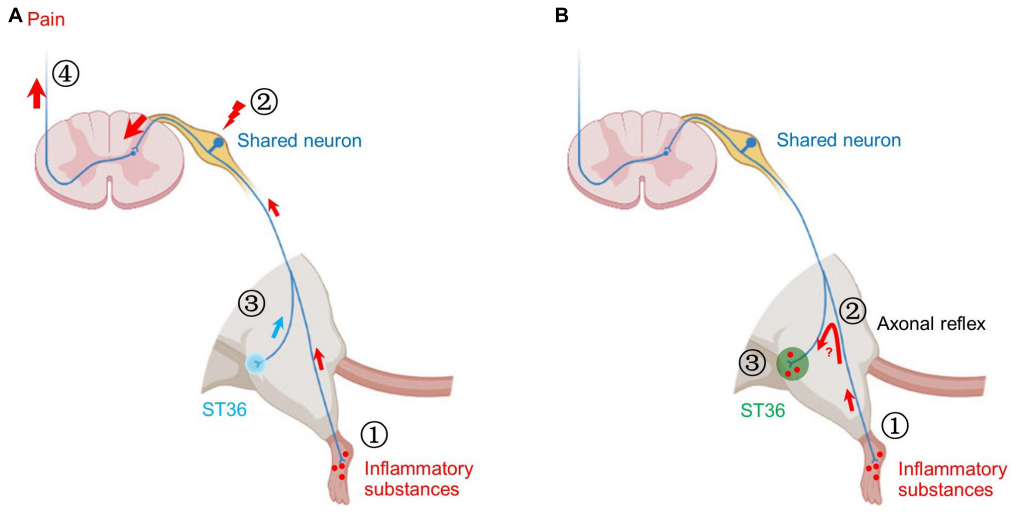

FIGURE 8
Two possible mechanisms of shared neurons participating in acupoint sensitization. **(A)** ① The inflammatory substances induced by CFA in the hind paw plantar stimulate the terminals of shared neurons. ② The pain signals are continuously transmitted to the somata of shared DRG neurons, resulting in increased neuronal excitability. ③ Mechanical stimulation of ST36 more readily activates shared neurons. ④ More pain signals are transmitted to the brain. Behaviorally, the pain threshold of ST36 acupoint decreased. **(B)** ① The inflammatory substances induced by CFA in the hind paw plantar stimulate the terminals of shared neurons. ② By the axonal reflex mechanism, the nerve impulses are transmitted to ST36 acupoint *via* axon bifurcation. ③ The persistent nerve impulses promote the release of pro-inflammatory molecules from the nerve terminal and recruit mast cells to aggregate, degranulate, etc. Locally enhanced neuroimmune responses lead to lower pain thresholds and enlarged receptive field of ST36 acupoint.

Leung et al., 2005; Kagitani et al., 2010; Lee et al., 2020; Qu et al., 2020). And our previous study reported that proprioceptive neurons are more likely to receive stimulation at acupoints by acupuncture (Li et al., 2022). Therefore, the neurons that receive acupuncture stimulation at acupoints and produce therapeutic effects may not be the same group of neurons that participate in acupoint sensitization.

Our behavioral studies revealed the role of shared neurons in the decreased pain threshold of sensitized acupoints, but cannot explain other immunological phenomena at sensitized acupoints yet, such as degranulation of local mast cells. The axonal reflex mechanism may be an appropriate explanation (Carlsson, 2002). The persistent pain signal from the hind paw may be transmitted retrogradely to the ST36 acupoint through the branch of afferent fibers, thereby promoting the release of pro-inflammatory molecules from the nerve terminal at the acupoint (Choi and Di Nardo, 2018). These secreted pro-inflammatory molecules recruit mast cells to aggregate, degranulate, etc. (**Figure 8B**). However, the following two issues still need to be verified by rigorous experiments: (1) Is there a true and continuous transmission of neural excitation from the plantar to the acupoint? (2) Whether the transmitted excitation results in the release of neurotransmitters necessary for local inflammatory responses? These are new research topics that require new research methods, especially *in vivo* studies.

Data availability statement

The raw data supporting the conclusions of this article will be made available by the authors, without undue reservation.

Ethics statement

The animal study was reviewed and approved by the Ethics Committee of the Laboratory Animal Center of Tongji University.

Author contributions

X-FG and LX conceived and supervised the project. WL, JL, AC, DD, and TZ conducted the experiments. QL and JS guided the experimental implementation. X-FG wrote the manuscript with inputs from all authors.

Funding

This work was sponsored by the Major Program of the National Natural Science Foundation of China (No. 82130121), the Key Subject Construction Project of Shanghai Municipal Health Commission (ZK2019B13), the Shanghai Pujiang Program (20PJ1412500), the Natural Science Foundation of Shanghai (21ZR1450100), the Fundamental Research Funds for the Central Universities (22120220196), and the Scientific Research Launch Project of Shanghai Fourth People's Hospital (sykyqd01101).

Conflict of interest

The authors declare that the research was conducted in the absence of any commercial or financial relationships that could be construed as a potential conflict of interest.

Publisher's note

All claims expressed in this article are solely those of the authors and do not necessarily represent those of their affiliated organizations, or those of the publisher, the editors and the reviewers. Any product that may be evaluated in this article, or claim that may be made by its manufacturer, is not guaranteed or endorsed by the publisher.

Supplementary material

The Supplementary Material for this article can be found online at: https://www.frontiersin.org/articles/10.3389/fnmol.2022.974007/full#supplementary-material

SUPPLEMENTARY FIGURE 1
The CFA models were successfully built. An equal volume of saline was injected into the left hind paw plantar as the control. **(A)** The mechanical pain thresholds of the hind paw were reduced significantly by CFA treatment from day 1. $n = 6$, t-test, $P_{CFAvs.saline} < 0.0001$ (D1). **(B)** The thermal pain thresholds of the hind paw were reduced significantly by CFA treatment from day 1. $n = 6$, t-test, $P_{CFAvs.saline} < 0.0001$ (D1).

SUPPLEMENTARY FIGURE 2
CNO did not change the pain thresholds of plantar both in the CFA model and in normal mice without expression of M4 muscarinic DREADD receptors. **(A)** The mechanical pain thresholds and thermal pain thresholds of the ipsilateral hind paw plantar were not changed by CNO treatment in the CFA model. $n = 6$. paired t-test. For mechanical pain thresholds, $P = 0.6109$. For thermal pain thresholds, $P = 0.0648$. **(B)** The mechanical pain thresholds and thermal pain thresholds of the ipsilateral hind paw plantar were not changed by CNO treatment in normal mice. $n = 6$, paired t-test. For mechanical pain thresholds, $P = 0.2374$. For thermal pain thresholds, $P = 0.4092$.

SUPPLEMENTARY FIGURE 3
CNO did not change the pain thresholds of ST36 acupoint or LST both in normal mice and in the CFA model without expression of M3 muscarinic DREADD receptors. **(A)** The mechanical pain thresholds of the ipsilateral ST36 acupoint and the LST in the normal mice were not changed by CNO treatment. $n = 6$, paired t-test. For ST36 acupoint, $P = 0.8053$. For LST, $P = 0.2892$. **(B)** The mechanical pain thresholds of the ipsilateral ST36 acupoint and the LST in the CFA model were not changed by CNO treatment. $n = 6$, paired t-test. For ST36 acupoint, $P = 0.3907$. For LST, $P = 0.4650$.

References

Bao, C. H., Wang, C. Y., Li, G. N., Yan, Y. L., Wang, D., Jin, X. M., et al. (2019). Effect of mild moxibustion on intestinal microbiota and NLRP6 inflammasome signaling in rats with post-inflammatory irritable bowel syndrome. *World J. Gastroenterol.* 25, 4696–4714. doi: 10.3748/wjg.v25.i32.4696

Carlsson, C. (2002). Acupuncture mechanisms for clinically relevant long-term effects–reconsideration and a hypothesis. *Acupunct. Med.* 20, 82–99. doi: 10.1136/aim.20.2-3.82

Chang, W., Kanda, H., Ikeda, R., Ling, J., DeBerry, J. J., and Gu, J. G. (2016). Merkel disc is a serotonergic synapse in the epidermis for transmitting tactile signals in mammals. *Proc. Natl. Acad. Sci. U.S.A.* 113, E5491–E5500. doi: 10.1073/pnas.1610176113

Chen, H. C., Chen, M. Y., Hsieh, C. L., Wu, S. Y., Hsu, H. C., and Lin, Y. W. (2018). TRPV1 is a responding channel for acupuncture manipulation in mice peripheral and central nerve system. *Cell. Physiol. Biochem.* 49, 1813–1824. doi: 10.1159/000493627

Choi, J. E., and Di Nardo, A. (2018). Skin neurogenic inflammation. *Semin. Immunopathol.* 40, 249–259.

Dai, Y. Q., Weng, H., Wang, Q., Guo, X. J., Wu, Q., Zhou, L., et al. (2022). Moxibustion for diarrhea-predominant irritable bowel syndrome: A systematic review and meta-analysis of randomized controlled trials. *Complement. Ther. Clin. Pract.* 46:101532.

Dong, F., Shi, H., Yang, L., Xue, H., Wei, M., Zhong, Y. Q., et al. (2020). FGF13 Is Required for Histamine-Induced Itch Sensation by Interaction with NaV1.7. *J. Neurosci.* 40, 9589–9601. doi: 10.1523/JNEUROSCI.0599-20.2020

Dorsher, P. T. (2008). Can classical acupuncture points and trigger points be compared in the treatment of pain disorders? Birch's analysis revisited. *J. Altern. Complement. Med.* 14, 353–359. doi: 10.1089/acm.2007.0810

Du, J., Fang, J., Xiang, X., Yu, J., Le, X., Liang, Y., et al. (2021). Effects of low- and high-frequency electroacupuncture on protein expression and distribution of TRPV1 and P2X3 in rats with peripheral nerve injury. *Acupunct. Med.* 39, 478–490. doi: 10.1177/0964528420968845

Fan, Y., Kim, D. H., Ryu, Y., Chang, S., Lee, B. H., Yang, C. H., et al. (2018). Neuropeptides SP and CGRP underlie the electrical properties of acupoints. *Front. Neurosci.* 12:907. doi: 10.3389/fnins.2018.00907

Fang, J., Wang, S., Zhou, J., Shao, X., Sun, H., Liang, Y., et al. (2021). Electroacupuncture regulates pain transition through inhibiting PKCEPSILON and TRPV1 expression in dorsal root ganglion. *Front. Neurosci.* 15:685715. doi: 10.3389/fnins.2021.685715

Fang, Y., Han, S., Li, X., Xie, Y., Zhu, B., Gao, X., et al. (2020). Cutaneous hypersensitivity as an indicator of visceral inflammation via C-Nociceptor axon bifurcation. *Neurosci. Bull.* 37, 45–54. doi: 10.1007/s12264-020-00577-5

Feng, X. J., Ma, L. X., Jiao, C., Kuang, H. X., Zeng, F., Zhou, X. Y., et al. (2019). Nerve injury elevates functional Cav3.2 channels in superficial spinal dorsal horn. *Mol. Pain* 15:1744806919836569. doi: 10.1177/1744806919836569

Ferrier, J., Bayet-Robert, M., Pereira, B., Daulhac, L., Eschalier, A., Pezet, D., et al. (2013). A polyamine-deficient diet prevents oxaliplatin-induced acute cold and mechanical hypersensitivity in rats. *PLoS One* 8:e77828. doi: 10.1371/journal.pone.0077828

Foreman, R. D., Garrett, K. M., and Blair, R. W. (2015). Mechanisms of cardiac pain. *Compr. Physiol.* 5, 929–960.

Gao, X. F., Feng, J. F., Wang, W., Xiang, Z. H., Liu, X. J., Zhu, C., et al. (2015). Pirt reduces bladder overactivity by inhibiting purinergic receptor P2X3. *Nat. Commun.* 6:7650. doi: 10.1038/ncomms8650

Gao, X., Qin, Q., Yu, X., Liu, K., Li, L., Qiao, H., et al. (2015). Acupuncture at heterotopic acupoints facilitates distal colonic motility via activating M3 receptors and somatic afferent C-fibers in normal, constipated, or diarrhoeic rats. *Neurogastroenterol. Motil.* 27, 1817–1830.

Gebhart, G. F., and Bielefeldt, K. (2016). Physiology of visceral pain. *Compr. Physiol.* 6, 1609–1633.

Goldman, N., Chen, M., Fujita, T., Xu, Q., Peng, W., Liu, W., et al. (2010). Adenosine A1 receptors mediate local anti-nociceptive effects of acupuncture. *Nat. Neurosci.* 13, 883–888.

Guo, Z. L., Fu, L. W., Su, H. F., Tjen, A. L. S. C., and Longhurst, J. C. (2018). Role of TRPV1 in acupuncture modulation of reflex excitatory cardiovascular responses. *Am. J. Physiol. Regul. Integr. Comp. Physiol.* 314, R655–R666. doi: 10.1152/ajpregu.00405.2017

He, W., Wu, M., Jing, X. H., Bai, W., Zhu, B., and Yu, X. (2015). [Entity of acupoint: Kinetic changes of acupoints in histocytochemistry]. *Zhongguo Zhen Jiu* 35, 1181–1186.

Huang, S., Li, L., Liu, J., Li, X., Shi, Q., Li, Y., et al. (2021). The preventive value of acupoint sensitization for patients with stable angina pectoris: A randomized, double-blind, positive-controlled, multicentre trial. *Evid. Based Complement. Alternat. Med.* 2021:7228033. doi: 10.1155/2021/7228033

Jung, W. M., Lee, S. H., Lee, Y. S., and Chae, Y. (2017). Exploring spatial patterns of acupoint indications from clinical data: A STROBE-compliant article. *Medicine* 96:e6768. doi: 10.1097/MD.0000000000006768

Kagitani, F., Uchida, S., and Hotta, H. (2010). Afferent nerve fibers and acupuncture. *Auton. Neurosci.* 157, 2–8.

Katz, I. R., Simpson, G. M., Jethanandani, V., Cooper, T., and Muhly, C. (1989). Steady state pharmacokinetics of nortriptyline in the frail elderly. *Neuropsychopharmacology* 2, 229–236. doi: 10.1016/0893-133x(89)90026-2

Lavian, H., and Korngreen, A. (2019). Short-term depression shapes information transmission in a constitutively active GABAergic synapse. *Sci. Rep.* 9:18092. doi: 10.1038/s41598-019-54607-y

Lee, J. H., Gang, J., Yang, E., Kim, W., and Jin, Y. H. (2020). Bee venom acupuncture attenuates oxaliplatin-induced neuropathic pain by modulating action potential threshold in A-fiber dorsal root ganglia neurons. *Toxins* 12:737. doi: 10.3390/toxins12120737

Leung, A., Khadivi, B., Duann, J. R., Cho, Z. H., and Yaksh, T. (2005). The effect of Ting point (tendinomuscular meridians) electroacupuncture on thermal pain: A model for studying the neuronal mechanism of acupuncture analgesia. *J. Altern. Complement. Med.* 11, 653–661. doi: 10.1089/acm.2005.11.653

Li, C. L., Li, K. C., Wu, D., Chen, Y., Luo, H., Zhao, J. R., et al. (2016). Somatosensory neuron types identified by high-coverage single-cell RNA-sequencing and functional heterogeneity. *Cell Res.* 26, 83–102.

Li, S., Huang, J., Guo, Y., Wang, J., Lu, S., Wang, B., et al. (2021). PAC1 receptor mediates electroacupuncture-induced neuro and immune protection during cisplatin chemotherapy. *Front Immunol.* 12:714244. doi: 10.3389/fimmu.2021.714244

Li, W., Dai, D., Chen, A., Gao, X. F., and Xiong, L. (2022). Characteristics of zusanli dorsal root ganglion neurons in rats and their receptor mechanisms in response to adenosine. *J. Pain.* doi: 10.1016/j.jpain.2022.04.003 [Epub ahead of print].

Li, Y., Yin, C., Li, X., Liu, B., Wang, J., Zheng, X., et al. (2019). Electroacupuncture alleviates paclitaxel-induced peripheral neuropathic pain in rats via suppressing TLR4 signaling and TRPV1 upregulation in sensory neurons. *Int. J. Mol. Sci.* 20:5917. doi: 10.3390/ijms20235917

Lin, X., Liu, X., Xu, J., Cheng, K. K., Cao, J., Liu, T., et al. (2019). Metabolomics analysis of herb-partitioned moxibustion treatment on rats with diarrhea-predominant irritable bowel syndrome. *Chin. Med.* 14:18. doi: 10.1186/s13020-019-0240-2

Liu, S., Wang, Z. F., Su, Y. S., Ray, R. S., Jing, X. H., Wang, Y. Q., et al. (2020). Somatotopic organization and intensity dependence in driving distinct NPY-expressing sympathetic pathways by electroacupuncture. *Neuron* 108, 436–450.e7. doi: 10.1016/j.neuron.2020.07.015

Liu, S., Wang, Z., Su, Y., Qi, L., Yang, W., Fu, M., et al. (2021). A neuroanatomical basis for electroacupuncture to drive the vagal-adrenal axis. *Nature* 598, 641–645.

Liu, Y. J., Lin, X. X., Fang, J. Q., and Fang, F. (2018). Involvement of MrgprC in electroacupuncture analgesia for attenuating CFA-induced thermal hyperalgesia by suppressing the TRPV1 pathway. *Evid. Based Complement. Alternat. Med.* 2018:9102107. doi: 10.1155/2018/9102107

Ma, S. X. (2021). Low electrical resistance properties of acupoints: Roles of NOergic signaling molecules and neuropeptides in skin electrical conductance. *Chin. J. Integr. Med.* 27, 563–569. doi: 10.1007/s11655-021-3318-5

Ma, Y., Guo, H., Bai, F., Zhang, M., Yang, L., Deng, J., et al. (2018). A rat model of knee osteoarthritis suitable for electroacupuncture study. *Exp. Anim.* 67, 271–280. doi: 10.1538/expanim.17-0142

Mao-Ying, Q. L., Wang, X. W., Yang, C. J., Li, X., Mi, W. L., Wu, G. C., et al. (2012). Robust spinal neuroinflammation mediates mechanical allodynia in Walker 256 induced bone cancer rats. *Mol. Brain* 5:16. doi: 10.1186/1756-6606-5-16

Ngai, S. P., Jones, A. Y., and Cheng, E. K. (2011). Lung meridian acupuncture point skin impedance in asthma and description of a mathematical relationship

with FEV1. *Respir. Physiol. Neurobiol.* 179, 187–191. doi: 10.1016/j.resp.2011.08.004

Oh, J. E., and Kim, S. N. (2021). Anti-Inflammatory effects of acupuncture at ST36 point: A literature review in animal studies. *Front. Immunol.* 12:813748. doi: 10.3389/fimmu.2021.813748

Pattwell, S. S., Liston, C., Jing, D., Ninan, I., Yang, R. R., Witztum, J., et al. (2016). Dynamic changes in neural circuitry during adolescence are associated with persistent attenuation of fear memories. *Nat. Commun.* 7:11475. doi: 10.1038/ncomms11475

Prato, V., Taberner, F. J., Hockley, J. R. F., Callejo, G., Arcourt, A., Tazir, B., et al. (2017). Functional and Molecular Characterization of Mechanoinsensitive "Silent" Nociceptors. *Cell Rep.* 21, 3102–3115. doi: 10.1016/j.celrep.2017.11.066

Qi, X., Chen, L., Zhang, X., Han, M., He, W., Su, Y., et al. (2017). [Distribution of algesia sensitized acupoints in the patients of intestinal cancer]. *Zhongguo Zhen Jiu* 37, 963–966.

Qin, Q. G., Fu, Y., Shi, J., Wu, Q., Wang, S. Y., Cao, Q. A., et al. (2020). [Myofascial trigger point: An indicator of acupoint sensitization]. *Zhen Ci Yan Jiu* 45, 57–61.

Qin, Q. G., Gao, X. Y., Liu, K., Yu, X. C., Li, L., Wang, H. P., et al. (2014). Acupuncture at heterotopic acupoints enhances jejunal motility in constipated and diarrheic rats. *World J. Gastroenterol.* 20, 18271–18283. doi: 10.3748/wjg.v20.i48.18271

Qu, Z., Liu, L., Yang, Y., Zhao, L., Xu, X., Li, Z., et al. (2020). Electro-acupuncture inhibits C-fiber-evoked WDR neuronal activity of the trigeminocervical complex: Neurophysiological hypothesis of a complementary therapy for acute migraine modeled rats. *Brain Res.* 1730:146670. doi: 10.1016/j.brainres.2020.146670

Ramires, C. C., Balbinot, D. T., Cidral-Filho, F. J., Dias, D. V., Dos Santos, A. R., and da Silva, M. D. (2021). Acupuncture reduces peripheral and brainstem cytokines in rats subjected to lipopolysaccharide-induced inflammation. *Acupunct. Med.* 39, 376–384. doi: 10.1177/0964528420938379

Rezende, B. M., Athayde, R. M., Goncalves, W. A., Resende, C. B., Teles de Toledo Bernardes, P., Perez, D. A., et al. (2017). Inhibition of 5-lipoxygenase alleviates graft-versus-host disease. *J. Exp. Med.* 214, 3399–3415. doi: 10.1084/jem.20170261

Shih, Y. W., Su, J. Y., Kung, Y. S., Lin, Y. H., To Anh, D. T., Ridwan, E. S., et al. (2021). Effectiveness of acupuncture in relieving chemotherapy-induced leukopenia in patients with breast cancer: A systematic review with a meta-analysis and trial sequential analysis. *Integr. Cancer Ther.* 20:15347354211063884. doi: 10.1177/15347354211063884

Shih, Y. W., Yang, S. F., Chien, M. H., Chang, C. W., Chang, V. H. S., and Tsai, H. T. (2018). Significant effect of acupressure in elevating blood stem cell factor during chemotherapy in patients with gynecologic cancer. *J. Nurs. Res.* 26, 411–419. doi: 10.1097/jnr.0000000000000257

Song, S., Xu, Y., Liu, J., Jia, Y., Lin, X., Liu, Y., et al. (2021). Strong twirling-rotating manual acupuncture with 4 r/s is superior to 2 r/s in relieving pain by activating C-fibers in rat models of CFA-Induced Pain. *Evid. Based Complement. Alternat. Med.* 2021:5528780. doi: 10.1155/2021/5528780

Stoodley, C. J., D'Mello, A. M., Ellegood, J., Jakkamsetti, V., Liu, P., Nebel, M. B., et al. (2017). Altered cerebellar connectivity in autism and cerebellar-mediated rescue of autism-related behaviors in mice. *Nat. Neurosci.* 20, 1744–1751.

Szawka, R. E., Poletini, M. O., Leite, C. M., Bernuci, M. P., Kalil, B., Mendonca, L. B., et al. (2013). Release of norepinephrine in the preoptic area activates anteroventral periventricular nucleus neurons and stimulates the surge of luteinizing hormone. *Endocrinology* 154, 363–374.

Tan, H., Tumilty, S., Chapple, C., Liu, L., McDonough, S., Yin, H., et al. (2019). Understanding acupoint sensitization: A narrative review on phenomena, Potential Mechanism, and Clinical Application. *Evid. Based Complement. Alternat. Med.* 2019:6064358. doi: 10.1155/2019/6064358

Tian, H., Huang, L., Sun, M., Xu, G., He, J., Zhou, Z., et al. (2022). Acupuncture for knee osteoarthritis: A systematic review of randomized clinical trials with meta-analyses and trial sequential analyses. *Biomed Res. Int.* 2022:6561633. doi: 10.1155/2022/6561633

Tjen, A. L. S. C., Fu, L. W., Zhou, W., Syuu, Z., and Longhurst, J. C. (2005). Role of unmyelinated fibers in electroacupuncture cardiovascular responses. *Auton. Neurosci.* 118, 43–50. doi: 10.1016/j.autneu.2004.12.006

Tong, J., Deng, C., Sun, G., Zhou, J., Zhong, P., Wang, T., et al. (2021). Electroacupuncture Upregulates HIF-1alpha and SOX9 Expression in Knee Osteoarthritis. *Evid. Based Complement. Alternat. Med.* 2021:2047097. doi: 10.1155/2021/2047097

Wang, L., Li, Z., and Guan, X. (1996). [The relationship of C fiber to 5-hydroxytryptamine in spinal cord of rat in electroacupuncture analgesia]. *Zhen Ci Yan Jiu* 21, 22–24.

Wang, X., Qi, Q., Wang, Y., Wu, H., Jin, X., Yao, H., et al. (2018). Gut microbiota was modulated by moxibustion stimulation in rats with irritable bowel syndrome. *Chin. Med.* 13:63. doi: 10.1186/s13020-018-0220-y

Wei, J., Liu, L., Li, Z., Lyu, T., Zhao, L., Xu, X., et al. (2022). Fire needling acupuncture suppresses cartilage damage by mediating macrophage polarization in mice with knee osteoarthritis. *J. Pain Res.* 15, 1071–1082. doi: 10.2147/JPR.S360555

Wong, Y. M. (2014). Preliminary investigation: Acupoint-skin conductance in stroke survivors. *Appl. Psychophysiol. Biofeedback* 39, 159–162. doi: 10.1007/s10484-014-9249-6

Wu, Y., Jiang, Y., Shao, X., He, X., Shen, Z., Shi, Y., et al. (2019). Proteomics analysis of the amygdala in rats with CFA-induced pain aversion with electro-acupuncture stimulation. *J. Pain Res.* 12, 3067–3078. doi: 10.2147/JPR.S211826

Zhang, K., Guo, X. M., Yan, Y. W., Liu, Y. Y., Xu, Z. F., Zhao, X., et al. (2018). Applying statistical and complex network methods to explore the key signaling molecules of acupuncture regulating neuroendocrine-immune network. *Evid. Based Complement. Alternat. Med.* 2018:9260630. doi: 10.1155/2018/9260630

Zhang, M., Guo, H., Ma, Y., Xu, F., Bai, F., Liang, S., et al. (2019). Acupoint sensitization is associated with increased excitability and hyperpolarization-activated current (Ih) in C- But Not Adelta-type neurons. *Neuroscience* 404, 499–509. doi: 10.1016/j.neuroscience.2019.02.028

Zhang, Z. J., Guo, J. S., Li, S. S., Wu, X. B., Cao, D. L., Jiang, B. C., et al. (2018). TLR8 and its endogenous ligand miR-21 contribute to neuropathic pain in murine DRG. *J. Exp. Med.* 215, 3019–3037. doi: 10.1084/jem.20180800

Zhu, B. (2015). [The plasticity of acupoint]. *Zhongguo Zhen Jiu* 35, 1203–1208.

Zhu, B. (2019). [The sensitization phenomenon of acupoint and biological significances]. *Zhongguo Zhen Jiu* 39, 115–121.

Zhu, Y. J., Wu, X. Y., Wang, W., Chang, X. S., Zhan, D. D., Diao, D. C., et al. (2022). Acupuncture for quality of life in gastric cancer patients undergoing adjuvant chemotherapy. *J. Pain Symptom Manage.* 63, 210–220. doi: 10.1016/j.jpainsymman.2021.09.009

frontiers | Frontiers in Molecular Neuroscience

TYPE Original Research
PUBLISHED 31 August 2022
DOI 10.3389/fnmol.2022.990260

OPEN ACCESS

EDITED BY
Yize Li,
Tianjin Medical University General Hospital, China

REVIEWED BY
Rao Fu,
Sun Yat-sen University, China
Nan Gu,
Fourth Military Medical University, China
Qi-Liang Mao-Ying,
Fudan University, China

*CORRESPONDENCE
Lingli Liang
ll2017@xjtu.edu.cn

SPECIALTY SECTION
This article was submitted to Pain Mechanisms and Modulators, a section of the journal Frontiers in Molecular Neuroscience

RECEIVED 09 July 2022
ACCEPTED 02 August 2022
PUBLISHED 31 August 2022

CITATION
Mao Q, Tian L, Wei J, Zhou X, Cheng H, Zhu X, Li X, Gao Z, Zhang X and Liang L (2022) Transcriptome analysis of microRNAs, circRNAs, and mRNAs in the dorsal root ganglia of paclitaxel-induced mice with neuropathic pain.
Front. Mol. Neurosci. 15:990260.
doi: 10.3389/fnmol.2022.990260

Transcriptome analysis of microRNAs, circRNAs, and mRNAs in the dorsal root ganglia of paclitaxel-induced mice with neuropathic pain

Qingxiang Mao[1], Lixia Tian[2,3], Jianxiong Wei[2,3], Xiaoqiong Zhou[2,3], Hong Cheng[2,3], Xuan Zhu[2,3], Xiang Li[2], Zihao Gao[2], Xi Zhang[2] and Lingli Liang[2,3]*

[1]Department of Anesthesiology, Daping Hospital, Army Medical University, Chongqing, China, [2]Department of Physiology and Pathophysiology, School of Basic Medical Sciences, Xi'an Jiaotong University Health Science Center, Xi'an, China, [3]Institute of Neuroscience, Translational Medicine Institute, Xi'an Jiaotong University Health Science Center, Xi'an, China

The microtubule-stabilizing drug paclitaxel (PTX) is a chemotherapeutic agent widely prescribed for the treatment of various tumor types. The main adverse effect of PTX-mediated therapy is chemotherapy-induced peripheral neuropathy (CIPN) and neuropathic pain, which are similar to the adverse effects associated with other chemotherapeutic agents. Dorsal root ganglia (DRG) contain primary sensory neurons; any damage to these neurons or their axons may lead to neuropathic pain. To gain molecular and neurobiological insights into the peripheral sensory system under conditions of PTX-induced neuropathic pain, we used transcriptomic analysis to profile mRNA and non-coding RNA expression in the DRGs of adult male C57BL/6 mice treated using PTX. RNA sequencing and in-depth gene expression analysis were used to analyze the expression levels of 67,228 genes. We identified 372 differentially expressed genes (DEGs) in the DRGs of vehicle- and PTX-treated mice. Among the 372 DEGs, there were 8 mRNAs, 3 long non-coding RNAs (lncRNAs), 16 circular RNAs (circRNAs), and 345 microRNAs (miRNAs). Moreover, the changes in the expression levels of several miRNAs and circRNAs induced by PTX have been confirmed using the quantitative polymerase chain reaction method. In addition, we compared the expression levels of differentially expressed miRNAs and mRNA in the DRGs of mice with PTX-induced neuropathic pain against those evaluated in other models of neuropathic pain induced by other chemotherapeutic agents, nerve injury, or diabetes. There are dozens of shared differentially expressed miRNAs between PTX and diabetes, but only a few shared miRNAs between PTX and nerve injury. Meanwhile, there is no shared differentially expressed mRNA between PTX and nerve injury. In conclusion, herein, we show that treatment with PTX induced

numerous changes in miRNA expression in DRGs. Comparison with other neuropathic pain models indicates that DEGs in DRGs vary greatly among different models of neuropathic pain.

KEYWORDS

paclitaxel, dorsal root ganglion, microRNA, circRNA, RNA sequencing

Introduction

Neuropathic pain can be caused by a lesion in, or disease of, the somatosensory nervous system. Some of the most common conditions involving peripheral neuropathic pain, listed in the new classification criteria from the International Association for the Study of Pain (IASP), include trigeminal neuralgia, peripheral nerve injury, painful polyneuropathy, postherpetic neuralgia, and painful radiculopathy (Scholz et al., 2019). The toxicity of chemotherapeutic agents to the peripheral nervous system can also induce peripheral neuropathy and neuropathic pain (Liang et al., 2020a; Starobova et al., 2020). Most patients with neuropathic pain report an ongoing or intermittent spontaneous pain and pain evoked by light touch or other stimuli (Finnerup et al., 2021). Ectopic activity in injured nerves or dorsal root ganglia (DRG), and peripheral and central sensitization, underlie spontaneous and evoked pain in different neuropathic pain conditions (Finnerup et al., 2021). Multiple mechanisms, including alteration in ion channel activity, activation of immune cells, glial-derived mediators, and epigenetic regulation in the peripheral sensory neurons, contribute to the neurogenesis of neuropathic pain (Liang et al., 2015; Finnerup et al., 2021). However, the various neuropathic pain conditions involve different underlying mechanisms.

Paclitaxel (PTX) is a well-known chemotherapeutic agent with a unique mechanism of action. PTX binds to microtubules in the cytoskeleton and enhances tubulin polymerization, resulting in cellular apoptosis (Jordan and Wilson, 2004). Treatment using PTX can also lead to peripheral neuropathy, which is similar to the adverse effects exerted by other chemotherapeutic agents (Mao et al., 2019; Liang et al., 2020a; Starobova et al., 2020; Kang et al., 2021). Previously, we have reported on an epigenetic regulation mechanism in paclitaxel-induced mouse model of neuropathic pain. In that study, we described that DNA methyltransferase DNMT3a triggers downregulation of *K2p 1.1* expression in the DRG, which contributes to paclitaxel-induced neuropathic pain (Mao et al., 2019). To elucidate more potential mechanisms driving PTX-induced neuropathic pain, herein we used high-throughput RNA sequencing (RNA-Seq) and transcriptomic analysis to evaluate gene expression changes in the DRGs of PTX-treated mice. Previous studies have utilized transcriptomic analysis conducted using high-throughput RNA-Seq or microRNA arrays to profile gene-expression changes in the DRGs of mice with neuropathic pain induced by nerve injury (Wu et al., 2016), diabetes (Zhang H. H. et al., 2020), or other chemotherapeutic agents (Starobova et al., 2020). Hence, we further compared PTX-induced differentially expressed miRNAs, circRNAs, and mRNAs with those described in other neuropathic pain models. RNA-Seq and in-depth gene expression analysis revealed that 345 microRNAs, 6 mRNAs, 3 lncRNAs, and 16 circRNAs were differentially expressed in response to treatment utilizing PTX. Nevertheless, there are only a few shared differentially expressed genes in these neuropathic pain models. Gene expression in the DRG varies depending on the type of insult to these neurons or their axons. Although transcriptomic gene expression profiling enhances our understanding of pain mechanisms under various neuropathic pain conditions, further investigations are needed to validate the potential molecular targets to develop individualized treatment strategies for patients with neuropathic pain.

Materials and methods

Animals

Adult male C57BL/6 mice (8–9 weeks old) were used in this study. Mice were housed (up to five per cage) at 25°C and maintained at a standard 12-h light/dark cycle, with water and food available *ad libitum*. The animal housing facility and all procedures involving animals were approved by the Institutional Animal Ethics Committee of the Xi'an Jiaotong University Health Science Center, and were conducted in accord with the ethical guidelines put forth by the International Association for the Study of Pain. All efforts were made to minimize the suffering of laboratory animals and to reduce the number of animals used in the study. All investigators performing experiments were blinded to the group designation of the mice.

Treatment using paclitaxel

Paclitaxel was prepared and administered as described previously (Liang et al., 2020a). Briefly, to prepare 1 mL of PTX stock solution at 6 mg/mL concentration, PTX (6 mg;

MedChemExpress, Monmouth Junction, NJ, United States) was dissolved in a 1:1 solution of Cremophor EL (500 μL; Sigma-Aldrich, St. Louis, MO, United States) and ethanol (500 μL). Prior to treatment, the PTX stock solution was diluted with 0.9% sterile sodium chloride (NaCl) to a final concentration of 0.4 mg/mL. Each mouse was injected with PTX (4 mg/kg) intraperitoneally (i.p.) every other day for a total of six times. The control mice received vehicle solution (Cremophor EL: ethanol, 1:1, diluted using 0.9% sterile NaCl solution) using the same schedule as that used for PTX mice.

Behavioral tests

All mice were habituated to the testing environment for 3 days prior to baseline testing. Von Frey filaments (0.07 and 0.40 g; Stoelting Co., Wood Dale, IL, United States) were used to evoke mechanical allodynia and hyperalgesia as described previously (Liang et al., 2020a,b). Briefly, each mouse was placed onto an elevated mesh screen within a Plexiglas chamber and was allowed an accommodation period until exploration and grooming behavior ceased. Each calibrated von Frey filament was applied to the left or right hind paw for approximately 1 s, and each trial was repeated 10 times at intervals of 3 min between each application. A positive response occurred when the mouse showed a strong paw withdrawal response to the von Frey filament. Both positive and negative responses were recorded in each trial and the number of positive responses in the 10 times was expressed as percentage of paw withdrawal frequency (PWF) [(number of paw withdrawals/10 times) × 100 = % PWF].

Evoked thermal hyperalgesia to noxious heat was assessed using a Model 37,370 Analgesic Meter (UGO Basile, Comerio, Italy) (Liang et al., 2020b,c). Briefly, each mouse was placed onto a glass plate within a Plexiglas chamber, and radiant heat was applied from below to the middle of the plantar surface of each hind paw until paw withdrawal occurred. When the mouse lifted its foot, the light beam was turned off automatically. The length of time from the starting of the light beam and the foot lift was defined as paw withdrawal latency (PWL). The cut-off time was 20 s to avoid tissue damage. Each trial was repeated five times for one paw at 5-min intervals.

RNA-seq, bioinformatics, and pathway analysis

Mice were euthanized and bilateral lumbar 3 (L3) to L5 DRGs were harvested and flash frozen in liquid nitrogen, and then stored at −80°C. Bilateral L3-L5 DRGs obtained from 2 mice suffering from PTX or vehicle injection were pooled and used as one biological replicate. Six independent biological replicates collected from twelve mice in the vehicle and PTX groups (three biological replicates per group) were sent to BGI Genomics Inc. (Wuhan, China) described previously (Liang et al., 2020a). Briefly, total RNA from each sample was extracted and purified using the TRIzol method. The quality of RNA was estimated by an RNA Integrity Number (RIN) between 1 and 10 with 10 being the highest quality samples showing the least degradation. The RIN scores of six samples were shown in **Supplementary Datasheet 1**. The RIN score of each sample is over 6, indicating that they are of sufficient quality to produce a library for sequencing (Kukurba and Montgomery, 2015). Then, RNA sequencing was conducted on a BGISEQ500 platform (BGI Genomics). Ten samples were evaluated using multiplexing, sequencing, differential gene expression analysis, and transcriptomic expression analysis. Raw data were quality controlled using SOAPnuke software (BGI Genomics) (Cock et al., 2010) and clean reads were obtained after filtering out reads with ribosome RNA (rRNA) and other contaminations. Clean reads were mapped to *Mus musculus* genome sequence (version GCF_000001635.26_GRCm38.p6) from the National Center for Biotechnology Information (NCBI) using hierarchical indexing for spliced alignment of transcripts (HISAT; Center for Computational Biology, Johns Hopkins University, Maryland, MD, United States), and to *Mus musculus* gene sequence using Bowtie2 (Langmead and Salzberg, 2012), to quantify mRNAs and long non-coding RNAs. To quantify circRNAs, clean reads were mapped to known *M. musculus* circRNAs. To detect small RNAs, clean tags were mapped to an miRNA database and *M. musculus* genome sequence, and then quantified. Mapped reads for each gene were calculated to determine the expression levels for that gene. Differential expression analysis was performed via MA-plot software using the DEGseq method (Wang et al., 2010). All expression values were transformed into $\log_2$ values. Comparisons of gene expression levels between groups were conducted using Student's *t*-test. Differentially expressed genes (DEGs) were designated as genes with adjusted *P*-values (*Q*-values) less than 0.05. Log_2 fold changes (FC) in miRNA expression were either more or less than 1. For analysis of DEG mRNA, functional classifications and pathways were evaluated using Gene Ontology (GO) Elite and DAVID Bioinformatics Resources 6.7 Kyoto Encyclopedia of Genes and Genomes (KEGG) pathways. All these data can be extracted manually by utilizing Dr. Tom on-line analysis system provided by BGI Genomics Inc.

Reverse transcription-polymerase chain reaction for detection of microRNA

Bilateral L3–L5 DRGs collected from each mouse were pooled to obtain a sufficient amount of RNA. Tissues were homogenized in, and total RNA was extracted using, Beyozol

(Beyotime, Shanghai, China) according to the manufacturers' protocol. For miRNA quantification, 200 ng total RNA was reverse-transcribed into cDNA using a stem-loop primer specific for each mature miRNA, and using an miRNA First Strand cDNA Synthesis kit (Stem-loop Method) (Sangon Biotech, Shanghai, China) according to manufacturer's instructions. Quantitative PCR was performed on a Real-time Detection System (Agilent Mx3005P qPCR system, Santa Clara, CA, United States) using Hieff® qPCR SYBR® Green Master Mix (Yeasen Biotechnology, Shanghai, China), and forward and reverse primers specific for each miRNA. All the primers used in this procedure (Table 1) were designed and synthesized by Sangon Biotech (Shanghai, China). PCR reactions were performed as follows: initial 3-min incubation at 95°C, followed by 40 cycles at 95°C for 10 s (s), 60°C for 30 s, 72°C for 30 s, 95°C for 5 s, 65°C for 15 s, and 95°C for 5 s. PCR products were verified using agarose gel electrophoresis and analysis of dissociation curve. U6 small nuclear RNA (Rnu6) was used as endogenous control to normalize differences in miRNA levels of each sample. Quantification was performed by normalizing target gene cycle threshold (Ct) values to that of Rnu6 Ct. The ratio of relative miRNA level in each sample to average miRNA level in vehicle-group samples was calculated using the $2^{-\Delta\Delta Ct}$ method.

Reverse transcription-polymerase chain reaction for detection of circRNA

For quantification of circRNA expression levels, total RNA was reverse-transcribed using ThermoScript reverse transcriptase and Random Hexamer Primer (Invitrogen/Thermo Fisher Scientific). For quantitative RT-PCR (qRT-PCR), each sample was run in triplicate using 20 μl reaction volume comprised of 10 μl Hieff® qPCR SYBR® Green Master Mix, 20 ng cDNA, and 2 μL 250 nM forward and reverse primers. All the primers used in this procedure (Table 2) were designed and synthesized by Sangon Biotech (Shanghai, China). PCR reactions were run on an Agilent Mx3005P qPCR system using the following conditions: initial 3-min incubation at 95°C, 40 cycles at 95°C for 10 s, 60°C for 30 s, 72°C for 30 s, 95°C for 5 s, 65°C for 15 s, and 95°C for 5 s. Agarose gel electrophoresis and analysis of dissociation curve were used to verify PCR products. All data were normalized to expression levels of *Gapdh* used as internal control. The ratio of mRNA level in each sample to average mRNA level in samples from the vehicle treatment group was calculated using the $2^{-\Delta\Delta CT}$ method.

TABLE 2 The primers for circRNAs and the internal control gene.

CircRNAs	Primers	Sequences (5′–3′)
mmu_circ_0009357	Forward	ACCACGAGAATGCGAAGGAACAAG
	Reverse	CCTCCTGTCATCCTCCTCATCTCC
mmu_circ_0013069	Forward	GGGGTGTAGAGGGCAAGGAGAG
	Reverse	TCTTGTTCTTCTTTCCTGCCTTCCC
mmu_circ_0006031	Forward	GTGGAGGTGAGGCAGGAGAGTC
	Reverse	ACCTGAGGTGTCCCGCTTCTTG
mmu_circ_0001817	Forward	ACCGGTCCTCCTCTATTCGG
	Reverse	CCAAACAAGCTCTCAAGGTCCA
mmu_circ_0011289	Forward	GGAGACTGTGCCTGTGGTTGTG
	Reverse	TCAGTCCTCTCAGCCTCCATATTCC
Gapdh	Forward	TCGGTGTGAACGGATTTGGC
	Reverse	TCCCATTCTCGGCCTTGACT

Statistical analysis

For behavioral tests, 24 mice were randomly distributed into the vehicle and PTX groups (12 mice/group). Data obtained using behavioral tests are expressed as means ± error of

TABLE 1 The miRNA primers.

MiRNAs	Primers	Sequences (5′–3′)
mmu-miR-376b-3p	RT	GTCGTATCCAGTGCAGGGTCCGAGGTATTCGCACTGGATACGACAAGTGG
	Forward	AAGCGCCTATCATAGAGGAACA
	Reverse	CAGTGCAGGGTCCGAGGT
mmu-miR-29c-3p	RT	GTCGTATCCAGTGCAGGGTCCGAGGTATTCGCACTGGATACGACTAACCG
	Forward	AGCTGGACTAGCACCATTTGAAA
	Reverse	AGTGCAGGGTCCGAGGTATT
mmu-miR-532-5p	RT	GTCGTATCCAGTGCAGGGTCCGAGGTATTCGCACTGGATACGACACGGTC
	Forward	AACCTCCCATGCCTTGAGTG
	Reverse	CAGTGCAGGGTCCGAGGT
Rnu6 (*Mus musculus*)	RT	GTCGTATCCAGTGCAGGGTCCGAGGTATTCGCACTGGATACGACAAAAAT
	Forward	GAAGATTTAGCATGGCCCCTGC
	Reverse	CAGTGCAGGGTCCGAGGT

RT, reverse transcription.

mean (SEM), and were statistically analyzed using two-way repeated measure (RM) ANOVA followed by *post hoc* Tukey test (SigmaPlot 12.5, San Jose, CA, United States). Three biological repeats (two mice/repeat) were selected randomly from 10 mice in each group and examined using RNA-Seq. Three to six mice (one mouse/repeat) per group were examined using RT-PCR and were statistically analyzed using two-tailed unpaired *t*-test (SigmaPlot 12.5). *P*-values less than 0.05 were considered statistically significant.

Results

Paclitaxel induces hypersensitivity to pain

We have previously shown that intraperitoneal injection of PTX induces pain hypersensitivity which peaks at approximately 10–14 days after the first injection (Mao et al., 2019). Therefore, day 10 was selected as time point for evaluation of PTX-induced transcriptomic changes in the DRG using RNA sequencing. To ensure that all mice treated using PTX showed pain hypersensitivity, paw withdrawal frequency (PWF) in response to mechanical stimulation and paw withdrawal latency (PWL) in response to thermal stimulation were assessed on day 10 following the first PTX injection and before the harvesting of DRGs (**Figure 1A**). In agreement with results obtained in our previous studies (Mao et al., 2019; Liang et al., 2020a), our present results show that treatment using PTX led to a dramatic increase in PWF response to 0.07- and 0.40-g von Frey filaments in both hind paws on day 10 compared with baseline response and that of the vehicle-treated group ($P < 0.05$ for 0.07-g von Frey filament; $P < 0.01$ for 0.40-g von Frey filament; **Figures 1B,C**). Similarly, treatment using PTX also induced thermal hyperalgesia in our mice, as shown by decreased PWL response in both hind paws compared with baseline response and that of the vehicle-treated group ($P < 0.01$; **Figure 1D**). Treatment with vehicle did not induce changes in either PWF or PWL of either hind paw compared to their respective baseline response levels (**Figures 1B–D**).

Paclitaxel induces transcriptomic changes in coding and non-coding RNAs

RNA-Seq and in-depth gene expression analysis were used to explore transcriptomic changes in mRNA and non-coding RNA expression in PTX-induced DRGs. Our analyses identified a total of 67,228 genes including 22,899 coding mRNAs, 24677 lncRNAs, 16127 circRNAs, 2959 microRNAs, and 554 pseudoRNAs. DEGs were first extracted based on their *Q*-values of being less than 0.05. Our results indicate that 345 microRNAs were differentially expressed in response to treatment using PTX, while only 8 mRNAs, 3 long non-coding RNAs (lncRNAs), and 16 circRNAs were extracted as DEGs after induction using PTX (**Figure 2A**).

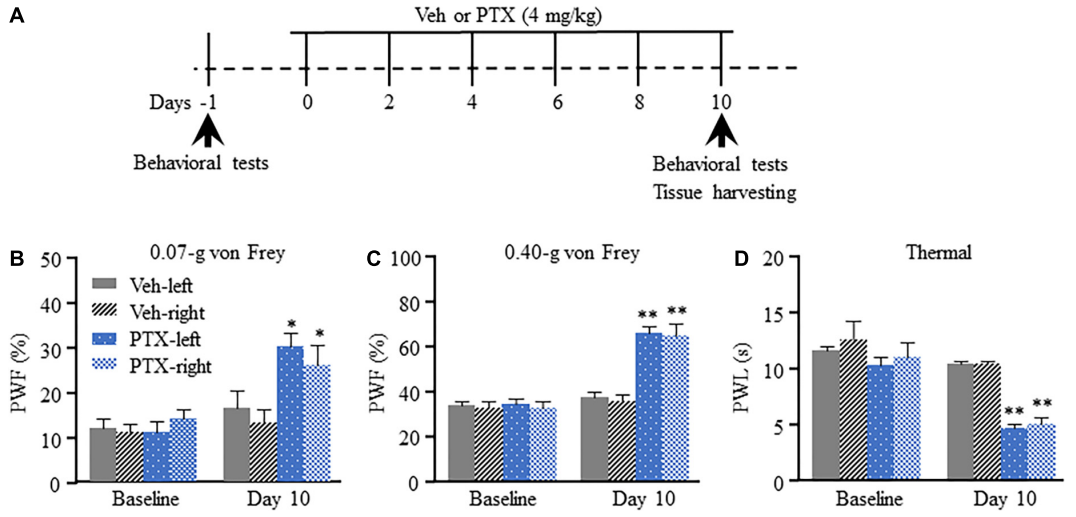

FIGURE 1
Mechanical allodynia and thermal hyperalgesia induced by paclitaxel (PTX) in mice. **(A)** A schematic of drug administrations and behavioral tests showed that mice were intraperitoneally injected with PTX (4 mg/kg) or vehicle solution (200 μl) every other day for a total of six times. **(B–D)** The paw withdrawal frequency (PWF) in response to a 0.07-g **(B)** and 0.40-g **(C)** von Frey filament, and the paw withdrawal latency (PWL), in response to thermal stimulation **(D)**, were assessed on day 10 after the first injection using PTX, and were compared with those of mice in the vehicle (Veh)-treated group. $n = 12$/group. Results are presented as mean ± SEM; $^{*}P < 0.05$, $^{**}P < 0.01$, compared with vehicle group by two-way ANOVA followed by *post hoc* Tukey test.

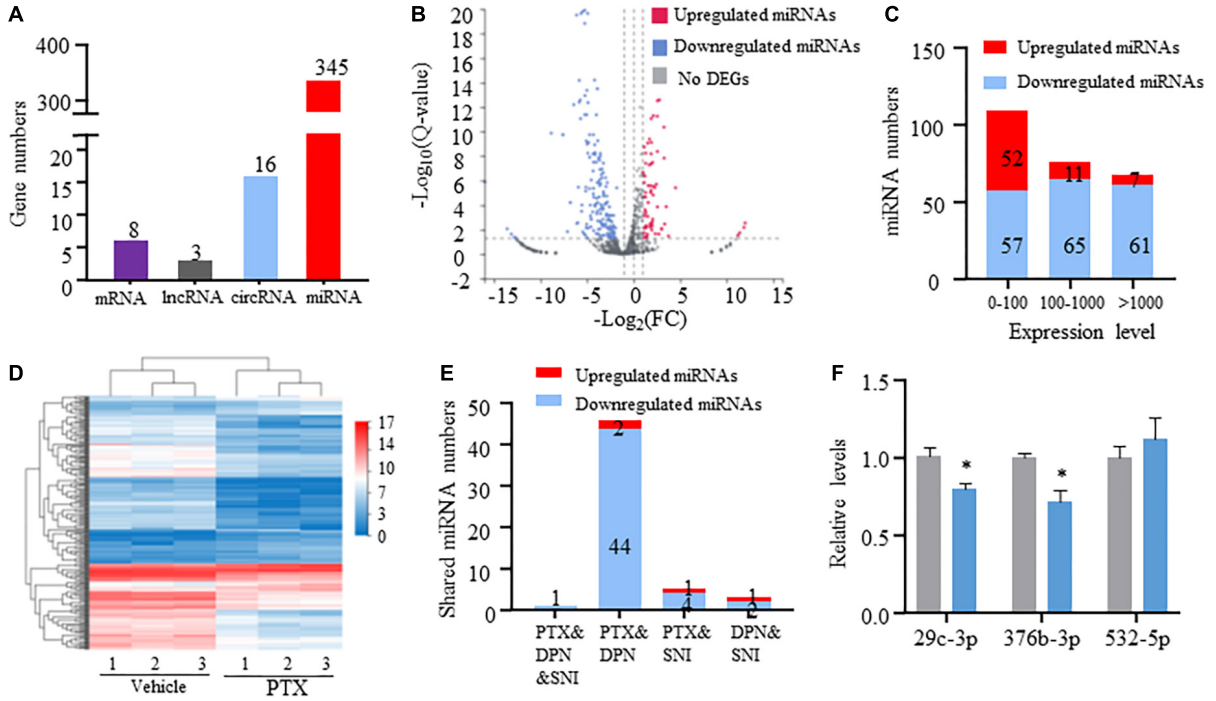

FIGURE 2
Transcriptome profiling of miRNAs in paclitaxel (PTX)-treated mice. **(A)** Numbers of differentially expressed genes (DEGs) were determined using transcriptome analysis. DEGs are genes having *Q*-values less than 0.05. **(B)** Volcano plot of differentially expressed miRNAs after PTX administration shows the most highly upregulated [$\log_2$(fold change, FC) > 1] or downregulated [log2(FC) < −1] genes. **(C)** Numbers of upregulated and downregulated miRNA showing low (0–100), medium (100–1,000), or high (more than 1,000) expression levels, based on respective expression level values in the vehicle group. **(D)** Hierarchical clustering analysis shows 253 differentially expressed miRNAs in vehicle and PTX groups. **(E)** Numbers of differentially expressed miRNA shared among PTX, diabetic peripheral neuropathy (DPN), and spared nerve injury (SNI) models. **(F)** Validation of PTX-induced downregulation of miR-376b-3p and miR-29c-3p expression as assessed using quantitative polymerase chain reaction. Results are presented as mean ± SEM of 3–6 independent experiments. $^*P < 0.05$ compared with the vehicle group by two-tailed unpaired *t*-test.

Differentially expressed miRNAs induced by paclitaxel treatment

Next, we used threshold values $\log_2FC > 1$ or $\log_2FC < -1$ to identify a total of 253 differentially expressed miRNAs that comprised 70 upregulated and 183 downregulated miRNAs (**Figures 2B,C** and **Supplementary Datasheet 2**). Hierarchical clustering analysis revealed 253 differentially expressed miRNAs in the vehicle and PTX groups (**Figure 2D**). We also defined miRNA expression levels as low (0–100), medium (100–1,000), or high (more than 1,000) based on their respective levels in the vehicle group (**Supplementary Datasheet 2**). Our results indicate that nearly equal numbers of miRNAs were upregulated or downregulated in the low expression group. However, PTX induced a downregulation in the expression levels of most miRNAs in the medium and high expression groups (**Figures 2B,C**). These findings suggest that miRNA basal expression levels are an important factor in their expression changes after treatment using PTX.

Of the identified 253 differentially expressed miRNAs, the top 11 significantly upregulated and top 22 significantly downregulated miRNAs with medium or high expression levels are listed in **Table 3**. We then searched studies in PubMED (up to July 09, 2022) to investigate whether these miRNAs have been previously reported in pain-related conditions. The results of our search indicate that 10 miRNAs in the DRGs were reported to be involved in pain regulation induced by nerve injury, diabetes, or inflammation (Rau et al., 2010; Zhang et al., 2011; Wang et al., 2014; Sakai et al., 2017; Jia et al., 2018; Dai et al., 2019; Zhang and Wang, 2019; Xu et al., 2020; Zhang Z. et al., 2020; Li et al., 2021) (**Table 3**). However, changes in the expression levels of some of these miRNAs are opposite under different pain conditions. Because changes in miRNA expression profiles have been reported in spared nerve injury (SNI)-induced neuropathic pain (Dai et al., 2019) and diabetic peripheral neuropathy (DPN) (Bali et al., 2021), we then compared PTX-induced DEGs in the DRGs of our mice with those in SNI-induced or diabetic neuropathic pain models. Our results indicate that only one miRNA, mmu-miR-532-5p, showed consistent changes in expression among these neuropathic pain models (**Table 4**). PTX and DPN shared the highest number of DEGs; among 46 DEGs in total, only 2

were upregulated and the remaining 44 were downregulated. PTX and nerve injury shared five differentially expressed miRNAs, while DPN and nerve injury shared three DEGs (**Figure 2E** and **Supplementary Datasheet 3**). The differentially expressed miRNAs shared among these models may contribute to neuropathic pain irrespective of causative origin. We then used qPCR to validate the expression levels of mmu-miR-29c-3p, mmu-miR-376b-3p, and mmu-miR-532-5p shown in **Tables 3**, **4**, respectively. Our results indicate that PTX induced a downregulation in the expression levels of mmu-miR-376b-3p and mmu-miR-29c-3p (**Figure 2F**), which agreed with our results obtained using RNA-Seq. Nonetheless, qPCR indicated that the expression level of mmu-miR-532-5p was not modified by treatment using PTX (**Figure 2F**).

Differentially expressed circRNAs induced by treatment using paclitaxel

CircRNAs, a type of non-coding RNAs, have been identified as miRNA sponges that regulate the expression and function of coding mRNAs, and are involved in various biological processes including pain (Wang et al., 2018; Zhang et al., 2019; Lin et al., 2020; Song et al., 2020; Zhang H. H. et al., 2020). From our

TABLE 3 The top upregulated or downregulated miRNAs induced by paclitaxel treatment.

Rank	Genes	Log2 (FC)	Expression level	Validated target	Changes under pain condition
1	mmu-miR-181a-2-3p	3.25	Medium		
2	mmu-miR-323-5p	2.76	Medium		
3	mmu-miR-485-5p	2.55	High	Cdc42 and Rac1 (Zhang Z. et al., 2020); ASIC1 (Xu et al., 2020)	Nerve injury↓ (Zhang Z. et al., 2020); Inflammation pain↓ (Xu et al., 2020)
4	mmu-miR-191-3p	2.54	Medium		
5	mmu-let-7d-3p	2.09	High	Oprm1 (Li et al., 2021)	
6	mmu-let-7e-3p	2.02	Medium		
7	mmu-miR-138-1-3p	1.88	Medium		
8	mmu-miR-211-5p	1.87	Medium		
9	mmu-miR-615-3p	1.87	Medium		
10	mmu-miR-139-3p	1.70	Medium		
11	mmu-miR-369-5p	1.51	High		
1	mmu-miR-362-3p	−8.85	Medium		
2	mmu-miR-466b-3p	−7.60	Medium		Nerve injury↓ (Rau et al., 2010)
3	mmu-miR-466c-3p	−7.60	Medium		
4	mmu-miR-466p-3p	−7.60	Medium		
5	mmu-miR-107-3p	−6.43	Medium		
6	mmu-miR-19b-3p	−6.13	High	Potassium channels (Sakai et al., 2017)	Nerve injury↑ (Sakai et al., 2017)
7	mmu-miR-339-5p	−5.85	Medium		Acupuncture↓ (Wang et al., 2014)
8	mmu-miR-365-3p	−5.85	Medium		
9	mmu-miR-1249-3p	−5.74	Medium		Nerve injury↓ (Dai et al., 2019)
10	mmu-miR-674-3p	−5.71	Medium		
11	mmu-miR-376b-5p	−5.66	High		
12	mmu-miR-30e-5p	−5.47	High		
13	mmu-miR-106b-5p	−5.26	Medium		
14	mmu-miR-29c-3p	−5.26	High	PRKCI (Jia et al., 2018)	diabetic db/db mice↑ (Jia et al., 2018)
15	mmu-miR-377-3p	−5.26	Medium		
16	mmu-miR-22-5p	−5.24	High		
17	mmu-miR-142a-3p	−5.11	High		
18	mmu-miR-144-5p	−5.04	Medium		Nerve injury↓ (Rau et al., 2010; Zhang et al., 2011)
19	mmu-miR-17-5p	−5.02	Medium	Potassium channels (Sakai et al., 2017)	Nerve injury↑ (Sakai et al., 2017)
20	mmu-miR-29a-5p	−4.99	Medium		
21	mmu-miR-29a-3p	−4.94	High		
22	mmu-miR-33-5p	−4.93	High	GDNF (Zhang et al., 2019)	Bupivacaine (Bv)-induced neural apoptosis↑ (Zhang et al., 2019); diabetic peripheral neuropathy (Bali et al., 2021)

TABLE 4 Shared differentially expressed miRNAs among neuropathic pain models.

MiRNAs	MiRNA changes		
	PTX	DPN (Bali et al., 2021)	SNI (Dai et al., 2019)
miR-532-5p	↓	↓	↓
miR-132-5p	↑	↓	↑
miR-376b-3p	↓	↓	↑

PTX, paclitaxel; DPN, diabetic peripheral neuropathy; SNI, spared nerve injury.

RNA-Seq data, 16 circRNAs were extracted as DEGs induced by treatment using PTX (Figure 3A and Table 5). RT-PCR was used to further validate several differentially expressed circRNAs showing high fold changes in expression or relative high expression levels. Our results show that the expression levels of mmu_circ_0009357, mmu_circ_0013069, mmu_circ_0006031, and mmu_circ_0001817 were increased by 1.37-, 1.33-, 1.40-, and 1.50-fold, respectively, by PTX treatment compared with their respective levels in control mice; these increases were statistically significant ($P < 0.05$) (Figure 3B). The expression level of mmu_circ_0011289 was also increased by 1.26-fold in response to PTX treatment compared with its levels in control mice, but this change did not reach statistical significance ($P = 0.25$) (Figure 3B).

Because circRNAs can function as miRNA sponges, thereby reducing miRNA ability to target mRNAs (Song et al., 2020), we used CircMIR software (BIOINF, The Affiliated Cancer Hospital of Nanjing Medical University, Nanjing, China) to predict miRNAs that interact with mmu_circ_0009357, mmu_circ_0013069, mmu_circ_0006031, and mmu_circ_0001817 (Figure 4). The predicted miRNAs, which were differentially expressed after induction using PTX, are shown in Figure 4 and Table 6.

TABLE 5 Differentially expressed circRNA induced by paclitaxel treatment.

Gene name	Gene symbol	Log2 (FC)	Q-value
mmu_circ_0013334	Dgki	−0.585	0.019
mmu_circ_0012312	Trrap	−0.485	0.043
mmu_circ_0006735	Tubb5	−0.413	0.030
mmu_circ_0009682	Stmn3	0.489	0.019
mmu_circ_0011019	Ssbp3	0.511	0.023
mmu_circ_0008020	Cox8a	0.541	0.002
mmu_circ_0006024	Arf3	0.609	< 0.001
mmu_circ_0002651	Slc25a39	0.658	< 0.001
mmu_circ_0005798	Grina	0.664	< 0.001
mmu_circ_0001817	None	0.832	< 0.001
mmu_circ_0008835	None	0.875	0.047
mmu_circ_0006881	Tubb4	1.012	< 0.001
mmu_circ_0006031	Mll2	1.276	0.001
mmu_circ_0013069	Ptms	1.314	< 0.001
mmu_circ_0009357	Prnp	1.443	0.007
mmu_circ_0011289	Arid1a	1.773	0.025

Analysis of differentially expressed mRNAs

From our RNA-Seq data, eight mRNAs and three lncRNAs were extracted as DEGs after treatment using PTX (Table 7). Most of these mRNAs showed minor changes in expression

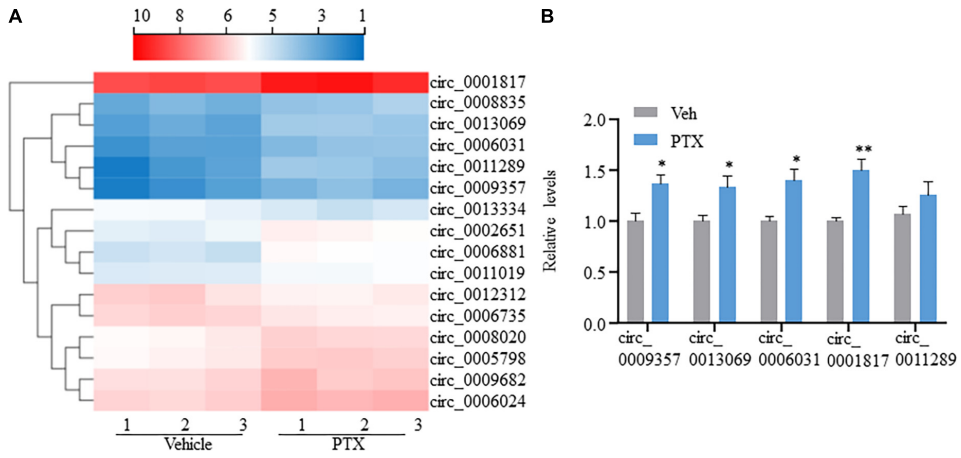

FIGURE 3
Transcriptome profiling and validation of circRNA expression in paclitaxel (PTX)-treated mice. **(A)** Hierarchical clustering analysis shows 16 differentially expressed circRNAs in vehicle and PTX groups. **(B)** Validation of differentially expressed circRNAs using quantitative polymerase chain reaction. Results are presented as mean ± SEM of 4–5 independent experiments. $^*P < 0.05$; $^{**}P < 0.01$ compared with vehicle group by two-tailed unpaired *t*-test.

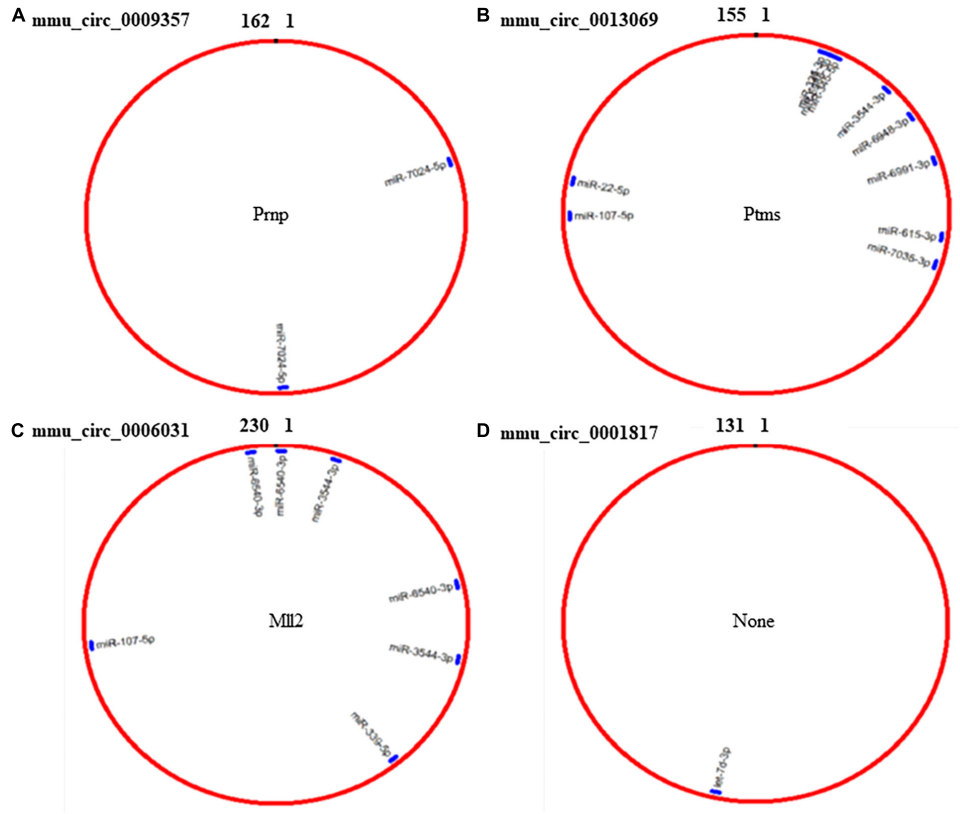

FIGURE 4
Prediction of miRNAs that interact with mmu_circ_0009357, mmu_circ_0013069, mmu_circ_0006031, and mmu_circ_0001817 by circMIR software. **(A)** Predicted binding site for miR-7024-5p on mmu_circ_0009357. **(B)** Combination site for 10 miRNAs on mmu_circ_0013069. **(C)** Predicted binding site for four miRNAs on mmu_circ_0006031. **(D)** Predicted binding site for let-7d-3p on mmu_circ_0001817.

(Table 7). The eight differentially expressed mRNAs upregulated by treatment using PTX were as follows: encoding parathymosin (Ptms); encoding cerebellar degeneration related protein 1 (Cdr1); encoding ribosomal protein L37, retrotransposed (Rpl37rt); encoding period circadian regulator 2 (Per2); encoding nuclear receptor subfamily 1 group D member 1 (Nr1d1), also known as Gvin2; encoding GTPase, very large interferon inducible, family member 2 (Gm4070); encoding D-box binding PAR bZIP transcription factor (Dbp); and encoding XK related X-linked (Xkrx) (Table 7 and Figures 5A,B).

The GO enrichment analysis indicated that these DEGs showed nucleus-, cytoplasm-, membrane-, and dendrite-related functions (Figure 6A), and were also associated with transcription-, translation-, and circadian rhythm-related signaling (Figures 6B,C).

The KEGG pathway analysis was conducted to evaluate the major pathways associated with these eight differentially expressed mRNAs showing upregulated expression. Our results indicate that among these eight mRNAs, Nr1d1 and Per2 were important in the regulation of circadian rhythm and were associated with environmental adaption (Figures 6D,E). Rpl37rt was enriched in ribosome and important in the regulation of translation (Figures 6D,E). KEGG network analysis showed that Nr1d1 and Per2 were connected to others, indicating that they may function jointly (Figure 6F). Protein-protein interactions (PPI) analysis also showed that Nr1d1, Per2, and Dbp shared a common network (Figure 6G).

Starobova et al. (2020) recently described changes in differential gene expression in the DRG following treatment using vincristine, oxaliplatin, or cisplatin. Therefore, we compared PTX-induced DEGs assessed in our present study with those induced by oxaliplatin or cisplatin (Starobova et al., 2020) (Supplementary Datasheet 4). Although five genes (*Alas2*, *Hbb-bt*, *Itgb2l*, *Ly6c2*, and *Nr4a3*) were shared among vincristine, oxaliplatin, and cisplatin (Starobova et al., 2020), none of these genes showed significant changes in expression following treatment with PTX. However, Dbp mRNA showed significant changes in expression levels following treatment using PTX or oxaliplatin (Supplementary Datasheet 4). Moreover, Cdr1 mRNA also showed significant changes in expression levels following treatment using PTX or cisplatin (Supplementary Datasheet 4). We then compared our results with those obtained in a previous study on cisplatin-induced

TABLE 6 CircRNA and miRNA interaction predicted by CircMir software.

PTX-induced differentially expressed circRNAs	PTX-induced differentially expressed miRNAs
mmu_circ_0009357	mmu-miR-7024-5p
mmu_circ_0013069	mmu-miR-326-3p
	mmu-miR-6988-3p
	mmu-miR-345-5p
	mmu-miR-3544-3p
	mmu-miR-6948-3p
	mmu-miR-6991-3p
	mmu-miR-615-3p
	mmu-miR-7035-3p
	mmu-miR-107-5p
	mmu-miR-22-5p
mmu_circ_0006031	mmu-miR-6540-3p
	mmu-miR-3544-3p
	mmu-miR-339-5p
	mmu-miR-107-5p
mmu_circ_0001817	mmu-let-7d-3p

TABLE 7 Differentially expressed mRNA and lncRNA induced by paclitaxel treatment.

Gene ID	Gene name	Type	Log2 (FC)	Q-value
100042856	Gm4070	mRNA	0.467	0.034
69202	Ptms	mRNA	0.514	< 0.001
631990	Cdr1	mRNA	0.627	< 0.001
18627	Per2	mRNA	0.710	0.023
217166	Nr1d1	mRNA	0.911	0.001
13170	Dbp	mRNA	1.096	0.002
331524	Xkrx	mRNA	1.520	< 0.001
100502825	Rpl37rt	mRNA	2.126	< 0.001
BGIG10090_45213	BGIG10090_45213	lncRNA	−0.566	0.023
105246404	Gm41696	lncRNA	0.701	< 0.001
BGIG10090_42549	BGIG10090_42549	lncRNA	2.515	< 0.001

gene expression changes in A/J mice (Lessans et al., 2019). Our results show that *Dbp* was also a shared gene induced by treatment using either PTX or cisplatin (**Supplementary Datasheet 5**). Megat et al. (2019) also sequenced input mRNA, equivalent to the DRG transcriptome, and translating ribosome affinity purification (TRAP) mRNAs associated with translating ribosomes in the Nav1.8 subset of DRG neurons (TRAP-seq) from naive mice and mice with treatment using PTX (at day 10 after treatment). Input transcriptome analysis revealed that only 4 genes were upregulated (Dpep2, Car3, Iah1, and Arhgef4) and 1 was downregulated (Plcb3) in the DRG by treatment using PTX (Megat et al., 2019). Yet, none of these genes were overlapped with the eight differentially expressed mRNAs in the current work.

We previously reported that nerve injury induces changes in thousands of coding and non-coding RNA in injured DRGs (Wu et al., 2016); therefore, in our present study, we compared DEGs in the DRGs induced using PTX with DEGs in the DRGs induced using nerve injury. Our results indicate that none of PTX-induced DEGs showed significant expression changes in the DRGs subjected to nerve injury (**Supplementary Table 1**).

Discussion

In this study, we used RNA-Seq and in-depth gene expression analysis to explore gene expression profiles in the DRGs of PTX-treated mice. Among the identified 67,228 genes, 345 microRNAs, 6 mRNAs, 3 lncRNAs, and 16 circRNAs were differentially expressed in response to treatment using PTX. Several previous studies have reported on DEGs in different neuropathic pain models; therefore, we compared DEG expression and summarized some of genes shared in these neuropathic pain models. We also used RT-PCR to validate the changes in the expression levels of several miRNAs and circRNAs.

MiRNAs are important in regulating pain transmission, and are, therefore, increasingly investigated for their emerging therapeutic potential (Sakai et al., 2017; Dai et al., 2019; Bali et al., 2021). In our present study, we identified 253 differentially expressed miRNAs (70 upregulated and 183 downregulated miRNAs) in PTX-treated mice. Among these miRNAs, several have been shown to contribute to pain regulation (Rau et al., 2010; Zhang et al., 2011; Wang et al., 2014; Sakai et al., 2017; Jia et al., 2018; Dai et al., 2019; Zhang and Wang, 2019; Xu et al., 2020; Zhang Z. et al., 2020; Li et al., 2021). Sakai et al. (2017) reported that miR-17-92 cluster members, including miR-17, miR-18a, miR-19a, miR-19b, miR-20a, and miR-92a, are consistently upregulated in primary sensory neurons after nerve injury, and that the miR-17-92 cluster cooperatively regulates the function of multiple voltage-gated potassium channel subunits, thereby perpetuating mechanical allodynia. However, another study reported that these miRNAs show unchanged expression levels in rats with SNI-induced neuropathic pain (Dai et al., 2019). Curiously, in our present study, most of these miRNAs were downregulated by PTX treatment, as shown by our RNA-Seq data. We then compared PTX induced-differentially expressed miRNAs with DEGs reported in nerve injury and diabetes induced-neuropathic pain models (Dai et al., 2019; Bali et al., 2021). Our results indicate that only mmu-miR-532-5p showed consistently downregulated expression among these three models of neuropathic pain. The shared differentially expressed miRNAs may be important in pain pathogenesis and warrant further investigation. Although the data obtained using high-throughput screening RNA-Seq provide many crucial clues

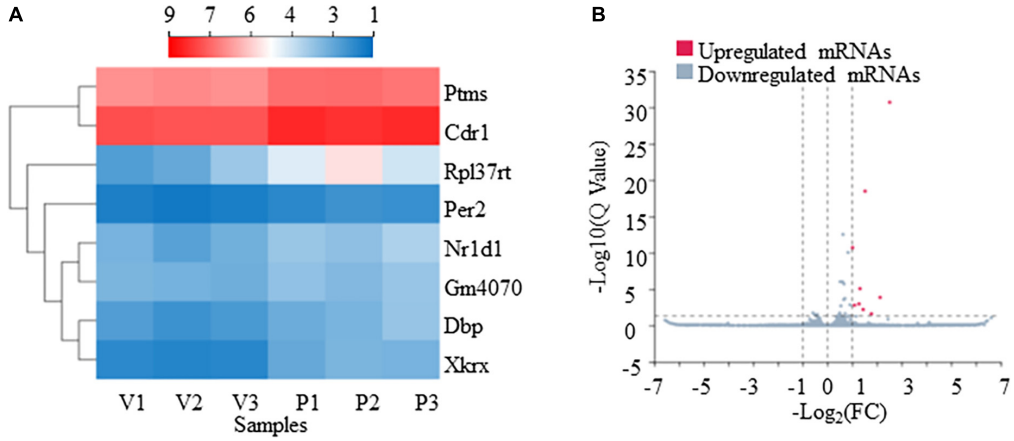

FIGURE 5
Transcriptome profiling of mRNAs in paclitaxel (PTX)-treated mice. **(A)** Hierarchical clustering analysis revealed eight differentially expressed mRNAs in vehicle and PTX groups. **(B)** Volcano plot of differentially expressed mRNAs following PTX administration.

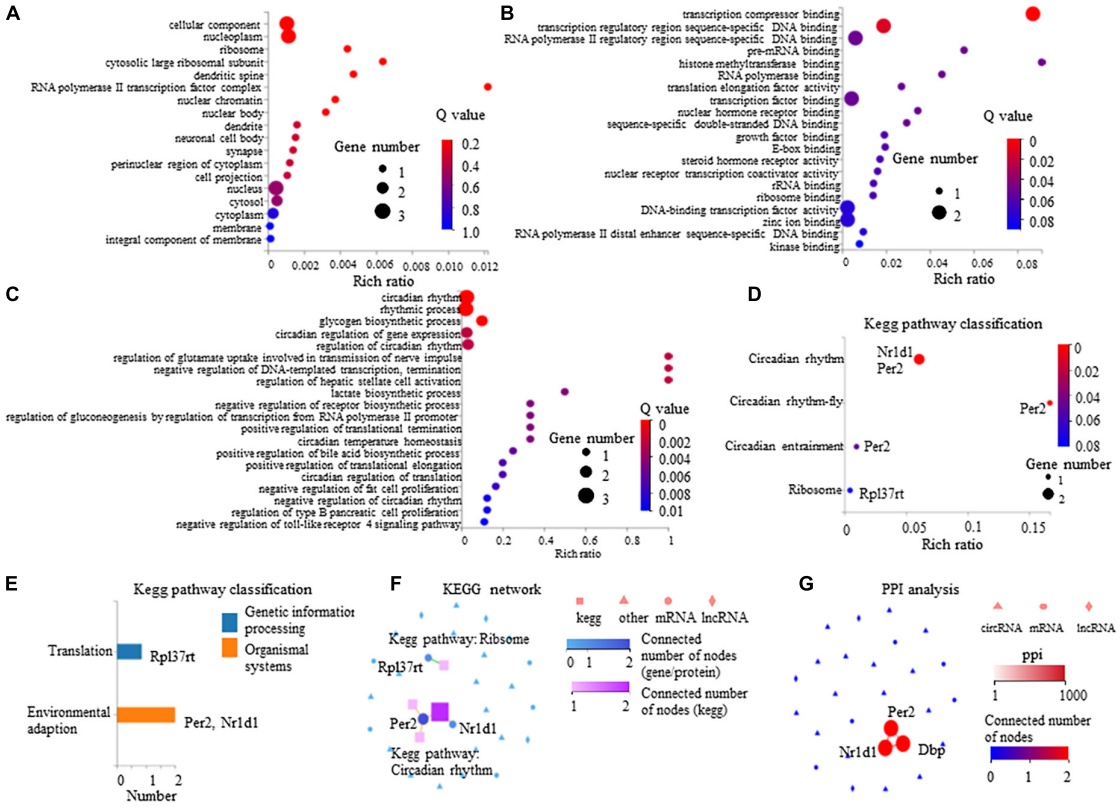

FIGURE 6
Gene Ontology (GO) enrichment analysis and Kyoto Encyclopedia of Genes and Genomes (KEGG) pathway of eight differentially expressed mRNAs in paclitaxel (PTX)-treated mice. **(A)** GO cellular component analysis. **(B)** GO molecular function analysis. **(C)** GO biological process analysis. **(D)** KEGG pathway enrichment analysis. **(E)** KEGG pathway classification analysis. **(F,G)** Connection between *Nr1d1*, *Per2*, and *Dbp* shown by KEGG network **(F)** and protein-protein interactions (PPI) analysis **(G)**.

in the study of pain genesis, further validation studies are necessary to elucidate the mechanisms involved in chronic pain development.

CircRNAs, a type of non-coding RNAs, can mediate the functions of diverse molecules including non-coding RNAs, mRNAs, DNA, and proteins. Thus, circRNAs play critical

roles in tumor genesis and development, in sensitivity to radiation and chemotherapy, and in pain (Wang et al., 2018; Kristensen et al., 2019; Zhang et al., 2019; Lin et al., 2020; Song et al., 2020; Zhang H. H. et al., 2020). In our present study, we found that 16 circRNAs in the DRG showed altered expression levels in response to treatment using PTX. However, no overlapping circRNAs were found in comparing these circRNAs with those dysregulated in mice with diabetes mellitus (Zhang H. H. et al., 2020). CircRNAs usually sponge microRNAs to regulate the expression and function of coding mRNA (Zhang et al., 2019). Our results also show that PTX-induced differentially expressed circRNAs interacted with one or several PTX-induced differentially expressed miRNAs. Among these miRNAs, miR-339 shows upregulated expression in acupuncture, indicating that miR-339 may be involved in acupuncture analgesia (Wang et al., 2014). The miRNA miR-15b plays a critical role in oxaliplatin-induced chronic neuropathic pain via downregulation of BACE1 expression (Ito et al., 2017). Therefore, it is interesting to find out whether a circRNA-miRNA regulatory pathway underlies PTX-induced neuropathic pain.

Chemotherapy-induced peripheral neuropathy and neuropathic pain can be induced by numerous anticancer agents, such as PTX, oxaliplatin, vincristine, and cisplatin, although these drugs have diverse mechanisms of action (Liang et al., 2020a; Starobova et al., 2020; Kang et al., 2021). PTX, which is a chemotherapeutic agent belonging to the taxane class, binds to cytoskeletal microtubules and enhances tubulin polymerization (Jordan and Wilson, 2004). Vincristine inhibits the assembly of β-tubulin (Gan et al., 2010). Platinum derivatives oxaliplatin and cisplatin bind to DNA and interfere with replication, transcription, and the cell cycle (Alcindor and Beauger, 2011; Dasari and Tchounwou, 2014). Several studies have reported on changes in differential gene expression in the DRG following treatment with PTX, vincristine, oxaliplatin, or cisplatin (Megat et al., 2019; Starobova et al., 2020; Kang et al., 2021). Megat et al. (2019) explored the changes of DRG transcriptome in the Nav1.8 subset of DRG neurons by PTX treatment and five differentially expressed genes were identified in the DRG by paclitaxel treatment. Sadly, none of them were overlapped with the PTX-induced differentially expressed mRNAs in the current study. In Dr. Megat's work, they gathered all DRGs from cervical, thoracic, and lumbar levels while we precisely gathered lumbar DRGs. This might be one of the reasons which cause the difference. In another recent work by Sun et al. (2022), RNA-Seq research identified 384 differentially expressed mRNAs in the DRG of rats 14 days after PTX injection. As a full list of 384 DEGs is not available, it is not clear whether some mRNAs were overlapped in these studies. Nevertheless, the genes *Dbp* and *Cdr1* were shared between PTX and other chemotherapeutic agents by comparison of the results obtained in our present study with those obtained in other studies. *Dbp* encodes D site albumin promoter binding protein, which is a member of the Par bZIP transcription factor family; this protein can bind DNA as a homo- or heterodimer and is involved in the regulation of several circadian rhythm genes (Lopez-Molina et al., 1997). *Cdr1* encodes cerebellar degeneration related antigen 1. Further investigation is necessary to explore the role of these genes in PTX-induced neuropathic pain.

Our present study had several limitations. In this study, our RNA-Seq analysis revealed several differentially expressed mRNAs following treatment with PTX. However, previous studies have reported on expression changes in hundreds of genes in PTX-induced DRGs (Zhang et al., 2016; Li et al., 2017; Mao et al., 2019). Previously, we found that PTX induces downregulation in the expression of *K2p1.1* mRNA and protein in DRG neurons (Mao et al., 2019). Downregulation of *K2p1.1* mRNA in the DRG is also attributed to paclitaxel-induced increase in DNMT3a expression levels in the DRG (Mao et al., 2019). However, changes in the expression levels of these genes were not observed in our present study. This is probably due to the large differences among animals treated with PTX. We also observed some miRNAs are oppositely regulated under different pain conditions. The different causative origin may be one of the reasons. On the other hand, the expression level of one miRNA is probably different in the development and maintenance of neuropathic pain. Finally, although transcriptomic analysis of nervous tissue has greatly extended our understanding of pain mechanisms and progression, validation and mechanistic exploration of DEG expression are essential and warrant further investigation.

Data availability statement

The data presented in the study are deposited in the BIG Sub repository (https://ngdc.cncb.ac.cn/gsa/), accession number CRA007673.

Ethics statement

The animal study was reviewed and approved by Institutional Animal Ethics Committee of the Xi'an Jiaotong University Health Science Center.

Author contributions

LL and QM initiated the project, designed the experiments, and analyzed the data. LT, JW, XQZ, HC, XuZ, XL, ZG, and XiZ did behavioral tests and molecular experiment. QM uploaded the RNA-Seq raw data to BIG Sub. LL wrote the manuscript. All authors read and approved the final manuscript.

Funding

This work was supported by the Natural Science Foundation of Chongqing (cstc2019jcyj-msxmX0018) to QM, the National Natural Science Foundation of China (31871065), the China Postdoctoral Science Foundation (2018M633527), and the Shaanxi Province Postdoctoral Science Foundation (2018BSHEDZZ147) to LL.

Conflict of interest

The authors declare that the research was conducted in the absence of any commercial or financial relationships that could be construed as a potential conflict of interest.

Publisher's note

Supplementary material

The Supplementary Material for this article can be found online at: https://www.frontiersin.org/articles/10.3389/fnmol.2022.990260/full#supplementary-material

References

Alcindor, T., and Beauger, N. (2011). Oxaliplatin: a review in the era of molecularly targeted therapy. *Curr. Oncol.* 18, 18–25. doi: 10.3747/co.v18i1.708

Bali, K. K., Gandla, J., Rangel, D. R., Castaldi, L., Mouritzen, P., Agarwal, N., et al. (2021). A genome-wide screen reveals microRNAs in peripheral sensory neurons driving painful diabetic neuropathy. *Pain* 162, 1334–1351. doi: 10.1097/j.pain.0000000000002159

Cock, P. J., Fields, C. J., Goto, N., Heuer, M. L., and Rice, P. M. (2010). The Sanger FASTQ file format for sequences with quality scores, and the Solexa/Illumina FASTQ variants. *Nucleic Acids Res.* 38, 1767–1771. doi: 10.1093/nar/gkp1137

Dai, D., Wang, J., Jiang, Y., Yuan, L., Lu, Y., Zhang, A., et al. (2019). Small RNA sequencing reveals microRNAs related to neuropathic pain in rats. *Braz. J. Med. Biol. Res.* 52:e8380. doi: 10.1590/1414-431X20198380

Dasari, S., and Tchounwou, P. B. (2014). Cisplatin in cancer therapy: molecular mechanisms of action. *Eur. J. Pharmacol.* 740, 364–378. doi: 10.1016/j.ejphar.2014.07.025

Finnerup, N. B., Kuner, R., and Jensen, T. S. (2021). Neuropathic pain: from mechanisms to treatment. *Physiol. Rev.* 101, 259–301. doi: 10.1152/physrev.00045.2019

Gan, P. P., McCarroll, J. A., Po'uha, S. T., Kamath, K., Jordan, M. A., and Kavallaris, M. (2010). Microtubule dynamics, mitotic arrest, and apoptosis: drug-induced differential effects of betaIII-tubulin. *Mol. Cancer Ther.* 9, 1339–1348. doi: 10.1158/1535-7163.MCT-09-0679

Ito, N., Sakai, A., Miyake, N., Maruyama, M., Iwasaki, H., Miyake, K., et al. (2017). miR-15b mediates oxaliplatin-induced chronic neuropathic pain through BACE1 down-regulation. *Br. J. Pharmacol.* 174, 386–395. doi: 10.1111/bph.13698

Jia, L., Wang, L., Chopp, M., Li, C., Zhang, Y., Szalad, A., et al. (2018). MiR-29c/PRKCI Regulates Axonal Growth of Dorsal Root Ganglia Neurons Under Hyperglycemia. *Mol. Neurobiol.* 55, 851–858. doi: 10.1007/s12035-016-0374-5

Jordan, M. A., and Wilson, L. (2004). Microtubules as a target for anticancer drugs. *Nat. Rev. Cancer* 4, 253–265. doi: 10.1038/nrc1317

Kang, L., Tian, Y., Xu, S., and Chen, H. (2021). Oxaliplatin-induced peripheral neuropathy: clinical features, mechanisms, prevention and treatment. *J. Neurol.* 268, 3269–3282. doi: 10.1007/s00415-020-09942-w

Kristensen, L. S., Andersen, M. S., Stagsted, L. V. W., Ebbesen, K. K., Hansen, T. B., and Kjems, J. (2019). The biogenesis, biology and characterization of circular RNAs. *Nat. Rev. Genet.* 20, 675–691. doi: 10.1038/s41576-019-0158-7

Kukurba, K. R., and Montgomery, S. B. (2015). RNA sequencing and analysis. *Cold Spring Harb. Protoc.* 2015, 951–969. doi: 10.1101/pdb.top084970

Langmead, B., and Salzberg, S. L. (2012). Fast gapped-read alignment with Bowtie 2. *Nat. Methods* 9, 357–359. doi: 10.1038/nmeth.1923

Lessans, S., Lassiter, C. B., Carozzi, V., Heindel, P., Semperboni, S., Oggioni, N., et al. (2019). Global transcriptomic profile of dorsal root ganglion and physiological correlates of cisplatin-induced peripheral neuropathy. *Nurs. Res.* 68, 145–155. doi: 10.1097/NNR.0000000000000338

Li, X., Chen, Y., Wang, J., Jiang, C., and Huang, Y. (2021). Lung cancer cell-derived exosomal let-7d-5p down-regulates OPRM1 to promote cancer-induced bone pain. *Front. Cell Dev. Biol.* 9:666857. doi: 10.3389/fcell.2021.666857

Li, Y., Tatsui, C. E., Rhines, L. D., North, R. Y., Harrison, D. S., Cassidy, R. M., et al. (2017). Dorsal root ganglion neurons become hyperexcitable and increase expression of voltage-gated T-type calcium channels (Cav3.2) in paclitaxel-induced peripheral neuropathy. *Pain* 158, 417–429. doi: 10.1097/j.pain.0000000000000774

Liang, L., Lutz, B. M., Bekker, A., and Tao, Y. X. (2015). Epigenetic regulation of chronic pain. *Epigenomics* 7, 235–245. doi: 10.2217/epi.14.75

Liang, L., Wei, J., Tian, L., Padma Nagendra, B. V., Gao, F., Zhang, J., et al. (2020a). Paclitaxel induces sex-biased behavioral deficits and changes in gene expression in mouse prefrontal cortex. *Neuroscience* 426, 168–178. doi: 10.1016/j.neuroscience.2019.11.031

Liang, L., Wu, S., Lin, C., Chang, Y. J., and Tao, Y. X. (2020b). Alternative splicing of Nrcam gene in dorsal root ganglion contributes to neuropathic pain. *J. Pain* 21, 892–904. doi: 10.1016/j.jpain.2019.12.004

Liang, L., Zhang, J., Tian, L., Wang, S., Xu, L., Wang, Y., et al. (2020c). AXL signaling in primary sensory neurons contributes to chronic compression of dorsal root ganglion-induced neuropathic pain in rats. *Mol. Pain* 16:1744806919900814. doi: 10.1177/1744806919900814

Lin, J., Shi, S., Chen, Q., and Pan, Y. (2020). Differential expression and bioinformatic analysis of the circRNA expression in migraine patients. *Biomed. Res. Int.* 2020:4710780. doi: 10.1155/2020/4710780

Lopez-Molina, L., Conquet, F., Dubois-Dauphin, M., and Schibler, U. (1997). The DBP gene is expressed according to a circadian rhythm in the suprachiasmatic nucleus and influences circadian behavior. *EMBO J.* 16, 6762–6771. doi: 10.1093/emboj/16.22.6762

Mao, Q., Wu, S., Gu, X., Du, S., Mo, K., Sun, L., et al. (2019). DNMT3a-triggered downregulation of K2p 1.1 gene in primary sensory neurons contributes to paclitaxel-induced neuropathic pain. *Int. J. Cancer* 145, 2122–2134. doi: 10.1002/ijc.32155

Megat, S., Ray, P. R., Moy, J. K., Lou, T. F., Barragan-Iglesias, P., Li, Y., et al. (2019). Nociceptor translational profiling reveals the ragulator-Rag GTPase complex as a critical generator of neuropathic pain. *J. Neurosci.* 39, 393–411. doi: 10.1523/JNEUROSCI.2661-18.2018

Rau, C. S., Jeng, J. C., Jeng, S. F., Lu, T. H., Chen, Y. C., Liliang, P. C., et al. (2010). Entrapment neuropathy results in different microRNA expression patterns from denervation injury in rats. *BMC Musculoskelet. Disord.* 11:181. doi: 10.1186/1471-2474-11-181

Sakai, A., Saitow, F., Maruyama, M., Miyake, N., Miyake, K., Shimada, T., et al. (2017). MicroRNA cluster miR-17-92 regulates multiple functionally related

voltage-gated potassium channels in chronic neuropathic pain. *Nat. Commun.* 8:16079. doi: 10.1038/ncomms16079

Scholz, J., Finnerup, N. B., Attal, N., Aziz, Q., Baron, R., Bennett, M. I., et al. (2019). The IASP classification of chronic pain for ICD-11: chronic neuropathic pain. *Pain* 160, 53–59. doi: 10.1097/j.pain.0000000000001365

Song, G., Yang, Z., Guo, J., Zheng, Y., Su, X., and Wang, X. (2020). Interactions among lncRNAs/circRNAs, miRNAs, and mRNAs in neuropathic pain. *Neurotherapeutics* 17, 917–931. doi: 10.1007/s13311-020-00881-y

Starobova, H., Mueller, A., Deuis, J. R., Carter, D. A., and Vetter, I. (2020). Inflammatory and neuropathic gene expression signatures of chemotherapy-induced neuropathy induced by vincristine, cisplatin, and oxaliplatin in C57BL/6J mice. *J. Pain* 21, 182–194. doi: 10.1016/j.jpain.2019.06.008

Sun, W., Yang, S., Wu, S., Ba, X., Xiong, D., Xiao, L., et al. (2022). Transcriptome analysis reveals dysregulation of inflammatory and neuronal function in dorsal root ganglion of paclitaxel-induced peripheral neuropathy rats. *Mol. Pain* [Epub ahead of print]. doi: 10.1177/17448069221106167

Wang, J. Y., Li, H., Zhang, L., Ma, C. M., Wang, J. L., Lai, X. S., et al. (2014). Adenosine as a probing tool for the mechanistic study of acupuncture treatment. *Clin. Exp. Pharmacol. Physiol.* 41, 933–939. doi: 10.1111/1440-1681.12304

Wang, L., Feng, Z., Wang, X., Wang, X., and Zhang, X. (2010). DEGseq: an R package for identifying differentially expressed genes from RNA-seq data. *Bioinformatics* 26, 136–138. doi: 10.1093/bioinformatics/btp612

Wang, L., Luo, T., Bao, Z., Li, Y., and Bu, W. (2018). Intrathecal circHIPK3 shRNA alleviates neuropathic pain in diabetic rats. *Biochem. Biophys. Res. Commun.* 505, 644–650. doi: 10.1016/j.bbrc.2018.09.158

Wu, S., Marie Lutz, B., Miao, X., Liang, L., Mo, K., Chang, Y. J., et al. (2016). Dorsal root ganglion transcriptome analysis following peripheral nerve injury in mice. *Mol. Pain* 12:1744806916629048. doi: 10.1177/1744806916629048

Xu, M., Wu, R., Zhang, L., Zhu, H. Y., Xu, G. Y., Qian, W., et al. (2020). Decreased MiR-485-5p contributes to inflammatory pain through post-transcriptional upregulation of ASIC1 in rat dorsal root ganglion. *J. Pain Res.* 13, 3013–3022. doi: 10.2147/JPR.S279902

Zhang, H., Li, Y., de Carvalho-Barbosa, M., Kavelaars, A., Heijnen, C. J., Albrecht, P. J., et al. (2016). Dorsal root ganglion infiltration by macrophages contributes to paclitaxel chemotherapy-induced peripheral neuropathy. *J. Pain* 17, 775–786. doi: 10.1016/j.jpain.2016.02.011

Zhang, H., and Wang, K. (2019). Downregulation of MicroRNA-33-5p protected bupivacaine-induced apoptosis in murine dorsal root ganglion neurons through GDNF. *Neurotox. Res.* 35, 860–866. doi: 10.1007/s12640-018-9994-z

Zhang, H. H., Zhang, Y., Wang, X., Yang, P., Zhang, B. Y., Hu, S., et al. (2020). Circular RNA profile in diabetic peripheral neuropathy: analysis of coexpression networks of circular RNAs and mRNAs. *Epigenomics* 12, 843–857. doi: 10.2217/epi-2020-0011

Zhang, H. Y., Zheng, S. J., Zhao, J. H., Zhao, W., Zheng, L. F., Zhao, D., et al. (2011). MicroRNAs 144, 145, and 214 are down-regulated in primary neurons responding to sciatic nerve transection. *Brain Res.* 1383, 62–70. doi: 10.1016/j.brainres.2011.01.067

Zhang, S. B., Lin, S. Y., Liu, M., Liu, C. C., Ding, H. H., Sun, Y., et al. (2019). CircAnks1a in the spinal cord regulates hypersensitivity in a rodent model of neuropathic pain. *Nat. Commun.* 10:4119. doi: 10.1038/s41467-019-12049-0

Zhang, Z., Li, X., Li, A., and Wu, G. (2020). miR-485-5p suppresses Schwann cell proliferation and myelination by targeting cdc42 and Rac1. *Exp. Cell Res.* 388:111803. doi: 10.1016/j.yexcr.2019.111803

frontiers | Frontiers in Molecular Neuroscience

TYPE Review
PUBLISHED 20 September 2022
DOI 10.3389/fnmol.2022.1007889

OPEN ACCESS

EDITED BY
Xin Zhang,
Duke University, United States

REVIEWED BY
Tong Liu,
Nantong University, China
Andrew M. Tan,
Yale University, United States
Olga Anna Korczeniewska,
The State University of New Jersey, United States

*CORRESPONDENCE
Xiaqing Ma
zxymxq@163.com

†These authors have contributed equally to this work

SPECIALTY SECTION
This article was submitted to Pain Mechanisms and Modulators, a section of the journal Frontiers in Molecular Neuroscience

RECEIVED 31 July 2022
ACCEPTED 30 August 2022
PUBLISHED 20 September 2022

CITATION
Cheng T, Xu Z and Ma X (2022) The role of astrocytes in neuropathic pain. *Front. Mol. Neurosci.* 15:1007889. doi: 10.3389/fnmol.2022.1007889

The role of astrocytes in neuropathic pain

Tong Cheng†, Zhongling Xu† and Xiaqing Ma*

Department of Anesthesiology, Affiliated Hospital of Nantong University, Medical School of Nantong University, Nantong, China

Neuropathic pain, whose symptoms are characterized by spontaneous and irritation-induced painful sensations, is a condition that poses a global burden. Numerous neurotransmitters and other chemicals play a role in the emergence and maintenance of neuropathic pain, which is strongly correlated with common clinical challenges, such as chronic pain and depression. However, the mechanism underlying its occurrence and development has not yet been fully elucidated, thus rendering the use of traditional painkillers, such as non-steroidal anti-inflammatory medications and opioids, relatively ineffective in its treatment. Astrocytes, which are abundant and occupy the largest volume in the central nervous system, contribute to physiological and pathological situations. In recent years, an increasing number of researchers have claimed that astrocytes contribute indispensably to the occurrence and progression of neuropathic pain. The activation of reactive astrocytes involves a variety of signal transduction mechanisms and molecules. Signal molecules in cells, including intracellular kinases, channels, receptors, and transcription factors, tend to play a role in regulating post-injury pain once they exhibit pathological changes. In addition, astrocytes regulate neuropathic pain by releasing a series of mediators of different molecular weights, actively participating in the regulation of neurons and synapses, which are associated with the onset and general maintenance of neuropathic pain. This review summarizes the progress made in elucidating the mechanism underlying the involvement of astrocytes in neuropathic pain regulation.

KEYWORDS

astrocytes, neuropathic pain, signal transduction, cytokine, chemokine

Introduction

Astrocytes or astroglia originate from radial glia cells that have been transformed from neuroepithelial precursor cells in the embryonic tube (Kriegstein and Noctor, 2004; Miller and Gauthier, 2007). As the most abundant and versatile glial cell type, accounting for approximately 20–40% of all glial cells in the central nervous system (CNS) (Colombo and Farina, 2016), astrocytes perform a broad range of different structural functions, including water and ion homeostasis, metabolism specialization, and brain oxidation, thus playing key roles in various levels of CNS function, such as growth, experience-dependent alignment, and maturation. In the absence of disease,

astrocytes assist neurons metabolically and help sustain normal metabolic levels of extracellular K + ions, glutamate, and water. Astrocytes communicate with one another *via* hemichannels that join neighboring cells to construct intercellular gap junction communication pathways. As a result, astrocytes potentially transmit calcium waves and participate in the dissemination of various long-distance signaling molecules. Astrocytes also form a physical barrier around synapses, thus "shielding" them from glutamate overflow while simultaneously providing metabolic support. Furthermore, owing to their proximity to synapses, astrocytes modulate the local intervening ionic and chemical environment during synaptic formation and propagation. Thus, astrocytes play a pivotal role in governing synaptic formation, maturation, removal, and maintenance as well as supporting synaptic activity *via* a combination of diffusible and interaction factors. Loss-of-function disorders of astrocytes may constitute the basis of various forms of neurological dysfunction and pathology, including trauma, stroke, multiple sclerosis, and Alzheimer's disease (Huynh et al., 1997; Weggen et al., 1998; Simpson et al., 2010).

Nociception is recognized as a negative sensorial feeling that is related to or described in terms of real or prospective tissue injury. While acute pain possesses an important protective function, chronic pain is often maladaptive, with no biological benefits. Chronic pain refers to a pain state that lasts for more than 1 month, and it can be derived from several different etiologies. An epidemiological study revealed that the prevalence of chronic pain in China was approximately 31.54%. Other studies have demonstrated that it affects up to 30% of adults worldwide and costs the United States economy over $600 billion per annum (Bouhassira et al., 2008). The long duration of hyperalgesia and ectopic pain has a negative impact on individuals' mental state and enjoyment; therefore, it qualifies as one of the major predisposing factors leading to depression and even suicide. Neuropathic pain is a kind of chronic pain that is common and greatly affects patients' lives, and it is defined by the International Association for the Study of Pain as "pain generated by a lesion or disease of the somatosensory nervous system" (Bouhassira, 2019). A considerable amount of research has been conducted on neuropathic pain in past decades, and it has generally been regarded a consequence of the complex mutual effect of mechanisms in the peripheral and central nervous systems. Importantly, consensus has increasingly corroborated the peculiar roles of reactive glial cells in the onset and persistence of neuropathic pain.

Overview of neuropathic pain

Pain can be perceived as a self-protective mechanism of the body, warning the body of ongoing or impending tissue damage. For example, the pain sensation that occurs when a finger is scraped by a knife is nociceptive pain. If the tissue is damaged, the body will follow up with an inflammatory response, which promotes tissue repair while releasing various mediators that stimulate injury receptors and cause pain. This pain is known as inflammatory pain. In contrast, neuropathic pain is defined as pain produced by injury or disease affecting the somatosensory nervous system and is distinguished by the following clinical presentations: spontaneous pain, nociceptive hyperalgesia, and pain triggered by touch. Neuropathic pain generally affects people more and lasts longer than other types (Torrance et al., 2006) of pain.

Neuropathic pain is typically characterized by both positive and negative sensory symptoms. Positive sensory symptoms include spontaneous positive sensations, such as paresthesia, dysesthesia, paroxysmal pain, and persistent superficial pain, and stimuli-induced positive sensations involving hyperalgesia and allodynia. Mechanical hyperalgesia, typically characterized by a mildly painful, prick-like, irritating stimulation, potentially leads to a more painful sensation. Mechanical dynamic nociception and mechanical static nociception are two terms used to characterize painful conditions caused by slight moving touch and pressure, respectively. In addition, defects in different somatosensory characteristics, including, but not limited to, numbness, deadness, tactile hypoesthesia, reduced heat sensitivity, and lack of vibratory feeling, although habitually overlooked, constitute manifestations of the negative symptoms of neuropathic pain.

Several different mechanisms that are required for neuropathic pain to develop are not limited to the periphery alone, but even extend all the way to the CNS, including the spinal cord, brain, and downstream modulatory system. These mechanisms have preliminarily been explored (Cohen and Mao, 2014). Several maladaptive mechanisms underlying these symptoms not only comprise peripheral hypersensitivity of nociception and hyperexcitability of afferent neurons but also central hypersensitivity, including vicarious pain facilitation, de-suppression of pain sensation, and central restructuring procedures, in addition to sympathetic persistent pain.

To study the occurrence and development of pain, highlight novel pain signaling pathways, and solve emerging issues in the field of pain, such as the development of more effective analgesic drugs and avoidance of adverse effects induced by analgesic drugs, several rodent models for pain research have been established to imitate human pain circumstances. In the course of neuropathic pain research, surgical models are crucial in establishing nociceptive states, predominantly comprising chronic constriction injury (CCI) to the sciatic nerve (Bridges et al., 2001; Hogan, 2002), partial sciatic nerve ligation (Seltzer et al., 1990), spinal nerve ligation (Challa, 2015), spare nerve injury (SNI) (Erichsen and Blackburn-Munro, 2002; Rode et al., 2005; Bourquin et al., 2006), brachial plexus avulsion (Carvalho et al., 1997; Rodrigues-Filho et al., 2003, 2004), spinal nerve transection (SNT) (Li et al., 2002), and sciatic nerve transection models (Wall et al., 1979). Most of these models

induced reactions comparable to those reported in causal pain, a persistent burning pain condition commonly exhibited in human distal limbs following damage to certain peripheral nerves. Under normal conditions, investigators apply different forms of pain to rodents in research projects to identify novel molecular substances and attain commendable achievements in the field of neuropathic pain (Challa, 2015).

Overview of astrocytes

In the CNS, glial cells outnumber neurons by a factor of 10–50, predominantly including astrocytes, microglia, and oligodendrocytes (Moalem and Tracey, 2006). Astrocytes are regarded the most numerous cells in terms of number and volume, accounting for >40% of all glial cells (Aldskogius and Kozlova, 1998). As a class of neural cells originating from the ectoderm and neurepithelium, a single astrocyte is estimated to be capable of wrapping around 140,000 synapses and four to six neuron somata and contacting 300–600 neuron dendrites in rodents (Bushong et al., 2002; Oberheim et al., 2009; Gao and Ji, 2010b). With these physiological strengths, astrocytes sustain homeostasis and are partly responsible for defending the CNS (Verkhratsky and Nedergaard, 2018).

Physiological functions of astrocytes

Utilizing multiple biologically based techniques and state-of-the-art *in vivo* non-traumatic approaches (e.g., positron emission tomography, magnetic resonance imaging scans, and magnetic resonance spectroscopy), astrocytes have been thoroughly studied, and their roles encompass a broad variety of dynamic physiological compositions and functionalized features: water and ion homeostasis, metabolic specialization, and brain oxidation (Volterra and Meldolesi, 2005; Haydon and Carmignoto, 2006; Romero-Sandoval et al., 2008; Fellin, 2009; Jiang et al., 2020).

Astrocytes play a role in neural tissue, closely combining with neural networks, and control the homeostatic balance between individual molecules in the CNS and individual tissues of the entire organ through the transportation of major ions and protons, clearance and decomposition of neurotransmitters, and release of neurotransmitter precursors and reactive oxygen scavengers. Astrocytes maintain neurotransmission as a consequence of providing neurotransmitter precursors for neurons and control cellular homeostasis through embryonic and adult neurogenesis. Moreover, regulating metabolic homeostasis by synthesizing glycogen and providing energy substrates for neurons is also a momentous routine of astrocytes. Disguised as glial cells, astrocytes constitute a cortical covering that envelops the CNS, manage the blood-brain barrier, and serve as chemoreceptors, thereby promoting dynamic homeostasis throughout the body. Traumatic brain injury, infection, and other diseases can increase astrocyte reactivity, thus transforming resting astrocytes into reactive astrocytes with abnormal characteristic behavior. Thus, astrocytes potentially represent the primary defense system of the CNS by increasing reactivity (**Figure 1**).

These routine structural, functional, and physiological strengths of astrocytes play crucial roles in various levels of CNS function, such as growth, experience-dependent alignment, and maturation (Verkhratsky and Nedergaard, 2018; Tsuda, 2019; Giovannoni and Quintana, 2020).

The role of astrocytes in synaptic transmission and synaptic plasticity

The special, close relationship between astrocyte membranes and synaptic structures, the high expression of neurotransmitters in astrocytes, and their regulation of synaptic transmission concertedly create a tripartite synaptic model (Araque et al., 1999; Halassa et al., 2007). Astrocytes potentially serve as a multifunctional key in controlling all aspects of synaptic connections: regulating the maturation of the synaptic network; maintaining the stability of the ionic dynamics of the synaptic cleft; monitoring and regulating the constant changes in neurotransmitters; and ultimately, participating in synaptic extinction (Nedergaard and Verkhratsky, 2012; Verkhratsky and Nedergaard, 2014). In addition, during synaptogenesis, astrocytes surprisingly possess a considerable degree of flexibility and mobility that helps stabilize new synapses. As the close relationship between astrocytes and synapses becomes better understood and more deeply studied, further possibilities for astrocytes in synaptic transmission and plasticity are unfolding (Barker and Ullian, 2010).

The role of astrocytes in memory

Astrocytes have been proven to be intimately involved in neuronal functions in memory formation (Haydon and Nedergaard, 2014; Moraga-Amaro et al., 2014). Suzuki et al. (2011) demonstrated that astrocyte glycogenolysis and lactate release contribute to the formation of long-term memory and maintenance of long-term enhancement of synaptic strength induced *in vivo*. In addition, we have learned that astrocyte-derived lactate produced by glycogenolysis is involved in regulating the changes in substances required for long-term memory formation, including, but not limited to, the expression of target genes and phosphorylation of the transcription factor CREB, among others, thus contributing significantly to long-term memory formation in rats (Suzuki et al., 2011).

Astrocytes in pathology

During the development of neurological diseases, astrocytes often exhibit different pathological manifestations successively

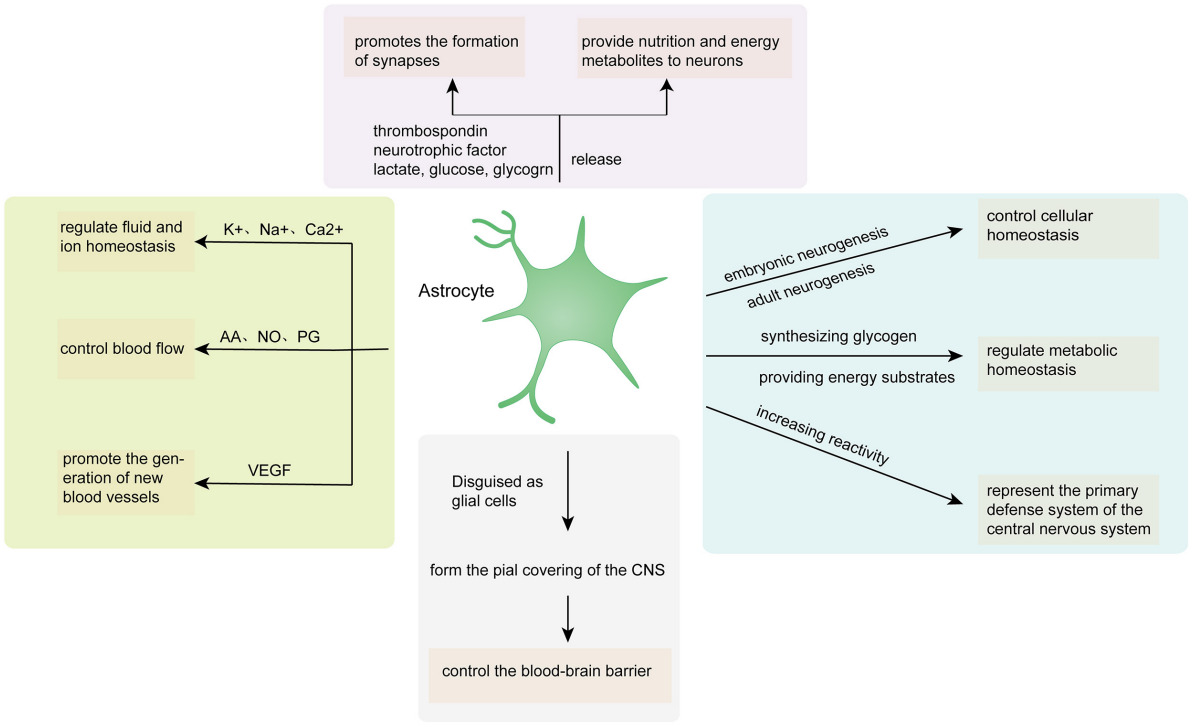

FIGURE 1
Astrocyte functions in the CNS. AA, arachidonic acid; NO, nitric oxide; PG, prostaglandin; VEGF, vascular endothelial growth factor.

or simultaneously, such as, dysfunctional astrocyte atrophy, pathological remodeling of astrocytes, and reactive astrocyte hyperplasia (Pekny et al., 2016). Disorders or loss of function may form the basis of various forms of neurological dysfunction and pathology, including, but not limited to, trauma, stroke, multiple sclerosis, and Alzheimer's disease, among others (Weggen et al., 1998; Simpson et al., 2010).

In addition, they have been linked to a worse prognosis of CNS injury, such as excitatory toxic neurodegeneration due to inadequate glutamate intake (Bush et al., 1999; Swanson et al., 2004) or a higher risk of invasion or injury resulting from astrocyte barrier dysfunction (Bush et al., 1999; Faulkner et al., 2004; Drögemüller et al., 2008; Herrmann et al., 2008; Voskuhl et al., 2009). Extensive molecular and cellular biological evidence has currently demonstrated that the harmful effects of reactive astrogliosis and glial scarring are typically manifested by the inhibition of axon regeneration (Silver and Miller, 2004). Furthermore, astrocytes have appeared in a variety of domestic and international studies on different disease pathological states (Swanson et al., 2004; Brambilla et al., 2005; Jansen et al., 2005; Tian et al., 2005; Hamby et al., 2006; Farina et al., 2007; Brambilla et al., 2009). Some researchers have that found seizures in epilepsy may be directly related to the dysfunction and denaturation of astrocytes triggered by abnormalities in cytotoxic T lymphocytic autoimmunity (Whitney and McNamara, 2000; Bauer et al., 2007). Other autoimmune inflammatory states involving the CNS have also been reasonably speculated to be associated with astrocytes, such as systemic lupus erythematosus; however, they have not been explicitly studied (Tomita et al., 2004). Furthermore, astrocytes have now been firmly considered to make a significant contribution to the pathophysiology of hepatic encephalopathy (Norenberg et al., 2005).

Activation of astrocytes in neuropathic pain

Astrocyte activation has been identified within a few layers of the CNS, such as the spinal cord and supraspinal center (Gao and Ji, 2010b). In fact, current research on the relationship between astrocytes and pain has predominantly focused on the spinal cord level. In pain research, astrocyte activation is commonly understood as the increased expression of the glial fibrillary acidic protein (GFAP) or astrogliosis.

In recent years, two distinct kinds of reactive astrocytes, A1-reactive and A2-reactive astrocytes, have been identified (Liddelow et al., 2017). Induced by neuroinflammation, A1 astrocytes potentially secrete neurotoxins leading to rapid death of neurons and other types of glial cells. Conversely, ischemia-induced A2 astrocytes contribute to more effective tissue healing and neuronal preservation (Liddelow et al., 2017; **Figure 2**).

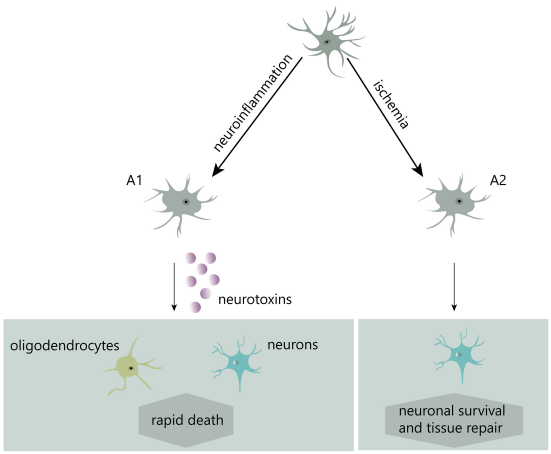

FIGURE 2
Two different types of reactive astrocytes.

A1-reactive astrocytes rather than A2 are mostly believed to be involved in the development of neuropathic pain, and much of the research in this area has focused on them.

Astrocytes from the CNS, particularly the spinal cord, have been shown to undergo morphophysiological and behavioral alterations, such as translation and transcription, following peripheral nerve injury, inflammation, or tumor invasion. Certain activation states, such as an increase in intracellular Ca2+ flux and phosphorylation of signaling molecules, are considered to be completed within minutes. Activation states that take tens of minutes (translation regulation) or hours (transcriptional regulation) to follow also exist. Longer activation states, such as astrogliosis, may require longer periods of time, such as tens of hours or even days to appear (Gao and Ji, 2010b).

Astrocytes are generally believed to regulate pain mainly through the following three activation states: (1) changes in glial signaling pathways, such as changes in the phosphorylation level of mitogen-activated protein kinase (MAPK) and expression of transcription factors; (2) changes in the expression of receptors and channel proteins, such as the upregulation of inflammatory factor receptors and gap junction proteins and downregulation of glutamate transporters; and (3) continuous production and excretion of various glia-derived factors, such as cellular factors, chemokines, and proteinases (Gao and Ji, 2010b; Ji et al., 2013).

Hofstetter et al. (2005) claimed that the transplantation of neural stem cells that can transform into astrocytes into damaged spinal cords resulted in an abnormal, pain-like hypersensitivity response in the front paw. Furthermore, the inhibition of astrocyte differentiation of transplanted cells by transducing neural stem cells with neurogenin-2 before transplanting potentially prevents graft-induced abnormal pain. Inhibitors of glial cells and astrocytes, in particular, fluoroacetate and its metabolite fluorocitrate (FC), only require considerably minute quantities to specifically interfere with astrocyte physiological metabolism *via* obstructing a glial cell enzyme in the astrocytic Krebs cycle. Several mouse models of pain that had undergone intrathecal injection of FC or fluoroacetate demonstrated relief from pain sensation (Milligan et al., 2003; Obata et al., 2006; Clark et al., 2007; Okada-Ogawa et al., 2009). In addition, astrocyte engagement in the ventrolateral periaqueductal gray (vlPAG) was found to be closely associated with pain response. Liu et al. (2022) injected FC into the vlPAG of diabetic neuropathic pain (DNP) rats and found the mechanical withdrawal threshold of DNP rats to decrease significantly, suggesting that the pain-relieving action of FC in DNP rats was related to the inhibition of astrocyte activation in the vlPAG. FC's pain-relieving action has been frequently validated in a wide range of different research topics on neuropathic pain, revealing a close relationship between astrocyte activation and neuropathic pain status.

Key signaling mechanisms and molecules regulating reactive astrocytes

Multiple signal transduction pathways are engaged in the process of converting resting astrocytes into reactive astrocytes (Karimi-Abdolrezaee and Billakanti, 2012). Many diverse cell types, such as neurons, glial cells, and inflammatory cells, release chemical signals that stimulate nascent astrocytes (Pekny et al., 2016). Chemical signals engaged in the regulation of astrocyte activation comprise proinflammatory cytokines [interleukin-1β (IL-1β), tumor necrosis factor α (TNF-α), and interleukin-6 (IL-6)], and gene transcription factors [signal transduction and transcriptional activator 3 (STAT3)], among others (Koyama, 2014; **Figure 3**).

Janus kinase-signal transduction and transcriptional activator 3 pathway

Tsuda demonstrated that astrocyte proliferation in neuropathic pain is regulated by the JAK-STAT3 signaling pathway. Moreover, the application of the janus kinase (JAK) inhibitors AG490 and JAK inhibitor I to the spine resulted in the inhibition of astrocyte proliferation during astrocyte restriction and STAT3 activation. Furthermore, the inhibition of astrocyte proliferation by JAK-STAT3 signaling inhibitors potentially leads to the recovery of haptic pain (Tsuda et al., 2011). Therefore, it is reasonable to conclude that the inhibition of JAK-STAT3 signaling leads to that of astrocyte proliferation in the dorsal horn.

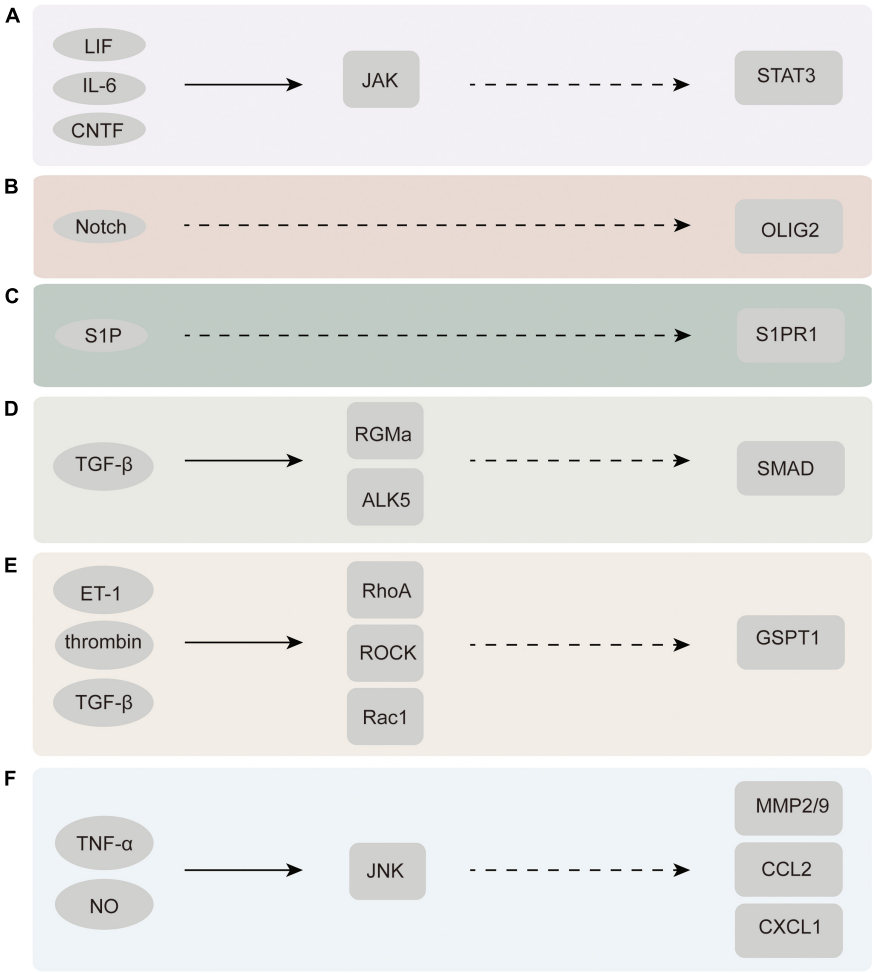

FIGURE 3
Chemicals and molecules that activate astrocytes and their upstream and downstream signaling pathways. **(A)** JAK-STAT3 signaling pathway. **(B)** Notch-Olig2 signaling pathway. **(C)** S1PR1 signaling pathway. **(D)** TGF-β-SMAD signaling pathway. **(E)** Rac1-GSPT1 signaling pathway. **(F)** JNK signaling pathway. LIF, leukemia inhibitory factor; CNTF, ciliary neurotrophic factor; ET-1, endothelin-1; ROCK, rho associated kinase; GSPT1, G1 to S phase transition 1; JNK, C-Jun N-terminal kinase; MMP2/9, matrix metalloproteinase-2/9.

Some experiments have demonstrated that the proliferative capacity of astrocytes intervened by AG490 or with STAT3 defects is reduced to a certain extent (Washburn and Neary, 2006; Sarafian et al., 2010). Liu et al. (2021) demonstrated that not only were the activation levels of JAK2 and STAT3 significantly reduced by miR-135-5p mimics intervention but also GFAP, IL-1β, and TNF-α expression, which was consistently decreased. Moreover, functional *in vitro* studies have also confirmed that miR-135-5p potentially inhibits the JAK2-STAT3 signaling pathway in bone cancer pain, and histological staining has proven that miR-135-5p can directly interrupt the activity process of JAK2 and its upstream and downstream molecules in astrocytes (Liu et al., 2021). These studies demonstrate that JAK-STAT3 signaling has a key contribution in the occurrence and progression of neuropathic pain *via* the modulation of astrocyte activation.

Notch–oligodendrocyte transcription factor 2 pathway

Oligodendrocyte transcription factor 2 (Olig2) is an essential transcription factor required for the proliferation and derivation of developmental astrocytes. Olig2-labeled subsets of astrocytes have been detected in clusters and in greater numbers in certain fixed zones of the thalamus, midbrain, and spinal cord of rodents (Wang et al., 2021). By ablating Olig2, Chen found reactive astrocyte proliferation to be reduced, demonstrating that Olig2 plays a key role in reactive astrocyte proliferation (Chen et al., 2008). A BrdU labeling experiment suggested that Notch molecules may contribute to the numerical increase and functional specialization of reactive astrocytes by regulating the nuclear cytoplasmic translocation of Olig2 (Marumo et al., 2013). Mice with exclusive Notch 1 knockout in GFAP-positive

reactive astrocytes also exhibited a significant reduction in proliferative reactive astrocytes (Shimada et al., 2011). Both mechanical and thermal hyperalgesia induced by CCI were effectively reduced by inhibiting the mRNA expression of Olig2, a marker of astrocyte activation (Bertozzi et al., 2017). The above findings suggest that the Olig2 signaling pathway is highly involved in astrocyte activation and the progression of neuropathic pain.

S1P receptor subtype 1 pathway

Chen et al. (2019) found that sphingosine-1-phosphate (S1P), which is produced in the spinal dorsal horn of CCI and SNI models, actuates neuropathic pain through targeted activation of S1P receptor subtype 1 (S1PR1) present in astrocytes. CCI and SNI models treated with an astrocyte-specific S1PR1 knockout were not observed to experience neuropathic pain. Therefore, astrocytes have been identified as the major cellular substrates for S1PR1 activity. In addition, their study also found that the relief of neuropathic pain induced by S1PR1 inhibition is mediated by interleukin-10 (IL-10), a cellular factor capable of participating in neuroprotection and fighting against inflammatory infections, thus identifying the S1PR1 axis as a key link in the developmental process and signaling pathways of neuropathic pain (Chen et al., 2019). Therefore, S1PR1 is expected to be a novel therapeutic target for neuropathic pain.

Transforming growth factor beta-Sma- and Mad-related protein pathway

Transforming growth factor betas (TGF-βs), as versatile growth factors, are involved in critical events in the body that regulate growth, illness, and wound healing. TGF-β1 has been extensively known to be a cytokine implicated in injury, especially in the activation of astrocytes and scar production (Diniz et al., 2019). TGFβ is immediately triggered following CNS damage and stimulates the Sma- and Mad-related protein (SMAD) family of transcription factors in astrocytes (Koyama, 2014). Ralay Ranaivo et al. (2010) successfully activated the SMAD pathway downstream of TGFβR using albumin in primary astrocyte cultures. Other studies have found that the knockdown of repulsive guidance molecule a (RGMa) eliminates TGFβ1-induced astrocyte proliferation and activation and proved that RGMa potentially promotes TGFβ1/SMAD2/3 signal transduction by binding to activin receptor-like kinase 5 and SMAD2/3 simultaneously, constituting a composite (Zhang et al., 2018). The above findings suggest that the TGF-SMAD signaling pathway is expected to become an important target for astrocyte activation and neuropathic pain treatment.

Rac1–G1 to S phase transition 1 pathway

As a member of the Ras homolog gene family, the small G protein RhoA is widely expressed in astrocytes and participates in cytoskeletal regulation together with its downstream effector Rho-dependent kinase (ROCK) by regulating myosin and actin (Tönges et al., 2011; Maldonado et al., 2017; Wen et al., 2019; Lu et al., 2021). The expression of RhoA and Rac1 in the glial scar area is significantly increased after injury (Erschbamer et al., 2005). Several experimental results reveal that the activation of RhoA/ROCK and its upstream and downstream molecules facilitates the occurrence and sustainment of neuropathic pain (Tatsumi et al., 2005; Hang et al., 2013). The inhibition of ROCK leads to rapid and reversible astral alignment of cultured astrocytes and increases their migratory activity. In one experiment, Rac1-KD or Rac1-KO astrocytes displayed significantly delayed cell cycle progression and decreased cell migration as well as the diminished expression of G1 to S phase transition 1 (GSPT1). In addition, the decreased expression and response of GSPT1 to lipopolysaccharide (LPS) treatment were observed. This suggests that GSPT1 is a downstream target of Rac1 (Ishii et al., 2017). Rac1-GSPT1, as a novel signaling axis in astrocytes, is an important factor in astrocyte activation after CNS injury. However, whether GSPT1 directly leads to neuropathic pain still warrants further research.

Intracellular kinases, channels, transporters, and receptors involved in neuropathic pain regulation in astrocytes

Many signaling molecules exist in astrocytes, including intracellular kinases, channels, receptors, and transcription factors, exhibiting pathological changes and playing a role in pain regulation after injury.

Intracellular kinases

The MAPK family, which is composed of P38, extracellular signal-regulated kinase (ERK), and C-Jun N-terminal kinase (JNK), plays a crucial role in pain regulation (Gao and Ji, 2010b). Different members exhibit specific expressions in various pain states (Ji et al., 2009); nonetheless, all of them have been proven effective in alleviating neuropathic pain in various pain models (Zhuang et al., 2005; Gao et al., 2009; Wang et al., 2012).

Phosphorylated ERK has been observed in spinal astrocytes during the late stage of pain induced by complete Freund's adjuvant (Weyerbacher et al., 2010). In an experiment, Yu used the mitogen-activated ERK kinase inhibitor U0126 to

inhibit astrocyte activation and moderate the release of proinflammatory cytokines (IL-1β and IL-6) by activated astrocytes. The ERK1/2 pathway was found to potentially mediate astrocyte activity through the PPARγ pathway in CCI rats (Zhong et al., 2019).

Choi et al. (2019) demonstrated that the neurosteroid-metabolizing enzyme cytochrome P450c17 stimulates astrocytes through the P38 phosphorylation pathway, eventually contributing to the occurrence of CCI-induced mechanical nociception in mice.

Janus kinase has been shown to engage in the regulation and sustainment of nociception by astrocytes after nerve damage (Cao et al., 2015). P-JNK inhibitors relieve neuropathic pain in mice by inhibiting JNK signaling in spinal cord astrocytes (Li et al., 2020). Tetramethylpyrazine selectively inhibits JNK activity, inhibits astrocyte activation, and reduces matrix metalloproteinase-2/9 (MMP-2/9) expression, thus alleviating the maintenance of neuropathic pain (Jiang et al., 2017). This suggests that JNK-MMP-2/9 is a potentially promising new focus for neuropathic pain relief.

Receptors

To date, relatively few ion channels and receptors that are involved in the activation of astrocytes, thus ultimately leading to the development of neuropathic pain, have been identified (**Table 1**).

Toll-like receptor 4 (TLR-4) is widely present throughout astrocytes. Overexpression of the high mobility group box-1 (HMGB1) protein potentially downregulates the paw withdrawal mechanical threshold and paw withdrawal thermal latency in CCI rodents by enhancing the activation of astrocytes, the TLR4/NF-κB axis, and its upstream and downstream molecules, resulting in the enhancement of neuropathic pain (Zhao et al., 2020). A subject of experimental observations in mice treated with toll-like receptor 2 (TLR2) knockout demonstrated that TLR2 expression is essential for neuropathic pain development. Neurodamage-induced astrocyte activation was also reduced in TLR2-knockout mice. The expression of TLRs has been found to enable astrocytes to release inflammatory mediators closely related to neuropathic pain, including, but not limited to, IL-6, monocyte chemoattractant protein-1 (MCP-1), and nitric oxide (NO) (Thakur et al., 2017). Thus, both TLR2 and TLR4 facilitate the progression and sustainment of pain caused by nerve damage (Kim et al., 2007).

A shortened isomeric form of tyrosine receptor kinase B (TrkB) has recently been found to be implicated in the pathological process of neuropathic pain (Renn et al., 2009). The TrkB.T1 isomeric form is generated through alternative splicing of TrkB. As the only isoform expressed in astrocytes (Rose et al., 2003; Dorsey et al., 2006; Ohira et al., 2007; Holt et al., 2019), Trkb.T1 has exhibited an increased expression in various experimental models of pain (Renn et al., 2009; Wu et al., 2013; Matyas et al., 2017) and attracted increasing attention. Antiretroviral treatment causes abnormal mechanical pain in mice through triggering the activity of brain-derived neurotrophic factor (BDNF) and consequently resulting in polyneuronal hyperactivity (Renn et al., 2011). Trkb.t1-specific knockout mice (Dorsey et al., 2006) were found to be relieved of abnormal pain sensation and heat hyperalgesia in the neuropathic pain model system (Renn et al., 2009). After RNA sequencing work on astrocytes extracted from TrkB.T1 KO mice, the researchers detected a downregulation in the ability

TABLE 1 Expression of ion channels and receptors in astrocytes.

Classifications	Name	Ligands	Mediators regulated *via* activation	Changes in expression in neuropathic pain	References
Ion channels	Connexin-43	Cx43 siRNA, Cx43 mimetic peptide, $Ca_V3.2$, CaMKII	CXCL12, LPS, IL-1β, IL-6, c-fos, ATP	Up-regulated	Gao and Ji, 2010b; Li et al., 2021; Zhu et al., 2022
	Connexin-30	–	IL-1β, IL-6	Up-regulated	Gao and Ji, 2010b
	AQP4	Anti-AQP4 recombinant autoantibodies (rAQP4 IgG), TGN-020, TNF-α	ATP, glutamate transporter 1, c-fos, ERK	Up-regulated	Wang et al., 2020; Ishikura et al., 2021; Guo et al., 2022
Receptors	IL-18 receptor	IL-18	Nuclear factor kappaB	Up-regulated	Miyoshi et al., 2008
	TLR2	Triacylated lipoproteins, peptidoglycan glycolipids, heat shock protein-60, heat shock protein-70	MCP-1, reactive oxygen species, CXCL8, NO, IL-6	Up-regulated	Bowman et al., 2003; Kawai and Akira, 2009; Milligan and Watkins, 2009
	TLR4	LPS, hyaluronate, envprost, heparin, taxol, HMGB1	MCP-1, TNF-α, IL-6, NO, IL-1α, IL-1β,	Up-regulated	Scholz and Woolf, 2007; Nicotra et al., 2012; Thakur et al., 2015
	Trkb.T1	BDNF, ligands of the G-protein-coupled receptor (GPCR) family of transmembrane receptors	Rho GDP dissociation inhibitor, Ca2 +	Up-regulated	Matyas et al., 2017; Cao et al., 2020

of their astrocytes to divide, differentiate, and migrate (Cao et al., 2020). These results suggest that the imbalance in the physiological state of astrocytes caused by the involvement of TrkB.T1 promotes neuropathic pain development.

Considering the prevalence of neuropathic pain and incurable suffering associated with it, the study of ion channels and receptors associated with astrocytes is a potentially new opportunity to bring hope to affected people worldwide. AV411 (ibudilast), an antagonist of TLR4, is currently undergoing phase II clinical trials and has previously been shown to exert satisfactory efficacy in various models of neuropathic pain by inhibiting cytokines produced by glial cells as well as promoting the production of the anti-inflammatory cytokine IL-10 and neurotrophic factors (Connolly and O'Neill, 2012). This presents new directions and possibilities to research on targeted therapy for neuropathic pain. The TLR family and Trkb.T1 deserve further investigation and deeper exploration as key components of astrocytes that are closely linked to neuropathic pain.

Gap junctions

Astrocytes form a network of gap junctions through Ca2+ signals in the form of calcium oscillations (Blomstrand et al., 1999; Haydon, 2001). The main structural components of gap junctions are connexins (CX), such as Cx26, Cx29, Cx30, Cx32, and Cx36, among others. Cx30 and Cx43 are specifically expressed in astrocytes (Giaume and McCarthy, 1996; Nagy et al., 2004). Astrocytic connexins not only regulate gap junction function but also act as semi-channels to transfer and release chemicals such as ATP from inside to outside the cell (Xing et al., 2019), thus regulating synaptic transmission and further leading to pain by directly interacting with injurious neurons (D'Hondt et al., 2014). Cx43 has been shown to effectively regulate the production and release of the chemokine CXCL12 in bone marrow stromal cells (Schajnovitz et al., 2011). Transfection of Cx43 can inhibit LPS-triggered hyperexcitability and upregulation of proinflammatory cellular factors and chemokines (Tsuchida et al., 2013). In addition, intrathecal injection of HIV1 GP120 is followed by a massive proliferation of IL-1β and IL-6 in the cerebrospinal fluid. Carboxy ketone (CBX), a non-specific gap junction antagonist, can block this in a timely and effective manner (Spataro et al., 2004). These behaviors are directly related to neuropathic pain.

Astrocyte-derived inflammatory mediators involved in neuropathic pain regulation

Astrocytes regulate neuropathic pain by releasing a series of mediators of different molecular weights. Macromolecular mediators are represented by cellular factors (e.g., TNF-α and IL-1β), chemokines (e.g., CCL2 and CXCL1), growth factors (e.g., BDNF and bFGF), and proteases (e.g., MMP-2 and tPA), among others. Small molecular media predominantly comprise glutamic acid and ATP, among others. These mediators actively participate in the regulation of neurons and synapses and are inextricably linked to the onset and maintenance of neuropathic pain.

Proinflammatory cytokines

IL-1β is a well-known proinflammatory cytokine. IL-1β upregulation has been observed in spinal cord astrocytes following peripheral nerve lesions. Increasing evidence suggests that IL-1β is involved in pain sensitivity (Cao and Zhang, 2008; Kiguchi et al., 2012). Intrathecal administration of IL-1β receptor antagonists alleviates inflammatory and neuropathic pain. Neuropathic pain was also significantly reduced in mice with IL-1β type I receptor knockout or those deliberately treated with an IL-1β antagonist. In contrast, IL-1β injected into the spinal canal induces pain hypersensitivity (Gao and Ji, 2010b; Ji et al., 2013). Further experiments have also shown that IL-1β is directly sensitive to thermally and chemically sensitive cationic channels in the transient receptor potential cation channel subfamily V member 1 (Kiguchi et al., 2012).

Chemokines

Chemokines, a specific group of cell factors possessing over 50 family components, are widely believed to exist in the blood and immune system and have recently been found to be widespread in the CNS and particularly active in astrocytes (Kiguchi et al., 2012). Chemokines predominantly perform their biological functions by binding to their G-protein-coupled receptors. Current studies have demonstrated that chemokines and corresponding receptors are usually present in different cell types to participate in their interaction and regulation (Gao and Ji, 2010a). CCL2, also called MCP-1, is mainly derived from astrocytes. A remarkable increase in JNK-dependent CCL2 in spinal astrocytes induced by peripheral nerve injury has also been observed, and it has been found to drive neuropathic pain with direct modulation of spinal neurons. CCL2 can rapidly increase the inward currents of spinal dorsal horn neurons induced by AMPA and NMDA. This indicates increased synaptic glutamate transmission, which is strongly associated with increased central sensitization and markedly diminished nociceptive sensation (Gao and Ji, 2010b; Nakagawa and Kaneko, 2010). Furthermore, CCL2 potentially stimulates the division and differentiation of spinal microglia to further support pain development (Nakagawa and Kaneko, 2010).

CCL3 has also been found to cause neuropathic pain through IL-1β upregulation (Kiguchi et al., 2012). CXCL1, an essential cytokine, potentially acts as a mediator, lubricating the communication between neurons and astrocytes (Kiguchi et al., 2012). In spinal nerve ligation models, CXCL1 and its receptor CXCR2 have been observed to undergo upregulation in spinal astrocytes and neurons (Zhang et al., 2013). Intrathecal injection of anti-CXCl1 antibodies has been found to successfully alleviate pain hypersensitivity induced by spinal nerve ligation, and CXCR2 antagonists can definitively terminate CXCl1-induced thermal pain allergy. This implies that CXCL1, CXCR2, and CCL3 are all involved in driving neuropathic pain.

Proteases

Proteases expressed in astrocytes, such as matrix metalloproteinases (MMPs) and tissue-type plasminogen activators (tPAs), have been found to play a key role in the development of neuropathic pain driven by astrocytes (Gao and Ji, 2010b). Different MMPs have been implicated in the progression of neuropathic pain at different periods of time after nerve injury. MMP-9 induces the early development of neuropathic pain by mediating the early cleavage of IL-1β and activation of microglia, while MMP-2 is engaged in the sustainment of neuropathic pain in late stages through modulating the cleavage of IL-1β and activation of astrocytes (Kawasaki et al., 2008).

As an extracellular serine protease, tPA participates in the regulation and revision of tissue components located outside the cell, leading to alterations in neuroplasticity (Kozai et al., 2007). One study found that reactive astrocytes express tPA following trauma to the spinal cord, and tPA inhibitors injected into the spinal canal successfully inhibit mechanical pain triggered by dorsal root ligature (Kozai et al., 2007).

Growth factors

In recent years, BDNF, which binds to TrkB, has been found to be closely associated with astrocyte activation in a rat model of spinal nerve ligation. In certain experimental studies, the BDNF inhibitor ANA-12 was found to inhibit astrocyte activation in the dorsal horn of the spinal cord and subsequently alleviate or even inhibit the onset of mechanical nociceptive hypersensitivity. Increased BDNF levels and proinflammatory cytokines have also been observed following astrocyte activation (Chiang et al., 2012). Similarly, mechanical pain alterations have been reversed using fluorotic acids that inhibit astrocyte activation to downregulate BDNF (Ding et al., 2020). These actions are all accomplished through the binding of BDNF to TrkB.T1, the only TrkB receptor subtype expressed on astrocytes (Wu et al., 2013). BDNF produced by astrocytes has also been found to enhance NMDA receptors in excitatory neurons and decrease inhibitory neuronal activity by accomplishing depolarization displacement of the transient reversal potential (E_{GABA}) and decreased conductance of presynaptic gamma-aminobutyric acid (GABA). These provide BDNF the ability to enhance the synaptic activity of excitatory neurons, thus promoting the development of neuropathic pain (Zhou et al., 2021).

Supraspinal astrocytes in neuropathic pain

As neuroplasticity advances in the spinal cord and ascending routes reach the upper spinal regions, the production and transmission of action potentials are facilitated, resulting in abnormal manifestations of pain behaviors. Of particular interest are the PAG and rostral ventromedial medulla (RVM), which play a key role in nociceptive regulation (Dubový et al., 2018). Belief in the elevated involvement of the PAG and RVM in nociceptive modulation is also growing. Other studies have revealed that unilateral sterile CCI (sCCI) or complete SNT (CSNT) for several weeks induces significant bilateral astrocyte activation in the dlPAG and vlPAG. Astrocyte activation is more extensive in CSNT than in sCCI, and more extensive astrocyte activation is also observed in the RVM. Although the ability of CSNT to trigger astrocyte transformation in the PAG and RVM into an active state is stronger, the ability of the two kinds of sciatic nerve damage to trigger an active state of microglia in upper spinal tectonics is similar. Furthermore, this suggests that reactive astrocytes in the PAG and RVM can be sustained to promote downstream structural groups and consequently maintain neuropathic pain, whereas reactive microglia tend to be involved in response to persistent peripheral nerve injuries. CCL2 secreted by neurons and astrocytes after PAG and RVM damage has the potential to trigger reactive microglia mediated by CCR2 (Dubový et al., 2018). Astrocyte activation in the PAG and RVM contributes indispensably to the progression and sustainment of neuropathic pain.

Astrocyte–microglia and astrocyte–neuron interactions

CCL2 and CXCL1 have been found to be expressed in spinal cord astrocytes, act on CCR2 and CXCR2 in spinal cord neurons, and thus potentially play a role in increasing excitatory synaptic transmission. Studies on electrophysiological aspects found CCL2 to immediately enhance NMDA-induced currents and increase the frequency of excitatory postsynaptic currents in spinal cord lamina II neurons. Co-stimulation of spinal cord neurons with CCL2

and GABA resulted in a dose-dependent and rapid decrease in GABA-induced inward currents (Zhang et al., 2017). CCL7 (monocyte chemotactic protein 3), produced by spinal astrocytes, has also been shown to act on CCR2 in microglia and induce the activation of spinal microglia (Imai et al., 2013). These findings demonstrate that astrocytes do not act independently. They are inextricably linked to neurons and microglia and concertedly contribute to the development of neuropathic pain. This aspect of research warrants deeper exploration.

New analgesic drugs targeting astrocytes

To date, no definitive effective treatment options for neuropathic pain are available worldwide. The most frequently used drugs include tricyclic antidepressants, ion channel-modulating drugs (gabapentin, pregabalin), and some anticonvulsants. These drugs only provide pain relief but do not completely eradicate neuropathic pain, and they often produce a number of side effects (O'Connor and Dworkin, 2009; Zychowska et al., 2015). Other analgesics, such as opioids, are even less effective in the clinical treatment of neuropathic pain (O'Connor and Dworkin, 2009). Although the clinical application of analgesic drugs targeting astrocytes has not yet commenced, targeted treatment of neuropathic pain *via* astrocytes may emerge as a new alternative for affected patients. In fact, several experimental studies are already underway. Dexmedetomidine has been found to effectively inhibit HMGB1-mediated astrocyte activation and the TLR4/NF-κB signaling pathway in CCI rats and successfully relieve neuropathic pain in rats (Zhao et al., 2020). Koumine has been found to exert analgesic effects by inhibiting astrocyte activation and the release of proinflammatory cytokines (Jin et al., 2018). Triptolide, the active component of *Tripterygium wilfordii* Hook F, in combination with MK-801, the non-competitive *N*-methyl-D-aspartate receptor antagonist, inhibits astrocyte activation and STAT phosphorylation, consequently exerting synergistic analgesic effects (Wang et al., 2017). All these drugs inhibit the contributory process of astrocytes to neuropathic pain to a certain extent and are expected to be new protocols and strategies for the treatment of neuropathic pain. However, most of these drugs remain at the animal testing stage, and their specific application methods and exact clinical effects require further investigation and exploration.

Conclusion

To conclude, astrocyte activation and the changes in the signaling pathways and molecular mechanisms involved in the spinal cord and supraspinal structures contribute indispensably to the progression and sustainment of neuropathic pain. Elucidating the mechanism underlying astrocyte activation is of great significance to the progress and development of pain management worldwide. Currently, the exploration of new targeted pain treatments in the wake of opioid overdependence and overuse is of particular importance. Research on the role played by astrocytes in neuropathic pain is expected to realize the clinical transformation of animal experimental research, which is of great significance for human happiness and quality of life.

Author contributions

XM: conceptualization, writing-reviewing, and editing. TC: writing-original draft preparation. ZX: supervision. All authors have approved the final version of the manuscript to be submitted.

Funding

This work was supported by Natural Science Foundation of Affiliated Hospital of Nantong University to XM (grant nos. 101964 and 102209).

Acknowledgments

We would like to thank Editage (www.editage.cn) for English language editing.

Conflict of interest

The authors declare that the research was conducted in the absence of any commercial or financial relationships that could be construed as a potential conflict of interest.

The reviewer TL declared a shared affiliation with the authors to the handling editor at the time of review.

Publisher's note

References

Aldskogius, H., and Kozlova, E. N. (1998). Central neuron-glial and glial-glial interactions following axon injury. *Prog. Neurobiol.* 55, 1–26. doi: 10.1016/s0301-0082(97)00093-2

Araque, A., Parpura, V., Sanzgiri, R. P., and Haydon, P. G. (1999). Tripartite synapses: Glia, the unacknowledged partner. *Trends Neurosci.* 22, 208–215. doi: 10.1016/s0166-2236(98)01349-6

Barker, A. J., and Ullian, E. M. (2010). Astrocytes and synaptic plasticity. *Neuroscientist* 16, 40–50. doi: 10.1177/1073858409339215

Bauer, J., Elger, C. E., Hans, V. H., Schramm, J., Urbach, H., Lassmann, H., et al. (2007). Astrocytes are a specific immunological target in Rasmussen's encephalitis. *Ann. Neurol.* 62, 67–80. doi: 10.1002/ana.21148

Bertozzi, M. M., Rossaneis, A. C., Fattori, V., Longhi-Balbinot, D. T., Freitas, A., Cunha, F. Q., et al. (2017). Diosmin reduces chronic constriction injury-induced neuropathic pain in mice. *Chem. Biol. Interact.* 273, 180–189. doi: 10.1016/j.cbi.2017.06.014

Blomstrand, F., Khatibi, S., Muyderman, H., Hansson, E., Olsson, T., and Rönnbäck, L. (1999). 5-Hydroxytryptamine and glutamate modulate velocity and extent of intercellular calcium signalling in hippocampal astroglial cells in primary cultures. *Neuroscience* 88, 1241–1253. doi: 10.1016/S0306-4522(98)00351-0

Bouhassira, D. (2019). Neuropathic pain: Definition, assessment and epidemiology. *Rev. Neurol.* 175, 16–25. doi: 10.1016/j.neurol.2018.09.016

Bouhassira, D., Lantéri-Minet, M., Attal, N., Laurent, B., and Touboul, C. (2008). Prevalence of chronic pain with neuropathic characteristics in the general population. *Pain* 136, 380–387. doi: 10.1016/j.pain.2007.08.013

Bourquin, A. F., Süveges, M., Pertin, M., Gilliard, N., Sardy, S., Davison, A. C., et al. (2006). Assessment and analysis of mechanical allodynia-like behavior induced by spared nerve injury (SNI) in the mouse. *Pain* 122, 14.e1–14. doi: 10.1016/j.pain.2005.10.036

Bowman, C. C., Rasley, A., Tranguch, S. L., and Marriott, I. (2003). Cultured astrocytes express toll-like receptors for bacterial products. *Glia* 43, 281–291. doi: 10.1002/glia.10256

Brambilla, R., Bracchi-Ricard, V., Hu, W. H., Frydel, B., Bramwell, A., Karmally, S., et al. (2005). Inhibition of astroglial nuclear factor kappaB reduces inflammation and improves functional recovery after spinal cord injury. *J. Exp. Med.* 202, 145–156. doi: 10.1084/jem.20041918

Brambilla, R., Persaud, T., Hu, X., Karmally, S., Shestopalov, V. I., Dvoriantchikova, G., et al. (2009). Transgenic inhibition of astroglial NF-kappa B improves functional outcome in experimental autoimmune encephalomyelitis by suppressing chronic central nervous system inflammation. *J. Immunol.* 182, 2628–2640. doi: 10.4049/jimmunol.0802954

Bridges, D., Thompson, S. W., and Rice, A. S. (2001). Mechanisms of neuropathic pain. *Br. J. Anaesth.* 87, 12–26. doi: 10.1093/bja/87.1.12

Bush, T. G., Puvanachandra, N., Horner, C. H., Polito, A., Ostenfeld, T., Svendsen, C. N., et al. (1999). Leukocyte infiltration, neuronal degeneration, and neurite outgrowth after ablation of scar-forming, reactive astrocytes in adult transgenic mice. *Neuron* 23, 297–308. doi: 10.1016/S0896-6273(00)80781-3

Bushong, E. A., Martone, M. E., Jones, Y. Z., and Ellisman, M. H. (2002). Protoplasmic astrocytes in CA1 stratum radiatum occupy separate anatomical domains. *J. Neurosci.* 22, 183–192. doi: 10.1523/JNEUROSCI.22-01-00183.2002

Cao, H., and Zhang, Y. Q. (2008). Spinal glial activation contributes to pathological pain states. *Neurosci. Biobehav. Rev.* 32, 972–983. doi: 10.1016/j.neubiorev.2008.03.009

Cao, J., Wang, J. S., Ren, X. H., and Zang, W. D. (2015). Spinal sample showing p-JNK and P38 associated with the pain signaling transduction of glial cell in neuropathic pain. *Spinal Cord* 53, 92–97. doi: 10.1038/sc.2014.188

Cao, T., Matyas, J. J., Renn, C. L., Faden, A. I., Dorsey, S. G., and Wu, J. (2020). Function and Mechanisms of Truncated BDNF Receptor TrkB.T1 in Neuropathic Pain. *Cells* 9:1194. doi: 10.3390/cells9051194

Carvalho, G. A., Nikkhah, G., and Samii, M. (1997). Pain management after post-traumatic brachial plexus lesions. Conservative and surgical therapy possibilities. *Orthopade* 26, 621–625. doi: 10.1007/PL00003420

Challa, S. R. (2015). Surgical animal models of neuropathic pain: Pros and Cons. *Int. J. Neurosci.* 125, 170–174. doi: 10.3109/00207454.2014.922559

Chen, Y., Miles, D. K., Hoang, T., Shi, J., Hurlock, E., Kernie, S. G., et al. (2008). The basic helix-loop-helix transcription factor olig2 is critical for reactive astrocyte proliferation after cortical injury. *J. Neurosci.* 28, 10983–10989. doi: 10.1523/JNEUROSCI.3545-08.2008

Chen, Z., Doyle, T. M., Luongo, L., Largent-Milnes, T. M., Giancotti, L. A., Kolar, G., et al. (2019). Sphingosine-1-phosphate receptor 1 activation in astrocytes contributes to neuropathic pain. *Proc. Natl. Acad. Sci. U. S. A.* 116, 10557–10562. doi: 10.1073/pnas.1820466116

Chiang, C. Y., Sessle, B. J., and Dostrovsky, J. O. (2012). Role of astrocytes in pain. *Neurochem. Res.* 37, 2419–2431. doi: 10.1007/s11064-012-0801-6

Choi, S. R., Beitz, A. J., and Lee, J. H. (2019). Inhibition of cytochrome P450c17 reduces spinal astrocyte activation in a mouse model of neuropathic pain via regulation of p38 MAPK phosphorylation. *Biomed. Pharmacother.* 118:109299. doi: 10.1016/j.biopha.2019.109299

Clark, A. K., Gentry, C., Bradbury, E. J., McMahon, S. B., and Malcangio, M. (2007). Role of spinal microglia in rat models of peripheral nerve injury and inflammation. *Eur. J. Pain* 11, 223–230. doi: 10.1016/j.ejpain.2006.02.003

Cohen, S. P., and Mao, J. (2014). Neuropathic pain: Mechanisms and their clinical implications. *BMJ* 348:f7656. doi: 10.1136/bmj.f7656

Colombo, E., and Farina, C. (2016). Astrocytes: Key Regulators of Neuroinflammation. *Trends Immunol.* 37, 608–620. doi: 10.1016/j.it.2016.06.006

Connolly, D. J., and O'Neill, L. A. (2012). New developments in Toll-like receptor targeted therapeutics. *Curr. Opin. Pharmacol.* 12, 510–518. doi: 10.1016/j.coph.2012.06.002

D'Hondt, C., Iyyathurai, J., Himpens, B., Leybaert, L., and Bultynck, G. (2014). Cx43-hemichannel function and regulation in physiology and pathophysiology: Insights from the bovine corneal endothelial cell system and beyond. *Front. Physiol.* 5:348. doi: 10.3389/fphys.2014.00348

Ding, H., Chen, J., Su, M., Lin, Z., Zhan, H., Yang, F., et al. (2020). BDNF promotes activation of astrocytes and microglia contributing to neuroinflammation and mechanical allodynia in cyclophosphamide-induced cystitis. *J. Neuroinflammation* 17:19. doi: 10.1186/s12974-020-1704-0

Diniz, L. P., Matias, I., Siqueira, M., Stipursky, J., and Gomes, F. C. A. (2019). Astrocytes and the TGF-β1 Pathway in the Healthy and Diseased Brain: A Double-Edged Sword. *Mol. Neurobiol.* 56, 4653–4679. doi: 10.1007/s12035-018-1396-y

Dorsey, S. G., Renn, C. L., Carim-Todd, L., Barrick, C. A., Bambrick, L., Krueger, B. K., et al. (2006). In vivo restoration of physiological levels of truncated TrkB.T1 receptor rescues neuronal cell death in a trisomic mouse model. *Neuron* 51, 21–28. doi: 10.1016/j.neuron.2006.06.009

Drögemüller, K., Helmuth, U., Brunn, A., Sakowicz-Burkiewicz, M., Gutmann, D. H., Mueller, W., et al. (2008). Astrocyte gp130 expression is critical for the control of Toxoplasma encephalitis. *J. Immunol.* 181, 2683–2693. doi: 10.4049/jimmunol.181.4.2683

Dubový, P., Klusáková, I., Hradilová-Svíženská, I., Joukal, M., and Boadas-Vaello, P. (2018). Activation of Astrocytes and Microglial Cells and CCL2/CCR2 Upregulation in the Dorsolateral and Ventrolateral Nuclei of Periaqueductal Gray and Rostral Ventromedial Medulla Following Different Types of Sciatic Nerve Injury. *Front. Cell Neurosci.* 12:40. doi: 10.3389/fncel.2018.00040

Erichsen, H. K., and Blackburn-Munro, G. (2002). Pharmacological characterisation of the spared nerve injury model of neuropathic pain. *Pain* 98, 151–161. doi: 10.1016/S0304-3959(02)00039-8

Erschbamer, M. K., Hofstetter, C. P., and Olson, L. (2005). RhoA, RhoB, RhoC, Rac1, Cdc42, and Tc10 mRNA levels in spinal cord, sensory ganglia, and corticospinal tract neurons and long-lasting specific changes following spinal cord injury. *J. Comp. Neurol.* 484, 224–233. doi: 10.1002/cne.20471

Farina, C., Aloisi, F., and Meinl, E. (2007). Astrocytes are active players in cerebral innate immunity. *Trends Immunol.* 28, 138–145. doi: 10.1016/j.it.2007.01.005

Faulkner, J. R., Herrmann, J. E., Woo, M. J., Tansey, K. E., Doan, N. B., and Sofroniew, M. V. (2004). Reactive astrocytes protect tissue and preserve function after spinal cord injury. *J. Neurosci.* 24, 2143–2155. doi: 10.1523/JNEUROSCI.3547-03.2004

Fellin, T. (2009). Communication between neurons and astrocytes: Relevance to the modulation of synaptic and network activity. *J. Neurochem.* 108, 533–544. doi: 10.1111/j.1471-4159.2008.05830.x

Gao, Y. J., and Ji, R. R. (2010b). Targeting astrocyte signaling for chronic pain. *Neurotherapeutics* 7, 482–493. doi: 10.1016/j.nurt.2010.05.016

Gao, Y. J., and Ji, R. R. (2010a). Chemokines, neuronal-glial interactions, and central processing of neuropathic pain. *Pharmacol. Ther.* 126, 56–68. doi: 10.1016/j.pharmthera.2010.01.002

Gao, Y. J., Zhang, L., Samad, O. A., Suter, M. R., Yasuhiko, K., Xu, Z. Z., et al. (2009). JNK-induced MCP-1 production in spinal cord astrocytes contributes to central sensitization and neuropathic pain. *J. Neurosci.* 29, 4096–4108. doi: 10.1523/JNEUROSCI.3623-08.2009

Giaume, C., and McCarthy, K. D. (1996). Control of gap-junctional communication in astrocytic networks. *Trends Neurosci.* 19, 319–325. doi: 10.1016/0166-2236(96)10046-1

Giovannoni, F., and Quintana, F. J. (2020). The Role of Astrocytes in CNS Inflammation. *Trends Immunol.* 41, 805–819. doi: 10.1016/j.it.2020.07.007

Guo, S., Song, Z., He, J., Yin, G., Zhu, J., Liu, H., et al. (2022). Akt/Aquaporin-4 Signaling Aggravates Neuropathic Pain by Activating Astrocytes after Spinal Nerve Ligation in Rats. *Neuroscience* 482, 116–131. doi: 10.1016/j.neuroscience.2021.12.015

Halassa, M. M., Fellin, T., and Haydon, P. G. (2007). The tripartite synapse: Roles for gliotransmission in health and disease. *Trends Mol. Med.* 13, 54–63. doi: 10.1016/j.molmed.2006.12.005

Hamby, M. E., Hewett, J. A., and Hewett, S. J. (2006). TGF-beta1 potentiates astrocytic nitric oxide production by expanding the population of astrocytes that express NOS-2. *Glia* 54, 566–577. doi: 10.1002/glia.20411

Hang, L. H., Shao, D. H., Chen, Z., and Sun, W. J. (2013). Spinal RhoA/Rho kinase signalling pathway may participate in the development of bone cancer pain. *Basic Clin. Pharmacol. Toxicol.* 113, 87–91. doi: 10.1111/bcpt.12069

Haydon, P. G. (2001). GLIA: Listening and talking to the synapse. *Nat. Rev. Neurosci.* 2, 185–193. doi: 10.1038/35058528

Haydon, P. G., and Carmignoto, G. (2006). Astrocyte control of synaptic transmission and neurovascular coupling. *Physiol. Rev.* 86, 1009–1031. doi: 10.1152/physrev.00049.2005

Haydon, P. G., and Nedergaard, M. (2014). How do astrocytes participate in neural plasticity?. *Cold Spring Harb. Perspect. Biol.* 7:a020438. doi: 10.1101/cshperspect.a020438

Herrmann, J. E., Imura, T., Song, B., Qi, J., Ao, Y., Nguyen, T. K., et al. (2008). STAT3 is a critical regulator of astrogliosis and scar formation after spinal cord injury. *J. Neurosci.* 28, 7231–7243. doi: 10.1523/JNEUROSCI.1709-08.2008

Hofstetter, C. P., Holmström, N. A., Lilja, J. A., Schweinhardt, P., Hao, J., Spenger, C., et al. (2005). Allodynia limits the usefulness of intraspinal neural stem cell grafts; directed differentiation improves outcome. *Nat. Neurosci.* 8, 346–353. doi: 10.1038/nn1405

Hogan, Q. (2002). Animal pain models. *Reg. Anesth. Pain Med.* 27, 385–401. doi: 10.1097/00115550-200207000-00009

Holt, L. M., Hernandez, R. D., Pacheco, N. L., Torres Ceja, B., Hossain, M., and Olsen, M. L. (2019). Astrocyte morphogenesis is dependent on BDNF signaling via astrocytic TrkB.T1. *Elife* 8:e44667. doi: 10.7554/eLife.44667

Huynh, D. P., Vinters, H. V., Ho, D. H., Ho, V. V., and Pulst, S. M. (1997). Neuronal expression and intracellular localization of presenilins in normal and Alzheimer disease brains. *J. Neuropathol. Exp. Neurol.* 56, 1009–1017. doi: 10.1097/00005072-199709000-00006

Imai, S., Ikegami, D., Yamashita, A., Shimizu, T., Narita, M., Niikura, K., et al. (2013). Epigenetic transcriptional activation of monocyte chemotactic protein 3 contributes to long-lasting neuropathic pain. *Brain* 136, 828–843. doi: 10.1093/brain/aws330

Ishii, T., Ueyama, T., Shigyo, M., Kohta, M., Kondoh, T., Kuboyama, T., et al. (2017). A Novel Rac1-GSPT1 Signaling Pathway Controls Astrogliosis Following Central Nervous System Injury. *J. Biol. Chem.* 292, 1240–1250. doi: 10.1074/jbc.M116.748871

Ishikura, T., Kinoshita, M., Shimizu, M., Yasumizu, Y., Motooka, D., Okuzaki, D., et al. (2021). Anti-AQP4 autoantibodies promote ATP release from astrocytes and induce mechanical pain in rats. *J. Neuroinflammation* 18:181. doi: 10.1186/s12974-021-02232-w

Jansen, L. A., Uhlmann, E. J., Crino, P. B., Gutmann, D. H., and Wong, M. (2005). Epileptogenesis and reduced inward rectifier potassium current in tuberous sclerosis complex-1-deficient astrocytes. *Epilepsia* 46, 1871–1880. doi: 10.1111/j.1528-1167.2005.00289.x

Ji, R. R., Berta, T., and Nedergaard, M. (2013). Glia and pain: Is chronic pain a gliopathy?. *Pain* 154, S10–S28. doi: 10.1016/j.pain.2013.06.022

Ji, R. R., Gereau, R. W. T., Malcangio, M., and Strichartz, G. R. (2009). MAP kinase and pain. *Brain Res. Rev.* 60, 135–148. doi: 10.1016/j.brainresrev.2008.12.011

Jiang, B. C., Liu, T., and Gao, Y. J. (2020). Chemokines in chronic pain: Cellular and molecular mechanisms and therapeutic potential. *Pharmacol. Ther.* 212:107581. doi: 10.1016/j.pharmthera.2020.107581

Jiang, L., Pan, C. L., Wang, C. Y., Liu, B. Q., Han, Y., Hu, L., et al. (2017). Selective suppression of the JNK-MMP2/9 signal pathway by tetramethylpyrazine attenuates neuropathic pain in rats. *J. Neuroinflammation* 14:174. doi: 10.1186/s12974-017-0947-x

Jin, G. L., Yue, R. C., He, S. D., Hong, L. M., Xu, Y., and Yu, C. X. (2018). Koumine Decreases Astrocyte-Mediated Neuroinflammation and Enhances Autophagy, Contributing to Neuropathic Pain From Chronic Constriction Injury in Rats. *Front. Pharmacol.* 9:989. doi: 10.3389/fphar.2018.00989

Karimi-Abdolrezaee, S., and Billakanti, R. (2012). Reactive astrogliosis after spinal cord injury-beneficial and detrimental effects. *Mol. Neurobiol.* 46, 251–264. doi: 10.1007/s12035-012-8287-4

Kawai, T., and Akira, S. (2009). The roles of TLRs, RLRs and NLRs in pathogen recognition. *Int. Immunol.* 21, 317–337. doi: 10.1093/intimm/dxp017

Kawasaki, Y., Xu, Z. Z., Wang, X., Park, J. Y., Zhuang, Z. Y., Tan, P. H., et al. (2008). Distinct roles of matrix metalloproteases in the early- and late-phase development of neuropathic pain. *Nat. Med.* 14, 331–336. doi: 10.1038/nm1723

Kiguchi, N., Kobayashi, Y., and Kishioka, S. (2012). Chemokines and cytokines in neuroinflammation leading to neuropathic pain. *Curr. Opin. Pharmacol.* 12, 55–61. doi: 10.1016/j.coph.2011.10.007

Kim, D., Kim, M. A., Cho, I. H., Kim, M. S., Lee, S., Jo, E. K., et al. (2007). A critical role of toll-like receptor 2 in nerve injury-induced spinal cord glial cell activation and pain hypersensitivity. *J. Biol. Chem.* 282, 14975–14983. doi: 10.1074/jbc.M607277200

Koyama, Y. (2014). Signaling molecules regulating phenotypic conversions of astrocytes and glial scar formation in damaged nerve tissues. *Neurochem. Int.* 78, 35–42. doi: 10.1016/j.neuint.2014.08.005

Kozai, T., Yamanaka, H., Dai, Y., Obata, K., Kobayashi, K., Mashimo, T., et al. (2007). Tissue type plasminogen activator induced in rat dorsal horn astrocytes contributes to mechanical hypersensitivity following dorsal root injury. *Glia* 55, 595–603. doi: 10.1002/glia.20483

Kriegstein, A. R., and Noctor, S. C. (2004). Patterns of neuronal migration in the embryonic cortex. *Trends Neurosci.* 27, 392–399. doi: 10.1016/j.tins.2004.05.001

Li, G. Z., Hu, Y. H., Lu, Y. N., Yang, Q. Y., Fu, D., Chen, F., et al. (2021). CaMKII and Ca(V)3.2 T-type calcium channel mediate Connexin-43-dependent inflammation by activating astrocytes in vincristine-induced neuropathic pain. *Cell. Biol. Toxicol.* [Epub ahead of print]. doi: 10.1007/s10565-021-09631-y

Li, L., Xian, C. J., Zhong, J. H., and Zhou, X. F. (2002). Effect of lumbar 5 ventral root transection on pain behaviors: A novel rat model for neuropathic pain without axotomy of primary sensory neurons. *Exp. Neurol.* 175, 23–34. doi: 10.1006/exnr.2002.7897

Li, R., Dang, S., Yao, M., Zhao, C., Zhang, W., Cui, J., et al. (2020). Osthole alleviates neuropathic pain in mice by inhibiting the P2Y(1)-receptor-dependent JNK signaling pathway. *Aging* 12, 7945–7962. doi: 10.18632/aging.103114

Liddelow, S. A., Guttenplan, K. A., Clarke, L. E., Bennett, F. C., Bohlen, C. J., Schirmer, L., et al. (2017). Neurotoxic reactive astrocytes are induced by activated microglia. *Nature* 541, 481–487. doi: 10.1038/nature21029

Liu, M., Cheng, X., Yan, H., Chen, J., Liu, C., and Chen, Z. (2021). MiR-135-5p Alleviates Bone Cancer Pain by Regulating Astrocyte-Mediated Neuroinflammation in Spinal Cord through JAK2/STAT3 Signaling Pathway. *Mol. Neurobiol.* 58, 4802–4815. doi: 10.1007/s12035-021-02458-y

Liu, X., He, J., Gao, J., and Xiao, Z. (2022). Fluorocitrate and neurotropin confer analgesic effects on neuropathic pain in diabetic rats via inhibition of astrocyte activation in the periaqueductal gray. *Neurosci. Lett.* 768:136378. doi: 10.1016/j.neulet.2021.136378

Lu, W., Chen, Z., and Wen, J. (2021). RhoA/ROCK signaling pathway and astrocytes in ischemic stroke. *Metab. Brain Dis.* 36, 1101–1108. doi: 10.1007/s11011-021-00709-4

Maldonado, H., Calderon, C., Burgos-Bravo, F., Kobler, O., Zuschratter, W., Ramirez, O., et al. (2017). Astrocyte-to-neuron communication through integrin-engaged Thy-1/CBP/Csk/Src complex triggers neurite retraction via the RhoA/ROCK pathway. *Biochim. Biophys. Acta Mol. Cell. Res.* 1864, 243–254. doi: 10.1016/j.bbamcr.2016.11.006

Marumo, T., Takagi, Y., Muraki, K., Hashimoto, N., Miyamoto, S., and Tanigaki, K. (2013). Notch signaling regulates nucleocytoplasmic Olig2 translocation in reactive astrocytes differentiation after ischemic stroke. *Neurosci. Res.* 75, 204–209. doi: 10.1016/j.neures.2013.01.006

Matyas, J. J., O'Driscoll, C. M., Yu, L., Coll-Miro, M., Daugherty, S., Renn, C. L., et al. (2017). Truncated TrkB.T1-Mediated Astrocyte Dysfunction Contributes to Impaired Motor Function and Neuropathic Pain after Spinal Cord Injury. *J. Neurosci.* 37, 3956–3971. doi: 10.1523/JNEUROSCI.3353-16.2017

Miller, F. D., and Gauthier, A. S. (2007). Timing is everything: Making neurons versus glia in the developing cortex. *Neuron* 54, 357–369. doi: 10.1016/j.neuron.2007.04.019

Milligan, E. D., Twining, C., Chacur, M., Biedenkapp, J., O'Connor, K., Poole, S., et al. (2003). Spinal glia and proinflammatory cytokines mediate mirror-image

neuropathic pain in rats. *J. Neurosci.* 23, 1026–1040. doi: 10.1523/JNEUROSCI.23-03-01026.2003

Milligan, E. D., and Watkins, L. R. (2009). Pathological and protective roles of glia in chronic pain. *Nat. Rev. Neurosci.* 10, 23–36. doi: 10.1038/nrn2533

Miyoshi, K., Obata, K., Kondo, T., Okamura, H., and Noguchi, K. (2008). Interleukin-18-mediated microglia/astrocyte interaction in the spinal cord enhances neuropathic pain processing after nerve injury. *J. Neurosci.* 28, 12775–12787. doi: 10.1523/JNEUROSCI.3512-08.2008

Moalem, G., and Tracey, D. J. (2006). Immune and inflammatory mechanisms in neuropathic pain. *Brain Res. Rev.* 51, 240–264. doi: 10.1016/j.brainresrev.2005.11.004

Moraga-Amaro, R., Jerez-Baraona, J. M., Simon, F., and Stehberg, J. (2014). Role of astrocytes in memory and psychiatric disorders. *J. Physiol.* 108, 240–251. doi: 10.1016/j.jphysparis.2014.08.005

Nagy, J. I., Dudek, F. E., and Rash, J. E. (2004). Update on connexins and gap junctions in neurons and glia in the mammalian nervous system. *Brain Res. Brain Res. Rev.* 47, 191–215. doi: 10.1016/j.brainresrev.2004.05.005

Nakagawa, T., and Kaneko, S. (2010). Spinal astrocytes as therapeutic targets for pathological pain. *J. Pharmacol. Sci.* 114, 347–353. doi: 10.1254/jphs.10R04CP

Nedergaard, M., and Verkhratsky, A. (2012). Artifact versus reality–how astrocytes contribute to synaptic events. *Glia* 60, 1013–1023. doi: 10.1002/glia.22288

Nicotra, L., Loram, L. C., Watkins, L. R., and Hutchinson, M. R. (2012). Toll-like receptors in chronic pain. *Exp. Neurol.* 234, 316–329. doi: 10.1016/j.expneurol.2011.09.038

Norenberg, M. D., Rao, K. V., and Jayakumar, A. R. (2005). Mechanisms of ammonia-induced astrocyte swelling. *Metab. Brain Dis.* 20, 303–318. doi: 10.1007/s11011-005-7911-7

Obata, H., Eisenach, J. C., Hussain, H., Bynum, T., and Vincler, M. (2006). Spinal glial activation contributes to postoperative mechanical hypersensitivity in the rat. *J. Pain* 7, 816–822. doi: 10.1016/j.jpain.2006.04.004

Oberheim, N. A., Takano, T., Han, X., He, W., Lin, J. H., Wang, F., et al. (2009). Uniquely hominid features of adult human astrocytes. *J. Neurosci.* 29, 3276–3287. doi: 10.1523/JNEUROSCI.4707-08.2009

O'Connor, A. B., and Dworkin, R. H. (2009). Treatment of neuropathic pain: An overview of recent guidelines. *Am. J. Med.* 122, S22–S32. doi: 10.1016/j.amjmed.2009.04.007

Ohira, K., Funatsu, N., Homma, K. J., Sahara, Y., Hayashi, M., Kaneko, T., et al. (2007). Truncated TrkB-T1 regulates the morphology of neocortical layer I astrocytes in adult rat brain slices. *Eur. J. Neurosci.* 25, 406–416. doi: 10.1111/j.1460-9568.2007.05282.x

Okada-Ogawa, A., Suzuki, I., Sessle, B. J., Chiang, C. Y., Salter, M. W., Dostrovsky, J. O., et al. (2009). Astroglia in medullary dorsal horn (trigeminal spinal subnucleus caudalis) are involved in trigeminal neuropathic pain mechanisms. *J. Neurosci.* 29, 11161–11171. doi: 10.1523/JNEUROSCI.3365-09.2009

Pekny, M., Pekna, M., Messing, A., Steinhäuser, C., Lee, J. M., Parpura, V., et al. (2016). Astrocytes: A central element in neurological diseases. *Acta Neuropathol.* 131, 323–345. doi: 10.1007/s00401-015-1513-1

Ralay Ranaivo, H., Patel, F., and Wainwright, M. S. (2010). Albumin activates the canonical TGF receptor-smad signaling pathway but this is not required for activation of astrocytes. *Exp. Neurol.* 226, 310–319. doi: 10.1016/j.expneurol.2010.09.005

Renn, C. L., Leitch, C. C., and Dorsey, S. G. (2009). In vivo evidence that truncated trkB.T1 participates in nociception. *Mol. Pain* 5:61. doi: 10.1186/1744-8069-5-61

Renn, C. L., Leitch, C. C., Lessans, S., Rhee, P., McGuire, W. C., Smith, B. A., et al. (2011). Brain-derived neurotrophic factor modulates antiretroviral-induced mechanical allodynia in the mouse. *J. Neurosci. Res.* 89, 1551–1565. doi: 10.1002/jnr.22685

Rode, F., Jensen, D. G., Blackburn-Munro, G., and Bjerrum, O. J. (2005). Centrally-mediated antinociceptive actions of GABA(A) receptor agonists in the rat spared nerve injury model of neuropathic pain. *Eur. J. Pharmacol.* 516, 131–138. doi: 10.1016/j.ejphar.2005.04.034

Rodrigues-Filho, R., Campos, M. M., Ferreira, J., Santos, A. R., Bertelli, J. A., and Calixto, J. B. (2004). Pharmacological characterisation of the rat brachial plexus avulsion model of neuropathic pain. *Brain Res.* 1018, 159–170. doi: 10.1016/j.brainres.2004.05.058

Rodrigues-Filho, R., Santos, A. R., Bertelli, J. A., and Calixto, J. B. (2003). Avulsion injury of the rat brachial plexus triggers hyperalgesia and allodynia in the hindpaws: A new model for the study of neuropathic pain. *Brain Res.* 982, 186–194. doi: 10.1016/S0006-8993(03)03007-5

Romero-Sandoval, E. A., Horvath, R. J., and DeLeo, J. A. (2008). Neuroimmune interactions and pain: Focus on glial-modulating targets. *Curr. Opin. Investig. Drugs* 9, 726–734.

Rose, C. R., Blum, R., Pichler, B., Lepier, A., Kafitz, K. W., and Konnerth, A. (2003). Truncated TrkB-T1 mediates neurotrophin-evoked calcium signalling in glia cells. *Nature* 426, 74–78. doi: 10.1038/nature01983

Sarafian, T. A., Montes, C., Imura, T., Qi, J., Coppola, G., Geschwind, D. H., et al. (2010). Disruption of astrocyte STAT3 signaling decreases mitochondrial function and increases oxidative stress in vitro. *PLoS One* 5:e9532. doi: 10.1371/journal.pone.0009532

Schajnovitz, A., Itkin, T., D'Uva, G., Kalinkovich, A., Golan, K., Ludin, A., et al. (2011). CXCL12 secretion by bone marrow stromal cells is dependent on cell contact and mediated by connexin-43 and connexin-45 gap junctions. *Nat. Immunol.* 12, 391–398. doi: 10.1038/ni.2017

Scholz, J., and Woolf, C. J. (2007). The neuropathic pain triad: Neurons, immune cells and glia. *Nat. Neurosci.* 10, 1361–1368. doi: 10.1038/nn1992

Seltzer, Z., Dubner, R., and Shir, Y. (1990). A novel behavioral model of neuropathic pain disorders produced in rats by partial sciatic nerve injury. *Pain* 43, 205–218. doi: 10.1016/0304-3959(90)91074-S

Shimada, I. S., Borders, A., Aronshtam, A., and Spees, J. L. (2011). Proliferating reactive astrocytes are regulated by Notch-1 in the peri-infarct area after stroke. *Stroke* 42, 3231–3237. doi: 10.1161/STROKEAHA.111.623280

Silver, J., and Miller, J. H. (2004). Regeneration beyond the glial scar. *Nat. Rev. Neurosci.* 5, 146–156. doi: 10.1038/nrn1326

Simpson, J. E., Ince, P. G., Lace, G., Forster, G., Shaw, P. J., Matthews, F., et al. (2010). Astrocyte phenotype in relation to Alzheimer-type pathology in the ageing brain. *Neurobiol. Aging* 31, 578–590. doi: 10.1016/j.neurobiolaging.2008.05.015

Spataro, L. E., Sloane, E. M., Milligan, E. D., Wieseler-Frank, J., Schoeniger, D., Jekich, B. M., et al. (2004). Spinal gap junctions: Potential involvement in pain facilitation. *J. Pain* 5, 392–405. doi: 10.1016/j.jpain.2004.06.006

Suzuki, A., Stern, S. A., Bozdagi, O., Huntley, G. W., Walker, R. H., Magistretti, P. J., et al. (2011). Astrocyte-neuron lactate transport is required for long-term memory formation. *Cell* 144, 810–823. doi: 10.1016/j.cell.2011.02.018

Swanson, R. A., Ying, W., and Kauppinen, T. M. (2004). Astrocyte influences on ischemic neuronal death. *Curr. Mol. Med.* 4, 193–205. doi: 10.2174/1566524043479185

Tatsumi, S., Mabuchi, T., Katano, T., Matsumura, S., Abe, T., Hidaka, H., et al. (2005). Involvement of Rho-kinase in inflammatory and neuropathic pain through phosphorylation of myristoylated alanine-rich C-kinase substrate (MARCKS). *Neuroscience* 131, 491–498. doi: 10.1016/j.neuroscience.2004.10.022

Thakur, K. K., Bolshette, N. B., Trandafir, C., Jamdade, V. S., Istrate, A., Gogoi, R., et al. (2015). Role of toll-like receptors in multiple myeloma and recent advances. *Exp. Hematol.* 43, 158–167. doi: 10.1016/j.exphem.2014.11.003

Thakur, K. K., Saini, J., Mahajan, K., Singh, D., Jayswal, D. P., Mishra, S., et al. (2017). Therapeutic implications of toll-like receptors in peripheral neuropathic pain. *Pharmacol. Res.* 115, 224–232. doi: 10.1016/j.phrs.2016.11.019

Tian, G. F., Azmi, H., Takano, T., Xu, Q., Peng, W., Lin, J., et al. (2005). An astrocytic basis of epilepsy. *Nat. Med.* 11, 973–981. doi: 10.1038/nm1277

Tomita, M., Khan, R. L., Blehm, B. H., and Santoro, T. J. (2004). The potential pathogenetic link between peripheral immune activation and the central innate immune response in neuropsychiatric systemic lupus erythematosus. *Med. Hypotheses* 62, 325–335. doi: 10.1016/j.mehy.2003.10.009

Tönges, L., Koch, J. C., Bähr, M., and Lingor, P. (2011). ROCKing Regeneration: Rho Kinase Inhibition as Molecular Target for Neurorestoration. *Front. Mol. Neurosci.* 4:39. doi: 10.3389/fnmol.2011.00039

Torrance, N., Smith, B. H., Bennett, M. I., and Lee, A. J. (2006). The epidemiology of chronic pain of predominantly neuropathic origin. Results from a general population survey. *J. Pain* 7, 281–289. doi: 10.1016/j.jpain.2005.11.008

Tsuchida, S., Arai, Y., Kishida, T., Takahashi, K. A., Honjo, K., Terauchi, R., et al. (2013). Silencing the expression of connexin 43 decreases inflammation and joint destruction in experimental arthritis. *J. Orthop. Res.* 31, 525–530. doi: 10.1002/jor.22263

Tsuda, M. (2019). Microglia-Mediated Regulation of Neuropathic Pain: Molecular and Cellular Mechanisms. *Biol. Pharm. Bull.* 42, 1959–1968. doi: 10.1248/bpb.b19-00715

Tsuda, M., Kohro, Y., Yano, T., Tsujikawa, T., Kitano, J., Tozaki-Saitoh, H., et al. (2011). JAK-STAT3 pathway regulates spinal astrocyte proliferation and

neuropathic pain maintenance in rats. *Brain* 134, 1127–1139. doi: 10.1093/brain/awr025

Verkhratsky, A., and Nedergaard, M. (2014). Astroglial cradle in the life of the synapse. *Philos. Trans. R. Soc. Lond. B Biol. Sci.* 369:20130595. doi: 10.1098/rstb.2013.0595

Verkhratsky, A., and Nedergaard, M. (2018). Physiology of Astroglia. *Physiol. Rev.* 98, 239–389. doi: 10.1152/physrev.00042.2016

Volterra, A., and Meldolesi, J. (2005). Astrocytes, from brain glue to communication elements: The revolution continues. *Nat. Rev. Neurosci.* 6, 626–640. doi: 10.1038/nrn1722

Voskuhl, R. R., Peterson, R. S., Song, B., Ao, Y., Morales, L. B., Tiwari-Woodruff, S., et al. (2009). Reactive astrocytes form scar-like perivascular barriers to leukocytes during adaptive immune inflammation of the CNS. *J. Neurosci.* 29, 11511–11522. doi: 10.1523/JNEUROSCI.1514-09.2009

Wall, P. D., Devor, M., Inbal, R., Scadding, J. W., Schonfeld, D., Seltzer, Z., et al. (1979). Autotomy following peripheral nerve lesions: Experimental anaesthesia dolorosa. *Pain* 7, 103–113. doi: 10.1016/0304-3959(79)90002-2

Wang, C., Wu, Q., Wang, Z., Hu, L., Marshall, C., and Xiao, M. (2020). Aquaporin 4 knockout increases complete freund's adjuvant-induced spinal central sensitization. *Brain Res. Bull.* 156, 58–66. doi: 10.1016/j.brainresbull.2020.01.004

Wang, H., Xu, L., Lai, C., Hou, K., Chen, J., Guo, Y., et al. (2021). Region-specific distribution of Olig2-expressing astrocytes in adult mouse brain and spinal cord. *Mol. Brain* 14:36. doi: 10.1186/s13041-021-00747-0

Wang, J., Qiao, Y., Yang, R. S., Zhang, C. K., Wu, H. H., Lin, J. J., et al. (2017). The synergistic effect of treatment with triptolide and MK-801 in the rat neuropathic pain model. *Mol. Pain* 13:1744806917746564. doi: 10.1177/1744806917746564

Wang, X. W., Li, T. T., Zhao, J., Mao-Ying, Q. L., Zhang, H., Hu, S., et al. (2012). Extracellular signal-regulated kinase activation in spinal astrocytes and microglia contributes to cancer-induced bone pain in rats. *Neuroscience* 217, 172–181. doi: 10.1016/j.neuroscience.2012.04.065

Washburn, K. B., and Neary, J. T. (2006). P2 purinergic receptors signal to STAT3 in astrocytes: Difference in STAT3 responses to P2Y and P2X receptor activation. *Neuroscience* 142, 411–423. doi: 10.1016/j.neuroscience.2006.06.034

Weggen, S., Diehlmann, A., Buslei, R., Beyreuther, K., and Bayer, T. A. (1998). Prominent expression of presenilin-1 in senile plaques and reactive astrocytes in Alzheimer's disease brain. *Neuroreport* 9, 3279–3283.

Wen, J. Y., Gao, S. S., Chen, F. L., Chen, S., Wang, M., and Chen, Z. W. (2019). Role of CSE-Produced H(2)S on Cerebrovascular Relaxation via RhoA-ROCK Inhibition and Cerebral Ischemia-Reperfusion Injury in Mice. *ACS Chem. Neurosci.* 10, 1565–1574. doi: 10.1021/acschemneuro.8b00533

Weyerbacher, A. R., Xu, Q., Tamasdan, C., Shin, S. J., and Inturrisi, C. E. (2010). N-Methyl-D-aspartate receptor (NMDAR) independent maintenance of inflammatory pain. *Pain* 148, 237–246. doi: 10.1016/j.pain.2009.11.003

Whitney, K. D., and McNamara, J. O. (2000). GluR3 autoantibodies destroy neural cells in a complement-dependent manner modulated by complement regulatory proteins. *J. Neurosci.* 20, 7307–7316. doi: 10.1523/JNEUROSCI.20-19-07307.2000

Wu, J., Renn, C. L., Faden, A. I., and Dorsey, S. G. (2013). TrkB.T1 contributes to neuropathic pain after spinal cord injury through regulation of cell cycle pathways. *J. Neurosci.* 33, 12447–12463. doi: 10.1523/JNEUROSCI.0846-13.2013

Xing, L., Yang, T., Cui, S., and Chen, G. (2019). Connexin Hemichannels in Astrocytes: Role in CNS Disorders. *Front. Mol. Neurosci.* 12:23. doi: 10.3389/fnmol.2019.00023

Zhang, R., Wu, Y., Xie, F., Zhong, Y., Wang, Y., Xu, M., et al. (2018). RGMa mediates reactive astrogliosis and glial scar formation through TGFβ1/Smad2/3 signaling after stroke. *Cell Death Differ.* 25, 1503–1516. doi: 10.1038/s41418-018-0058-y

Zhang, Z. J., Cao, D. L., Zhang, X., Ji, R. R., and Gao, Y. J. (2013). Chemokine contribution to neuropathic pain: Respective induction of CXCL1 and CXCR2 in spinal cord astrocytes and neurons. *Pain* 154, 2185–2197. doi: 10.1016/j.pain.2013.07.002

Zhang, Z. J., Jiang, B. C., and Gao, Y. J. (2017). Chemokines in neuron-glial cell interaction and pathogenesis of neuropathic pain. *Cell. Mol. Life Sci.* 74, 3275–3291. doi: 10.1007/s00018-017-2513-1

Zhao, E., Bai, L., Li, S., Li, L., Dou, Z., Huang, Y., et al. (2020). Dexmedetomidine Alleviates CCI-Induced Neuropathic Pain via Inhibiting HMGB1-Mediated Astrocyte Activation and the TLR4/NF-κB Signaling Pathway in Rats. *Neurotox. Res.* 38, 723–732. doi: 10.1007/s12640-020-00245-6

Zhong, Y., Chen, J., Chen, J., Chen, Y., Li, L., and Xie, Y. (2019). Crosstalk between Cdk5/p35 and ERK1/2 signalling mediates spinal astrocyte activity via the PPARγ pathway in a rat model of chronic constriction injury. *J. Neurochem.* 151, 166–184. doi: 10.1111/jnc.14827

Zhou, W., Xie, Z., Li, C., Xing, Z., Xie, S., Li, M., et al. (2021). Driving effect of BDNF in the spinal dorsal horn on neuropathic pain. *Neurosci. Lett.* 756:135965. doi: 10.1016/j.neulet.2021.135965

Zhu, D., Fan, T., Chen, Y., Huo, X., Li, Y., Liu, D., et al. (2022). CXCR4/CX43 Regulate Diabetic Neuropathic Pain via Intercellular Interactions between Activated Neurons and Dysfunctional Astrocytes during Late Phase of Diabetes in Rats and the Effects of Antioxidant N-Acetyl-L-Cysteine. *Oxid. Med. Cell. Longev.* 2022:8547563. doi: 10.1155/2022/8547563

Zhuang, Z. Y., Gerner, P., Woolf, C. J., and Ji, R. R. (2005). ERK is sequentially activated in neurons, microglia, and astrocytes by spinal nerve ligation and contributes to mechanical allodynia in this neuropathic pain model. *Pain* 114, 149–159. doi: 10.1016/j.pain.2004.12.022

Zychowska, M., Rojewska, E., Makuch, W., Przewlocka, B., and Mika, J. (2015). The influence of microglia activation on the efficacy of amitriptyline, doxepin, milnacipran, venlafaxine and fluoxetine in a rat model of neuropathic pain. *Eur. J. Pharmacol.* 749, 115–123. doi: 10.1016/j.ejphar.2014.11.022

frontiers | Frontiers in Molecular Neuroscience

TYPE Review
PUBLISHED 05 October 2022
DOI 10.3389/fnmol.2022.1006908

OPEN ACCESS

EDITED BY
Sung Jun Jung,
Hanyang University, South Korea

REVIEWED BY
Sun Wook Hwang,
Korea University, South Korea
Joo Min Park,
Institute for Basic Science, South Korea

*CORRESPONDENCE
Linlin Zhang
linlinzhang@tmu.edu.cn
Qing Li
anelivea@126.com

†These authors have contributed equally to this work

SPECIALTY SECTION
This article was submitted to Pain Mechanisms and Modulators, a section of the journal Frontiers in Molecular Neuroscience

RECEIVED 29 July 2022
ACCEPTED 13 September 2022
PUBLISHED 05 October 2022

CITATION
Li Z, Zhang H, Wang Y, Li Y, Li Q and Zhang L (2022) The distinctive role of menthol in pain and analgesia: Mechanisms, practices, and advances.
Front. Mol. Neurosci. 15:1006908.
doi: 10.3389/fnmol.2022.1006908

The distinctive role of menthol in pain and analgesia: Mechanisms, practices, and advances

Ziping Li[1†], Haoyue Zhang[1,2†], Yigang Wang[1,2†], Yize Li[2], Qing Li[2*] and Linlin Zhang[2*]

[1]The Graduate School, Tianjin Medical University, Tianjin, China, [2]Department of Anesthesiology, Tianjin Medical University General Hospital, Tianjin, China

Menthol is an important flavoring additive that triggers a cooling sensation. Under physiological condition, low to moderate concentrations of menthol activate transient receptor potential cation channel subfamily M member 8 (TRPM8) in the primary nociceptors, such as dorsal root ganglion (DRG) and trigeminal ganglion, generating a cooling sensation, whereas menthol at higher concentration could induce cold allodynia, and cold hyperalgesia mediated by TRPM8 sensitization. In addition, the paradoxical irritating properties of high concentrations of menthol is associated with its activation of transient receptor potential cation channel subfamily A member 1 (TRPA1). Under pathological situation, menthol activates TRPM8 to attenuate mechanical allodynia and thermal hyperalgesia following nerve injury or chemical stimuli. Recent reports have recapitulated the requirement of central group II/III metabotropic glutamate receptors (mGluR) with endogenous κ-opioid signaling pathways for menthol analgesia. Additionally, blockage of sodium channels and calcium influx is a determinant step after menthol exposure, suggesting the possibility of menthol for pain management. In this review, we will also discuss and summarize the advances in menthol-related drugs for pathological pain treatment in clinical trials, especially in neuropathic pain, musculoskeletal pain, cancer pain and postoperative pain, with the aim to find the promising therapeutic candidates for the resolution of pain to better manage patients with pain in clinics.

KEYWORDS

menthol, pain, transient receptor potential channel, opioid receptor, analgesia

Introduction

Chronic pain affecting more than 30% of people worldwide (Cohen et al., 2021) with enormous personal and financial burdens. Concerns about the adverse effects, interactions, and potential for abuse of analgesic drugs have forced the search for alternative methods to manage pain effectively and safely. Although several therapies

have been proposed, inadequate knowledge of the underlying pathophysiological mechanisms is one of the reasons for the current lack of pain relief.

Menthol have been used for pain relief since ancient times, first described by Hippocrates (Sprengell, 1708) and Galen (Siegel, 1970). Hippocrates considered mint as a cooling agent for peripheral pain. Galen expanded the use of menthol even further, so that existing topical analgesic containing menthol were named "Menthol Galen-Pharma." Menthol is a cyclic monoterpene alcohol, which is derived primarily from aromatic plants. It is a natural compound with three asymmetric carbon atoms and, thus occurs as four pairs of optical isomers namely (+)- and (-)-isomenthol, (+)- and (-)- menthol, (+)- and (-)-neumenthol, (+)- and (-)-neoisomenthol. The principal form of menthol found in nature is (-)-menthol (L-menthol), and the main supply is obtained naturally. The Nobel Prize for chemistry was awarded to Ryoji Noyori in 2001 for the work on asymmetric catalysis for menthol chemical synthesis (Kamatou et al., 2013).

Menthol is one of the most important flavorings additives besides vanilla and citrus (Kamatou et al., 2013) and is used as a cooling and/or flavors enhancing ingredient in medicines, cosmetics and insecticides, confectionery, chewing gum, liqueurs, toothpaste, shampoos, and soaps (Patel et al., 2007; Kolassa, 2013). Menthol exhibits unique, multiple, and paradoxical sensory effects when applied externally to the skin or mucous membranes. menthol application at low doses produces a cooling sensation, whereas at higher doses, it evokes burning, irritation, and pain (Wei and Seid, 1983; Wasner et al., 2004; Namer et al., 2005; Proudfoot et al., 2006). In practice, various topical over-the-counter products containing menthol for pain relief have concentrations ranging 5−16% (320−1024 mM) (Oz et al., 2017).

Several *in vitro* and *in vivo* studies have demonstrated menthol's biological properties, such as its analgesic, antibacterial, antifungal, anesthetic, and osmotic enhancement, as well as chemoprophylaxis and immunomodulatory effects (Kamatou et al., 2013). The multiple physiological effects of menthol appear to depend on its interaction with a variety of receptors throughout the body. It has been proposed to sensitize transient receptor potential cation channel subfamily M member 8 (TPRM8) and transient receptor potential cation channel subfamily V member 3 (TRPV3), desensitize transient receptor potential cation channel subfamily A member 1 (TRPA1) and transient receptor potential cation channel subfamily V member 1 (TRPV1), stimulate κ-opioid systems, and enhance central glutamate dependent gate control mechanisms (Green and McAuliffe, 2000; Macpherson et al., 2006; Proudfoot et al., 2006; Zanotto et al., 2008). This complex and unique effect of menthol has contributed to its potential as a promising area of pain research. This review summarizes the current pre-clinical results and clinical practice evidence on menthol in analgesic research.

Analgesic mechanism of menthol

Menthol and transient receptor potential family

Transient receptor potential (TRP) channels are a family of proteins which are present in nociceptors and allow organisms to transduce environmental signals that produce pain (Rosenbaum et al., 2022), of which, the discovery is a Nobel physiology and medicine-awarded subject in 2021. Currently, menthol is considered to be the activity regulator of TRPM8, TRPA1 and TRPV1, etc., in the TRP family, and thus menthol and its chemically modified derivatives are currently highlighted again.

Transient receptor potential cation channel subfamily M member 8

In general, menthol selectively acts on TRPM8, a non-selective calcium-permeable channel expressed in a subset of sensory neurons in the dorsal root ganglion (DRG) and trigeminal ganglion (Galeotti et al., 2002; McKemy et al., 2002), which are thought to be the main molecular sensor of cold somatosensation in human body (activation temperature is 8−28°C) (Andersen et al., 2014; Olsen et al., 2014). In addition to menthol and low temperature, TRPM8 channels can be activated by a variety of stimuli (Izquierdo et al., 2021), including the menthol analog icilin (Colburn et al., 2007; Izquierdo et al., 2021), changes in voltage (Fernández et al., 2011; Raddatz et al., 2014) and extracellular osmotic pressure (Parra et al., 2014; Quallo et al., 2015).

Transient receptor potential cation channel subfamily M member 8 participates in cold signal transmission in two general ways: one that transduces innocuous cool temperatures to trigger cool sensation, behavioral thermoregulation, and analgesia; and another that transmits nociceptive signals to trigger more overtly nocifensive behaviors (Chung and Caterina, 2007). For the body in physiological state, TRPM8 predominantly activate the first, but in pathological conditions such as nerve injury or inflammation, TRPM8 mainly plays the second role (Marwaha et al., 2016; De Caro et al., 2019). To understand how interactions among different concentrations of menthol, different chemical or physical stimuli, and the structure of the TRPM8 channel determines pain states, it is necessary to understand that there are three important properties of their function that may be affected to modulate their gating (closing and opening of the ion conduction pathway): *activation*, *sensitization* and *desensitization* (Rosenbaum et al., 2022). To be more specific, in physiological states, low to moderate concentrations of menthol activate TRPM8 receptors to produce a feeling of coolness; at higher concentration, menthol could induce cold allodynia, and cold hyperalgesia mediated by TRPM8 sensitization; following nerve injury or chemical stimuli, menthol activates TRPM8 to

mediate relief of mechanical allodynia and thermal hyperalgesia; long-term local exposure to menthol also desensitizes TRPM8-sensitive fibers. Based on the results of experiments with topical menthol solutions applied to rodents, the dividing line between "low" and "high" concentrations we refer to here is 10% wt/vol or 640 mM.

TRPM8 activation

Almost all the analgesic potency of menthol comes from its activation of TRPM8. It is worth noting that the term "analgesia" specifically refers to the relief of noxious heat, chemical stimuli, and mechanical allodynia. In patch-clamp recordings, menthol activated wild-type TRPM8 with the half maximal effective concentration (EC_{50}) of 185.4 ± 69.4 μM (Xu et al., 2020). TRPM8 activation evokes an influx of Ca^{2+} into the primary sensory neuron, leading to its activation and the propagation of action potentials. The activation of TRPM8 by menthol has been extensively studied in a variety of *in vivo* rodent models. Proudfoot et al. (2006) demonstrated that peripherally (4 mM) or centrally (200 nM) applied menthol, in a model of neuropathic pain (chronic compressive nerve injury, CCI) marked reverse behavioral reflex sensitization to noxious heat and mechanical stimulation. In addition, sensitization specific thermal and mechanical analgesia induced by TRPM8 activation has also been observed in focal demyelination of the sciatic nerve (Proudfoot et al., 2006), Complete Freund's adjuvant (CFA) intra plantar injection (Proudfoot et al., 2006; Pan et al., 2012), and chemical stimulus (such as capsaicin, acrolein or cinnamaldehyde) (Proudfoot et al., 2006; Liu et al., 2013). Systemic or topical application of menthol can dose-dependently increase pain threshold in rodents in hot plate tests (Galeotti et al., 2002; Klein et al., 2010; Liu et al., 2013). In addition, direct evidence that TRPM8 may explain all the analgesic activity of menthol was provided by Liu et al. (2013) using genetic and pharmacological approaches in mice: the gene deletion and selective inhibitor (AMG2850) of TRPM8 completely eliminated the TRPM8-dependent analgesia on chemical stimuli, noxious heat, and inflammation. It is worth noting that the activation of TRPM8 can be regulated by neurotrophic factors (Lippoldt et al., 2013, 2016), phosphatidylinositol bisphosphate (PIP_2) (Premkumar et al., 2005; Rohács et al., 2005), Ca^{2+}-independent phospholipase A2 (iPLA2) and polyunsaturated fatty acids (Andersson et al., 2007), forming a complex network.

It is important to note that in the above study, menthol produced TRPM8-dependent analgesia of acute and inflammatory pain over a wide range of concentrations and administration routes (oral, intraperitoneal, intraplantar or topical), from estimated systemic levels of 60−120 μM, to a topical concentration in the molar range (30% wt/vol) (Liu et al., 2013). This means, that this concentration range may be lower than the reported TRPM8 activation concentration; means that cause analgesia in the sensitized pain state with lower doses of TRPM8 activation.

TRPM8 sensitization

In the physiological state, high concentrations of menthol can induce TRPM8 sensitization and promote the development of cold allodynia and cold hyperalgesia by excessively lowering the cold pain threshold. Menthol-induced cold hypersensitivity is believed to primarily rely on direct sensitization of TRPM8 on Aδ and C-fibers (Andersen et al., 2014). Numerous studies indicate that high concentration of menthol can cause hyperalgesia in cold perception in rodents (>10% wt/vol or >640 mM for mice topically, Tajino et al., 2007), which may make menthol valuable in pre-clinical screening of analgesic agents for cold hyperalgesia (Rossi et al., 2006; Tajino et al., 2007), and it provides a theoretical basis for the establishment of experimental cold hyperalgesia pain model in human with topically high concentration of menthol (>30% wt/vol for healthy subjects, Hatem et al., 2006).

In contrast to the peripheral sensitization of TRPM8 neurons by menthol under physiological conditions, the actual conditions leading to hypersensitivity under pathological conditions are complex (Andersen et al., 2014). In the periphery, nociceptive cold fibers can become sensitized upon axonal degeneration leading to dysregulation of TRP channel expression, resulting in a more excitable phenotype (Gold et al., 2003). Preclinical studies have shown that TRPM8 expression in sensory neurons (DRG and superficial dorsal horn) is increased with the development of hypersensitivity to mechanical, thermal, and cold stimuli in rats with CCI (Proudfoot et al., 2006; Colburn et al., 2007; Frederick et al., 2007; Xing et al., 2007; Su et al., 2011, 2017) and L5 and L6 spinal nerve ligation (SNL) (Katsura et al., 2006; Patel et al., 2014; Koh et al., 2016). Overexpression of TRPM8 has been linked to development of cold allodynia. Evaporative cooling of acetone may represent an inherently less toxic cold stimulus, so it is common to assess cold sensitivity by measuring the response of laboratory animals to acetone application. Colburn et al. (2007) used CCI rodent model to observe significant sensitivity to acetone application. In contrast, TRPM8 gene deletion mice showed no significant increase in acetone sensitivity at any time after ligation (Rimola et al., 2021). This sensory disturbance was also successfully reversed by TRPM8 mRNA antisense (Su et al., 2011). Administration of oxaliplatin and other chemotherapeutic agents can lead to chemotherapy-induced peripheral neuropathy (CIPN), which is characterized by cold abnormal pain and mechanical hyperalgesia. Oxaliplatin treatment has been shown to induce an increase in TRPM8 expression in DRG (Kawashiri et al., 2012; Mizuno et al., 2014; Yamamoto et al., 2018), and that oxaliplatin-induced cold hypersensitivity is diminished in TRPM8 knockout mice (Descoeur et al., 2011). Recently updated studies have shown

that the activity of the TRPM8 but not the activity of any other member of the TRP channel family is transiently increased after oxaliplatin treatment (Rimola et al., 2021). These changes will increase the body's sensitivity to cold and thus reduce the perception of pathological pain, which may represent a protective effect of self-pain reduction in biological evolution.

TRPM8 desensitization

Desensitization occurs when the channel becomes refractory to an activating stimulus by adopting a conformational state where the passage of ions is not allowed. In the context of the nociceptive system, desensitization may function as a protective mechanism in which hyperexcitation or cell death by ion-dependent signaling pathways is avoided (Rosenbaum et al., 2022). To be specific, the activity of the cold- and menthol-activated TRPM8 diminishes over time in the presence of extracellular Ca^{2+} (Yudin et al., 2011; Diver et al., 2019), which is manifested by a decrease in the cooling effect over time when exposed to menthol, along with a decrease in TRPM8 activity (Cliff and Green, 1994; Reid and Flonta, 2001; Matsu-ura et al., 2006; Daniels et al., 2009). In addition, menthol can cause a short-lasting cross-desensitization of other irritant chemicals-induced stimulus including capsaicin (Cliff and Green, 1996; Green and McAuliffe, 2000; Naganawa et al., 2015), citric acid (Morice et al., 1994; Plevkova et al., 2013), cinnamaldehyde (Zanotto et al., 2008; Klein et al., 2011), and nicotine (Dessirier et al., 2001; Fan et al., 2016; Huynh et al., 2020, etc.), that is, a reduction in irritation evoked by compounds other than itself (Dessirier et al., 2001).

Transient receptor potential cation channel subfamily A member 1

However, abnormal pain induced by high menthol concentration still exists experimental fact that is difficult to be explained by sensitization of TRPM8. Fan et al. (2016) demonstrated that mice showed a concentration-dependent oral aversion of menthol (>100 μg/mL or >640 mM), and that gene deletion of TRPM8 did not reduce this aversion. Lemon et al. (2019) conducted a brief-access exposure tests in mice to measure reduction in orosensory avoidance behaviors to aqueous menthol solutions and showed that oral aversion to menthol was reduced in mice deficient for TRPA1 but not TRPM8.

Due to the low selectivity of menthol (Macpherson et al., 2006; Vogt-Eisele et al., 2007), it can also activate TRPA1 (Karashima et al., 2007; Xiao et al., 2008), which is a member of the TRP family with TRPM8. Expression of TRPA1 is limited in a subset of nociceptive neurons of the trigeminal ganglion and DRG (Story et al., 2003; Kobayashi et al., 2005) and is a sensor for a wide variety of environmental stimuli, such as intense cold activation temperature is <18°C (Story et al., 2003), close to 8°C, the reported threshold of noxious cold, Wahren et al. (1989), Tillman et al. (1995), and Harrison and Davis (1999) irritating compounds, reactive chemicals, and endogenous signals associated with cell injury (Talavera et al., 2020) to elicit protective responses. Although both respond to cold stimuli, TRPM8 and TRPA1 are activated by harmless cooling and harmful cold (Caterina et al., 1997; Bandell et al., 2004), respectively. Irritating compounds that directly activate TRPA1 and may cause pain in humans include cinnamaldehyde, allyl isothiocyanate, allicin, formalin (Bandell et al., 2004; Bautista et al., 2005; Moran et al., 2011), and bradykinin as inflammatory mediators (Bandell et al., 2004; Obata et al., 2005). TRPA1 has been implicated in several painful and inflammatory conditions and is considered a promising potential target for the development of, amongst others, analgesic, antipruritic and anti-inflammatory pharmacotherapeutics (Andrade et al., 2012; Koivisto et al., 2012; Preti et al., 2015). The irritating properties of menthol have been shown to be associated with this activation of TRPA1 (Karashima et al., 2007; Fan et al., 2016). In concert with the sensitivity of TRPM8 for menthol, Karashima et al. (2007) showed bell-shaped dose-response curve of menthol to channels by whole-cell and single-channel recordings of heterologously expressed TRPA1, demonstrate a bimodal sensitivity of TRPA1 to menthol, further proved that menthol acts as an effective agonist of TRPA1 at relative low concentrations (100−300 μM), but acts as an antagonist at higher concentrations [≥300 mM (Karashima et al., 2007)] by causing reversible channel blocking, although this high-concentration blocking effect was only found in rodent models, not human models (Macpherson et al., 2006; Karashima et al., 2007; Xiao et al., 2008; Lemon et al., 2019).

Transient receptor potential cation channel subfamily V member 1

Menthol also causes analgesic effects through TRPM8-independent mechanisms, such as the TRPV1, which is involved in the transmission and modulation of nociception, as well as the molecular integration of diverse painful stimuli (Huang et al., 2002; Cui et al., 2006). The activators of TRPV1 are noxious heat [activation temperature is >42°C, in the range of perception that shifts from innocuous warmth to noxious heat; the reported threshold of noxious heat is 55°C (Patapoutian et al., 2003)], acidic pH, capsaicin (the irritating compound in hot chili peppers), and allyl isothiocyanate (Everaerts et al., 2011). TRPV1 is a non-selective cation channel; when it is activated, Na^{+} and Ca^{2+} flowing into the cell to depolarize nociceptive neurons, leading to action potential firing and finally leads to a painful, burning sensation (Caterina et al., 1997). In particular, the functions of TRPV1 and TRPA1 interlink with each other to a considerable extent. This is especially clear in relation to pain and neurogenic inflammation where TRPV1 is co-expressed on the vast majority of TRPA1-expressing sensory nerves and both integrate a variety of noxious stimuli (Fernandes et al., 2012). At the same time, TRPV1 also has a bimodal characteristic similar to TRPA1, which is activated by low menthol concentration

and inhibited by high menthol concentration. Nguyen et al. (2021) observed that TRPV1 was activated by 3 mM menthol (HEK293T cells expressing rat TRPV1) and Takaishi et al. (2016) found *in vitro* that the TRPV1 current was completely inhibited at higher concentrations (>10 mM, HEK293T cells expressing human TRPV1), and this concentration is sufficient to activate TRPM8 and induce anti-nociceptive effects in response to thermal and mechanical stimuli in practice. This may be related to an important feature of TRPV1, which is rapid desensitization after activation, making the channel refractory to further stimulation (Szallasi and Blumberg, 1999). Thus, TRPV1 agonist that can cause desensitization and TRPV1 antagonists can both be considered as promising novel types of analgesics in therapeutic regimen (Gavva et al., 2008; Gunthorpe and Chizh, 2009). This suggests that the desensitization/inhibition of menthol on TRPV1 may be one of the potential mechanisms to explain the analgesic effect of menthol, and menthol and its derivatives could be promising molecules to develop TRPV1 antagonists (Takaishi et al., 2016).

In addition, menthol activates TRPV3, which specifically expressed in keratinocytes (skin cells) to produce a "warm" sensation at innocuous temperatures (activation temperature is about 34−38°C) (Peier et al., 2002; Xu et al., 2002; Macpherson et al., 2006), which would seem to explain one of the curious effects of menthol administration is that it can make human subjects report spontaneous sensations of warmth (Green, 1985; Hatem et al., 2006). *In vitro* heterologous TRPV3 expressing CHO cells, 0.5−2 mM menthol induced TRPV3 currents in a concentration dependent manner, while TRPA1 and TRPV1 currents were inhibited. Also, the sensitization to TRPV3 currents was observed with repeated application of 0.5 mM menthol (Macpherson et al., 2006). Although TRPV3 and TRPV1 share over 40% identity (Peier et al., 2002; Smith et al., 2002; Xu et al., 2002), little research has been done on the structural features that make them functionally so different.

As mentioned above, menthol induces analgesia through several different TRP mechanisms. For example, the simultaneous administration of menthol in response to capsaicin-induced hyperalgesia may also be involved: activation and desensitization of TRPM8 by menthol, activation of TRPA1 by menthol at higher concentrations, activation of TRPV1 and TRPA1 by capsaicin, inhibition of TRPV1 by menthol, and other mechanisms. The resulting analgesic effect of menthol should be the net effect of this complex network of mechanisms. Rodent models of menthol and its analogs are shown in **Table 1**.

Menthol and glutamate receptor

Activation of TRPM8 by menthol analog icilin is reported to produce analgesia by activating central inhibitory pathways (Chung and Caterina, 2007; Dhaka et al., 2007), which make use of inhibitory group II/III metabotropic glutamate receptors in the spinal cord (mGluRs). Numerous studies revealed that the mGluRs play a major role in modulatory central nervous system pathways and have been suggested to have pharmacological antinociceptive implications in inflammatory, neuropathic, and acute pain (Fisher et al., 2002; Simmons et al., 2002; Chen and Pan, 2005).

Proudfoot et al. (2006) demonstrated that intrathecal administration of group II and group III mGluRs antagonists prevented the reversal of thermal and mechanical sensitization of intrathecal menthol (200 nM) and topical icilin (200 μM) after CCI in rats, from which they hypothesized that: the activation of TRPM8 by menthol or icilin in a subpopulation of afferents results in the release of glutamate from central synapses, which then acts through inhibitory group II/III mGluRs located either pre-synaptically on injury-activated nociceptive afferents or perhaps also post-synaptically on dorsal-horn neurons, thereby attenuating neuropathic sensitization. These findings highlight the possible value of menthol and its analogs as TRPM8 activators and downstream central targets of TRPM8 action as novel analgesics for development.

Menthol and opioid

Transient receptor potential cation channel subfamily M member 8-mediated menthol antinociception was found to be dependent on activation of the endogenous opioid pathway (Galeotti et al., 2002; Liu et al., 2013; Patel et al., 2014), and intensive opioid receptors stimulation can also suppresses TRPM8 activity in DRG neurons, lead to the internalization of TRPM8 to pain relief (Shapovalov et al., 2013), suggesting that the two share a common pathway for modulating pain sensation in general. The non-selective opioid receptor antagonist naloxone (Liu et al., 2013; Shapovalov et al., 2013), and the selective κ-antagonist nor-NBI significantly reduced the TRPM8-dependent analgesia of acute and inflammatory pain (Galeotti et al., 2002), whereas the selective μ-antagonist CTOP and δ1-antagonist 7-benzylidenenal-trexone (BNTX) and δ2-antagonist naltriben did not prevent menthol-induced antinociception, therefore, the menthol-induced TRPM8-dependent analgesia is more likely mediated by the activation of the central κ-opioid system, excluding the involvement of μ and δ opioid systems (Galeotti et al., 2002).

Opioid tolerance and opioid-induced hyperalgesia is common in patients who have for chronically treated with opioids (Colvin et al., 2019). Cold allodynia is also a common complaint of patients chronically treated with opioids. In contrast with the findings that acute morphine triggers TRPM8 internalization (Shapovalov et al., 2013) and Gong and Jasmin (2017) demonstrated in rodent models that chronic

TABLE 1 Rodent models of menthol and its analogs.

Rodent models	Compound	Route of administration	Concentration	Effects	References
CCI, SD rats	L-Menthol	Subcutaneously	10%	Cold hypersensitivity exacerbated	Zuo et al., 2013
CCI, Wistar rats	Icilin	Topical	<500 μM	Behavioral-reflex sensitization reversed in thermal and mechanical tests	Proudfoot et al., 2006
			>5000 μM	Hyperalgesia effects	
		Intrathecal injection	<10 nM	Behavioral-reflex sensitization reversed in thermal and mechanical tests	
	L-Menthol	Topical	4 mM		
		Intrathecal injection	200 nM		
SNL, SD rats	Icilin	Topical	1 mM	Nociceptive behaviors enhanced	Ji et al., 2007
SNL, SD rats	Icilin	Topical	10−200 μM	Not affected tactile allodynia or thermal hyperalgesia, but cold allodynia increased	Hagenacker et al., 2014
		Intrathecal injection	0.1 nM−1 μM		
SNL, SD rats	L-Menthol	Topical	10% and 40%	Alleviate cooling hypersensitivity; no significant effect in mechanical withdrawal thresholds	Patel et al., 2014
	M8-Ag	Subcutaneously	30 $mg{\cdot}kg^{-1}$	Reverse behavioral hypersensitivity to cooling	
Hot-plate and abdominal constriction, Swiss albino mice	L-Menthol	Oral	3−10 $mg{\cdot}kg^{-1}$	The pain threshold increased dose-dependently	Galeotti et al., 2002
		Intracerebroventricularly	10 μg		
Thermal Paw Withdrawal, SD rats	L-Menthol	Topical	0.1−10%, and 40%	Withdrawal latency increased	Klein et al., 2010
Von Frey Paw Withdrawal, SD rats				Only the 40% menthol group was significantly different from all other groups indicating allodynia	
Two-temperature preference test, SD rats				Low cold sensitivity at high concentration (10% and 40%); cold allergy at low concentrations (0.01−1%)	
Cold plate test, SD rats				Cold antinociceptive effect of 40% menthol	
CFA-induced inflammatory pain, CD-1 mice	L-Menthol	Intraperitoneal injection	100 $mg{\cdot}kg^{-1}$	Thermal and mechanical hypersensitivity reduced	Pan et al., 2012
Formalin-Induced Spontaneous Nociceptive Behavior, CD-1 mice				Nociception decreased	
Hot plate test, C57BL/6 mice	L-Menthol	Oral	10 $mg{\cdot}kg^{-1}$	Approximately doubled paw withdrawal latencies at both temperature (52°C or 55°C)	Liu et al., 2013
Hot plate test, C57BL/7 mice		Topical	30%	Analgesic effect	
Hot plate test, C57BL/8 mice		Intraperitoneal injection	20 $mg{\cdot}kg^{-1}$	Tail flick latencies increased	
Capsaicin-induced nocifensive behavior, C57BL/8 mice		Injected into the plantar surface of the hind paw	20 μM	Mechanical hyperalgesia inhibited	
Capsaicin-induced mechanical hyperalgesia, C57BL/8 mice			1 mM	Nocifensive behavior inhibited	
Acrolein-induced TRPA1-dependent nocifensive behavior, C57BL/8 mice					
SNL, SD rats	L-Menthol	Injected into the plantar surface of the hind paw	1%, 10%, and 40%	Cold hypersensitivity alleviated, no change in receptive field size was observed or in heat, dynamic brush, or electrically evoked responses	Patel et al., 2014
$TRPM8^{+/+}$ mice	Icilin	Intraperitoneal injection	60 $mg{\cdot}kg^{-1}$	Robust jumping response	Colburn et al., 2007
CCI, C57/B6 mice	L-Menthol	Topical	40 μL	Licking duration increased, also displayed behaviors such as flinching of the paw and brushing of the affected area	Caspani et al., 2009

(*Continued*)

TABLE 1 (Continued)

Rodent models	Compound	Route of administration	Concentration	Effects	References
WT, C57BL/6 mice	L-Menthol	Oral	>50 μg/mL	Consumed less mentholated water and more plain water	Fan et al., 2016
WT, C57BL/6 mice	L-Menthol	Oral	>0.7 mM	Oral aversion	Lemon et al., 2019
PpIX phototoxicity pain, NIH SWISS mice	L-Menthol	Topical	2% and 16%	Pain behavior reduced	Wright et al., 2018
CFA, Wistar rats	L-Menthol	Intraperitoneal injection	100 $mg{\cdot}kg^{-1}$	Anti-hyperalgesia properties and no negative locomotor side effects	Hilfiger et al., 2021
AmmVIII intraperitoneally, C57BL/6 mice	L-Menthol	Subcutaneously	1 mM	Analgesic effects of mechanical hypersensitivity	Gaudioso et al., 2012

CCI, chronic constriction injury; CFA, complete Freund's adjuvant; SD rats, Sprague-Dawley rats; SNL, spinal nerve ligation; TRPA1, transient receptor potential ankyrin 1.

morphine administration induced cold hyperalgesia and up-regulation of TRPM8. However, knockdown, or selective blocking of TRPM8 can reduce cold hyperalgesia caused by morphine. Iftinca et al. (2020) further confirmed that chronic morphine enhances cold hypersensitivity by increasing excitability and reduction desensitization in TRPM8-expressing neurons through activation of μ-opioid-receptor-protein kinase C beta (MOR-PKCβ) signaling pathway, which can be reversed by a follow-up treatment with the inverse non-selective opioid receptor antagonist naloxone (Shapovalov et al., 2013).

In addition to TRPM8, a strong connection has been suggested between the TRPV1 and the opioid pathway. Chronic administration of morphine up-regulates TRPV1 expression in spinal cord, DRG and sciatic nerve (Niiyama et al., 2007; Chen et al., 2008; Vardanyan et al., 2009); blocking TRPV1 by SB366971 (Chen et al., 2008) and capsazepine (Nguyen et al., 2010) or destructing TRPV1-expressing sensory neurons by resiniferatoxin (Chen and Pan, 2006) significantly inhibited morphine tolerance in rodents. TRPV1 has also been reported to be a physiological regulator of opioid receptors through a β-arrestin2 and PKA-dependent manner (Bao et al., 2015; Scherer et al., 2017; Basso et al., 2019). Thus, it is conceivable that menthol-mediated modulation of TRPV1, and thus regulation of opioid pathways affording a promising avenue to improve the therapeutic profile of opioid medications.

In addition, studies have shown that TRPA1, which is involved in the formation of harmful signals, significantly attenuates its association with μ-opioid receptors in the DRG, spinal cord and brain areas under the mediation by calcium-activated calmodulin in formalin-induced inflammatory pain and CCI-induced neuropathic pain in mice (Cortés-Montero et al., 2020).

In conclusion, existing studies demonstrate cross-talk interactions between opioid pathways and TRP, these mechanisms could provide a basis for better understanding general analgesia associated with opiate administration and hyperalgesia associated with abstinence. We illustrate the possible mechanisms of menthol action on the DRG or trigeminal ganglion (**Figure 1**).

Other potential mechanisms

In addition to the above mentioned, a number of different kinds of ligand and voltage-gated ion channels for menthol mediated analgesia have been proposed, and these mechanisms may partially explain the TRP-independent mechanisms are responsible for menthol analgesia.

Voltage-gated Na^+ channels

Menthol has local anesthetic activity. Galeotti et al. (2001) found that menthol significantly reduced electrically induced contractions of rat phrenic hemidiaphragm in a dose-dependent manner; the number of stimuli necessary to provoke the rabbit conjunctival reflex increased in a dose-dependent manner. By recording heterologously expressed whole-cell sodium inward currents in rat neuronal and human skeletal muscle, Haeseler et al. (2002) used patch-clamp to demonstrate that menthol acts like the local anesthetic lidocaine to suppress whole cell Na^+ currents with an IC_{50} of 571 and 376 μM for neuronal cells and skeletal muscle fibers, respectively. In another electrophysiological study, Gaudioso et al. (2012) conclude that menthol inhibits Nav1.8, Nav1.9, and TTX-sensitive Na^+ channels in a concentration-, voltage-, and frequency-dependent manner. It is worth mentioning that eucalyptol (an agonist of TRPM8, 1 mM), and BCTC (a TRPM8 antagonist, IC_{50} = 0.8 μM) had no effect on the above Na^+ currents, indicating that the blocking effect of menthol on Na^+ channels is independent of TRPM8. Another study on cortical neurons reported that menthol (250 μM) dampens the generation of action potentials in TRPM8 knock-out mice and in the presence of a TRPM8 blocker, suggest that menthol can modulate voltage-gated sodium channels in cortical neurons through a TRP-independent pathway (Pezzoli et al., 2014).

Voltage-gated Ca^{2+} channels

Several reports have demonstrated that menthol modulates the functional properties of voltage-gated Ca^{2+} channels. *In vitro* studies have shown that menthol blocks Ca^{2+} influx in Helix neurons (Swandulla et al., 1986), cultured DRG cells

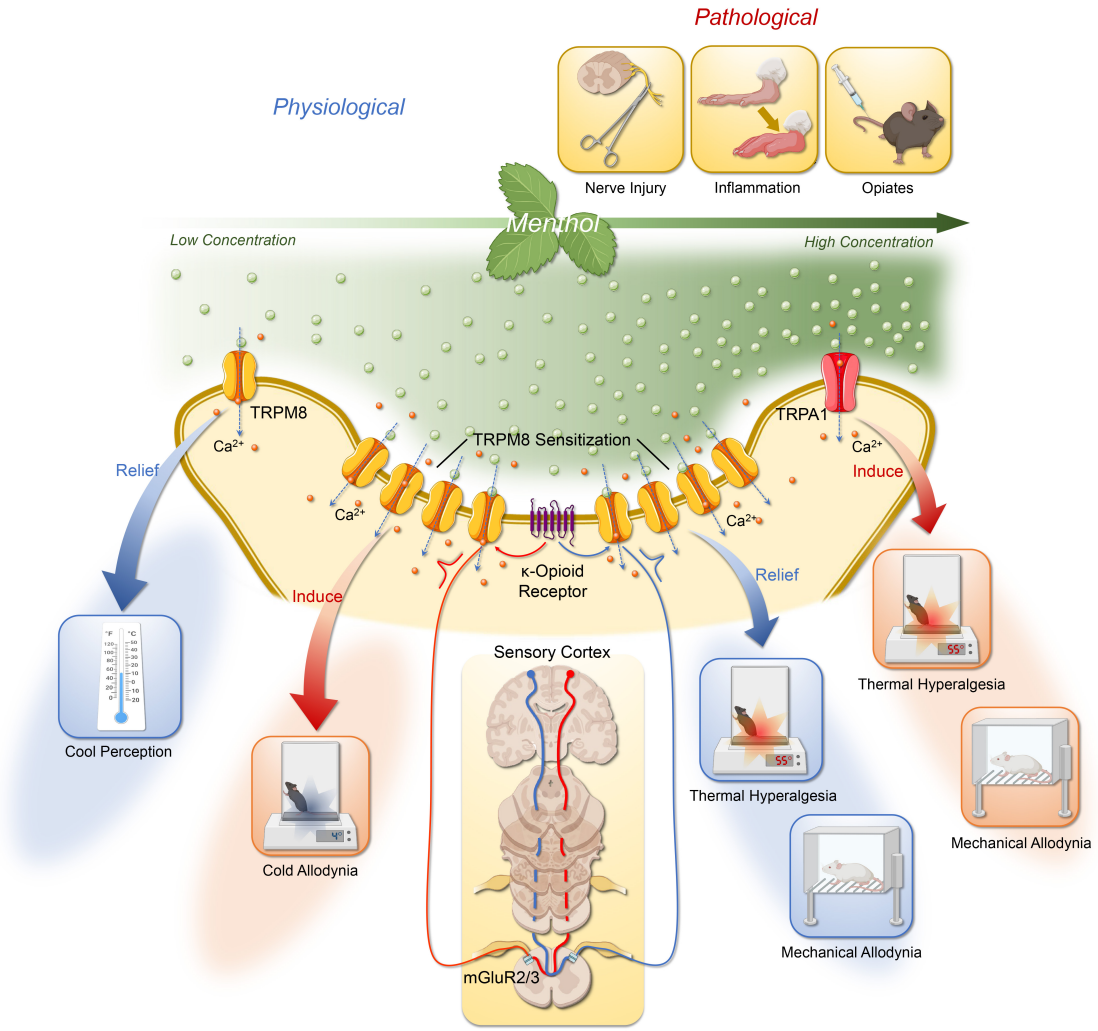

FIGURE 1
The possible mechanisms of menthol action on the DRG or trigeminal ganglion *via* TRPM8 and TRPA1. The effects of menthol are concentration dependent. Low to moderate concentrations of menthol activate TRPM8 in the DRG and trigeminal ganglion to produce a cooling sensation; at higher concentration, menthol could induce cold allodynia, and cold hyperalgesia mediated by TRPM8 sensitization; following nerve injury or chemical stimuli, menthol activates TRPM8 to mediate relief of mechanical allodynia and thermal hyperalgesia. Its analgesic effect is also dependent on the activation of central group II/III mGluR with endogenous κ-opioid signaling pathways. In addition, the thermal and mechanical allodynia of high concentrations of menthol is associated with its activation of TRPA1. Created with BioRender.com.

(Swandulla et al., 1987), LA-N-5 human neuroblastoma cells (Sidell et al., 1990), leech neurons (Dierkes et al., 1997), guinea-pig ileal smooth muscle, rat and guinea-pig atrial and papillary muscle, rat brain synaptosomes and chick retinal neurons (Hawthorn et al., 1988). In addition, menthol decreased the muscle contractures of tracheal (Ito et al., 2008; Wang et al., 2016), bronchial (Wright et al., 1997), vas deference (Filippov et al., 2009; Vladymyrova et al., 2011), colon (Amato et al., 2014), and aortae, mesenteric, coronary arteries (Cheang et al., 2013) smooth muscle by inhibiting of L-type voltage-gated calcium channels. Ramos-Filho et al. (2014) proved that menthol (300 μM) or nifedipine (1 μM) inhibited carbachol and electrical field stimulation induced contractions in both wild type and TRPM8 knockout bladder strips, conclude that menthol inhibits smooth muscle contraction by blocking L-type Ca^{2+} channels in a manner independent of TRPM8 activation. Menthol not only limits Ca^{2+} influx through voltage-gated Ca^{2+} channels, but also induces Ca^{2+} release from intracellular storage pools (endoplasmic reticulum and Golgi) in a TRP-independent manner (Palade, 1987; Tsuzuki et al., 2004; Lu et al., 2006; Mahieu et al., 2007; Wondergem and Bartley, 2009; Neumann and Copello, 2011; Melanaphy et al., 2016). Based on these findings, Melanaphy et al. (2016) revealed that the vasorelaxation effect of menthol and other TRPM8 agonists on isolated rat tail artery myocytes is the net effect of non-specific inhibition of L-type Ca^{2+} channels and activation of Ca^{2+} release in the sarcoplasmic reticulum. These findings will promote the understanding of the vascular effects of TRPM8,

particularly the well-known hypotensive effects of menthol (Sun et al., 2014), and may also have translational implications (Melanaphy et al., 2016).

In addition, menthol can potently inhibit $K_v7.2/3$ channels (a voltage-gated K^+ channel) isoforms (IC_{50} = 289 μM) and their mediated M currents. These mechanisms may be helpful in explaining TRPM8-mediated cooling and analgesic effects (Vetter et al., 2013).

$GABA_A$ receptors

In the central nervous system, γ-amino butyric acid (GABA) is the major inhibitory neurotransmitter. In responding to an action potential, it is released from the pre-synaptic button into the synaptic cleft and acts on either ionotropic $GABA_A$ receptors or metabotropic G-protein coupled $GABA_B$ receptors. Among them, the activation of $GABA_A$ receptors causes hyperpolarization and eventually the suppression of neuronal activity (Fritschy et al., 2012; Sigel and Steinmann, 2012). In practice, $GABA_A$ are the main targets of many sedatives and general anesthetics (Millan, 2003; Hemmings et al., 2005). Menthol acts as a potent positive allosteric modulator at $GABA_A$ (Hall et al., 2004; Corvalán et al., 2009). Menthol can enhance the $GABA_A$-mediated currents in the spinal dorsal horn (Pan et al., 2012), CA1 pyramidal neurons of the hippocampus (Zhang X. B. et al., 2008), periaqueductal grey (PAG) neurons in midbrain slices (Lau et al., 2014) and *Xenopus oocytes* (Watt et al., 2008) *in vitro*. In particular, the TRPM8 agonist icilin, the non-selective TRPM8/TRPV1 antagonist Capsazepine or the TRPA1 antagonist HC-030031 did not affect menthol potentiation of $GABA_A$ receptor-mediated currents in PAG neurons in midbrain slices from rats, indicating that the menthol actions occur independently of TRP channel activation (Lau et al., 2014). Just like propofol, which acts on a similar site in the $GABA_A$ receptor and has a general anesthetic effect, menthol has been shown to be a moderate anesthetic with an EC_{50} of 23 μM, about 10-fold less potent anesthesia than propofol (Thorup et al., 1983; Krasowski et al., 2001). While menthol was far less potent than propofol in producing anesthesia its toxicity is minimal (Thorup et al., 1983) and therefore point to menthol as a lead compound for the development of novel GABAergic modulatory drugs (Watt et al., 2008).

Nicotinic acetylcholine receptors

Menthol is also often added to tobacco products because of the "coolness" of smoke, which is believed to bring pleasure to smokers (Werley et al., 2007); at the same time, menthol may reduce respiratory irritation response found in tobacco smoke (Hans et al., 2012). These applications have been proved to be related to possible functional interaction between menthol and nicotinic acetylcholine receptors (nAChRs) (Dessirier et al., 2001; Ruskin et al., 2008; Willis et al., 2011; Hans et al., 2012; Ashoor et al., 2013a). The nAChRs are cation-permeable ion channel-receptor complex activated by the neurotransmitter acetylcholine, which play important roles in several physiological functions and pathological conditions (Dani and Bertrand, 2007; Dineley et al., 2015). *In vitro* electrophysiologic studies showed that menthol was a negative allosteric regulator of α4β2 subtypes of nAChRs (Hans et al., 2012); menthol can even desensitize α3β4 subtype of nAChRs through allosteric mechanism (Ton et al., 2015); and menthol can also inhibit the α7 subtype of nAChRs non-competitively (Ashoor et al., 2013a). In addition, Henderson et al. (2016) demonstrated that chronic menthol induces cell-type-selective up-regulation of α4* subtype of nAChRs and also alters midbrain dopamine neuron function; more importantly, since menthol plus nicotine can produce greater reward-related behavior than nicotine alone (Henderson et al., 2017), this may explain the difficulty in quitting smoking (Foulds et al., 2010), whereas menthol can enhance smoking behavior and stimulate adverse effect of smoking on health as an additive to tobacco products (Kabbani, 2013; Wickham, 2015).

Menthol is also an allosteric non-competitive inhibitor of the 5-hydroxytryptamine type 3 ($5\text{-}HT_3$) receptor (Heimes et al., 2011; Ashoor et al., 2013b; Walstab et al., 2014; Ziemba et al., 2015), which may explain its effective antiemetic properties.

It is worth noting that Liu et al. (2013) pointed out in their study on the role of TRPM8 in menthol induced analgesia that, in addition to activating TRPM8 channels, the concentration in the experiment (60−120 μM for systemic use and 30% wt/vol for external use) was sufficient or far more than the concentration required for pharmacological effects on other potential targets involved in menthol induced analgesia mediator mentioned above. However, any residual analgesic effect of menthol was not observed in TRPM8 knockout mice, which may imply these alternative targets: 1. may have little or no interaction with menthol to affect pain perception; 2. may only play a role in menthol analgesia under specific situations; 3. may have specific analgesic effect for other menthol isoforms (Liu et al., 2013). Therefore, further studies are needed to explore the interaction between menthol and these other potential alternative targets in analgesic effects.

Menthol in clinical practice

Over the past 15 years, a large number of menthol and its derivatives have been described by large pharmaceutical companies, small biotech companies and the academic community, but only a few have made it into clinical trials and even fewer have completed clinical trials.

Menthol-induced human cold hyperalgesia pain model

Under pathophysiological conditions, normally innocuous skin cooling can induce pain. This cold hyperalgesia (allodynia)

is a striking symptom in patients with neuropathic pain (Lindblom and Verrillo, 1979; Wahren and Torebjörk, 1992; Woolf and Mannion, 1999; Baron, 2000). Translational surrogate models of pain, allodynia and hyperalgesia make it possible to evaluate the efficacy of drugs in pre-clinical settings and contribute to improved screening, diagnosis and treatment strategies for patients by applying these models in healthy volunteers to narrow the gap between animals and patients (Arendt-Nielsen and Yarnitsky, 2009). However, pathological animal models such as CCI, SNL and CIPN that induce neuropathic pain or hyperalgesia are often irreversible and invasive and cannot be used as human replacement models *per se*. As above, there have been numerous pre-clinical studies using menthol to establish cold hypersensitivity. In view of this, topical high concentration of L-menthol is the only human experimental pain model established to investigate the mechanism of cold hyperalgesia (Andersen et al., 2015). The work of Andersen et al. (2014) summarized the topical application of menthol in humans as a transformational model for cold abnormal pain and hyperalgesia. According to their findings, most of the menthol was applied to the volar forearm (Wasner et al., 2004; Namer et al., 2005; Hatem et al., 2006; Flühr et al., 2009); the highest menthol concentration that can actually be triggered effectively is about 40% (Wasner et al., 2004, 2008; Namer et al., 2005, 2008; Seifert and Maihöfner, 2007; Altis et al., 2009; Flühr et al., 2009; Binder et al., 2011; Mahn et al., 2014), but a 30% menthol ethanol solution proved to be the ideal formulation because of its effectiveness and safety (Hatem et al., 2006); the most common spontaneous sensation reported by subjects during application was coldness or mild pain; all studies reviewed consistently found a significant increase in cold pain threshold in healthy volunteers (Andersen et al., 2015). Human studies on topical menthol induced cold pain are summarized in **Table 2**.

Musculoskeletal pain

Knowledge about the feasibility of topical menthol for musculoskeletal pain dates back centuries, as topical menthol has been widely used to treat muscle soreness (Silva, 2020). The most common musculoskeletal pain is low back pain, which affects 30% to 40% of the general population and is the leading cause of disability (Hartvigsen et al., 2018). Using a randomized controlled design, Zhang J. et al. (2008) determined to add Biofreeze (Performance Health Inc., Export, PA, United States), a locally applied pain-killing agent containing menthol, to the chiropractic treatment plan for patients with low back pain, with significant pain relief effect. However, there were no significant changes in Roland-Morris Disability Questionnaire (RMDQ), heart rate variability, or LBP electromyography (EMG) compared with the control group, and further studies with a larger sample size are needed to confirm the findings (Zhang J. et al., 2008). In addition, NCT03012503 has compared the effects of Biofreeze with placebo on neck pain after cervical massage with chiropractic, but no results have been published to date.

Osteoarthritis (OA) is the main cause of disability in the elderly (Glyn-Jones et al., 2015). Topp et al. compare the ability to complete functional tasks and knee pain while completing functional tasks among 20 patients with knee OA after topical application of either 3.5% menthol gel or an inert placebo gel, but no differences were found in functional tasks or pain (Topp et al., 2013). NCT03888807 attempted to determine the effects of Biofreeze vs. placebo on walking gait characteristics and walking pain in patients with bilateral knee OA but announced early termination due to difficulty in enrolling subjects. In addition, NCT03888807, NCT04351594, and NCT01565070 have been evaluating the effect of Biofreeze on knee OA, but no results have been obtained.

Post-exercise myalgia and delayed onset muscle soreness (DOMS) are common symptoms after exercise and physical activity. Stefanelli et al. (2019) found that DOMS reduced corticospinal excitability and after the administration of menthol-based topical analgesic, there was a reduction in pain, which was accompanied by increased corticospinal inhibition. Although ice application is considered the traditional method for post-exercise pain relief, Johar et al. (2012) demonstrated that compared to ice, the topical menthol-based analgesic decreased perceived discomfort to a greater extent and permitted greater tetanic forces to be produced, and the effectiveness of ice for acute injury has not been proven in any clinical trials and may even be harmful (Bleakley et al., 2004). Airaksinen et al. (2003) showed that topical menthol gels not only provide excellent pain relief, but also promote recovery in patients with exercise-related soft tissue injuries. Higashi et al. (2010) reported in a double-blind randomized controlled trial that a single 8-h patch containing methyl salicylate and menthol significantly alleviated pain associated with mild to moderate muscle strain in these adult patients compared to patients receiving a placebo patch. NCT02100670 is a multicenter, randomized, double-blind, placebo-controlled, parallel-group trial performed to evaluate topical 1% diclofenac/3% menthol gel in treating ankle sprain, but no significant improvement was observed with topical 1% diclofenac/3% menthol gel compared with placebo, 1% diclofenac, or 3% menthol gel in treating pain from ankle sprain (Lai et al., 2017).

Carpal tunnel syndrome is a neuromuscular disease caused by increased pressure on the median nerve of the wrist, with common symptoms include wrist and hand pain, paresthesia, thenar muscle weakness and loss of flexibility (Padua et al., 2016). A three-blind randomized placebo-controlled crossover trial demonstrated that topical menthol significantly reduced pain intensity compared with placebo in abattoir workers with chronic pain and carpal tunnel syndrome symptoms (Sundstrup et al., 2014).

TABLE 2 Human models of menthol and its products.

Compound	Route of administration	Indication	Effects	Clinical trial number	References
10 mM menthol	Oral	Healthy subjects	Transiently desensitize capsaicin-sensitive fibers	NA	Proudfoot et al., 2006
40% Menthol	Topical	Healthy subjects	Topical menthol induced cold allodynia	NA	Wasner et al., 2004, 2008; Namer et al., 2005, 2008; Seifert and Maihöfner, 2007; Altis et al., 2009; Flühr et al., 2009; Binder et al., 2011; Mahn et al., 2014
30% Menthol	Topical	Healthy subjects	30% Topical menthol can induce cold hyperalgesia with effectively and safely	NA	Hatem et al., 2006
10% Menthol	Topical	Healthy subjects	No significant to histamine-induced itch and pain sensation	NA	Yosipovitch et al., 1996
Tetracaine gel with vs. without menthol	Topical	Healthy subjects	Improved the analgesic efficacy of the tetracaine gel in part through enhanced percutaneous permeation	NA	Liu et al., 2005
Menthol smokers vs. non-menthol smokers	NA	Healthy subjects	Less pain and pain-related functional interference	NA	Kosiba et al., 2019
0%, 10%, 20% and 30% menthol	Topical	Healthy subjects	The concentration-dependent grading response elicits a range of sensations	NA	Wright et al., 2019
Topical pain-relieving patch (containing 6% menthol) vs. placebo	Topical	Mild to moderate pain condition	Significant relief of pain	NA	Gudin et al., 2020
40% Menthol	Topical	Upper limb amputees	Induce hypersensitivity	NA	Vase et al., 2013
40% Menthol vs. placebo	Topical	Healthy subjects, Trans-cinnamaldehyde-induced hyperalgesia	*No Results Posted*	NCT02653703	Andersen et al., 2016
5% Menthol cream vs. placebo	Topical	After photodynamic therapy	*No Results Posted*	NCT02984072	
Menthol (Biofreeze) vs. placebo	Topical	Acute LBP	Significant relief of pain	NA	Zhang J. et al., 2008
Menthol (Biofreeze) vs. placebo	Topical	Non-radicular mechanical neck pain	*No Results Posted*	NCT03012503	
3.5% Menthol gel vs. inert placebo gel	Topical	OA	No significant improvement	NA	Topp et al., 2013
Menthol (Biofreeze) vs. placebo	Topical	OA	*No Results Posted*	NCT03888807, NCT04351594, NCT01565070	
Menthol (Biofreeze) vs. placebo	Topical	EIMD	Menthol may reduce the sensation of muscle soreness and may influence recovery of lower-body power	NA	Gillis et al., 2020
Menthol (Biofreeze) vs. placebo	Topical	DOMS	Significant relief of pain associated with increased corticospinal inhibition	NA	Stefanelli et al., 2019
3.5% menthol gel vs. application of ice	Topical	DOMS	Decreased perceived discomfort to a greater extent and permitted greater tetanic forces to be produced.	NA	Johar et al., 2012
3.5% menthol gel vs. inert placebo gel	Topical	Soft tissue injuries	Significant relief of pain	NA	Airaksinen et al., 2003
3% menthol + ibuprofen vs. gel ibuprofen gel alone/diclofenac gel	Topical	Soft tissue injuries	Significant relief of pain	NA	Wade et al., 2019
Mentholated cream only vs. MC containing oxygenated glycerol triesters	Topical	Acute musculoskeletal pain	The combination resulted in a gradual reduction in pain, lower VAS scores, and greater improvements in lifestyle and mobility improvements	NCT01387750	Taylor et al., 2012
3.5% Menthol patch vs. placebo patch	Topical	Mild to moderate musculoskeletal strain	Significant relief of pain	NA	Higashi et al., 2010
1% Diclofenac/3% menthol gel vs. inert placebo gel	Topical	Acute ankle sprain	No significant improvement	NCT02100670	Lai et al., 2017
Menthol (Biofreeze) vs. placebo	Topical	CTS	*No Results Posted*	NCT01716767	

(*Continued*)

TABLE 2 (Continued)

Compound	Route of administration	Indication	Effects	Clinical trial number	References
Menthol (Biofreeze) vs. placebo	Topical	CTS	Significant relief of pain	NA	Sundstrup et al., 2014
Neat peppermint oil (containing 10% menthol)*	Topical	Postherpetic neuralgia	Significant relief of pain	NA	Davies et al., 2002
Menthol (Biofreeze) vs. placebo	Topical	MPS	Increase in the mouth opening size	NA	Yaman et al., 2021
1% Menthol cream	Topical	CIPN, PMPS	Significant relief of pain	NA	Fallon et al., 2015
1% Menthol cream*	Topical	CIPN	Significant relief of pain	NA	Cortellini et al., 2017
5% Menthol cream*	Topical	CIPN	Significant relief of pain	NA	Brid et al., 2015
7.5% Methyl salicylate/2% menthol lotion vs. placebo	Topical	CIPN	*No Results Posted*	NCT01855607	
3.5% Menthol gel vs. inert placebo gel	Topical	CIPN	*No Results Posted*	NCT04276727	
Mannitol + menthol cream vs. menthol cream	Topical	PDPN	*No Results Posted*	NCT02728687	
No cooling vs. menthol-containing cooling bandage vs. ice containing cold pack	Topical	Undergoing anterior cruciate ligament reconstruction	Positive subjective comfort feedback	NA	Engelhard et al., 2019
Menthol 10% solution vs. menthol 0.5% solution	Topical	Migraine	Significant relief of pain	NA	Borhani Haghighi et al., 2010
6% Menthol gel (STOPAIN)	Topical	Migraine	Significant relief of pain	NCT01687101	St Cyr et al., 2015; Kayama et al., 2018
40% Menthol	Topical	Histamine-induced itch	An inhibitory effect on histaminergic itch	NA	Andersen et al., 2017; Engelhard et al., 2019
Menthol based aromatic therapy vs. placebo	NA	Second trimester genetic amniocentesis	No significant improvement	NA	Hanprasertpong et al., 2015

* Case reports. CTS, carpal tunnel syndrome; CIPN, chemotherapy-induced peripheral neuropathy; DOMS, delayed-onset muscle soreness; EIMD, exercise-induced muscle damage; LBP, low back pain; MPS, Masticatory myofascial pain syndrome; OA, osteoarthritis; PDPN, painful diabetic peripheral neuropathy; PMPS, post-mastectomy pain syndrome; VAS, Visual Analog Scale.

Neuropathic pain

Neuropathic pain is defined as pain caused by a lesion or disease of the somatosensory nervous system and is a major therapeutic challenge. Common causes of neuropathic pain include cerebrovascular accident, multiple sclerosis or spinal cord injury, or peripheral nervous system, for example, painful diabetic neuropathy, postherpetic neuralgia, or surgery (Boyd et al., 2019). The first reported use of menthol in neuropathic pain dates to 1870, when menthol oil was successfully used to treat neuropathic facial pain.

Chemotherapy-induced peripheral neuropathy is a severe and painful adverse reaction of cancer treatment in patients. CIPN that occurs during chemotherapy, sometimes requiring dose reduction or cessation, impacting on survival (Colvin, 2019). Menthol activated TRPM8 channels are a promising therapeutic target in CIPN (Colvin, 2019). In Fallon et al. (2015), in a proof-of-concept study, determined that 82% of evaluable patients had an improvement in their total pain scores after 4−6 weeks of treatment with topical 1% menthol cream, and 50% had a clinically relevant reduction in pain scores of at least 30%. Cortellini et al. (2017) reported the remarkable treatment with menthol cream of a male patient with a history of metastatic colon cancer and previous chemotherapies who had neuropathy that impaired his quality of life and limited further chemotherapy. Another clinical study (NCT01855607, as shown in **Table 2**) assessed whether 6 weeks of treatment with topical menthol twice daily would reduce CIPN in patients have completed adjuvant or neo-adjuvant Taxane based breast cancer therapy or Oxaliplatin based colon cancer chemotherapy. Recently, a phase II study (NCT04276727, as shown in **Table 2**) used a special brain scan called functional magnetic resonance imaging (fMRI) to help determine whether topical menthol therapy has potential for CIPN patients. In a word, CIPN patients may benefit from the use of menthol, either during the treatment of patients complain of subjective improvement, lead to a better quality of life, and can be implemented without interruption of chemotherapy and effective chemotherapy dose delivery, which in turn lead to longer survival, is likely to be an effective potential palliative treatment option.

Neuropathy is one of the most common long-term complications of diabetes, characterized by altered thermal, mechanical, and chemical sensation. Of three large, clinic-based studies from Europe, the prevalence of diabetic neuropathy varied from 23–29% (Young et al., 1993; Tesfaye et al., 1996; Cabezas-Cerrato, 1998). Preclinical studies have shown that there was an increase in TRPV1-mediated currents but a decrease in TRPM8-mediated currents in DRG isolated from diabetic hyperalgesia mice. Therefore, menthol, which has the effect of targeting TRPV1 or TRPM8, may be a useful approach to treat pain associated with diabetic neuropathy (Pabbidi and Premkumar, 2017). There has been a randomized, double-blind, placebo-controlled crossover trial of the efficacy and safety of

menthol topically alone or in combination with mannitol in the relief of diabetic neuropathy (NCT02728687), with no results have been reported.

In addition, Davies et al. (2002) reported successful relief of postherpetic neuralgia using topical peppermint oil in combination with other interventions.

Others

Management of postoperative pain relieve suffering and leads to earlier mobilization, shortened hospital stay, reduced hospital costs, and increased patient satisfaction (Gupta et al., 2010). Engelhard et al. (2019) observed a beneficial effect of cooling by a menthol-containing bandage during the rehabilitation phase after anterior cruciate ligament reconstruction. The reduction of muscle cross section within 30 days after surgery was prevented by menthol dressings, which highly contributed to rehabilitation success after 90 days of therapy and can reduce painkiller consumption (Engelhard et al., 2019).

Genome-wide association analysis have revealed that TRPM8 is associated with susceptibility to migraine without aura (Freilinger et al., 2012), and reduced TRPM8 expression (rs10166942 carriers) helps reduce migraine risk in humans (Gavva et al., 2019), which may provide the rationale for the topical menthol as an alternative treatment option for migraine patients. A randomized, triple-blind, placebo-controlled, crossed-over study demonstrated the efficacy, safety, and relative tolerability of cutaneous application of 10% menthol solution in the treatment of migraine without aura (Borhani Haghighi et al., 2010). An open-label pilot study showed that 52% of subjects experienced at least one statistically significant improvement in migraine severity 2 h after using topical menthol (St Cyr et al., 2015). Due to the limitations of these studies, larger placebo-controlled clinical trials are needed.

Pruritus and pain are closely related but distinct sensations. There is a broad overlap between pain- and itch-related peripheral mediators and/or receptors, and there are astonishingly similar mechanisms of neuronal sensitization in the peripheral and central (Ikoma et al., 2006). Analgesia and antipruritic therapy should have common targets. In 1995, Bromm et al. found that topical menthol had a central inhibitory effect on histamine-induced pruritus of the lower left arm in 15 healthy male volunteers (Bromm et al., 1995). Andersen et al. (2017) conducted a similar study and got the same conclusion, further verified the antipruritic effect of menthol like doxepin. Using a combination of pharmacologic, genetic, and mouse behavioral assays, Palkar et al. (2018) found that the inhibition of pruritus by menthol requires TRPM8 channels or intact and functional TRPM8-expressing afferent neurons. Menthol and its analogs that rely on TRPM8 channels are a promising target for the development of pruritus therapies, and further clinical trials could significantly improve the management of pruritus.

Conclusion

We summarize the progress of menthol in pain and analgesia research based on existing evidence and demonstrate the important role of menthol in clinical analgesia. Although TRPM8 may explain the analgesic effect of menthol, the molecular mechanism between upstream and downstream has not been fully elucidated, and the exact association between menthol, TRP family, mGluRs and endogenous κ-opioid signaling pathway has not been established. Furthermore, menthol interactions with TRPA1 and other targets may have pro-nociceptive and inflammatory effects. In fact, topical menthol treatment is often accompanied by skin irritation, and inhalation of menthol can aggravate asthma in some patients, which may be the role of TRPA1 (Bautista et al., 2006; Zhang X. B. et al., 2008; Caceres et al., 2009). This is very similar to the action of beta-adrenergic receptors in the circulatory system. Therefore, it is urgent to develop TRPM8-specific drugs to replace menthol in analgesic and anti-irritant therapy, to prevent these adverse effects and allow more effective analgesic treatment.

Author contributions

LZ, ZL, and HZ designed and collected the literatures, and wrote the manuscript. YW and YL collected some literatures and created the figure and tables. LZ and QL revised the manuscript. All authors contributed to the article and approved the submitted version.

Funding

This work was supported by research grants of National Natural Science Foundation of China to LZ (Grant nos. 82171205 and 81801107) and National Natural Science Foundation of China to YL (Grant no. 82071243).

Conflict of interest

The authors declare that the research was conducted in the absence of any commercial or financial relationships that could be construed as a potential conflict of interest.

Publisher's note

References

Airaksinen, O. V., Kyrklund, N., Latvala, K., Kouri, J. P., Grönblad, M., and Kolari, P. (2003). Efficacy of cold gel for soft tissue injuries: A prospective randomized double-blinded trial. *Am. J. Sports Med.* 31, 680–684. doi: 10.1177/03635465030310050801

Altis, K., Schmidtko, A., Angioni, C., Kuczka, K., Schmidt, H., Geisslinger, G., et al. (2009). Analgesic efficacy of tramadol, pregabalin and ibuprofen in menthol-evoked cold hyperalgesia. *Pain* 147, 116–121. doi: 10.1016/j.pain.2009.08.018

Amato, A., Liotta, R., and Mulè, F. (2014). Effects of menthol on circular smooth muscle of human colon: Analysis of the mechanism of action. *Eur. J. Pharmacol.* 740, 295–301. doi: 10.1016/j.ejphar.2014.07.018

Andersen, H. H., Gazerani, P., and Arendt-Nielsen, L. (2016). High-concentration L-menthol exhibits counter-irritancy to neurogenic inflammation, thermal and mechanical hyperalgesia caused by trans-cinnamaldehyde. *J. Pain* 17, 919–929. doi: 10.1016/j.jpain.2016.05.004

Andersen, H. H., Melholt, C., Hilborg, S. D., Jerwiarz, A., Randers, A., Simoni, A., et al. (2017). Antipruritic effect of cold-induced and transient receptor potential-agonist-induced counter-irritation on histaminergic itch in humans. *Acta Derm. Venereol.* 97, 63–67. doi: 10.2340/00015555-2447

Andersen, H. H., Olsen, R. V., Møller, H. G., Eskelund, P. W., Gazerani, P., and Arendt-Nielsen, L. (2014). A review of topical high-concentration L-menthol as a translational model of cold allodynia and hyperalgesia. *Eur. J. Pain* 18, 315–325. doi: 10.1002/j.1532-2149.2013.00380.x

Andersen, H. H., Poulsen, J. N., Uchida, Y., Nikbakht, A., Arendt-Nielsen, L., and Gazerani, P. (2015). Cold and L-menthol-induced sensitization in healthy volunteers–a cold hypersensitivity analogue to the heat/capsaicin model. *Pain* 156, 880–889. doi: 10.1097/j.pain.0000000000000123

Andersson, D. A., Nash, M., and Bevan, S. (2007). Modulation of the cold-activated channel TRPM8 by lysophospholipids and polyunsaturated fatty acids. *J. Neurosci.* 27, 3347–3355. doi: 10.1523/jneurosci.4846-06.2007

Andrade, E. L., Meotti, F. C., and Calixto, J. B. (2012). TRPA1 antagonists as potential analgesic drugs. *Pharmacol. Ther.* 133, 189–204. doi: 10.1016/j.pharmthera.2011.10.008

Arendt-Nielsen, L., and Yarnitsky, D. (2009). Experimental and clinical applications of quantitative sensory testing applied to skin, muscles and viscera. *J. Pain* 10, 556–572. doi: 10.1016/j.jpain.2009.02.002

Ashoor, A., Nordman, J. C., Veltri, D., Yang, K. H., Al Kury, L., Shuba, Y., et al. (2013a). Menthol binding and inhibition of α7-nicotinic acetylcholine receptors. *PLoS One* 8:e67674. doi: 10.1371/journal.pone.0067674

Ashoor, A., Nordman, J. C., Veltri, D., Yang, K. H., Shuba, Y., Al Kury, L., et al. (2013b). Menthol inhibits 5-HT3 receptor-mediated currents. *J. Pharmacol. Exp. Ther.* 347, 398–409. doi: 10.1124/jpet.113.203976

Bandell, M., Story, G. M., Hwang, S. W., Viswanath, V., Eid, S. R., Petrus, M. J., et al. (2004). Noxious cold ion channel TRPA1 is activated by pungent compounds and bradykinin. *Neuron* 41, 849–857. doi: 10.1016/s0896-6273(04)00150-3

Bao, Y., Gao, Y., Yang, L., Kong, X., Yu, J., Hou, W., et al. (2015). The mechanism of μ-opioid receptor (MOR)-TRPV1 crosstalk in TRPV1 activation involves morphine anti-nociception, tolerance and dependence. *Channels (Austin)* 9, 235–243. doi: 10.1080/19336950.2015.1069450

Baron, R. (2000). Peripheral neuropathic pain: From mechanisms to symptoms. *Clin. J. Pain* 16, S12–S20. doi: 10.1097/00002508-200006001-00004

Basso, L., Aboushousha, R., Fan, C. Y., Iftinca, M., Melo, H., Flynn, R., et al. (2019). TRPV1 promotes opioid analgesia during inflammation. *Sci. Signal.* 12:eaav0711. doi: 10.1126/scisignal.aav0711

Bautista, D. M., Jordt, S. E., Nikai, T., Tsuruda, P. R., Read, A. J., Poblete, J., et al. (2006). TRPA1 mediates the inflammatory actions of environmental irritants and proalgesic agents. *Cell* 124, 1269–1282. doi: 10.1016/j.cell.2006.02.023

Bautista, D. M., Movahed, P., Hinman, A., Axelsson, H. E., Sterner, O., Högestätt, E. D., et al. (2005). Pungent products from garlic activate the sensory ion channel TRPA1. *Proc. Natl. Acad. Sci. U.S.A.* 102, 12248–12252. doi: 10.1073/pnas.0505356102

Binder, A., Stengel, M., Klebe, O., Wasner, G., and Baron, R. (2011). Topical high-concentration (40%) menthol-somatosensory profile of a human surrogate pain model. *J. Pain* 12, 764–773. doi: 10.1016/j.jpain.2010.12.013

Bleakley, C., McDonough, S., and MacAuley, D. (2004). The use of ice in the treatment of acute soft-tissue injury: A systematic review of randomized controlled trials. *Am. J. Sports Med.* 32, 251–261. doi: 10.1177/0363546503260757

Borhani Haghighi, A., Motazedian, S., Rezaii, R., Mohammadi, F., Salarian, L., Pourmokhtari, M., et al. (2010). Cutaneous application of menthol 10% solution as an abortive treatment of migraine without aura: A randomised, double-blind, placebo-controlled, crossed-over study. *Int. J. Clin. Pract.* 64, 451–456. doi: 10.1111/j.1742-1241.2009.02215.x

Boyd, A., Bleakley, C., Hurley, D. A., Gill, C., Hannon-Fletcher, M., Bell, P., et al. (2019). Herbal medicinal products or preparations for neuropathic pain. *Cochrane Database Syst. Rev.* 4:Cd010528. doi: 10.1002/14651858.CD010528.pub4

Brid, T., Miranda, G., Lozano, B., and Baamonde, A. (2015). Topical L-menthol for postradiotherapy neuropathic pain: A case report. *J. Pain Symptom Manage.* 50, e2–e4. doi: 10.1016/j.jpainsymman.2015.04.024

Bromm, B., Scharein, E., Darsow, U., and Ring, J. (1995). Effects of menthol and cold on histamine-induced itch and skin reactions in man. *Neurosci Lett.* 187, 157–160. doi: 10.1016/0304-3940(95)11362-z

Cabezas-Cerrato, J. (1998). The prevalence of clinical diabetic polyneuropathy in Spain: A study in primary care and hospital clinic groups. Neuropathy spanish study group of the spanish diabetes society (SDS). *Diabetologia* 41, 1263–1269. doi: 10.1007/s001250051063

Caceres, A. I., Brackmann, M., Elia, M. D., Bessac, B. F., del Camino, D., D'Amours, M., et al. (2009). A sensory neuronal ion channel essential for airway inflammation and hyperreactivity in asthma. *Proc. Natl. Acad. Sci. U.S.A.* 106, 9099–9104. doi: 10.1073/pnas.0900591106

Caspani, O., Zurborg, S., Labuz, D., and Heppenstall, P. A. (2009). The contribution of TRPM8 and TRPA1 channels to cold allodynia and neuropathic pain. *PLoS One* 4:e7383. doi: 10.1371/journal.pone.0007383

Caterina, M. J., Schumacher, M. A., Tominaga, M., Rosen, T. A., Levine, J. D., and Julius, D. (1997). The capsaicin receptor: A heat-activated ion channel in the pain pathway. *Nature* 389, 816–824. doi: 10.1038/39807

Cheang, W. S., Lam, M. Y., Wong, W. T., Tian, X. Y., Lau, C. W., Zhu, Z., et al. (2013). Menthol relaxes rat aortae, mesenteric and coronary arteries by inhibiting calcium influx. *Eur. J. Pharmacol.* 702, 79–84. doi: 10.1016/j.ejphar.2013.01.028

Chen, S. R., and Pan, H. L. (2005). Distinct roles of group III metabotropic glutamate receptors in control of nociception and dorsal horn neurons in normal and nerve-injured Rats. *J. Pharmacol. Exp. Ther.* 312, 120–126. doi: 10.1124/jpet.104.073817

Chen, S. R., and Pan, H. L. (2006). Loss of TRPV1-expressing sensory neurons reduces spinal mu opioid receptors but paradoxically potentiates opioid analgesia. *J. Neurophysiol.* 95, 3086–3096. doi: 10.1152/jn.01343.2005

Chen, Y., Geis, C., and Sommer, C. (2008). Activation of TRPV1 contributes to morphine tolerance: Involvement of the mitogen-activated protein kinase signaling pathway. *J. Neurosci.* 28, 5836–5845. doi: 10.1523/jneurosci.4170-07.2008

Chung, M. K., and Caterina, M. J. (2007). TRP channel knockout mice lose their cool. *Neuron* 54, 345–347. doi: 10.1016/j.neuron.2007.04.025

Cliff, M. A., and Green, B. G. (1994). Sensory irritation and coolness produced by menthol: Evidence for selective desensitization of irritation. *Physiol. Behav.* 56, 1021–1029. doi: 10.1016/0031-9384(94)90338-7

Cliff, M. A., and Green, B. G. (1996). Sensitization and desensitization to capsaicin and menthol in the oral cavity: Interactions and individual differences. *Physiol. Behav.* 59, 487–494. doi: 10.1016/0031-9384(95)02089-6

Cohen, S. P., Vase, L., and Hooten, W. M. (2021). Chronic pain: An update on burden, best practices, and new advances. *Lancet* 397, 2082–2097. doi: 10.1016/s0140-6736(21)00393-7

Colburn, R. W., Lubin, M. L., Stone, D. J. Jr., Wang, Y., Lawrence, D., D'Andrea, M. R., et al. (2007). Attenuated cold sensitivity in TRPM8 null mice. *Neuron* 54, 379–386. doi: 10.1016/j.neuron.2007.04.017

Colvin, L. A. (2019). Chemotherapy-induced peripheral neuropathy: Where are we now? *Pain* 160 Suppl 1, S1–S10. doi: 10.1097/j.pain.0000000000001540

Colvin, L. A., Bull, F., and Hales, T. G. (2019). Perioperative opioid analgesia-when is enough too much? A review of opioid-induced tolerance and hyperalgesia. *Lancet* 393, 1558–1568. doi: 10.1016/s0140-6736(19)30430-1

Cortellini, A., Verna, L., Cannita, K., Napoleoni, L., Parisi, A., Ficorella, C., et al. (2017). Topical menthol for treatment of chemotherapy-induced peripheral neuropathy. *Indian J. Palliat. Care* 23, 350–352. doi: 10.4103/ijpc.Ijpc_23_17

Cortés-Montero, E., Rodríguez-Muñoz, M., Ruiz-Cantero, M. D. C., Cobos, E. J., Sánchez-Blázquez, P., and Garzón-Niño, J. (2020). Calmodulin supports TRPA1 channel association with opioid receptors and glutamate NMDA receptors in the nervous tissue. *Int. J. Mol. Sci.* 22:229. doi: 10.3390/ijms22010229

Corvalán, N. A., Zygadlo, J. A., and García, D. A. (2009). Stereo-selective activity of menthol on GABA(A) receptor. *Chirality* 21, 525–530. doi: 10.1002/chir.20631

Cui, M., Honore, P., Zhong, C., Gauvin, D., Mikusa, J., Hernandez, G., et al. (2006). TRPV1 receptors in the CNS play a key role in broad-spectrum analgesia of TRPV1 antagonists. *J. Neurosci.* 26, 9385–9393. doi: 10.1523/jneurosci.1246-06.2006

Dani, J. A., and Bertrand, D. (2007). Nicotinic acetylcholine receptors and nicotinic cholinergic mechanisms of the central nervous system. *Annu. Rev. Pharmacol. Toxicol.* 47, 699–729. doi: 10.1146/annurev.pharmtox.47.120505.105214

Daniels, R. L., Takashima, Y., and McKemy, D. D. (2009). Activity of the neuronal cold sensor TRPM8 is regulated by phospholipase C *via* the phospholipid phosphoinositol 4,5-bisphosphate. *J. Biol. Chem.* 284, 1570–1582. doi: 10.1074/jbc.M807270200

Davies, S. J., Harding, L. M., and Baranowski, A. P. (2002). A novel treatment of postherpetic neuralgia using peppermint oil. *Clin. J. Pain* 18, 200–202. doi: 10.1097/00002508-200205000-00011

De Caro, C., Cristiano, C., Avagliano, C., Bertamino, A., Ostacolo, C., Campiglia, P., et al. (2019). Characterization of new TRPM8 modulators in pain perception. *Int. J. Mol. Sci.* 20:5544. doi: 10.3390/ijms20225544

Descoeur, J., Pereira, V., Pizzoccaro, A., Francois, A., Ling, B., Maffre, V., et al. (2011). Oxaliplatin-induced cold hypersensitivity is due to remodelling of ion channel expression in nociceptors. *EMBO Mol. Med.* 3, 266–278. doi: 10.1002/emmm.201100134

Dessirier, J. M., O'Mahony, M., and Carstens, E. (2001). Oral irritant properties of menthol: Sensitizing and desensitizing effects of repeated application and cross-desensitization to nicotine. *Physiol. Behav.* 73, 25–36. doi: 10.1016/s0031-9384(01)00431-0

Dhaka, A., Murray, A. N., Mathur, J., Earley, T. J., Petrus, M. J., and Patapoutian, A. (2007). TRPM8 is required for cold sensation in mice. *Neuron* 54, 371–378. doi: 10.1016/j.neuron.2007.02.024

Dierkes, P. W., Hochstrate, P., and Schlue, W. R. (1997). Voltage-dependent Ca2+ influx into identified leech neurones. *Brain Res.* 746, 285–293. doi: 10.1016/s0006-8993(96)01264-4

Dineley, K. T., Pandya, A. A., and Yakel, J. L. (2015). Nicotinic ACh receptors as therapeutic targets in CNS disorders. *Trends Pharmacol. Sci.* 36, 96–108. doi: 10.1016/j.tips.2014.12.002

Diver, M. M., Cheng, Y., and Julius, D. (2019). Structural insights into TRPM8 inhibition and desensitization. *Science* 365, 1434–1440. doi: 10.1126/science.aax6672

Engelhard, D., Hofer, P., and Annaheim, S. (2019). Evaluation of the effect of cooling strategies on recovery after surgical intervention. *BMJ Open Sport Exerc. Med.* 5:e000527. doi: 10.1136/bmjsem-2019-000527

Everaerts, W., Gees, M., Alpizar, Y. A., Farre, R., Leten, C., Apetrei, A., et al. (2011). The capsaicin receptor TRPV1 is a crucial mediator of the noxious effects of mustard oil. *Curr. Biol.* 21, 316–321. doi: 10.1016/j.cub.2011.01.031

Fallon, M. T., Storey, D. J., Krishan, A., Weir, C. J., Mitchell, R., Fleetwood-Walker, S. M., et al. (2015). Cancer treatment-related neuropathic pain: Proof of concept study with menthol–a TRPM8 agonist. *Support. Care Cancer* 23, 2769–2777. doi: 10.1007/s00520-015-2642-8

Fan, L., Balakrishna, S., Jabba, S. V., Bonner, P. E., Taylor, S. R., Picciotto, M. R., et al. (2016). Menthol decreases oral nicotine aversion in C57BL/6 mice through a TRPM8-dependent mechanism. *Tob. Control.* 25, ii50–ii54. doi: 10.1136/tobaccocontrol-2016-053209

Fernandes, E. S., Fernandes, M. A., and Keeble, J. E. (2012). The functions of TRPA1 and TRPV1: Moving away from sensory nerves. *Br. J. Pharmacol.* 166, 510–521. doi: 10.1111/j.1476-5381.2012.01851.x

Fernández, J. A., Skryma, R., Bidaux, G., Magleby, K. L., Scholfield, C. N., McGeown, J. G., et al. (2011). Voltage- and cold-dependent gating of single TRPM8 ion channels. *J. Gen. Physiol.* 137, 173–195. doi: 10.1085/jgp.201010498

Filippov, I. B., Vladymyrova, I. A., Kuliieva Ie, M., Skryma, R., Prevarskaia, N., Shuba, et al. (2009). [Modulation of the smooth muscle contractions of the rat vas deferens by TRPM8 channel agonist menthol]. *Fiziol Zh (1994)* 55, 30–40.

Fisher, K., Lefebvre, C., and Coderre, T. J. (2002). Antinociceptive effects following intrathecal pretreatment with selective metabotropic glutamate receptor compounds in a rat model of neuropathic pain. *Pharmacol. Biochem. Behav.* 73, 411–418. doi: 10.1016/s0091-3057(02)00832-8

Flühr, K., Neddermeyer, T. J., and Lötsch, J. (2009). Capsaicin or menthol sensitization induces quantitative but no qualitative changes to thermal and mechanical pain thresholds. *Clin. J. Pain* 25, 128–131. doi: 10.1097/AJP.0b013e3181817aa2

Foulds, J., Hooper, M. W., Pletcher, M. J., and Okuyemi, K. S. (2010). Do smokers of menthol cigarettes find it harder to quit smoking? *Nicotine Tob. Res.* 12 Suppl 2, S102–S109. doi: 10.1093/ntr/ntq166

Frederick, J., Buck, M. E., Matson, D. J., and Cortright, D. N. (2007). Increased TRPA1, TRPM8, and TRPV2 expression in dorsal root ganglia by nerve injury. *Biochem. Biophys. Res. Commun.* 358, 1058–1064. doi: 10.1016/j.bbrc.2007.05.029

Freilinger, T., Anttila, V., de Vries, B., Malik, R., Kallela, M., Terwindt, G. M., et al. (2012). Genome-wide association analysis identifies susceptibility loci for migraine without aura. *Nat. Genet.* 44, 777–782. doi: 10.1038/ng.2307

Fritschy, J. M., Panzanelli, P., and Tyagarajan, S. K. (2012). Molecular and functional heterogeneity of GABAergic synapses. *Cell. Mol. Life Sci.* 69, 2485–2499. doi: 10.1007/s00018-012-0926-4

Galeotti, N., Di Cesare Mannelli, L., Mazzanti, G., Bartolini, A., and Ghelardini, C. (2002). Menthol: A natural analgesic compound. *Neurosci. Lett.* 322, 145–148. doi: 10.1016/s0304-3940(01)02527-7

Galeotti, N., Ghelardini, C., Mannelli, L., Mazzanti, G., Baghiroli, L., and Bartolini, A. (2001). Local anaesthetic activity of (+)- and (-)-menthol. *Planta Med.* 67, 174–176. doi: 10.1055/s-2001-11515

Gaudioso, C., Hao, J., Martin-Eauclaire, M. F., Gabriac, M., and Delmas, P. (2012). Menthol pain relief through cumulative inactivation of voltage-gated sodium channels. *Pain* 153, 473–484. doi: 10.1016/j.pain.2011.11.014

Gavva, N. R., Sandrock, R., Arnold, G. E., Davis, M., Lamas, E., Lindvay, C., et al. (2019). Reduced TRPM8 expression underpins reduced migraine risk and attenuated cold pain sensation in humans. *Sci. Rep.* 9:19655. doi: 10.1038/s41598-019-56295-0

Gavva, N. R., Treanor, J. J., Garami, A., Fang, L., Surapaneni, S., Akrami, A., et al. (2008). Pharmacological blockade of the vanilloid receptor TRPV1 elicits marked hyperthermia in humans. *Pain* 136, 202–210. doi: 10.1016/j.pain.2008.01.024

Gillis, D. J., Vellante, A., Gallo, J. A., and D'Amico, A. P. (2020). Influence of menthol on recovery from exercise-induced muscle damage. *J. Strength Cond. Res.* 34, 451–462. doi: 10.1519/jsc.0000000000002833

Glyn-Jones, S., Palmer, A. J., Agricola, R., Price, A. J., Vincent, T. L., Weinans, H., et al. (2015). Osteoarthritis. *Lancet* 386, 376–387. doi: 10.1016/s0140-6736(14)60802-3

Gold, M. S., Weinreich, D., Kim, C. S., Wang, R., Treanor, J., Porreca, F., et al. (2003). Redistribution of Na(V)1.8 in uninjured axons enables neuropathic pain. *J. Neurosci.* 23, 158–166. doi: 10.1523/jneurosci.23-01-00158.2003

Gong, K., and Jasmin, L. (2017). Sustained morphine administration induces TRPM8-dependent cold hyperalgesia. *J. Pain* 18, 212–221. doi: 10.1016/j.jpain.2016.10.015

Green, B. G. (1985). Menthol modulates oral sensations of warmth and cold. *Physiol. Behav.* 35, 427–434. doi: 10.1016/0031-9384(85)90319-1

Green, B. G., and McAuliffe, B. L. (2000). Menthol desensitization of capsaicin irritation. Evidence of a short-term anti-nociceptive effect. *Physiol. Behav.* 68, 631–639. doi: 10.1016/s0031-9384(99)00221-8

Gudin, J. A., Dietze, D. T., and Hurwitz, P. L. (2020). Improvement of pain and function after use of a topical pain relieving patch: Results of the RELIEF study. *J. Pain Res.* 13, 1557–1568. doi: 10.2147/jpr.S258883

Gunthorpe, M. J., and Chizh, B. A. (2009). Clinical development of TRPV1 antagonists: Targeting a pivotal point in the pain pathway. *Drug Discov. Today* 14, 56–67. doi: 10.1016/j.drudis.2008.11.005

Gupta, A., Kaur, K., Sharma, S., Goyal, S., Arora, S., and Murthy, R. S. (2010). Clinical aspects of acute post-operative pain management & its assessment. *J. Adv. Pharm. Technol. Res.* 1, 97–108.

Haeseler, G., Maue, D., Grosskreutz, J., Bufler, J., Nentwig, B., Piepenbrock, S., et al. (2002). Voltage-dependent block of neuronal and skeletal muscle sodium channels by thymol and menthol. *Eur. J. Anaesthesiol.* 19, 571–579. doi: 10.1017/s0265021502000923

Hagenacker, T., Lampe, M., and Schäfers, M. (2014). Icilin reduces voltage-gated calcium channel currents in naïve and injured DRG neurons in the rat spinal nerve ligation model. *Brain Res.* 1557, 171–179. doi: 10.1016/j.brainres.2014.02.022

Hall, A. C., Turcotte, C. M., Betts, B. A., Yeung, W. Y., Agyeman, A. S., and Burk, L. A. (2004). Modulation of human GABAA and glycine receptor currents by menthol and related monoterpenoids. *Eur. J. Pharmacol.* 506, 9–16. doi: 10.1016/j.ejphar.2004.10.026

Hanprasertpong, T., Kor-anantakul, O., Leetanaporn, R., Suwanrath, C., Suntharasaj, T., Pruksanusak, N., et al. (2015). Reducing pain and anxiety during second trimester genetic amniocentesis using aromatic therapy: A randomized trial. *J. Med. Assoc. Thai.* 98, 734–738.

Hans, M., Wilhelm, M., and Swandulla, D. (2012). Menthol suppresses nicotinic acetylcholine receptor functioning in sensory neurons *via* allosteric modulation. *Chem. Senses* 37, 463–469. doi: 10.1093/chemse/bjr128

Harrison, J. L., and Davis, K. D. (1999). Cold-evoked pain varies with skin type and cooling rate: A psychophysical study in humans. *Pain* 83, 123–135. doi: 10.1016/s0304-3959(99)00099-8

Hartvigsen, J., Hancock, M. J., Kongsted, A., Louw, Q., Ferreira, M. L., Genevay, S., et al. (2018). What low back pain is and why we need to pay attention. *Lancet* 391, 2356–2367. doi: 10.1016/s0140-6736(18)30480-x

Hatem, S., Attal, N., Willer, J. C., and Bouhassira, D. (2006). Psychophysical study of the effects of topical application of menthol in healthy volunteers. *Pain* 122, 190–196. doi: 10.1016/j.pain.2006.01.026

Hawthorn, M., Ferrante, J., Luchowski, E., Rutledge, A., Wei, X. Y., and Triggle, D. J. (1988). The actions of peppermint oil and menthol on calcium channel dependent processes in intestinal, neuronal and cardiac preparations. *Aliment. Pharmacol. Ther.* 2, 101–118. doi: 10.1111/j.1365-2036.1988.tb00677.x

Heimes, K., Hauk, F., and Verspohl, E. J. (2011). Mode of action of peppermint oil and (-)-menthol with respect to 5-HT3 receptor subtypes: Binding studies, cation uptake by receptor channels and contraction of isolated rat ileum. *Phytother. Res.* 25, 702–708. doi: 10.1002/ptr.3316

Hemmings, H. C. Jr., Akabas, M. H., Goldstein, P. A., Trudell, J. R., Orser, B. A., and Harrison, N. L. (2005). Emerging molecular mechanisms of general anesthetic action. *Trends Pharmacol. Sci.* 26, 503–510. doi: 10.1016/j.tips.2005.08.006

Henderson, B. J., Wall, T. R., Henley, B. M., Kim, C. H., McKinney, S., and Lester, H. A. (2017). Menthol enhances nicotine reward-related behavior by potentiating nicotine-induced changes in nAChR function, nAChR upregulation, and DA neuron excitability. *Neuropsychopharmacology* 42, 2285–2291. doi: 10.1038/npp.2017.72

Henderson, B. J., Wall, T. R., Henley, B. M., Kim, C. H., Nichols, W. A., Moaddel, R., et al. (2016). Menthol alone upregulates midbrain nachrs, alters nachr subtype stoichiometry, alters dopamine neuron firing frequency, and prevents nicotine reward. *J. Neurosci.* 36, 2957–2974. doi: 10.1523/jneurosci.4194-15.2016

Higashi, Y., Kiuchi, T., and Furuta, K. (2010). Efficacy and safety profile of a topical methyl salicylate and menthol patch in adult patients with mild to moderate muscle strain: A randomized, double-blind, parallel-group, placebo-controlled, multicenter study. *Clin. Ther.* 32, 34–43. doi: 10.1016/j.clinthera.2010.01.016

Hilfiger, L., Triaux, Z., Marcic, C., Héberlé, E., Emhemmed, F., Darbon, P., et al. (2021). Anti-hyperalgesic properties of menthol and pulegone. *Front. Pharmacol.* 12:753873. doi: 10.3389/fphar.2021.753873

Huang, S. M., Bisogno, T., Trevisani, M., Al-Hayani, A., De Petrocellis, L., Fezza, F., et al. (2002). An endogenous capsaicin-like substance with high potency at recombinant and native vanilloid VR1 receptors. *Proc. Natl. Acad. Sci. U.S.A.* 99, 8400–8405. doi: 10.1073/pnas.122196999

Huynh, Y. W., Raimondi, A., Finkner, A., Kuck, J. D., Selleck, C., and Bevins, R. A. (2020). Menthol blunts the interoceptive discriminative stimulus effects of nicotine in female but not male rats. *Psychopharmacology (Berl)* 237, 2395–2404. doi: 10.1007/s00213-020-05542-8

Iftinca, M., Basso, L., Flynn, R., Kwok, C., Roland, C., Hassan, A., et al. (2020). Chronic morphine regulates TRPM8 channels *via* MOR-PKCβ signaling. *Mol Brain* 13:61. doi: 10.1186/s13041-020-00599-0

Ikoma, A., Steinhoff, M., Ständer, S., Yosipovitch, G., and Schmelz, M. (2006). The neurobiology of itch. *Nat. Rev. Neurosci.* 7, 535–547. doi: 10.1038/nrn1950

Ito, S., Kume, H., Shiraki, A., Kondo, M., Makino, Y., Kamiya, K., et al. (2008). Inhibition by the cold receptor agonists menthol and icilin of airway smooth muscle contraction. *Pulm. Pharmacol. Ther.* 21, 812–817. doi: 10.1016/j.pupt.2008.07.001

Izquierdo, C., Martín-Martínez, M., Gómez-Monterrey, I., and González-Muñiz, R. (2021). TRPM8 channels: Advances in structural studies and pharmacological modulation. *Int. J. Mol. Sci.* 22:8502. doi: 10.3390/ijms22168502

Ji, G., Zhou, S., Kochukov, M. Y., Westlund, K. N., and Carlton, S. M. (2007). Plasticity in intact A delta- and C-fibers contributes to cold hypersensitivity in neuropathic rats. *Neuroscience* 150, 182–193. doi: 10.1016/j.neuroscience.2007.09.002

Johar, P., Grover, V., Topp, R., and Behm, D. G. (2012). A comparison of topical menthol to ice on pain, evoked tetanic and voluntary force during delayed onset muscle soreness. *Int. J. Sports. Phys. Ther.* 7, 314–322.

Kabbani, N. (2013). Not so Cool? Menthol's discovered actions on the nicotinic receptor and its implications for nicotine addiction. *Front. Pharmacol.* 4:95. doi: 10.3389/fphar.2013.00095

Kamatou, G. P., Vermaak, I., Viljoen, A. M., and Lawrence, B. M. (2013). Menthol: A simple monoterpene with remarkable biological properties. *Phytochemistry* 96, 15–25. doi: 10.1016/j.phytochem.2013.08.005

Karashima, Y., Damann, N., Prenen, J., Talavera, K., Segal, A., Voets, T., et al. (2007). Bimodal action of menthol on the transient receptor potential channel TRPA1. *J. Neurosci.* 27, 9874–9884. doi: 10.1523/jneurosci.2221-07.2007

Katsura, H., Obata, K., Mizushima, T., Yamanaka, H., Kobayashi, K., Dai, Y., et al. (2006). Antisense knock down of TRPA1, but not TRPM8, alleviates cold hyperalgesia after spinal nerve ligation in rats. *Exp. Neurol.* 200, 112–123. doi: 10.1016/j.expneurol.2006.01.031

Kawashiri, T., Egashira, N., Kurobe, K., Tsutsumi, K., Yamashita, Y., Ushio, S., et al. (2012). L type Ca^2+ channel blockers prevent oxaliplatin-induced cold hyperalgesia and TRPM8 overexpression in rats. *Mol. Pain* 8:7. doi: 10.1186/1744-8069-8-7

Kayama, Y., Shibata, M., Takizawa, T., Ibata, K., Shimizu, T., Ebine, T., et al. (2018). Functional interactions between transient receptor potential M8 and transient receptor potential V1 in the trigeminal system: Relevance to migraine pathophysiology. *Cephalalgia* 38, 833–845. doi: 10.1177/0333102417712719

Klein, A. H., Carstens, M. I., Zanotto, K. L., Sawyer, C. M., Ivanov, M., Cheung, S., et al. (2011). Self- and cross-desensitization of oral irritation by menthol and cinnamaldehyde (CA) *via* peripheral interactions at trigeminal sensory neurons. *Chem. Sense* 36, 199–208. doi: 10.1093/chemse/bjq115

Klein, A. H., Sawyer, C. M., Carstens, M. I., Tsagareli, M. G., Tsiklauri, N., and Carstens, E. (2010). Topical application of L-menthol induces heat analgesia, mechanical allodynia, and a biphasic effect on cold sensitivity in rats. *Behav. Brain. Res.* 212, 179–186. doi: 10.1016/j.bbr.2010.04.015

Kobayashi, K., Fukuoka, T., Obata, K., Yamanaka, H., Dai, Y., Tokunaga, A., et al. (2005). Distinct expression of TRPM8, TRPA1, and TRPV1 mRNAs in rat primary afferent neurons with adelta/c-fibers and colocalization with trk receptors. *J. Comp. Neurol.* 493, 596–606. doi: 10.1002/cne.20794

Koh, W. U., Choi, S. S., Kim, J. H., Yoon, H. J., Ahn, H. S., Lee, S. K., et al. (2016). The preventive effect of resiniferatoxin on the development of cold hypersensitivity induced by spinal nerve ligation: Involvement of TRPM8. *BMC Neurosci.* 17:38. doi: 10.1186/s12868-016-0273-8

Koivisto, A., Hukkanen, M., Saarnilehto, M., Chapman, H., Kuokkanen, K., Wei, H., et al. (2012). Inhibiting TRPA1 ion channel reduces loss of cutaneous nerve fiber function in diabetic animals: Sustained activation of the TRPA1 channel contributes to the pathogenesis of peripheral diabetic neuropathy. *Pharmacol. Res.* 65, 149–158. doi: 10.1016/j.phrs.2011.10.006

Kolassa, N. (2013). Menthol differs from other terpenic essential oil constituents. *Regul. Toxicol. Pharmacol.* 65, 115–118. doi: 10.1016/j.yrtph.2012.11.009

Kosiba, J. D., Hughes, M. T., LaRowe, L. R., Zvolensky, M. J., Norton, P. J., Smits, J. A. J., et al. (2019). Menthol cigarette use and pain reporting among African American adults seeking treatment for smoking cessation. *Exp. Clin. Psychopharmacol.* 27, 276–282. doi: 10.1037/pha0000254

Krasowski, M. D., Jenkins, A., Flood, P., Kung, A. Y., Hopfinger, A. J., and Harrison, N. L. (2001). General anesthetic potencies of a series of propofol analogs correlate with potency for potentiation of gamma-aminobutyric acid (GABA) current at the GABA(A) receptor but not with lipid solubility. *J. Pharmacol. Exp. Ther.* 297, 338–351.

Lai, P. M., Collaku, A., and Reed, K. (2017). Efficacy and safety of topical diclofenac/menthol gel for ankle sprain: A randomized, double-blind, placebo- and active-controlled trial. *J. Int. Med. Res.* 45, 647–661. doi: 10.1177/0300060517700322

Lau, B. K., Karim, S., Goodchild, A. K., Vaughan, C. W., and Drew, G. M. (2014). Menthol enhances phasic and tonic GABAA receptor-mediated currents in midbrain periaqueductal grey neurons. *Br. J. Pharmacol.* 171, 2803–2813. doi: 10.1111/bph.12602

Lemon, C. H., Norris, J. E., and Heldmann, B. A. (2019). The TRPA1 ion channel contributes to sensory-guided avoidance of menthol in mice. *eNeuro* 6, 304–319. doi: 10.1523/eneuro.0304-19.2019

Lindblom, U., and Verrillo, R. T. (1979). Sensory functions in chronic neuralgia. *J. Neurol. Neurosurg. Psychiatry* 42, 422–435. doi: 10.1136/jnnp.42.5.422

Lippoldt, E. K., Elmes, R. R., McCoy, D. D., Knowlton, W. M., and McKemy, D. D. (2013). Artemin, a glial cell line-derived neurotrophic factor family member, induces TRPM8-dependent cold pain. *J. Neurosci.* 33, 12543–12552. doi: 10.1523/jneurosci.5765-12.2013

Lippoldt, E. K., Ongun, S., Kusaka, G. K., and McKemy, D. D. (2016). Inflammatory and neuropathic cold allodynia are selectively mediated by the neurotrophic factor receptor GFRα3. *Proc. Natl. Acad. Sci. U.S.A.* 113, 4506–4511. doi: 10.1073/pnas.1603294113

Liu, B., Fan, L., Balakrishna, S., Sui, A., Morris, J. B., and Jordt, S. E. (2013). TRPM8 is the principal mediator of menthol-induced analgesia of acute and inflammatory pain. *Pain* 154, 2169–2177. doi: 10.1016/j.pain.2013.06.043

Liu, Y., Ye, X., Feng, X., Zhou, G., Rong, Z., Fang, C., et al. (2005). Menthol facilitates the skin analgesic effect of tetracaine gel. *Int. J. Pharm.* 305, 31–36. doi: 10.1016/j.ijpharm.2005.08.005

Lu, H. F., Hsueh, S. C., Yu, F. S., Yang, J. S., Tang, N. Y., Chen, S. C., et al. (2006). The role of Ca2+ in (-)-menthol-induced human promyelocytic leukemia HL-60 cell death. *In. Vivo* 20, 69–75.

Macpherson, L. J., Hwang, S. W., Miyamoto, T., Dubin, A. E., Patapoutian, A., and Story, G. M. (2006). More than cool: Promiscuous relationships of menthol and other sensory compounds. *Mol. Cell. Neurosci.* 32, 335–343. doi: 10.1016/j.mcn.2006.05.005

Mahieu, F., Owsianik, G., Verbert, L., Janssens, A., De Smedt, H., Nilius, B., et al. (2007). TRPM8-independent menthol-induced Ca2+ release from endoplasmic reticulum and Golgi. *J. Biol. Chem.* 282, 3325–3336. doi: 10.1074/jbc.M605213200

Mahn, F., Hüllemann, P., Wasner, G., Baron, R., and Binder, A. (2014). Topical high-concentration menthol: Reproducibility of a human surrogate pain model. *Eur. J. Pain* 18, 1248–1258. doi: 10.1002/j.1532-2149.2014.484.x

Marwaha, L., Bansal, Y., Singh, R., Saroj, P., Bhandari, R., and Kuhad, A. (2016). TRP channels: Potential drug target for neuropathic pain. *Inflammopharmacology* 24, 305–317. doi: 10.1007/s10787-016-0288-x

Matsu-ura, T., Michikawa, T., Inoue, T., Miyawaki, A., Yoshida, M., and Mikoshiba, K. (2006). Cytosolic inositol 1,4,5-trisphosphate dynamics during intracellular calcium oscillations in living cells. *J. Cell. Biol.* 173, 755–765. doi: 10.1083/jcb.200512141

McKemy, D. D., Neuhausser, W. M., and Julius, D. (2002). Identification of a cold receptor reveals a general role for TRP channels in thermosensation. *Nature* 416, 52–58. doi: 10.1038/nature719

Melanaphy, D., Johnson, C. D., Kustov, M. V., Watson, C. A., Borysova, L., Burdyga, T. V., et al. (2016). Ion channel mechanisms of rat tail artery contraction-relaxation by menthol involving, respectively, TRPM8 activation and L-type Ca2+ channel inhibition. *Am. J. Physiol. Heart Circ. Physiol.* 311, H1416–H1430. doi: 10.1152/ajpheart.00222.2015

Millan, M. J. (2003). The neurobiology and control of anxious states. *Prog. Neurobiol.* 70, 83–244. doi: 10.1016/s0301-0082(03)00087-x

Mizuno, K., Kono, T., Suzuki, Y., Miyagi, C., Omiya, Y., Miyano, K., et al. (2014). Goshajinkigan, a traditional Japanese medicine, prevents oxaliplatin-induced acute peripheral neuropathy by suppressing functional alteration of TRP channels in rat. *J. Pharmacol. Sci.* 125, 91–98. doi: 10.1254/jphs.13244fp

Moran, M. M., McAlexander, M. A., Bíró, T., and Szallasi, A. (2011). Transient receptor potential channels as therapeutic targets. *Nat. Rev. Drug Discov.* 10, 601–620. doi: 10.1038/nrd3456

Morice, A. H., Marshall, A. E., Higgins, K. S., and Grattan, T. J. (1994). Effect of inhaled menthol on citric acid induced cough in normal subjects. *Thorax* 49, 1024–1026. doi: 10.1136/thx.49.10.1024

Naganawa, T., Baad-Hansen, L., Ando, T., and Svensson, P. (2015). Influence of topical application of capsaicin, menthol and local anesthetics on intraoral somatosensory sensitivity in healthy subjects: Temporal and spatial aspects. *Exp. Brain. Res.* 233, 1189–1199. doi: 10.1007/s00221-015-4200-5

Namer, B., Kleggetveit, I. P., Handwerker, H., Schmelz, M., and Jorum, E. (2008). Role of TRPM8 and TRPA1 for cold allodynia in patients with cold injury. *Pain* 139, 63–72. doi: 10.1016/j.pain.2008.03.007

Namer, B., Seifert, F., Handwerker, H. O., and Maihöfner, C. (2005). TRPA1 and TRPM8 activation in humans: Effects of cinnamaldehyde and menthol. *Neuroreport* 16, 955–959. doi: 10.1097/00001756-200506210-00015

Neumann, J. T., and Copello, J. A. (2011). Cross-reactivity of ryanodine receptors with plasma membrane ion channel modulators. *Mol. Pharmacol.* 80, 509–517. doi: 10.1124/mol.111.071167

Nguyen, T. H. D., Itoh, S. G., Okumura, H., and Tominaga, M. (2021). Structural basis for promiscuous action of monoterpenes on TRP channels. *Commun. Biol.* 4:293. doi: 10.1038/s42003-021-01776-0

Nguyen, T. L., Nam, Y. S., Lee, S. Y., Kim, H. C., and Jang, C. G. (2010). Effects of capsazepine, a transient receptor potential vanilloid type 1 antagonist, on morphine-induced antinociception, tolerance, and dependence in mice. *Br. J. Anaesth.* 105, 668–674. doi: 10.1093/bja/aeq212

Niiyama, Y., Kawamata, T., Yamamoto, J., Omote, K., and Namiki, A. (2007). Bone cancer increases transient receptor potential vanilloid subfamily 1 expression within distinct subpopulations of dorsal root ganglion neurons. *Neuroscience* 148, 560–572. doi: 10.1016/j.neuroscience.2007.05.049

Obata, K., Katsura, H., Mizushima, T., Yamanaka, H., Kobayashi, K., Dai, Y., et al. (2005). TRPA1 induced in sensory neurons contributes to cold hyperalgesia after inflammation and nerve injury. *J. Clin. Invest.* 115, 2393–2401. doi: 10.1172/jci25437

Olsen, R. V., Andersen, H. H., Møller, H. G., Eskelund, P. W., and Arendt-Nielsen, L. (2014). Somatosensory and vasomotor manifestations of individual and combined stimulation of TRPM8 and TRPA1 using topical L-menthol and trans-cinnamaldehyde in healthy volunteers. *Eur. J. Pain* 18, 1333–1342. doi: 10.1002/j.1532-2149.2014.494.x

Oz, M., El Nebrisi, E. G., Yang, K. S., Howarth, F. C., and Al Kury, L. T. (2017). Cellular and molecular targets of menthol actions. *Front. Pharmacol.* 8:472. doi: 10.3389/fphar.2017.00472

Pabbidi, M. R., and Premkumar, L. S. (2017). Role of transient receptor potential channels Trpv1 and trpm8 in diabetic peripheral neuropathy. *J Diabetes Treat.* 2017:029.

Padua, L., Coraci, D., Erra, C., Pazzaglia, C., Paolasso, I., Loreti, C., et al. (2016). Carpal tunnel syndrome: Clinical features, diagnosis, and management. *Lancet Neurol.* 15, 1273–1284. doi: 10.1016/s1474-4422(16)30231-9

Palade, P. (1987). Drug-induced Ca2+ release from isolated sarcoplasmic reticulum. II. Releases involving a Ca2+-induced Ca2+ release channel. *J. Biol. Chem.* 262, 6142–6148.

Palkar, R., Ongun, S., Catich, E., Li, N., Borad, N., Sarkisian, A., et al. (2018). Cooling relief of acute and chronic itch requires TRPM8 channels and neurons. *J. Invest. Dermatol.* 138, 1391–1399. doi: 10.1016/j.jid.2017.12.025

Pan, R., Tian, Y., Gao, R., Li, H., Zhao, X., Barrett, J. E., et al. (2012). Central mechanisms of menthol-induced analgesia. *J. Pharmacol. Exp. Ther.* 343, 661–672. doi: 10.1124/jpet.112.196717

Parra, A., Gonzalez-Gonzalez, O., Gallar, J., and Belmonte, C. (2014). Tear fluid hyperosmolality increases nerve impulse activity of cold thermoreceptor endings of the cornea. *Pain* 155, 1481–1491. doi: 10.1016/j.pain.2014.04.025

Patapoutian, A., Peier, A. M., Story, G. M., and Viswanath, V. (2003). ThermoTRP channels and beyond: Mechanisms of temperature sensation. *Nat. Rev. Neurosci.* 4, 529–539. doi: 10.1038/nrn1141

Patel, R., Gonçalves, L., Leveridge, M., Mack, S. R., Hendrick, A., Brice, N. L., et al. (2014). Anti-hyperalgesic effects of a novel TRPM8 agonist in neuropathic rats: A comparison with topical menthol. *Pain* 155, 2097–2107. doi: 10.1016/j.pain.2014.07.022

Patel, T., Ishiuji, Y., and Yosipovitch, G. (2007). Menthol: A refreshing look at this ancient compound. *J. Am. Acad. Dermatol.* 57, 873–878. doi: 10.1016/j.jaad.2007.04.008

Peier, A. M., Reeve, A. J., Andersson, D. A., Moqrich, A., Earley, T. J., Hergarden, A. C., et al. (2002). A heat-sensitive TRP channel expressed in keratinocytes. *Science* 296, 2046–2049. doi: 10.1126/science.1073140

Pezzoli, M., Elhamdani, A., Camacho, S., Meystre, J., González, S. M., le Coutre, J., et al. (2014). Dampened neural activity and abolition of epileptic-like activity in cortical slices by active ingredients of spices. *Sci. Rep.* 4:6825. doi: 10.1038/srep06825

Plevkova, J., Kollarik, M., Poliacek, I., Brozmanova, M., Surdenikova, L., Tatar, M., et al. (2013). The role of trigeminal nasal TRPM8-expressing afferent neurons in the antitussive effects of menthol. *J. Appl. Physiol. (1985)* 115, 268–274. doi: 10.1152/japplphysiol.01144.2012

Premkumar, L. S., Raisinghani, M., Pingle, S. C., Long, C., and Pimentel, F. (2005). Downregulation of transient receptor potential melastatin 8 by protein kinase C-mediated dephosphorylation. *J. Neurosci.* 25, 11322–11329. doi: 10.1523/jneurosci.3006-05.2005

Preti, D., Saponaro, G., and Szallasi, A. (2015). Transient receptor potential ankyrin 1 (TRPA1) antagonists. *Pharm. Pat. Anal.* 4, 75–94. doi: 10.4155/ppa.14.60

Proudfoot, C. J., Garry, E. M., Cottrell, D. F., Rosie, R., Anderson, H., Robertson, D. C., et al. (2006). Analgesia mediated by the TRPM8 cold receptor in chronic neuropathic pain. *Curr. Biol.* 16, 1591–1605. doi: 10.1016/j.cub.2006.07.061

Quallo, T., Vastani, N., Horridge, E., Gentry, C., Parra, A., Moss, S., et al. (2015). TRPM8 is a neuronal osmosensor that regulates eye blinking in mice. *Nat. Commun.* 6:7150. doi: 10.1038/ncomms8150

Raddatz, N., Castillo, J. P., Gonzalez, C., Alvarez, O., and Latorre, R. (2014). Temperature and voltage coupling to channel opening in transient receptor potential melastatin 8 (TRPM8). *J. Biol. Chem.* 289, 35438–35454. doi: 10.1074/jbc.M114.612713

Ramos-Filho, A. C., Shah, A., Augusto, T. M., Barbosa, G. O., Leiria, L. O., de Carvalho, H. F., et al. (2014). Menthol inhibits detrusor contractility independently of TRPM8 activation. *PLoS One* 9:e111616. doi: 10.1371/journal.pone.0111616

Reid, G., and Flonta, M. L. (2001). Physiology. Cold current in thermoreceptive neurons. *Nature* 413:480. doi: 10.1038/35097164

Rimola, V., Osthues, T., Königs, V., Geißlinger, G., and Sisignano, M. (2021). Oxaliplatin causes transient changes in TRPM8 channel activity. *Int. J. Mol. Sci.* 22:4962. doi: 10.3390/ijms22094962

Rohács, T., Lopes, C. M., Michailidis, I., and Logothetis, D. E. (2005). PI(4,5)P2 regulates the activation and desensitization of TRPM8 channels through the TRP domain. *Nat. Neurosci.* 8, 626–634. doi: 10.1038/nn1451

Rosenbaum, T., Morales-Lázaro, S. L., and Islas, L. D. (2022). TRP channels: A journey towards a molecular understanding of pain. *Nat. Rev. Neurosci.* doi: 10.1038/s41583-022-00611-7 [Epub ahead of print].

Rossi, H. L., Vierck, C. J. Jr., Caudle, R. M., and Neubert, J. K. (2006). Characterization of cold sensitivity and thermal preference using an operant orofacial assay. *Mol. Pain* 2:37. doi: 10.1186/1744-8069-2-37

Ruskin, D. N., Anand, R., and LaHoste, G. J. (2008). Chronic menthol attenuates the effect of nicotine on body temperature in adolescent rats. *Nicotine Tob. Res.* 10, 1753–1759. doi: 10.1080/14622200802443734

Scherer, P. C., Zaccor, N. W., Neumann, N. M., Vasavda, C., Barrow, R., Ewald, A. J., et al. (2017). TRPV1 is a physiological regulator of μ-opioid receptors. *Proc. Natl. Acad. Sci. U.S.A.* 114, 13561–13566. doi: 10.1073/pnas.1717005114

Seifert, F., and Maihöfner, C. (2007). Representation of cold allodynia in the human brain–a functional MRI study. *Neuroimage* 35, 1168–1180. doi: 10.1016/j.neuroimage.2007.01.021

Shapovalov, G., Gkika, D., Devilliers, M., Kondratskyi, A., Gordienko, D., Busserolles, J., et al. (2013). Opiates modulate thermosensation by internalizing cold receptor TRPM8. *Cell Rep.* 4, 504–515. doi: 10.1016/j.celrep.2013.07.002

Sidell, N., Verity, M. A., and Nord, E. P. (1990). Menthol blocks dihydropyridine-insensitive Ca2+ channels and induces neurite outgrowth in human neuroblastoma cells. *J. Cell. Physiol.* 142, 410–419. doi: 10.1002/jcp.1041420226

Siegel, R. E. (1970). *Galen on sense perception*. Basel: Karger Publishers.

Sigel, E., and Steinmann, M. E. (2012). Structure, function, and modulation of GABA(A) receptors. *J. Biol. Chem.* 287, 40224–40231. doi: 10.1074/jbc.R112.386664

Silva, H. (2020). A descriptive overview of the medical uses given to mentha aromatic herbs throughout history. *Biology (Basel)* 9:484. doi: 10.3390/biology9120484

Simmons, R. M., Webster, A. A., Kalra, A. B., and Iyengar, S. (2002). Group II mGluR receptor agonists are effective in persistent and neuropathic pain models in rats. *Pharmacol. Biochem. Behav.* 73, 419–427. doi: 10.1016/s0091-3057(02)00849-3

Smith, G. D., Gunthorpe, M. J., Kelsell, R. E., Hayes, P. D., Reilly, P., Facer, P., et al. (2002). TRPV3 is a temperature-sensitive vanilloid receptor-like protein. *Nature* 418, 186–190. doi: 10.1038/nature00894

Sprengell, C. J. (1708). *Aphorisms of hippocrates: And the sentences of celsus; with explanations and references to the most considerable writers in physick and philosophy, both ancient and modern*. London: R. Bonwick.

St Cyr, A., Chen, A., Bradley, K. C., Yuan, H., Silberstein, S. D., and Young, W. B. (2015). Efficacy and tolerability of STOPAIN for a migraine attack. *Front. Neurol.* 6:11. doi: 10.3389/fneur.2015.00011

Stefanelli, L., Lockyer, E. J., Collins, B. W., Snow, N. J., Crocker, J., Kent, C., et al. (2019). Delayed-onset muscle soreness and topical analgesic alter corticospinal excitability of the biceps brachii. *Med. Sci. Sports Exerc.* 51, 2344–2356. doi: 10.1249/mss.0000000000002055

Story, G. M., Peier, A. M., Reeve, A. J., Eid, S. R., Mosbacher, J., Hricik, T. R., et al. (2003). ANKTM1, a TRP-like channel expressed in nociceptive neurons, is activated by cold temperatures. *Cell* 112, 819–829. doi: 10.1016/s0092-8674(03)00158-2

Su, L., Shu, R., Song, C., Yu, Y., Wang, G., Li, Y., et al. (2017). Downregulations of TRPM8 expression and membrane trafficking in dorsal root ganglion mediate the attenuation of cold hyperalgesia in CCI rats induced by GFRα3 knockdown. *Brain Res. Bull.* 135, 8–24. doi: 10.1016/j.brainresbull.2017.08.002

Su, L., Wang, C., Yu, Y. H., Ren, Y. Y., Xie, K. L., and Wang, G. L. (2011). Role of TRPM8 in dorsal root ganglion in nerve injury-induced chronic pain. *BMC Neurosci.* 12:120. doi: 10.1186/1471-2202-12-120

Sun, J., Yang, T., Wang, P., Ma, S., Zhu, Z., Pu, Y., et al. (2014). Activation of cold-sensing transient receptor potential melastatin subtype 8 antagonizes vasoconstriction and hypertension through attenuating RhoA/Rho kinase pathway. *Hypertension* 63, 1354–1363. doi: 10.1161/hypertensionaha.113.02573

Sundstrup, E., Jakobsen, M. D., Brandt, M., Jay, K., Colado, J. C., Wang, Y., et al. (2014). Acute effect of topical menthol on chronic pain in slaughterhouse workers with carpal tunnel syndrome: Triple-blind, randomized placebo-controlled trial. *Rehabil. Res. Pract.* 2014:310913. doi: 10.1155/2014/310913

Swandulla, D., Carbone, E., Schäfer, K., and Lux, H. D. (1987). Effect of menthol on two types of Ca currents in cultured sensory neurons of vertebrates. *Pflugers Arch.* 409, 52–59. doi: 10.1007/bf00584749

Swandulla, D., Schäfer, K., and Lux, H. D. (1986). Calcium channel current inactivation is selectively modulated by menthol. *Neurosci. Lett.* 68, 23–28. doi: 10.1016/0304-3940(86)90223-5

Szallasi, A., and Blumberg, P. M. (1999). Vanilloid (Capsaicin) receptors and mechanisms. *Pharmacol. Rev.* 51, 159–212.

Tajino, K., Matsumura, K., Kosada, K., Shibakusa, T., Inoue, K., Fushiki, T., et al. (2007). Application of menthol to the skin of whole trunk in mice induces autonomic and behavioral heat-gain responses. *Am. J. Physiol. Regul. Integr. Comp. Physiol.* 293, R2128–R2135. doi: 10.1152/ajpregu.00377.2007

Takaishi, M., Uchida, K., Suzuki, Y., Matsui, H., Shimada, T., Fujita, F., et al. (2016). Reciprocal effects of capsaicin and menthol on thermosensation through regulated activities of TRPV1 and TRPM8. *J. Physiol. Sci.* 66, 143–155. doi: 10.1007/s12576-015-0427-y

Talavera, K., Startek, J. B., Alvarez-Collazo, J., Boonen, B., Alpizar, Y. A., Sanchez, A., et al. (2020). Mammalian transient receptor potential TRPA1 channels: From structure to disease. *Physiol. Rev.* 100, 725–803. doi: 10.1152/physrev.00005.2019

Taylor, R. Jr., Gan, T. J., Raffa, R. B., Gharibo, C., Pappagallo, M., Sinclair, N. R., et al. (2012). A randomized, double-blind comparison shows the addition of oxygenated glycerol triesters to topical mentholated cream for the treatment of acute musculoskeletal pain demonstrates incremental benefit over time. *Pain Pract.* 12, 610–619. doi: 10.1111/j.1533-2500.2012.00529.x

Tesfaye, S., Stevens, L. K., Stephenson, J. M., Fuller, J. H., Plater, M., Ionescu-Tirgoviste, C., et al. (1996). Prevalence of diabetic peripheral neuropathy and its relation to glycaemic control and potential risk factors: The EURODIAB IDDM Complications Study. *Diabetologia* 39, 1377–1384. doi: 10.1007/s001250050586

Thorup, I., Würtzen, G., Carstensen, J., and Olsen, P. (1983). Short term toxicity study in rats dosed with pulegone and menthol. *Toxicol. Lett.* 19, 207–210. doi: 10.1016/0378-4274(83)90120-0

Tillman, D. B., Treede, R. D., Meyer, R. A., and Campbell, J. N. (1995). Response of C fibre nociceptors in the anaesthetized monkey to heat stimuli: Correlation with pain threshold in humans. *J. Physiol.* 485 (Pt 3), 767–774. doi: 10.1113/jphysiol.1995.sp020767

Ton, H. T., Smart, A. E., Aguilar, B. L., Olson, T. T., Kellar, K. J., and Ahern, G. P. (2015). Menthol enhances the desensitization of human α3β4 nicotinic acetylcholine receptors. *Mol. Pharmacol.* 88, 256–264. doi: 10.1124/mol.115.098285

Topp, R., Brosky, J. A. Jr., and Pieschel, D. (2013). The effect of either topical menthol or a placebo on functioning and knee pain among patients with knee OA. *J. Geriatr. Phys. Ther.* 36, 92–99. doi: 10.1519/JPT.0b013e318268dde1

Tsuzuki, K., Xing, H., Ling, J., and Gu, J. G. (2004). Menthol-induced Ca2+ release from presynaptic Ca2+ stores potentiates sensory synaptic transmission. *J. Neurosci.* 24, 762–771. doi: 10.1523/jneurosci.4658-03.2004

Vardanyan, A., Wang, R., Vanderah, T. W., Ossipov, M. H., Lai, J., Porreca, F., et al. (2009). TRPV1 receptor in expression of opioid-induced hyperalgesia. *J. Pain* 10, 243–252. doi: 10.1016/j.jpain.2008.07.004

Vase, L., Svensson, P., Nikolajsen, L., Arendt-Nielsen, L., and Jensen, T. S. (2013). The effects of menthol on cold allodynia and wind-up-like pain in upper limb amputees with different levels of phantom limb pain. *Neurosci. Lett.* 534, 52–57. doi: 10.1016/j.neulet.2012.11.005

Vetter, I., Hein, A., Sattler, S., Hessler, S., Touska, F., Bressan, E., et al. (2013). Amplified cold transduction in native nociceptors by M-channel inhibition. *J. Neurosci.* 33, 16627–16641. doi: 10.1523/jneurosci.1473-13.2013

Vladymyrova, I. A., Filippov, I. B., Kuliieva Ie, M., Iurkevych, A., Skryma, R., Prevarskaia, N., et al. (2011). [Comparative effects of menthol and icilin on the induced contraction of the smooth muscles of the vas deferens of normal and castrated rats]. *Fiziol Zh (1994)* 57, 21–33.

Vogt-Eisele, A. K., Weber, K., Sherkheli, M. A., Vielhaber, G., Panten, J., Gisselmann, G., et al. (2007). Monoterpenoid agonists of TRPV3. *Br. J. Pharmacol.* 151, 530–540. doi: 10.1038/sj.bjp.0707245

Wade, A. G., Crawford, G. M., Young, D., Corson, S., and Brown, C. (2019). Comparison of diclofenac gel, ibuprofen gel, and ibuprofen gel with levomenthol for the topical treatment of pain associated with musculoskeletal injuries. *J. Int. Med. Res.* 47, 4454–4468. doi: 10.1177/0300060519859146

Wahren, L. K., and Torebjörk, E. (1992). Quantitative sensory tests in patients with neuralgia 11 to 25 years after injury. *Pain* 48, 237–244. doi: 10.1016/0304-3959(92)90063-h

Wahren, L. K., Torebjörk, E., and Jörum, E. (1989). Central suppression of cold-induced C fibre pain by myelinated fibre input. *Pain* 38, 313–319. doi: 10.1016/0304-3959(89)90218-2

Walstab, J., Wohlfarth, C., Hovius, R., Schmitteckert, S., Röth, R., Lasitschka, F., et al. (2014). Natural compounds boldine and menthol are antagonists of

human 5-HT3 receptors: Implications for treating gastrointestinal disorders. *Neurogastroenterol. Motil.* 26, 810–820. doi: 10.1111/nmo.12334

Wang, H. W., Liu, S. C., Chao, P. Z., and Lee, F. P. (2016). Menthol inhibiting parasympathetic function of tracheal smooth muscle. *Int. J. Med. Sci.* 13, 923–928. doi: 10.7150/ijms.17042

Wasner, G., Naleschinski, D., Binder, A., Schattschneider, J., McLachlan, E. M., and Baron, R. (2008). The effect of menthol on cold allodynia in patients with neuropathic pain. *Pain Med.* 9, 354–358. doi: 10.1111/j.1526-4637.2007.00290.x

Wasner, G., Schattschneider, J., Binder, A., and Baron, R. (2004). Topical menthol–a human model for cold pain by activation and sensitization of C nociceptors. *Brain* 127, 1159–1171. doi: 10.1093/brain/awh134

Watt, E. E., Betts, B. A., Kotey, F. O., Humbert, D. J., Griffith, T. N., Kelly, E. W., et al. (2008). Menthol shares general anesthetic activity and sites of action on the GABA(A) receptor with the intravenous agent, propofol. *Eur. J. Pharmacol.* 590, 120–126. doi: 10.1016/j.ejphar.2008.06.003

Wei, E. T., and Seid, D. A. (1983). AG-3-5: A chemical producing sensations of cold. *J. Pharm. Pharmacol.* 35, 110–112. doi: 10.1111/j.2042-7158.1983.tb04279.x

Werley, M. S., Coggins, C. R., and Lee, P. N. (2007). Possible effects on smokers of cigarette mentholation: A review of the evidence relating to key research questions. *Regul. Toxicol. Pharmacol.* 47, 189–203. doi: 10.1016/j.yrtph.2006.09.004

Wickham, R. J. (2015). How menthol alters tobacco-smoking behavior: A biological perspective. *Yale J. Biol. Med.* 88, 279–287.

Willis, D. N., Liu, B., Ha, M. A., Jordt, S. E., and Morris, J. B. (2011). Menthol attenuates respiratory irritation responses to multiple cigarette smoke irritants. *Faseb J.* 25, 4434–4444. doi: 10.1096/fj.11-188383

Wondergem, R., and Bartley, J. W. (2009). Menthol increases human glioblastoma intracellular Ca2+, BK channel activity and cell migration. *J. Biomed. Sci.* 16:90. doi: 10.1186/1423-0127-16-90

Woolf, C. J., and Mannion, R. J. (1999). Neuropathic pain: Aetiology, symptoms, mechanisms, and management. *Lancet* 353, 1959–1964. doi: 10.1016/s0140-6736(99)01307-0

Wright, A., Benson, H. A. E., and Moss, P. (2019). Development of a topical menthol stimulus to evaluate cold hyperalgesia. *Musculoskelet Sci. Pract.* 41, 55–63. doi: 10.1016/j.msksp.2019.03.010

Wright, C. E., Laude, E. A., Grattan, T. J., and Morice, A. H. (1997). Capsaicin and neurokinin A-induced bronchoconstriction in the anaesthetised guinea-pig: Evidence for a direct action of menthol on isolated bronchial smooth muscle. *Br. J. Pharmacol.* 121, 1645–1650. doi: 10.1038/sj.bjp.0701319

Wright, L., Baptista-Hon, D., Bull, F., Dalgaty, F., Gallacher, M., Ibbotson, S. H., et al. (2018). Menthol reduces phototoxicity pain in a mouse model of photodynamic therapy. *Pain* 159, 284–297. doi: 10.1097/j.pain.0000000000001096

Xiao, B., Dubin, A. E., Bursulaya, B., Viswanath, V., Jegla, T. J., and Patapoutian, A. (2008). Identification of transmembrane domain 5 as a critical molecular determinant of menthol sensitivity in mammalian TRPA1 channels. *J. Neurosci.* 28, 9640–9651. doi: 10.1523/jneurosci.2772-08.2008

Xing, H., Chen, M., Ling, J., Tan, W., and Gu, J. G. (2007). TRPM8 mechanism of cold allodynia after chronic nerve injury. *J. Neurosci.* 27, 13680–13690. doi: 10.1523/jneurosci.2203-07.2007

Xu, H., Ramsey, I. S., Kotecha, S. A., Moran, M. M., Chong, J. A., Lawson, D., et al. (2002). TRPV3 is a calcium-permeable temperature-sensitive cation channel. *Nature* 418, 181–186. doi: 10.1038/nature00882

Xu, L., Han, Y., Chen, X., Aierken, A., Wen, H., Zheng, W., et al. (2020). Molecular mechanisms underlying menthol binding and activation of TRPM8 ion channel. *Nat. Commun.* 11:3790. doi: 10.1038/s41467-020-17582-x

Yamamoto, S., Egashira, N., Tsuda, M., and Masuda, S. (2018). Riluzole prevents oxaliplatin-induced cold allodynia *via* inhibition of overexpression of transient receptor potential melastatin 8 in rats. *J. Pharmacol. Sci.* 138, 214–217. doi: 10.1016/j.jphs.2018.10.006

Yaman, D., Alpaslan, C., and Kalaycioglu, O. (2021). The effects of Biofreeze and superficial heat on masticatory myofascial pain syndrome. *Eur. Oral. Res.* 55, 133–138. doi: 10.26650/eor.2021858837

Yosipovitch, G., Szolar, C., Hui, X. Y., and Maibach, H. (1996). Effect of topically applied menthol on thermal, pain and itch sensations and biophysical properties of the skin. *Arch. Dermatol. Res.* 288, 245–248. doi: 10.1007/bf02530092

Young, M. J., Boulton, A. J., MacLeod, A. F., Williams, D. R., and Sonksen, P. H. (1993). A multicentre study of the prevalence of diabetic peripheral neuropathy in the United Kingdom hospital clinic population. *Diabetologia* 36, 150–154. doi: 10.1007/bf00400697

Yudin, Y., Lukacs, V., Cao, C., and Rohacs, T. (2011). Decrease in phosphatidylinositol 4,5-bisphosphate levels mediates desensitization of the cold sensor TRPM8 channels. *J. Physiol.* 589, 6007–6027. doi: 10.1113/jphysiol.2011.220228

Zanotto, K. L., Iodi Carstens, M., and Carstens, E. (2008). Cross-desensitization of responses of rat trigeminal subnucleus caudalis neurons to cinnamaldehyde and menthol. *Neurosci. Lett.* 430, 29–33. doi: 10.1016/j.neulet.2007.10.008

Zhang, X. B., Jiang, P., Gong, N., Hu, X. L., Fei, D., Xiong, Z. Q., et al. (2008). A-type GABA receptor as a central target of TRPM8 agonist menthol. *PLoS One* 3:e3386. doi: 10.1371/journal.pone.0003386

Zhang, J., Enix, D., Snyder, B., Giggey, K., and Tepe, R. (2008). Effects of Biofreeze and chiropractic adjustments on acute low back pain: A pilot study. *J. Chiropr. Med.* 7, 59–65. doi: 10.1016/j.jcme.2008.02.004

Ziemba, P. M., Schreiner, B. S., Flegel, C., Herbrechter, R., Stark, T. D., Hofmann, T., et al. (2015). Activation and modulation of recombinantly expressed serotonin receptor type 3A by terpenes and pungent substances. *Biochem. Biophys. Res. Commun.* 467, 1090–1096. doi: 10.1016/j.bbrc.2015.09.074

Zuo, X., Ling, J. X., Xu, G. Y., and Gu, J. G. (2013). Operant behavioral responses to orofacial cold stimuli in rats with chronic constrictive trigeminal nerve injury: Effects of menthol and capsazepine. *Mol. Pain* 9:28. doi: 10.1186/1744-8069-9-28

frontiers | Frontiers in Molecular Neuroscience

TYPE Original Research
PUBLISHED 06 October 2022
DOI 10.3389/fnmol.2022.1008203

OPEN ACCESS

EDITED BY
Xin Zhang,
Duke University, United States

REVIEWED BY
Bao-Chun Jiang,
Zhejiang University, China
Hui-Jing Wang,
Shanghai University of Medicine and Health Sciences, China
Shaofeng Pu,
Shanghai Jiao Tong University, China

*CORRESPONDENCE
Qi-Liang Mao-Ying
maoyql@fudan.edu.cn

SPECIALTY SECTION
This article was submitted to Pain Mechanisms and Modulators, a section of the journal Frontiers in Molecular Neuroscience

RECEIVED 31 July 2022
ACCEPTED 12 September 2022
PUBLISHED 06 October 2022

CITATION
Chen Y, Chen H, Li X-C, Mi W-L, Chu Y-X, Wang Y-Q and Mao-Ying Q-L (2022) Neuronal toll like receptor 9 contributes to complete Freund's adjuvant-induced inflammatory pain in mice.
Front. Mol. Neurosci. 15:1008203.
doi: 10.3389/fnmol.2022.1008203

Neuronal toll like receptor 9 contributes to complete Freund's adjuvant-induced inflammatory pain in mice

Yu Chen[1], Hui Chen[1], Xiao-Chen Li[1], Wen-Li Mi[1,2], Yu-Xia Chu[1,2], Yan-Qing Wang[1,2,3] and Qi-Liang Mao-Ying[1,2]*

[1]Department of Integrative Medicine and Neurobiology, School of Basic Medical Sciences, Shanghai Medical College, Institute of Acupuncture Research, Institutes of Integrative Medicine, Fudan University, Shanghai, China, [2]Shanghai Key Laboratory of Acupuncture Mechanism and Acupoint Function, Fudan University, Shanghai, China, [3]State Key Laboratory of Medical Neurobiology and MOE Frontiers Center for Brain Science, Institutes of Brain Science, Fudan University, Shanghai, China

Toll like receptor 9 (TLR9) is a critical sensor for danger-associated molecular patterns (DAMPs) and a crucial marker of non-sterile/sterile inflammation among all TLRs. However, the significance of TLR9 in inflammatory pain remains unclear. Here, we subcutaneously injected Complete Freund's adjuvant (CFA) into the plantar surface of the hind paw, to established a mouse model of inflammatory pain, and we examined expression and distribution of TLR9 in this model. There was a significant increase of TLR9 mRNA and reduction of mechanical paw withdrawal threshold in mice intraplantar injected with CFA. By contrast, mechanical paw withdrawal threshold significantly increased in mice treated with TLR9 antagonist ODN2088. Furthermore, TLR9 is found predominantly distributed in the neurons by immunofluorescence experiment. Accordingly, neuronal TLR9 downregulation in the spinal cord prevented CFA-induced persistent hyperalgesia. Overall, these findings indicate that neuronal TLR9 in the spinal cord is closely related to CFA-induced inflammatory pain. It provides a potential treatment option for CFA-induced inflammatory pain by applying TLR9 antagonist.

KEYWORDS

inflammatory pain, toll-like receptor 9, toll-like receptor 9 antagonist, CpG ODN, spinal cord, neuron

Introduction

Toll-like receptors (TLRs) are a class of pattern-recognition receptors that are inherited from the germ line and trigger innate immune responses by recognizing pathogen associated molecular patterns (PAMPs) (Akira et al., 2006). Some endogenous ligands such as danger-associated molecular patterns (DAMPs) can also be recognized by TLRs after tissue injury or cellular stress. When activated, TLRs are known to promote the production of a wide variety of inflammatory mediators including cytokines (e.g., TNF-α), chemokines [e.g., monocyte chemotactic protein-1 (MCP-1)], enzymes (e.g., cyclooxygenase-2 and matrix metalloproteinase 9), and other inflammatory mediators (e.g., prostaglandins) (Basbaum et al., 2009; Buchanan et al., 2010; Chen and Nunez, 2010; Lehnardt, 2010; Okun et al., 2011). Therefore, TLRs play a significant part in the pathogenesis of various CNS disorders, including infectious diseases such as spinal cord injury (Pallottie et al., 2018; Li et al., 2019), Parkinson's disease (Maatouk et al., 2018), neuropathic pain (Liu et al., 2016), pruritus (Liu et al., 2010), stroke (Caso et al., 2007), and multiple sclerosis (Prinz et al., 2006). Proinflammatory central immune signaling pathway plays an important role in the induction and maintenance of heightened pain condition (Nicotra et al., 2012).

TLRs have been involved in the pain process in a growing number of studies, including cancer induced bone pain (Li et al., 2013), neuropathic pain (Wang et al., 2013; Liu et al., 2016, 2017; Zhang et al., 2018) and inflammatory pain (Guan et al., 2016; Liu et al., 2016; Zhang and Deng, 2017; Sun et al., 2018). TLR9 is a critical sensor for DAMPs and a crucial marker of non-sterile/sterile inflammation among all TLRs. TLR9, in particular, is of special role because it localizes in endolysosomes and has distinct ligand, the unmethylated CpG motifs of bacterial DNA (Krieg et al., 1998; Hemmi et al., 2000; Park et al., 2008). Cytidine-phosphateguanosine oligodeoxynucleotide 2088 (CpG ODN 2088) has been used as TLR9 antagonist in numerous studies (David et al., 2013, 2014; Qin et al., 2014; Acioglu et al., 2016). According to the literature, CpG ODN 2088 reduces injury-induced thermal hypersensitivity by inhibiting inflammatory response and TNF-α expression, suggesting that TLR9 may play potential a role in SCI-induced pain (David et al., 2013). Although research efforts have been made on other TLRs, such as TLR4 in inflammatory pain (Zhao et al., 2015), the significance of TLR9 in inflammatory pain is yet unknown.

The current study aims to investigate the role of neuronal TLR9 in the spinal dorsal horn in CFA-induced inflammatory pain. CFA treatment induced upregulation of TLR9 mRNA in the spinal cord, and inhibition of TLR9 by TLR9 antagonist significantly relieved CFA-induced mechanical allodynia. The role of neuronal TLR9 in CFA-induced inflammatory pain was observed by an adeno associated virus (AAV) virus with a neuronal specific promoter SYN delivering TLR9 shRNA to downregulate neuronal TLR9. The present study revealed that neuronal TLR9 might serve as a promising therapeutic approach for inflammatory pain treatment.

Materials and methods

Experimental animals

Adult male C57BL/6 mice were purchased from Shanghai SLAC Laboratory Animal Co., Ltd., China. Mice were reared under a 12 h light and dark cycle with free access to food and water. Before experimental operation, mice were acclimated for at least 1 week after being received. The virus injection was applied on mice at the age of 5–6 weeks, while other experiments were performed on mice at the age of 8–10 weeks. This study was approved by the local ethical committee at School of Basic Medical Sciences, Fudan University, People's Republic of China (Agreement No. 20140226-087). All procedures covered in the study were in accordance with the National Institutes of Health Guide for the Care and Use of Laboratory Animals and the Ethical Issues of the International Association for the Study of Pain. As for behavioral test, prior to formal test, mice were habituated in the testing environment without any stimulation 1 h per day for 2 consecutive days and the experimenters were blinded to the treatment.

Establishment of complete Freund's adjuvant-induced inflammatory pain model and intrathecal injection

According to previous study (Ghasemlou et al., 2015), 20 μl of CFA (Sigma, F5881-10ML) was delivered into the plantar surface of hind paw in mice via subcutaneous injection to induce inflammatory-pain related response. The control group was injected with the same volume of normal saline.

Intrathecal injection of ODN 2088 (InvivoGen, tlrl-2088) or ODN 2088 control (InvivoGen, tlrl-2088c-1) (150 ng/g) (David et al., 2014) started on the 5th and 14th day after the CFA injection. A 30 1/2 gauge needle connected with a 10 μl Hamilton syringe was inserted into the intervertebral space between the fifth and sixth lumbar as previously described (Hu et al., 2018). The instant mechanical allodynia was measured every 1 h. ODN 2088 was dissolved in double distilled water. Mice were assigned to the experimental groups at random, and they were anesthetized with isoflurane (1.0 L/min at a concentration of 3.0% in oxygen).

Real-time PCR

Total RNA of the samples from L4-L6 spinal dorsal horn was isolated with RNSiso Plus (Takara, 9109)

following manufacturer's instructions and then measured with Nanodrop (Thermo). The sequences of primers for each target mRNA are as follows (Acioglu et al., 2016): GAPDH, forward: 5′-AAA TGG TGA AGG TCG GTG TG-3′, reverse: 5′-AGG TCA ATG AAG GGG TCG TT-3′, TLR9, forward: 5′-GCGGCAGCATCCTGCTCCAA-3′, reverse: 5′-GGGGGCTAAGGCCAGTGGGT-3′;. All primers used for PCR analysis are synthesized by Sangon Biotech (Shanghai) Co., Ltd. Reverse transcription was conducted by employing PrimeScript^{TM} RT reagent Kit with gDNA Eraser (Takara, RR047A) and SYBR Premix Ex Taq^{TM} II (Takara, RR820A).

Behavioral tests

Up-and-down method

According to previous research (Hu et al., 2018), a series of von Frey hairs (0.02, 0.04, 0.07, 0.16, 0.4, 0.6, 1.0, and 1.4 g) (Stoelting, Wood Dale, Illinois, USA) were applied to measure mechanical paw withdrawal threshold. In short, mice were acclimated in a plexiglass box separately for 30 min. A von Frey hair was accordingly employed and held for about 3 s. There was a 10-min interval between von Frey hair applications. For each test, 0.16 g von Frey hair was chosen as the first application, and the hair force was then decreased or increased according to the reaction. A rapid withdrawal of the hind paw was defined as positive reaction. There are five more stimuli during the test following the first shift in reaction occurred. Final scores were converted to a 50% von Frey threshold using the Dixon up-and-down paradigm (Dixon, 1980).

Hargreave's test and hot plate assay

Thermal hyperalgesia was measured according to our previous study (Mao-Ying et al., 2006). In brief, mice were put into a clear plastic chamber on an elevated glass pane. Radiant heat was then applied to the plantar surface of the hind paw until the mouse lifted its paw. The cut-off time was set to 20 s so as to avoid damage of tissue.

As for hot plate, according to our previous study (Mao-Ying et al., 2006), the temperature was set to 52°C. Withdrawal latency began when the mouse was placed on the plate and terminated when either a rapid withdrawal or paw flinching was observed. Likewise, the cut-off time was set to 20 s so as to avoid damage of tissue. As for the test, there were three replicates in each mouse with enough interval between applications and calculated by the mean value.

Open field test replications

Open field test (OFT) was applied to identify whether AAV injection would influence mice's locomotive ability. The open box device contains a 50 × 50 cm white floor with an opaque wall (40 cm height). It was cleaned up with 5% aqueous acetic acid before each trial. The performance of mice in the open field was recorded with a camera. Finally, the horizontal movement and the vertical movement (two front paws in the air or the mice climbing the wall) of the mice within 5 min were analyzed by the OFT video analysis system, as described previously (Wang et al., 2019).

Rotarod test

To evaluate the mice's acquisition of skillful motor behavior, a rotarod machine with an automatic timer and a falling sensor (ENV-575M, Med Associates, USA) was used. Before test sessions, mice were trained on the static drum for 5 min (two sessions per day) at a relatively slow speed (5 rpm/min) for 2 consecutive days. To test the accelerating rotarod, the rod speed was set to accelerate from 4 to 40 rpm in 300 s. The falling latency was recorded automatically by photocells. As for the test, there were three replicates in each mouse with at least 30-min intervals between applications, and the mean value of falling latency was calculated.

Intraspinal adeno associated virus delivery

According to our previous study (Ma et al., 2021), mice aged 5–6 weeks received virus delivery 3 weeks before the CFA injection. Mice were deeply anesthetized and placed on a stereotaxic frame. The spine was fixed with the help of two spinal adaptors to fully expose the L4-L5 lumbar space. A glass microelectrode for Nanoliter (with 1.14 mm of outer diameter, 0.53 mm of inner diameter) was applied to insert into the spinal dorsal horn intervertebral space at a depth of 200–300 μm. A motorized perfusion system (Nanoliter 2010, World Precision Instruments) was used to control the rate of virus delivery (60 nl/min). Delivery finished, and the glass microelectrode was then left in spinal dorsal horn for 5 min. With wounds sutured, mice were placed on a heating pad to support recovery. AAV virus vectors employed in our study were purchased from OBiO Technology (Shanghai, China).

Transfection with TLR9-GFP plasmid and western blot

The plasmid of TLR9 shRNA was designed by OBiO Technology (Shanghai, China). The micro30 shRNA (Tlr9) sequence was cloned into the *Hin*dIII(1494) and *Age*I(1503) sites of the adeno-associated virus vector AOV062 pAAV-SYN-MCS-EGFP-3FLAG. Neuroblastoma cells SY5Y cells were provided by the Shanghai Institute of Cell Biology, Chinese Academy of Sciences (Shanghai, China), according to previous study from our lab (Cui et al., 2020). Dulbecco's modified Eagles medium (Gibco, USA) containing 10% fetal bovine serum were used to cultivate SY5Y cells. The cells were stored

in the cell incubator, with temperature of 37°C and CO_2 of 5% concentration. Following the manufacturer's instructions, SY5Y cells were harvested and transfected with 1 μg of cDNA coding for TLR9-GFP with Lipofectamine 3000 (Invitrogen). The cells were lysed using RIPA Lysis Buffer (100 μl/g, Beyotime Biotechology, P0013B). Applying SDS-PAGE, samples were separated with 10% acrylamide gels and then transferred onto polyvinylidene fluoride membranes. The membranes were incubated overnight with TLR9 (Abcam, ab37154) or β-actin (ProteinTech, HRP-60008) primary antibody at 4°C on a shaker table. On the following day, they were washed with TBST. After that, the membranes were incubated with corresponding HRP-conjugated secondary antibody for 2 h at room temperature. The target bands were detected with ImageQuant LAS4000 miniimage analyzer (GE Healthcare, Buckinghamshire, UK) and the gray value of target bands was analyzed by ImageJ software (version 1.47).

Immunofluorescence

Mice were anesthetized with 10% chloral hydrate. Then they were transcardially perfused with saline and perfused with 4% formaldehyde. L4-L6 segment of the mice spinal cord was soaked in 4% formaldehyde for 4 h, and subsequently in 20 and 30% sucrose. The 30 μm-thick sections were incubated in Superblock Buffer (Thermo, 37580) for 1 h at room temperature, reacted with mouse anti-NeuN (Millipore) or anti-TLR9 (Abcam, ab37154) overnight at 4°C, and then reacted with Alexa-594-conjugated donkey anti-mouse IgG secondary antibodies (Invitrogen) for 2 h at room temperature. After three washes with PBST, the sections were attached using mounting media containing DAPI and were analyzed by confocal microscope (FV1000, Olympus). The mean gray value and the cell amount were analyzed by ImageJ. The Pearson's R value was measured by the coloc 2 function of ImageJ.

Statistical analysis

All data analysis was performed through the use of the Prism7 software packages and IBM SPSS 22.0. All data are presented as mean ± standard error of the mean (SEM). A *t*-test was used for direct comparisons between the two groups. Significant differences among groups were checked by two-way ANOVA. Repeated-measures ANOVA was applied to compare the differences between TLR9 shRNA group and the control group. Significance was assumed when $p < 0.05$.

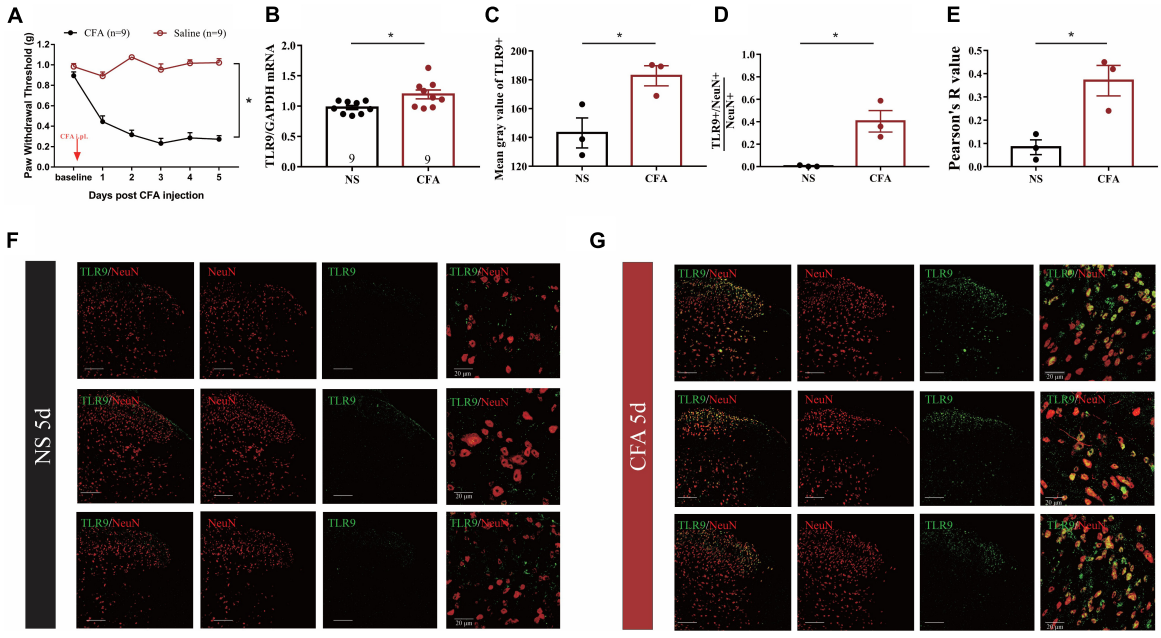

FIGURE 1
(A) The mechanical threshold decreased after CFA injection. The statistical method is repeated measures ANOVA. *$p < 0.05$. **(B)** Real-time PCR analysis showed that TLR9 increased in inflammatory pain. Results are normalized to GAPDH. Values are represented as mean ± SEM. *$p < 0.05$. Student's *t*-test was used for comparisons. **(C)** The mean gray value of TLR9 immunostaining from **(F,G)** between NS- and CFA-treated group. Values are represented as mean ± SEM. *$p < 0.05$. **(D)** The proportion of TLR9 + /NeuN + colocalization between NS- and CFA-treated group. The numbers of cells were counted by ImageJ. Values are represented as mean ± SEM. *$p < 0.05$. **(E)** The Pearson's R value of TLR9 and NeuN represented the correlation between NS- and CFA-treated group. The value was measured by coloc 2 in ImageJ. **(F,G)** The immunofluorescence of spinal cord form NS- and CFA-treated group, respectively. Double immunostaining of TLR9 (green) with NeuN (a neuronal marker, red). Scale bars = 100 μm.

Results

Toll like receptor 9, probably neuronal toll like receptor 9, increased in complete Freund's adjuvant-induced inflammatory pain in mice

We initially established a mouse model of CFA-induced inflammatory pain to observe whether spinal TLR9 was involved in inflammatory pain. In accordance with the previous report (Gao et al., 2018), a significant decline of mechanical paw withdrawal threshold can be observed in CFA-treated mice as compared with normalsaline (NS) treated mice (**Figure 1A**). Moreover, the results showed that the expression of TLR9 mRNA was increased ($^*p < 0.05$, **Figure 1B**) in the L4-L6 lumbar segment of the spinal dorsal horn on the 5th day in CFA-treated mice, compared with normal saline-treated mice. Moreover, we measured TLR9 protein levels in NS- and CFA-treated mice by immunofluorescence (**Figures 1F,G**). The mean gray value of TLR9 increased on the 5th day after the CFA injection (**Figure 1C**). The proportion of TLR9 + /NeuN + (neuronal nuclei, a neuronal marker) in NeuN + cell was raised in CFA-treated mice compared with NS-treated mice, indicating that the increased TLR9 in CFA-treated mice mainly occurred in neurons (**Figure 1D**). Further, the Pearson correlation coefficient (Pearson's *R* value) was higher in CFA-treated mice on the 5th day than that in NS-treated mice, indicating that the positive linear relationship between TLR9 and NeuN was stronger on the 5th day after the CFA injection (**Figure 1E**). These results showed that CFA-induced inflammation might result in an increase of TLR9 level, especially in neurons.

Distribution of toll like receptor 9 in the spinal cord of complete Freund's adjuvant -induced inflammatory mice

TLR9 was then doubly immunostained with GFAP (glial fibrillary acidic protein, an astrocytic marker), and Iba-1 (ionized calcium-binding adapter molecule 1, a microglial marker) (**Figures 2A,B**). According to the color code of the heatmap, the proportion of colocalization between TLR9 + and NeuN + was generally greater than that between GFAP + and Iba1 + (**Figure 2C**). Moreover, we adopted the Pearson correlation coefficient (Pearson's R value) to analyze the specific relevance on individual variables (**Figure 2D**). The Pearson's R values were 0.42, 0.45, and 0.24 between TLR9 immunoreactivity (IR) and NeuN-IR, representing the positive linear specific relevance (R = [0, 1]) of TLR9 to NeuN. The Pearson's *R* values of TLR9-IR and NeuN-IR were generally higher than those of GFAP-IR and Iba1-IR. These indicated that in CFA-treated mice, the positive linear specific relevance of TLR9-IR to NeuN-IR were stronger than TLR9-IR to GFAP-IR or Iba-1-IR. TLR9-IR was mainly colocalized with NeuN-IR, suggesting that the alteration of TLR9 was predominantly distributed in neuron in CFA-induced inflammation.

Toll like receptor 9 was involved in complete Freund's adjuvant -induced inflammatory pain

According to **Figure 3A**, CFA-treated mice exhibited a significant decrease of mechanical paw withdrawal threshold as compared with NS-treated mice on the 5th day after the CFA injection ($^*p < 0.05$). Functional inhibition of TLR9 by intrathecal injection of TLR9 antagonist ODN2088 (150 ng/g body weight; David et al., 2014) significantly increased mechanical paw withdrawal threshold 2 h after the ODN2088 injection ($^*p < 0.05$, **Figure 3B**), compared to the group with ODN2088 control injection.

Moreover, to evaluate the involvement of TLR9 in long-term inflammation, we also functionally inhibited TLR9 by intrathecally injecting TLR9 antagonist ODN2088 on the 14th day after the CFA injection. CFA-treated mice exhibited a significant decrease of mechanical paw withdrawal threshold as compared with NS-treated mice on the 14th day ($^*p < 0.05$, **Figure 3C**). TLR9 antagonist ODN2088 significantly increased mechanical paw withdrawal threshold 2 h after the ODN2088 injection ($^*p < 0.05$, **Figure 3D**), which was alike to the results on day 5.

Neuronal toll like receptor 9 in the spinal cord contributed to complete Freund's adjuvant-induced inflammatory pain

For the purpose of achieving downregulation of TLR9 *in vivo* by AAV, we first constructed a plasmid with effective downregulation of TLR9 in SY5Y cells, according to the previous study from our lab (Cui et al., 2020). The micro30 shRNA (Tlr9) sequence was cloned into the *Hin*dIII(1494) and *Age*I(1503) sites of the AAV vector AOV062 pAAV-SYN-MCS-EGFP-3FLAG (**Figure 4A**). Western blot analysis showed significant knock-down effects of this plasmid (**Figure 4B**). Taking SYN as a promoter of mature neurons, the plasmid was packaged into the AAV2/9 vector, which can specifically transfect mature neurons. To assess whether neuronal TLR9 in the spinal cord was involved in CFA-induced persistent hyperalgesia, the virus with the neuronal specific promoter SYN delivering TLR9 shRNA was injected into the L4-L5 lumbar segment (**Figure 4C**). The EGFP image (green) was highly colocalized with neurons (red) in the dorsal spinal cord (**Figure 4D**).

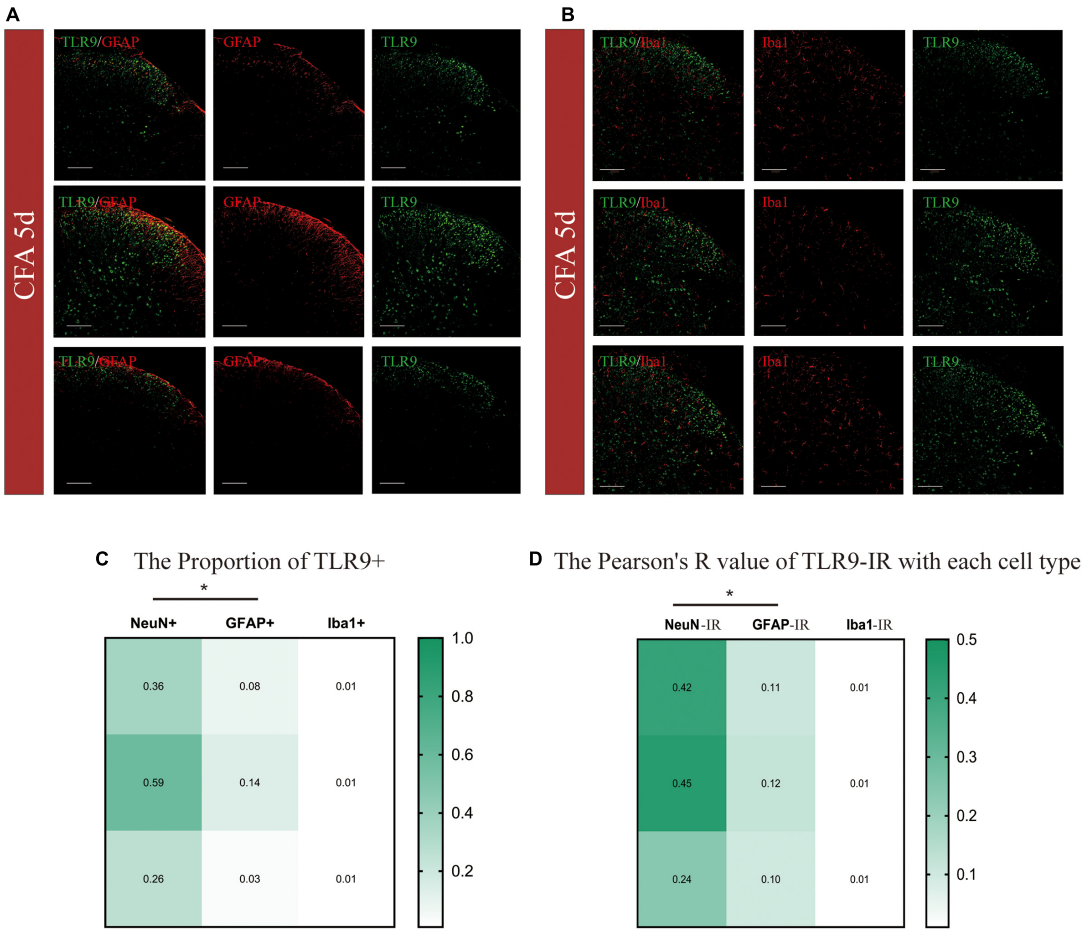

FIGURE 2
(A,B) Cellular distributions of TLR9 in the spinal cords of CFA mice. Double immunostaining of TLR9 (green) with GFAP (an astrocytic marker, red), and Iba-1 (a microglial marker, red) in the spinal dorsal horn. Scale bars = 100 μm. **(C)** The heatmap showed TLR9 + /NeuN + proportion was generally higher than TLR9 + with GFAP + or Iba1 + with proportions of colocalization color-coded in the scale shown. *$p < 0.05$. Student's *t*-test was used for comparisons. **(D)** The heatmap showed the Pearson's *R*-value of TLR9 with each cell type with values color-coded in the scale shown. *$p < 0.05$.

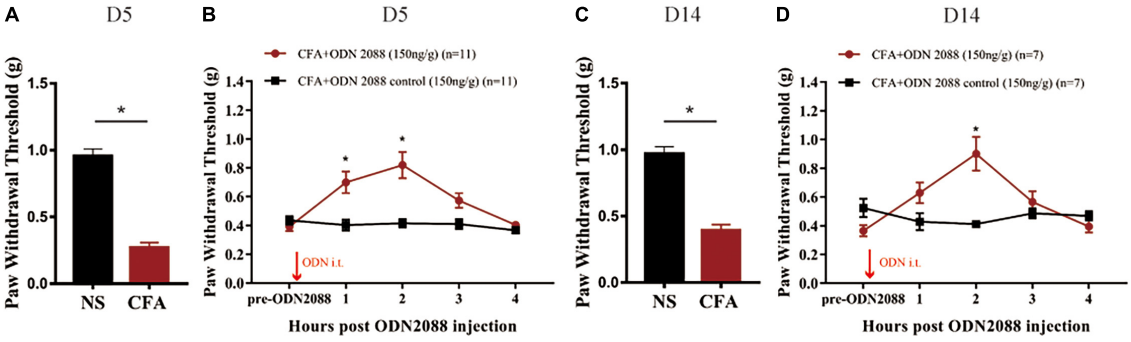

FIGURE 3
(A) The von Frey test showed that the mechanical paw withdrawal threshold decreased at the 5th day after CFA injection. Values are represented as mean ± SEM. *$p < 0.05$. Student's *t*-test was used for comparisons. **(B)** TLR9 inhibition raised mechanical paw withdrawal threshold 2 h after the ODN2088 injection at D5. **(C)** The von Frey test showed that the mechanical paw withdrawal threshold decreased at the 14th day after CFA injection. Values are represented as mean ± SEM. *$p < 0.05$. Student's *t*-test was used for comparisons. **(D)** TLR9 inhibition raised mechanical paw withdrawal threshold 2 h after the antagomir injection at D14. The arrows indicated the moment of the ODN 2088 or control administrations.

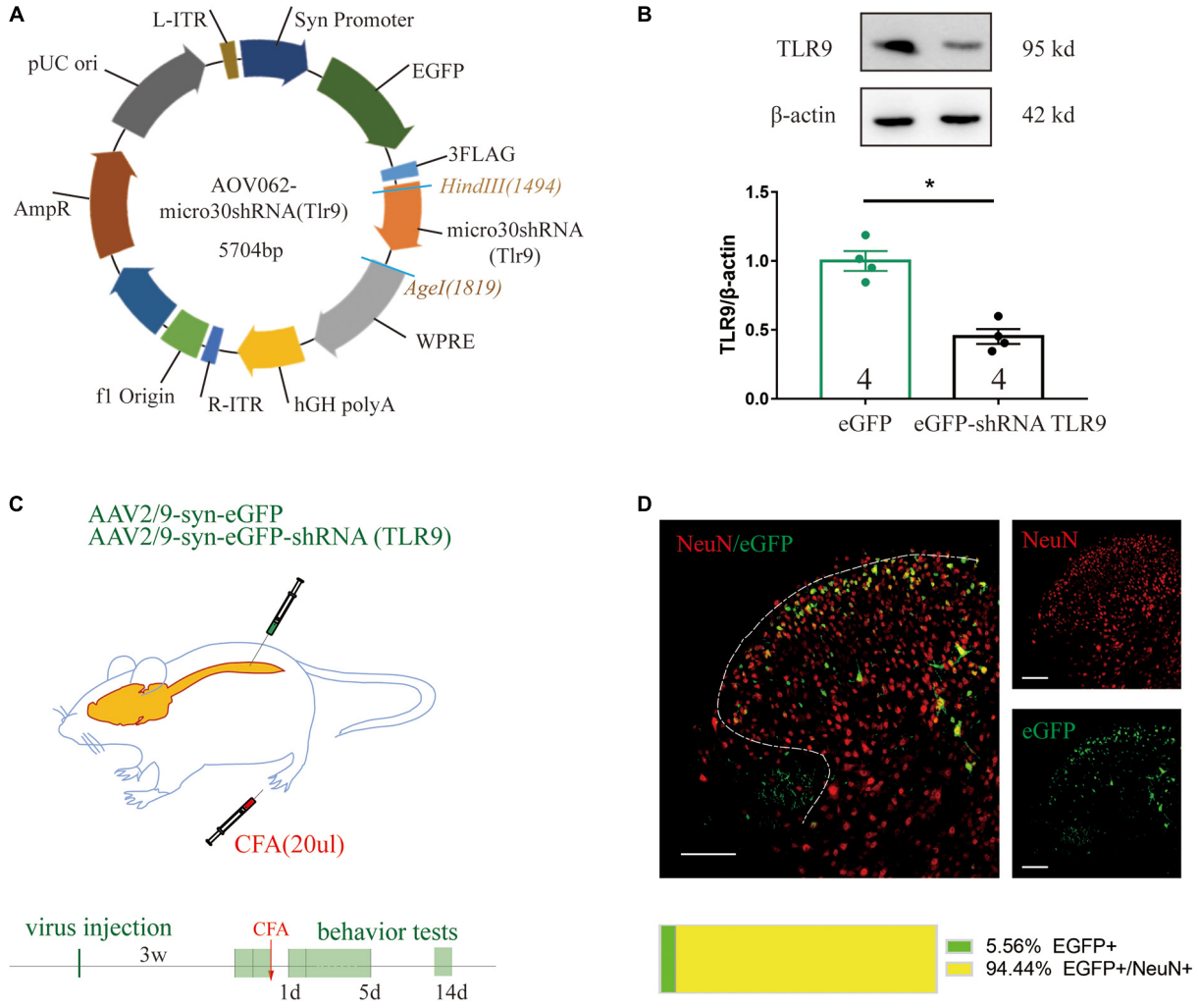

FIGURE 4
(A) The construction of a recombinant plasmid containing shRNA TLR9. **(B)** Western blot analysis showed that TLR9 protein expression was downregulated in SY5Y transfected with TLR9-GFP plasmid. Results are normalized to β-actin and shown as ratios to eGFP control group. Values are represented as mean ± SEM. *$p < 0.05$ vs. eGFP control group. Student's *t*-test had been utilized to compare. **(C)** The neuron-specific promoter SYN was used in an experiment to suppress spinal cord neuronal TLR9 expression. **(D)** Representative images showed NeuN labeling (red) and eGFP-tagged (green) AAV-eGFP-shRNA TLR9 in the spinal cord. Scale bar, 100 μm. The percentage of the colocalization was displayed below.

In the CFA-treated mice, downregulation of neuronal TLR9 increased the mechanical paw withdrawal threshold as compared to the group with empty vector virus injection (Figure 5A), which indicated that neuronal TLR9 downregulation in the spinal cord prevented CFA-induced inflammatory pain.

Previous studies indicated that TLR9 deficiency impacted motor and sensory behaviors (Khariv et al., 2013). Thus, we detected whether downregulation of TLR9 in spinal neurons would affect sensory and motor behaviors. Downregulation of TLR9 in spinal neurons had no effect on locomotor activity (the index of the number of rearings and the traveled distance in Open Field Test, latency to fall in Rotarod test), mechanical sensitivity (von Frey test), and thermal sensitivity (Radiant heat and Hot plate) ($p > 0.05$, Figures 5B–G).

Discussion

Our study for the first time demonstrates that TLR9 antagonist via intrathecal administration or downregulation of neuronal TLR9 attenuates CFA-induced inflammatory pain in mice. Thus, TLR9, particularly neuronal TLR9, may serve as a potential therapeutic target against inflammatory pain.

According to previous reports, there are several TLRs expressing in spinal cord including TLR2, TLR3, TLR4, TLR8,

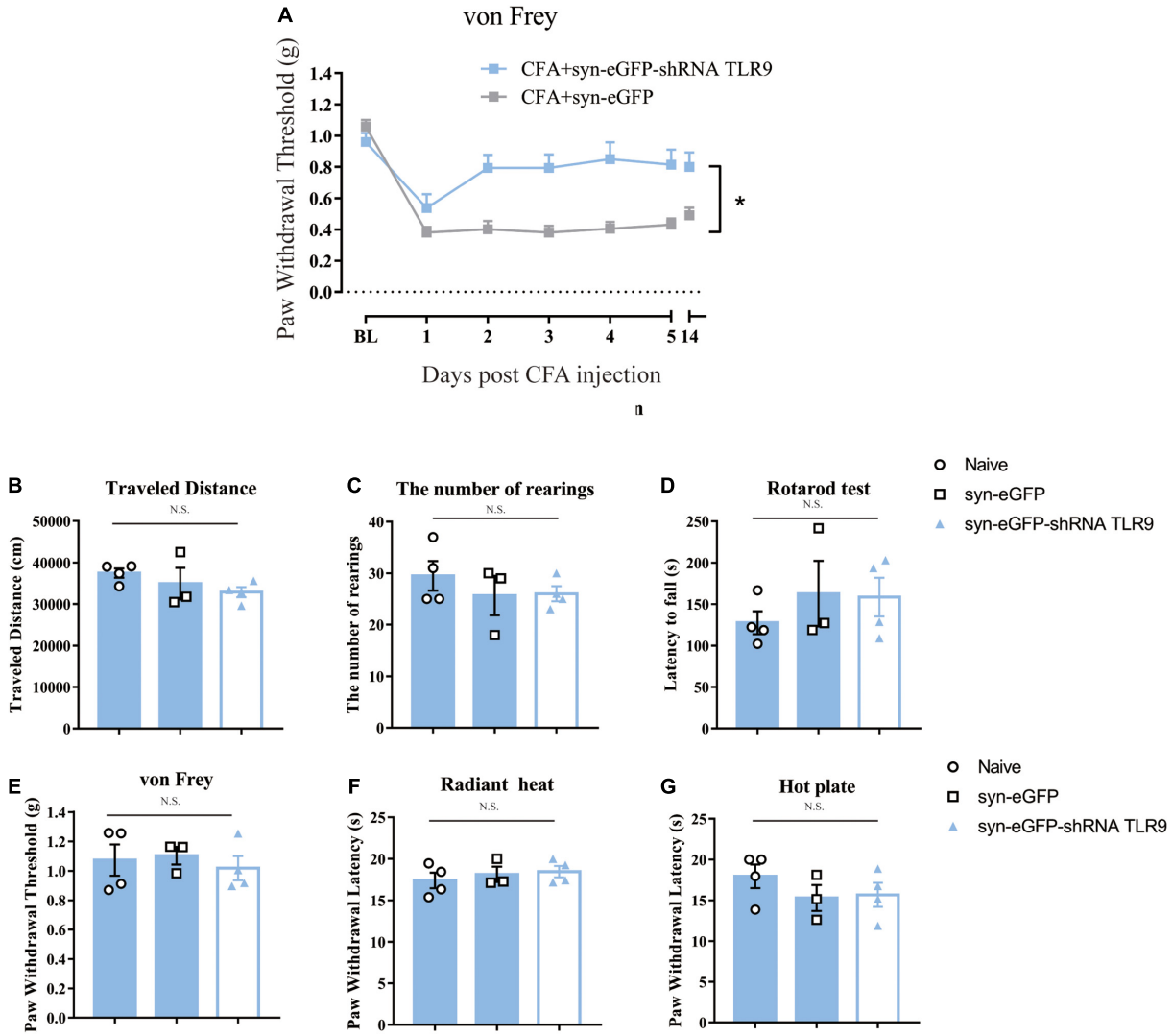

FIGURE 5
(A) Downregulation of neuronal TLR9 in the spinal cord increased the mechanical paw withdrawal threshold in CFA mice. Data are expressed as means ± SEM. Repeated measurements ANOVA is the statistical approach used. **(B–G)** The locomotive ability (open field, rotarod test), the mechanical sensitivity (von Frey) and thermal (radiant heat, hot plate) sensitivity was unaffected by virus to downregulate the neuronal TLR9 $p > 0.05$. Multiple comparisons using two-way ANOVA are the statistical approach.

and TLR9 (Kigerl and Popovich, 2009; Heiman et al., 2014). The role of TLRs in all kinds of pain has been extensively studied (Liu et al., 2012; Ji, 2015). For instance, there are deferred and decreased mechanical allodynia and heat hyperalgesia post L5 spinal nerve transection in TLR2 knock-out mice (Kim et al., 2007). TLR4 ablation or inhibition by siRNA or antagonist attenuates arthritic pain (Christianson et al., 2011) and bone cancer pain (Wu et al., 2010). Taken together, these findings imply that TLRs have distinct and non-redundant functions. Earlier studies reveal that when intrathecally administrated, TLR9 agonist induces an inflammatory response in the spinal cord of intact mice (Li et al., 2019). TLR9 antagonist blocks tumor-induced pain sensitivity (Qi et al., 2011). In this study, the expression of TLR9 was increased by CFA-injection, and inhibition or downregulation of TLR9 alleviated CFA-induced mechanical pain, which supports the idea that TLR9 plays a detrimental role in CFA-induced inflammatory pain. TLR9 antagonists have been shown to preserve injured proximal axons, control glial scarring, and minimize detrimental inflammation through the action of ODN 2088 (Li et al., 2019). Recently, Dynavax Technologies (DT) has designed immunoregulatory oligonucleotides with unique inhibitory sequences for TLR9 that suppress autoimmune and inflammatory diseases (Patra and Choi, 2016). All the evidences above imply that TLR9 antagonist can be effective therapies for TLR9-mediated inflammatory disorders.

TLR9 has been lately confirmed to be expressed in different cell types in CNS. In diabetic encephalopathy, Sun et al. found a drastic increase for TLR9 expression in neurons cultivated in high-glucose media (Sun et al., 2017; Zhao et al., 2018). Our study indicated that TLR9 was mainly distributed in neuron in CFA-induced inflammation, and that neuronal TRL9 contributed to CFA-induced inflammatory pain. The Pearson's *R* value were 0.37 ± 0.11 between TLR9-IR and NeuN-IR, representing the positive linear specific relevance between TLR9 and NeuN (R = [0, 1]). However, the proportion of TLR9 + in GFAP + were 0.08 ± 0.06, while the Pearson's *R* value were 0.11 ± 0.01, representing weak specific relevance of TLR9-IR to GFAP-IR in CFA-induced inflammation. These results suggested that although we detected few TLR9-IR colocalized with GFAP-IR, there was still less relevance of TLR9 to GFAP in CFA-induced inflammatory pain. Even though TLR9 in astrocytes was found to be involved in SCI (spinal cord injury), and TLR9 antagonist could selectively affect astroglial glutamate transporters (Pallottie et al., 2018), whether astroglial TLR9 is involved in CFA-induced inflammatory pain still needs to be confirmed.

It has been reported that TLR9 deficient ($TLR9^{-/-}$) mice displayed hypersensitivity to thermal stimuli and enhanced motor-responsivity compared to wide type mice. This indicated that TLR9 was probably of essential part for the development of sensory and motor behaviors (Khariv et al., 2013). In this study, downregulated neuronal TLR9 by AAV vector did not affect locomotor activity or sensitivity to mechanical and thermal stimulations. It should be noted that, in this study, the virus injection was performed on the mice aged 5–6 weeks and that we only downregulated TLR9 in neuron. This is quite different from the TLR9 deficient mice. The neural development of mice might be close to maturity when they are 5–6 weeks old, and further downregulation of TLR9 at this age is not enough to affect sensory-motor ability. On the other hand, despite the downregulation of TLR9 in some neurons, TLR9 in other cells has already met the normal neural development and function needs. Therefore, this experiment is different from that of TLR9 knockout mice. The downregulation of neuronal TLR9 did not show a hyper-responsive sensory and motor phenotype.

It is plausible that CpG ODN 2088 could confer neuronal protection by interfering with the binding or function of DAMPs that activate TLR9. However, there have been only a few identified TLR9 endogenous activators up to now. Fortunately, a number of host TLR9 stimulants have been discovered in the domain of sterile inflammation, such as mitochondrial DNA (Oka et al., 2012) and DNA-high-mobility group protein B1 (HMGB1) complex (Ivanov et al., 2007; Tian et al., 2007). Whereas the identification of DAMPs in CFA-affected spinal cord is beyond the scope of today's investigation, future studies are in need to unravel such ligands.

Data availability statement

The datasets used or analyzed during the current study are available from the corresponding author on reasonable request.

Ethics statement

The animal study was reviewed and approved by local Ethical Committee at Fudan University of Basic Medical Sciences, People's Republic of China (Agreement No. 20140 226-087).

Author contributions

YC carried out the major part of the study and drafted the manuscript. HC and X-CL performed part of the study. W-LM and Y-XC revised the manuscript. Y-QW and Q-LM-Y conceived, designed the study, and revised the manuscript. All authors contributed to the article and approved the submitted version.

Funding

This work was supported by the National Key R&D Program of China (2017YFB0403803) and the National Natural Science Funds of China (81873101, 81473749, 81371247, 81771202, and 81971056).

Acknowledgments

We are grateful for the support from the Innovative Research Team of High-level Local Universities in Shanghai, the Development Project of Shanghai Peak Disciplines-Integrated Chinese and Western Medicine, and the Shanghai Municipal Science and Technology Major Project (No. 2018SHZDZX01) and ZJLab.

Conflict of interest

The authors declare that the research was conducted in the absence of any commercial or financial relationships that could be construed as a potential conflict of interest.

Publisher's note

References

Acioglu, C., Mirabelli, E., Baykal, A. T., Ni, L., Ratnayake, A., Heary, R. F., et al. (2016). Toll like receptor 9 antagonism modulates spinal cord neuronal function and survival: direct versus astrocyte-mediated mechanisms. *Brain Behav. Immun.* 56, 310–324. doi: 10.1016/j.bbi.2016.03.027

Akira, S., Uematsu, S., and Takeuchi, O. (2006). Pathogen recognition and innate immunity. *Cell* 124, 783–801.

Basbaum, A. I., Bautista, D. M., Scherrer, G., and Julius, D. (2009). Cellular and molecular mechanisms of pain. *Cell* 139, 267–284. doi: 10.1177/0022034515612022

Buchanan, M. M., Hutchinson, M., Watkins, L. R., and Yin, H. (2010). Toll-like receptor 4 in CNS pathologies. *J. Neurochem.* 114, 13–27.

Caso, J. R., Pradillo, J. M., Hurtado, O., Lorenzo, P., Moro, M. A., and Lizasoain, I. (2007). Toll-like receptor 4 is involved in brain damage and inflammation after experimental stroke. *Circulation* 115, 1599–1608.

Chen, G. Y., and Nunez, G. (2010). Sterile inflammation: sensing and reacting to damage. *Nat. Rev. Immunol.* 10, 826–837.

Christianson, C. A., Dumlao, D. S., Stokes, J. A., Dennis, E. A., Svensson, C. I., Corr, M., et al. (2011). Spinal TLR4 mediates the transition to a persistent mechanical hypersensitivity after the resolution of inflammation in serum-transferred arthritis. *Pain* 152, 2881–2891. doi: 10.1016/j.pain.2011.09.020

Cui, W. Q., Chu, Y. X., Xu, F., Chen, T., Gao, L., Feng, Y., et al. (2020). Calcium channel alpha2delta1 subunit mediates secondary orofacial hyperalgesia through PKC-TRPA1/Gap junction signaling. *J. Pain* 21, 238–257. doi: 10.1016/j.jpain.2019.08.012

David, B. T., Ratnayake, A., Amarante, M. A., Reddy, N. P., Dong, W., Sampath, S., et al. (2013). A toll-like receptor 9 antagonist reduces pain hypersensitivity and the inflammatory response in spinal cord injury. *Neurobiol. Dis.* 54, 194–205. doi: 10.1016/j.nbd.2012.12.012

David, B. T., Sampath, S., Dong, W., Heiman, A., Rella, C. E., Elkabes, S., et al. (2014). A toll-like receptor 9 antagonist improves bladder function and white matter sparing in spinal cord injury. *J. Neurotrauma* 31, 1800–1806. doi: 10.1089/neu.2014.3357

Dixon, W. J. (1980). Efficient analysis of experimental observations. *Ann. Rev. Pharmacol. Toxicol.* 20, 441–462.

Gao, F., Xiang, H. C., Li, H. P., Jia, M., Pan, X. L., Pan, H. L., et al. (2018). Electroacupuncture inhibits NLRP3 inflammasome activation through CB2 receptors in inflammatory pain. *Brain Behav. Immun.* 67, 91–100. doi: 10.1016/j.bbi.2017.08.004

Ghasemlou, N., Chiu, I. M., Julien, J.-P., and Woolf, C. J. (2015). CD11b+Ly6G- myeloid cells mediate mechanical inflammatory pain hypersensitivity. *Proc. Natl. Acad. Sci. U.S.A* 112, E6808–E6817. doi: 10.1073/pnas.1501372112

Guan, Z., Hellman, J., and Schumacher, M. (2016). Contemporary views on inflammatory pain mechanisms: TRPing over innate and microglial pathways. *F1000Res.* 5:F1000FacultyRev–2425. doi: 10.12688/f1000research.8710.1

Heiman, A., Pallottie, A., Heary, R. F., and Elkabes, S. (2014). Toll-like receptors in central nervous system injury and disease: a focus on the spinal cord. *Brain Behav. Immun.* 42, 232–245.

Hemmi, H., Takeuchi, O., Kawai, T., Kaisho, T., Sato, S., Sanjo, H., et al. (2000). A toll-like receptor recognizes bacterial DNA. *Nature* 408, 740–745.

Hu, L. Y., Zhou, Y., Cui, W. Q., Hu, X. M., Du, L. X., Mi, W. L., et al. (2018). Triggering receptor expressed on myeloid cells 2 (TREM2) dependent microglial activation promotes cisplatin-induced peripheral neuropathy in mice. *Brain Behav. Immun.* 68, 132–145. doi: 10.1016/j.bbi.2017.10.011

Ivanov, S., Dragoi, A. M., Wang, X., Dallacosta, C., Louten, J., Musco, G., et al. (2007). A novel role for HMGB1 in TLR9-mediated inflammatory responses to CpG-DNA. *Blood* 110, 1970–1981. doi: 10.1182/blood-2006-09-044776

Ji, R. R. (2015). Neuroimmune interactions in itch: Do chronic itch, chronic pain, and chronic cough share similar mechanisms? *Pulm. Pharmacol. Ther.* 35, 81–86. doi: 10.1016/j.pupt.2015.09.001

Khariv, V., Pang, K., Servatius, R. J., David, B. T., Goodus, M. T., Beck, K. D., et al. (2013). Toll-like receptor 9 deficiency impacts sensory and motor behaviors. *Brain Behav. Immun.* 32, 164–172. doi: 10.1016/j.bbi.2013.04.007

Kigerl, K. A., and Popovich, P. G. (2009). Toll-like receptors in spinal cord injury. *Curr. Top. Microbiol. Immunol.* 336, 121–136.

Kim, D., Kim, M. A., Cho, I. H., Kim, M. S., Lee, S., Jo, E. K., et al. (2007). A critical role of toll-like receptor 2 in nerve injury-induced spinal cord glial cell activation and pain hypersensitivity. *J. Biol. Chem.* 282, 14975–14983.

Krieg, A. M., Wu, T., Weeratna, R., Efler, S. M., Love-Homan, L., Yang, L., et al. (1998). Sequence motifs in adenoviral DNA block immune activation by stimulatory CpG motifs. *Proc. Natl. Acad. Sci. U.S.A.* 95, 12631–12636. doi: 10.1073/pnas.95.21.12631

Lehnardt, S. (2010). Innate immunity and neuroinflammation in the CNS: the role of microglia in Toll-like receptor-mediated neuronal injury. *Glia* 58, 253–263. doi: 10.1002/glia.20928

Li, L., Ni, L., Eugenin, E. A., Heary, R. F., and Elkabes, S. (2019). Toll-like receptor 9 antagonism modulates astrocyte function and preserves proximal axons following spinal cord injury. *Brain Behav. Immun.* 80, 328–343. doi: 10.1016/j.bbi.2019.04.010

Li, X., Wang, X.-W., Feng, X.-M., Zhou, W.-J., Wang, Y.-Q., and Mao-Ying, Q.-L. (2013). Stage-dependent anti-allodynic effects of intrathecal Toll-like receptor 4 antagonists in a rat model of cancer induced bone pain. *J. Physiol. Sci.* 63, 203–209. doi: 10.1007/s12576-012-0244-5

Liu, F., Wang, Z., Qiu, Y., Wei, M., Li, C., Xie, Y., et al. (2017). Suppression of MyD88-dependent signaling alleviates neuropathic pain induced by peripheral nerve injury in the rat. *J. Neuroinflammation* 14:70.

Liu, T., Gao, Y. J., and Ji, R. R. (2012). Emerging role of Toll-like receptors in the control of pain and itch. *Neurosci. Bull.* 28, 131–144.

Liu, T., Xu, Z. Z., Park, C. K., Berta, T., and Ji, R. R. (2010). Toll-like receptor 7 mediates pruritus. *Nat. Neurosci.* 13, 1460–1462.

Liu, X. J., Liu, T., Chen, G., Wang, B., Yu, X. L., Yin, C., et al. (2016). TLR signaling adaptor protein MyD88 in primary sensory neurons contributes to persistent inflammatory and neuropathic pain and neuroinflammation. *Sci. Rep.* 6:28188. doi: 10.1038/srep28188

Ma, X., Chen, Y., Li, X. C., Mi, W. L., Chu, Y. X., Wang, Y. Q., et al. (2021). Spinal neuronal GRK2 contributes to preventive effect by electroacupuncture on cisplatin-induced peripheral neuropathy in mice. *Anesth. Analg.* 134, 204–215. doi: 10.1213/ANE.0000000000005768

Maatouk, L., Compagnion, A. C., Sauvage, M. C., Bemelmans, A. P., Leclere-Turbant, S., Cirotteau, V., et al. (2018). TLR9 activation via microglial glucocorticoid receptors contributes to degeneration of midbrain dopamine neurons. *Nat. Commun.* 9:2450.

Mao-Ying, Q. L., Cui, K. M., Liu, Q., Dong, Z. Q., Wang, W., Wang, J., et al. (2006). Stage-dependent analgesia of electro-acupuncture in a mouse model of cutaneous cancer pain. *Eur. J. Pain* 10, 689–694. doi: 10.1016/j.ejpain.2005.11.001

Nicotra, L., Loram, L. C., Watkins, L. R., and Hutchinson, M. R. (2012). Toll-like receptors in chronic pain. *Exp. Neurol.* 234, 316–329.

Oka, T., Hikoso, S., Yamaguchi, O., Taneike, M., Takeda, T., Tamai, T., et al. (2012). Mitochondrial DNA that escapes from autophagy causes inflammation and heart failure. *Nature* 485, 251–255. doi: 10.1038/nature10992

Okun, E., Griffioen, K. J., and Mattson, M. P. (2011). Toll-like receptor signaling in neural plasticity and disease. *Trends Neurosci.* 34, 269–281.

Pallottie, A., Ratnayake, A., Ni, L., Acioglu, C., Li, L., Mirabelli, E., et al. (2018). A toll-like receptor 9 antagonist restores below-level glial glutamate transporter

expression in the dorsal horn following spinal cord injury. *Sci. Rep.* 8:8723. doi: 10.1038/s41598-018-26915-2

Park, B., Brinkmann, M. M., Spooner, E., Lee, C. C., Kim, Y. M., and Ploegh, H. L. (2008). Proteolytic cleavage in an endolysosomal compartment is required for activation of Toll-like receptor 9. *Nat. Immunol.* 9, 1407–1414. doi: 10.1038/ni.1669

Patra, M. C., and Choi, S. (2016). Recent progress in the development of Toll-like receptor (TLR) antagonists. *Expert. Opin. Ther. Pat.* 26, 719–730.

Prinz, M., Garbe, F., Schmidt, H., Mildner, A., Gutcher, I., Wolter, K., et al. (2006). Innate immunity mediated by TLR9 modulates pathogenicity in an animal model of multiple sclerosis. *J. Clin. Invest.* 116, 456–464. doi: 10.1172/JCI26078

Qi, J., Buzas, K., Fan, H., Cohen, J. I., Wang, K., Mont, E., et al. (2011). Painful pathways induced by TLR stimulation of dorsal root ganglion neurons. *J. Immunol.* 186, 6417–6426. doi: 10.4049/jimmunol.1001241

Qin, M., Li, Y., Yang, X., and Wu, H. (2014). Safety of Toll-like receptor 9 agonists: a systematic review and meta-analysis. *Immunopharmacol. Immunotoxicol.* 36, 251–260. doi: 10.3109/08923973.2013.861481

Sun, X., Zeng, H., Wang, Q., Yu, Q., Wu, J., Feng, Y., et al. (2018). Glycyrrhizin ameliorates inflammatory pain by inhibiting microglial activation-mediated inflammatory response via blockage of the HMGB1-TLR4-NF-kB pathway. *Exp. Cell Res.* 369, 112–119. doi: 10.1016/j.yexcr.2018.05.012

Sun, Y., Xiao, Q., Luo, C., Zhao, Y., Pu, D., Zhao, K., et al. (2017). High-glucose induces tau hyperphosphorylation through activation of TLR9-P38MAPK pathway. *Exp. Cell Res.* 359, 312–318. doi: 10.1016/j.yexcr.2017.07.032

Tian, J., Avalos, A. M., Mao, S. Y., Chen, B., Senthil, K., Wu, H., et al. (2007). Toll-like receptor 9-dependent activation by DNA-containing immune complexes is mediated by HMGB1 and RAGE. *Nat. Immunol.* 8, 487–496. doi: 10.1038/ni1457

Wang, J., Yu, R., Han, Q.-Q., Huang, H.-J., Wang, Y.-L., Li, H.-Y., et al. (2019). G-1 exhibit antidepressant effect, increase of hippocampal ERs expression and improve hippocampal redox status in aged female rats. *Behav. Brain Res.* 359, 845–852. doi: 10.1016/j.bbr.2018.07.017

Wang, X., Grace, P. M., Pham, M. N., Cheng, K., Strand, K. A., Smith, C., et al. (2013). Rifampin inhibits Toll-like receptor 4 signaling by targeting myeloid differentiation protein 2 and attenuates neuropathic pain. *FASEB J.* 27, 2713–2722. doi: 10.1096/fj.12-222992

Wu, F. X. B. J., Miao, X. R., Huang, S. D., Xu, X. W., Gong, D. J., Sun, Y. M., et al. (2010). Intrathecal siRNA against Toll-like receptor 4 reduces nociception in a rat model of neuropathic pain. *Int. J. Med. Sci.* 7, 251–259. doi: 10.7150/ijms.7.251

Zhang, J., and Deng, X. (2017). Bupivacaine effectively relieves inflammation-induced pain by suppressing activation of the NF−κB signalling pathway and inhibiting the activation of spinal microglia and astrocytes. *Exp. Therap. Med.* 13, 1074–1080. doi: 10.3892/etm.2017.4058

Zhang, Z. J., Guo, J. S., Li, S. S., Wu, X. B., Cao, D. L., Jiang, B. C., et al. (2018). TLR8 and its endogenous ligand miR-21 contribute to neuropathic pain in murine DRG. *J. Exp. Med.* 215, 3019–3037. doi: 10.1084/jem.20180800

Zhao, X.-H., Zhanga, T., and Li, Y.-Q. (2015). The up-regulation of spinal Toll-like receptor 4 in rats with inflammatory pain induced by complete Freund's adjuvant. *Brain Res. Bull.* 111, 97–103. doi: 10.1016/j.brainresbull.2015.01.002

Zhao, Y., Pu, D., Sun, Y., Chen, J., Luo, C., Wang, M., et al. (2018). High glucose-induced defective thrombospondin-1 release from astrocytes via TLR9 activation contributes to the synaptic protein loss. *Exp. Cell Res.* 363, 171–178. doi: 10.1016/j.yexcr.2017.12.030

frontiers | Frontiers in Molecular Neuroscience

TYPE Original Research
PUBLISHED 25 October 2022
DOI 10.3389/fnmol.2022.1026593

OPEN ACCESS

EDITED BY
Xin Zhang,
Duke University, United States

REVIEWED BY
Yan-Qing Wang,
Fudan University, China
Ceng Luo,
Fourth Military Medical University, China
Zilong Wang,
Southern University of Science and Technology, China

*CORRESPONDENCE
Xingji You
yoyo1976@shu.edu.cn
Jingxiang Wu
wjx1132@163.com

†These authors have contributed equally to this work

SPECIALTY SECTION
This article was submitted to Pain Mechanisms and Modulators, a section of the journal Frontiers in Molecular Neuroscience

RECEIVED 24 August 2022
ACCEPTED 03 October 2022
PUBLISHED 25 October 2022

CITATION
Li X, Wang W, Zhang X, Gong Z, Tian M, Zhang Y, You X and Wu J (2022) Neuroinflammation in the medial prefrontal cortex exerts a crucial role in bone cancer pain. *Front. Mol. Neurosci.* 15:1026593. doi: 10.3389/fnmol.2022.1026593

Neuroinflammation in the medial prefrontal cortex exerts a crucial role in bone cancer pain

Xin Li[1,2†], Wei Wang[1†], Xiaoxuan Zhang[1,2], Zhihao Gong[1], Mi Tian[3], Yuxin Zhang[1], Xingji You[2*] and Jingxiang Wu[1*]

[1]Department of Anesthesiology, Shanghai Chest Hospital, Shanghai Jiao Tong University, Shanghai, China, [2]School of Medicine, Shanghai University, Shanghai, China, [3]Department of Critical Care Medicine, Huashan Hospital, Fudan University, Shanghai, China

Bone cancer pain (BCP) is one of the most common types of pain in cancer patients which compromises the patient's functional status, quality of life, and survival. Central hyperalgesia has increasingly been identified as a crucial factor of BCP, especially in the medial prefrontal cortex (mPFC) which is the main cortical area involved in the process of pain and consequent negative emotion. To explore the genetic changes in the mPFC during BCP occurrence and find possible targets for prediction, we performed transcriptome sequencing of mPFC in the BCP rat model and found a total of 147 differentially expressed mRNAs (DEmRNAs). A protein-protein interaction (PPI) network revealed that the DEmRNAs mainly participate in the inflammatory response. Meanwhile, microglia and astrocytes were activated in the mPFC of BCP rats, further confirming the presence of neuroinflammation. In addition, Gene Ontology (GO) analysis showed that DEmRNAs in the mPFC are mainly involved in antigen processing, presentation of peptide antigen, and immune response, occurring in the MHC protein complex. Besides, the Kyoto Encyclopedia of Genes and Genomes (KEGG) analysis revealed that DEmRNAs are mainly enriched in the pathways of phagosome, staphylococcus aureus infection, and antigen processing, in which MHCII participate. Furthermore, immunostaining showed that MHCII is mainly located in the microglia. Microglia are believed to be involved in antigen processing, a key cause of BCP. *In vivo*, minocycline (MC) treatment inhibits the activation of microglia and reduces the expression of MHCII and proinflammatory cytokines, thereby alleviating BCP and pain-related anxiety. Taken together, our study identified differentially expressed genes in the BCP process and demonstrated that the activation of microglia participates in the inflammatory response and antigen process, which may contribute to BCP.

KEYWORDS

transcriptome sequencing, bone cancer pain, medial prefrontal cortex, microglia, immune inflammation, major histocompatibility complex class II

Introduction

The incidence of cancer worldwide has increased steadily in the past 10 years (Miller et al., 2020), advanced cancer metastasis to bone is one of the most common complications (Meuser et al., 2001; Clézardin et al., 2021), inflicting patients with severe and chronic pain. Unfortunately, current pain management interventions are still insufficient (Kapoor et al., 2021). Several causes of bone cancer pain (BCP) have been proposed, including structural reorganization of sensory and sympathetic nerve fibers in the bone, combined with the cellular and neurochemical reorganization in the spinal cord and brain (Mantyh, 2013; Zajączkowska et al., 2019). More and more evidence has been accumulated to support the role of central nociceptive hypersensitivity in BCP (Hou et al., 2020; Wu et al., 2021).

The medial prefrontal cortex (mPFC) is a central mediator in the pain pathway, which is crucial as an integrator of ascending sensory information, cognitive and emotional responses, and descending inhibitory control (Ong et al., 2019; Kummer et al., 2020). Changes in gene expression in the PFC play a role in acute and chronic pain development and maintenance (Yan et al., 2019; Cai et al., 2020; Qian et al., 2020; Shiers and Price, 2020; Topham et al., 2020). During chronic pain states, it has been reported that mPFC undergoes structural and functional plasticity (Obermann et al., 2013; Liu et al., 2018; Sang et al., 2018; Huang et al., 2020). Transcriptome analysis of the mPFC using ribonucleic acid (RNA) sequencing and further RT-qPCR has also shown that rodents with neuropathic pain displayed an increase in genes including NMDA receptor, BDNF, and κ-opioid receptor (Alvarado et al., 2013; Palmisano et al., 2019). Most recently, DNA methylation in the PFC was found to be highly correlated with both pain and comorbid behaviors in a mouse model of neuropathic pain (Tajerian et al., 2013; Topham et al., 2020). In addition, mPFC microglia have been shown to cause pain in the model of the peripheral nerve injury (Fiore and Austin, 2019). Therapeutic mechanisms targeting mPFC may have efficacy across various pain disorders and simultaneously address associated cognitive and emotional comorbidities (Nashed et al., 2015). However, when BCP occurs, the expression profile and specific BCP regulation mechanisms of mRNA in the prefrontal cortex are largely unknown.

To detect transcriptomic changes in the mPFC of the BCP process and explore the potential therapeutic targets, we established the widely used BCP rat model and performed transcriptome sequencing to explore expression profile changes of mRNAs, and functional analysis of differential genes to provide new insights on the mechanism of BCP. Differentially expressed mRNAs (DEmRNAs) were subjected to Gene Ontology (GO) and Kyoto Encyclopedia of Genes and Genomes (KEGG) pathway analyses to evaluate their functions and possible mechanisms. Our study may provide new insights into understanding the central mechanisms of BCP and help to find promising genes or signaling pathways that could be manipulated to treat BCP disorders.

Materials and methods

Bone cancer pain animal model

Female Sprague-Dawley (200–250 g) and Wistar rats (60–70 g) were purchased from B&K Universal Group Limited (Shanghai, China) and housed in cages at a temperature of 24 ± 1°C under 12/12 h light-dark cycles with free access to food and water. All animal handling and surgical procedures were carried out in accordance with the guidelines of the International Association for the Study of Pain, approved by the Animal Care and Use Committee of Shanghai Chest Hospital, Shanghai Jiao Tong University. In the study, Sprague-Dawley rats weighing 200–250 g were randomly divided into three groups: Sham group, BCP + normal saline group (BCP group), and BCP + 20 mg/kg MC group (BCP + MC group).

BCP was induced in rats as previously described (Brigatte et al., 2007). Briefly, female Wistar rats received an intraperitoneal inoculation of Walker 256 mammary gland carcinoma cells (purchased from ATCC). After 1 week, cells in the ascites were collected and resuspended in saline to a final concentration of 2×10^7 cells/ml. Next, female Sprague Dawley rats were anesthetized with pentobarbital (50 mg/kg, i.p.), and a 23-gauge needle was inserted into the intramedullary canal of the right tibia at one-third of the length from the lower end, to create a cavity for the injection of saline (10 μl, Sham) or Walker 256 cell suspension (10 μl, containing 2×10^5 cells in total, BCP). The cavity was sealed with bone wax and the incision was closed with stitches. Upon waking from anesthesia, the animals were returned to their home cages.

Pain behavioral tests

Mechanical allodynia was evaluated by measuring the paw withdrawal thresholds (PWT) in response to a series of calibrated von Frey filaments (Remeniuk et al., 2015). In brief, rats were transferred to a chamber with a metal mesh floor and allowed to acclimatize for 30 min. Then, von Frey filaments were applied to the plantar surface of the right hind paw in ascending order (1, 1.4, 2, 4, 6, 8, 10, and 15 g). Abrupt paw withdrawal, licking, and shaking are defined as positive responses. Once a positive response was observed, the rat was allowed to rest for 5 min. PWT was defined as the lowest force that elicited a positive response and averaged across three repeats of measurement.

Movement-evoked pain was assessed with the limb use score (LUS) (Remeniuk et al., 2015). Rats were permitted to move spontaneously on a smooth plastic table (50 × 50 cm). The limb

use during spontaneous ambulation was scored on a scale of 4–0 (4: normal use; 3: slightly limping; 2: limping; 1: no use of the limbs, partial; 0: no use of the limbs, complete).

Microglia-activated inhibitor MC was purchased from MedChemExpress (Monmouth Junction, NJ, USA), dissolved in saline (20 mg/ml, stored at −20°C for use), and administrated every other day from 1 day after surgery (D1, 20 mg/kg, i.p.). All behavioral tests were performed by an investigator who was blinded to the experimental design.

Elevated plus maze test

Anxiety-like behavior was measured using the elevated plus-maze (Shanghai Jiliang Software Technology Co., Ltd.). It consisted of two opposing open arms (50 × 10 × 0.5 cm), two opposing closed arms (50 × 10 × 40 cm), and a central open platform (10 × 10 cm). Each rat was placed on the central platform facing one of the open arms and allowed to explore the apparatus for 5 min. We analyzed the time spent in the open arms and total numbers of entries by JLBehv-EPMG software, based on previous literature (Masukawa et al., 2020).

Tissue collection and ribonucleic acid extraction

On day 17, rats were deeply anesthetized with sodium pentobarbital (40 mg/kg, i.p.) and perfused through the ascending aorta with 0.9% saline (4°C). After the perfusion, the medial prefrontal central (mPFC) was collected. Total RNA was extracted from the Sham and BCP group tissues using Trizol reagent (Invitrogen, Carlsbad, CA, USA), following the manufacturer's instructions. For tissue samples, about 60 mg of liquid nitrogen was ground into powder and the powder samples were transferred into 1.5 ml Trizol reagent. The mixture was centrifuged at 12,000 × *g* for 5 min at 4°C. The supernatant was transferred to a new 2.0-ml tube with 0.3 ml of chloroform/isoamyl alcohol (24:1) per 1.5 ml of Trizol reagent. After the mixture was centrifuged at 12,000 × *g* for 10 min at 4°C, the aqueous phase was transferred to a new 1.5 ml tube which was added with an equal volume of supernatant of isopropyl alcohol. The mixture was centrifuged at 12,000 × *g* for 20 min at 4°C and then the supernatant was removed. After being washed with 1 ml 75% ethanol, the RNA pellet was air-dried in the biosafety cabinet and then dissolved by adding 25 ∼ 100 μl DEPC-treated water. Subsequently, total RNA was qualified and quantified using a Nano Drop and Agilent 2100 Bioanalyzer (Yin et al., 2021) (Thermo Fisher Scientific, MA, USA).

RNA-seq library establishment and RNA-seq

Approximately 1 μg total RNA per sample was treated with Ribo-Zero® Magnetic Kit (Epicenter) to deplete rRNA. First-strand cDNA was generated using random primers reverse transcription, followed by second-strand cDNA synthesis. The synthesized cDNA was subjected to end-repair and then was 3′ adenylated. Adapters were ligated to the ends of these 3′ adenylated cDNA fragments. Several rounds of PCR amplification with PCR Primer Cocktail and PCR Master Mix are performed to enrich the cDNA fragments. Then the PCR products are purified with Ampure XP Beads. The final library was quality and quantitated in two methods: checking the distribution of the fragment size using the Agilent 2100 Bioanalyzer and quantifying the library using real-time quantitative PCR (qPCR) (TaqMan Probe). The qualified libraries were sequenced pair end on the Hiseq 4000 platform (Fang et al., 2018) (BGI-Shenzhen, China).

Bioinformatics analysis

Primary sequencing data produced by RNA-Seq (raw reads) were subjected to quality control (QC). The sequencing data was filtered with SOAPnuke (v1.5.2) by removing reads containing sequencing adapter; removing reads whose low-quality base ratio (base quality less than or equal to 5) is more than 20%, and removing reads whose unknown base ("N" base) ratio is more than 5%; afterward, clean reads were obtained and stored in FASTQ format. The clean reads were mapped to the reference genome using HISAT2 (v2.0.4). After that, Ericscript (v0.5.5) and rMATS (V3.2.5) were used to detect fusion genes and differential splicing genes (DSGs), respectively. Bowtie2 (v2.2.5) was applied to align the clean reads to the gene set, a database built by BGI (Beijing Genomic Institute in Shenzhen), in which known and novel, coding and non-coding transcripts were included, then the expression level of the gene was calculated by RSEM (v1.2.12). The heatmap was drawn by pheatmap (v1.0.8) according to the gene expression in different samples. Essentially, differential expression analysis was performed using the DESeq2(v1.4.5) with q-value ≤ 0.05.

Cluster analysis and screening of differentially expressed genes

Distances of expressed genes were calculated using the Euclidean method. The sum of the squared deviations algorithm was used to calculate distance. The cluster analysis and heat map visualization of gene expression patterns were performed using the "pheatmap" package in the R software of Bioconductor. DEmRNAs with statistical significance were identified through

Scatter Plot filtering as we reported before. The threshold required for the results to be considered significant was as follows: q-value ≤ 0.01 and the absolute value of $|\log2$ (fold change)$| \geq 0.58$ as in our previous study. To take an insight into the change of phenotype, GO and KEGG enrichment analysis of annotated different expression genes was performed by bioinformatics.[1]

Western blot

Animals were deeply anesthetized with sodium pentobarbital (50 mg/kg, i.p.) and rapidly sacrificed by cervical dislocation. The mPFC was homogenized in RIPA buffer containing 1 mM PMSF (Beyotime) and centrifuged at 13,000 × g for 30 min. The supernatant was collected, and the total protein concentration was titrated using a bicinchoninic acid kit. An equivalent amount of protein (50 μg) was fractionated on 10% polyacrylamide gel. Proteins were then transferred to nitrocellulose membranes (Millipore) at 300 mA for 90 min. Membranes were blocked with 5% BSA in Tris-buffered saline (TBS, 50 mM Tris-HCl, 150 mM NaCl, pH 7.5) for 2 h at room temperature and incubated overnight at 4°C with primary antibodies (anti-CD74 at 1:500, sc-6262, SANTA CRUZ; anti-CTSS at 1:1,000, ab92780, Abcam; anti-CIITA at 1:1,000, sc-13556, SANTA CEUZ; anti-Vinculin at 1:1,000, A2752, ABclonal; anti-MHCII at 1:1,000, sc06-78, invitrogen) in TBS containing 5% BSA. Following three washes with TBS, membranes were incubated with horseradish peroxidase-conjugated secondary antibodies (goat anti-rabbit at 1:2,000, ab205718, Abcam; goat anti-mouse at 1:2,000, ab205719, Abcam) in TBS containing 5% BSA for 2 h at room temperature. Immunoreactive proteins were visualized using the enhanced chemiluminescence western blotting detection system (Santa Cruz). The membranes were analyzed with a computerized image analysis system (ChemiDoc XRS1, Bio-Rad, Hercules, CA), and the intensity of the protein bands was quantified with Image Lab software (ImageJ). All protein expression was normalized to Vinculin.

Bone histomorphometric analysis

The ipsilateral tibia of BCP rats was fixed in 4% paraformaldehyde for 48 h, followed by decalcification in 10% EDTA for 3–4 weeks, and 6-μm sections were prepared on a rotating microtome. Paraffin-embedded sections were deparaffinized in xylene, rehydrated, and stained with hematoxylin-eosin (H&E; Sigma, St Louis, MO, USA) according to the manufacturer's protocol (Wang et al., 2019).

1 www.bioinformatics.com.cn

Enzyme-linked immunosorbent assay

ELISA was used to determine the inflammatory cytokines (IL-1β, TNF-α, and IL-18) in the mPFC. The samples were weighed and then homogenized completely in phosphate-buffered solution (PBS). After centrifugation (1,000 × g, 10 min) of the homogenates at 4°C, supernatants were collected and stored at -80°C. The concentrations of TNF-α (ml002859-C), IL-1β (ml037361-C), and IL-18 (ml002816-C) were detected following the instruction of ELISA kits (Shanghai Enzyme-linked Biotechnology Co., Ltd.).

Real-time quantitative polymerase chain reaction

Total RNA was extracted from mPFC using a total RNA Kit (Vazyme Biotech Co., Ltd., China), and complementary DNA (cDNA) was generated using a cDNA Synthesis Kit (DBI® Bioscience Co., Ltd., Germany), according to instructions provided by the manufacturers. RT-qPCR was carried out using an SYBR Green assay (DBI® Bioscience) on a StepOnePlus Real—Time PCR System (Applied Biosystems®, Thermo Fisher Scientific, Waltham, MA, USA), and the relative gene expression was determined using the comparative Ct ($\Delta\Delta$Ct) method. GAPDH was used as a housekeeping gene. The primer sequences are as **Supplementary Table 1**.

Immunofluorescence

Animals were deeply anesthetized with sodium pentobarbital (50 mg/kg, i.p.) and underwent sternotomy, followed by intracardiac perfusion with 200 ml saline and 200 ml 4% ice-cold paraformaldehyde in 0.1 M phosphate-buffered saline. The brain was removed, postfixed in 4% paraformaldehyde for 4 h, and subsequently allowed to equilibrate in 30% sucrose in phosphate-buffered saline overnight at 4°C. Brain samples were embedded in Tissue-Tek O.C.T., cut at a thickness of 20 μM using a cryostat (Leica CM1850-1-1), and mounted on slides. All Brain samples were thoroughly rinsed in PBS to remove any residual OCT. The samples were then blocked in 0.3% Triton-X 100 and 5% normal donkey serum (NDS) in PBS for 1 h, and incubated overnight with anti-MHCII (1:50, MCA46GA, BIO-RAD), anti-IBA-1 (1:100, ab178847, Abcam), anti-GFAP (1:100, ab254082, Abcam), anti-NEUN (1:100, ab177487, Abcam). On the next day, the samples were rinsed in PBS and incubated for 1 h in PBS containing appropriate secondary antibody (1:500) from Jackson ImmunoResearch (catalog nos. 711-545-152 or 715-585-150) or Cell Signaling Technology (catalog nos. 8,889 or 4,408). The samples were then rinsed in PBS and coverslipped with Antifade Mounting Medium with DAPI

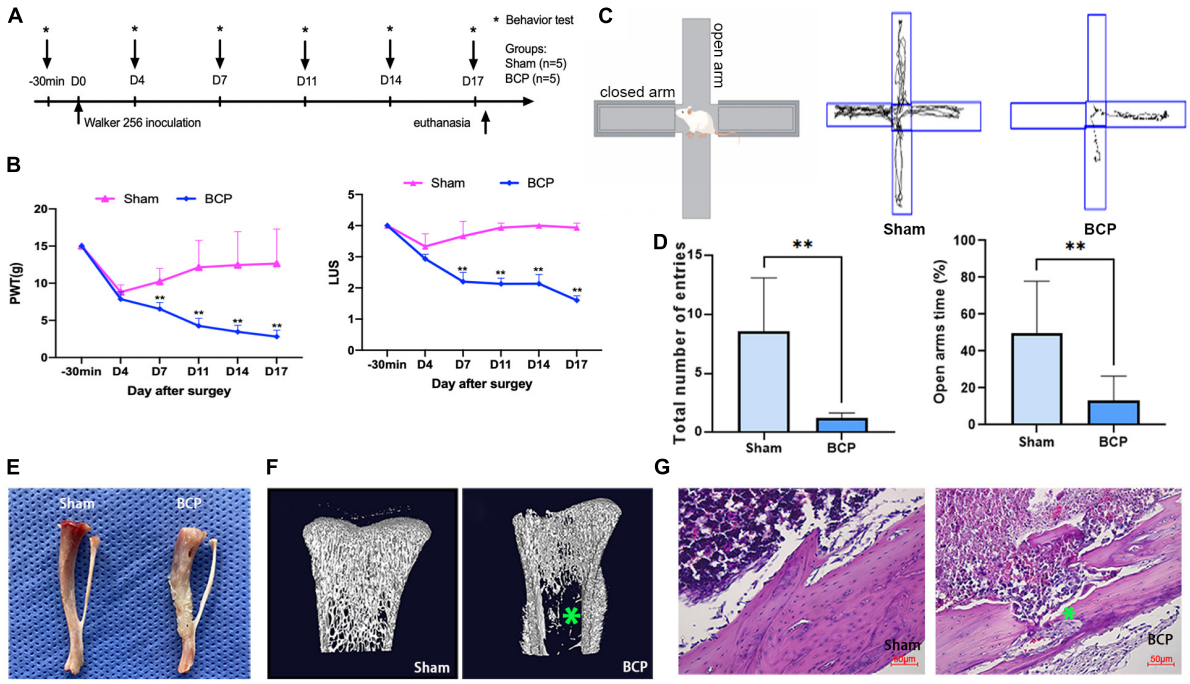

FIGURE 1
Induction of bone cancer pain (BCP) in rats. **(A)** Experimental timeline showing the dates of surgery (D0) and behavioral tests (−30 min, D4, D7, D11, D14, and D17). On D0, saline (Sham) or Walker 256 mammary gland carcinoma cells (BCP) were injected into the tibia in rats and pain sensation was assessed before and after through behavioral tests. **(B)** Induction of significant hyperalgesia in the tumor-bearing hind paw, as assessed through the paw withdrawal threshold (PWT, **Left**) and the limb use score (LUS, **Right**). **(C,D)** Track and result in an analysis of cross maze. A total number of entries and times in open arms were used to measure the degree of walking ability and pain-related anxiety. Compared with the Sham group, the walking ability of BCP group was decreased and exerted pain-related anxiety. **(E)** Photograph of the tibia from a BCP rat on D17 shows obvious tumor growth and bone mass destruction **(Right)** compared to the one from a Sham rat **(Left)**. **(F)** Representative micro-CT images showing the bone microstructure of two tibias from a Sham rat **(Left)** and a BCP rat **(Right)** on D17. Note the reduction in medullary bone and the increase in lesions in cortical bone with the tibia from the BCP rat. **(G)** Hematoxylin and eosin-stained histological sections show obvious medullary bone loss and bone destruction in the tibia of a BCP rat on D17 **(Right)** when compared to the one from a Sham rat **(Left)**. Data are expressed as mean ± SD and statistically analyzed by Two-way ANOVA followed by Turkey's multiple comparisons test with repeated measurements, the behavior test has been repeated 3 times, and $p < 0.05$ was considered statistically significant. $n = 5$ per group. $^{*}p < 0.05$, $^{**}p < 0.01$ vs. Sham groups.

(Beyotime, Nanjing, China). The imaging and subsequent analysis were performed using a Confocal Microscope (TCS SP8, Leica Microsystems, Mannheim, Germany).

Statistics

Data are reported as the mean ± standard deviation. The data were analyzed using GraphPad Prism 8.0 for Windows (San Diego, CA, USA). Results from behavioral testing were analyzed using ANOVA for repeated measures. For all other measures between the 2 groups, the Student's *t*-test was used for the comparisons of variables with normal distribution from independent samples. For comparisons among > 2 groups, a one-way ANOVA with Turkey's multiple comparisons test was applied. Two-way ANOVA followed by Turkey's multiple comparisons test with repeated measurements was used to determine the interaction between time and two groups. Fisher's least significant difference test for pairwise comparisons, all statistical tests were two-sided, and $p < 0.05$ was considered statistically significant.

Results

Rats developed mechanical hypersensitivity and osteolytic lesions after tumor cells inoculation

To induce BCP in rats, we injected Walker 256 mammary gland carcinoma cells into the intramedullary canal of the right tibia. Behavioral tests were performed 30 min before the operation and on D4, D7, D11, D14, and D17 (Figure 1A). BCP rats exhibited a significant decrease in PWT and LUS when compared to the Sham rats (Figure 1B), consistent with previously reported values (Remeniuk et al., 2015). Meanwhile, the elevated plus-maze experiment carried out on D17 showed

the total number of entries and open arms time (%) of BCP rats were reduced (**Figures 1C,D**), indicating that they suffered from pain-related anxiety and impaired walking ability (Blaszczyk et al., 2018). Next, a pathological examination was conducted on D17 after the animals were sacrificed. We found that in gross images the surface of the tibia of Sham rats was smooth while that of BCP rats was swollen and uneven (**Figure 1E**). Furthermore, we found bone destruction in BCP rats, in contrast to uniform bone quality in Sham rats with tibia micro-CT (**Figure 1F**). Lastly, we performed hematoxylin and eosin staining of the tibia and found tumor cell proliferation and invasion of the bone cortex in BCP rats, but not in Sham rats (**Figure 1G**). Taken together, these behavioral and pathological results strongly suggested that BCP was successfully induced in rats.

Transcriptomic high-throughput sequencing revealed changes in gene expression profiles

The count and fold change of DEmRNAs were visualized by a gene map (**Figure 2A**). The expression of ten mRNAs was changed more than 20 times in the mPFC of BCP. Hierarchical clustering of the expression of mRNA showed obvious discrimination between BCP and Sham rats (**Figure 2B**). The results were visualized through a volcano plot (**Figure 2C**). These results indicated that tumor inoculation in the tibia shifted expression profiles of mRNA in mPFC, and 147 DEmRNAs (136 upregulated and 11 downregulated) were found in the transcriptomic sequencing, which may account for the development of hyperalgesia in BCP rats.

To validate the reliability of sequencing quantification, 18 DEmRNAs (10 upregulated and 8 downregulated) were selected to undergo RT-qPCR on another batch of samples (n = 5 per group), independent of the ones used for RNA-seq. As shown in **Figure 2D**, RT-qPCR quantification of top DEmRNA was consistent with RNA sequencing; Impad1, Ubd, RT1-Ba, RT1-Da, RT1-Db, CXCL9, Cd74, C3, and CXCL9, were all significantly upregulated (**Figure 2D**), and Prg4, Gprin3, Npnt, Gjb2, Co16a3, and Cntnap5c were downregulated (**Figure 2E**).

Protein-protein interaction network of differentially expressed mRNAs

For the 147 DEmRNAs, we obtained the PPI network containing 112 nodes and 674 edges. The network was set to the default cutoff (interaction score > 0.4) in the STRING online database (**Figure 3A**). It showed extensive interaction among them and 7 subnetworks were clustered, which may represent more compact functional blocks (**Figure 3B**). Moreover, functional analysis of these genes showed that they were mainly involved in immunological processes/pathways, indicating they were crucial to the pathogenesis of BCP (**Figure 3C**). In the central system, astrocytes and microglia may release various inflammatory mediators that stimulate nociceptive neurons and reinforce glial activation, thereby promoting neuronal sensitization and behavioral hypersensitivity observed in neuropathic pain (Blaszczyk et al., 2018). In our study, immunostaining showed that morphology and number of astrocytes and microglia are changed in the mPFC of BCP rats (**Figures 3D,E**). Furthermore, ELISA analysis showed that the pro-inflammatory cytokines level of IL-1β, IL-18, and TNF-α were upregulated in the mPFC of BCP rats (**Figure 3F**), suggesting the inflammatory response.

Gene ontology analysis and Kyoto Encyclopedia of Genes and Genomes analysis of differentially expressed mRNAs

In order to further explore the function of DEmRNAs, GO enrichment analysis was conducted on 147 DEmRNAs, and results showed that the DEmRNAs were mainly involved in the following biological process (BP) terms: antigen processing and presentation of peptide antigen, leukocyte mediated immunity, antigen processing and presentation, and so forth (**Figure 4A**). Most DEmRNAs were enriched in the following cellular component (CC) terms: external side of the plasma membrane, MHC protein complex, MHC class II protein complex, and so forth (**Figure 4B**). Meanwhile, the following molecular function (MF) terms were enriched including peptide antigen binding, and immunity receptor activity (**Figure 4C**).

Similarly, KEGG analysis of these dysregulated genes showed that, neglecting unrelated pathways, DEmRNAs were primarily enriched in antigen processing and presentation, phagosome, staphylococcus aureus infection, etc. (**Figure 4D**). These results also indicated the involvement of extra-/intra-cellular pathways in inflammatory and immunologic processes.

MHCII in microglia of medial prefrontal cortex may participate in the process of bone cancer pain

We aimed to explore the underlying neuroimmune mechanism of BCP and find several valuable pain biomarkers. It was found that MHCII may be involved in the top three pathways: antigen processing and presentation, phagosomes, and staphylococcus aureus infection (**Figure 5A**). We investigated the expression of MHCII in the mPFC after BCP. RT1-Da and RT1-Bb, two subunits of MHCII, were strongly upregulated at the mRNA level in BCP rats when compared to Sham rats (**Figure 2D** and **Supplementary Figure 1**).

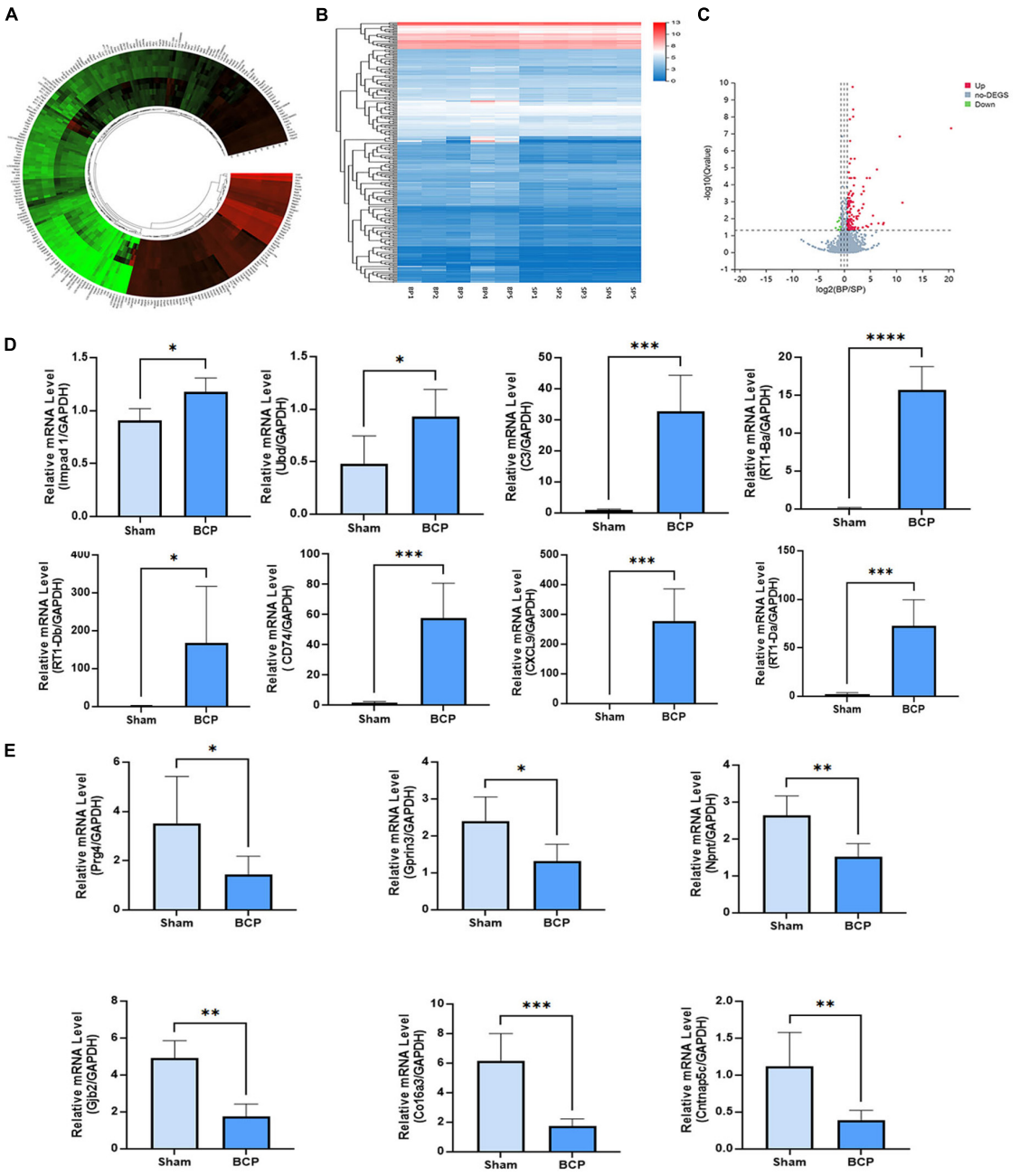

FIGURE 2
DEmRNAs in the mPFC were found between Sham and BCP rats at D17. **(A)** The gene map of the different expression mRNAs (DEmRNAs) in the mPFC between Sham and BCP rats. **(B)** The heatmap of the DEmRNAs in the mPFC between Sham and BCP rats. **(C)** The volcano plot of DEmRNAs in the mPFC between Sham and BCP rats. **(D,E)** The expression level of up-regulated mRNAs **(D)** and downregulated mRNAs **(E)**, with gene names on each bar graph. Data are expressed as mean ± SD and statistically analyzed by Student's *t*-test. $n = 5$ per group. $^{*}p < 0.05$, $^{**}p < 0.01$, $^{***}p < 0.001$, $^{****}p < 0.0001$ vs. Sham group.

Consistently, both western blot and immunostaining confirmed increased expression of MHCII in the mPFC of BCP rats at the protein level (Figures 5B–D). Remarkably, the expression of CD74 and CTSS, two binding partners of MHCII in downstream antigen presentation, and the class II trans-activator (CIITA), a key transcription factor for MHCII, were all significantly increased in BCP rats when compared to Sham rats ($p < 0.05$, Figures 5E,F). Therefore, MHCII may be involved in the process of BCP. In addition, double immunostaining revealed that MHCII was localized mainly in microglia, not in astrocytes (Figures 5G,H). Microglial cells, rather than astrocytes, are considered to be the main antigen-presenting cells in the central

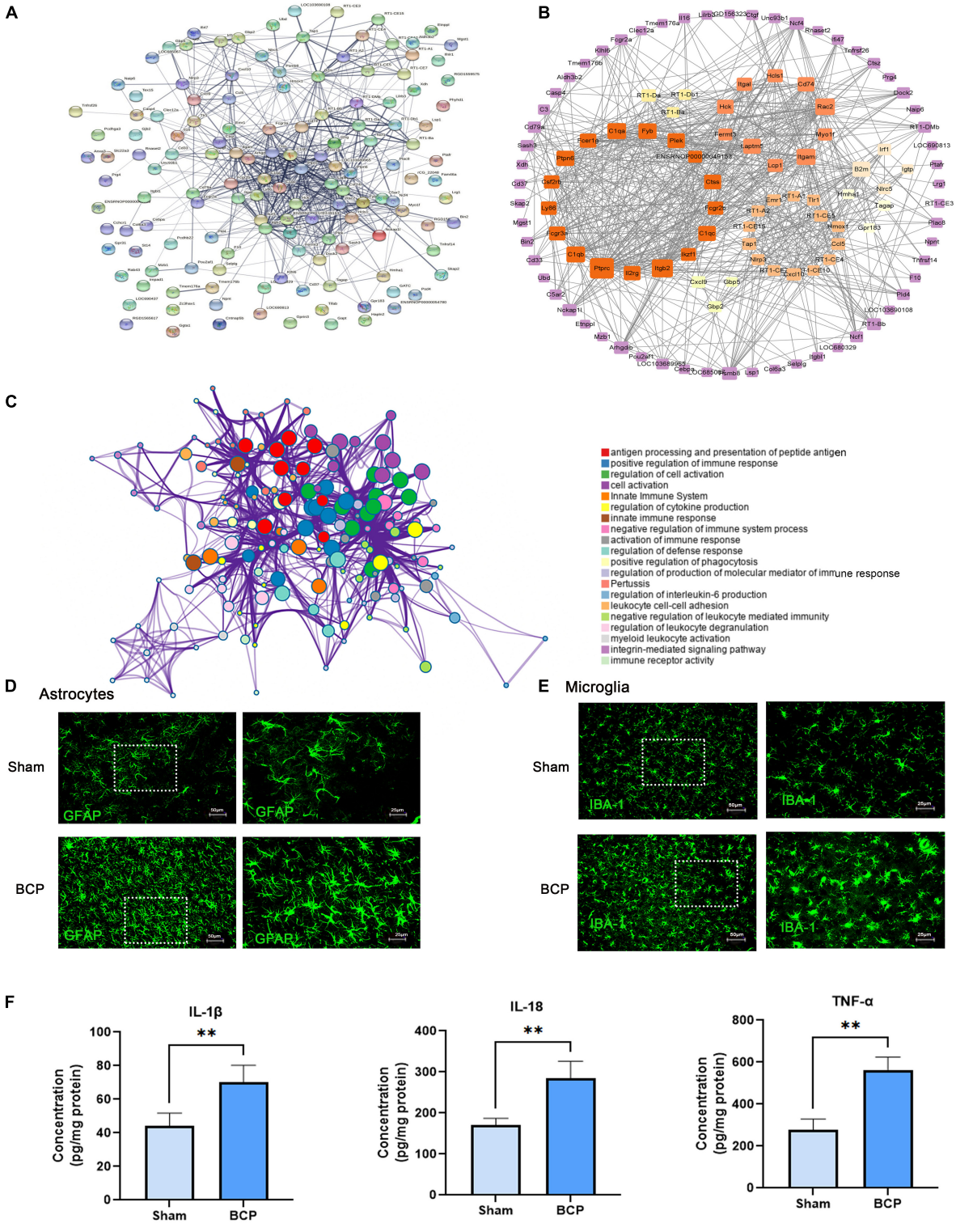

FIGURE 3

Immune inflammation exerts a crucial role in bone cancer pain at D17. **(A)** PPI network constructed by the 147 DEmRNA-coding protein. **(B)** The node's color scale indicates connectivity with other nodes, and the edge's thickness indicates the interaction's combined score. The clusters were the top seven subnetworks calculated by MCODE. **(C)** A functional enrichment network is constructed by nodes representing terms. **(D,E)** Astrocyte and microglia activated in the mPFC of BCP rats. Representative immunofluorescence images showing the morphologies of the astrocyte labeled with GFAP **(D)**, microglia labeled with Iba1 **(E)** in the mPFC. **(F)** The pro-inflammatory cytokines upregulated in the mPFC of BCP rats. Data are expressed as mean ± SD and statistically analyzed by Student's *t*-test. $n = 5$ per group. $^{**}p < 0.01$, vs. Sham groups.

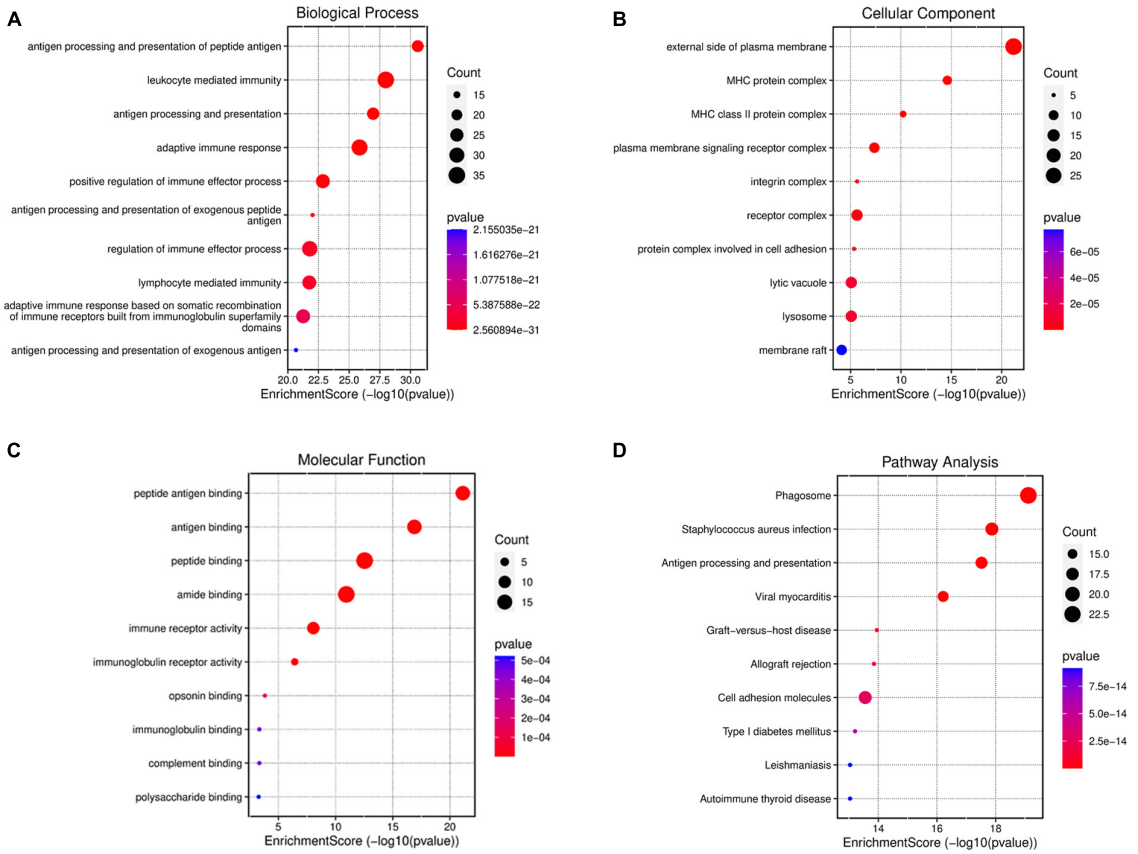

FIGURE 4
GO and KEGG enrichment analysis for DEmRNAsof mPFC in the progress of BCP. GO enrichment of DEmRNAs shows the top 10 terms (according to *p*-value) in three types of GO terms, biological process **(A)**, cellular component **(B)**, and molecular function **(C)**. **(D)** KEGG enrichment analysis shows the top 10 pathways in the progress of BCP. The size of the bubble indicates the number of enriched DEmRNAs, the color indicates the *p*-value and the position indicates the rich factor.

nervous system (Almolda et al., 2011; Dasgupta and Dasgupta, 2017), suggesting that MHCII in the mPFC may be a biomarker of activated microglia which participate in the antigen process to contribute to BCP.

In order to further investigate whether activation of microglia in mPFC plays a crucial role in the process of BCP, minocycline (MC) was administered in BCP rats to inhibit microglia activation (20 mg/kg, every other day from D1, intraperitoneally) (**Figure 6A**). Rats were randomly divided into three groups; Sham, BCP (+ saline), and BCP + MC. The reduction of PWT and LUS in BCP rats can be reversed by MC treatment (**Figure 6B**). Meanwhile, the elevated plus-maze experiment carried out at D14 showed that the MC treatment increased the total number of entries and open arms time (%) (**Figures 6C,D**), indicating improvement of walking ability and relief of pain-related anxiety. In addition, the upregulation of pro-inflammatory cytokines of BCP was reversed in the BCP + MC group (**Figure 6E**), confirming the inhibition of microglia activation may relieve the symptom of BCP. To detect the expression of antigen process, RT-PCR, western blot, and immunofluorescent staining showed that the upregulation of MHCII in the mPFC microglia was decreased (**Figures 6F–I**) and the upregulation of its downstream binding partners (CD74 and CTSS) and key transcription factor (CIITA) (**Figures 6H,I**) were also reversed after the treatment of MC. It indicates that MHCII and its related pathway may be decreased after the inhibition of microglia activation. Thus, we proposed that MHCII in the mPFC may be a biomarker for microglia activation to participate in antigen processing and further promote BCP.

Discussion

In this study, the whole genome of mPFC from rats with BCP was sequenced for the first time, revealing the key genes, which was a highlight. Firstly, the transcription sequence showed that there are 147 DEmRNAs in the mPFC of the BCP rat. Secondly, KEGG and GO enrichment indicated that the DEmRNAs are mainly involved in immune inflammation.

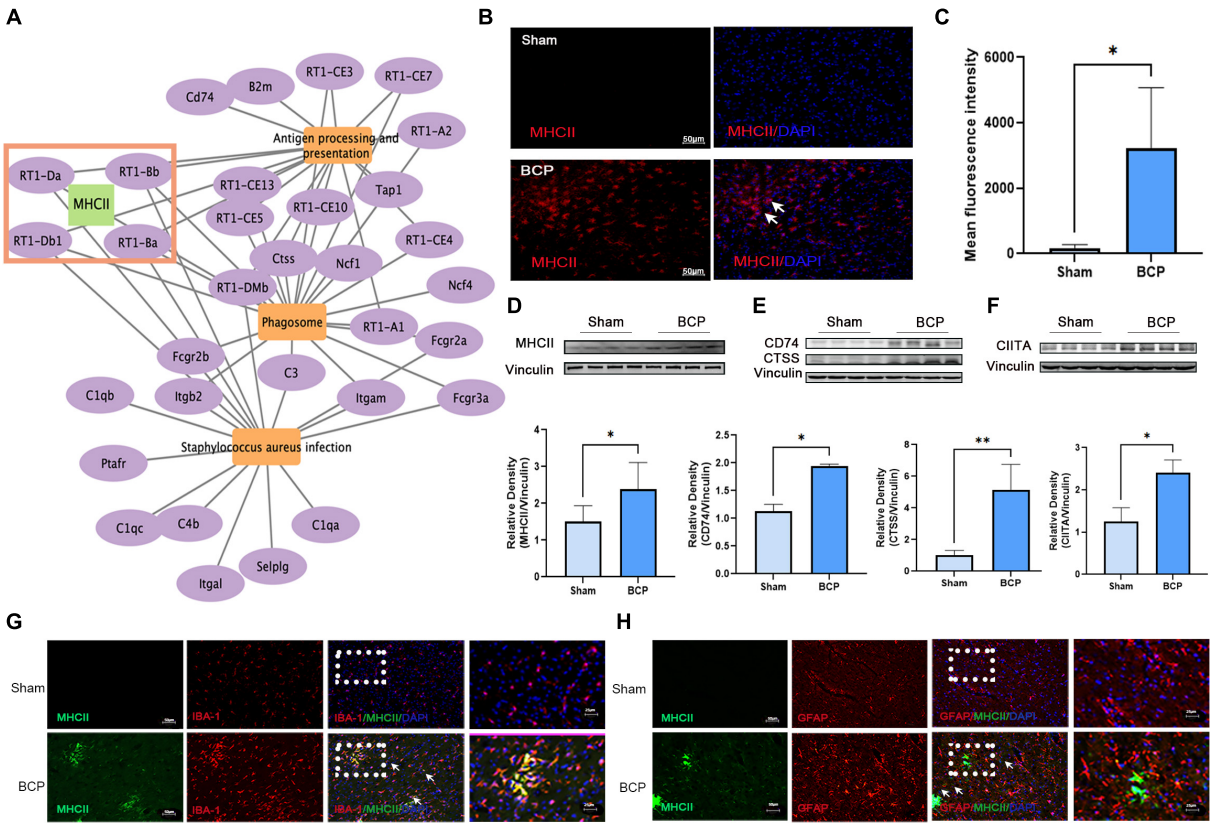

FIGURE 5
Increased expression of MHCII in the medial prefrontal cortex (mPFC) in rats with BCP at D17. **(A)** The interaction of the top 3 pathways and genes showed that MHCII may exert a crucial role. **(B,C)** Immunofluorescent showed the increased expression of MHCII. **(D–F)** Western blot also revealed that MHCII was upregulated **(D)**. Western blot revealed that the CD74 and CTSS upstream of MHCII and CIITA downstream of MHCII were upregulated in the mPFC of BCP rats **(E)**. $*p < 0.05$, $**p < 0.01$ vs. Sham group. **(G,H)** Double immunofluorescent staining of MHCII and cell type-specific markers revealed that the increased expression of MHCII in the mPFC of rats with BCP occurred mainly in microglia **(G)**, but not in astrocytes **(H)**.

Thirdly, we displayed that MHCII, which is the key gene in the enrichment, was increased in the microglia of BCP rats' mPFC. Lastly, we confirmed that the pain and pain-related anxiety were relieved by administrating MC to inhibit microglia activation, accompanied by the reversal of the upregulation of MHCII, indicating that MHCII related to microglia activation plays a crucial role in the mPFC of BCP.

A wealth of evidence has suggested that BCP is a complex clinical syndrome, that shares several features with inflammatory and neuropathic pain (Falk and Dickenson, 2014) and which often comes with concurrent depression, cognitive impairment, and other diseases (Feller et al., 2019; Liu et al., 2021). The mPFC is a main cortical area involved in processing both pain and consequent negative emotion (Salomons et al., 2015; Mecca et al., 2021), notably, it has been reported that dysfunction of mPFC neurons may be implicated in neuropathic pain-related anxiety (Du et al., 2022). Most, recently, Dai et al. (2022) performed a gene set enrichment analysis in the mPFC of neuropathic pain, and they found that there are 49 different expression genes. To further explore the potential targets in the mPFC of BCP, we established a comprehensive transcription sequence. The analysis showed that there were 147 DEmRNAs. PPI network analysis showed that DEmRNAs in mPFC were mainly involved in immune inflammation. Meanwhile, in the mPFC of BCP rats, microglia and astrocytes were activated, and pro-inflammatory cytokines were released, indicating an immune inflammation response. In addition, accumulating evidence suggests that in the central nervous system non-neuronal cells interact with nociceptive neurons by secreting neuroactive signaling molecules that modulate pain (Ji et al., 2016; Totsch and Sorge, 2017).

In the analysis of neuropathic pain, the most significantly regulated gene sets included oligodendrocyte differentiation, semaphoring plexin signaling pathway, negative regulation of gliogenesis, neuron fate commitment, intrinsic component of external side of plasma membrane, and germ cell nucleus (Dai et al., 2022). While, in our study, different from neuropathic pain, we found that the BP, CC, and MF was related to the

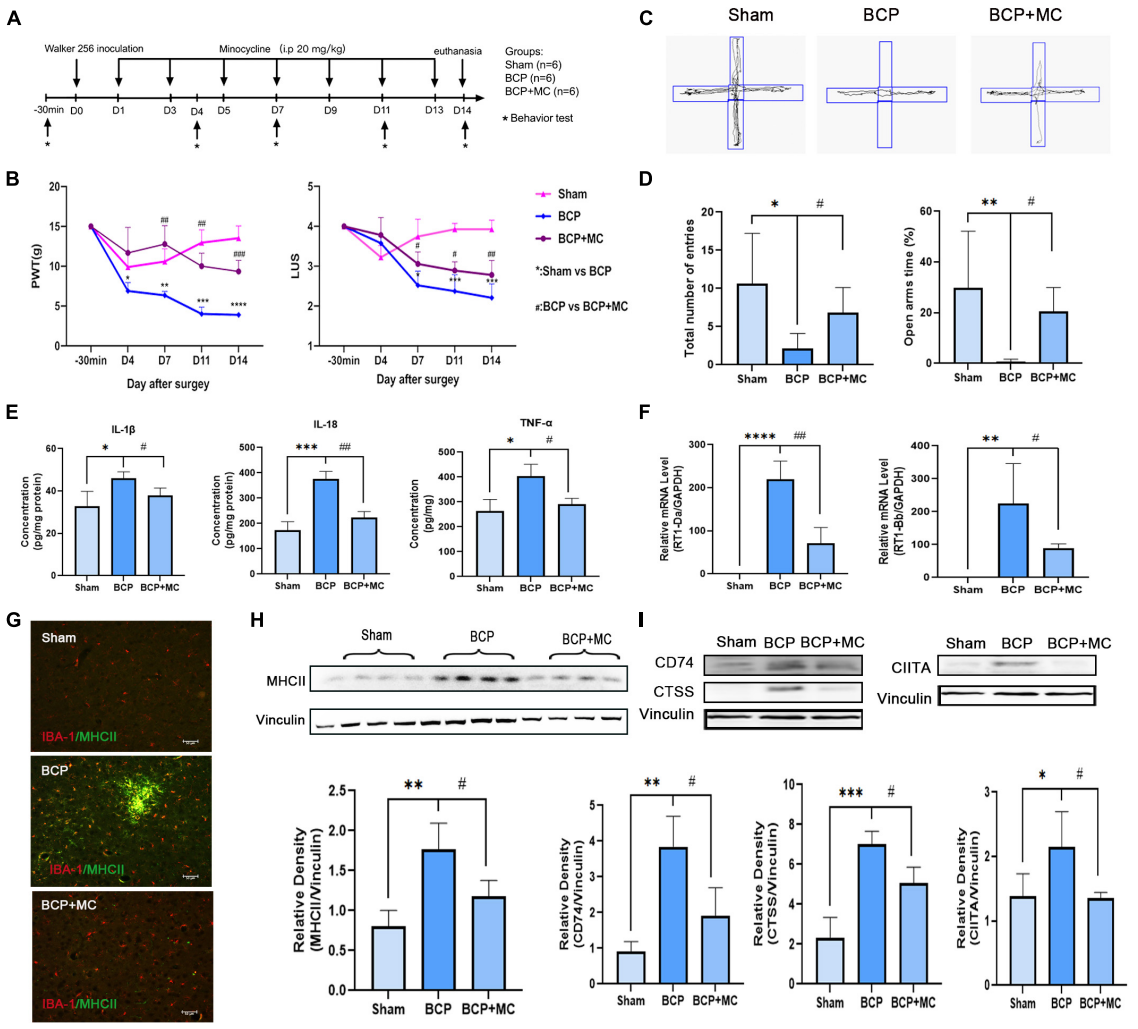

FIGURE 6
The inhibition of activation of microglia administrated relieved hyperalgesia and pain-related anxiety at D14. **(A)** Experimental timeline showing injection of minocycline (20 mg/kg, i.p.) every other day from D1. **(B)** Both PWT (left) and LUS (right) of BCP rats were elevated by minocycline **(C,D)**. Total number of entries and times in open arms reduced in the BCP rats reversed after the treatment of minocycline. **(E)** The increased expression of proinflammatory cytokines was downregulated in the BCP + MC group. **(F–I)** The upregulated expression of MHCII **(F–H)** and the related protein CIITA, CTSS, and CD74 were both decreased in the BCP + MC group **(I)**. $^{*}p < 0.05$, $^{**}p < 0.01$, $^{***}p < 0.001$, $^{****}p < 0.0001$ vs. Sham group; $^{\#}p < 0.05$, $^{\#\#}p < 0.01$, $^{\#\#\#}p < 0.001$ vs. BCP group. Error bars are represented as mean ± SD, one-way analysis of variance (ANOVA) followed by Tukey's multiple comparison test, $n = 4$ per group.

MHC complex and antigen process in the mPFC of BCP rats. As previous research reported that infiltrated $CD4^{+}$T lymphocytes might interact with MHCII-presented antigen in the spinal cord and contribute to BCP (Song et al., 2017). As such, our study proposed that MHCII in the mPFC may exert a crucial role in the process of BCP. Besides, KEGG enrichment also displayed that 32 genes were involved in the top three pathways: Phagosome, Staphylococcus aureus infection, Antigen processing, and presentation. Further, MHCII was involved in all three pathways, indicating MHCII in the mPFC plays an important role in the occurrence of BCP.

In line with the literature, MHCII has been shown to participate in the occurrence of different chronic pain (Dominguez et al., 2008a,b; Liu et al., 2012; Hartlehnert et al., 2017; Dorsey et al., 2019). In the present study, the expression of MHCII was upregulated in the mPFC of BCP rats, confirming the key role of MHCII. To further investigate the function of MHCII in the process of BCP, we found that MHCII was located in the activated microglia which is the main antigen-presenting cells population in the central nervous system. Although some studies have shown that activated microglia in the spinal cord and hippocampus may modulate BCP in rats' model (Dai et al., 2019; Diaz-delCastillo et al., 2020), there are no typical markers indicating the types of microglia involved in pain. In our study, we found that inhibition of the activation of microglia by MC could relieve BCP as well

as pain-related anxiety. It is worth noting that the upregulated expression of MHCII could be reversed by the treatment of MC, as such, we speculated that microglia co-labeled with MHCII in the mPFC may participate in BCP. Since MC was administered systemically, its analgesic effect may partly due to inhibit microglia and MHCII in other areas of the nervous system, such as spinal cord. However, in this study, we found that MC inhibited microglia and MHCII activation in mPFC, suggesting that at least mPFC play a role in analgesia. To further investigate this mechanism, our future study may focus on mPFC in BCP rats.

In summary, by high-throughput sequencing of the transcriptome, we found 147 DEmRNAs (136 upregulated and 11 downregulated) in the mPFC of BCP rats established by implantation of Walker 256 carcinoma cells into the right tibia. MHCII exerts a crucial role in the transcription analysis and our research supposed that MHCII in the mPFC may be a biomarker for microglia activation to participate in antigen processing and further promote BCP. These findings shed new light on the mechanisms of BCP and open a new venue for designing treatment plans to alleviate BCP in patients with advanced cancer, and additional tests are necessary to provide a more comprehensive picture.

Data availability statement

The original contributions presented in this study are publicly available. This data can be found here: https://www.ncbi.nlm.nih.gov/, PRJNA876307.

Ethics statement

This animal study was reviewed and approved by the Animal Care and Use Committee of Shanghai Chest Hospital, Shanghai Jiao Tong University [permission no. KS (Y)20170] and carried out in accordance with the guidelines of the International Association for the Study of Pain.

Author contributions

JW and XY designed the study. XL, WW, XZ, ZG, MT, and YZ performed the experiments. ZG, XZ, MT, and XY analyzed the data. XL and WW wrote the manuscript. All authors reviewed and approved the manuscript.

Funding

This work was supported by the National Natural Science Foundation of China (82071233), the Shanghai Sailing Program (21YF1442900), and the Nurture projects for basic research of Shanghai Chest Hospital (2019YNJCM08) and (2020YNJCQ13).

Acknowledgments

We thank Mr. Wang Kai of the Central Laboratory of Shanghai Chest Hospital for his help in animal feeding and model establishment and Mr. Yang Xiaohua of Shanghai Chest Hospital for his help in the preparation of brain slices.

Conflict of interest

The authors declare that the research was conducted in the absence of any commercial or financial relationships that could be construed as a potential conflict of interest.

The reviewer Y-QW declared a shared affiliation with the author MT to the handling editor at the time of review.

Publisher's note

Supplementary material

The Supplementary Material for this article can be found online at: https://www.frontiersin.org/articles/10.3389/fnmol.2022.1026593/full#supplementary-material

SUPPLEMENTARY FIGURE 1
The expression level of upregulated mRNAs (RT1-Bb and CTSS) in the mPFC of BCP rats. Data are expressed as mean ± SD and statistically analyzed by Student's *T*-test. $n = 5$ per group. $^{*}p < 0.05$, $^{**}p < 0.01$ vs. Sham group.

SUPPLEMENTARY TABLE 1
The primer sequences are listed in the **Supplementary Table 1**.

SUPPLEMENTARY TABLE 2
A total of 20,258 genes were detected in the mPFC between Sham and BCP rats, each group with $n = 5$.

SUPPLEMENTARY TABLE 3
The count and fold change of the 147 DEmRNAs in the mPFC between Sham and BCP rats.

SUPPLEMENTARY TABLE 4
The details of the interactions between the 147 DEmRNA-coding proteins.

References

Almolda, B., Gonzalez, B., and Castellano, B. (2011). Antigen presentation in EAE: Role of microglia, macrophages and dendritic cells. *Front. Biosci. (Landmark Ed)* 16, 1157–1171. doi: 10.2741/3781

Alvarado, S., Tajerian, M., Millecamps, M., Suderman, M., Stone, L. S., and Szyf, M. (2013). Peripheral nerve injury is accompanied by chronic transcriptome-wide changes in the mouse prefrontal cortex. *Mol. Pain* 9:21. doi: 10.1186/1744-8069-9-21

Blaszczyk, L., Maître, M., Lesté-Lasserre, T., Clark, S., Cota, D., Oliet, S. H. R., et al. (2018). Sequential alteration of microglia and astrocytes in the rat thalamus following spinal nerve ligation. *J. Neuroinflammation* 15:349. doi: 10.1186/s12974-018-1378-z

Brigatte, P., Sampaio, S. C., Gutierrez, V. P., Guerra, J. L., Sinhorini, I. L., Curi, R., et al. (2007). Walker 256 tumor-bearing rats as a model to study cancer pain. *J. Pain* 8, 412–421. doi: 10.1016/j.jpain.2006.11.006

Cai, G., Zhu, Y., Zhao, Y., Chen, J., Guo, C., Wu, F., et al. (2020). Network analysis of miRNA and mRNA changes in the prelimbic cortex of rats with chronic neuropathic pain: Pointing to inflammation. *Front. Genet.* 11:612. doi: 10.3389/fgene.2020.00612

Clézardin, P., Coleman, R., Puppo, M., Ottewell, P., Bonnelye, E., Paycha, F., et al. (2021). Bone metastasis: Mechanisms, therapies, and biomarkers. *Physiol. Rev.* 101, 797–855.

Dai, J., Ding, Z., Zhang, J., Xu, W., Guo, Q., Zou, W., et al. (2019). Minocycline relieves depressive-like behaviors in rats with bone cancer pain by inhibiting microglia activation in hippocampus. *Anesth. Analg.* 129, 1733–1741. doi: 10.1213/ANE.0000000000004063

Dai, W., Huang, S., Luo, Y., Cheng, X., Xia, P., Yang, M., et al. (2022). Sex-specific transcriptomic signatures in brain regions critical for neuropathic pain-induced depression. *Front. Mol. Neurosci.* 15:886916. doi: 10.3389/fnmol.2022.886916

Dasgupta, S., and Dasgupta, S. (2017). Antigen presentation for priming T cells in central system. *Int. J. Biochem. Cell Biol.* 82, 41–48.

Diaz-delCastillo, M., Hansen, R. B., Appel, C. K., Nielsen, L., Nielsen, S. N., Karyniotakis, K., et al. (2020). Modulation of rat cancer-induced bone pain is independent of spinal microglia activity. *Cancers (Basel)* 12:2740. doi: 10.3390/cancers12102740

Dominguez, C. A., Li, L., Lidman, O., Olsson, T., Wiesenfeld-Hallin, Z., Piehl, F., et al. (2008a). Both MHC and non-MHC genes regulate development of experimental neuropathic pain in rats. *Neurosci. Lett.* 442, 284–286. doi: 10.1016/j.neulet.2008.07.027

Dominguez, C. A., Lidman, O., Hao, J. X., Diez, M., Tuncel, J., Olsson, T., et al. (2008b). Genetic analysis of neuropathic pain-like behavior following peripheral nerve injury suggests a role of the major histocompatibility complex in development of allodynia. *Pain* 136, 313–319. doi: 10.1016/j.pain.2007.07.009

Dorsey, S. G., Renn, C. L., Griffioen, M., Lassiter, C. B., Zhu, S., Huot-Creasy, H., et al. (2019). Whole blood transcriptomic profiles can differentiate vulnerability to chronic low back pain. *PLoS One* 14:e0216539. doi: 10.1371/journal.pone.0216539

Du, Y., Xu, C. L., Yu, J., Liu, K., Lin, S. D., Hu, T. T., et al. (2022). HMGB1 in the mPFC governs comorbid anxiety in neuropathic pain. *J. Headache Pain* 23:102. doi: 10.1186/s10194-022-01475-z

Falk, S., and Dickenson, A. H. (2014). Pain and nociception: Mechanisms of cancer-induced bone pain. *J. Clin. Oncol.* 32, 1647–1654.

Fang, C., Zhong, H., Lin, Y., Chen, B., Han, M., Ren, H., et al. (2018). Assessment of the cPAS-based BGISEQ-500 platform for metagenomic sequencing. *Gigascience* 7, 1–8. doi: 10.1093/gigascience/gix133

Feller, L., Khammissa, R. A. G., Bouckaert, M., Ballyram, R., Jadwat, Y., and Lemmer, J. (2019). Pain: Persistent postsurgery and bone cancer-related pain. *J. Int. Med. Res.* 47, 528–543.

Fiore, N. T., and Austin, P. J. (2019). Peripheral nerve injury triggers neuroinflammation in the medial prefrontal cortex and ventral hippocampus in a subgroup of rats with coincident affective behavioural changes. *Neuroscience* 416, 147–167. doi: 10.1016/j.neuroscience.2019.08.005

Hartlehnert, M., Derksen, A., Hagenacker, T., Kindermann, D., Schäfers, M., Pawlak, M., et al. (2017). Schwann cells promote post-traumatic nerve inflammation and neuropathic pain through MHC class II. *Sci. Rep.* 7:12518. doi: 10.1038/s41598-017-12744-2

Hou, X., Weng, Y., Guo, Q., Ding, Z., Wang, J., Dai, J., et al. (2020). Transcriptomic analysis of long noncoding RNAs and mRNAs expression profiles in the spinal cord of bone cancer pain rats. *Mol. Brain* 13:47. doi: 10.1186/s13041-020-00589-2

Huang, S., Zhang, Z., Gambeta, E., Xu, S. C., Thomas, C., Godfrey, N., et al. (2020). Dopamine inputs from the ventral tegmental area into the medial prefrontal cortex modulate neuropathic pain-associated behaviors in mice. *Cell Rep.* 31:107812.

Ji, R. R., Chamessian, A., and Zhang, Y. Q. (2016). Pain regulation by non-neuronal cells and inflammation. *Science* 354, 572–577.

Kapoor, R., Saxena, A. K., Vasudev, P., Sundriyal, D., and Kumar, A. (2021). Cancer induced bone pain: Current management and future perspectives. *Med. Oncol.* 38:134.

Kummer, K. K., Mitrić, M., Kalpachidou, T., and Kress, M. (2020). The medial prefrontal cortex as a central hub for mental comorbidities associated with chronic pain. *Int. J. Mol. Sci.* 21:3440. doi: 10.3390/ijms21103440

Liu, H., Shiryaev, S. A., Chernov, A. V., Kim, Y., Shubayev, I., Remacle, A. G., et al. (2012). Immunodominant fragments of myelin basic protein initiate T cell-dependent pain. *J. Neuroinflammation* 9:119. doi: 10.1186/1742-2094-9-119

Liu, P., Wang, G., Zeng, F., Liu, Y., Fan, Y., Wei, Y., et al. (2018). Abnormal brain structure implicated in patients with functional dyspepsia. *Brain Imaging Behav.* 12, 459–466.

Liu, X., Xie, Z., Li, S., He, J., Cao, S., and Xiao, Z. (2021). PRG-1 relieves pain and depressive-like behaviors in rats of bone cancer pain by regulation of dendritic spine in hippocampus. *Int. J. Biol. Sci.* 17, 4005–4020. doi: 10.7150/ijbs.59032

Mantyh, P. (2013). Bone cancer pain: Causes, consequences, and therapeutic opportunities. *Pain* 154(Suppl. 1), S54–S62.

Masukawa, M. Y., Correa-Netto, N. F., Silva-Gomes, A. M., Linardi, A., and Santos-Junior, J. G. (2020). Anxiety-like behavior in acute and protracted withdrawal after morphine-induced locomotor sensitization in C57BL/6 male mice: The role of context. *Pharmacol. Biochem. Behav.* 194:172941. doi: 10.1016/j.pbb.2020.172941

Mecca, C. M., Chao, D., Yu, G., Feng, Y., Segel, I., Zhang, Z., et al. (2021). Dynamic change of endocannabinoid signaling in the medial prefrontal cortex controls the development of depression after neuropathic pain. *J. Neurosci.* 41, 7492–7508. doi: 10.1523/JNEUROSCI.3135-20.2021

Meuser, T., Pietruck, C., Radbruch, L., Stute, P., Lehmann, K. A., and Grond, S. (2001). Symptoms during cancer pain treatment following WHO-guidelines: A longitudinal follow-up study of symptom prevalence, severity and etiology. *Pain* 93, 247–257. doi: 10.1016/S0304-3959(01)00324-4

Miller, K. D., Fidler-Benaoudia, M., Keegan, T. H., Hipp, H. S., Jemal, A., and Siegel, R. L. (2020). Cancer statistics for adolescents and young adults, 2020. *CA Cancer J. Clin.* 70, 443–459. doi: 10.3322/caac.21637

Nashed, M. G., Seidlitz, E. P., Frey, B. N., and Singh, G. (2015). Depressive-like behaviours and decreased dendritic branching in the medial prefrontal cortex of mice with tumors: A novel validated model of cancer-induced depression. *Behav. Brain Res.* 294, 25–35. doi: 10.1016/j.bbr.2015.07.040

Obermann, M., Rodriguez-Raecke, R., Naegel, S., Holle, D., Mueller, D., Yoon, M. S., et al. (2013). Gray matter volume reduction reflects chronic pain in trigeminal neuralgia. *Neuroimage* 74, 352–358. doi: 10.1016/j.neuroimage.2013.02.029

Ong, W. Y., Stohler, C. S., and Herr, D. R. (2019). Role of the prefrontal cortex in pain processing. *Mol. Neurobiol.* 56, 1137–1166.

Palmisano, M., Caputi, F. F., Mercatelli, D., Romualdi, P., and Candeletti, S. (2019). Dynorphinergic system alterations in the corticostriatal circuitry of neuropathic mice support its role in the negative affective component of pain. *Genes Brain Behav.* 18:e12467. doi: 10.1111/gbb.12467

Qian, Y., Wang, Z., Zhou, S., Zhao, W., Yin, C., Cao, J., et al. (2020). MKP1 in the medial prefrontal cortex modulates chronic neuropathic pain via regulation of p38 and JNK1/2. *Int. J. Neurosci.* 130, 643–652. doi: 10.1080/00207454.2019.1667785

Remeniuk, B., Sukhtankar, D., Okun, A., Navratilova, E., Xie, J. Y., King, T., et al. (2015). Behavioral and neurochemical analysis of ongoing bone cancer pain in rats. *Pain* 156, 1864–1873. doi: 10.1097/j.pain.0000000000000218

Salomons, T. V., Nusslock, R., Detloff, A., Johnstone, T., and Davidson, R. J. (2015). Neural emotion regulation circuitry underlying anxiolytic effects of perceived control over pain. *J. Cogn. Neurosci.* 27, 222–233. doi: 10.1162/jocn_a_00702

Sang, K., Bao, C., Xin, Y., Hu, S., Gao, X., Wang, Y., et al. (2018). Plastic change of prefrontal cortex mediates anxiety-like behaviors associated with chronic pain in neuropathic rats. *Mol. Pain* 14:1744806918783931. doi: 10.1177/1744806918783931

Shiers, S., and Price, T. J. (2020). Molecular, circuit, and anatomical changes in the prefrontal cortex in chronic pain. *Pain* 161, 1726–1729. doi: 10.1097/j.pain.0000000000001897

Song, Z., Xiong, B., Zheng, H., Manyande, A., Guan, X., Cao, F., et al. (2017). STAT1 as a downstream mediator of ERK signaling contributes to bone cancer pain by regulating MHC II expression in spinal microglia. *Brain Behav. Immun.* 60, 161–173. doi: 10.1016/j.bbi.2016.10.009

Tajerian, M., Alvarado, S., Millecamps, M., Vachon, P., Crosby, C., Bushnell, M. C., et al. (2013). Peripheral nerve injury is associated with chronic, reversible changes in global DNA methylation in the mouse prefrontal cortex. *PLoS One* 8:e55259. doi: 10.1371/journal.pone.0055259

Topham, L., Gregoire, S., Kang, H., Salmon-Divon, M., Lax, E., Millecamps, M., et al. (2020). The transition from acute to chronic pain: Dynamic epigenetic reprogramming of the mouse prefrontal cortex up to 1 year after nerve injury. *Pain* 161, 2394–2409. doi: 10.1097/j.pain.0000000000001917

Totsch, S. K., and Sorge, R. E. (2017). Immune system involvement in specific pain conditions. *Mol. Pain* 13:1744806917724559.

Wang, W., Jiang, Q., Wu, J., Tang, W., and Xu, M. (2019). Upregulation of bone morphogenetic protein 2 (Bmp2) in dorsal root ganglion in a rat model of bone cancer pain. *Mol. Pain* 15:1744806918824250. doi: 10.1177/1744806918824250

Wu, S., Chen, X., Huang, F., Lin, M., Chen, P., Wan, H., et al. (2021). Transcriptomic analysis of long noncoding RNA and mRNA expression profiles in the amygdala of rats with bone cancer pain-depression comorbidity. *Life (Basel)* 11:834. doi: 10.3390/life11080834

Yan, X. T., Xu, Y., Cheng, X. L., He, X. H., Wang, Y., Zheng, W. Z., et al. (2019). SP1. MYC, CTNNB1, CREB1, JUN genes as potential therapy targets for neuropathic pain of brain. *J. Cell Physiol.* 234, 6688–6695. doi: 10.1002/jcp.27413

Yin, M., Chu, S., Shan, T., Zha, L., and Peng, H. (2021). Full-length transcriptome sequences by a combination of sequencing platforms applied to isoflavonoid and triterpenoid saponin biosynthesis of *Astragalus mongholicus* bunge. *Plant Methods* 17:61. doi: 10.1186/s13007-021-00762-1

Zajączkowska, R., Kocot-Kępska, M., Leppert, W., and Wordliczek, J. (2019). Bone pain in cancer patients: Mechanisms and current treatment. *Int. J. Mol. Sci.* 20:6047.

frontiers | Frontiers in Molecular Neuroscience

TYPE Original Research
PUBLISHED 07 December 2022
DOI 10.3389/fnmol.2022.1083671

OPEN ACCESS

EDITED BY
Xin Zhang,
Duke University,
United States

REVIEWED BY
Chun Yang,
Nanjing Medical University,
China
Mu Huo Ji,
Nanjing Medical University,
China
Jian-Jun Yang,
Zhengzhou University,
China

*CORRESPONDENCE
Jun-Li Cao
caojl0310@aliyun.com

†These authors have contributed equally to this work

SPECIALTY SECTION
This article was submitted to Pain Mechanisms and Modulators, a section of the journal Frontiers in Molecular Neuroscience

RECEIVED 29 October 2022
ACCEPTED 21 November 2022
PUBLISHED 07 December 2022

CITATION
Abdul M, Yan H-Q, Zhao W-N, Lyu X-B, Xu Z, Yu X-L, Gao Y-H and Cao J-L (2022) VTA-NAc glutaminergic projection involves in the regulation of pain and pain-related anxiety.
Front. Mol. Neurosci. 15:1083671.
doi: 10.3389/fnmol.2022.1083671

VTA-NAc glutaminergic projection involves in the regulation of pain and pain-related anxiety

Mannan Abdul[1,2,3,4†], Hao-Qi Yan[1†], Wei-Nan Zhao[1†], Xiao-Bin Lyu[1], Zheng Xu[1,2], Xiao-Lu Yu[1,2], Yi-Hong Gao[1] and Jun-Li Cao[1,2,3,4*]

[1]Jiangsu Province Key Laboratory of Anesthesiology, Xuzhou Medical University, Xuzhou, China, [2]Jiangsu Province Key Laboratory of Anesthesia and Analgesia Application Technology, Xuzhou Medical University, Xuzhou, China, [3]NMPA Key Laboratory for Research and Evaluation of Narcotic and Psychotropic Drugs, Xuzhou Medical University, Xuzhou, China, [4]Department of Anesthesiology, The Affiliated Hospital of Xuzhou Medical University, Xuzhou, China

Background: Besides the established role of dopamine neurons and projections in nociceptive stimuli, the involvement of ventral tegmental area (VTA) glutamatergic projections to nucleus accumbens (NAc) in pain remains unknown. In the present study, we aimed to examine the role of VTA glutamatergic projections to NAc in painful stimuli and its related behavioral changes.

Methods: Unilateral chronic constrictive injury (CCI) of sciatic nerve or intraplantar hind paw injections (i.pl.) of complete Freund's adjuvant (CFA) were used to develop pathological pain models in wild-type and VGluT2-Cre mice. The involvement of VTA glutamatergic neurons with projections to NAc in CCI-induced pain model was noted by c-Fos labeling and firing rate recordings. Pain response and pain-related behavior changes to the artificial manipulation of the VTA glutamatergic projections to NAc were observed by Hargreaves tests, von Frey tests, open field tests, elevated maze tests, and sucrose preference tests.

Results: Glutamatergic neurons in VTA had efferent inputs to shell area of the NAc. The CCI pain model significantly increased neuronal activity and firing rate in VTA glutamate neurons with projections to NAc. The photoinhibition of these glutamatergic projections relieved CCI-induced neuropathic pain and CFA-induced acute and chronic inflammatory pain. Moreover, pathological neuropathic pain-induced anxiety and less sucrose preference were also relieved by inhibiting the VTA glutamatergic projections to NAc.

Conclusion: Together, glutamatergic inputs from VTA to NAc contribute to chronic neuropathic and inflammatory pain and pain-related anxiety and depressive behaviors, providing a mechanism for developing novel therapeutic methods.

KEYWORDS

VTA, NAc, chronic pain, anxiety, glutamate

Introduction

Chronic pain is a hostile sensory and emotional experience related to established or potential tissue damage (Raja et al., 2020). Its negative affective states could also lead to adverse emotional conditions such as anhedonia, fear, anxiety, and depression (Markovic et al., 2021). Nevertheless, the mechanism of chronic pain involves neural complexity among many brain circuits.

Dopamine (DA) release from ventral tegmental area (VTA) neurons is known to provoke pain behavior persistence, stress, anxiety, and addiction (Trainor, 2011). In contrast to the well-studied and established functions of DA neurons, the functional role of VTA glutamate neurons is less studied. It could be due to the relatively small population of glutamate neurons in VTA compared to DA and GABA neurons (Holly and Miczek, 2016; Zhang et al., 2017; Adeniyi et al., 2020). Emerging studies have begun to reveal the reputation of glutamate release from VTA neurons in regulating diverse behavioral repertoire through a complex intra-VTA and long-range neuronal network. The VTA glutamate neurons send projections parallel with VTA DA neurons, such as the nucleus accumbens (NAc) and prefrontal cortex (PFC), and to regions with few VTA dopaminergic inputs, such as lateral habenula (LHb) and ventral pallidum (VP). Some studies reported the role of these glutamate projections in driving aversion and promoting wakefulness, etc. (Zell et al., 2020; Cai and Tong, 2022). Other data suggested that VTA glutamate neurons are more excitable than different types of neurons, as they exhibit increased overall firing to both fear-inducing context memories and increased response to behavioral avoidance, allodynia, and dysregulation of innate defensive behaviors in mice (Root et al., 2018; Barbano et al., 2020; Xia and Kheirbek, 2020). Thus, the VTA glutamatergic neurons may play an important role in pain behavior release.

As mentioned above, NAc is an important down steam nucleus of VTA, which is involved in mediating the reinforcing actions and responses to noxious stimuli. It is also considered that, following peripheral nerve injury, a cell-specific regulation in NAc worsens tactile allodynia (Ren et al., 2016). Besides, deep brain stimulation of the NAc has elicited successful analgesia by forwarding inhibitory projection to the medial thalamus (Strasser et al., 2019; Harris and Peng, 2020).

Even though VTA glutamate and its projections to NAc are being studied in some psychological changes, its role in chronic pain and related emotional behavior remains unclear. Thus, we speculated that VTA-NAc glutamatergic projection regulates pain and pain-related anxiety. In the present study, we investigated the role of VTA glutamatergic projections to NAc in nociceptive response and their related behavioral variations in acute and chronic pain states influenced by the chemogenetic and optogenetic manipulation of VTA-NAc glutamatergic-specific projections.

Materials and methods

Animals

Male C57BL/6J mice (Experimental Animal Center of the Xuzhou Medical University, China) and VGluT2-Cre mice (Jackson Lab, America) were used in the study (Male D1-Cre & D2-Cre mice from Jackson Lab, America, were used in the supplementary experiments). Mice (Maximum, 5 per cage) were housed in a vivarium (22°C–25°C) with free access to food and water under a light/dark cycle of 12 h. All the mice were randomly grouped and subjected to experiments during the light time of the cycle. All the investigators were blinded to experimental conditions during testing. All the experiments were permitted by the Animal Care and Use Committee of Xuzhou Medical University and performed following the Guide for the Care and Use of Laboratory Animals of the National Institutes of Health.

Adenovirus-associated virus vectors

Adenovirus-associated virus (AAV) vectors purchased from Brain VTA were: rAAV-CaMKIIa-CRE-WPRE-hGH PA AAV2/R; rAAV-Ef1α-DIO-EYFP-WPRE pA; rAAV-Ef1α-DIO-eNpHR3.0-EYFP-WPRE pA; rAAV-EF1α-DIO-hChR2(H134R)-EYFP-WPRE-hGH pA; and rAAV-Ef1α-DIO-hM4D (Gi)-EYFP-WPREs AAV2/R. The virus vectors were of the same batch and title for one complete experiment.

Stereotaxic surgery and microinjection

Mice were primarily anesthetized with sodium pentobarbital (40 mg/kg, i.p.) and fixed on the small animal stereotaxic apparatus (RWD). After the initial disinfection, the scalp skin was cut to expose the skull's cranium; 3% hydrogen peroxide was applied to remove the periosteum on the incisional area, and the residual was washed off with the application of normal saline. For the microinjection, the AAV vectors of 200–300 nl volume were injected into the VTA of wild-type mice (AP: 1.05 mm; ML: ±3.20 mm; DV: −4.6 mm; 7° angle) and VTA of VGluT2-Cre mice (AP: 0.4 mm; ML: ±3.10 mm; DV: −4.6 mm) and NAc of wild-type/VGluT2-Cre mice (AP: 1.1 mm; ML: ±0.87 mm; DV: −4.67 mm) by a Hamilton syringe needle, United States (33 gauge) at a rate of 0.1 ml/min, followed by a 10 min pause to minimize backflow. Erythromycin ointment was applied to the wounded site to avoid infection. The ceramic fiber-optic cannulas were implanted bilaterally above the NAc (AP: 1.5 mm; ML: ±1.5 mm; DV: −4.67 mm; 10° angle) and VTA (AP: 1.05 mm; ML: ±3.05 mm; DV: −4.6 mm; 7° angle) of wild-type and VGluT2-Cre mice through the dental cement. Lastly, the mice were placed in sterilized cages with a heating cushion underneath, and these mice were returned to their respective cages on gaining consciousness from anesthesia.

Pain models

Chronic constriction injury of the sciatic nerve

Chronic Constriction Injury of the Sciatic Nerve (CCI) was performed to establish the neuropathic pain model as previously reported (Medeiros et al., 2021). Mice were anesthetized with sodium pentobarbital (40 mg/kg, i.p.). After fur removal and disinfecting of the surgical area, blunt dissection was made to expose the sciatic nerve at the mid-thigh level. Three nonabsorbable 4–0 silks were lightly tied around the sciatic nerve at intervals of 1.0 mm. sham surgery was done without such constrictive ligation as control. After suturing, erythromycin ointment was applied locally on the wound opening. Lastly, the mice were placed in sterilized cages with a heating cushion underneath, and these mice were returned to their respective cages on gaining consciousness from anesthesia.

Intraplantar complete Freund's adjuvant

Complete Freund's adjuvant (CFA) was injected to establish the inflammatory pain model, as previously reported (Larson et al., 1986). Mice were injected subcutaneously with CFA (10 µl, Beyotime China # P2036) into the plantar surface of the left hind paw plantar (i.pl.) with a 20-gauge micro-injector. Controls were injected with 10 µl saline at the same site of the hind paw.

Optogenetic stimulation

For optogenetic manipulations, optical fibers in VTA or NAc were connected to a combined laser generator and stimulator (Newdoon, Hangzhou, China), which was used to generate a 594 nm wavelength of the yellow laser, or a 473 nm of a blue laser, with specific output patterns as described in the figures. The three-time periods were selected for "Pre" (baseline observations), "Light" (manipulation through the laser stimulus at 3 h after the baseline readings were observed), and "Post" (4 h post the light stimulus).

Behavioral tests

Paw withdrawal latency

Paw withdrawal latencies (PWLs) were measured using the Hargreaves test (Hargreaves et al., 1988) with the IITC plantar analgesia meter (IITC Life Science). In a quiet environment, these mice were placed in polyethylene cages separately on a glass platform and allowed to accommodate the apparatus for 1–2 h. A radiant heat source beneath the glass was used to stimulate the plantar surface of the hind paw. Before testing, heat intensity was adjusted to produce a baseline of 10–15 s. A cutoff time was set at 25 s to prevent tissue damage. Flinching, flicking, and trembling were considered positive responses. The measurements were triplicated at 10 min intervals, and the mean was calculated as the PWL.

50% paw withdrawal threshold

For the estimation of 50% paw withdrawal threshold (50% PWT), the up- and down-method with von Frey filaments was used. In brief, mice were placed in polyethylene cages separately on an elevated metallic wire mesh platform. Before testing, mice were allowed to acclimatize to the environment for 1–2 h. Testing started with the midrange filament of 0.16 g strength. Subsequent filaments were proceeded according to the up-down method, and 5 consecutive touches were applied at 5 min intervals for rest. The filaments were pressed against the plantar surface and held for 3 s. Positive responses were noted when mice withdrew their hind paw during this time. Finally, 50% PWTs were calculated as described in the previous study (Bonin et al., 2014).

Open field test

Open field test (OFT) was conducted with a white plastic open field apparatus (40 cm × 40 cm). This field was artificially divided into a 20 cm × 20 cm center zone and a rest peripheral zone. After sterilization with 75% alcohol, mice were put into the center zone and allowed to travel freely within 10 min. The ANY-maze tracking system recorded the traveling trace, the number of entries into the center zone, and the time spent in the center zone for each mouse.

Elevated plus maze

An elevated apparatus with a digital camera was used to perform the EPM test. The maze, 70 cm above the floor, consists of two open arms (30 cm × 5 cm) and two closed arms (30 cm × 5 cm) with 15 cm high opaque walls. When testing, mice were placed in the center area facing an open arm and allowed to travel freely for 5 min. The traveling trace, number of entries into the open arms, and time spent in the open arms for each mouse were recorded by the ANY maze tracking system.

Sucrose preference test

Mice were singly housed in two identical leak-resistant bottles containing tap water for 3 days before testing. On testing day, mice first underwent water restriction for 8 h. They were given two identical leak-resistant bottles containing tap water solutions and 1% sucrose solutions. The two bottles of each mouse were exchanged every 6 h. To facilitate the Clozapine-N-oxide (CNO) delivery, the mice were placed under an inverted light/dark cycle, where light onset occurs in the evening. As invasive injections of CNO can manipulate the results, we used the oral route by first dissolving Clozapine-N-oxide (CNO, 5 mg) in 1 ml of 0.9% sterile saline solution and refrigerating the stock solution at 4°C. On test day, we filled the bottles with 10 ml of water +1% sucrose + CNO (1 mg/kg) and 10 ml of water + CNO (1 mg/kg) for the subjected mice, and the control group was placed without the presence of CNO, but with 0.9% sterile saline (1 ml/kg), we noted both the preference in 24 h cycle as reported (Zhan et al., 2019). Following the testing, the percentage of sucrose solution intake was calculated to reflect the sucrose preference.

Immunohistology and confocal imaging

With deep anesthesia by sodium pentobarbital (40 mg/kg, i.p.), mice were subjected to intracardial perfusion with 40 ml PBS, pH 7.4, and 20 ml 4% PFA. Later, the brain samples were extracted and postfixed in 4% PFA at 4°C for 6–8 h, then kept in 30% sucrose solution for 48 h. Coronal brain sections (40 mm thick) were prepared by a frozen-section microtome (VT1000S, Leica Microsystems). The brain sections with fluorescent protein expression were directly covered, slipped in a mounting medium, and envisioned by a laser scanning confocal microscope (LSM 880, Carl Zeiss). For the desired immunofluorescent staining, all the sections were washed in PBS for 15 min, incubated with an antigen retrieval solution (P0090, Biyuntian) for 5 min, and subsequentially blocked for a nominated period of 1 h with a PBS solution containing 1% BSA and 0.25% Triton X-100. According to the experimental needs of the respected protocols, the sections were incubated with the primary antibodies overnight, including mouse rabbit anti-c-Fos (1:500, 2,250, Cell Signaling Technology). After being washed in PBS for 15 min, the sections were tagged with secondary antibodies for 2 h, like anti-rabbit Alexa-594 (1:200, A21207, Thermo Fisher Scientific). As controls, adjacent sections were incubated without primary antibodies. Lastly, the sections were mounted onto glass slides; images were obtained using a confocal microscope (LSM 880, Carl Zeiss).

Electrophysiology

The brain was placed after the immediate decapitation at a high concentration of sucrose solution at −4°C, and the brain sheet containing 250 μm thick with VTA and NAc was cut with a vibrating slice. The ingredients of high sugar artificial cerebrospinal fluid are (mm): 254 Sucrose, 1.25 NaH_2PO_4, 10 D-Glucose, 24 $NaHCO_3$, 3 KCl, 2 $CaCl_2$, and 2 $MgSO_4$ (PH 7.35, 295–305 MOSM). The brain slice was placed in a 35°C artificial cerebrospinal fluid (ACSF) with 95% O_2 + 5% CO_2 mixture for 1 h, and after that, it was placed in 1.25 NaH_2PO_4, 10 D-Glucose, 24 $NaHCO_3$, 3 KCl, 2 $CaCl_2$, and 2 $MgSO_4$ (pH 7.35, 295–305 MOSM). After the glass microelectrode (3–5 mΩ) is sealed, the discharge frequency is recorded in the Cell-Attach recording mode. Filtering and collection of the MULTI CLAMP 700B diaphragm amplifier were performed, and light stimulation was given to validate the VTA glutamate neuron downstream toward the NAc for the optogenetic viral vector.

Statistical analysis

All experiments were replicated in 3–8 mice of each group with the same generation and age, with the data randomly collected and processed. Mice were excluded from data collection and analysis because of the following reasons: (a) because of off-target or poor expression for virus vectors; (b) because of health complications after surgical intervention (e.g., body weight drops 20% in a day) and experimental failures; (c) because of the mortality of mice. No data points were excluded after data acquisition was accomplished. Data were analyzed offline, and experimenters were not blinded to the experimental group during the analyses. All data were expressed as the mean ± SEM. The statistical graph plot and data calculation were performed with GraphPad Prism8. *Two-way ANOVA* with repeated measures followed by *Bonferroni post-tests* was used to compare the differences between the groups with multiple time points of "Pre," "Light" and "Post." *Unpaired sample t-tests* were performed in comparing the differences between two groups, *One-Way ANOVA* followed by the *Dunnett's post-tests* were used in comparing the differences between four groups. Statistical significance was defined as $p < 0.05$. Detailed descriptions can be found in the figure legends. The number of cells expressing c-Fos is compared by using Image-Pro. Plus (Version 6.0.260, Media Cybernetics, United States).

Results

CCI surgery increased the excitation level of the glutamatergic neurons projected from VTA to NAc

We targeted VTA-Glutamatergic neurons and their axons by injecting DIO-EYFP viral vector in the VTA of VGluT2-Cre mice (Figures 1A,B). We found that VTA glutamatergic projection to NAc was localized predominantly in the shell area, and sometimes these fibers are extended into the ventromedial shell and olfactory tubercle (Figure 1C). Then, c-Fos staining was also performed in the VGluT2-Cre mice to determine the neuronal activity in response to painful stimuli. VTA sections were prepared from sham or CCI mice on day 7 post-surgery. The staining results showed that CCI surgery resulted in an increased number of the c-Fos-positive cells in VTA, compared with their sham counterparts (Figures 1D,E). The population of glutamatergic neurons in VTA is reported to be less than other types of neurons like GABA and DA, and we only wanted these glutamatergic projections to be NAc-specific rather than VTA glutamatergic projection to other brain regions in VGluT2-Cre mice. We used the CaMKII tracing method in the wild-type mice because CaMKII was reported to colonize predominantly with the glutamate neurons (Zhu et al., 2014; Basting et al., 2018; Liu et al., 2020; Sheng et al., 2020; Zhang et al., 2020; Li et al., 2022). For this, a retrograde CaMKIIa-CRE viral vector was injected into the NAc, and DIO-EYFP was injected in the VTA of the wild-type mice (Figure 1F). Confocal imaging confirmed that somatic bodies of VTA glutamate neurons had axonal projections to NAc sections were prepared from sham or CCI mice on the day 7 post-surgery (Figure 1G). The firing rates of these VTA glutamatergic somatic bodies were recorded using MULTI CLAMP 700B diaphragm amplifier. We noted a significantly increased firing rate of the

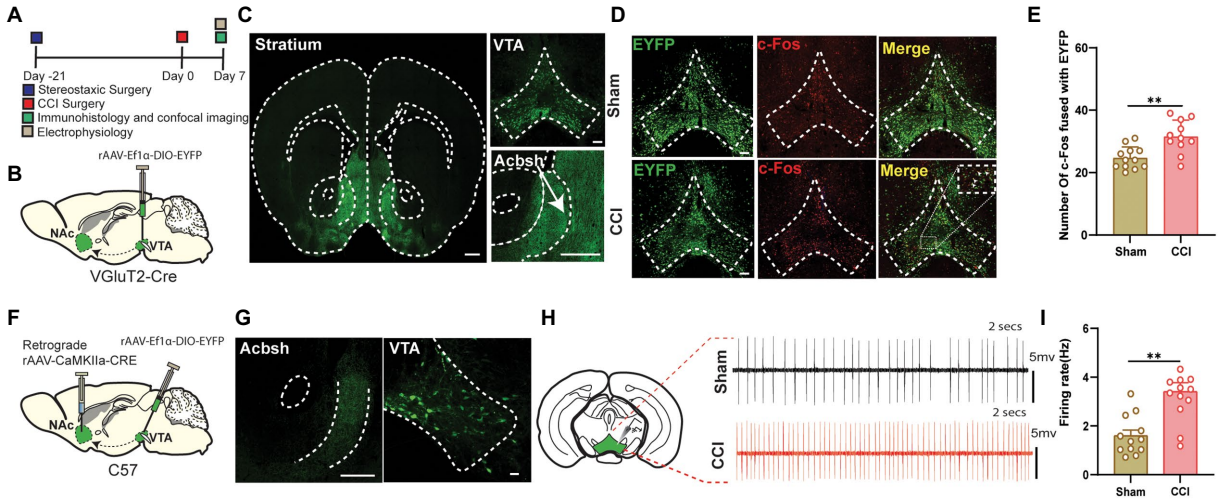

FIGURE 1
The neuropathic pain can induce hyperactivity in the VTA Glutamate neurons projecting to NAc. **(A)** Experimental timeline. For the immunohistological expression, the DIO-EYFP viral vector was injected in the VTA brain region and VGluT2-Cre mice were given 21days for the expression of the virus before the CCI surgery. The c-Fos labeling was performed on day 7 after the sham or CCI surgery (unilateral sciatic nerve ligation) in mice. **(B)** Schematic illustration depicting viral constructs and experimental surgery in VGluT2-Cre mice. **(C)** Confocal image of VTA somatic expression of DIO-EYFP (Scale bar=200μm) and VTA VGluT2 fibers projecting to NAc (Scale bar=500μm and Scale bar=200μm); these fibers are highly concentrated in NAc shell. **(D)** Representative confocal images of VTA glutamatergic somatic cell bodies infected by DIO-EYFP and stained with c-Fos of both sham (without nerve ligation) and CCI mice (unilateral sciatic nerve ligation); these images were demarcated as DIO-EYFP only, c-Fos labeled only and merged image of DIO-EYFP infected somatic bodies coupled with c-Fos protein. Scale bar=200μm. **(E)** Quantitative data regarding the comparison between c-Fos protein expression coupled with DIO-EYFP infected glutamatergic somatic cell bodies of VTA brain region in the sham group vs. CCI group of the VGluT2-Cre mice (n=12 slices/group from 3, 3 mice; $^{**}p<0.01$, unpaired-sample t-test). **(F)** Experimental timeline. For the immunohistological expression, retrograde CaMKIIa-CRE viral vector was injected in the NAc brain region, DIO-EYFP viral vector was injected in the VTA brain region, and wild-type mice were given 21days for the expression of the virus before the CCI surgery. The electrophysiological recordings for the firing rate were done on day 7 after the sham or CCI surgery (unilateral sciatic nerve ligation) in wild-type mice. **(G)** Confocal images showing virus expression in the VTA somatic body and NAc axon terminals in the brain region of wild-type mice infected by the viral vector of CaMKIIa-CRE and DIO-EYFP for the labeling of the glutamatergic projections. Scale bar=200μm and Scale bar=100μm. **(H)** Traces of firing activity of the glutamatergic somatic bodies of VTA (with axonal projections to NAc) in wild-type mice. **(I)** Quantitative data regarding the firing activity of glutamate neurons in VTA (with axonal projections to NAc) of sham and CCI groups (24 neurons from 6, 6 mice, $^{**}p< 0.01$, unpaired-sample t-test).

neurons in the CCI mice compared to its sham-controlled subjects (Figures 1H,I). The data indicate that the glutamatergic projections from VTA to NAc are involved in the chronic pain mechanism.

The photoinhibition of the glutamatergic neurons projected from VTA to NAc suppressed CCI-induced pain behavior

We wanted to investigate the pain-relieving effect of VTA glutamatergic projections to NAc in the CCI-induced neuropathic pain model of wild-type and VGluT2-Cre mice. First, we used two different methods for manipulating the VTA glutamatergic neurons with projections to NAc in wild-type mice. For the somatic inhibition in mice induced by the CCI surgery, A retrograde CaMKIIa-CRE virus was injected into NAc. DIO-EYFP-NpHR injection with optical fibers implantation was performed on the wild-type mice's VTA brain region. For the control groups, the DIO-EYFP was injected in the VTA without the presence of NpHR (Figure 2A). For terminal inhibition in mice induced by the CCI surgery, a retrograde CaMKIIa-CRE injection with optical fibers implantation was performed onto the NAc brain region, and DIO-EYFP-pHR was injected into VTA of the wild-type mice. For the control groups, the DIO-EYFP was injected in the VTA without the presence of NpHR. For terminal inhibition in wild-type naïve mice, a retrograde CaMKIIa-CRE injection with optical fibers implantation was performed onto the NAc brain region, and DIO-EYFP-NpHR was injected into VTA of the wild-type mice, For the control groups, the DIO-EYFP was injected in the VTA without the presence of NpHR. For terminal activation in wild-type naïve mice, a retrograde CaMKIIa-CRE injection with optical fibers implantation was performed onto the NAc brain region, and DIO-EYFP-ChR2 was injected into VTA of the wild-type mice, For the control groups, the DIO-EYFP was injected in the VTA without the presence of ChR2. Besides, electrophysiological stimulation was also done to verify the effective manipulation of the viral vector (Figures 2D,G). Confocal imaging was performed for the viral expression in VTA and NAc (Figures 2B,E). We noted that the mice had a pain-reducing effect through optogenetic inhibition of VTA glutamatergic projections to NAc in CCI mice infected with DIO-EYFP-NpHR compared to control groups (Figures 2C,F).

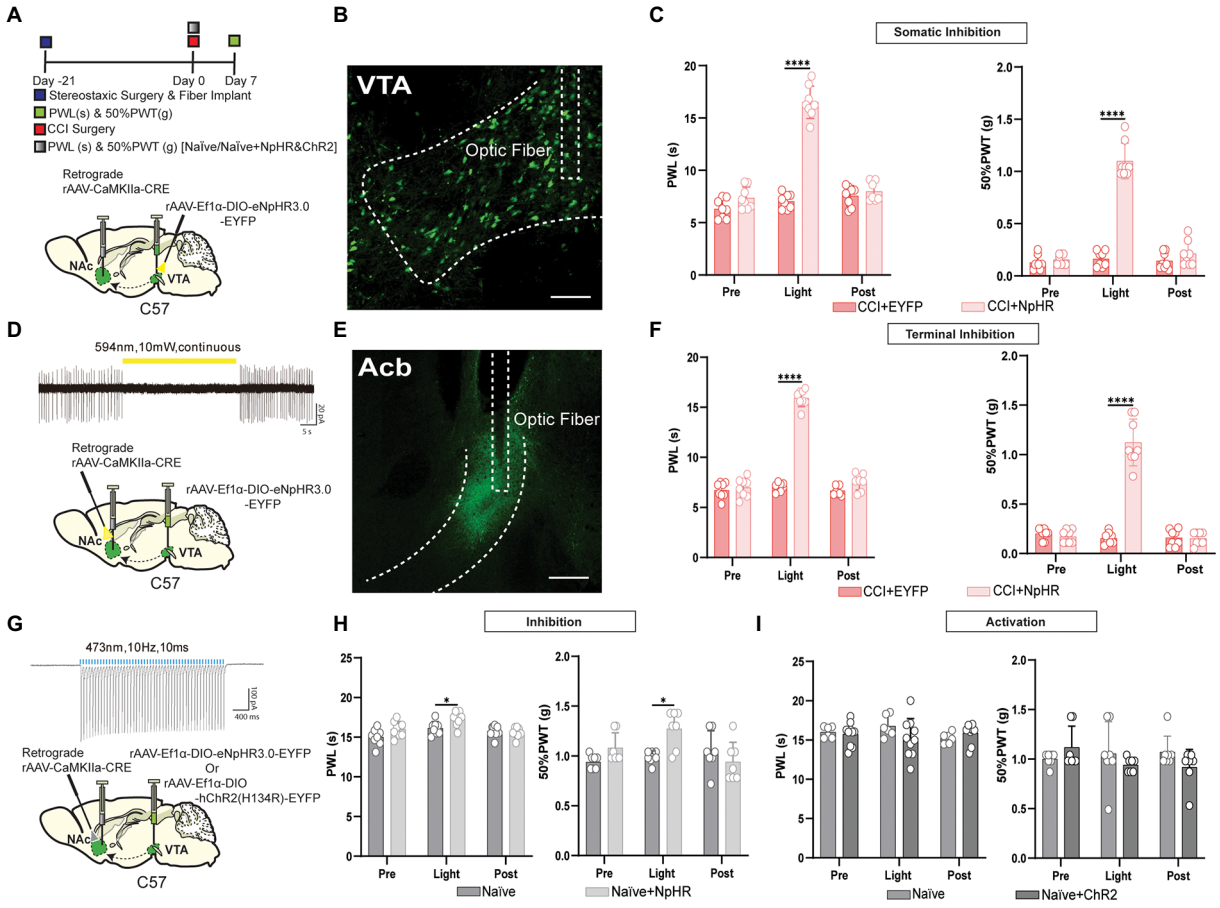

FIGURE 2
Inhibition of the glutamatergic neurons projected from VTA to NAc has relieved neuropathic pain in wild-type mice. **(A)** Experimental timeline. Schematic illustration depicting viral constructs. For the somatic stimulation, a retrograde CaMKIIa-CRE viral vector was injected in the NAc brain region and DIO-NpHR-EYFP injection with fiber implantation was performed on the VTA, wild-type mice were given 21days for the expression of the virus before the CCI surgery, PWLs and 50% PWTs of the hind paws were assessed on day 7 after CCI surgery in wild-type mice. **(B)** Representative confocal image for somatic virus expression in VTA of wild-type mice infected by the viral vector of CaMKIIa-CRE and DIO-NpHR-EYFP for labeling glutamatergic projections. Scale bar = 200μm. **(C)** The quantitative comparison of PWLs and 50% PWTs between the two groups (with and without light stimulation). Statistics show that PWLs of CCI+NpHR group exhibited a significant increase in withdrawal latency during the somatic light stimulation period [Light phase] compared with the CCI+EYFP group (n=8, 8 mice; ****p<0.0001), also 50% PWTs of CCI+NpHR group were also significantly increased during the somatic light stimulation [Light phase] compared with the CCI+EYFP group (n=8, 8 mice; ***p<0.001) of the wild-type mice. **(D)** 594nm yellow laser stimulation-induced inhibition of firing activity in VTA glutamatergic neuron expressing NpHR with axonal projections to NAc (10mW, continuous stimulation). For the terminal light stimulation, a retrograde CaMKIIa-CRE viral vector injection with fiber implantation was performed in the NAc brain region, and DIO-NpHR-EYFP was injected into the VTA, wild-type mice were given 21days for the expression of the virus before the CCI surgery, PWLs and 50% PWTs were assessed on day 7 after CCI surgery. **(E)** Confocal images showing virus expression NAc axon terminals in the brain region of wild-type mice infected by the viral vector of CaMKIIa-CRE and DIO-NpHR-EYFP for labeling glutamatergic projections. Scale bar = 200μm. **(F)** The quantitative comparison of PWLs and 50% PWTs between the two groups (with and without light stimulation). Statistics showing that CCI+NpHR group exhibited a significant increase in PWLs during the terminal light stimulation [Light phase] compared with the CCI+EYFP group (n=8, 8 mice; ****p<0.0001), 50% PWTs of CCI+NpHR group were also increased during the terminal light stimulation [Light phase] compared with the CCI+EYFP group (n=8, 8 mice; ***p<0.0001) in wild-type mice. **(G)** For the somatic activation of this pathway, a retrograde viral vector CaMKIIa-CRE viral vector were injected in the NAc brain region and DIO-ChR2-EYFP or DIO-NpHR-EYFP was injected in the VTA of naïve mice, 473nm blue laser stimulation-induced excitation of firing activity in VTA glutamatergic neuron expressing ChR2 with axonal projections to NAc brain region (473nm, 10Hz, 10ms; the validation of EYFP-NpHR viral was described previously for the somatic inhibition) and wild-type mice were given 21days for the expression of the virus. **(H)** The comparison of PWLs and 50% PWTs between the two groups (with and without light stimulation). Statistics showing that Naïve + NpHR group exhibited a less significant increase in PWLs during the somatic light stimulation [Light phase] compared with the naïve group (n=7, 7 mice; *p<0.05), 50% PWTs of the Naïve + NpHR group also exhibited a less significant increase by the somatic light stimulation [Light phase] compared with the naïve group (n=7, 7 mice; *p<0.05). **(I)** During the terminal activation, the quantitative comparison (with and without light stimulation) of PWLs and 50% PWTs between the two groups showed Naïve + NpHR group exhibited no significant difference in PWLs by the somatic stimulation compared with the naïve group (n=7, 7 mice; p>0.05), 50% PWTs of the Naïve+ChR2 group also exhibited no significance with the naïve group (n=7, 7 mice; p>0.05) of the wild-type mice (All the readings were measured during 3 consecutive periods, and all the comparisons were performed by the *two-way ANOVA test* followed by *Bonferroni post-test*).

In addition, this inhibitory effect of the VTA glutamatergic projections to NAc was bidirectional, as the somatic and terminal stimulation both induce the same pain-relieving effect of the neuropathic pain. The naïve mice with artificial inhibition of glutamatergic neurons projected from VTA to NAc showed less elevation in the pain intensity. Surprisingly, the activation of these neurons through DIO-ChR2-EYFP could not induce any change in the thermal and mechanical pain thresholds (Figures 2H,I). Although multiple types of VTA VGluT2 neurons may target the same output structure, it has so far been shown that VGluT2-only neurons project to the nucleus accumbens (Root et al., 2018). To further reveal this, we injected DIO-EYFP-NpHR in VTA, and the optical fibers were planted in the NAc brain region of VGluT2-Cre mice induced by the CCI surgery (Figure 3A). Similar to the results in wild-type mice, we found that optogenetic inhibition of specific VTA glutamate projections to NAc suppressed the thermal and mechanical pain threshold in CCI mice (Figures 3B,C). Besides, artificial activation through the DIO-ChR2 viral vector or inhibition through DIO-NpHR of these VTA-NAc glutamate projections did not affect the pain behavior in the naïve VGluT2-Cre mice (Figure 3D).

The photoinhibition of glutamatergic neurons projected from VTA to NAc suppressed CFA injection-induced acute and chronic inflammatory pain

Is the pain-reducing effect of suppressing VTA-NAc glutamatergic projection sustained in acute and chronic inflammatory pain? To answer this question, the short-term and long-term CFA injection-induced pain models were prepared as acute and chronic stages of pain reported previously (Ling et al., 2020). For the somatic stimulation in wild-type mice induced by the intraplantar hind paw injection of CFA, a retrograde CaMKIIa-CRE virus was injected into NAc, and DIO-EYFP-NpHR was injected with optical fiber implantation on VTA. For terminal stimulation in wild-type mice induced by the intraplantar hind paw injection of CFA, a retrograde CaMKIIa-CRE was injected with fiber implantation onto NAc, and DIO-EYFP-NpHR was injected into VTA (Figure 4A). The data showed that inhibiting VTA-NAc glutamatergic projection shows a decrease in pain intensity at 3 h and at 3 days after CFA injection (Figures 4B–E). For further confirmation, the VGluT2-Cre mice induced by intraplantar hind paw injection of CFA were

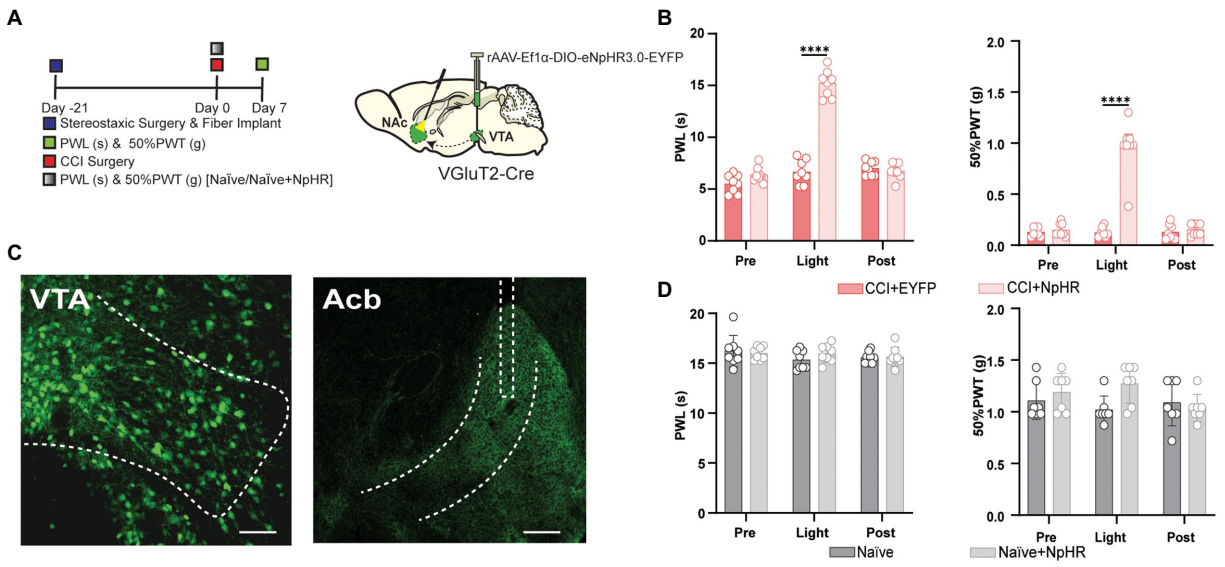

FIGURE 3
Inhibition of the glutamatergic neurons projected from VTA to NAc has relieved neuropathic pain in VGluT2-Cre mice. **(A)** Experimental timeline. Schematic illustration depicting viral constructs. For the terminal stimulation, DIO-NpHR-EYFP was injected in the VTA, the optical fiber was planted at the NAc in VGluT2-Cre mice, and mice were given 21days for the expression of the virus before the CCI surgery or before PWLs and 50% PWTs measurement in naïve mice. PWLs and 50% PWTs of the hind paws were assessed on day 7 after CCI surgery in VGluT2-Cre mice. **(B)** The quantitative comparison of PWLs and 50% PWTs between the two groups (with and without light stimulation). Statistics showing that CCI+NpHR group exhibited a significant increase in PWLs during the terminal light stimulation period [Light phase] compared with the CCI+EYFP group (n=8, 8 mice; ****p<0.0001), 50% PWTs of CCI+NpHR group were also significantly increased during the terminal light stimulation [Light phase] compared with the CCI+EYFP group (n=8, 8 mice; ***p<0.0001) in VGluT2-Cre mice. **(C)** Confocal images showing virus expression in the somatic bodies of VTA and terminal projection in NAc brain region of the VGluT2-Cre mice. Scale bar=200μm and scale bar=200μm. **(D)** The comparison of PWLs and 50% PWTs between the two groups of the naïve mice (with and without light stimulation), Statistics showing Naïve + NpHR group exhibited no significant difference in PWLs and 50% PWTs compared with the Naïve group (n=7, 7 mice; p>0.05) of the VGluT2-Cre mice (All the readings were measured during 3 consecutive periods and the comparisons were performed by the *two-way ANOVA test* followed by *Bonferroni post-test*).

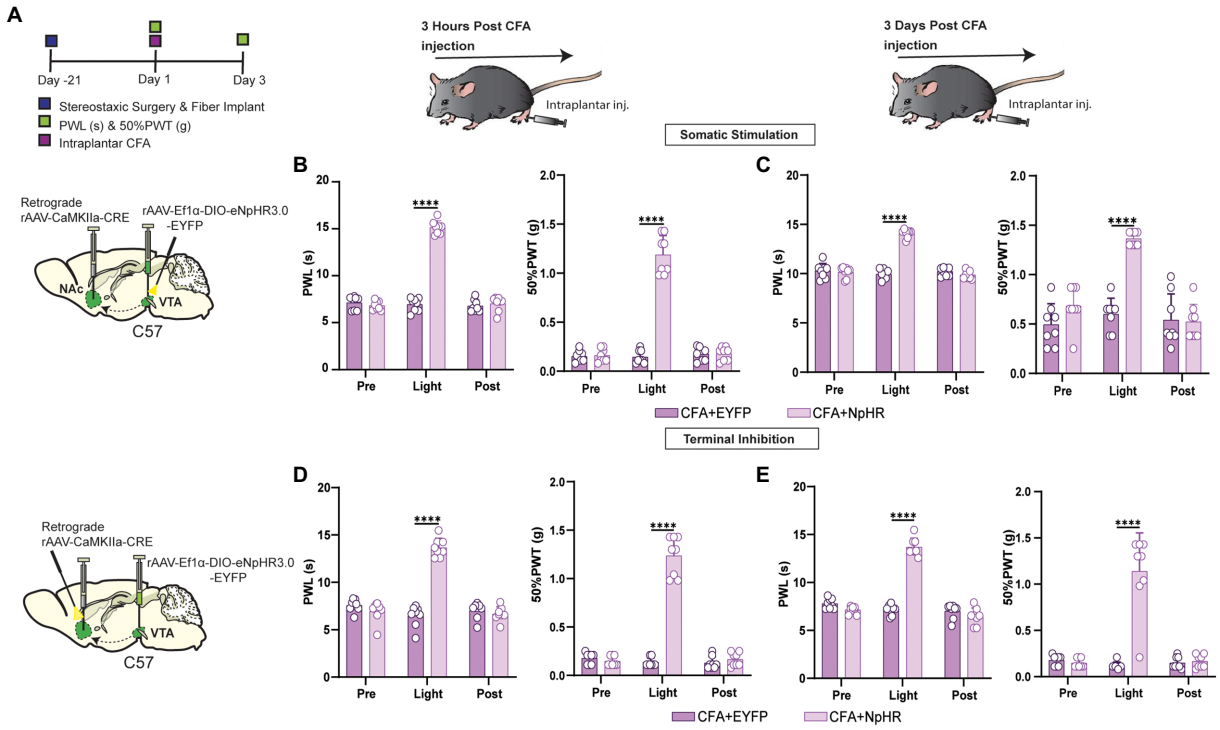

FIGURE 4
Inhibition of this pathway can affect both short-term and long-term inflammatory pain in wild-type mice. **(A)** Experimental timeline. Schematic illustration depicting viral constructs. For the somatic stimulation, a retrograde CaMKIIa-CRE viral vector was injected in the NAc brain region, and DIO-NpHR-EYFP injection with fiber implantation was performed on the VTA, and wild-type mice were given 21days for the expression of the virus before the ip.l. CFA injection. 50% PWTs and PWLs of the hind paws were assessed at 3h and day 3 after ip.l. CFA injection in wild-type mice. **(B)** The quantitative comparison of PWLs and 50% PWTs between the two groups (with and without light stimulation). Statistics show that PWLs of CFA+NpHR group exhibited a significant increase in withdrawal latency by the somatic light stimulation [Light phase] compared to the CFA+EYFP group (n=8, 8 mice ****p<0.0001), also 50% PWTs of CFA+NpHR group were significantly increased during the somatic light stimulation [Light phase] compared with the CFA+EYFP group (n=8, 8 mice; ***p<0.0001) of the wild-type mice after 3h of ip.l. CFA injection. **(C)** The quantitative comparison of PWLs and 50% PWTs between the two groups (with and without light stimulation). Statistics showing that PWLs of the CFA+NpHR group exhibited a significant increase in withdrawal latency during the somatic light stimulation [Light phase] compared with the CFA+EYFP group (n=8, 8 mice ****p<0.0001). Also, 50% PWTs of CFA+NpHR group were significantly increased during the somatic light stimulation [Light phase] compared with the CFA+EYFP group (n=8, 8 mice; ***p<0.0001) of the wild-type mice after 3days of ip.l. CFA injection. **(D)** For the terminal stimulation, a retrograde CaMKIIa-CRE viral vector injection with fiber implantation was performed on the NAc brain region, and DIO-NpHR-EYFP was injected in the VTA. PWLs and 50% PWTs of the hind paws were assessed at 3h and day 3 after ip.l. CFA injection in wild-type mice. The quantitative comparison (with and without light stimulation) of PWLs and 50% PWTs between the two groups. Statistics showing that PWLs of CFA+NpHR group exhibited a significant increase in withdrawal latency during the terminal light stimulation [Light phase] period compared with the CFA+EYFP group (n=8, 8 mice; ****p<0.0001). Also, 50% PWTs of CFA+NpHR group were significantly increased during the terminal light stimulation [Light phase] compared with the CFA+EYFP group (n=8, 8 mice; ****p<0.0001) of the wild-type mice after 3h of ip.l. CFA injection. **(E)** Statistics showing that PWLs of CFA+NpHR group exhibited a significant increase in withdrawal latency during the terminal light stimulation period [Light phase] compared with the CFA+EYFP group (n=8, 8 mice; ****p<0.0001). Also, 50% PWTs of CFA+NpHR group were significantly increased during the terminal light stimulation period [Light phase] compared with the CFA+EYFP group (n=8, 8 mice; ****p<0.0001) of the wild-type mice after 3days of ip.l. CFA injection (All the readings were measured during 3 consecutive periods, and the comparisons were performed by the *two-way ANOVA test* followed by *Bonferroni post-test*).

used. We injected DIO-EYFP-NpHR in VTA, and the optical fibers were planted on NAc in VGluT2-Cre mice (Figure 5A). Inhibiting VTA-NAc glutamatergic projection among VGluT2-Cre mice also showed a decrease in pain intensity at 3 h and at 3 days after CFA injection (Figures 5B,C). These data suggested that VTA glutamatergic projections to NAc are equally effective in both acute and chronic inflammatory pain states. In contrast, the optogenetic inhibition by DIO-EYFP-NpHR or activation by DIO-EYFP-ChR2 of VTA glutamatergic projections to NAc did not effect the pain state in VGluT2-Cre mice.

The inhibition of glutamatergic neurons projected from VTA to NAc released chronic pain-related anxiety

Previously researchers reported that animal subjects suffering from chronic pain could develop anxiety-like behavior (Li et al., 2014; Zhou et al., 2020; Liu et al., 2021). The open field and elevated maze tests (Murasawa et al., 2020) were used for testing anxiety 21 days after CCI or sham surgery. For the somatic stimulation in wild-type mice, a retrograde CaMKIIa-CRE virus was injected into NAc, and DIO-EYFP-NpHR injection with fiber

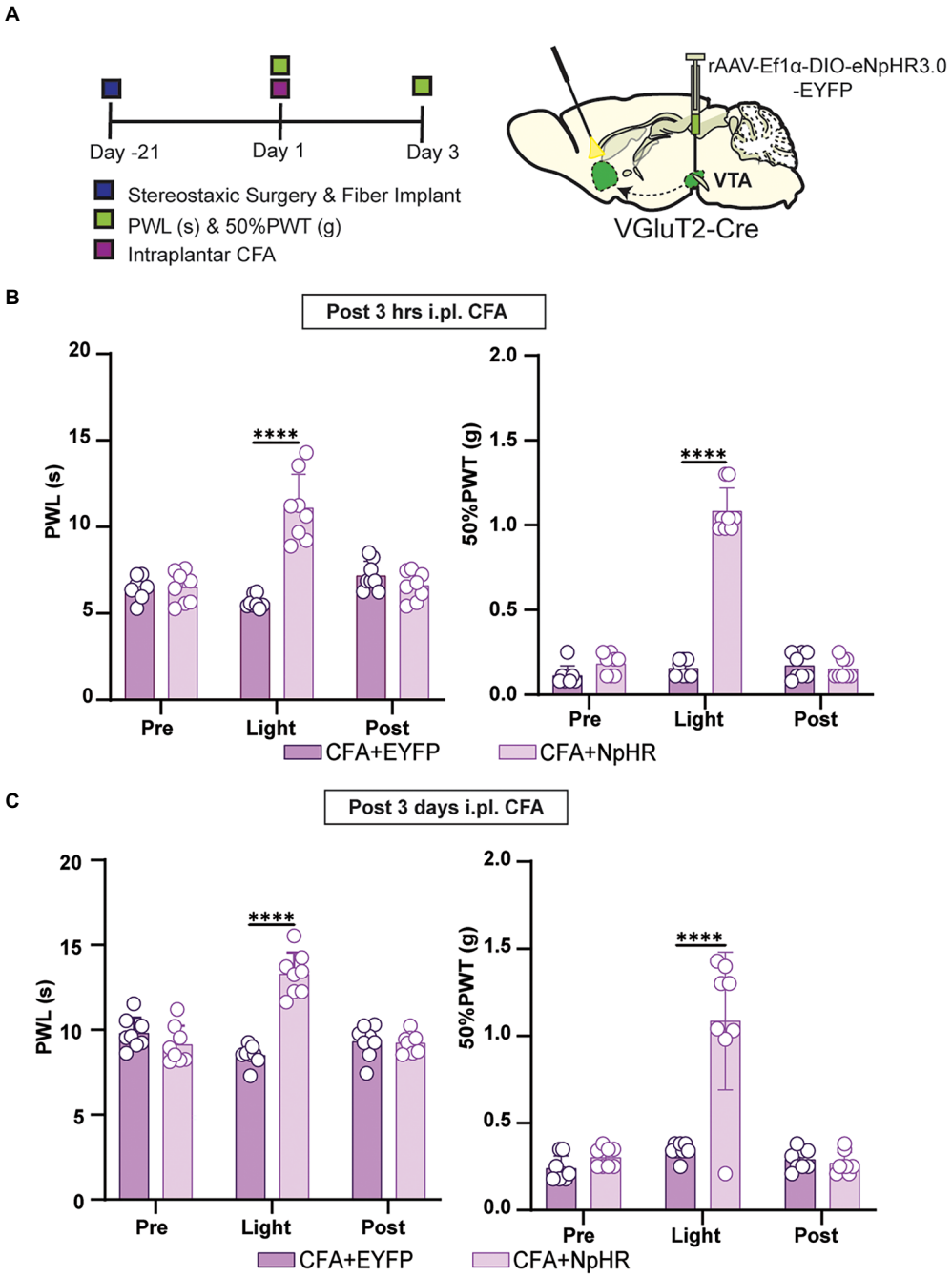

FIGURE 5
Inhibition of this pathway can affect both short-term and long-term inflammatory pain in VGluT2-Cre mice. **(A)** Experimental timeline. Schematic illustration depicting viral constructs. For stimulation, DIO-NpHR-EYFP was injected in the VTA, the optical fiber was planted at the NAc in VGluT2-Cre mice, mice were given 21days for the expression of the virus before the ip.l. CFA injection. PWLs and 50% PWTs of the hind paws were assessed at 3h and day 3 after ip.l. CFA injection in VGluT2-Cre mice. **(B)** The quantitative comparison of PWLs and 50% PWTs between the two groups (with and without light stimulation). Statistics showing that CFA+NpHR group exhibited a significant increase in PWLs during the terminal light stimulation [Light phase] compared with the CFA+EYFP group (n=8, 8 mice; ****p<0.0001), 50% PWTs of CFA+NpHR group were also increased by the terminal light stimulation [Light phase] compared with the CFA+EYFP group (n=8, 8 mice; ***p<0.0001) in VGluT2-Cre mice after 3h of ip.l. CFA injection. **(C)** The quantitative comparison of PWLs and 50% PWTs between the two groups (with and without light stimulation). Statistics showing that CFA+NpHR group exhibited a significant increase in PWLs by the terminal light stimulation period [Light phase] compared with the CFA+EYFP group (n=8, 8 mice; ****p<0.0001), 50% PWTs of CFA+NpHR group were also increased during the terminal light stimulation phase [Light phase] compared with the CFA+EYFP group (n=8, 8 mice; ****p<0.0001) in VGluT2-Cre mice after 3days of ip.l. CFA injection (All the readings were measured during 3 consecutive periods, and the comparisons were performed by the *two-way ANOVA test* followed by *Bonferroni post-test*).

implantation was placed on the VTA brain region, (Figures 6A,B). Compared with the control subject, CCI surgery resulted in decreased latency to enter the center area after being placed into the apparatus, and the photoinhibition of VTA-NAc glutamatergic pathway improved the exploratory behavior of CCI mice compared to its control counterparts and sham groups (Figures 6C,D). Besides this, the locomotion rate has not been influenced among all the groups (Figures 6E,F). Secondly, we performed the elevated maze test (EMT), 21 days after CCI or sham surgery. Again, for the somatic stimulation in wild-type mice, a retrograde CaMKIIa-CRE virus was injected into NAc, and DIO-EYFP-NpHR was injected with fiber implantation placed on VTA of the wild-type mice (Figures 6G,H). The EMT showed that CCI surgery resulted in a decreased duration of time spent and the number of entries in the open arms; the optogenetic inhibition of VTA-NAc glutamatergic pathway rescued this decrease among CCI-NpHR group significantly (Figures 6I–K). These data suggested that glutamatergic neurons projected from VTA to NAc contributed to pain-related anxiety behaviors.

The inhibition of glutamatergic neurons projected from VTA to NAc released chronic pain-related depression

It was reported that pain-induced depression evolves after pain has lasted at least 4–5 weeks (Llorca-Torralba et al., 2022), and the sucrose preference test is known for measuring stress-induced anhedonia in mice (Li et al., 2017; Liu et al., 2018). The intraperitoneal injection of CNO could create a bias in the experiment, so we utilized the infusion of CNO by mixing it with the desired solution as described previously (Zhan et al., 2019). We injected retrograde CaMKIIa-CRE into NAc and EYFP-hM4D (Gi) into the VTA of the wild-type mice (Figures 7A,B). The sucrose preference was recorded within 24 h among mice after 32 days of CCI surgery, and at the same time for the mice without the CCI surgery. Compared to control group, CCI-induced pain mice resulted in a reluctance and a significant decline in the preference for drinking the 1% sucrose water. The chemogenetical inhibition of the glutamatergic neurons projected from VTA to NAc could significantly improve the sucrose preference among mice suffering from CCI-induced pain compared to its control counterparts (Figure 7C). These data suggested that glutamatergic neurons projected from VTA to NAc contributed to pain-related depression behaviors too (Figure 8).

Discussion

Pain triggers maladaptive changes within the mesolimbic system (Massaly et al., 2016), leading to negative affective states such as anxiety and other related behavioral changes (Sieberg et al., 2018). The DA neurons in the VTA are considered the famous therapeutic target for treating reward-related behaviors, such as drug addictions and mood disorders, due to their crucial roles in directing reward-related responses. VTA GABA neurons have also been found to regulate reward consumption, depression, stress, and sleep by altering DA release from adjacent DA neurons, suggesting that the function of VTA GABA neurons is partially dependent on DA release. DA neurons are nominated explicitly for addiction (Pascoli et al., 2015), and relatively fewer researchers have focused on VTA glutamate signaling due to their intermittent existence in the VTA. However, recent studies suggested that VTA glutamate neurons regulate reward reinforcement, aversive behaviors, wakefulness, and defensive behaviors. However, its role in pain and related behavioral changes needs more detailed investigations.

In our study, we observed that glutamatergic neurons of VTA had efferent inputs to the NAc, which was constant in the previous study (Qi et al., 2016), and these VTA glutamatergic projections to NAc could be triggered for an increased firing rate and neuronal activity by inducing pathological pain of chronic constrictive injury providing a well-defined proposal that these glutamatergic projections from VTA to NAc also contributes to pain.

Acute activation of VTA glutamatergic terminals in the LHb, VP, and NAc induces self-stimulation and aversion through glutamate-mediated action (Qi et al., 2016), and the local VGluT2 levels in the nucleus accumbens are reported to remain unaltered in the pain state (Yamaguchi et al., 2007). In contrast, another report suggested that VGluT2 expression is essential in pain behavior (Scherrer et al., 2010). We found that activation of both CaMKII coupled and VGluT2 projections of VTA had no-significant changes in pain behavior. Still, in comparison, the inhibition of these projections can induce pain relief effects for both acute and chronic pain. In our idea, the VGluT2 inputs from VTA produce an inhibitory response to pain behavior by creating a rewarding aspect of relief in NAc (Harris and Peng, 2020).

People with chronic pain have three times the average risk of developing psychiatric symptoms like anxiety disorders and depression (Woo, 2010; Wilmer et al., 2021). Measurements of anxiety with chronic pain also show a strong association with depression. Neuropathic pain, initiated by constriction of the sciatic nerve, can induce anxiety-like behavior in mice, and the mice could develop a fear (Kamonseki et al., 2021). VTA-glutamate neuronal activity response to innate threatening stimuli (Barbano et al., 2020) and inhibitory response of NAc local glutamate receptors can prevent depressive symptoms. Moreover, neuropathic pain can induce anxiety, depression, and pain-related fear (Bagot et al., 2015; Xu et al., 2020). Our finding also proposed that chronic pathological pain can cause anxiety-like fear behavior in mice which can be reduced by inhibiting VTA glutamate projections to NAc. We can propose that this can be due to the way VTA glutamate neurons regulates the activity of D1 and D2 receptors in NAc (Sato et al., 2022) and inhibition of the D2 receptor alone can reduce the pain behavior among mice (Supplementary Figure 1). Another proposal could be the interneurons signaling in dopamine/glutamate interaction at different sites for behavioral responses (Richard and Berridge, 2011; Xiao et al., 2021). However, it is still unclear how the

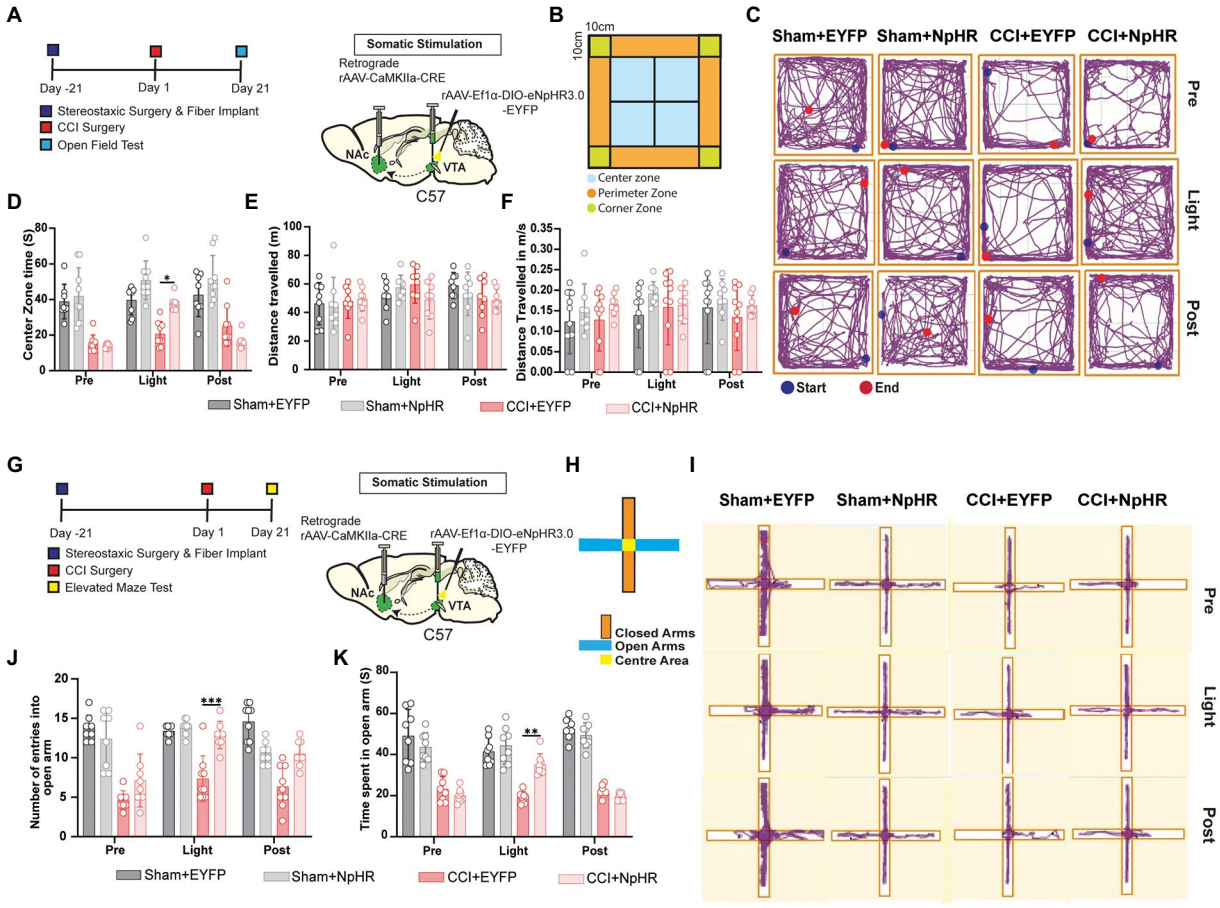

FIGURE 6
Inhibition of glutamatergic neurons projected from VTA to NAc decreases anxiety and improves the exploratory behavior of mice. **(A)** Experimental timeline. Schematic illustration depicting viral constructs. For the somatic stimulation, a retrograde viral vector CaMKIIa-CRE viral vector was injected in the NAc brain region and DIO-NpHR-EYFP was injected in the VTA, and the optical fibers were also planted at the VTA, mice were given 21days for the expression of the virus before the CCI or sham surgery. OFT was performed on day 21 after CCI surgery was established by the ligation of sciatic nerve and sham was produced with only an incision but without the ligation of sciatic nerve in wild-type mice. **(B)** Illustrated design of the field area for the OFT behavioral tests. **(C)** Tracing image of Sham + EYFP, Sham + NpHR, CCI+EYFP, and CCI+NpHR groups defining the roaming field of mice in different time periods. **(D)** The quantitative comparison regarding the time spent in the center zone by the groups of Sham + EYFP, Sham + NpHR, CCI+EYFP and CCI+NpHR (with and without light stimulation). Statistics showing that there is a significant difference regarding time duration spent in the center zone of CCI+NpHR group compared with the CCI+EYFP group (n=8, 8, 8, 8 mice; *p<0.05) but no significant difference compared to Sham + EYFP and Sham + NpHR (n=8, 8, 8, 8 mice; p>0.05) during the light stimulation period [Light phase]. **(E)** The quantitative comparison regarding distance traveled by the groups of Sham + EYFP, Sham +N pHR, CCI+EYFP, and CCI+NpHR. Statistics showing that all the groups showed no statistical difference in any time period. (n=8, 8, 8, 8 mice; p>0.05). **(F)** The quantitative comparison regarding speeds of Sham + EYFP, Sham + NpHR, CCI+EYFP, and CCI+NpHR. Statistics showing that all the groups showed no statistical difference in any time period. (n=8, 8, 8, 8 mice; p>0.05). **(G)** Experimental timeline. Schematic illustration depicting viral constructs. For the somatic stimulation a retrograde viral vector CaMKIIa-CRE viral vector was injected in the NAc brain region and DIO-NpHR-EYFP was injected in the VTA, the optical fiber was also implanted at the VTA, mice were given 21days for the expression of the virus before the CCI or sham surgery. EMT was performed on day 21 after CCI surgery in wild-type mice. The ligation of sciatic nerve established the CCI pain model. Sham was produced with only an incision but without sciatic nerve ligation. **(H)** Illustrated design regarding the arms of elevated maze. **(I)** Tracing image of Sham + EYFP, Sham + NpHR, CCI+EYFP, and CCI+NpHR groups defining the roaming field of mice in different time periods. **(J)** The quantitative comparison regarding the number of entries in the open arms of elevated maze by the mice of the groups of Sham + EYFP, Sham + NpHR, CCI+EYFP, and CCI+NpHR (with and without light stimulation). Statistics show that CCI+EYFP group exhibited a significant decrease in the number of entries in open area compared with CCI+NpHR group (n=8, 8, 8, 8 mice; ***p<0.001), but CCI+NpHR had no significant difference compared to Sham + EYFP, Sham + NpHR during the somatic light stimulation [Light phase] (n=8, 8, 8, 8 mice; p>0.05). **(K)** Statistics showing that CCI+EYFP group exhibited a significant decrease in the time spent in open area compared with CCI+NpHR group (n=8, 8, 8, 8 mice; **p<0.01), but CCI+NpHR had no significant difference compared to Sham + EYFP, and Sham + NpHR during the somatic light stimulation [Light phase] (n=8, 8, 8, 8 mice; p>0.05; all comparisons were done by *two-way ANOVA test* followed by *Bonferroni post-tests*).

VTA-NAc-specific molecular mechanisms modulate pain perception. Future studies could use the projection- and cell-type-specific gene analysis techniques and live single-cell sequencing techniques for further exploration.

Our study has some limitations. Firstly, this only defines the role of VTA glutamatergic inputs to the NAc brain region. We have planned future studies to compare different brain regions and types of neurons like DA and GABA for a comparative outcome.

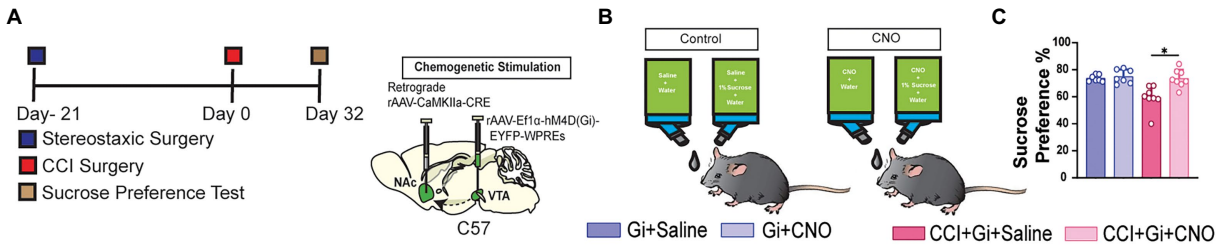

FIGURE 7
Inhibition of glutamatergic neurons projected from VTA to NAc can reduce the pain-induced decrease in sucrose preference, and this behavior. **(A)** Experimental timeline. Schematic illustration depicting viral constructs. For the chemogenetic stimulation a retrograde CaMKIIa-CRE viral vector was injected in the NAc brain region, and DIO-hM4D(Gi)-EYFP was injected in the VTA, mice were given 21days for the expression of the virus before the CCI surgery, the sucrose test was performed at the 32days post-surgery in the CCI-induced mice along with the mice without CCI surgery. **(B)** The illustration of the oral route of CNO infusion, CNO was mixed with water and 1% sucrose solution and the control group fluids were prepared without the presence of CNO drug. **(C)** Statistics data showing that CCI+Gi+Saline exhibited a significant decrease compared with CCI+Gi+CNO, Gi+Saline and Gi+CNO (n=7, 7, 8, 8 mice; *p<0.05) during the testing of sucrose preference of 24h (All the data were measured by *one-way ANOVA* followed by the *Dunnett's test*).

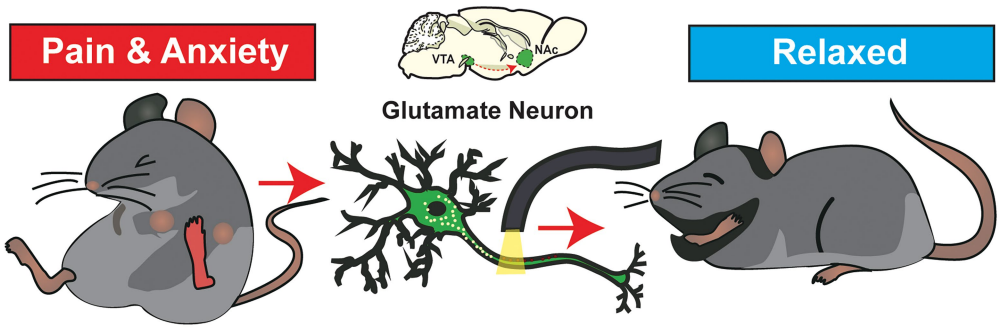

FIGURE 8
Schematic of theoretical pathway involvement in pain and pain-related behavior. Illustrated figure shows the VTA glutamate afferents to the NAc. These projections played a role in causing unrest and anxiety-like psychological mood change among the subjected mice suffering from pain stimuli. When these projections are silenced, it can relieve the mice from pain and pain-induced anxiety.

In our study, we used CCI pain as the primary pain model for all the anxiety and depressive changes that could cause different approaches in molecular-level mechanisms of CFA. We presumed that the behavioral response remains the same as reported in a study done previously (Zhou et al., 2021). Third, although D2 receptors positive neurons in the NAc contributed to the pain behavior, we did not examine the directed role of the glutamatergic inputs from VTA on these subtype neurons in the pain and pain-related behaviors, which needs to be further investigated.

Conclusion

We can summarize that VTA glutamatergic neurons with projections to NAc are as critical as the role of dopamine neurons in pain and pain-induced anxiety. We proposed that this inhibitory pathway could reduce the dopamine-only mediated side effects observed in recreational and clinical settings. The study is one of the first to discover the inhibition role of the VTA-glutamatergic pathway in pain mechanism and nociceptive induce anxiety. It may enlighten further studies focusing on understanding the multiple functions of VTA glutamatergic neurons.

Data availability statement

The original contributions presented in the study are included in the article/Supplementary material, further inquiries can be directed to the corresponding author.

Author contributions

MA and J-LC designed the study, critically reviewed the manuscript, approved the final version, and was accountable for the work. MA and H-QY designed the study, analyzed the data, interpreted the data, prepared the manuscript, critically reviewed the manuscript, approved the final version, were accountable for

the work, and assisted with the sample testing and data analysis. MA, H-QY, W-NZ, X-BL, ZX, X-LY, and J-LC conducted the study and critically reviewed the data. All authors contributed to the article and approved the submitted version.

Funding

This work was supported by the National Key R&D Program of China-the Sci-Tech Innovation 2030 Major Project (2021ZD0203100 to J-LC), the National Natural Science Foundation of China (81720108013, 82130033, and 82293641 to J-LC), the Natural Science Foundation of the Jiangsu Higher Education Institutions of China (19KJB320023 to X-LY), the Innovation and Entrepreneurship Program of Xuzhou Medical University (2021CXFUZX002 to X-LY), and Innovation Training Program for College Students in Jiangsu Province (201910313023Z).

Acknowledgments

We acknowledge the National Natural Science Foundation of China and Innovation Training Program for College Students in Jiangsu Province and the National Demonstration Centre for Experimental Basic Medical Science Education (Xuzhou Medical University).

Conflict of interest

The authors declare that the research was conducted in the absence of any commercial or financial relationships that could be construed as a potential conflict of interest.

Publisher's note

Supplementary material

The Supplementary material for this article can be found online at: https://www.frontiersin.org/articles/10.3389/fnmol.2022.1083671/full#supplementary-material

SUPPLEMENTARY FIGURE 1
Optogenetical inhibition of NAc D2 MSNs suppressed pain behavior. **(a)** Experimental timeline. Schematic illustration depicting viral constructs, mice were given 21days for the expression of the virus. For the stimulation, DIO-NpHR-EYFP was injected in the NAc and optical fiber was planted at the NAc in D1-Cre/D2-Cre mice. **(b)** PWLs (n=8, 8) and 50% PWTs (n=8, 8) were measured during three consecutive periods with or without 594nm laser stimulation in D1-Cre mice exhibited no significant difference (n=8, 8 $p>0.05$). **(c)** The quantitative comparison of PWLs and 50% PWTs between the two groups. Statistics showing that PWLs (n=8, 8 ****$p<0.0001$) and PWTs (n=8, 8 ****$p<0.0001$) exhibited a significant decrease in PWLs and 50% PWTs measured during 3 consecutive periods during laser stimulation [Light phase] in D2-Cre mice. All the readings were measured during 3 consecutive periods and all the comparisons were performed by *two-way ANOVA test* followed by *Bonferroni post-test*.

SUPPLEMENTARY FIGURE 2
Neuronal Activity of Glutamate neurons was intact in the chronic pain stage. **(a)** Experimental timeline. For the immunohistological expression. **(b)** The DIO-EYFP viral vector was injected in the VTA brain region and mice were given 21days for the expression of the virus before the CCI surgery and immunohistological and confocal imaging was performed 30days after CCI surgery. **(c)** Confocal image of VTA somatic expression of DIO-EYFP in VGluT2-Cre mice (Scale bar=200μm).

References

Adeniyi, P. A., Shrestha, A., and Ogundele, O. M. (2020). Distribution of VTA glutamate and dopamine terminals, and their significance in CA1 neural network activity. *Neuroscience* 446, 171–198. doi: 10.1016/j.neuroscience.2020.06.045

Bagot, R. C., Parise, E. M., Pena, C. J., Zhang, H. X., Maze, I., Chaudhury, D., et al. (2015). Ventral hippocampal afferents to the nucleus accumbens regulate susceptibility to depression. *Nat. Commun.* 6:7062. doi: 10.1038/ncomms8062

Barbano, M. F., Wang, H. L., Zhang, S., Miranda-Barrientos, J., Estrin, D. J., Figueroa-Gonzalez, A., et al. (2020). VTA glutamatergic neurons mediate innate defensive behaviors. *Neuron* 107, 368.e8–382.e8. doi: 10.1016/j.neuron.2020.04.024

Basting, T., Xu, J., Mukerjee, S., Epling, J., Fuchs, R., Sriramula, S., et al. (2018). Glutamatergic neurons of the paraventricular nucleus are critical contributors to the development of neurogenic hypertension. *J. Physiol.* 596, 6235–6248. doi: 10.1113/JP276229

Bonin, R. P., Bories, C., and De Koninck, Y. (2014). A simplified up-down method (SUDO) for measuring mechanical nociception in rodents using von Frey filaments. *Mol. Pain* 10:1744-8069-10-26. doi: 10.1186/1744-8069-10-26

Cai, J., and Tong, Q. (2022). Anatomy and function of ventral tegmental area glutamate neurons. *Front. Neural Circuits* 16:867053. doi: 10.3389/fncir.2022.867053

Hargreaves, K., Dubner, R., Brown, F., Flores, C., and Joris, J. (1988). A new and sensitive method for measuring thermal nociception in cutaneous hyperalgesia. *Pain* 32, 77–88. doi: 10.1016/0304-3959(88)90026-7

Harris, H. N., and Peng, Y. B. (2020). Evidence and explanation for the involvement of the nucleus accumbens in pain processing. *Neural Regen. Res.* 15, 597–605. doi: 10.4103/1673-5374.266909

Holly, E. N., and Miczek, K. A. (2016). Ventral tegmental area dopamine revisited: effects of acute and repeated stress. *Psychopharmacology (Berl)* 233, 163–186. doi: 10.1007/s00213-015-4151-3

Kamonseki, D. H., Christenson, P., Rezvanifar, S. C., and Calixtre, L. B. (2021). Effects of manual therapy on fear avoidance, kinesiophobia and pain catastrophizing in individuals with chronic musculoskeletal pain: systematic review and meta-analysis. *Musculoskelet. Sci. Pract.* 51:102311. doi: 10.1016/j.msksp.2020.102311

Larson, A. A., Brown, D. R., El-Atrash, S., and Walser, M. M. (1986). Pain threshold changes in adjuvant-induced inflammation: a possible model of chronic pain in the mouse. *Pharmacol. Biochem. Behav.* 24, 49–53. doi: 10.1016/0091-3057(86)90043-2

Li, Y. C., Wang, Q., Li, M. G., Hu, S. F., and Xu, G. Y. (2022). A paraventricular hypothalamic nucleus input to ventral of lateral septal nucleus controls chronic visceral pain. *Pain*. doi: 10.1097/j.pain.0000000000002750. [Epub ahead of print].

Li, Y., Wang, Y., Xuan, C., Li, Y., Piao, L., Li, J., et al. (2017). Role of the lateral Habenula in pain-associated depression. *Front. Behav. Neurosci.* 11:31. doi: 10.3389/fnbeh.2017.00031

Li, Q., Yue, N., Liu, S. B., Wang, Z. F., Mi, W. L., Jiang, J. W., et al. (2014). Effects of chronic electroacupuncture on depression- and anxiety-like behaviors in rats with

chronic neuropathic pain. *Evid. Based Complement. Alternat. Med.* 2014:158987. doi: 10.1155/2014/158987

Ling, Y. J., Ding, T. Y., Dong, F. L., Gao, Y. J., and Jiang, B. C. (2020). Intravenous Administration of Triptonide Attenuates CFA-induced pain hypersensitivity by inhibiting DRG AKT signaling pathway in mice. *J. Pain Res.* 13, 3195–3206. doi: 10.2147/JPR.S275320

Liu, P., Chen, J., Ma, S., Zhang, J., and Zhou, J. (2021). Albiflorin attenuates mood disorders under neuropathic pain state by suppressing the hippocampal NLRP3 Inflammasome activation during chronic constriction injury. *Int. J. Neuropsychopharmacol.* 24, 64–76. doi: 10.1093/ijnp/pyaa076

Liu, D., Tang, Q. Q., Wang, D., Song, S. P., Yang, X. N., Hu, S. W., et al. (2020). Mesocortical BDNF signaling mediates antidepressive-like effects of lithium. *Neuropsychopharmacology* 45, 1557–1566. doi: 10.1038/s41386-020-0713-0

Liu, M. Y., Yin, C. Y., Zhu, L. J., Zhu, X. H., Xu, C., Luo, C. X., et al. (2018). Sucrose preference test for measurement of stress-induced anhedonia in mice. *Nat. Protoc.* 13, 1686–1698. doi: 10.1038/s41596-018-0011-z

Llorca-Torralba, M., Camarena-Delgado, C., Suarez-Pereira, I., Bravo, L., Mariscal, P., Garcia-Partida, J. A., et al. (2022). Pain and depression comorbidity causes asymmetric plasticity in the locus coeruleus neurons. *Brain* 145, 154–167. doi: 10.1093/brain/awab239

Markovic, T., Pedersen, C. E., Massaly, N., Vachez, Y. M., Ruyle, B., Murphy, C. A., et al. (2021). Pain induces adaptations in ventral tegmental area dopamine neurons to drive anhedonia-like behavior. *Nat. Neurosci.* 24, 1601–1613. doi: 10.1038/s41593-021-00924-3

Massaly, N., Moron, J. A., and Al-Hasani, R. (2016). A trigger for opioid misuse: chronic pain and stress dysregulate the mesolimbic pathway and kappa opioid system. *Front. Neurosci.* 10:480. doi: 10.3389/fnins.2016.00480

Medeiros, P., Dos Santos, I. R., Junior, I. M., Palazzo, E., da Silva, J. A., Machado, H. R., et al. (2021). An adapted chronic constriction injury of the sciatic nerve produces sensory, affective, and cognitive impairments: a peripheral Mononeuropathy model for the study of comorbid neuropsychiatric disorders associated with neuropathic pain in rats. *Pain Med.* 22, 338–351. doi: 10.1093/pm/pnaa206

Murasawa, H., Kobayashi, H., Saeki, K., and Kitano, Y. (2020). Anxiolytic effects of the novel alpha 2delta ligand mirogabalin in a rat model of chronic constriction injury, an experimental model of neuropathic pain. *Psychopharmacology (Berl)* 237, 189–197. doi: 10.1007/s00213-019-05356-3

Pascoli, V., Terrier, J., Hiver, A., and Luscher, C. (2015). Sufficiency of mesolimbic dopamine neuron stimulation for the progression to addiction. *Neuron* 88, 1054–1066. doi: 10.1016/j.neuron.2015.10.017

Qi, J., Zhang, S., Wang, H. L., Barker, D. J., Miranda-Barrientos, J., and Morales, M. (2016). VTA glutamatergic inputs to nucleus accumbens drive aversion by acting on GABAergic interneurons. *Nat. Neurosci.* 19, 725–733. doi: 10.1038/nn.4281

Raja, S. N., Carr, D. B., Cohen, M., Finnerup, N. B., Flor, H., Gibson, S., et al. (2020). The revised International Association for the Study of Pain definition of pain: concepts, challenges, and compromises. *Pain* 161, 1976–1982. doi: 10.1097/j.pain.0000000000001939

Ren, W., Centeno, M. V., Berger, S., Wu, Y., Na, X., Liu, X., et al. (2016). The indirect pathway of the nucleus accumbens shell amplifies neuropathic pain. *Nat. Neurosci.* 19, 220–222. doi: 10.1038/nn.4199

Richard, J. M., and Berridge, K. C. (2011). Nucleus accumbens dopamine/glutamate interaction switches modes to generate desire versus dread: D (1) alone for appetitive eating but D (1) and D (2) together for fear. *J. Neurosci.* 31, 12866–12879. doi: 10.1523/JNEUROSCI.1339-11.2011

Root, D. H., Estrin, D. J., and Morales, M. (2018). Aversion or salience signaling by ventral tegmental area glutamate neurons. *iScience* 2, 51–62. doi: 10.1016/j.isci.2018.03.008

Sato, D., Narita, M., Hamada, Y., Mori, T., Tanaka, K., Tamura, H., et al. (2022). Relief of neuropathic pain by cell-specific manipulation of nucleus accumbens dopamine D1- and D2-receptor-expressing neurons. *Mol. Brain* 15:10. doi: 10.1186/s13041-021-00896-2

Scherrer, G., Low, S. A., Wang, X., Zhang, J., Yamanaka, H., Urban, R., et al. (2010). VGLUT2 expression in primary afferent neurons is essential for normal acute pain and injury-induced heat hypersensitivity. *Proc. Natl. Acad. Sci. U. S. A.* 107, 22296–22301. doi: 10.1073/pnas.1013413108

Sheng, H. Y., Lv, S. S., Cai, Y. Q., Shi, W., Lin, W., Liu, T. T., et al. (2020). Activation of ventrolateral orbital cortex improves mouse neuropathic pain-induced anxiodepression. *JCI Insight* 5:e133625. doi: 10.1172/jci.insight.133625

Sieberg, C. B., Taras, C., Gomaa, A., Nickerson, C., Wong, C., Ward, C., et al. (2018). Neuropathic pain drives anxiety behavior in mice, results consistent with anxiety levels in diabetic neuropathy patients. *Pain Rep.* 3:e651. doi: 10.1097/PR9.0000000000000651

Strasser, A., Xin, L., Gruetter, R., and Sandi, C. (2019). Nucleus accumbens neurochemistry in human anxiety: a 7 T (1) H-MRS study. *Eur. Neuropsychopharmacol.* 29, 365–375. doi: 10.1016/j.euroneuro.2018.12.015

Trainor, B. C. (2011). Stress responses and the mesolimbic dopamine system: social contexts and sex differences. *Horm. Behav.* 60, 457–469. doi: 10.1016/j.yhbeh.2011.08.013

Wilmer, M. T., Anderson, K., and Reynolds, M. (2021). Correlates of quality of life in anxiety disorders: review of recent research. *Curr. Psychiatry Rep.* 23:77. doi: 10.1007/s11920-021-01290-4

Woo, A. K. (2010). Depression and anxiety in pain. *Rev. Pain.* 4, 8–12. doi: 10.1177/204946371000400103

Xia, F., and Kheirbek, M. A. (2020). Circuit-based biomarkers for mood and anxiety disorders. *Trends Neurosci.* 43, 902–915. doi: 10.1016/j.tins.2020.08.004

Xiao, Q., Zhou, X., Wei, P., Xie, L., Han, Y., Wang, J., et al. (2021). A new GABAergic somatostatin projection from the BNST onto accumbal parvalbumin neurons controls anxiety. *Mol. Psychiatry* 26, 4719–4741. doi: 10.1038/s41380-020-0816-3

Xu, L., Nan, J., and Lan, Y. (2020). The nucleus Accumbens: a common target in the comorbidity of depression and addiction. *Front. Neural Circuits.* 14:37. doi: 10.3389/fncir.2020.00037

Yamaguchi, T., Sheen, W., and Morales, M. (2007). Glutamatergic neurons are present in the rat ventral tegmental area. *Eur. J. Neurosci.* 25, 106–118. doi: 10.1111/j.1460-9568.2006.05263.x

Zell, V., Steinkellner, T., Hollon, N. G., Warlow, S. M., Souter, E., Faget, L., et al. (2020). VTA glutamate neuron activity drives positive reinforcement absent dopamine co-release. *Neuron* 107, 864.e4–873.e4. doi: 10.1016/j.neuron.2020.06.011

Zhan, J., Komal, R., Keenan, W. T., Hattar, S., and Fernandez, D. C. (2019). Non-invasive strategies for chronic manipulation of DREADD-controlled neuronal activity. *J. Vis. Exp.* 10.3791/59439. doi: 10.3791/59439

Zhang, H., Qian, Y. L., Li, C., Liu, D., Wang, L., Wang, X. Y., et al. (2017). Brain-derived neurotrophic factor in the mesolimbic reward circuitry mediates nociception in chronic neuropathic pain. *Biol. Psychiatry* 82, 608–618. doi: 10.1016/j.biopsych.2017.02.1180

Zhang, T., Yanagida, J., Kamii, H., Wada, S., Domoto, M., Sasase, H., et al. (2020). Glutamatergic neurons in the medial prefrontal cortex mediate the formation and retrieval of cocaine-associated memories in mice. *Addict. Biol.* 25:e12723. doi: 10.1111/adb.12723

Zhou, Z., Qiu, N., Ou, Y., Wei, Q., Tang, W., Zheng, M., et al. (2021). N-Demethylsinomenine, an active metabolite of sinomenine, attenuates chronic neuropathic and inflammatory pain in mice. *Sci. Rep.* 11:9300. doi: 10.1038/s41598-021-88521-z

Zhou, C., Wu, Y., Ding, X., Shi, N., Cai, Y., and Pan, Z. Z. (2020). SIRT1 decreases emotional pain vulnerability with associated CaMKIIalpha deacetylation in central amygdala. *J. Neurosci.* 40, 2332–2342. doi: 10.1523/JNEUROSCI.1259-19.2020

Zhu, H., Pleil, K. E., Urban, D. J., Moy, S. S., Kash, T. L., and Roth, B. L. (2014). Chemogenetic inactivation of ventral hippocampal glutamatergic neurons disrupts consolidation of contextual fear memory. *Neuropsychopharmacology* 39, 1880–1892. doi: 10.1038/npp.2014.35

frontiers | Frontiers in Molecular Neuroscience

TYPE Original Research
PUBLISHED 23 January 2023
DOI 10.3389/fnmol.2023.1119667

OPEN ACCESS

EDITED BY
Linlin Zhang,
Tianjin Medical University General Hospital,
China

REVIEWED BY
Daojie Xu,
Fudan University,
China
Yongzheng Han,
Peking University Third Hospital,
China

*CORRESPONDENCE
Tao Xu
✉ balor@sjtu.edu.cn

†These authors have contributed equally to this work

SPECIALTY SECTION
This article was submitted to Pain Mechanisms and Modulators, a section of the journal Frontiers in Molecular Neuroscience

RECEIVED 09 December 2022
ACCEPTED 09 January 2023
PUBLISHED 23 January 2023

CITATION
Teng Q, Wang C, Dong J, Yan H, Chen M and Xu T (2023) Ultrasound-guided anterior iliopsoas muscle space block effectively reduces intraoperative hypotension in elderly adults undergoing hip surgery: A randomised controlled trial.
Front. Mol. Neurosci. 16:1119667.
doi: 10.3389/fnmol.2023.1119667

Ultrasound-guided anterior iliopsoas muscle space block effectively reduces intraoperative hypotension in elderly adults undergoing hip surgery: A randomised controlled trial

Qingyu Teng[1†], Chengyu Wang[1†], Jing Dong[1], Hai Yan[1], Moxi Chen[1] and Tao Xu[1,2*]

[1]Department of Anaesthesiology, Shanghai Sixth People's Hospital Affiliated to Shanghai Jiao Tong University School of Medicine, Shanghai, China, [2]Department of Anaesthesiology, Suzhou Hospital of Anhui Medical University, Suzhou, Anhui, China

Background: Hypotension often occurs during hip surgery in elderly adults with conventional posterior lumbosacral plexus block.

Purpose: We conducted a randomised controlled trial to determine if simple iliopsoas space block can lower the incidence of intraoperative hypotension (IOH) and provide sufficient perioperative pain relief during hip fracture surgery in elderly adults.

Methods: Patients undergoing surgery for elderly hip fracture were randomised to receive either an anterior iliopsoas space block with a lateral femoral cutaneous nerve block or a posterior lumbosacral plexus block. The primary outcome was a composite measure of IOH incidence comprising frequency, absolute and relative hypotension durations.

Results: Compared to the posterior group, the iliopsoas space block group had a decreased median frequency of IOH [1.09 (0–2. 14) vs. 3 (1.6–4.8), p =0.001, respectively] along with lower absolute [5 (0–10) min] and relative [minutes below systolic blood pressure of 100 mmHg in % of total anaesthesia time, 6.67 (0–7.65)] duration of IOH compared to the posterior group [35 (10–45) min, p=0.008; 37.6 (12.99–66.18), p=0.004, respectively]. The median pain levels in the post-anaesthesia care unit and median intraoperative sufentanil usage were comparable between the iliopsoas space group [2 (1–3); 8 (6–10) μg] and posterior group [1 (0–3); 5 (5–8) μg]. Thermal imaging revealed that the limb injected with the iliopsoas space block had a higher skin temperature than the unblocked limb in the sacral plexus innervated region.

Conclusion: A single iliopsoas space block lowers the IOH incidence and provides comparable perioperative analgesia to conventional lumbosacral plexus block.

Clinical Trial Registration: Trial registration at www.chictr.org.cn (ChiCTR2100051394); registered 22 September 2021.

KEYWORDS

hip fracture surgery, iliopsoas space block, intraoperative hypotension, perioperative analgesia, lumbosacral plexus block

Introduction

One of the most common fractures in senior people are hip fractures, which affect millions of people every year, causing pain, disability, and socioeconomic difficulty (Tajeu et al., 2014). The best therapy for hip fracture, particularly in the elderly, is internal fixation and arthroplasty, which permits early ambulation and decreases the likelihood of fracture consequences (Bhandari and Swiontkowski, 2017).

For hip fracture surgery, in addition to endotracheal-intubation, general and spinal anaesthesia, the lumbosacral plexus combined with laryngeal-mask general anaesthesia is currently widely promoted, especially for high-risk patients (de Visme et al., 2000; Ho and Karmakar, 2002; Strid et al., 2017). Compared with the previous two techniques, conventional posterior lumbosacral plexus block with laryngeal-mask general anaesthesia provided adequate pain relief during surgery, shortened hospital stays, and decreased mortality (Chen et al., 2018; Scurrah et al., 2018). However, the posterior lumbosacral plexus also has some disadvantages, such as multiple puncture injections, turning over to change the patient's position, and intraoperative hypotension (IOH; Aksoy et al., 2014; Zhang et al., 2022), which may be due to the diffusing local anaesthetics into the epidural area, sympathetic nerve block, or excessive analgesia (Lee and Braehler, 2017).

IOH is often used to characterise arterial hypotension in patients undergoing surgery under general anaesthesia (Bijker et al., 2007). In patients undergoing general surgery, neurological surgery, geriatric hip surgery, or cardiovascular surgery, reductions in arterial blood pressure below the lower limit of the vascular autoregulation curve are related to ischemia of vital organs (Bayliss, 1902; Mosher et al., 1964; Harper, 1966) and adverse organ outcomes (e.g., myocardial injury, stroke, and acute renal injury; Bijker et al., 2012; Aronson et al., 2013; Walsh et al., 2013). In addition, IOH is connected with prolonged hospital stays, surgical morbidity (Tassoudis et al., 2011), and even death (Monk et al., 2015).

Previously, we proposed the iliopsoas space block technique to provide equivalent analgesic effects to the traditional posterior lumbosacral plexus approach (Dong et al., 2021), which was still paired with sacral plexus block of the supine posture. The lumbosacral trunk walks below the psoas major and above the sacroiliac joint (Miniato and Varacallo, 2022); therefore, bolus injection of regional anaesthetic into the iliopsoas space could theoretically block the lumbosacral trunk by spreading around the psoas major space. In this randomised clinical trial, it was hypothesised that the single iliopsoas muscle space block might provide older patients undergoing surgical repair for hip fractures with a decreased incidence of IOH and better analgesia comparable to traditional posterior lumbosacral plexus block.

Materials and methods

Study design

Between October 2021 and August 2022, we performed a double-blind, randomised, controlled trial to compare the hemodynamic effects of ultrasound-guided iliopsoas block and posterior lumbosacral plexus block in elderly patients with hip fractures undergoing surgery. The Shanghai Sixth People's Hospital Ethics Committee (Ethical Committee Number 2021-221) approved the trial, which was registered at[1] (ChiCTR2100051394, principal investigator: Tao Xu).

Study population

Between October 2021 and August 2022, patients aged ≥65 years, with American Society of Anaesthesiologists (ASA) physical status class I-III and scheduled for unilateral hip surgery under general anaesthesia were recruited. All participants or their legal representatives gave their written, informed permission. Infection at the puncture site, history of hip surgery, preexisting neurological deficiency in the lower extremities, contraindications for regional anaesthesia, history of allergy to local anaesthetics, coagulopathy, substance addiction, or daily use of analgesics were exclusion criteria. Patients who refused to cooperate with the researchers were excluded from the study. Most surgeries for hip fractures took <2 h, while those that took longer were also excluded from the study.

Randomisation

All individuals were randomly assigned to either the iliopsoas muscle space group or the posterior lumbosacral plexus group by a physician not blinded to the experimental condition. Every ultrasound-guided nerve block was administered by a professional anaesthesiologist. The next step was conducted by a research coordinator or investigator who was blinded while collecting the data.

Anaesthetic management

All patients underwent fasting according to the ASA guidelines and were not premedicated. A peripheral intravenous access was established as well. The nerve block was administered by a senior anaesthesiologist with >10 y of expertise in ultrasound-guided nerve blocks. The skin of the block region was cleansed with iodophor and both the sterile window sheets and probe were covered with sterile drapes. A standardised amount of local anaesthetic was administered utilising ultrasound guidance and a portable ultrasound system (M-Turbo; SonoSite, Bothell, WA), a 2- to 5-MHz curved array transducer, and a 22-G needle (KDL; Shanghai KDL Medical Instruments, China). The impact and scope of the nerve blocks were assessed and documented. Using thermal imaging and infrared (IR) cameras (FLIR Systems, Wilsonville, OR), we measured bilateral lower limb skin temperature 20 min after completion of nerve block, based on previous research regarding the onset time of nerve block (Dong et al., 2021).

In the posterior lumbosacral plexus group, the lumbar plexus block was conducted using 30 ml of 0.333% ropivacaine at L2-3 and L3-4 utilising a longitudinal paravertebral scan and out-of-plane injection approach, as described by Kirchmair et al. (2001). As documented by Bendtsen et al. (2014), the patients also underwent a sacral plexus block consisting 30 ml of 0.333% ropivacaine. In accordance with our previous procedure, a transverse-section ultrasound scan was used to guide the

1 http://www.Chictr.org.cn

placement of 50 ml of 0. 333% ropivacaine in the lower region of the abdominal wall, 3–4 cm medial to the anterior superior iliac spine in a spine position (Figure 1; Dong et al., 2021) along with a lateral femoral cutaneous nerve block using 10 ml of 0.333% ropivacaine, as described by Thybo et al. (2016).

Propofol (2–3 mg/kg) and sufentanil (5 μg) were subsequently administered to establish general anaesthesia, and a laryngeal-mask airway (Auraonce; Ambu, Xiamen, China) was implanted. Sevoflurane administration and spontaneous breathing helped maintain the minimum alveolar concentration of sevoflurane between 0.8 and 1. Intraoperatively, a bolus dose of 2–3 μg of sufentanil was administered if the surgical stimuli caused an increase of 10 beats per minute (bpm) in heart rate or an increase of 20 mmHg in systolic blood pressure (SBP) at baseline. Sufentanil was adjusted to keep the respiratory rate < 20 bpm. The entire intraoperative sufentanil dosage was documented. During the perioperative phase, SBP, diastolic blood pressure (DBP), mean arterial pressure (MAP), heart rate (HR), and pulse oxygen saturation were recorded with invasive arterial blood-pressure monitoring.

The anaesthesiologist immediately delivers 3–5 mg ephedrine or 30-60 μg phenylephrine intravenously whenever IOH occurs, SBP <100 mmHg. The anaesthesiologist will administer 0.4–0.5 mg of atropine intravenously when the patient's heart rate falls below 50 beats per minute. All cardiovascular drugs used during the surgery were documented.

Every patient was admitted to the post-anaesthesia care unit (PACU) after surgery. The nursing personnel and a study coordinator blinded to conditions assessed the pain score 60 min after surgery. Using a visual analogue scale (VAS) ranging from 0 to 10, pain ratings were assessed (0 = no pain, 10 = greatest agony). In the PACU, opioids were given intravenously as necessary.

Outcomes

The definition of IOH remains controversial (Filiberto et al., 2021). Based on the Perioperative Quality Initiative (POQI) statement (Sessler et al., 2019) and related studies, we defined IOH as a SBP < 100 mmHg (Weinberg et al., 2022). As primary endpoints, a composite measure of IOH incidence, including frequency, absolute duration, and relative duration (percentage of total anaesthesia time), was established for this investigation, as stated by Schneck et al. (2020), while secondary endpoints included the pain score recorded 60 min after surgery and perioperative sufentanil dose.

Sample size

Based on the clinical data from our studies, we deemed a difference (confidence interval) of 2 in the frequency of IOH to be statistically significant. Assuming a standard deviation (SD) of 1.75 in each group, 36 participants would give 90% power to deliver an iliopsoas space block, which is related with a lower incidence of IOH than a lumbosacral posterior plexus block for senior hip fractures. Considering a drop-out rate of 20%, 44 patients were required to be enrolled in this study.

Statistical analysis

Demographic information, clinical features, and hemodynamic data were included in descriptive statistics. Non-normally distributed variables are shown as medians and interquartile ranges, as opposed to means and SDs for regularly distributed data. Numeral and percentage representations of categorical variables are used.

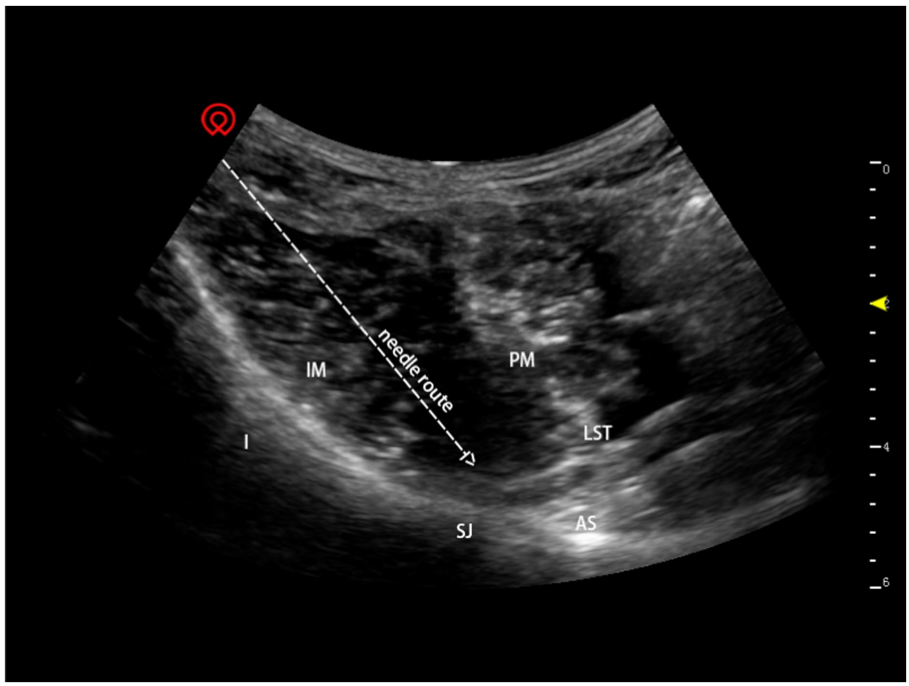

FIGURE 1
Ultrasound-guided anterior iliopsoas muscle space block. I: ilium; IM: iliac muscle; LST: lumbosacral trunk; PM: psoas muscle; SJ: sacroiliac joint; AS: alae sacralis.

Independent Student's t-tests were used to analyse differences in main outcomes across groups for continuous variables, while non-parametric tests were used for nominal variables. The significance threshold was fixed at $p < 0.05$. GraphPad Prism 6 was used to conduct statistical analysis (GraphPad Software, San Diego, CA). Two one-sided test (TOST) protocols were used to assess the secondary outcome across groups and determine if they were equivalent (2 equivalency margin).

Results

This research involved 48 individuals. Four individuals were excluded, and 44 patients were finally recruited in the trial (Figure 2). Six were excluded from analysis as the procedure lasted >2 h; 38 patients were included in the final analysis: 21 in the iliopsoas muscle space group and 17 in the posterior lumbosacral plexus group. Table 1 provides a summary of patient characteristics for the two groups.

Iliopsoas muscle space block reduces the incidence of IOH

The IOH frequency was considerably lower in the iliopsoas space block group than that in the posterior lumbosacral plexus group {all values in median interquartile [IQR] and shown as numbers of hypotensive events per hour (n/h); 1.09 (0–2.14), 3 (1.6–4.8); $p = 0.001$,

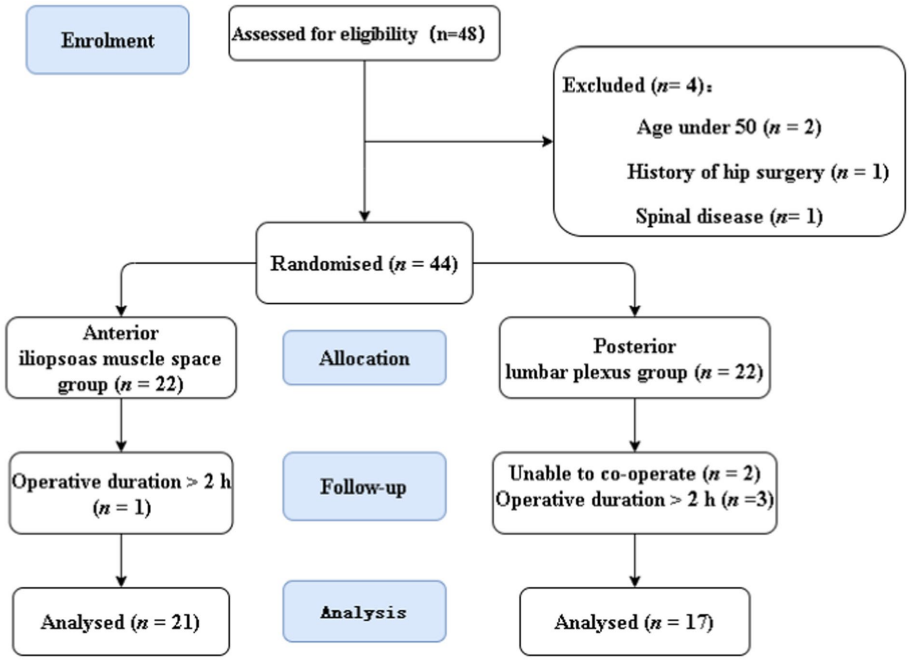

FIGURE 2
CONSORT flow diagram.

TABLE 1 General patient and surgery characteristics.

Characteristics	Iliopsoas space group (*n*=21)	Posterior lumbosacral plexus group (*n*=17)	*p* value
Sex, F (M)	12 (9)	7 (10)	0. 328
Height (cm)	160. 00 ± 7. 16	164. 00 ± 7. 25	0. 097
Weight (kg)	58. 38 ± 10. 41	60. 71 ± 10. 05	0. 492
BMI (kg/m^2)	22. 84 ± 3. 98	22. 47 ± 2. 63	0. 745
Age (years)	73. 33 ± 13. 10	76. 76 ± 9. 13	0. 367
Operation duration (min)	59. 05 ± 24. 18	62. 94 ± 18. 88	0. 591
Duration of general anaesthesia (min)	76. 57 ± 31. 46	79. 00 ± 20. 40	0. 785
PACU 1-h VAS score	2 (1–3)	1 (0–3)	0. 279
Perioperative propofol dose (mg)	130 (110–160)	130 (102–150)	0. 554
Perioperative dose of sufentanil (μg)	8 (6–10)	5 (5–8)	0. 176

Data are expressed as mean ± SD or median (interquartile range). SD: standard deviation; BMI: body mass index; VAS: visual analogue scale; PACU: post-anaesthesia care unit.

respectively}. In comparison to the posterior lumbosacral plexus group, the iliopsoas space block group had considerably shorter absolute [5 (0–10) min, 35 (10–45) min; $p = 0.008$, respectively] and relative [minutes below SBP 100 mmHg in % of total anaesthesia time, 6.67 (0–17.65), 37.6 (12.99–66.18); $p = 0.004$, respectively] durations of IOH (Figure 3; Table 2). However, neither the number nor the duration of hypotension events (SBP < 90 mmHg) differed substantially between groups.

Pain scores in the PACU

Receivers of a posterior lumbar plexus block ($n = 17$) had a median IQR pain score of 1 (0–3), whereas those receiving an iliopsoas muscle space block ($n = 21$) received a score of 2(1–3), resulting in a group difference of −1 (95% confidence interval [CI], −0.614 to 2.065; $p = 0.279$; Figure 4). Since the CI fell within the predetermined range of-2.0 to 2.0, the effects of the two therapies on postoperative pain were comparable. Using the non-parametric TOST, equivalence was measured (Figure 5).

Perioperative sufentanil usage

Sufentanil was administered in the iliopsoas space block group at a median IQR dose of 8 (6–10) μg and in the posterior group at a median IQR dose of 5 (5–8) μg (Table 1). There was no significant difference between the two groups ($p = 0.176$) indicating that both the iliopsoas space block and posterior lumbosacral plexus block may be useful for providing analgesia during hip surgery.

Iliopsoas space block's blocking range

FLIR imaging revealed the body surface temperature at the same selected points on the patients' blocked and unblocked sides. The selected point temperature of the heel (sacral plexus innervation area) on the nerve-blocked side was 26.3°C while that of the unblocked side was 24.8°C. The temperature at the base of the foot (sacral plexus innervation area) on the blocked side was 25.7°C and that on the unblocked side was 23.4°C. The temperature at selected points of the distal femur (lumbar plexus innervation) on the nerve-blocked side was

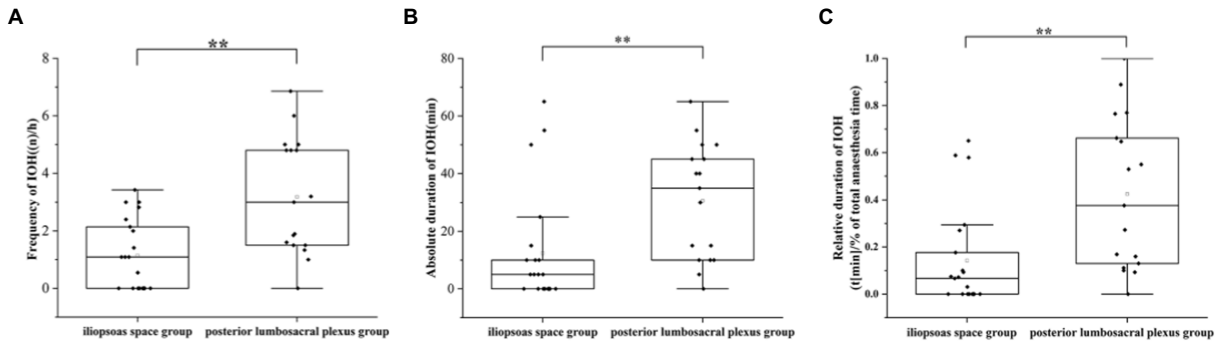

FIGURE 3
Graphs demonstrating the frequency **(A)**, absolute **(B)**, and relative duration **(C)** of hypotensive events in the study. IOH: intraoperative hypotension. **p<0.01.

TABLE 2 Overview of primary endpoint parameters.

Characteristics	Iliopsoas space group (n=21)	Posterior lumbosacral plexus group (n=17)	P value
Frequency of IOH, n/h	1. 09 (0–2. 14)	3 (1. 6–4. 8)	0. 001**
Absolute duration of IOH (min)	5 (0–10)	35 (10–45)	0. 008**
Relative duration of IOH%	6. 67 (0–17. 65)	37. 6 (12. 99–66. 18)	0. 004**
Number of hypotension (SBP < 90 mmHg)	0 (0–1)	1 (0–2)	0. 238
Duration of hypotension (SBP < 90 mmHg) (min)	0 (0–5)	5 (0–15)	0. 181
Number of hypotension (SBP < 100 mmHg)	1 (0–2)	4 (2–4)	0. 001**
Duration of hypotension (SBP < 100 mmHg) (min)	5 (0–10)	35 (10–45)	0. 008**
Surgery type (no. of cases)			0. 264
Total hip arthroplasty	10	10	
Hemi-arthroplasty	7	3	
Internal fixation of intertrochanteric fracture of femur	0	2	
Internal fixation of intertrochanteric fracture of femur	2	0	
Internal fixation of femoral neck fracture	2	2	

Values are shown as median [interquartile range] or number. n/h: numbers of hypotensive events per hour; IOH: intraoperative hypotension; SBP: systolic blood pressure. **p < 0.01.

27.2°C and that on the unblocked side was 26°C. The medial (lumbar plexus innervation region) side of the thigh had a temperature of 29.5°C whereas the unblocked side had 28.9°C. The darker the colour of the corresponding region, the lower the temperature. After the nerve block, the blocked sacral plexus innervation area (sciatic innervation area) had a brighter colour, indicating a higher skin temperature and nerve blockage, compared to the unblocked side (Supplementary Figure 1). After the nerve block was administered, the limb skin temperature of the region innervated by the femoral nerve, obturator nerve, and sciatic nerve was higher on the blocked side than on the unblocked side, indicating that both the lumbar plexus and lumbosacral trunk were successfully blocked.

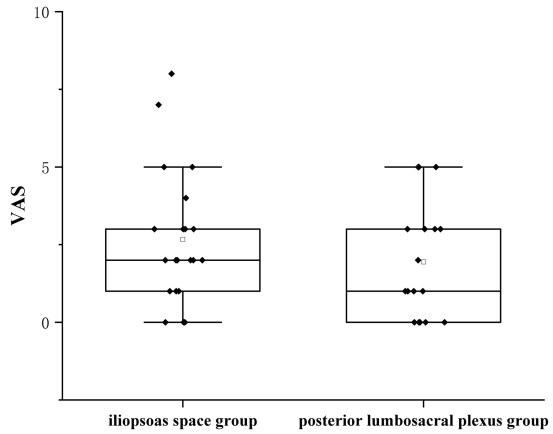

FIGURE 4
Effect of either an anterior iliopsoas space or posterior lumbosacral plexus block on postoperative pain after hip surgery with an injection of 0.33% ropivacaine. Data are expressed as median [interquartile range]. The 95% confidence intervals for the estimated group differences were prespecified tolerances and therefore deemed equivalent. VAS, visual analogue scale.

Discussion

Building on our previous work (Dong et al., 2021), we compared the incidence of hypotension and analgesic effects of a single iliopsoas space block to those of a posterior lumbosacral plexus block in hip surgery. Significantly lesser IOH occurred in the iliopsoas plexus group than in the posterior lumbosacral plexus group. In addition, the pain relief after surgery was comparable across groups, indicating that a single iliopsoas space block not only minimises the incidence of IOH but also has the same pain-relieving effect as a posterior lumbosacral plexus block.

Posterior lumbosacral plexus block is often utilised in hip surgery; however, IOH frequently occurs and has unanticipated outcomes (Aksoy et al., 2014; Zhang et al., 2022). Evidence has demonstrated that longer periods of SBP < 100 mmHg following non-cardiac surgery are related with an increased risk of organ damage and death (Sessler et al., 2019). Based on Weinberg et al. (2022), 153 studies (48.1%) did not include any duration variable in the definition of hypotension; however, IOH should be defined using the absolute values indicated in the POQI statement (Sessler et al., 2019); that is, MAP <60–70 mmHg or SBP < 100 mmHg. Accordingly, we defined IOH as SBP < 100 mmHg in the current study. Here, we demonstrated that the incidence of IOH considerably decreased in elderly patients undergoing hip fracture surgery using an iliopsoas space block compared to the posterior lumbosacral plexus block.

Possible causes of IOH after traditional posterior lumbosacral plexus block include nerve root block, local anaesthetics' epidural space

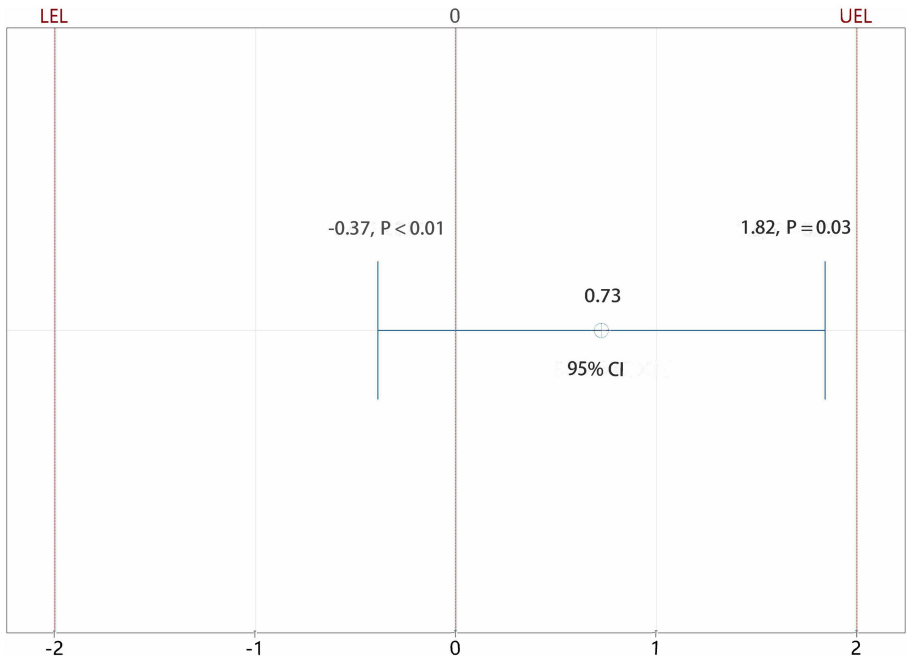

FIGURE 5
Equivalent test results of iliopsoas muscle space group and posterior lumbar plexus group. CI: confidence interval; LEL: lower equivalence limit; UEL: upper equivalence limit. Using the non-parametric TOST, the CI fell within the predetermined range of −2.0 to 2.0, the effects of the two therapies on postoperative pain were comparable.

diffusion, sympathetic nerve block, and excessive analgesia (Lee and Braehler, 2017). When performing a lumbosacral plexus block, if the needle point is placed extremely near the foraminal opening, the medication may transfer down the foraminal to the epidural area, resulting in an epidural block (Lee and Braehler, 2017). Furthermore, since the lumbar sympathetic nerve is positioned between the anterolateral lumbar vertebrae and the medial psoas major muscle (Feigl et al., 2011), it may be blocked simultaneously during the lumbar plexus block. Above all, a lumbosacral plexus block may cause blood vessel dilation of the lower extremities and blood pressure decline, which happens in up to 81% of non-cardiac procedures and is related with a higher 30-day death rate (van Waes et al., 2016). A single anterior iliopsoas space block can effectively avoid these potential problems. With this newly introduced technique, the local anaesthetic rarely enters the epidural diffusion, and the block is relatively restricted. Compared with the posterior lumbosacral plexus, the anterior iliopsoas space block migrates more to the periphery to achieve accurate block and provide relative analgesia without being excessive. Therefore, an iliopsoas anterior space block can effectively decrease the occurrence of IOH and provide an appropriate analgesic effect to the elderly during hip surgery.

As the lumbosacral trunk passes medially to the psoas major muscle at the level of the first sacral vertebra (Miniato and Varacallo, 2022), it can be blocked by injecting a high-volume of local anaesthetic into the iliopsoas space, diffusing medially into the psoas major. Despite the fact that the iliopsoas space block requires a longer onset time than the posterior lumbosacral plexus block (Dong et al., 2021), the iliopsoas space block can not only block the femoral nerve, obturator nerve, and lateral femoral cutaneous nerve, but also the lumbosacral trunk, thereby providing adequate analgesia for hip fracture surgery without additional sacral plexus block. However, variations in the abnormally high VAS score 1 h after surgery also indicate that the possible local anaesthetic diffusion in the space around the psoas major muscle may also result in imperfect blockade.

In addition, the anterior iliopsoas block has many other advantages over the posterior lumbosacral plexus block, such as avoiding the risk of cardiovascular disturbances caused by the pain of turning over in the fracture patient, risk of thrombus dislodging from the leg vein caused by turning over, and risk of aggravated fracture injury caused by postural changes. Additionally, the anterior iliopsoas block may minimise the number of punctures and/or repeated blocks (sacral plexus), and the occurrence of blockage-related haemorrhage, nerve damage, and total spinal anaesthesia. The anterior block provides separation from the abdominal cavity to protect the kidneys and intestines from possible injury. Therefore, it is beneficial to promote anterior iliopsoas space block in the supine posture.

The present research has certain limitations. First, propofol causes hypotension following anaesthesia induction; on the other hand, age-related changes in vascular tone, homeostatic disturbances, and sympathetic nervous system tonic activity render the elderly more vulnerable to IOH. The perioperative bispectral index should be monitored to avoid the effect of anaesthesia depth on blood pressure fluctuations. Second, local anaesthetic concentration and volumetric titration were not assessed to obtain more accurate injection volumes and concentrations.

In conclusion, this study demonstrated that a single iliopsoas muscle space block not only provides as much perioperative analgesia as the traditional lumbosacral plexus block, but also reduces the number of punctures, helps avoid position changes of the patient, and effectively reduces the incidence of IOH, thus improving patient prognosis and increasing perioperative safety.

Data availability statement

The original contributions presented in the study are included in the article/Supplementary material, further inquiries can be directed to the corresponding author.

Ethics statement

The Shanghai Sixth People's Hospital Ethics Committee (Ethical Committee Number 2021-221) approved the trial. The patients/participants provided their written informed consent to participate in this study.

Author contributions

TX conceived and designed the experiments. The data collection was performed by QT, HY and JD. QT and CW analysed the data. The manuscript was written by TX, QT and CW. MC contributed materials and analysis tool. All authors contributed to the article and approved the submitted version.

Funding

This work was supported by grant from the Natural Science Foundation of China (82171486), the Interdisciplinary Program of Shanghai Jiao Tong University to TX (YG2021ZD23), General Science Foundation of Shanghai Sixth People's Hospital to TX (YNMS202114) and Scientific research fund of Shanghai Sixth People's Hospital to MC (YNTS202005).

Conflict of interest

The authors declare that the research was conducted in the absence of any commercial or financial relationships that could be construed as a potential conflict of interest.

Publisher's note

Supplementary material

The Supplementary material for this article can be found online at: https://www.frontiersin.org/articles/10.3389/fnmol.2023.1119667/full#supplementary-material

References

Aksoy, M., Dostbil, A., Ince, I., Ahiskalioglu, A., Alici, H. A., Aydin, A., et al. (2014). Continuous spinal anaesthesia versus ultrasound-guided combined psoas compartment-sciatic nerve block for hip replacement surgery in elderly high-risk patients: a prospective randomised study. *BMC Anesthesiol.* 14:99. doi: 10.1186/1471-2253-14-99

Aronson, S., Phillips-Bute, B., Stafford-Smith, M., Fontes, M., Gaca, J., Mathew, J. P., et al. (2013). The association of postcardiac surgery acute kidney injury with intraoperative systolic blood pressure hypotension. *Anesthesiol Res Pract* 2013:174091. doi: 10.1155/2013/174091

Bayliss, W. M. (1902). On the local reactions of the arterial wall to changes of internal pressure. *J. Physiol.* 28, 220–231. doi: 10.1113/jphysiol.1902.sp000911

Bendtsen, T. F., Pedersen, E. M., Haroutounian, S., et al. (2014). The suprasacral parallel shift vs lumbar plexus blockade with ultrasound guidance in healthy volunteers--a randomised controlled trial. *Anaesthesia* 69, 1227–1240. doi: 10.1111/anae.12753

Bhandari, M., and Swiontkowski, M. (2017). Management of Acute hip Fracture. *N. Engl. J. Med.* 377, 2053–2062. doi: 10.1056/NEJMcp1611090

Bijker, J. B., Persoon, S., Peelen, L. M., Moons, K. G. M., Kalkman, C. J., Kappelle, L. J., et al. (2012). Intraoperative hypotension and perioperative ischemic stroke after general surgery: a nested case-control study. *Anesthesiology* 116, 658–664. doi: 10.1097/ALN.0b013e3182472320

Bijker, J. B., van Klei, W. A., Kappen, T. H., van Wolfswinkel, L., Moons, K. G. M., and Kalkman, C. J. (2007). Incidence of intraoperative hypotension as a function of the chosen definition: literature definitions applied to a retrospective cohort using automated data collection. *Anesthesiology* 107, 213–220. doi: 10.1097/01.anes.0000270724.40897.8e

Chen, W. Q., Guo, N., Wang, S. S., Wang, R., Huang, F., and Li, S. R. (2018). General laryngeal mask airway anesthesia with lumbar plexus and sciatic block provides better outcomes than general anesthesia and endotracheal intubation in elderly patients undergoing hip surgery. *Arch. Gerontol. Geriatr.* 78, 227–232. doi: 10.1016/j.archger.2018.07.005

de Visme, V., Picart, F., Le Jouan, R., et al. (2000). Combined lumbar and sacral plexus block compared with plain bupivacaine spinal anesthesia for hip fractures in the elderly. *Reg. Anesth. Pain Med.* 25, 158–162. doi: 10.1053/rapm.2000.0250158

Dong, J., Zhang, Y., Chen, X., Ni, W., Yan, H., Liu, Y., et al. (2021). Ultrasound-guided anterior iliopsoas muscle space block versus posterior lumbar plexus block in hip surgery in the elderly: a randomised controlled trial. *Eur. J. Anaesthesiol.* 38, 366–373. doi: 10.1097/EJA.0000000000001452

Feigl, G. C., Kastner, M., Ulz, H., Breschan, C., Dreu, M., and Likar, R. (2011). Topography of the lumbar sympathetic trunk in normal lumbar spines and spines with spondylophytes. *Br. J. Anaesth.* 106, 260–265. doi: 10.1093/bja/aeq345

Filiberto, A. C., Loftus, T. J., Elder, C. T., Hensley, S., Frantz, A., Efron, P., et al. (2021). Intraoperative hypotension and complications after vascular surgery: a scoping review. *Surgery* 170, 311–317. doi: 10.1016/j.surg.2021.03.054

Harper, A. M. (1966). Autoregulation of cerebral blood flow: influence of the arterial blood pressure on the blood flow through the cerebral cortex. *J. Neurol. Neurosurg. Psychiatry* 29, 398–403. doi: 10.1136/jnnp.29.5.398

Ho, A. M., and Karmakar, M. K. (2002). Combined paravertebral lumbar plexus and parasacral sciatic nerve block for reduction of hip fracture in a patient with severe aortic stenosis. *Can. J. Anaesth.* 49, 946–950. doi: 10.1007/BF03016880

Kirchmair, L., Entner, T., Wissel, J., Moriggl, B., Kapral, S., and Mitterschiffthaler, G. (2001). A study of the paravertebral anatomy for ultrasound-guided posterior lumbar plexus block. *Anesth. Analg.* 93, 477–481. doi: 10.1097/00000539-200108000-00047

Lee, B. H., and Braehler, M. (2017). Use of test dose allows early detection of subdural local anesthetic injection with lumbar plexus block. *J. Clin. Anesth.* 37, 111–113. doi: 10.1016/j.jclinane.2016.11.011

Miniato, M. A., and Varacallo, M. *Anatomy, Back*, Lumbosacral Trunk. Treasure Island (FL). (2022).

Monk, T. G., Bronsert, M. R., Henderson, W. G., Mangione, M. P., Sum-Ping, S. T. J., Bentt, D. R., et al. (2015). Association between intraoperative hypotension and hypertension and 30-day postoperative mortality in noncardiac surgery. *Anesthesiology* 123, 307–319. doi: 10.1097/aln.0000000000000756

Mosher, P., Ross, J. Jr., McFate, P. A., and Shaw, R. F. (1964). Control of coronary blood flow by an autoregulatory mechanism. *Circ. Res.* 14, 250–259. doi: 10.1161/01.res.14.3.250

Schneck, E., Schulte, D., Habig, L., Ruhrmann, S., Edinger, F., Markmann, M., et al. (2020). Hypotension prediction index based protocolized haemodynamic management reduces the incidence and duration of intraoperative hypotension in primary total hip arthroplasty: a single Centre feasibility randomised blinded prospective interventional trial. *J. Clin. Monit. Comput.* 34, 1149–1158. doi: 10.1007/s10877-019-00433-6

Scurrah, A., Shiner, C. T., Stevens, J. A., and Faux, S. G. (2018). Regional nerve blockade for early analgesic management of elderly patients with hip fracture - a narrative review. *Anaesthesia* 73, 769–783. doi: 10.1111/anae.14178

Sessler, D. I., Bloomstone, J. A., Aronson, S., Berry, C., Gan, T. J., Kellum, J. A., et al. (2019). Perioperative quality initiative consensus statement on intraoperative blood pressure, risk and outcomes for elective surgery. *Br. J. Anaesth.* 122, 563–574. doi: 10.1016/j.bja.2019.01.013

Strid, J. M. C., Sauter, A. R., Ullensvang, K., Andersen, M. N., Daugaard, M., Bendtsen, M. A. F., et al. (2017). Ultrasound-guided lumbar plexus block in volunteers; a randomized controlled trial. *Br. J. Anaesth.* 118, 430–438. doi: 10.1093/bja/aew464

Tajeu, G. S., Delzell, E., Smith, W., Arora, T., Curtis, J. R., Saag, K. G., et al. (2014). Death, debility, and destitution following hip fracture. *J. Gerontol. A Biol. Sci. Med. Sci.* 69, 346–353. doi: 10.1093/gerona/glt105

Tassoudis, V., Vretzakis, G., Petsiti, A., Stamatiou, G., Bouzia, K., Melekos, M., et al. (2011). Impact of intraoperative hypotension on hospital stay in major abdominal surgery. *J. Anesth.* 25, 492–499. doi: 10.1007/s00540-011-1152-1

Thybo, K. H., Schmidt, H., and Hagi-Pedersen, D. (2016). Effect of lateral femoral cutaneous nerve-block on pain after total hip arthroplasty: a randomised, blinded, placebo-controlled trial. *BMC Anesthesiol.* 16:21. doi: 10.1186/s12871-016-0183-4

van Waes, J. A., van Klei, W. A., Wijeysundera, D. N., et al. (2016). Association between intraoperative hypotension and myocardial injury after vascular surgery. *Anesthesiology* 124, 35–44. doi: 10.1097/ALN.0000000000000922

Walsh, M., Devereaux, P. J., Garg, A. X., Kurz, A., Turan, A., Rodseth, R. N., et al. (2013). Relationship between intraoperative mean arterial pressure and clinical outcomes after noncardiac surgery: toward an empirical definition of hypotension. *Anesthesiology* 119, 507–515. doi: 10.1097/ALN.0b013e3182a10e26

Weinberg, L., Li, S. Y., Louis, M., Karp, J., Poci, N., Carp, B. S., et al. (2022). Reported definitions of intraoperative hypotension in adults undergoing non-cardiac surgery under general anaesthesia: a review. *BMC Anesthesiol.* 22:69. doi: 10.1186/s12871-022-01605-9

Zhang, Q., Ling, M., Wang, X., and Cui, D. (2022). A comparison of two peripheral nerve blocks combined with general anesthesia in elderly patients undergoing Arthroplasty for hip fractures: a pilot randomized controlled trial. *Front Surg* 9:715422. doi: 10.3389/fsurg.2022.715422

frontiers | Frontiers in Molecular Neuroscience

TYPE Review
PUBLISHED 09 February 2023
DOI 10.3389/fnmol.2023.1128974

OPEN ACCESS

EDITED BY
Linlin Zhang,
Tianjin Medical University General Hospital, China

REVIEWED BY
Shunmei Lu,
Wuxi People's Hospital Affiliated to Nanjing Medical University, China
Zilong Qiu,
Shanghai Jiaotong University School of Medicine, China

*CORRESPONDENCE
Tao Xu
✉ balor@sjtu.edu.cn

†These authors have contributed equally to this work

SPECIALTY SECTION
This article was submitted to Pain Mechanisms and Modulators, a section of the journal Frontiers in Molecular Neuroscience

RECEIVED 21 December 2022
ACCEPTED 18 January 2023
PUBLISHED 09 February 2023

CITATION
Huang M, Qi Q and Xu T (2023) Targeting Shank3 deficiency and paresthesia in autism spectrum disorder: A brief review. *Front. Mol. Neurosci.* 16:1128974. doi: 10.3389/fnmol.2023.1128974

Targeting Shank3 deficiency and paresthesia in autism spectrum disorder: A brief review

Min Huang[1,2†], Qi Qi[1,2†] and Tao Xu[1,2*]

[1]Department of Anesthesiology, Sixth People's Hospital Affiliated to Shanghai Jiao Tong University School of Medicine, Shanghai, China, [2]Department of Anesthesiology, Suzhou Hospital of Anhui Medical University, Suzhou, China

Autism spectrum disorder (ASD) includes a group of multifactorial neurodevelopmental disorders characterized by impaired social communication, social interaction, and repetitive behaviors. Several studies have shown an association between cases of ASD and mutations in the genes of SH3 and multiple ankyrin repeat domain protein 3 (SHANK3). These genes encode many cell adhesion molecules, scaffold proteins, and proteins involved in synaptic transcription, protein synthesis, and degradation. They have a profound impact on all aspects of synaptic transmission and plasticity, including synapse formation and degeneration, suggesting that the pathogenesis of ASD may be partially attributable to synaptic dysfunction. In this review, we summarize the mechanism of synapses related to Shank3 in ASD. We also discuss the molecular, cellular, and functional studies of experimental models of ASD and current autism treatment methods targeting related proteins.

KEYWORDS

autism spectrum disorder, ASD, synapse, Shank3, treatment

1. Introduction

1.1. Autism

Autism spectrum disorder (ASD) is a term widely used to describe multiple multifactorial neurodevelopmental (Sharma et al., 2018) and grouping disorders (Becerra et al., 2014), including autism (Jiang and Ehlers, 2013), Asperger's syndrome (Berkel et al., 2018), and no other general developmental disorders (Thapar et al., 2017). However, the updated diagnostic criteria for ASD mainly focus on two core areas: social communication disorder and alternative interests/repetitive behaviors (Kales et al., 2015; Kodak and Bergmann, 2020; Srivastava et al., 2021).

The prevalence of ASD has increased steadily (Kincaid et al., 2017; Hyman et al., 2020). Genetic factors, parental history of mental illness, premature birth, and oxygen exposure to psychotropic drugs or pesticides are associated with a higher risk of ASD (Kincaid et al., 2017; Masi et al., 2017; Crump et al., 2021). Various scales, such as the Childhood Autism Rating Scale (CARS; Moon et al., 2019), Childhood Autism Spectrum Disorder Observation (ASD-OC; Neal et al., 2012), and Developmental, Dimensional, and Diagnostic Interview (3Di; Randall et al., 2018), can be used to assess abnormal behaviors and symptoms in ASD efficiently. Nearly 75% of patients with ASD have coexisting mental illnesses or complications, including ADHD, epilepsy, anxiety, bipolar disorder, depression, Tourette's syndrome, and inpatient diseases (Tuchman et al., 2010; Doshi-Velez et al., 2014).

Pharmacological and non-pharmacological interventions are used for ASD treatment (Sharma et al., 2018). Existing drug treatments, including psychostimulants, atypical antipsychotics, antidepressants, and α-2 adrenergic receptor agonists, can partially relieve the core symptoms of

ASD and control comorbidities (Aman, 2004; Muskens et al., 2017). Moreover, non-pharmacological interventions, including music therapy and cognitive and social behavioral therapies, improve the social interaction and oral communication of patients with ASD (Sharma et al., 2018; Esposito et al., 2020). The combined use of vitamins, herbs, nutritional supplements, and behavioral therapy improves ASD symptoms; however, the specific efficacy needs further investigation (Guang et al., 2018; Sharma et al., 2018).

1.2. Shank3

Shank (also known as ProSAP) protein has three main subtypes, Shank1, Shank2, and Shank3, with similar structural domains: N-terminal ankyrin repeats, an Src homology 3 (SH3) domain, a PSD-95/Discs large/ZO-1 (PDZ) domain, an extended proline-rich region, and a sterile alpha motif (SAM) domain (Saupe et al., 2011; Costales and Kolevzon, 2015; Varghese et al., 2017; Sgritta et al., 2019).

As the main scaffold protein of excitatory synaptic PSD, Shank protein interacts with more than 30 types of postsynaptic proteins through these domains. These domains are critical for synapse formation, glutamate receptor transport, and neuronal signal transmission (Monteiro and Feng, 2017; Orefice et al., 2019). Shank3 is encoded by the *SHANK3* gene located on chromosome 22q13.3. The 22q13.3 deletion syndrome [also known as Phelan-McDermid syndrome (PMS)] is found and characterized by marked developmental deterioration (Phelan et al., 2001; Phelan and McDermid, 2012). More than 50% of patients with PMS have identified *SHANK3* abnormalities, including complete deletions, insertions, splicing mutations, and point mutations (Durand et al., 2007; Gauthier et al., 2009; Boccuto et al., 2013). Mutations in *SHANK3* are estimated to occur in 1–2% of people with autism and intellectual disabilities, while mutations in *SHANK1* and *SHANK2* are less common (Boccuto et al., 2013; Leblond et al., 2014; Roberts et al., 2014). Shank3 deficient neurons showed reduced overall expression levels of PSD protein, including GKAP, Homer1b/c, AMPAR subunit GluA1, and NMDAR subunit NR2A (Wang et al., 2011; Peça et al., 2011a). The disruption of the interaction and connection between Shank3, GKAP, and Homer1b/c may cause the redistribution and disruption of the activity-dependent GluA1 subunit. Consequently, posterior tonicity increases, and hippocampal LTP decreases (Wang et al., 2011). In patients with PMS, neurons induced by pluripotent stem cells (iPSCs) showed significantly impaired NMDAR and AMPAR-mediated synaptic transmission (Shcheglovitov et al., 2013; Speed et al., 2015; Qin et al., 2018; Tatavarty et al., 2020). Shank3-deficient mice showed repetitive self-harm and social interaction defects. In addition, mEPSC frequency and amplitude were significantly reduced, indicating a reduction in the number of functional synapses and a decrease in the postsynaptic responses of available synapses (Peça et al., 2011b; Lee et al., 2021). In contrast, overexpression of Shank3 resulted in a sharp increase in the amplitude of AMPAR-mediated NMDAR and NMDAR-mediated EPSC and a high frequency of AMPAR-mediated mEPSC (Arons et al., 2012).

1.3. Risk factors of ASD

The prevalence of ASD in boys is four to five times that in girls (Christensen et al., 2018). Patients with genetic and chromosomal diseases tend to show more symptoms of ASD (Ogata et al., 2014). About 10% of children with ASD also have Down syndrome or Fragile X syndrome (DiGuiseppi et al., 2010; Auerbach et al., 2021). The psychiatric history of biological parents, especially the history of schizophrenia and affective disorder, is associated with an increased incidence of ASD (Jokiranta et al., 2013). Fetal exposure to pesticides is associated with a decrease in infant weight and length, delay in psychomotor development, and high risk of autism (Landrigan, 2010). In addition, epidemiological studies have shown that exposure of pregnant mothers to viral or bacterial infections, especially in the first trimester or middle of pregnancy, promotes the mother's immune activation (MIA) and increases the risks of children's neuropsychiatric disease, including ASD (Estes and McAllister, 2016). MIA is related to an increase in neuroinflammatory cytokines, abnormal expression of synaptic proteins, and abnormal development of synaptic connections, all of which may contribute to the pathophysiology of ASD (Pendyala et al., 2017). Consuming psychotropic drugs during pregnancy is considered a risk factor for autism. Several studies have demonstrated that prescribing antidepressants to pregnant women increases the risk of autism moderately (Gidaya et al., 2014; Siu and Weksberg, 2017). Certain limitations, including failure to carefully adjust the mother's psychiatric history (Hoover and Kaufman, 2018; Bai et al., 2020), genetic susceptibility to ASD (Pardo and Eberhart, 2007; Wei et al., 2021), and variable molecular and clinical effects of different antidepressants (McCarthy et al., 2016; Soler et al., 2018; Johannessen et al., 2019), may lead to differences in findings of current and repeated studies. However, a recent 12-year study (including full-term live births by mothers who received antidepressants during pregnancy) concluded that the period of antidepressant use did increase the risk of autism in children (Boukhris et al., 2016; Modabbernia et al., 2017). A previous pilot study evaluated medical screening results at the time of referral for children and adolescents with different mental disorders. They found newly developed somatic functions in 56% of the subjects (Muskens et al., 2015). These findings include a wide range of medical problems, including weight and height problems (Dhaliwal et al., 2019), high thyroid hormone levels (Needham et al., 2021), dyslipidemia (Panjwani et al., 2020), anemia (Wiegersma et al., 2019), vitamin D and B12 deficiency (Raghavan et al., 2018; Wang Z. et al., 2020), and malformations (Grafodatskaya et al., 2010). Some of these results require consultation with other medical experts. In contrast, other results directly impact daily medical practice, such as adjusting psycho-drug logic therapy and participating in overweight prevention plans (Vannucchi et al., 2014; Mansouri et al., 2020). These studies contribute to improving people's understanding of the relationship between somatic and mental symptoms in developmental disorders. It points to common genetic pathways and other potential mechanisms that may be involved (Dovey et al., 2019; Frolli et al., 2021). In addition, the simultaneous assessment of medical and psychiatric disorders may be of great value. Clinicians can then relate somatic functions to different diagnostic considerations for medical and psychological intervention (Rodin et al., 2021).

2. Shank3 and ASD

2.1. Links between Shank3 genes and ASD

The *SHANK* gene was first found to be related to neurodevelopmental disorders in the study of PMS (Costales and Kolevzon, 2015; Frank, 2021). PMS is a neurodevelopmental disorder caused by the deletion of 22q13.3, characterized by autistic behavior, hypotonia, and continuous

or even nonexistent speech (Burdeus-Olavarrieta et al., 2021). Genome rearrangements in patients with PMS include deletions, chromosomal, mesenchymal deletions, and unbalanced translocations (Bonaglia et al., 2011; Leblond et al., 2014; Tammimies, 2019). In almost all reported cases (Wilson et al., 2003; Wilson et al., 2008), the loss of Shank3 was observed. These cases support the theory that PMS symptoms are caused by the loss of the SHANK3 haplotype (Phelan and McDermid, 2012) or complete *SHANK3* gene on chromosome 22 (Grabrucker et al., 2011a,b). In addition to the symptoms of autism, genetic screening of patients with ASD who have not yet been diagnosed with PMS also revealed many *SHANK3* mutations (Durand et al., 2007; Moessner et al., 2007; Gauthier et al., 2009; Boccuto et al., 2013; Leblond et al., 2014). These mutations include small deletions, nonsense mutations, breakpoints, and missense mutations. A meta-analysis study found that mutations or disruptions in the SHANK gene family accounted for about 1–2% of all patients with ASD (Leblond et al., 2014; Zhou et al., 2016). The degree of related mutations and cognitive impairment between SHANK1-3 also differs: patients with *SHANK3* mutations suffer more cognitive impairment than those with *SHANK1* or *SHANK2* mutations (Qin et al., 2022). In addition, patients with *SHANK3* mutations have severe cognitive deficits (Chevallier et al., 2012; Zhou et al., 2016). These findings together indicate that the common neurobiological effects shared by all members of the *SHANK* gene family may be related to the pathophysiology of ASD. Furthermore, the degree of cognitive impairment in ASD may be due to mutations in the *SHANK* family members, the most significant being *SHANK3* (Chevallier et al., 2012; Baum et al., 2015; Monteiro and Feng, 2017; Banker et al., 2021). The difference in the severity of symptoms can be determined by the mutation of the specific *SHANK* gene (Jiang and Ehlers, 2013; Gong and Wang, 2015; Li and Pozzo-Miller, 2020). The results of the study suggest that mutations in the *SHANK3* gene are the primary cause of ASD and that the expression of the other two remaining *SHANK* subtypes can (or cannot) compensate for its loss (Mashayekhi et al., 2021; Salomaa et al., 2021). Family mutations are comprehensive and should be screened in clinical practice. Many human *SHANK3* mutations map to exon 21 and are associated with moderate to severe intellectual disability (D'Antoni et al., 2014; Mossa et al., 2021; Purushotham et al., 2022). Mutations in the pro-domain region of exon 21 were not associated with altered pathophysiology (Shi et al., 2017; Moutin et al., 2021). One possible explanation is that exon 21 is present in most *SHANK3* isotype surrogates (Moutin et al., 2021). Therefore, mutations in this exon may have more severe effects (Speed et al., 2019). Given the nature of these genes in ASD, it becomes imperative to understand their usual role in synapses and how mutations disrupt them (Figure 1).

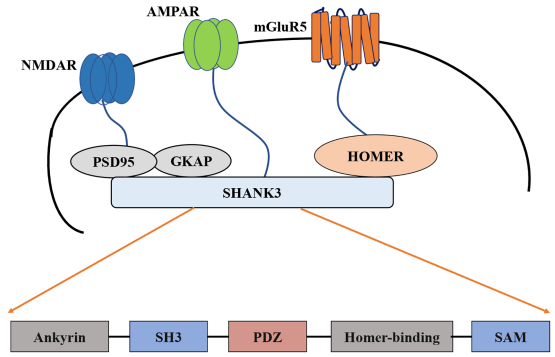

FIGURE 1
Schematic diagram of postsynaptic density and construction of Shank3. PSD-95, Postsynaptic density-95; SH3, Src homology 3; PDZ, PSD95/DlgA/Zo-1; SAM, Sterile alpha motif; mGluR5, metabotropic glutamate receptor 5; AMPAR, The α-amino-3-hydroxy-5-methyl-4-isoxazolepropionic acid receptor; NMDAR, The N-methyl-D-aspartate receptor; GKAP, guanylate kinase-associated protein.

2.2. Neurobiological characteristics of ASD models with alterations in the Shank gene

The expression of different Shank3 subtypes varies with different brain regions and ages (Wang et al., 2014b; Vyas et al., 2021), complicating the analysis and establishment of animal models. Studies on various mouse models of Shank3 heterozygous deletion have recorded changes in the transport of glutamate transmitters or synapses (Yi et al., 2016; Lutz et al., 2020). For example, the Shank3 (Shank3α) model, by deleting exons 4–9, shows reduced immunoreactivity of the glutamate receptor 1 in hippocampal CA1 (Bozdagi et al., 2010; Epstein et al., 2014). In Shank3B$^{-/-}$ mice, gene deletion of two consecutive Shank3 isoforms (Shank3α and β) increases the length and complexity of dendrites and decreases the synaptic density of spinal neurons in the striatum and PSD length and thickness (Peça et al., 2011a; Balaan et al., 2019; Rendall et al., 2019). Purkinje cells of Shank3$^{+/\Delta C}$ mice have Shank3 C-terminal deletions, although the density does not change, and they have a robust dendritic complexity in the body and reduced synaptic density (Kloth et al., 2015; Zhu et al., 2018). The expression of NMDA receptors in the PFC of these mice was reduced; however, the density of synapses did not change (Duffney et al., 2015). The dendrites on the CA1 neurons of Shank3$^{\Delta C/\Delta C}$ mice reduced LTP and NMDA/AMPA ratios in the hippocampus; however, their complexity or synapse density did not change (Bangash et al., 2011; Kouser et al., 2013). In a KO mouse model (Shank3Δe4–22$^{-/-}$ mice) that eliminated all Shank3 subtypes, the PSD length and thickness of the striatum were reduced (Pagliardini et al., 2005; Bey et al., 2018). Restoring Shank3 expression in adult Shank3-deficient mice can reverse the destruction of dendritic spines in the striatum and stimulate synaptic function (Peça et al., 2011a; Mei et al., 2016; Hsueh, 2019). The above findings confirmed the role of Shank3 in mobilizing multiple glutamate receptor assemblies at the PSD and synaptic signal substitution and dynamics (Jeong et al., 2021). Although the loss of heterozygosity in Shank3 is more representative of the defects observed in human PMS, the researchers still focused on the homozygous Shank3 KO (Han et al., 2016; Yi et al., 2016; Jacot-Descombes et al., 2020).

Based on the molecular and physiological abnormalities in SHANK3-deficient animals (Delling and Boeckers, 2021), various pharmaceutical compounds have been proposed as possible therapeutic options for SHANK3-related neuropsychiatric disorders (Wang X. et al., 2016; Vicidomini et al., 2017). For example, modulation of glutamate receptors may be beneficial, as AMPAR, NMDAR, or GRM5 hypofunction may lead to excitation/inhibition imbalance, contributing to ASD-like phenotypes in SHANK3-mutant mice (Guo et al., 2019; Rhine et al., 2019; Nuzzo et al., 2020).

3. Comorbidity of Shank3 deficiency and paresthesia

Hypersensitivity, hyposensitivity, or abnormal interest in sensory stimuli are common features of patients with ASD (Lord et al., 2020) and PMS, who usually show increased pain tolerance (Zencica et al., 2010;

Soorya et al., 2013). Abnormal sensory function in *SHANK3*-deficient rodents can be analyzed in various ways. The most used paradigm focuses on the perception of injury or somatic sensory function. Examples of the methods used include the tail-flick, Frey, and hot plate tests. However, other methods have also been investigated, including auditory, olfactory, visual, vestibular function, and sensorimotor gating (Bruno et al., 2021). In rat models, exons 4–22 (Han et al., 2013; Drapeau et al., 2018), exon 11 (Vicidomini et al., 2017), exon 21 (Kouser et al., 2013), and exons 11–21 (Song et al., 2019) describe general somatic dysfunction, especially low pain sensitivity. Targeted destruction of SHANK3 in tail embryo cells, somatosensory neurons [exon 13–16 (Orefice et al., 2019)], and cells expressing SCN10A [commonly known as Nav1.8, exon 4–22 (Han et al., 2013)] can induce somatosensory dysfunction. Two studies examining the constitutive SHANK3 defect model exon 13–16 (Chen et al., 2020; Kabitzke et al., 2020) described somatosensory dysfunction related to light touch stimulation. In contrast, in other studies, the somatosensory function examined by heat/injury perception was not affected in these mice (Dhamne et al., 2017; Schroeder et al., 2017). Additionally, there is mixed evidence regarding the mouse model of exons 4–9 (Yang et al., 2012; Orefice et al., 2019), while the somatic sensory function of mice with exon 8 appears unaffected (Yoo et al., 2019).

These previous studies suggest that ASD subjects express their pain perception through various behaviors, including typical reactions similar to those seen in the general population. Crying, shouting, protecting the painful parts, or seeking comfort are examples. However, the behaviors are more specific and less easily recognized as pain-related behaviors (making specific sounds, playing posture, etc.; Dubois et al., 2017). Despite these findings, the version of the Diagnostic and Statistical Manual of Mental Disorders (DSM 5) still mentions sensitivity to pain as a diagnostic standard and uses the term "obvious pain indication." Pain sensitivity is a critical issue for patients with autism because they experience pain more frequently than others (Gillberg and Coleman, 1996; Lee et al., 2008). The sensitivity of patients with autism to pain may affect their medical pain management. This may lead to an insufficient treatment or a lack of evaluation. Therefore, this assumption needs to be tested.

Although some adults with ASD may also experience reduced pain sensitivity, lack of pain perception may not be considered a classic characteristic of ASD populations. To understand the pain in ASD and explain its lack of reactivity, it is necessary to focus on multiple components of pain rather than just the mechanism of pain and consider pain as part of a broader conceptual framework (Hadjistavropoulos and Craig, 2002; Dubois et al., 2010; Rattaz et al., 2013; Moore, 2015). Conceptualizing pain expression from the perspective of multiple factors requires individual pain management strategies and evaluation according to the clinical characteristics of patients with autism.

4. Treatment of ASD and paresthesia by targeting Shank3

Current treatment options for ASD include pharmacological and non-pharmacological interventions. Pharmacological interventions include psychostimulants, atypical antipsychotics, antidepressants, alpha-2 adrenergic receptor agonists, NMDA receptor antagonists, and antiepileptic mood stabilizers (Aman et al., 2008; Costales and Kolevzon, 2015; Bicker et al., 2021). This section focuses on the safety and tolerability profiles of the main strategies used to treat children and adults with ASD (Table 1).

Because the genome of human mutations associated with ASD is very complex, animal models are the basis for studying specific mutations and establishing beneficial genotype-cell phenotypes (De Rubeis et al., 2018; Zhou et al., 2019; Reed et al., 2020). New approaches to preclinical animal studies should take into account evidence that certain therapeutic windows affect specific circuits and associated behavioral phenotypes, but also potentially reopen those critical plasticity periods to enhance therapeutic effectiveness. In particular, the advantage of the SHANK3 gene is that different mouse models can be designed, including different Shank3 gene deletions or failures (Engineer et al., 2018; Poleg et al., 2021). In addition, the SHANK3 protein has a precise location in the glutamatergic synapse. The study of the Shank3 gene is less complicated than that of other autism-related genes (Uchino and Waga, 2015; Tao-Cheng et al., 2016; Wang L. et al., 2020; Golden et al., 2021). Since autism is a neurodevelopmental disorder (symptoms appearing before age three; Lord et al., 2000; Bonaglia et al., 2001), one of the critical questions in autism research is whether the symptoms are reversible in adulthood. Recently, in a study, mice with Shank3-KO (with the deletion of the PDZ domain) had an inverted PDZ domain so that they could be repositioned at any point in the growth phase to re-express the Shank3 gene (Jaramillo et al., 2016, 2017; Jacot-Descombes et al., 2020). This gene design is crucial because it keeps the Shank3 gene under the control of its endogenous genome and

TABLE 1 Targets in Shank3 and treatment effects.

Target	Edit	Related factors	Effect
PDZ domain	Inverted	Homer, GluN2A, GluN2B and GluR2	Repetitive modification, anxiety, social interaction deficits and impaired motor coordination
	Restored in adulthood		All the changes restored
Full length Shank3 gene	Knock-out	mGluR5, AMPAR and NMDAR	Repetitive modification, anxiety, social interaction deficits and impaired motor coordination
	Re-expression in adulthood		Reduce repetitive behaviors and social interaction defects, but cannot relieve anxiety or motor coordination defects,
Exon 11	Knock-out	RAC1 and PAK	Social behavior defects
Exon 6 and 7	Knock-out	GABA	Spatial memory deficits

PDZ, PSD95/DlgA/Zo-1; GluN2A, NMDA receptor 2A; GluN2B, NMDA receptor 2B; GluR2, Glutamate ionotropic receptor AMPA type subunit 2; mGluR5, metabotropic glutamate receptor 5; AMPAR, The α-amino-3-hydroxy-5-methyl-4-isoxazolepropionic acid receptor; NMDAR, The N-methyl-D-aspartate receptor; RAC1, Rac Family Small GTPase 1; PAK, p21-activated kinase; GABA, gamma-aminobutyric acid.

avoids the expression of the SHANK3 gene at a non-physiological level, which may cause potential confusion (Saré et al., 2020). These Shank3-KO mice had defects in neurotransmission in the striatum. As a result, the striatum's synapse density and the levels of essential PSD proteins (SAPAP3, Homer, GluN2A, GluN2B, and GluR2) were reduced. Behaviorally, these Shank3-KO mice showed repetitive self-harm modification, anxiety, social interaction deficits (decreased frequency and duration of social interaction), and impaired motor coordination. By restoring the expression of the Shank3 gene, all these changes could be restored in adulthood (Mei et al., 2016; Guo et al., 2019; Lee et al., 2021).

Re-expression of Shank3 in adulthood can reduce repetitive self-harm behaviors and social interaction deficits but not anxiety or motor coordination defects. Accordingly, this re-expression can only save a portion of the behavioral manifestations of autism (Grabrucker et al., 2011a; Peça et al., 2011a; Tai et al., 2020). A similar study showed that early postpartum intervention could improve irreversible behavioral defects in adulthood (Jin et al., 2018; Bukatova et al., 2021). Therefore, this phenomenon emphasizes the unique performance of SHANK3 expression at specific developmental stages and throughout life. Relying on the emergence of novel gene editing methods (such as CRISPR; Liu et al., 2018; Tu et al., 2019; Chiola et al., 2021), repairing the SHANK3 gene in adulthood can alleviate some synaptic and behavioral disorders related to SHANK3 mutations. Although there are still technical limitations to the genetic manipulation of mature neurons in the fully adult brain, recent research has promoted the application of CRISPR to adult brain repair (Swiech et al., 2015; Lee et al., 2017). More importantly, this work shows the possibility of treating patients with SHANK3 mutations or deletions during adulthood (either pharmacologically or through future genetic modification methods).

Some studies have shown that the re-expression of the Shank3 gene in the brain leads to a complete reversal of the expression of the SHANK3 protein. Previous studies have verified this result (Speed et al., 2015). However, we cannot conclude that this biochemical rescue leads to the rescue of some behaviors or synaptic phenotypes in mutants. Transgene seems to have complex effects on wild-type mouse synaptic transmission (Han et al., 2013; Lin R. et al., 2021). Nevertheless, some scholars have successfully replicated the previous behavioral and electrophysiological findings in Shank3 mutant mouse models (Kouser et al., 2013; Speed et al., 2015).

In summary, these studies indicate that restoring Shank3 levels or downstream signals in adults may be one of the therapeutic ways to alleviate certain synaptic and behavioral disorders associated with Shank3 mutations (Bariselli et al., 2016; Jaramillo et al., 2020; Reichova et al., 2020). As downstream mediators and proteins related to the Shank3 network are regulated, two groups have recently studied mGluR5 and Homer as potential therapeutic targets in ASD (Kouser et al., 2013; Wang X. et al., 2016; Vicidomini et al., 2017; Huang et al., 2021). Using complete Shank3-KO mice (Wang X. et al., 2016), they demonstrated that inhibition of mGluR5 activity could reduce excessive licking, while positive agonists of mGluR5 aggravated self-licking. In another study (Vicidomini et al., 2017), the pharmacological enhancement of mGluR5 activity improved repetitive behavior and rescued other behavioral defects in Shank3-KO mice (Verpelli et al., 2011; Lin et al., 2014). Although these studies may seem contradictory, the mGluR5 positive agonist CDPPB exacerbated self-modification in these studies. These results are based on different Shank3-mutant transgenic mice, which can lead to different results. However, the findings from both studies are consistent in other respects. According to another study (Vicidomini et al., 2017), pharmacological activation of mGluR5 activity alleviated functional (NMDA-induced synaptic membrane depolarization; Arvanov and Wang, 1997; Pisani et al., 2001) and behavioral defects (social interaction and Morris water maze; Wang Y. et al., 2016) in mice with exon 11 deletion. Another study reported that the cortical actin filaments of mice lacking exon 11 were significantly reduced (Duffney et al., 2015). This was attributed to the reduced activity of RAC1 and PAK, as well as the enhanced activity of cofilin (the main factor involved in actin depolymerization; Al-Ayadhi and Halepoto, 2013; Sarowar and Grabrucker, 2016; Yi et al., 2016). This suggests that actin modulators may be another potential molecular target for treating ASD. The increase of RAC1 activity in the PFC of these mice improved their social behavior defects and NMDAR function (Park et al., 2003; Duffney et al., 2013, 2015). In contrast, inhibition of PAK or RAC1 function resulted in social behavior defects and dysregulation of NMDAR function in wild-type mice (Bennett and Lagopoulos, 2014; Lin Y. et al., 2021). The use of drugs in Shank3 mutant mice to reverse their symptoms highlights the potential target pathway. NMDA hypofunction is a potential mechanism of ASD behavior (Won et al., 2012; Lee et al., 2015). Social interaction could be improved by treating mice with CDPPB (probably due to the enhancement of NMDAR function through mGluR5 activation; Won et al., 2012). In recent years, many studies have investigated NMDA-dependent inhibitors, demonstrating their therapeutic efficacy in ASD (King et al., 2001; Minshawi et al., 2016; Wink et al., 2017). The mechanism of the NMDAR antagonist, ketamine, acting on the nervous system, significantly overlaps with the pathophysiological theory of ASD, including destroying synaptic connections and neuronal networks (Wang et al., 2014a,b; Krüttner et al., 2022). However, despite the broad interest throughout psychopharmacology research, ketamine has not been explored in clinical trials of ASD. Furthermore, mice lacking exons 6 and 7 have impaired GABAergic neurotransmission (Orefice et al., 2016; Lim et al., 2017). Collectively, these studies suggest that NMDAR hypofunction leads to specific ASD-like phenotypes in Shank-mutant mice, and other related molecular targets may be used to regulate NMDAR activity. Direct gene targeting in humans appears to be a future treatment option for some types of ASDs, as the recent success of many techniques related to detecting and treating genetic disorders may provide the necessary tools.

5. Conclusion

Although Shank3 mutation is heterozygous in humans, the analysis and identification of Shank3 homozygous mutant mice are imperative for understanding the physiological role of Shank3 and its functional consequences. In addition, the mutation has destructive effects. In terms of the treatment window, the earlier the treatment is administered, the better the outcome. However, interventions in adulthood may still be useful for reducing some of the symptoms associated with SHANK3 mutations. It is necessary to carefully analyze the specific phenotype of a genotype before trying a drug alone. Exploring the *SHANK3* gene may help uncover some of the neurobiological aspects of autism.

Author contributions

MH and TX performed the conceptualization. MH and QQ searched the literature and prepared the draft. All authors contributed to the article and approved the submitted version.

Funding

This work was supported by grant from the Natural Science Foundation of China (82171486), Natural Science Foundation of Shanghai to TX (21ZR1448400), the Interdisciplinary Program of Shanghai Jiao Tong University to TX (YG2021ZD23), and General Science Foundation of Shanghai Sixth People's Hospital to TX (YNMS202114).

Acknowledgments

We thank the lab members for their help on this manuscript.

Conflict of interest

The authors declare that the research was conducted in the absence of any commercial or financial relationships that could be construed as a potential conflict of interest.

The reviewer ZQ declared a shared parent affiliation with the authors to the handling editor at the time of review.

Publisher's note

References

Al-Ayadhi, L., and Halepoto, D. M. (2013). Role of proteomics in the discovery of autism biomarkers. *J. Coll. Physicians Surg. Pak.* 23, 137–143.

Aman, M. G. (2004). Management of hyperactivity and other acting-out problems in patients with autism spectrum disorder. *Semin. Pediatr. Neurol.* 11, 225–228. doi: 10.1016/j.spen.2004.07.006

Aman, M. G., Farmer, C. A., Hollway, J., and Arnold, L. E. (2008). Treatment of inattention, overactivity, and impulsiveness in autism spectrum disorders. *Child Adolesc. Psychiatr. Clin. N. Am.* 17, 713–738. doi: 10.1016/j.chc.2008.06.009

Arons, M. H., Thynne, C. J., Grabrucker, A. M., Li, D., Schoen, M., Cheyne, J. E., et al. (2012). Autism-associated mutations in ProSAP2/Shank3 impair synaptic transmission and neurexin-neuroligin-mediated transsynaptic signaling. *J. Neurosci.* 32, 14966–14978. doi: 10.1523/JNEUROSCI.2215-12.2012

Arvanov, V. L., and Wang, R. Y. (1997). NMDA-induced response in pyramidal neurons of the rat medial prefrontal cortex slices consists of NMDA and non-NMDA components. *Brain Res.* 768, 361–364. doi: 10.1016/S0006-8993(97)00842-1

Auerbach, B. D., Manohar, S., Radziwon, K., and Salvi, R. (2021). Auditory hypersensitivity and processing deficits in a rat model of fragile X syndrome. *Neurobiol. Dis.* 161:105541. doi: 10.1016/j.nbd.2021.105541

Bai, D., Marrus, N., Yip, B. H. K., Reichenberg, A., Constantino, J. N., and Sandin, S. (2020). Inherited risk for autism through maternal and paternal lineage. *Biol. Psychiatry* 88, 480–487. doi: 10.1016/j.biopsych.2020.03.013

Balaan, C., Corley, M. J., Eulalio, T., Leite-Ahyo, K., Pang, A. P. S., Fang, R., et al. (2019). Juvenile Shank3b deficient mice present with behavioral phenotype relevant to autism spectrum disorder. *Behav. Brain Res.* 356, 137–147. doi: 10.1016/j.bbr.2018.08.005

Bangash, M. A., Park, J. M., Melnikova, T., Wang, D., Jeon, S. K., Lee, D., et al. (2011). Enhanced polyubiquitination of Shank3 and NMDA receptor in a mouse model of autism. *Cells* 145, 758–772. doi: 10.1016/j.cell.2011.03.052

Banker, S. M., Gu, X., Schiller, D., and Foss-Feig, J. H. (2021). Hippocampal contributions to social and cognitive deficits in autism spectrum disorder. *Trends Neurosci.* 44, 793–807. doi: 10.1016/j.tins.2021.08.005

Bariselli, S., Tzanoulinou, S., Glangetas, C., Prévost-Solié, C., Pucci, L., Viguié, J., et al. (2016). SHANK3 controls maturation of social reward circuits in the VTA. *Nat. Neurosci.* 19, 926–934. doi: 10.1038/nn.4319

Baum, S. H., Stevenson, R. A., and Wallace, M. T. (2015). Behavioral, perceptual, and neural alterations in sensory and multisensory function in autism spectrum disorder. *Prog. Neurobiol.* 134, 140–160. doi: 10.1016/j.pneurobio.2015.09.007

Becerra, T. A., Von Ehrenstein, O. S., Heck, J. E., Olsen, J., Arah, O. A., Jeste, S. S., et al. (2014). Autism spectrum disorders and race, ethnicity, and nativity: a population-based study. *Pediatrics* 134, e63–e71. doi: 10.1542/peds.2013-3928

Bennett, M. R., and Lagopoulos, J. (2014). Stress and trauma: BDNF control of dendritic-spine formation and regression. *Prog. Neurobiol.* 112, 80–99. doi: 10.1016/j.pneurobio.2013.10.005

Berkel, S., Eltokhi, A., Fröhlich, H., Porras-Gonzalez, D., Rafiullah, R., Sprengel, R., et al. (2018). Sex hormones regulate SHANK expression. *Front. Mol. Neurosci.* 11:337. doi: 10.3389/fnmol.2018.00337

Bey, A. L., Wang, X., Yan, H., Kim, N., Passman, R. L., Yang, Y., et al. (2018). Brain region-specific disruption of Shank3 in mice reveals a dissociation for cortical and striatal circuits in autism-related behaviors. *Transl. Psychiatry* 8:94. doi: 10.1038/s41398-018-0142-6

Bicker, F., Nardi, L., Maier, J., Vasic, V., and Schmeisser, M. J. (2021). Criss-crossing autism spectrum disorder and adult neurogenesis. *J. Neurochem.* 159, 452–478. doi: 10.1111/jnc.15501

Boccuto, L., Lauri, M., Sarasua, S. M., Skinner, C. D., Buccella, D., Dwivedi, A., et al. (2013). Prevalence of SHANK3 variants in patients with different subtypes of autism spectrum disorders. *Eur. J. Hum. Genet.* 21, 310–316. doi: 10.1038/ejhg.2012.175

Bonaglia, M. C., Giorda, R., Beri, S., De Agostini, C., Novara, F., Fichera, M., et al. (2011). Molecular mechanisms generating and stabilizing terminal 22q13 deletions in 44 subjects with Phelan/McDermid syndrome. *PLoS Genet.* 7:e1002173. doi: 10.1371/journal.pgen.1002173

Bonaglia, M. C., Giorda, R., Borgatti, R., Felisari, G., Gagliardi, C., Selicorni, A., et al. (2001). Disruption of the ProSAP2 gene in a t(12,22)(q24.1;q13.3) is associated with the 22q13.3 deletion syndrome. *Am. J. Hum. Genet.* 69, 261–268. doi: 10.1086/321293

Boukhris, T., Sheehy, O., Mottron, L., and Bérard, A. (2016). Antidepressant use during pregnancy and the risk of autism spectrum disorder in children. *JAMA Pediatr.* 170, 117–124. doi: 10.1001/jamapediatrics.2015.3356

Bozdagi, O., Sakurai, T., Papapetrou, D., Wang, X., Dickstein, D. L., Takahashi, N., et al. (2010). Haploinsufficiency of the autism-associated Shank3 gene leads to deficits in synaptic function, social interaction, and social communication. *Mol. Autism.* 1:15. doi: 10.1186/2040-2392-1-15

Bruno, L. P., Doddato, G., Valentino, F., Baldassarri, M., Tita, R., Fallerini, C., et al. (2021). New candidates for autism/intellectual disability identified by whole-exome sequencing. *Int. J. Mol. Sci.* 22:22. doi: 10.3390/ijms222413439

Bukatova, S., Renczes, E., Reichova, A., Filo, J., Sadlonova, A., Mravec, B., et al. (2021). Shank3 deficiency is associated with altered profile of neurotransmission markers in pups and adult mice. *Neurochem. Res.* 46, 3342–3355. doi: 10.1007/s11064-021-03435-6

Burdeus-Olavarrieta, M., San José-Cáceres, A., García-Alcón, A., González-Peñas, J., Hernández-Jusdado, P., and Parellada-Redondo, M. (2021). Characterisation of the clinical phenotype in Phelan-McDermid syndrome. *J. Neurodev. Disord.* 13:26. doi: 10.1186/s11689-021-09370-5

Chen, Q., Deister, C. A., Gao, X., Guo, B., Lynn-Jones, T., Chen, N., et al. (2020). Dysfunction of cortical GABAergic neurons leads to sensory hyper-reactivity in a Shank3 mouse model of ASD. *Nat. Neurosci.* 23, 520–532. doi: 10.1038/s41593-020-0598-6

Chevallier, C., Kohls, G., Troiani, V., Brodkin, E. S., and Schultz, R. T. (2012). The social motivation theory of autism. *Trends Cogn. Sci.* 16, 231–239. doi: 10.1016/j.tics.2012.02.007

Chiola, S., Napan, K. L., Wang, Y., Lazarenko, R. M., Armstrong, C. J., Cui, J., et al. (2021). Defective AMPA-mediated synaptic transmission and morphology in human neurons with hemizygous SHANK3 deletion engrafted in mouse prefrontal cortex. *Mol. Psychiatry* 26, 4670–4686. doi: 10.1038/s41380-021-01023-2

Christensen, D. L., Braun, K. V. N., Baio, J., Bilder, D., Charles, J., Constantino, J. N., et al. (2018). Prevalence and characteristics of autism Spectrum disorder among children aged 8 years - autism and developmental disabilities monitoring network, 11 sites, United States, 2012. *MMWR Surveill. Summ.* 65, 1–23. doi: 10.15585/mmwr.ss6513a1

Costales, J. L., and Kolevzon, A. (2015). Phelan-McDermid syndrome and SHANK3: implications for treatment. *Neurotherapeutics* 12, 620–630. doi: 10.1007/s13311-015-0352-z

Crump, C., Sundquist, J., and Sundquist, K. (2021). Preterm or early term birth and risk of autism. *Pediatrics* 148:e2020032300. doi: 10.1542/peds.2020-032300

D'antoni, S., Spatuzza, M., Bonaccorso, C. M., Musumeci, S. A., Ciranna, L., Nicoletti, F., et al. (2014). Dysregulation of group-I metabotropic glutamate (mGlu) receptor mediated signalling in disorders associated with intellectual disability and autism. *Neurosci. Biobehav. Rev.* 46, 228–241. doi: 10.1016/j.neubiorev.2014.02.003

De Rubeis, S., Siper, P. M., Durkin, A., Weissman, J., Muratet, F., Halpern, D., et al. (2018). Delineation of the genetic and clinical spectrum of Phelan-McDermid syndrome caused by SHANK3 point mutations. *Mol. Autism.* 9:31. doi: 10.1186/s13229-018-0205-9

Delling, J. P., and Boeckers, T. M. (2021). Comparison of SHANK3 deficiency in animal models: phenotypes, treatment strategies, and translational implications. *J. Neurodev. Disord.* 13:55. doi: 10.1186/s11689-021-09397-8

Dhaliwal, K. K., Orsso, C. E., Richard, C., Haqq, A. M., and Zwaigenbaum, L. (2019). Risk factors for unhealthy weight gain and obesity among children with autism Spectrum disorder. *Int. J. Mol. Sci.* 20:3285. doi: 10.3390/ijms20133285

Dhamne, S. C., Silverman, J. L., Super, C. E., Lammers, S. H. T., Hameed, M. Q., Modi, M. E., et al. (2017). Replicable in vivo physiological and behavioral phenotypes of the Shank3B null mutant mouse model of autism. *Mol. Autism.* 8:26. doi: 10.1186/s13229-017-0142-z

Diguiseppi, C., Hepburn, S., Davis, J. M., Fidler, D. J., Hartway, S., Lee, N. R., et al. (2010). Screening for autism spectrum disorders in children with down syndrome: population prevalence and screening test characteristics. *J. Dev. Behav. Pediatr.* 31, 181–191. doi: 10.1097/DBP.0b013e3181d5aa6d

Doshi-Velez, F., Ge, Y., and Kohane, I. (2014). Comorbidity clusters in autism spectrum disorders: an electronic health record time-series analysis. *Pediatrics* 133, e54–e63. doi: 10.1542/peds.2013-0819

Dovey, T. M., Kumari, V., and Blissett, J. (2019). Eating behaviour, behavioural problems and sensory profiles of children with avoidant/restrictive food intake disorder (ARFID), autistic spectrum disorders or picky eating: same or different? *Eur. Psychiatry* 61, 56–62. doi: 10.1016/j.eurpsy.2019.06.008

Drapeau, E., Riad, M., Kajiwara, Y., and Buxbaum, J. D. (2018). Behavioral phenotyping of an improved mouse model of Phelan-McDermid syndrome with a complete deletion of the Shank3 gene. *eNeuro* 5:ENEURO.0046-18.2018. doi: 10.1523/ENEURO.0046-18.2018

Dubois, A., Michelon, C., Rattaz, C., Zabalia, M., and Baghdadli, A. (2017). Daily living pain assessment in children with autism: exploratory study. *Res. Dev. Disabil.* 62, 238–246. doi: 10.1016/j.ridd.2017.01.003

Dubois, A., Rattaz, C., Pry, R., and Baghdadli, A. (2010). Autism and pain - a literature review. *Pain Res. Manag.* 15, 245–253. doi: 10.1155/2010/749275

Duffney, L. J., Wei, J., Cheng, J., Liu, W., Smith, K. R., Kittler, J. T., et al. (2013). Shank3 deficiency induces NMDA receptor hypofunction via an actin-dependent mechanism. *J. Neurosci.* 33, 15767–15778. doi: 10.1523/JNEUROSCI.1175-13.2013

Duffney, L. J., Zhong, P., Wei, J., Matas, E., Cheng, J., Qin, L., et al. (2015). Autism-like deficits in Shank3-deficient mice are rescued by targeting actin regulators. *Cell Rep.* 11, 1400–1413. doi: 10.1016/j.celrep.2015.04.064

Durand, C. M., Betancur, C., Boeckers, T. M., Bockmann, J., Chaste, P., Fauchereau, F., et al. (2007). Mutations in the gene encoding the synaptic scaffolding protein SHANK3 are associated with autism spectrum disorders. *Nat. Genet.* 39, 25–27. doi: 10.1038/ng1933

Engineer, C. T., Rahebi, K. C., Borland, M. S., Buell, E. P., Im, K. W., Wilson, L. G., et al. (2018). Shank3-deficient rats exhibit degraded cortical responses to sound. *Autism Res.* 11, 59–68. doi: 10.1002/aur.1883

Epstein, I., Tushev, G., Will, T. J., Vlatkovic, I., Cajigas, I. J., and Schuman, E. M. (2014). Alternative polyadenylation and differential expression of Shank mRNAs in the synaptic neuropil. *Philos. Trans. R. Soc. Lond. Ser. B Biol. Sci.* 369:20130137. doi: 10.1098/rstb.2013.0137

Esposito, D., Belli, A., Ferri, R., and Bruni, O. (2020). Sleeping without prescription: Management of Sleep Disorders in children with autism with non-pharmacological interventions and over-the-counter treatments. *Brain Sci.* 10:441. doi: 10.3390/brainsci10070441

Estes, M. L., and Mcallister, A. K. (2016). Maternal immune activation: implications for neuropsychiatric disorders. *Science* 353, 772–777. doi: 10.1126/science.aag3194

Frank, Y. (2021). The neurological manifestations of Phelan-McDermid syndrome. *Pediatr. Neurol.* 122, 59–64. doi: 10.1016/j.pediatrneurol.2021.06.002

Frolli, A., Bosco, A., Di Carmine, F., Cavallaro, A., Lombardi, A., Sergi, L., et al. (2021). Parent training and therapy in children with autism. *Pediatr. Rep.* 13, 216–226. doi: 10.3390/pediatric13020030

Gauthier, J., Spiegelman, D., Piton, A., Lafrenière, R. G., Laurent, S., St-Onge, J., et al. (2009). Novel de novo SHANK3 mutation in autistic patients. *Am. J. Med. Genet. B Neuropsychiatr. Genet.* 150b, 421–424. doi: 10.1002/ajmg.b.30822

Gidaya, N. B., Lee, B. K., Burstyn, I., Yudell, M., Mortensen, E. L., and Newschaffer, C. J. (2014). In utero exposure to selective serotonin reuptake inhibitors and risk for autism spectrum disorder. *J. Autism Dev. Disord.* 44, 2558–2567. doi: 10.1007/s10803-014-2128-4

Gillberg, C., and Coleman, M. (1996). Autism and medical disorders: a review of the literature. *Dev. Med. Child Neurol.* 38, 191–202. doi: 10.1111/j.1469-8749.1996.tb15081.x

Golden, C. E. M., Wang, V. X., Harony-Nicolas, H., Hof, P. R., and Buxbaum, J. D. (2021). Reduced brain volume and white matter alterations in Shank3-deficient rats. *Autism Res.* 14, 1837–1842. doi: 10.1002/aur.2568

Gong, X., and Wang, H. (2015). SHANK1 and autism spectrum disorders. *Sci. China Life Sci.* 58, 985–990. doi: 10.1007/s11427-015-4892-6

Grabrucker, A. M., Knight, M. J., Proepper, C., Bockmann, J., Joubert, M., Rowan, M., et al. (2011a). Concerted action of zinc and ProSAP/Shank in synaptogenesis and synapse maturation. *EMBO J.* 30, 569–581. doi: 10.1038/emboj.2010.336

Grabrucker, A. M., Schmeisser, M. J., Schoen, M., and Boeckers, T. M. (2011b). Postsynaptic ProSAP/Shank scaffolds in the cross-hair of synaptopathies. *Trends Cell Biol.* 21, 594–603. doi: 10.1016/j.tcb.2011.07.003

Grafodatskaya, D., Chung, B., Szatmari, P., and Weksberg, R. (2010). Autism spectrum disorders and epigenetics. *J. Am. Acad. Child Adolesc. Psychiatry* 49, 794–809. doi: 10.1016/j.jaac.2010.05.005

Guang, S., Pang, N., Deng, X., Yang, L., He, F., Wu, L., et al. (2018). Synaptopathology involved in autism spectrum disorder. *Front. Cell. Neurosci.* 12:470. doi: 10.3389/fncel.2018.00470

Guo, B., Chen, J., Chen, Q., Ren, K., Feng, D., Mao, H., et al. (2019). Anterior cingulate cortex dysfunction underlies social deficits in Shank3 mutant mice. *Nat. Neurosci.* 22, 1223–1234. doi: 10.1038/s41593-019-0445-9

Hadjistavropoulos, T., and Craig, K. D. (2002). A theoretical framework for understanding self-report and observational measures of pain: a communications model. *Behav. Res. Ther.* 40, 551–570. doi: 10.1016/s0005-7967(01)00072-9

Han, K., Holder, J. L. Jr., Schaaf, C. P., Lu, H., Chen, H., Kang, H., et al. (2013). SHANK3 overexpression causes manic-like behaviour with unique pharmacogenetic properties. *Nature* 503, 72–77. doi: 10.1038/nature12630

Han, Q., Kim, Y. H., Wang, X., Liu, D., Zhang, Z. J., Bey, A. L., et al. (2016). SHANK3 deficiency impairs heat hyperalgesia and TRPV1 signaling in primary sensory neurons. *Neuron* 92, 1279–1293. doi: 10.1016/j.neuron.2016.11.007

Hoover, D. W., and Kaufman, J. (2018). Adverse childhood experiences in children with autism spectrum disorder. *Curr. Opin. Psychiatry* 31, 128–132. doi: 10.1097/YCO.0000000000000390

Hsueh, Y. P. (2019). Synaptic formation, neural circuits and neurodevelopmental disorders controlled by signaling, translation, and epigenetic regulation. *Dev. Neurobiol.* 79, 2–7. doi: 10.1002/dneu.22655

Huang, M., Pu, S., Jiang, W., Worley, P. F., and Xu, T. (2021). Deficiency of SHANK3 isoforms impairs thermal hyperalgesia and dysregulates the expression of postsynaptic proteins in the spinal cord. *Neurosci. Res.* 163, 26–33. doi: 10.1016/j.neures.2020.03.001

Hyman, S. L., Levy, S. E., and Myers, S. M. (2020). Identification, evaluation, and management of children with autism spectrum disorder. *Pediatrics* 145:e20193447. doi: 10.1542/peds.2019-3447

Jacot-Descombes, S., Keshav, N. U., Dickstein, D. L., Wicinski, B., Janssen, W. G. M., Hiester, L. L., et al. (2020). Altered synaptic ultrastructure in the prefrontal cortex of Shank3-deficient rats. *Mol. Autism.* 11:89. doi: 10.1186/s13229-020-00393-8

Jaramillo, T. C., Speed, H. E., Xuan, Z., Reimers, J. M., Escamilla, C. O., Weaver, T. P., et al. (2017). Novel Shank3 mutant exhibits behaviors with face validity for autism and altered striatal and hippocampal function. *Autism Res.* 10, 42–65. doi: 10.1002/aur.1664

Jaramillo, T. C., Speed, H. E., Xuan, Z., Reimers, J. M., Liu, S., and Powell, C. M. (2016). Altered striatal synaptic function and abnormal behaviour in Shank3 Exon4-9 deletion mouse model of autism. *Autism Res.* 9, 350–375. doi: 10.1002/aur.1529

Jaramillo, T. C., Xuan, Z., Reimers, J. M., Escamilla, C. O., Liu, S., and Powell, C. M. (2020). Early restoration of Shank3 expression in Shank3 Knock-out mice prevents Core ASD-like behavioral phenotypes. *eNeuro* 7:ENEURO.0332-19.2020. doi: 10.1523/ENEURO.0332-19.2020

Jeong, J., Li, Y., and Roche, K. W. (2021). CaMKII phosphorylation regulates synaptic enrichment of Shank3. *eNeuro* 8, ENEURO.0481–ENEU20.2021. doi: 10.1523/ENEURO.0481-20.2021

Jiang, Y. H., and Ehlers, M. D. (2013). Modeling autism by SHANK gene mutations in mice. *Neuron* 78, 8–27. doi: 10.1016/j.neuron.2013.03.016

Jin, C., Kang, H., Ryu, J. R., Kim, S., Zhang, Y., Lee, Y., et al. (2018). Integrative brain transcriptome analysis reveals region-specific and broad molecular changes in Shank3-overexpressing mice. *Front. Mol. Neurosci.* 11:250. doi: 10.3389/fnmol.2018.00250

Johannessen, M., Haugen, I. B., Bakken, T. L., and Braaten, Ø. (2019). A 22q13.33 duplication harbouring the SHANK3 gene: does it cause neuropsychiatric disorders? *BMJ Case Rep.* 12:e228258. doi: 10.1136/bcr-2018-228258

Jokiranta, E., Brown, A. S., Heinimaa, M., Cheslack-Postava, K., Suominen, A., and Sourander, A. (2013). Parental psychiatric disorders and autism spectrum disorders. *Psychiatry Res.* 207, 203–211. doi: 10.1016/j.psychres.2013.01.005

Kabitzke, P., Morales, D., He, D., Cox, K., Sutphen, J., Thiede, L., et al. (2020). Mouse model systems of autism spectrum disorder: replicability and informatics signature. *Genes Brain Behav.* 19:e12676. doi: 10.1111/gbb.12676

Kales, H. C., Gitlin, L. N., and Lyketsos, C. G. (2015). Assessment and management of behavioral and psychological symptoms of dementia. *BMJ* 350:h369. doi: 10.1136/bmj.h369

Kincaid, D. L., Doris, M., Shannon, C., and Mulholland, C. (2017). What is the prevalence of autism spectrum disorder and ASD traits in psychosis? A systematic review. *Psychiatry Res.* 250, 99–105. doi: 10.1016/j.psychres.2017.01.017

King, B. H., Wright, D. M., Handen, B. L., Sikich, L., Zimmerman, A. W., Mcmahon, W., et al. (2001). Double-blind, placebo-controlled study of amantadine hydrochloride in the treatment of children with autistic disorder. *J. Am. Acad. Child Adolesc. Psychiatry* 40, 658–665. doi: 10.1097/00004583-200106000-00010

Kloth, A. D., Badura, A., Li, A., Cherskov, A., Connolly, S. G., Giovannucci, A., et al. (2015). Cerebellar associative sensory learning defects in five mouse autism models. *elife* 4:e06085. doi: 10.7554/eLife.06085

Kodak, T., and Bergmann, S. (2020). Autism Spectrum disorder: characteristics, associated behaviors, and early intervention. *Pediatr. Clin. N. Am.* 67, 525–535. doi: 10.1016/j.pcl.2020.02.007

Kouser, M., Speed, H. E., Dewey, C. M., Reimers, J. M., Widman, A. J., Gupta, N., et al. (2013). Loss of predominant Shank3 isoforms results in hippocampus-dependent impairments in behavior and synaptic transmission. *J. Neurosci.* 33, 18448–18468. doi: 10.1523/JNEUROSCI.3017-13.2013

Krüttner, S., Falasconi, A., Valbuena, S., Galimberti, I., Bouwmeester, T., Arber, S., et al. (2022). Absence of familiarity triggers hallmarks of autism in mouse model through aberrant tail-of-striatum and prelimbic cortex signaling. *Neuron* 110, 1468–1482.e5. doi: 10.1016/j.neuron.2022.02.001

Landrigan, P. J. (2010). What causes autism? Exploring the environmental contribution. *Curr. Opin. Pediatr.* 22, 219–225. doi: 10.1097/MOP.0b013e328336eb9a

Leblond, C. S., Nava, C., Polge, A., Gauthier, J., Huguet, G., Lumbroso, S., et al. (2014). Meta-analysis of SHANK mutations in autism spectrum disorders: a gradient of severity in cognitive impairments. *PLoS Genet.* 10:e1004580. doi: 10.1371/journal.pgen.1004580

Lee, J., Chung, C., Ha, S., Lee, D., Kim, D. Y., Kim, H., et al. (2015). Shank3-mutant mice lacking exon 9 show altered excitation/inhibition balance, enhanced rearing, and spatial memory deficit. *Front. Cell. Neurosci.* 9:94. doi: 10.3389/fncel.2015.00094

Lee, L. C., Harrington, R. A., Chang, J. J., and Connors, S. L. (2008). Increased risk of injury in children with developmental disabilities. *Res. Dev. Disabil.* 29, 247–255. doi: 10.1016/j.ridd.2007.05.002

Lee, D. K., Li, S. W., Bounni, F., Friedman, G., Jamali, M., Strahs, L., et al. (2021). Reduced sociability and social agency encoding in adult Shank3-mutant mice are restored through gene re-expression in real time. *Nat. Neurosci.* 24, 1243–1255. doi: 10.1038/s41593-021-00888-4

Lee, B., Zhang, Y., Kim, Y., Kim, S., Lee, Y., and Han, K. (2017). Age-dependent decrease of GAD65/67 mRNAs but normal densities of GABAergic interneurons in the brain regions of Shank3-overexpressing manic mouse model. *Neurosci. Lett.* 649, 48–54. doi: 10.1016/j.neulet.2017.04.016

Li, W., and Pozzo-Miller, L. (2020). Dysfunction of the corticostriatal pathway in autism spectrum disorders. *J. Neurosci. Res.* 98, 2130–2147. doi: 10.1002/jnr.24560

Lim, C. S., Kim, H., Yu, N. K., Kang, S. J., Kim, T., Ko, H. G., et al. (2017). Enhancing inhibitory synaptic function reverses spatial memory deficits in Shank2 mutant mice. *Neuropharmacology* 112, 104–112. doi: 10.1016/j.neuropharm.2016.08.016

Lin, C. W., Chen, C. Y., Cheng, S. J., Hu, H. T., and Hsueh, Y. P. (2014). Sarm1 deficiency impairs synaptic function and leads to behavioral deficits, which can be ameliorated by an mGluR allosteric modulator. *Front. Cell. Neurosci.* 8:87. doi: 10.3389/fncel.2014.00087

Lin, R., Learman, L. N., Bangash, M. A., Melnikova, T., Leyder, E., Reddy, S. C., et al. (2021). Homer1a regulates Shank3 expression and underlies behavioral vulnerability to stress in a model of Phelan-McDermid syndrome. *Cell Rep.* 37:110014. doi: 10.1016/j.celrep.2021.110014

Lin, Y., Li, H., Peng, J., Li, C., Zhu, C., Zhou, Y., et al. (2021). Decrease of morphine-CPP by sinomenine via mediation of tyrosine hydroxylase, NMDA receptor subunit 2B and opioid receptor in the zebrafish brain. *Pak. J. Pharm. Sci.* 34, 1659–1665.

Liu, C. X., Li, C. Y., Hu, C. C., Wang, Y., Lin, J., Jiang, Y. H., et al. (2018). CRISPR/Cas9-induced shank3b mutant zebrafish display autism-like behaviors. *Mol. Autism.* 9:23. doi: 10.1186/s13229-018-0204-x

Lord, C., Brugha, T. S., Charman, T., Cusack, J., Dumas, G., Frazier, T., et al. (2020). Autism spectrum disorder. *Nat. Rev. Dis. Primers* 6:5. doi: 10.1038/s41572-019-0138-4

Lord, C., Cook, E. H., Leventhal, B. L., and Amaral, D. G. (2000). Autism spectrum disorders. *Neuron* 28, 355–363. doi: 10.1016/S0896-6273(00)00115-X

Lutz, A. K., Pfaender, S., Incearap, B., Ioannidis, V., Ottonelli, I., Föhr, K. J., et al. (2020). Autism-associated SHANK3 mutations impair maturation of neuromuscular junctions and striated muscles. *Sci. Transl. Med.* 12:eaaz3267. doi: 10.1126/scitranslmed.aaz3267

Mansouri, M., Pouretemad, H., Roghani, M., Wegener, G., and Ardalan, M. (2020). Autistic-like behaviours and associated brain structural plasticity are modulated by oxytocin in maternally separated rats. *Behav. Brain Res.* 393:112756. doi: 10.1016/j.bbr.2020.112756

Mashayekhi, F., Mizban, N., Bidabadi, E., and Salehi, Z. (2021). The association of SHANK3 gene polymorphism and autism. *Minerva Pediatr.* 73, 251–255. doi: 10.23736/S2724-5276.16.04539-4

Masi, A., Demayo, M. M., Glozier, N., and Guastella, A. J. (2017). An overview of autism Spectrum disorder, heterogeneity and treatment options. *Neurosci. Bull.* 33, 183–193. doi: 10.1007/s12264-017-0100-y

Mccarthy, A., Wafford, K., Shanks, E., Ligocki, M., Edgar, D. M., and Dijk, D. J. (2016). REM sleep homeostasis in the absence of REM sleep: effects of antidepressants. *Neuropharmacology* 108, 415–425. doi: 10.1016/j.neuropharm.2016.04.047

Mei, Y., Monteiro, P., Zhou, Y., Kim, J. A., Gao, X., Fu, Z., et al. (2016). Adult restoration of Shank3 expression rescues selective autistic-like phenotypes. *Nature* 530, 481–484. doi: 10.1038/nature16971

Minshawi, N. F., Wink, L. K., Shaffer, R., Plawecki, M. H., Posey, D. J., Liu, H., et al. (2016). A randomized, placebo-controlled trial of D-cycloserine for the enhancement of social skills training in autism spectrum disorders. *Mol. Autism.* 7:2. doi: 10.1186/s13229-015-0062-8

Modabbernia, A., Velthorst, E., and Reichenberg, A. (2017). Environmental risk factors for autism: an evidence-based review of systematic reviews and meta-analyses. *Mol. Autism.* 8:13. doi: 10.1186/s13229-017-0121-4

Moessner, R., Marshall, C. R., Sutcliffe, J. S., Skaug, J., Pinto, D., Vincent, J., et al. (2007). Contribution of SHANK3 mutations to autism spectrum disorder. *Am. J. Hum. Genet.* 81, 1289–1297. doi: 10.1086/522590

Monteiro, P., and Feng, G. (2017). SHANK proteins: roles at the synapse and in autism spectrum disorder. *Nat. Rev. Neurosci.* 18, 147–157. doi: 10.1038/nrn.2016.183

Moon, S. J., Hwang, J. S., Shin, A. L., Kim, J. Y., Bae, S. M., Sheehy-Knight, J., et al. (2019). Accuracy of the childhood autism rating scale: a systematic review and meta-analysis. *Dev. Med. Child Neurol.* 61, 1030–1038. doi: 10.1111/dmcn.14246

Moore, D. J. (2015). Acute pain experience in individuals with autism spectrum disorders: a review. *Autism* 19, 387–399. doi: 10.1177/1362361314527839

Mossa, A., Pagano, J., Ponzoni, L., Tozzi, A., Vezzoli, E., Sciaccaluga, M., et al. (2021). Developmental impaired Akt signaling in the Shank1 and Shank3 double knock-out mice. *Mol. Psychiatry* 26, 1928–1944. doi: 10.1038/s41380-020-00979-x

Moutin, E., Sakkaki, S., Compan, V., Bouquier, N., Giona, F., Areias, J., et al. (2021). Restoring glutamate receptosome dynamics at synapses rescues autism-like deficits in Shank3-deficient mice. *Mol. Psychiatry* 26, 7596–7609. doi: 10.1038/s41380-021-01230-x

Muskens, J. B., Velders, F. P., and Staal, W. G. (2017). Medical comorbidities in children and adolescents with autism spectrum disorders and attention deficit hyperactivity disorders: a systematic review. *Eur. Child Adolesc. Psychiatry* 26, 1093–1103. doi: 10.1007/s00787-017-1020-0

Muskens, J. B., Vermeulen, K., Van Deurzen, P. A., Tomesen, E. M., Van Der Gaag, R. J., Buitelaar, J. K., et al. (2015). Somatic screening in child and adolescent psychiatry: a descriptive pilot study. *Tijdschr. Psychiatr.* 57, 710–718.

Neal, D., Matson, J. L., and Hattier, M. A. (2012). A comparison of diagnostic criteria on the autism Spectrum disorder observation for children (ASD-OC). *Dev. Neurorehabil.* 15, 329–335. doi: 10.3109/17518423.2012.697492

Needham, B. D., Adame, M. D., Serena, G., Rose, D. R., Preston, G. M., Conrad, M. C., et al. (2021). Plasma and fecal metabolite profiles in autism spectrum disorder. *Biol. Psychiatry* 89, 451–462. doi: 10.1016/j.biopsych.2020.09.025

Nuzzo, T., Sekine, M., Punzo, D., Miroballo, M., Katane, M., Saitoh, Y., et al. (2020). Dysfunctional d-aspartate metabolism in BTBR mouse model of idiopathic autism. *Biochim. Biophys. Acta, Proteins Proteomics* 1868:140531. doi: 10.1016/j.bbapap.2020.140531

Ogata, H., Ihara, H., Murakami, N., Gito, M., Kido, Y., and Nagai, T. (2014). Autism spectrum disorders and hyperactive/impulsive behaviors in Japanese patients with Prader-Willi syndrome: a comparison between maternal uniparental disomy and deletion cases. *Am. J. Med. Genet. A* 164a, 2180–2186. doi: 10.1002/ajmg.a.36615

Orefice, L. L., Mosko, J. R., Morency, D. T., Wells, M. F., Tasnim, A., Mozeika, S. M., et al. (2019). Targeting peripheral somatosensory neurons to improve tactile-related phenotypes in ASD models. *Cells* 178, 867–886.e824. doi: 10.1016/j.cell.2019.07.024

Orefice, L. L., Zimmerman, A. L., Chirila, A. M., Sleboda, S. J., Head, J. P., and Ginty, D. D. (2016). Peripheral mechanosensory neuron dysfunction underlies tactile and behavioral deficits in mouse models of ASDs. *Cells* 166, 299–313. doi: 10.1016/j.cell.2016.05.033

Pagliardini, S., Ren, J., Wevrick, R., and Greer, J. J. (2005). Developmental abnormalities of neuronal structure and function in prenatal mice lacking the prader-willi syndrome gene necdin. *Am. J. Pathol.* 167, 175–191. doi: 10.1016/S0002-9440(10)62964-1

Panjwani, A. A., Ji, Y., Fahey, J. W., Palmer, A., Wang, G., Hong, X., et al. (2020). Maternal dyslipidemia, plasma branched-chain amino acids, and the risk of child autism spectrum disorder: evidence of sex difference. *J. Autism Dev. Disord.* 50, 540–550. doi: 10.1007/s10803-019-04264-x

Pardo, C. A., and Eberhart, C. G. (2007). The neurobiology of autism. *Brain Pathol.* 17, 434–447. doi: 10.1016/j.cell.2019.12.036

Park, E., Na, M., Choi, J., Kim, S., Lee, J. R., Yoon, J., et al. (2003). The Shank family of postsynaptic density proteins interacts with and promotes synaptic accumulation of the beta PIX guanine nucleotide exchange factor for Rac1 and Cdc42. *J. Biol. Chem.* 278, 19220–19229. doi: 10.1074/jbc.M301052200

Peça, J., Feliciano, C., Ting, J. T., Wang, W., Wells, M. F., Venkatraman, T. N., et al. (2011a). Shank3 mutant mice display autistic-like behaviours and striatal dysfunction. *Nature* 472, 437–442. doi: 10.1038/nature09965

Peça, J., Ting, J., and Feng, G. (2011b). SnapShot: autism and the synapse. *Cells* 147:706.e701. doi: 10.1016/j.cell.2011.10.015

Pendyala, G., Chou, S., Jung, Y., Coiro, P., Spartz, E., Padmashri, R., et al. (2017). Maternal immune activation causes behavioral impairments and altered cerebellar

cytokine and synaptic protein expression. *Neuropsychopharmacology* 42, 1435–1446. doi: 10.1038/npp.2017.7

Phelan, K., and Mcdermid, H. E. (2012). The 22q13.3 deletion syndrome (Phelan-McDermid syndrome). *Mol. Syndromol.* 2, 186–201. doi: 10.1159/000334260

Phelan, M. C., Rogers, R. C., Saul, R. A., Stapleton, G. A., Sweet, K., Mcdermid, H., et al. (2001). 22q13 deletion syndrome. *Am. J. Med. Genet.* 101, 91–99. doi: 10.1177/000992280404300106

Pisani, A., Gubellini, P., Bonsi, P., Conquet, F., Picconi, B., Centonze, D., et al. (2001). Metabotropic glutamate receptor 5 mediates the potentiation of N-methyl-D-aspartate responses in medium spiny striatal neurons. *Neuroscience* 106, 579–587. doi: 10.1016/s0306-4522(01)00297-4

Poleg, S., Kourieh, E., Ruban, A., Shapira, G., Shomron, N., Barak, B., et al. (2021). Behavioral aspects and neurobiological properties underlying medical cannabis treatment in Shank3 mouse model of autism spectrum disorder. *Transl. Psychiatry* 11:524. doi: 10.1038/s41398-021-01612-3

Purushotham, S. S., Reddy, N. M. N., D'souza, M. N., Choudhury, N. R., Ganguly, A., Gopalakrishna, N., et al. (2022). A perspective on molecular signalling dysfunction, its clinical relevance and therapeutics in autism spectrum disorder. *Exp. Brain Res.* 240, 2525–2567. doi: 10.1007/s00221-022-06448-x

Qin, Y., Du, Y., Chen, L., Liu, Y., Xu, W., Liu, Y., et al. (2022). A recurrent SHANK1 mutation implicated in autism spectrum disorder causes autistic-like core behaviors in mice via downregulation of mGluR1-IP3R1-calcium signaling. *Mol. Psychiatry* 27, 2985–2998. doi: 10.1038/s41380-022-01539-1

Qin, L., Ma, K., Wang, Z. J., Hu, Z., Matas, E., Wei, J., et al. (2018). Social deficits in Shank3-deficient mouse models of autism are rescued by histone deacetylase (HDAC) inhibition. *Nat. Neurosci.* 21, 564–575. doi: 10.1038/s41593-018-0110-8

Raghavan, R., Riley, A. W., Volk, H., Caruso, D., Hironaka, L., Sices, L., et al. (2018). Maternal multivitamin intake, plasma folate and vitamin B (12) levels and autism Spectrum disorder risk in offspring. *Paediatr. Perinat. Epidemiol.* 32, 100–111. doi: 10.1111/ppe.12414

Randall, M., Egberts, K. J., Samtani, A., Scholten, R. J., Hooft, L., Livingstone, N., et al. (2018). Diagnostic tests for autism spectrum disorder (ASD) in preschool children. *Cochrane Database Syst. Rev.* 7:Cd009044. doi: 10.1002/14651858.CD009044

Rattaz, C., Dubois, A., Michelon, C., Viellard, M., Poinso, F., and Baghdadli, A. (2013). How do children with autism spectrum disorders express pain? A comparison with developmentally delayed and typically developing children. *Pain* 154, 2007–2013. doi: 10.1016/j.pain.2013.06.011

Reed, M. D., Yim, Y. S., Wimmer, R. D., Kim, H., Ryu, C., Welch, G. M., et al. (2020). IL-17a promotes sociability in mouse models of neurodevelopmental disorders. *Nature* 577, 249–253. doi: 10.1038/s41586-019-1843-6

Reichova, A., Bacova, Z., Bukatova, S., Kokavcova, M., Meliskova, V., Frimmel, K., et al. (2020). Abnormal neuronal morphology and altered synaptic proteins are restored by oxytocin in autism-related SHANK3 deficient model. *Mol. Cell. Endocrinol.* 518:110924. doi: 10.1016/j.mce.2020.110924

Rendall, A. R., Perrino, P. A., Buscarello, A. N., and Fitch, R. H. (2019). Shank3B mutant mice display pitch discrimination enhancements and learning deficits. *Int. J. Dev. Neurosci.* 72, 13–21. doi: 10.1016/j.ijdevneu.2018.10.003

Rhine, M. A., Parrott, J. M., Schultz, M. N., Kazdoba, T. M., and Crawley, J. N. (2019). Hypothesis-driven investigations of diverse pharmacological targets in two mouse models of autism. *Autism Res.* 12, 401–421. doi: 10.1002/aur.2066

Roberts, J. L., Hovanes, K., Dasouki, M., Manzardo, A. M., and Butler, M. G. (2014). Chromosomal microarray analysis of consecutive individuals with autism spectrum disorders or learning disability presenting for genetic services. *Gene* 535, 70–78. doi: 10.1016/j.gene.2013.10.020

Rodin, R. E., Dou, Y., Kwon, M., Sherman, M. A., Dgama, A. M., Doan, R. N., et al. (2021). The landscape of somatic mutation in cerebral cortex of autistic and neurotypical individuals revealed by ultra-deep whole-genome sequencing. *Nat. Neurosci.* 24, 176–185. doi: 10.1038/s41593-020-00765-6

Salomaa, S. I., Miihkinen, M., Kremneva, E., Paatero, I., Lilja, J., Jacquemet, G., et al. (2021). SHANK3 conformation regulates direct actin binding and crosstalk with Rap1 signaling. *Curr. Biol.* 31, 4956–4970.e4959. doi: 10.1016/j.cub.2021.09.022

Saré, R. M., Lemons, A., Song, A., and Smith, C. B. (2020). Sleep duration in mouse models of neurodevelopmental disorders. *Brain Sci.* 11:31. doi: 10.3390/brainsci11010031

Sarowar, T., and Grabrucker, A. M. (2016). Actin-dependent alterations of dendritic spine morphology in Shankopathies. *Neural Plast.* 2016:8051861. doi: 10.1155/2016/8051861

Saupe, J., Roske, Y., Schillinger, C., Kamdem, N., Radetzki, S., Diehl, A., et al. (2011). Discovery, structure-activity relationship studies, and crystal structure of nonpeptide inhibitors bound to the Shank3 PDZ domain. *ChemMedChem* 6, 1411–1422. doi: 10.1002/cmdc.201100094

Schroeder, J. C., Reim, D., Boeckers, T. M., and Schmeisser, M. J. (2017). Genetic animal models for autism spectrum disorder. *Curr. Top. Behav. Neurosci.* 30, 311–324. doi: 10.1007/7854_2015_407

Sgritta, M., Dooling, S. W., Buffington, S. A., Momin, E. N., Francis, M. B., Britton, R. A., et al. (2019). Mechanisms underlying microbial-mediated changes in social behavior in mouse models of autism spectrum disorder. *Neuron* 101, 246–259.e246. doi: 10.1016/j.neuron.2018.11.018

Sharma, S. R., Gonda, X., and Tarazi, F. I. (2018). Autism spectrum disorder: classification, diagnosis and therapy. *Pharmacol. Ther.* 190, 91–104. doi: 10.1016/j.pharmthera.2018.05.007

Shcheglovitov, A., Shcheglovitova, O., Yazawa, M., Portmann, T., Shu, R., Sebastiano, V., et al. (2013). SHANK3 and IGF1 restore synaptic deficits in neurons from 22q13 deletion syndrome patients. *Nature* 503, 267–271. doi: 10.1038/nature12618

Shi, R., Redman, P., Ghose, D., Hwang, H., Liu, Y., Ren, X., et al. (2017). Shank proteins differentially regulate synaptic transmission. *eNeuro* 4:ENEURO.0163-15.2017. doi: 10.1523/ENEURO.0163-15.2017

Siu, M. T., and Weksberg, R. (2017). Epigenetics of autism spectrum disorder. *Adv. Exp. Med. Biol.* 978, 63–90. doi: 10.1007/978-3-319-53889-1_4

Soler, J., Fañanás, L., Parellada, M., Krebs, M. O., Rouleau, G. A., and Fatjó-Vilas, M. (2018). Genetic variability in scaffolding proteins and risk for schizophrenia and autism-spectrum disorders: a systematic review. *J. Psychiatry Neurosci.* 43, 223–244. doi: 10.1503/jpn.170066

Song, T. J., Lan, X. Y., Wei, M. P., Zhai, F. J., Boeckers, T. M., Wang, J. N., et al. (2019). Altered behaviors and impaired synaptic function in a novel rat model with a complete Shank3 deletion. *Front. Cell. Neurosci.* 13:111. doi: 10.3389/fncel.2019.00111

Soorya, L., Kolevzon, A., Zweifach, J., Lim, T., Dobry, Y., Schwartz, L., et al. (2013). Prospective investigation of autism and genotype-phenotype correlations in 22q13 deletion syndrome and SHANK3 deficiency. *Mol. Autism.* 4:18. doi: 10.1186/2040-2392-4-18

Speed, H. E., Kouser, M., Xuan, Z., Liu, S., Duong, A., and Powell, C. M. (2019). Apparent genetic rescue of adult Shank3 exon 21 insertion mutation mice tempered by appropriate control experiments. *eNeuro* 6:ENEURO.0317-19.2019. doi: 10.1523/ENEURO.0317-19.2019

Speed, H. E., Kouser, M., Xuan, Z., Reimers, J. M., Ochoa, C. F., Gupta, N., et al. (2015). Autism-associated insertion mutation (InsG) of Shank3 exon 21 causes impaired synaptic transmission and behavioral deficits. *J. Neurosci.* 35, 9648–9665. doi: 10.1523/JNEUROSCI.3125-14.2015

Srivastava, S., Condy, E., Carmody, E., Filip-Dhima, R., Kapur, K., Bernstein, J. A., et al. (2021). Parent-reported measure of repetitive behavior in Phelan-McDermid syndrome. *J. Neurodev. Disord.* 13:53. doi: 10.1186/s11689-021-09398-7

Swiech, L., Heidenreich, M., Banerjee, A., Habib, N., Li, Y., Trombetta, J., et al. (2015). In vivo interrogation of gene function in the mammalian brain using CRISPR-Cas9. *Nat. Biotechnol.* 33, 102–106. doi: 10.1038/nbt.3055

Tai, C., Chang, C. W., Yu, G. Q., Lopez, I., Yu, X., Wang, X., et al. (2020). Tau reduction prevents key features of autism in mouse models. *Neuron* 106, 421–437.e411. doi: 10.1016/j.neuron.2020.01.038

Tammimies, K. (2019). Genetic mechanisms of regression in autism spectrum disorder. *Neurosci. Biobehav. Rev.* 102, 208–220. doi: 10.1016/j.neubiorev.2019.04.022

Tao-Cheng, J. H., Toy, D., Winters, C. A., Reese, T. S., and Dosemeci, A. (2016). Zinc stabilizes Shank3 at the postsynaptic density of hippocampal synapses. *PLoS One* 11:e0153979. doi: 10.1371/journal.pone.0153979

Tatavarty, V., Torrado Pacheco, A., Groves Kuhnle, C., Lin, H., Koundinya, P., Miska, N. J., et al. (2020). Autism-associated Shank3 is essential for homeostatic compensation in rodent V1. *Neuron* 106, 769–777.e764. doi: 10.1016/j.neuron.2020.02.033

Thapar, A., Cooper, M., and Rutter, M. (2017). Neurodevelopmental disorders. Lancet. *Psychiatry* 4, 339–346. doi: 10.1016/S2215-0366(16)30376-5

Tu, Z., Zhao, H., Li, B., Yan, S., Wang, L., Tang, Y., et al. (2019). CRISPR/Cas9-mediated disruption of SHANK3 in monkey leads to drug-treatable autism-like symptoms. *Hum. Mol. Genet.* 28, 561–571. doi: 10.1093/hmg/ddy367

Tuchman, R., Cuccaro, M., and Alessandri, M. (2010). Autism and epilepsy: historical perspective. *Brain Dev.* 32, 709–718. doi: 10.1016/j.braindev.2010.04.008

Uchino, S., and Waga, C. (2015). Novel therapeutic approach for autism spectrum disorder: focus on SHANK3. *Curr. Neuropharmacol.* 13, 786–792. doi: 10.2174/1570159x13666151029105547

Vannucchi, G., Masi, G., Toni, C., Dell'osso, L., Erfurth, A., and Perugi, G. (2014). Bipolar disorder in adults with Asperger's syndrome: a systematic review. *J. Affect. Disord.* 168, 151–160. doi: 10.1016/j.jad.2014.06.042

Varghese, M., Keshav, N., Jacot-Descombes, S., Warda, T., Wicinski, B., Dickstein, D. L., et al. (2017). Autism spectrum disorder: neuropathology and animal models. *Acta Neuropathol.* 134, 537–566. doi: 10.1007/s00401-017-1736-4

Verpelli, C., Dvoretskova, E., Vicidomini, C., Rossi, F., Chiappalone, M., Schoen, M., et al. (2011). Importance of Shank3 protein in regulating metabotropic glutamate receptor 5 (mGluR5) expression and signaling at synapses. *J. Biol. Chem.* 286, 34839–34850. doi: 10.1074/jbc.M111.258384

Vicidomini, C., Ponzoni, L., Lim, D., Schmeisser, M. J., Reim, D., Morello, N., et al. (2017). Pharmacological enhancement of mGlu5 receptors rescues behavioral deficits in SHANK3 knock-out mice. *Mol. Psychiatry* 22, 689–702. doi: 10.1038/mp.2016.30

Vyas, Y., Cheyne, J. E., Lee, K., Jung, Y., Cheung, P. Y., and Montgomery, J. M. (2021). Shankopathies in the developing brain in autism Spectrum disorders. *Front. Neurosci.* 15:775431. doi: 10.3389/fnins.2021.775431

Wang, L., Adamski, C. J., Bondar, V. V., Craigen, E., Collette, J. R., Pang, K., et al. (2020). A kinome-wide RNAi screen identifies ERK2 as a druggable regulator of Shank3 stability. *Mol. Psychiatry* 25, 2504–2516. doi: 10.1038/s41380-018-0325-9

Wang, X., Bey, A. L., Chung, L., Krystal, A. D., and Jiang, Y. H. (2014a). Therapeutic approaches for shankopathies. *Dev. Neurobiol.* 74, 123–135. doi: 10.1002/dneu.22084

Wang, X., Bey, A. L., Katz, B. M., Badea, A., Kim, N., David, L. K., et al. (2016). Altered mGluR5-Homer scaffolds and corticostriatal connectivity in a Shank3 complete knockout model of autism. *Nat. Commun.* 7:11459. doi: 10.1038/ncomms11459

Wang, Z., Ding, R., and Wang, J. (2020). The association between vitamin D status and autism Spectrum disorder (ASD): a systematic review and meta-analysis. *Nutrients* 13:86. doi: 10.3390/nu13010086

Wang, Y., Ma, Y., Hu, J., Zhang, X., Cheng, W., Jiang, H., et al. (2016). Sex-specific effects of prenatal chronic mild stress on adult spatial learning capacity and regional glutamate receptor expression profiles. *Exp. Neurol.* 281, 66–80. doi: 10.1016/j.expneurol.2016.04.016

Wang, X., Mccoy, P. A., Rodriguiz, R. M., Pan, Y., Je, H. S., Roberts, A. C., et al. (2011). Synaptic dysfunction and abnormal behaviors in mice lacking major isoforms of Shank3. *Hum. Mol. Genet.* 20, 3093–3108. doi: 10.1093/hmg/ddr212

Wang, X., Xu, Q., Bey, A. L., Lee, Y., and Jiang, Y. H. (2014b). Transcriptional and functional complexity of Shank3 provides a molecular framework to understand the phenotypic heterogeneity of SHANK3 causing autism and Shank3 mutant mice. *Mol. Autism.* 5:30. doi: 10.1186/2040-2392-5-30

Wei, H., Zhu, Y., Wang, T., Zhang, X., Zhang, K., and Zhang, Z. (2021). Genetic risk factors for autism-spectrum disorders: a systematic review based on systematic reviews and meta-analysis. *J. Neural Transm. (Vienna)* 128, 717–734. doi: 10.1007/s00702-021-02360-w

Wiegersma, A. M., Dalman, C., Lee, B. K., Karlsson, H., and Gardner, R. M. (2019). Association of Prenatal Maternal Anemia with Neurodevelopmental Disorders. *JAMA Psychiat.* 76, 1294–1304. doi: 10.1001/jamapsychiatry.2019.2309

Wilson, H. L., Crolla, J. A., Walker, D., Artifoni, L., Dallapiccola, B., Takano, T., et al. (2008). Interstitial 22q13 deletions: genes other than SHANK3 have major effects on cognitive and language development. *Eur. J. Hum. Genet.* 16, 1301–1310. doi: 10.1038/ejhg.2008.107

Wilson, H. L., Wong, A. C., Shaw, S. R., Tse, W. Y., Stapleton, G. A., Phelan, M. C., et al. (2003). Molecular characterisation of the 22q13 deletion syndrome supports the role of haploinsufficiency of SHANK3/PROSAP2 in the major neurological symptoms. *J. Med. Genet.* 40, 575–584. doi: 10.1136/jmg.40.8.575

Wink, L. K., Minshawi, N. F., Shaffer, R. C., Plawecki, M. H., Posey, D. J., Horn, P. S., et al. (2017). D-Cycloserine enhances durability of social skills training in autism spectrum disorder. *Mol. Autism.* 8:2. doi: 10.1186/s13229-017-0116-1

Won, H., Lee, H. R., Gee, H. Y., Mah, W., Kim, J. I., Lee, J., et al. (2012). Autistic-like social behaviour in Shank2-mutant mice improved by restoring NMDA receptor function. *Nature* 486, 261–265. doi: 10.1038/nature11208

Yang, M., Bozdagi, O., Scattoni, M. L., Wöhr, M., Roullet, F. I., Katz, A. M., et al. (2012). Reduced excitatory neurotransmission and mild autism-relevant phenotypes in adolescent Shank3 null mutant mice. *J. Neurosci.* 32, 6525–6541. doi: 10.1523/JNEUROSCI.6107-11.2012

Yi, F., Danko, T., Botelho, S. C., Patzke, C., Pak, C., Wernig, M., et al. (2016). Autism-associated SHANK3 haploinsufficiency causes Ih channelopathy in human neurons. *Science* 352:aaf2669. doi: 10.1126/science.aaf2669

Yoo, Y. E., Yoo, T., Lee, S., Lee, J., Kim, D., Han, H. M., et al. (2019). Shank3 mice carrying the human Q321R mutation display enhanced self-grooming, abnormal electroencephalogram patterns, and suppressed neuronal excitability and seizure susceptibility. *Front. Mol. Neurosci.* 12:155. doi: 10.3389/fnmol.2019.00155

Zencica, P., Chaloupka, R., Hladíková, J., and Krbec, M. (2010). Adjacent segment degeneration after lumbosacral fusion in spondylolisthesis: a retrospective radiological and clinical analysis. *Acta Chir. Orthop. Traumatol. Cechoslov.* 77, 124–130. PMID: 20447355

Zhou, Y., Kaiser, T., Monteiro, P., Zhang, X., Van Der Goes, M. S., Wang, D., et al. (2016). Mice with Shank3 mutations associated with ASD and schizophrenia display both shared and distinct defects. *Neuron* 89, 147–162. doi: 10.1016/j.neuron.2015.11.023

Zhou, Y., Sharma, J., Ke, Q., Landman, R., Yuan, J., Chen, H., et al. (2019). Atypical behaviour and connectivity in SHANK3-mutant macaques. *Nature* 570, 326–331. doi: 10.1038/s41586-019-1278-0

Zhu, M., Idikuda, V. K., Wang, J., Wei, F., Kumar, V., Shah, N., et al. (2018). Shank3-deficient thalamocortical neurons show HCN channelopathy and alterations in intrinsic electrical properties. *J. Physiol.* 596, 1259–1276. doi: 10.1113/JP275147

frontiers | Frontiers in Molecular Neuroscience

TYPE Original Research
PUBLISHED 14 February 2023
DOI 10.3389/fnmol.2023.1096930

OPEN ACCESS

EDITED BY
Xin Zhang,
Duke University, United States

REVIEWED BY
Xinying Guo,
Guangzhou Women and Children's Medical Center, China
Li Zhang,
Shenzhen University, China

*CORRESPONDENCE
Yinghui Hua
✉ hua_cosm@aliyun.com
He Wang
✉ hewang@fudan.edu.cn

†These authors have contributed equally to this work and share first authorship

SPECIALTY SECTION
This article was submitted to Pain Mechanisms and Modulators, a section of the journal Frontiers in Molecular Neuroscience

RECEIVED 13 November 2022
ACCEPTED 16 January 2023
PUBLISHED 14 February 2023

CITATION
Wang Y, Li Q, Xue X, Xu X, Tao W, Liu S, Li Y, Wang H and Hua Y (2023) Neuroplasticity of pain processing and motor control in CAI patients: A UK Biobank study with clinical validation. *Front. Mol. Neurosci.* 16:1096930. doi: 10.3389/fnmol.2023.1096930

Neuroplasticity of pain processing and motor control in CAI patients: A UK Biobank study with clinical validation

Yiran Wang[1†], Qianru Li[1†], Xiao'ao Xue[1†], Xiaoyun Xu[2], Weichu Tao[2], Sixu Liu[3], Yunyi Li[3], He Wang[4,5,6*] and Yinghui Hua[1,7*]

[1]Department of Sports Medicine, Fudan University, Shanghai, China, [2]School of Exercise and Health, Shanghai University of Sport, Shanghai, China, [3]Department of Biomedical Engineering, Shanghai University of Traditional Chinese Medicine, Shanghai, China, [4]Institute of Science and Technology for Brain-Inspired Intelligence, Fudan University, Shanghai, China, [5]Human Phenome Institute, Fudan University, Shanghai, China, [6]Key Laboratory of Computational Neuroscience and Brain-Inspired Intelligence, Ministry of Education, Fudan University, Shanghai, China, [7]Yiwu Research Institute of Fudan University, Yiwu, China

Background: Pain plays an important role in chronic ankle instability (CAI), and prolonged pain may be associated with ankle dysfunction and abnormal neuroplasticity.

Purpose: To investigate the differences in resting-state functional connectivity among the pain-related brain regions and the ankle motor-related brain regions between healthy controls and patients with CAI, and explore the relationship between patients' motor function and pain.

Study design: A cross-database, cross-sectional study.

Methods: This study included a UK Biobank dataset of 28 patients with ankle pain and 109 healthy controls and a validation dataset of 15 patients with CAI and 15 healthy controls. All participants underwent resting-state functional magnetic resonance imaging scanning, and the functional connectivity (FC) among the pain-related brain regions and the ankle motor-related brain regions were calculated and compared between groups. The correlations between the potentially different functional connectivity and the clinical questionnaires were also explored in patients with CAI.

Results: The functional connection between the cingulate motor area and insula significantly differed between groups in both the UK Biobank ($p = 0.005$) and clinical validation dataset ($p = 0.049$), which was also significantly correlated with Tegner scores ($r = 0.532$, $p = 0.041$) in patients with CAI.

Conclusion: A reduced functional connection between the cingulate motor area and the insula was present in patients with CAI, which was also directly correlated with reduction in the level of patient physical activity.

KEYWORDS

ankle injuries, functional magnetic resonance imaging, functional connection, pain, central nervous system

1. Introduction

Lateral ankle sprain is one of the most common sports injuries (McCriskin et al., 2015; Jiang et al., 2018). Although approximately 80% of acute injuries have shown recovery with conservative treatments, the remaining 20% have demonstrated chronic ankle instability (CAI) and have suffered from a range of symptoms (e.g., persistent pain, impaired proprioception, and

repetitive re-injury) (Safran et al., 1999; Alghadir et al., 2020). The long-term chronic course can also lead to a reduced quality of life and the development of ankle osteoarthritis (Thompson et al., 2019). Despite a variety of currently utilized conservative treatments and surgery to treat CAI, the outcomes have been far from satisfactory. It is apparent, therefore, that additional research elucidating the pathological mechanisms is essential to deepen our understanding of CAI which could form the basis for more effective clinical intervention (Doherty et al., 2017).

To emphasize the vital role pain plays in CAI, current evidence suggests it is present in 58% of these patients, yet most studies on CAI have continued to ignore pain in their inclusion criteria or primary outcomes (Gribble et al., 2014; Al Adal et al., 2019, 2020). Ankle dysfunction associated with CAI, such as the sense of ankle instability, has been accompanied with pain (Gribble et al., 2014; Al Adal et al., 2020; Xue et al., 2021a). Moreover, persistent pain has been reported to disturb proprioception thereby jeopardizing safe return to sports (RTS) in patients with CAI (Al Adal et al., 2020). However, although pain and the corresponding ankle dysfunction are among the most common symptoms of CAI, existing studies have not thoroughly explained the underlying mechanisms. Recently, a growing number of studies have suggested that long-term pain and dysfunction of musculoskeletal disorders may be associated with maladaptive neuroplasticity in the central nervous system, and we postulated that this upstream mechanism might exist in CAI (Pelletier et al., 2015).

The concept of neuroplasticity suggests that the central nervous system has the ability to adapt to both the external environment and internal factors, which can change the degree of involvement of certain connections or brain areas through different neural circuits (Sharma et al., 2013). In recent years, functional magnetic resonance imaging (fMRI) has gradually shown its value in neurological studies of neuroplasticity, especially the functional connectivity (FC) evaluated by the between-region correlation of the blood oxygen level-dependent (BOLD) signal that reflects the simultaneous nature of blood flow in different brain tissues (Ogawa et al., 1990, 1993). Of particular interest, in musculoskeletal disorders, such as lower back pain and knee ligament injuries, altered FC has been recognized between patients and healthy controls that might negatively affect the time of returning to sports, especially the FC between the pain-related and motor-related areas that are associated with emotional processes, perception of visual motion and body form (e.g., the amygdala, postcentral gyrus, temporal-parietal junction, and middle temporal visual cortex) (Needle et al., 2017; Gandhi et al., 2020; Conboy et al., 2021; Xue et al., 2021b). However, similar evidence of an abnormality relative to FC in CAI has not been demonstrated.

Therefore, we aimed to analyze the functional connectivity between the ankle motor-related and pain-related areas in patients with CAI, to obtain evidence on whether pain is related to motor function and time to return to exercise, based on the initial exploration in patients with ankle pain of the UK Biobank (currently the most extensive human genetic cohort sample library), and further validation in patients with CAI enrolled from a sports medicine clinic. We hypothesized that there was an abnormal functional connection between the pain-brain region and the ankle-motor brain region in patients with CAI, which might also correlate with the clinical outcomes of the patients.

2. Methods

Participants and data acquisition

The study was designed with two parts of cross-sectional analyses to explore the pain symptoms in patients with CAI. Ethical approval was granted for the UK Biobank data usage, and the present research was prospectively registered online (No. 62721). Validation for using the dataset and all study protocols was approved by the Institutional Review Board Huashan Hospital, Fudan University (No. 2016M-008). Informed consent was obtained, and the rights of all subjects were protected.

Part 1 was an initial analysis based on existing MRI data in the UK Biobank (http://www.ukbiobank.ac.uk/). Participants were included if they met the diagnosis based on the ICD10 disease diagnostic classification codes M25.57 Pain in joint (Ankle and foot), and M79.67 Pain in limb (Ankle and foot). Exclusion criteria included patients with painful symptoms due to other factors, joint instability beyond the ankle, no brain imaging, not right-handed, lack of demographic data, and other excluded diseases. Brain images were acquired after the diagnosis of their disease. The diagnosis code of chronic ankle pain and the excluded codes can be found in supplemental digital content (Supplementary Table 1). The final patient group was matched to healthy controls in a 1:4 ratio using sex, age, BMI, and ethnic background.

Part 2 was a validation study using the participants we enrolled from February 2021 to July 2021. CAI patients were recruited by the sports medicine department at the Huashan Hospital, Fudan University. Adult patients were selected if they met the following recommendation of the International Ankle Consortium: (1) history of at least one significant ankle sprain, which occurred at least 12 months prior to the study, resulting in pain, swelling, and at least one interrupted day of normal physical activity; and (2) a score of < 24 on the Cumberland Ankle Instability Tool (CAIT) questionnaire (Hiller et al., 2006; Gribble et al., 2014). Additionally, all participants had been diagnosed with anterior talofibular ligament injuries through physical examinations (positive anterior drawer test) and imaging assessments (ultrasonic or ankle MRI) by an experienced orthopedist (Prof. Yinghui Hua) (Song et al., 2019). Furthermore, all participants were right-footed, defined by the limb they preferred to kick a ball. Exclusion criteria included: (1) a history of other musculoskeletal problems or surgeries of the lower extremities (except the CAI in the patient group); (2) acute ankle sprains or other injuries in the previous 3 months; (3) the medical history of or current medication usage for major medical illnesses, such as cardiovascular, respiratory, neurological, autoimmune, or mental disorders.

2.2. Data acquisition

MRI data acquisition protocols of the UK Biobank are presented online (https://biobank.ctsu.ox.ac.uk/crystal/crystal/docs/brain_mri.pdf). For the validation dataset, the Tegner Activity Rating Scale score and American Orthopedic Foot and Ankle Society Score (AOFAS) were measured prior to MRI scanning. The validation dataset MRI scanning was performed on a 7T scanner (MAGNETOM Terra, Siemens Healthcare, Erlangen, Germany) equipped with a 1Tx/32Rx head coil (Nova Medical, Wilmington, MA, USA). Subjects were reminded to lie still at

rest, looking at a cross reflected on a projector without thinking about anything. First, a MPRAGE sequence was used to acquire high resolution 3D T1-weighted images (sagittal): TR = 8.1 ms, TE = 3.7 ms; field of view = 256 × 256 mm; matrix = 256 × 256; inplane resolution = 1 × 1 mm; slice thickness = 1 mm; number of slices = 180. Second, fMRI data of resting-state were acquired with the following parameters: TR = 650 ms; TE = 30 ms; flip angle = 53°; field of view = 200 × 200 mm; acquisition matrix = 68 × 66; SENSE factor = 1.5; reconstructed in-plane resolution = 2.5 × 2.5; slice thickness = 3.5 mm; number of slices = 40; multi-band factor = 4. In total, 500 frames of data were collected, and the total time for the resting-state fMRI sessions was approximately 5.5 min.

2.3. Data analysis

For preprocessing of the images, Restplus (version 2019) software of Matlab2014a was used, including slice timing and realign, normalization to Montreal Neurological Institute (MNI) template space (resampled to 2 mm isotropic), and smoothing (8 mm full-width half-max kernel). Participants with movement outlier were confirmed using mean frame-wise displacement (FD) >0.2 mm, which would be excluded from the analysis.

For ROIs analysis, 5 mm spheres with combined left and right ankle motor-related regions related to motor were created based on previously published fMRI data of ankle movements, including 9 regions, such as bilateral primary sensorimotor cortex (SM1), supplementary motor area (SMA-proper), cingulate motor area (CMA), premotor cortex (PMC), secondary sensory cortex (SII), basal ganglia, and cerebellum (vermis, anterior lobes). The thalamus was excluded because the coordinates of bilateral brain regions were not available (Kapreli et al., 2007). Also, the 159 pre-defined pain-related ROIs (4 mm sphere) were evenly placed out in pain-related brain regions that were selected from a meta-analysis automatically generated from 516 articles labeled with the term "pain" in the framework of neurosynth (www.neurosyntsh.org) (Woo et al., 2014; Flodin et al., 2016) (Figure 2A). The volume of the ROI spheres was used to represent the total voxel size of this brain region, and the time series of BOLD signal under this ROI was extracted. The FCs calculated by the Fisher-z transformed Pearson correlation coefficients between the ankle motor-related and pain-related ROIs to identify neural differences in brain connectivity between ankle motor control and pain processing (Diekfuss et al., 2019).

The remainder of the statistical analyses were performed by Graphpad Prism Version 9.0. Data normality was tested using the Kolmogorov-Smirnov test. Chi2 tests, Mann Whitney U-tests, and independent two-sample *t*-tests were applied to examine the equivalence of demographic variables and the differences in clinical features between groups. Independent two-sample *t*-tests were used for comparisons between groups in both parts, and the two-tailed threshold of $p < 0.01$ was used to identify the potentially altered connectivity in the initial exploration of part 1, and the one-tailed threshold of $p < 0.05$ was used to validate the altered connectivity in part 2. Two-tailed Pearson correlation was also used to estimate the correlation between the significantly different FCs and the clinical questionnaires (i.e., AOFAS and Tegner scores) in patients with CAI, with the absolute values of correlation coefficients (r) classified as weak (0–0.4), moderate (0.4–0.7), or strong (0.7–1.0).

3. Results

3.1. Demographic and clinical features

A total of 502,461 participants were screened from the UK Biobank Resource, of which 463,486 were removed because they had no brain imaging, 4,274 were removed because they were not right-handed, 8,753 were excluded for disease, 879 were removed because they had no demographic data. The remaining 25,069 participants were screened based on the ICD10 disease diagnostic classification. After the exclusion of major illnesses/traumas, joint instability beyond the ankle, inclusion of ankle instability and selecting fMRI data quality, 28 participants were included in the chronic ankle pain group and 109 in the healthy control group for part 1, the detailed ICD10 codes and diagnosis are presented in Supplementary Tables 1–3. The flowchart of the participant selection in part 1 is presented in Figure 1A. Individual demographic data are shown in Table 1. In Group Chronic Ankle pain, there were 17 females and 11 males, and in Group Healthy Control, there were 63 females and 46 males. No significant differences were observed between the two groups for sex, age, BMI, and ethnic background ($p > 0.05$).

In part 2, 16 CAI patients and 18 healthy controls were recruited, while four subjects were excluded due to excessive head motion, leaving 15 in each of the patient groups for further data analysis. The flowchart of participant selection in part 2 is also presented in Figure 1B. Demographic data are shown in Table 2. In Group CAI, there were 2 females and 13 males, and in Group Healthy Control, there were 3 females and 12 males. No significant differences were observed between the two groups for sex, age, BMI, and ethnic background ($p > 0.05$). The CAI patients had significantly worse sports level (Tegner) and ankle function (AOFAS) ($p<0.001$) when compared with healthy controls.

3.2. FC analysis

A Heatmap of the t value of the between-group comparisons of the FCs between 9 ROIs of ankle activity and 159 ROIs of pain in the global brain is shown in Figure 2B. As compared to group healthy controls, brain FC was significantly lower in group chronic ankle pain in brain ROIs, including CMA and Insula ($p = 0.005$), CMA and Putamen ($p = 0.004$), CMA and Rolandic Operculum ($p = 0.004$), SII and Putamen ($p = 0.009$). These ROIs were used in the validation study in part 2; only the CMA and Insula persisted in patients with CAI ($p = 0.049$) (Table 3, Figure 3). The FC of CMA and Insula had a moderate correlation with Tegner scores ($r = 0.532$, $p = 0.041$), as shown in Figure 3D, while there was no significant correlation with the AOFAS scores ($r = 0.2738$, $p = 0.3234$).

4. Discussion

The most important finding of this study was that FC between CMA and insula was reduced in patients with CAI and the degree of

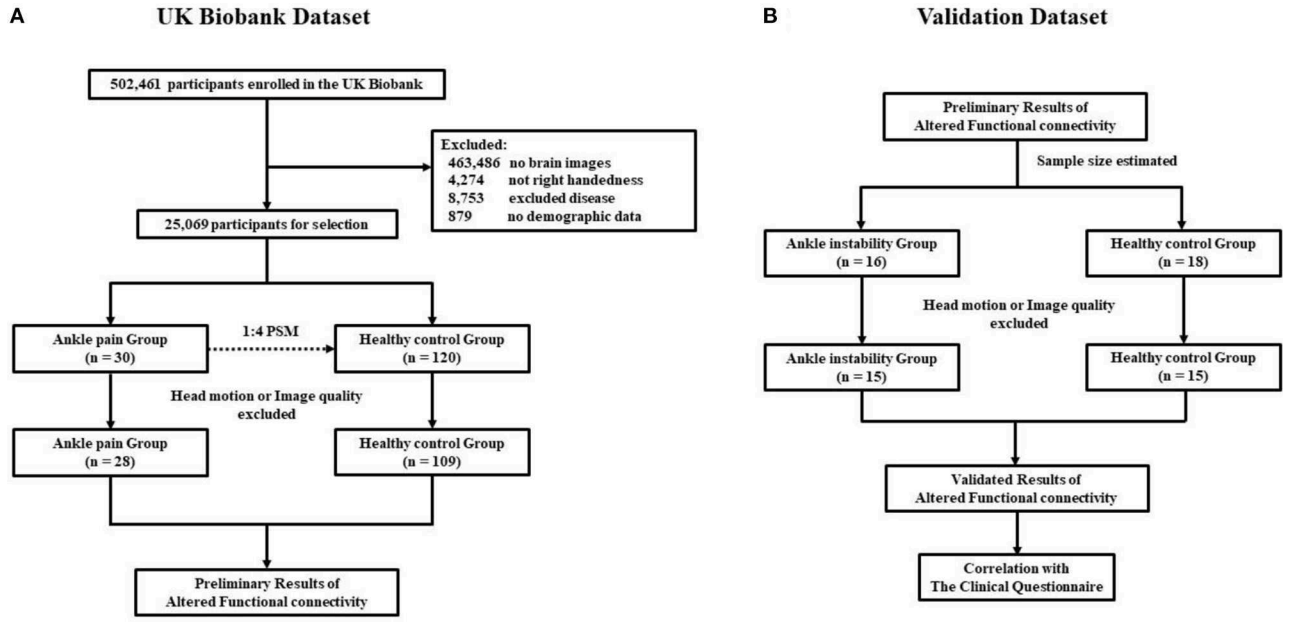

FIGURE 1
(A) Flowchart of the participants selection in part 1; **(B)** Flowchart of the participants selection in part 2.

TABLE 1 Demographic variables of ankle pain group and healthy control group presented as mean (SD).

UK Biobank set	Ankle pain ($n = 28$)	Healthy control ($n = 109$)	*P* value
Sex (female/male)	17/11	63/46	0.949
Age (years)	64.86 ± 7.08	63.93 ± 6.97	0.531
BMI (kg/m^2)	26.82 ± 4.28	27.13 ± 5.71	0.791
Ethnic background			0.872
A	26 (92.9%)	96 (88.1%)	
B	0 (0.0%)	3 (2.8%)	
C	1 (3.6%)	3 (2.8%)	
D	0 (0.0%)	1 (0.9%)	
E	0 (0.0%)	1 (0.9%)	
F	1 (3.6%)	2 (1.8%)	
G	0 (0.0%)	3 (2.8%)	

TABLE 2 Demographic variables of chronic ankle instability group and healthy control group presented as mean (SD).

Validation set	Ankle pain ($n = 15$)	Healthy control ($n = 15$)	*P* value
Sex (female/male)	2/13	3/12	1.000
Age (years)	26.20 ± 6.12	26.53 ± 2.39	0.846
BMI (kg/m^2)	24.13 ± 2.26	23.19 ± 2.30	0.265
Ethnic background			1.000
H	15 (100%)	15 (100%)	
Tegner scores	3.27 ± 1.71	5.07 ± 1.10	0.002
AOFAS	99.33 ± 2.58	69.87 ± 17.26	<0.001

connectivity was positively correlated with impaired motor function. To our knowledge, this study is the first fMRI study to evaluate the neuroplasticity of pain processing and motor control in patients with CAI.

The insula, a region involved in pain processing, is usually divided into partial subregions based on anatomy and connectivity (Centanni et al., 2021). Generally, the insula is thought to affect somatosensory, nociceptive, and affective functions (Starr et al., 2009; Segerdahl et al., 2015). Meanwhile, integration of information inputs in the insula provides the prediction of a combination of pain, perceptual errors, or a variety of other current conditions (Geuter et al., 2017; Centanni et al., 2021). The integration of emotional and somatosensory signals is a crucial function of the insula (Gonsalves et al., 2021). Previous studies have confirmed that enhanced nociceptive sensitization in patients with chronic pain may be associated with overlapping pain activation in the insula (Ploghaus et al., 2001; Zhuo, 2016). In addition, reduced pain inhibition is associated with stronger resting-state FC in relation to the insula and other cortical brain regions (Huynh et al., 2022). Furthermore, impaired insula function can also produce or enhance emotions such as anxiety (Paulus and Stein, 2010; Avery et al., 2014; Zhuo, 2016). Therefore, we believe that the insula has a valuable research significance in patients with chronic pain, not only in relation to their pain management but also in terms of predicting their psychological patterns and behavior.

The CMA area is anatomically divided into four regions and is not perfectly aligned in function (Lu et al., 1994; He et al., 1995; Wessel et al., 1995). Numerous studies have demonstrated that the CMA is significantly activated during lower limb movements, even activated before active awareness during voluntary activity

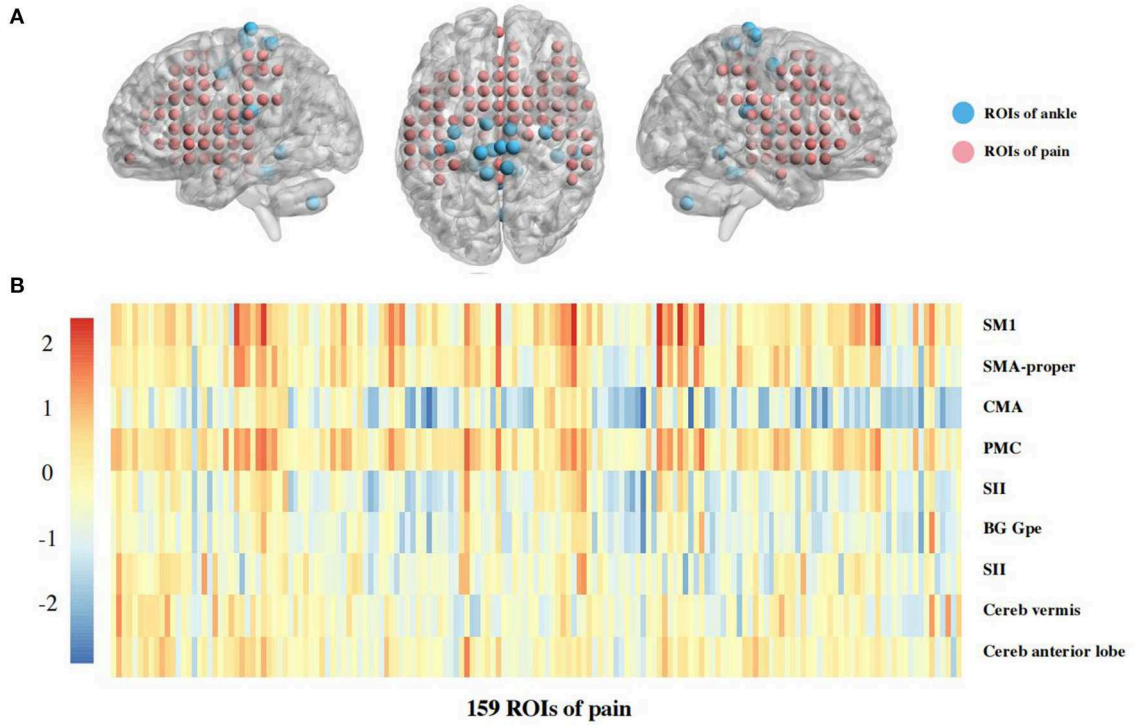

FIGURE 2
(A) The ROIs in global brain as sphere. Each ROI was put in a brain as sphere, for blue color was ROIs of ankle motor regions, and for red color was ROIs of pain regions. **(B)** Heatmaps of functional connectivity between 9 ROIs of ankle activity and 159 ROIs of pain in the global brain. Warmer colors (red and yellow regions) indicate stronger connectivities whereas cooler colors (blue and green regions) indicate weaker connectivity. The 9 ROIs associated with ankle activity are primary sensorimotor cortex (SM1); supplementary motor area (SMA-proper); cingulate motor area (CMA); premotor cortex (PMC); secondary sensory cortex (SII); basal ganglia (BG); external segment of globus pallidus (Gpe); cerebellum (Cereb), in which signsificant differences presented between CMA and Insula ($p = 0.005$), CMA and Putamen ($p = 0.004$), CMA and Rolandic Operculum ($p = 0.004$), SII and Putamen ($p = 0.009$). These ROIs were validated in part 2 of this study.

TABLE 3 Comparison of functional connectivity between the group chronic ankle pain and healthy control in two parts of study.

UK Biobank dataset	Ankle pain ($n = 28$)	Healthy control ($n = 109$)	Direction of difference	P value[#]
CMA–Insula	0.67 (0.30)	0.84 (0.28)	<	0.005**
CMA–Putamen	0.57 (0.31)	0.73 (0.25)	<	0.004**
CMA–Rolandic Operculum	0.65 (0.31)	0.83 (0.28)	<	0.004**
SII–Putamen	0.50 (0.30)	0.65 (0.27)	<	0.009**
Validation dataset	**Ankle pain ($n = 15$)**	**Healthy control ($n = 15$)**	**Direction of difference**	**P value[%]**
CMA–Insula	**0.56 (0.29)**	**0.75 (0.33)**	**<**	**0.049***
CMA–Putamen	0.59 (0.28)	0.55 (0.41)	>	0.380
CMA–Rolandic Operculum	0.70 (0.25)	0.70 (0.37)	>	0.499
SII–Putamen	0.55 (0.29)	0.45 (0.27)	>	0.186

ns, not significant**Significant ($p < 0.001$); *Significant ($p < 0.05$).

(Ball et al., 1999). Increased functional connectivity can be thought of as increased neuronal activity (Lin et al., 2008). In contrast, repetitive somatosensory and motor stimuli, and cognitive stimuli reflect increased resting-state functional connectivity (rsFC) in the brain network, which may be related to the aggregation of neurotransmitter receptors at synaptic terminals (Tung et al., 2013; Wei et al., 2014). Some studies have shown increased rsFC of the CMA with other motor-related cortical brain regions in stroke patients (Liu et al., 2020), which contradicts the results of the present study, but may indicate that the CMA and insula have different patterns from normal activity in processing movements related to pain sensation.

The present study links the insula to the CMA is an attempt to explain its reduced connectivity with decreased motor function. The conclusion that weaker intensity connectivity between the CMA and insula implies that these two brain regions failed to work well together, resulting in a temporal difference of activation in sequence, which forms the theoretical basis for further correlation analysis with pain and ankle dysfunction. We suggest that this

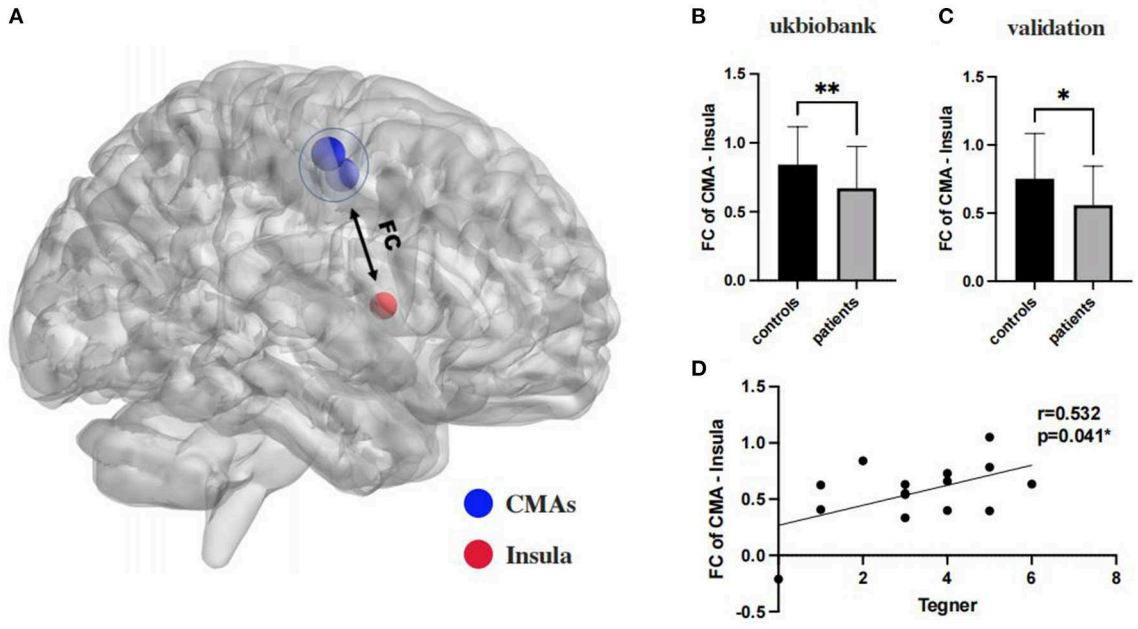

FIGURE 3
(A) The insula and CMAs ROIs in global brain as sphere, in which blue color was ROIs of CMAs, and for red color was ROIs of Insula; **(B, C)**: the functional connectivity between CMA and insula are significant on a corrected cluster level in ukbiobank ($p = 0.005$) and clinical validation ($p = 0.049$) both; **(D)**: functional connectivity of CMA and insulation significantly correlated with Tegner scores ($r = 0.532$, $p = 0.041$). **Significant ($p < 0.001$); *Significant ($p < 0.05$).

reduction in FC may indicate neuroplasticity in CAI patients. It should be noted that if the conflict exists between brain regions during processing information when exercising, this may be the cause of many CAI failures to recover motor function. Due to prolonged chronic pain, patients develop a lower response-ability to pain which in turn adjusts motor behavior. Based on our clinical experience, CAI patients with pain often have a greater fear of rehabilitation. Whether this occurs earlier or later than neuroplastic changes is uncertain, but clearly this psychological change delays their RTS. After participants became aware of their motor intentions, fear of movement-related pain caused hyperactivation in the cingulate motor area. This hyperactivation may result from a conflict between the unrealized desire to avoid the painful experience and the motivation to perform the desired motor task (Osumi et al., 2021). This may in part explain the poorer RTS function and longer RTS times in patients with CAI who experience long-term chronic pain. As some studies have similarly identified a progression of pain sensitization in the follow-up of post-operative CAI patients, the critical role of pain in clinical prognosis is emphasized. Our findings may further explain the process of injury-related outcomes in patients with CAI.

To further investigate the clinical significance of pain in patients with CAI, we assessed the relationship between CMA, insula and clinical scores. Tegner scores were designed to provide a standardized method of assessing the level of motor function through physical activity, and a two-year follow-up of athletes showed that t-scores also provided valid information in predicting RTS function in impaired patients (Klasan et al., 2021). In other words, reduced connectivity of the CMA to the insula directly correlated with the Tegner score. To some extent, it also indicated reduced RTS motor function. However, no significant correlation between rsFC and AOFAS scores was found in this study, which may be principally attributed to the following: (1) AOFAS is used in the clinic mostly to assess patient activity function, and the assessment of pain is less accurate than a VAS; (2) AOFAS is more subjective, and pain perception in different states varies greatly for CAI patients.

Through validation in clinical populations, we found a reduced regional connectivity between the insula and CMA in CAI, but in the UK Biobank data, we also found a significant results between the CMA and putamen, Rolandic operculum, even SII and putamen. This represents an interaction between pain and motor function that does not necessarily exist solely between the CMA and the insula. However, due to the false positives, we were unable to verify all their authenticity, which suggests that future work needs to focus more on the full range of symptoms in CAI patients rather than instability alone.

Current research regarding pain-sensitized brain function has emphasized abnormal connectivity between brain regions, rather than simply abnormal activation of brain regions. These intrinsic connectivity networks offer exciting new avenues for subsequent in-depth research: to perform functional analyses between brain regions in pain and further investigate the presence of neuroplasticity between the "upstream and downstream of pain". This, in turn, may shift attention to pain-induced central changes such as functional brain connectivity, abnormal activation of associated brain regions, and even large-scale brain network analysis. Concomitantly, we can optimize the clinical questionnaire evaluation system to determine more concordance with rsFC to help predict patient clinical symptoms and psychological status (Gonsalves et al., 2021).

We have also noted that many sports injuries produce pain that is not easily eliminated, so research on the FC between pain sensation and sports injuries can help us understand more about sports injuries. Additionally, due to the limitations of existing treatments, more treatments for pain after sports injuries should be developed. Several studies have shown that TMS can be used to enhance neuroplasticity and reduce pain after injuries (Lu et al., 2015; Shin et al., 2018; Krishnan et al., 2019). It is expected to facilitate more specific interventions in the process of passive assessment of injury-related stimuli to improve future surgical outcomes in patients with cerebral infarction and even other motor injuries.

4.1. Limitation

Several limitations should be noted. First, the increased false-positive rate associated with comparisons between multiple ROIs in our exploratory and preliminary study should be acknowledged. However, two sub-studies were performed with inter-validation, which may help to reduce the false-positive rate. Second, although similar to the sample size of previous studies of FC, ours was still smaller. To compensate, we used imaging of two groups, which may have reduced the false positive rate, and the use of a 7T MRI machine can also improve accuracy to a certain extent. Additionally, during data analysis, bilateral foot injuries were combined due to the deficiencies of the UK Biobank itself. The inclusion of more clinical subjects with more detailed clinical evaluations would certainly provide more accurate interindividual variability.

4.2. Conclusion

Reduced FC between the CMAs and the insula was present in patients with ankle instability and ankle pain, which was also directly correlated with reduction in the level of physical activity.

Data availability statement

The original contributions presented in the study are included in the article/Supplementary material, further inquiries can be directed to the corresponding authors.

Ethics statement

The studies involving human participants were reviewed and approved by Institutional Review Board Huashan Hospital, Fudan University. The patients/participants provided their written informed consent to participate in this study. Written informed consent was obtained from the individual(s) for the publication of any potentially identifiable images or data included in this article.

Author contributions

YW carried out the study design, data collection, quality rating, statistical analysis, and manuscript writing. XXue carried out the study design, data collection, quality rating, statistical analysis, and manuscript reviewing. QL carried out the study design, data collection, quality rating, and manuscript reviewing. XXu carried out the study design and manuscript reviewing. YH carried out the study design, supervision of the literature search, data collection and quality rating, and manuscript reviewing. All authors have read, approved the final version of the manuscript, and agree with the order of presentation of the authors.

Funding

This work was supported by the National Natural Science Foundation of China (Nos. 81871823, 81971583, 81671652, and 8207090113), National Key R&D Program of China (No. 2018YFC1312900), Shanghai Natural Science Foundation (No. 20ZR1406400), Science and Technology Commission of Shanghai Municipality (No. 18JC1410403), and Shanghai Municipal Science and Technology Major Project (Nos. 2017SHZDZX01 and 2018SHZDZX01).

Acknowledgments

The authors would like to express their gratitude to EditSprings (https://www.editsprings.cn) for the expert linguistic services provided.

Conflict of interest

The authors declare that the research was conducted in the absence of any commercial or financial relationships that could be construed as a potential conflict of interest.

Publisher's note

Supplementary material

The Supplementary Material for this article can be found online at: https://www.frontiersin.org/articles/10.3389/fnmol.2023.1096930/full#supplementary-material

References

Al Adal, S., Mackey, M., Pourkazemi, F., Hiller, C. E. (2020). The relationship between pain and associated characteristics of chronic ankle instability: a retrospective study. *J. Sport Heal. Sci.* 9, 96–101. doi: 10.1016/j.jshs.2019.07.009

Al Adal, S., Pourkazemi, F., Mackey, M., and Hiller, C. E. (2019). The prevalence of pain in people with chronic ankle instability: a systematic review. *J. Athl. Train.* 54, 662–670. doi: 10.4085/1062-6050-531-17

Alghadir, A. H., Iqbal, Z. A., Iqbal, A., Ahmed, H., and Ramteke, S. U. (2020). Effect of chronic ankle sprain on pain, range of motion, proprioception, and balance among athletes. *Int. J. Environ. Res. Public Health* 17, 1–11. doi: 10.3390/ijerph17155318

Avery, J. A., Drevets, W. C., Moseman, S. E., Bodurka, J., Barcalow, J. C., Simmons, W. K., et al. (2014). Major depressive disorder is associated with abnormal interoceptive activity and functional connectivity in the insula. *Biol. Psychiatry*. 76, 258–266. doi: 10.1016/j.biopsych.2013.11.027

Ball, T., Schreiber, A., Feige, B., Wagner, M., Lü, C. H., Kristeva-Feige, R., et al. (1999). The role of higher-order motor areas in voluntary movement as revealed by high-resolution EEG and fMRI. *Neuroimage*. 10, 682–694. doi: 10.1006/nimg.1999.0507

Centanni, S. W., Janes, A. C., Haggerty, D. L., Atwood, B., and Hopf, F. W. (2021). Better living through understanding the insula: Why subregions can make all the difference. *Neuropharmacology*. 198, 108765. doi: 10.1016/j.neuropharm.2021.108765

Conboy, V., Edwards, C., Ainsworth, R., Natusch, D., Burcham, C., Danisment, B., et al. (2021). Chronic musculoskeletal impairment is associated with alterations in brain regions responsible for the production and perception of movement. *J. Physiol.* 599, 2255–2272. doi: 10.1113/JP281273

Diekfuss, J. A., Grooms, D. R., Yuan, W., Dudley, J., Barber Foss, K. D., Thomas, S., et al. (2019). Does brain functional connectivity contribute to musculoskeletal injury? A preliminary prospective analysis of a neural biomarker of ACL injury risk. *J. Sci. Med. Sport.* 22, 169–174. doi: 10.1016/j.jsams.2018.07.004

Doherty, C., Bleakley, C., Delahunt, E., and Holden, S. (2017). Treatment and prevention of acute and recurrent ankle sprain: an overview of systematic reviews with meta-analysis. *Br. J. Sports Med.* 51, 113–125. doi: 10.1136/bjsports-2016-096178

Flodin, P., Martinsen, S., Altawil, R., Waldheim, E., Lampa, J., Kosek, E., et al. (2016). Intrinsic brain connectivity in chronic pain: a resting-state fMRI study in patients with rheumatoid arthritis. *Front. Hum. Neurosci.* 10, 107. doi: 10.3389/fnhum.2016.00107

Gandhi, W., Rosenek, N. R., Harrison, R., and Salomons, T. V. (2020). Functional connectivity of the amygdala is linked to individual differences in emotional pain facilitation. *Pain*. 161, 300–307. doi: 10.1097/j.pain.0000000000001714

Geuter, S., Boll, S., Eippert, F., and Büchel, C. (2017). Functional dissociation of stimulus intensity encoding and predictive coding of pain in the insula. *Elife*. 6, e24770. doi: 10.7554/eLife.24770.016

Gonsalves, M., Beck, Q., Fukuda, A., Tirrell, E., Kokdere, F., Kronenberg, E., et al. (2021). Mechanical Affective Touch Therapy (MATT) for anxiety disorders: effects on resting state functional connectivity. Brain Stimul. 14, 1630–1631. doi: 10.1016/j.brs.2021.10.137

Gribble, P. A., Delahunt, E., Bleakley, C. M., Caulfield, B., Docherty, C. L., Fong, D. T. P., et al. (2014). Selection criteria for patients with chronic ankle instability in controlled research: a position statement of the international ankle consortium. *J. Athl. Train.* 49, 121–7. doi: 10.4085/1062-6050-49.1.14

He, S.-., Q., and Dum, R. P. (1995). Strickia2a3 PL. Topographic organization of corticospinal projections from the frontal lobe: motor areas on the medial surface of the hemisphere. *J. Neurosci.* 5, 3284–3306. doi: 10.1523/JNEUROSCI.15-05-03284.1995

Hiller, C. E., Refshauge, K. M., Bundy, A. C., Herbert, R. D., and Kilbreath, S. L. (2006). The cumberland ankle instability tool: a report of validity and reliability testing. *Arch. Phys. Med. Rehabil.* 87, 1235–1241. doi: 10.1016/j.apmr.2006.05.022

Huynh, V., Lütolf, R., Rosner, J., Luechinger, R., Curt, A., Kollias, S., et al. (2022). Descending pain modulatory efficiency in healthy subjects is related to structure and resting connectivity of brain regions. *Neuroimage*. 247, 118742. doi: 10.1016/j.neuroimage.2021.118742

Jiang, D., Ao, Y., Jiao, C., Xie, X., Chen, L., Guo, Q., et al. (2018). Concurrent arthroscopic osteochondral lesion treatment and lateral ankle ligament repair has no substantial effect on the outcome of chronic lateral ankle instability. *Knee Surgery, Sport Traumatol Arthrosc* 26, 3129–3134. doi: 10.1007/s00167-017-4774-5

Kapreli, E., Athanasopoulos, S., Papathanasiou, M., Van Hecke, P., Kelekis, D., Peeters, R., et al. (2007). Lower limb sensorimotor network: issues of somatotopy and overlap. *Cortex*. 43, 219–232. doi: 10.1016/S0010-9452(08)70477-5

Klasan, A., Putnis, S. E., Grasso, S., Kandhari, V., Oshima, T., Parker, D. A., et al. (2021). Tegner level is predictive for successful return to sport 2 years after anterior cruciate ligament reconstruction. *Knee Surgery, Sport Traumatol Arthrosc*. 29, 3010–3016. doi: 10.1007/s00167-020-06335-4

Krishnan, V. S., Shin, S. S., Belegu, V., Celnik, P., Reimers, M., Smith, K. R., et al. (2019). Multimodal evaluation of TMS - Induced somatosensory plasticity and behavioral recovery in rats with contusion spinal cord injury. *Front. Neurosci.* 13, 387. doi: 10.3389/fnins.2019.00387

Lin, W., Zhu, Q., Gao, W., Chen, Y., Toh, C. H., Styner, M., et al. (2008). Functional connectivity MR imaging reveals cortical functional connectivity in the developing brain. *Am. J. Neuroradiol.* 29, 1883–1889. doi: 10.3174/ajnr.A1256

Liu, H., Cai, W., Xu, L., Li, W., and Qin, W. (2020). Differential reorganization of SMA subregions after stroke: a subregional level resting-state functional connectivity study. *Front Hum.* 13, 468. doi: 10.3389/fnhum.2019.00468

Lu, H., Kobilo, T., Robertson, C., Tong, S., Celnik, P., Pelled, G., et al. (2015). Transcranial magnetic stimulation facilitates neurorehabilitation after pediatric traumatic brain injury. *Sci. Rep.* 5, 14769. doi: 10.1038/srep14769

Lu, M. T., Preston, J. B., and Strick, P. L. (1994). Interconnections between the prefrontal cortex and the premotor areas in the frontal lobe. *JCN*. 341, 375–392. doi: 10.1002/cne.903410308

McCriskin, B. J., Cameron, K. L., Orr, J. D., and Waterman, B. R. (2015). Management and prevention of acute and chronic lateral ankle instability in athletic patient populations. *World J. Orthop.* 6, 161–171. doi: 10.5312/wjo.v6.i2.161

Needle, A. R., Lepley, A. S., and Grooms, D. R. (2017). Central nervous system adaptation after ligamentous injury: a summary of theories, evidence, and clinical interpretation. *Sport Med.* 47, 1271–1288. doi: 10.1007/s40279-016-0666-y

Ogawa, S., Lee, T. M., and Barrere, B. (1993). The sensitivity of magnetic resonance a rat brain to changes in the cerebral oxygenation. *Magn. Reson. Med.* 29, 205–210. doi: 10.1002/mrm.1910290208

Ogawa, S., Lee, T. M., Kay, A. R., and Tank, D. W. (1990). Brain magnetic resonance imaging with contrast dependent on blood oxygenation (cerebral blood flow/brain metabolism/oxygenation). *Proc. Natl. Acad. Sci. U S A.* 87, 9868–72. doi: 10.1073/pnas.87.24.9868

Osumi, M., Sumitani, M., Nishi, Y., Nobusako, S., Dilek, B., Morioka, S., et al. (2021). Fear of movement-related pain disturbs cortical preparatory activity after becoming aware of motor intention. *Behav. Brain Res.* 411, 113379. doi: 10.1016/j.bbr.2021.113379

Paulus, M. P., and Stein, M. B. (2010). Interoception in anxiety and depression. *Brain Struct. Funct.* 214, 451–463. doi: 10.1007/s00429-010-0258-9

Pelletier, R., Higgins, J., and Bourbonnais, D. (2015). Is neuroplasticity in the central nervous system the missing link to our understanding of chronic musculoskeletal disorders? *BMC Musculoskelet. Disord.* 16, 25. doi: 10.1186/s12891-015-0480-y

Ploghaus, A., Narain, C., Beckmann, C. F., Clare, S., Bantick, S., Wise, R., et al. (2001). Exacerbation of pain by anxiety is associated with activity in a hippocampal network. *J. Neurosci.* 21, 9896–9903. doi: 10.1523/JNEUROSCI.21-24-09896.2001

Safran, M. R., Benedetti, R. S., Bartolozzi, A. R., and Mandelbaum, B. R. (1999). Lateral ankle sprains: a comprehensive review part 1: etiology, pathoanatomy, histopathogenesis, and diagnosis. *Med. Sci. Sports Exerc.* 31, S429–37. doi: 10.1097/00005768-199907001-00004

Segerdahl, A. R., Mezue, M., Okell, T. W., Farrar, J. T., and Tracey, I. (2015). The dorsal posterior insula subserves a fundamental role in human pain. *Nat. Neurosci.* 18, 499–500. doi: 10.1038/nn.3969

Sharma, N., Classen, J., and Cohen, L. G. (2013). Neural plasticity and its contribution to functional recovery. *Handb. Clin. Neurol.* 110, 3–12. doi: 10.1016/B978-0-444-52901-5.00001-0

Shin, S. S., Krishnan, V., Stokes, W., Robertson, C., Celnik, P., Chen, Y., et al. (2018). Transcranial magnetic stimulation and environmental enrichment enhances cortical excitability and functional outcomes after traumatic brain injury. *Brain Stimul.* 11, 1306–1313. doi: 10.1016/j.brs.2018.07.050

Song, Y., Li, H., Sun, C., Zhang, J., Gui, J., Guo, Q., et al. (2019). Clinical guidelines for the surgical management of chronic lateral ankle instability: a consensus reached by systematic review of the available data. *Orthop. J. Sport Med.* 7, 232596711987385. doi: 10.1177/2325967119873852

Starr, C. J., Sawaki, L., Wittenberg, G. F., Burdette, J. H., Oshiro, Y., Quevedo, A. S., et al. (2009). Roles of the insular cortex in the modulation of pain: Insights from brain lesions. *J. Neurosci.* 29, 2684–2694. doi: 10.1523/JNEUROSCI.5173-08.2009

Thompson, C. S., Hiller, C. E., and Schabrun, S. M. (2019). Altered spinal-level sensorimotor control related to pain and perceived instability in people with chronic ankle instability. *J. Sci. Med. Sport* 22, 425–429. doi: 10.1016/j.jsams.2018.10.009

Tung, K. C., Uh, J., Mao, D., Xu, F., Xiao, G., Lu, H., et al. (2013). Alterations in resting functional connectivity due to recent motor task. *Neuroimage*. 78, 316–324. doi: 10.1016/j.neuroimage.2013.04.006

Wei, D., Yang, J., Li, W., Wang, K., Zhang, Q., Qiu, J., et al. (2014). Increased resting functional connectivity of the medial prefrontal cortex in creativity by means of cognitive stimulation. *Cortex*. 51, 92–102. doi: 10.1016/j.cortex.2013.09.004

Wessel, K., Zeffiro, T., Lou, J. S., Toro, C., and Hallett, M. (1995). Regional cerebral blood flow during a self-paced sequential finger opposition task in patients with cerebellar degeneration. *Brain*. 118, 379–393. doi: 10.1093/brain/118.2.379

Woo, C. W., Krishnan, A., and Wager, T. D. (2014). Cluster-extent based thresholding in fMRI analyses: pitfalls and recommendations. *Neuroimage*. 91, 412–419. doi: 10.1016/j.neuroimage.2013.12.058

Xue, X., Li, S., Li, H., Li, Q., and Hua, Y. (2021a). Deactivation of the dorsal anterior cingulate cortex indicated low postoperative sports levels in presurgical patients with chronic ankle instability. *BMC Sports Sci. Med. Rehabil*. 13, 121. doi: 10.1186/s13102-021-00353-6

Xue, X., Zhang, Y., Li, S., Xu, H., Chen, S., Hua, Y., et al. (2021b). Lateral ankle instability-induced neuroplasticity in brain grey matter: a voxel-based morphometry MRI study. *J. Sci. Med. Sport*. 24, 1240–1244. doi: 10.1016/j.jsams.2021.06.013

Zhuo, M. (2016). Neural mechanisms underlying anxiety-chronic pain interactions. *Trends Neurosci*. 39, 136–145. doi: 10.1016/j.tins.2016.01.006

frontiers | Frontiers in Molecular Neuroscience

TYPE Review
PUBLISHED 20 February 2023
DOI 10.3389/fnmol.2023.1102808

OPEN ACCESS

EDITED BY
Zilong Wang,
Southern University of Science and Technology, China

REVIEWED BY
Xin Luo,
Guangdong-Hong Kong-Macao Greater Bay Area Center for Brain Science and Brain-Inspired Intelligence, China
Xu-Hui Li,
Xi'an Jiaotong University, China

*CORRESPONDENCE
Jin Yu
✉ yujin@shmu.edu.cn
Na Yue
✉ dongdingbaiheyue@126.com

†These authors have contributed equally to this work

SPECIALTY SECTION
This article was submitted to Pain Mechanisms and Modulators, a section of the journal Frontiers in Molecular Neuroscience

RECEIVED 19 November 2022
ACCEPTED 16 January 2023
PUBLISHED 20 February 2023

CITATION
Shen Z, Li W, Chang W, Yue N and Yu J (2023) Sex differences in chronic pain-induced mental disorders: Mechanisms of cerebral circuitry. *Front. Mol. Neurosci.* 16:1102808. doi: 10.3389/fnmol.2023.1102808

Sex differences in chronic pain-induced mental disorders: Mechanisms of cerebral circuitry

Zuqi Shen[1†], Wei Li[1†], Weiqi Chang[1], Na Yue[2*] and Jin Yu[1,3*]

[1]Department of Integrative Medicine and Neurobiology, School of Basic Medical Sciences, Shanghai Medical College, Fudan University, Shanghai, China, [2]Weifang Maternal and Child Health Hospital, Weifang, China, [3]Shanghai Key Laboratory of Acupuncture Mechanism and Acupoint Function, Fudan University, Shanghai, China

Mental disorders such as anxiety and depression induced by chronic pain are common in clinical practice, and there are significant sex differences in their epidemiology. However, the circuit mechanism of this difference has not been fully studied, as preclinical studies have traditionally excluded female rodents. Recently, this oversight has begun to be resolved and studies including male and female rodents are revealing sex differences in the neurobiological processes behind mental disorder features. This paper reviews the structural functions involved in the injury perception circuit and advanced emotional cortex circuit. In addition, we also summarize the latest breakthroughs and insights into sex differences in neuromodulation through endogenous dopamine, 5-hydroxytryptamine, GABAergic inhibition, norepinephrine, and peptide pathways like oxytocin, as well as their receptors. By comparing sex differences, we hope to identify new therapeutic targets to offer safer and more effective treatments.

KEYWORDS

sex differences, pain, anxiety, depression, neural circuit

1. Introduction

Chronic pain has a high comorbidity rate with anxiety and depression, and the incidence is as high as 50% (Vos et al., 2020). Epidemiology suggests that there are sex differences in pain-induced mental disorders, and sex factors also affect the efficacy of clinical anti-anxiety and antidepressant drugs (Sramek et al., 2016; LeGates et al., 2019). Most of the experimental studies in neuroscience are carried out in male animals. The excessive dependence on male animals and cells in preclinical studies may mask the key sex differences that may guide clinical research (Madla et al., 2021). Therefore, this paper reviews the research on sex differences in the field of pain and related mental behaviors in recent years, analyzes the sex differences of dopamine, serotonin, GABA, oxytocin, and norepinephrine pathways involved in pain and related emotional behaviors, and combs out the brain circuit mechanism that may be involved in the regulation of sex differences in pain-induced mental disorders. In the era of individualized medical care, emphasis on sex medicine is essential to promote personalized care for patients.

2. Sex differences in neural circuits

Many brain regions, such as the anterior cingulate cortex, thalamus, amygdala, medial prefrontal cortex, and periaqueductal gray, are involved in the regulation of both chronic pain and emotions (Bushnell et al., 2013). However, a growing number of researchers believe that no neuron is an isolated island and that the connections between brain regions are more critical than brain subdivisions (Han and Domaille, 2022). Identifying specific or shared circuits that regulate pain and emotions is the key to unraveling the complex manifestations of pain and emotions.

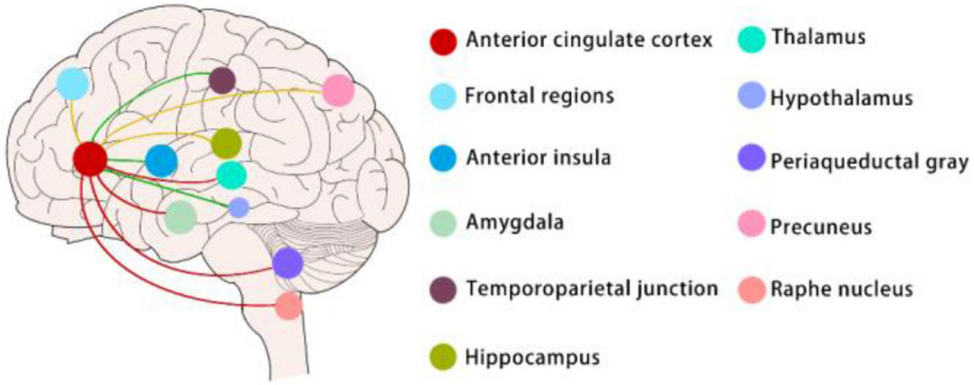

FIGURE 1
Sex differences in neural circuits (mainly in clinical experiments).

In clinical experiments, graph theory, modular analysis, and machine learning were used to analyze the default mode, central, visual, and sensorimotor modules in patients with chronic pain (Figure 1). In preclinical experiments, there were also more nuanced circuit manipulation experiments which were now being carried out extensively in animal experiments (Figure 2). Interestingly, both the clinical and preclinical results showed that sex difference was a non-negligible factor in the study of pain and emotions (Mogil, 2020). Brain regions and connections related to pain and emotions such as anterior cingulate cortex, amygdala, locus coeruleus, ventral tegmental area, and periaqueductal gray were all sexually differentiated.

Sex-difference neural circuits mentioned in this article are mainly about the functional connectivity (FC) of ACC. The red lines indicate that women exhibit greater FC between the anterior cingulate cortex and the thalamus, amygdala, periaqueductal gray, and raphe nucleus than men when chronic pain and pain emotions exist; The green lines indicate that men exhibit greater FC between the anterior cingulate cortex and temporoparietal junction, anterior insula, and hypothalamus than women when chronic pain and pain emotions exist. The yellow lines indicate that only women with chronic pain had greater ACC FC to the precuneus and lower FC to the hippocampus and frontal regions, men with chronic pain have no change in these connectivities compared to healthy men.

The green lines indicate that activation of the pathways induces pain-related depression in males but not females. Activation of the LC → ACC pathway leads to pain-induced depression in males, but it remains unknown whether the LC → ACC pathway conducts the same function in females. Increased VTA DA neuronal activity was associated with chronic neuropathic pain-induced depression-like behaviors. The activation of the Sp5C-LPBN^{Glu}-VTA^{DA} pathway was directly involved in the modulation of pain-related depression in males, but this circuit was not manipulated in females. Activation of the terminals in vlPAG/DR^{DA+} neurons or vlPAG/DR^{DA+}-BNST can reduce nociceptive sensitivity in naïve male mice and inflammatory pain states in males, whereas in female mice resulted in increased locomotion in the presence of significant stimuli. The purple lines indicate that activation of the pathways induces pain-related depression both in males and females. The inhibition of DRN serotonergic neurons → CeA somatostatin neurons pathway produces depression-like behaviors both in male and female mice models with chronic pain. There are also no sex differences in the regulation of the RMTg^{GABA}-VTA^{DA} circuit for chronic pain-induced pleasure deficits.

2.1. Anterior cingulate cortex (ACC)

Recent studies indicate that the anterior cingulate cortex (ACC) plays a critical role in chronic pain and pain-related emotional responses (Li et al., 2021). As an important part of the limbic system, ACC involves in pain and pain-related emotions *via* connectivity with other brain regions such as the descending pain antinociceptive system and so on (Chen et al., 2021). In a cross-sectional resting-state functional connectivity (RSFC) study among

Abbreviations: CGRP1, calcitonin gene-related peptide 1; CeA, central nucleus of the amygdala; DRN, dorsal raphe nucleus; LC, locus coeruleus; ACC, anterior cingulate cortex; sgACC, subgenual ACC; FC, functional connectivity; LTD, long-term depression; LTP, long-term potentiation; VTA, ventral tegmental area; PFC, prefrontal cortex; NAc, nucleus ambiguus; RMTg, rostromedial tegmental nucleus; DA, dopamine; Sp5C-LPBN, spinal trigeminal subnucleus caudalis to the lateral parabrachial nucleus; BNST, bed nucleus of the stria terminalis; vlPAG/DR, ventral lateral aqueduct periaqueductal gray/dorsal fissure; RVM, rostral ventromedial medulla; NE, norepinephrine; SNRI, serotonin-noradrenaline reuptake inhibitors; TH, tyrosine hydroxylase; CRF, corticotropin-releasing factor; D1 and D2, dopamine receptor 1 and 2; CCI, chronic constriction injury; NAc, nucleus accumbens; ADHD, attention-deficit/hyperactivity disorder; SSRI, selective serotonin reuptake inhibitor; 5-HIAA, 5-Hydroxy indoleacetic acid; IDO, indoleamine-2,3-dioxygenase; TRYCAT, tryptophan catabolite pathways; 5-HTT, 5-HT transporter; rs-fMRI, resting-state functional magnetic resonance imaging; GABA, gamma-aminobutyric acid; $GABA_{A/BR}$, $GABA_{A/B}$ receptors; GIRK, G proteingated inwardly-rectifying K^+; GAD, glutamic acid decarboxylase; GAT, GABA transporter; STG, superior cerebral gyrus; SPECT, single-photon emission computed tomography; $GABA_A$-BZR, $GABA_A$-benzodiazepine receptor; DMN, dorsomedial nucleus; Oxt, Oxytocin; PVN, paraventricular; SON, supraoptic nuclei; ICV, intracerebroventricular.

older adults, researchers found that the strongest evidence for sex differences emerged in the associations of thermal pain with RSFC between the ACC and amygdala and between the ACC and PAG in older females relative to older males (Figure 1) (Monroe et al., 2018). Researchers also investigated whether women have stronger functional connectivity (FC) and greater structural connectivity (SC) compared to men between the subgenual ACC (sgACC) and the descending antinociceptive system. They revealed that brain circuitry in women may provide for greater engagement of the descending modulation system mediating pain habituation but not in men. Between the sgACC and the periaqueductal gray (PAG), raphe nucleus, medial thalamus, and anterior midcingulate cortex (aMCC) women exhibited greater FC than men (Figure 1) (Wang et al., 2014). There were also findings indicating that abnormal sgACC circuitry is unique to women but not men with ankylosing spondylitis-related chronic pain. Compared to men, women had greater sgACC FC to the default mode and sensorimotor networks (Figure 1) (Osborne et al., 2021). Besides the connectivity, the anatomy of the ACC of rats was also sexually dimorphic with males having greater dendritic spine density as well as arborization. And this reduction was more pronounced for males with increasing age (Markham and Juraska, 2002). Synaptic plasticity is a key cellular mechanism for pain perception and emotional regulation. In preclinical studies, excitatory transmission and plasticity in the anterior cingulate cortex are critical in chronic pain-related emotions. Researchers used a 64-channel multielectrode (MED64) system to record synaptic plasticity in the ACC and found that long-term depression (LTD) was greater in ACC in male mice than females while long-term potentiation (LTP) did not show a sex-related difference (Liu et al., 2020). Besides, some studies reported that Sex differences in GABAergic gene expression occur in the ACC in schizophrenia (Bristow et al., 2015). It remains unknown whether Sex-difference GABAergic gene expression involves in pain and pain-related emotion.

2.2. Amygdala

It has been suggested that the amygdala receives inputs from the parabrachial nucleus and mediates differentiated pain and affective responses in males and females (Sun et al., 2020). Calcitonin gene-related peptide 1 (CGRP1) receptors in the central nucleus of the amygdala (CeA) are involved in neuropathic pain-related amygdala activity and contribute to nociception in both sexes (Presto and Neugebauer, 2022). However, they elicit emotional-affective pain responses such as ultrasound onset and anxiety-like behaviors mainly in females (Neugebauer et al., 2020). The dorsal raphe nucleus (DRN) is the main brain region for the synthesis and release of serotonin, and its involvement in pain-affective reactions has been discussed previously. It has been suggested that the inhibition of DRN serotonergic neurons → CeA somatostatin neurons pathway produces depression-like behaviors in male mice models with chronic pain. Activation of this pathway using pharmacological or optogenetic approaches reduced depression-like behavior in these mice (Figure 2) (Zhou et al., 2019). In this study, the researchers also included MRI data of the patient's FC to corroborate this finding. However, these data were not sex-differentiated, which seems to indicate that this circuit is not sexually dimorphic.

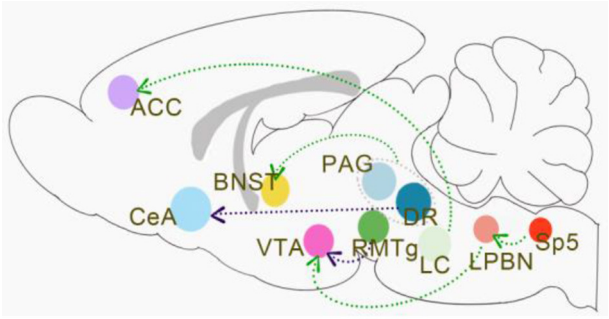

FIGURE 2
Sex differences in neural circuits (mainly in preclinical experiments).

2.3. Locus coeruleus (LC)

The locus coeruleus (LC) acts as a nucleus that regulates pain and emotion (Hirschberg et al., 2017). Resilience to chronic stress is mediated by the noradrenergic regulation of dopamine neurons (Llorca-Torralba et al., 2016). The circuits in which it is involved have also received considerable attention. In studies performed on male rats only, it was believed that bilateral chemogenetic inhibition of the LC → ACC pathway relieves pain-induced depression (Figure 2) (Llorca-Torralba et al., 2022), while activation of the noradrenergic LC → spinal cord pathway relieves pain. However, the noradrenergic system is considered to be sexually dimorphic in much of the literature. Studies have shown differences in the structure and function of LC between male and female rodents in many ways (Bangasser et al., 2015). The dendrites of the neurons in the LC of female rodents were more complex than those of the males (Bangasser et al., 2011), and the female LC dendrites further extended to the areas around the LC, as well as the afferent limbic systems involved in the stress response, such as the central nucleus of the amygdala and the bed nucleus of the stria terminalis (Van Bockstaele et al., 2001). And due to the increased synaptic density in females relative to males, female LC dendrites may receive more synaptic input (Bangasser et al., 2011). This means that anatomically the noradrenergic neurons of the LC may then form different circuits from other brain regions. Therefore, it remains unknown whether inhibition of the LC → ACC pathway relieves pain-induced depression is applicable to female rats.

2.4. Ventral tegmental area (VTA)

In addition to the involvement of the LC noradrenergic system in pain and depression co-morbidity, dopaminergic neuronal projections from the ventral tegmental area (VTA) to the prefrontal cortex (PFC), amygdala and nucleus ambiguus (NAc) play a key role in the perception and regulation of chronic pain symptoms (Hipólito et al., 2015). Rostromedial tegmental nucleus (RMTg) GABA hyperinhibition of the VTA dopamine (DA) neurons mediates pain-induced pleasure deprivation (Figure 2). In their experiments, the researchers concluded that no differences were found in the behaviors of males and females in the disease state or the alterations in their behaviors after the manipulation of the circuits (Markovic et al.,

2021). This suggests that there are no sex differences in the regulation of the RMTg GABA-VTA DA circuit for chronic pain-induced pleasure deficits (Figure 2) (Lowes et al., 2021). In another study, it was suggested that chronic neuropathic pain-induced depression-like behaviors were associated with increased VTA DA neuronal activity and that upstream spinal trigeminal sub-nucleus caudalis to the lateral parabrachial nucleus (Sp5C-LPBN) glutamatergic neuronal projections were directly involved in the modulation of VTA DA neurons (Figure 2) (Zhang et al., 2021). However, this circuit was not manipulated in female rats. Some studies support that the projections, gene expression levels, and electrical activity of VTA DA neurons do not differ significantly in males and females, which may explain the absence of functional differences in VTA DA-involved circuits in the co-morbidity of chronic pain and depression (Chung et al., 2017).

2.5. Periaqueductal gray (PAG)

In contrast, the DA neuron to the bed nucleus of the stria terminalis (BNST) projection circuit in the ventral lateral aqueduct periaqueductal gray/dorsal fissure (vlPAG/DR) has male and female differences in pain-related behaviors (Figure 2) (Yu et al., 2021). It has been found that activation of the terminals in vlPAG/DR^{DA+} neurons or vlPAG/DR^{DA+}-BNST can reduce nociceptive sensitivity in naïve male mice and inflammatory pain states in males, whereas activation of this pathway in female mice resulted in increased locomotion in the presence of significant stimuli (Yu et al., 2021). There is still insufficient fundamental research to answer the question of whether DA in PAG/DR is indeed sex-differentiated in projections and functions. Early studies suggested that the projection from the PAG to the rostral ventromedial medulla (RVM) is sexually dimorphic and that systemic administration of morphine significantly inhibited pain-induced PAG activation in male rather than female rats. It has also been suggested that microglia (Doyle et al., 2017) in the PAG, opioid receptor signaling (Loyd and Murphy, 2006), morphine metabolites (Doyle and Murphy, 2018), and endocannabinoids (Llorente-Berzal et al., 2022) are all sexually differentiated in their involvement in pain regulation. The PAG is a key structure in a number of regulatory pathways of nociception, emitting neuro fibers projections to the amygdala, hypothalamus, frontal cortex, hippocampus, and BNST to regulate the generation of pain and pain-related behaviors. We thus hypothesize, with little knowledge, that the brain circuits involving PAG are more likely to exhibit sexual dimorphism in their involvement in pain and related emotions.

In conclusion, whether different brain circuits are sexually dimorphic in their involvement in pain and related emotions may be related to differences in their own anatomies, molecular levels, and electrophysiological activities *per se*, and cannot be generalized in a simple way.

3. Sex differences in neurotransmitters and neuromodulators

The past and current literature have indicated that neurotransmitters and neuromodulators systems such as norepinephrine (Joshi and Chandler, 2020), dopamine (Hasbi et al., 2020), serotonin (Zhang et al., 2017), GABA (Cerne et al., 2022), and oxytocin (Tamborski et al., 2016; Aulino and Caldwell, 2020) seemed to be strongly involved in pain-related sexually dimorphic mental disorders (Dazzi and Scicchitano, 2014). Differences in concentrations (Busch et al., 1997), receptors (Hasbi et al., 2020), and transporters (Zachry et al., 2021) of these neurotransmitters and neuromodulators sexual differences may be potential targets for explaining sex differences in pain-related mental disorders.

3.1. Norepinephrine

Norepinephrine (NE) mediates the pathogenesis of pain and anxiety co-morbidity (Phillips et al., 2018). Serotonin-noradrenaline reuptake inhibitors (SNRI) antidepressants are widely used in anxiety disorders and they block the reuptake of NE and 5-HT, making them psychotropic drugs for the treatment of neuropathic pain in clinical settings as well (Fava et al., 2018). Norepinephrinergic neurons are mainly found in the LC and widely project to the cerebral cortex, hippocampus, hypothalamus, cerebellum, brainstem nuclei, and spinal cord (Mason, 1979). Previous studies have suggested that sex differences in the locus coeruleus noradrenergic system (Bangasser et al., 2015; Mulvey et al., 2018; Joshi and Chandler, 2020) may be one of the reasons why pain and depression occur frequently in females.

It has been reported that the LC of adult female rats is larger than that of male rats (Pinos et al., 2001) and contains more NE-ergic neurons (Guillamón et al., 1988), which corresponds to the phenomenon in humans (Busch et al., 1997). This may have increased the capacity for NE generation and release in females. In addition to differences in the number of neurons, there are also sex differences in the LC dendritic morphology (Bangasser et al., 2011). Morphological analysis of individual LC neurons by the researchers revealed that female LC dendrites are longer and more complex than those of males, which may increase synaptic afferent contacts in the peri-LC region (Mulvey et al., 2018). For example, increased nociception introduced by PAG (Bangasser et al., 2011) may be one of the neurobiological mechanisms underlying the sex differences in pain.

Apart from the differences in the number and morphology of NE-ergic neurons in LC, it has been reported that estradiol treatment increases NE levels in the ventral hippocampus, cortex, and hypothalamus of ovariectomized female rats (Bangasser et al., 2011). In addition, estrogen can increase NE synthesis and decrease NE degradation, while ovarian hormones increase NE levels in LC target regions through presynaptic modulation of NE release (Vathy and Etgen, 1988). This can occur through estrogenic regulation of the NE biosynthetic enzyme tyrosine hydroxylase (TH) (Serova et al., 2002; Dalla et al., 2010). The widespread projection system of the LC can release NE into the forebrain and regulate emotional behaviors by targeting forebrain regions. LC activation in animal models of chronic pain exhibited an anxiolytic-depressive phenotype (Landau et al., 2015) but these experiments did not involve females (Alba-Delgado et al., 2013).

However, in reports on other excitatory mediators associated with LC and neuropathic pain, the main excitatory neurotransmitter of the associated stress response, corticotropin-releasing factor (CRF), was enhanced in LC with sex differences. The expression of the CRF1 receptor was increased in the LC of male mice (Bangasser et al., 2013) with chronic pain and anxiogenic phenotypes, whereas this receptor

was weakly expressed in anxiety-resilient female mice with pain. Interestingly, increased sensitivity of LC to CRF signaling in females leads to enhanced LC responses of females to non-pain stresses.

In conclusion, sex differences in the locus coeruleus norepinephrine system in the phenotype of pain and related anxiety and depression is an area of research interest.

3.2. Dopamine

Dopaminergic neurons in the brain are widely distributed in the substantia nigra pars compacta (Poulin et al., 2018), ventral tegmental area (Markovic et al., 2021), hypothalamus (Kim et al., 2019) and periventricular area, periaqueductal gray, dorsal raphe nucleus (Yu et al., 2021), and the olfactory bulb (Pignatelli and Belluzzi, 2017). Regions such as the prefrontal cortex (Bhattacherjee et al., 2019), striatum (Dentresangle et al., 2001), nucleus ambiguus, amygdala (Janak and Tye, 2015), thalamus, hippocampus, periaqueductal gray (Yu et al., 2021), and dorsal horn of the spinal cord are all innervated by dopaminergic neurons and are involved in the transduction of pain and related behaviors (Mercer Lindsay et al., 2021; Yang H. et al., 2021). The nigrostriatal dopaminergic system affects pain transduction and perception through the ascending and descending pathways (Dieb et al., 2016). The mesolimbic dopaminergic system regulates pain perception mainly through the reward or motivational pathways in the ventral tegmental area innervating the vomeronasal nucleus, amygdala, thalamus, and hippocampus (Serafini et al., 2020). It also influences learning and memory as well as sensory evaluation of pain through projections to the prefrontal cortex (Huang et al., 2020).

In recent years, it has become a consensus that there are sex differences in the incidence of dopamine-related neuropsychiatric disorders and sensitivity to dopamine-enhancing drugs such as stimulants, and previous studies have shown that dopaminergic circuits often act through dopamine receptors D1 and D2 (Fasano et al., 2013; Stalter et al., 2020; Allichon et al., 2021). It has been shown in the chronic constriction injury (CCI) pain model of the sciatic nerve in mice that dopaminergic projections from the VTA to the nucleus accumbens (NAc) are involved in pain modulation (Ding et al., 2021). In addition, optogenetic activation of dopaminergic neurons in the VTA and their nerve endings in the NAc significantly increases the nociceptive threshold in CCI rats, and the analgesic effect is exerted mainly through D2 (Gao et al., 2020). D1 and D2 may be involved in pain and analgesia in different ways. In the PAG, an important component of the nociceptive descending regulatory system, the analgesic efficacy of opioid receptor agonists on thermal pain stimuli in mice is significantly reduced following damage to dopaminergic nerve endings. Microinjection of D1 antagonists attenuated the analgesic effect of opioids in the hot plate tests, whereas D2 antagonists showed no such effect (Tobaldini et al., 2018). In another study, pharmacological experiments revealed that both D1 and D2 antagonists significantly antagonized the analgesic effects of opioids. Injections of D2 agonists into PAG increased the nociceptive threshold in mice, and the analgesic effects of D2 agonists were blocked by D2 antagonists and γ-aminobutyric acid receptor agonists or opioid receptor antagonists. This study also demonstrated that the combination of D1 and D2 agonists had a greater anti-injurious effect than any one of the receptor agonists alone (Wang et al., 2021).

More interestingly, a number of studies have found that D1 and D2 are involved in sex-differentiated regulation of pain and related behaviors such as anxiety and depression (Hasbi et al., 2020). For example, in the caudate nucleus of non-human primates and the rat striatum, females express a higher density of D1–D2 heteromeric complexes and more D1–D2-expressing neurons compared to males (Hasbi et al., 2020). Signaling pathway analysis showed that sex differences in D1–D2 heteromer expression resulted in differences in the basal and heteromer-stimulated activity of two important signaling pathways, BDNF/TrkB and Akt/GSK3/β-linked protein. The dopamine D1–D2 heteromeric complex is involved in depressive and anxiety-like behaviors, and higher D1–D2 heteromer expression in females may significantly increase the propensity for depressive- and anxiety-like behaviors (Hasbi et al., 2020). Furthermore, in the field of non-pain-related emotions, it has been demonstrated that sex differences in D1 receptor-regulated molecular pathways lead to sex differences in social withdrawal behaviors (Campi et al., 2014). Although social defeat increased dopamine levels in male and female NAc, social withdrawal was induced only in female California mice, but not in male ones. Pharmacological experiments showed that D1 receptor activation was sufficient to induce social withdrawal in females, but not in males. D1 antagonists increased social approach behavior in females exposed to social defeat but did not affect naïve females (Campi et al., 2014). Apart from the fact that D1 and D2 are differentially expressed between males and females, they may be a potential target for revealing the differences in pain-related emotions between the two sexes. Sex differences in neurological dopamine sensitivity as well as in the balanced dopamine release among the circuits could be another area of concern.

In clinical and preclinical studies, using pharmacological methods combined with PET-CT imaging, researchers have suggested that the increased sensitivity of the striatal dopamine reward system in females compared to males may underlie the sex differences in substance use disorders and attention-deficit/hyperactivity disorder (ADHD) (Manza et al., 2022). However, some researchers pointed out that there is little sex difference in the encoding of VTA neurons as well as dopamine release and vesicle depletion in the NAc during the learning process of cue-action-reward instrumental tasks, and that dopamine-related sex differences may be mediated by secondary mechanisms that flexibly affect dopamine cell and circuit functions (Rivera-Garcia et al., 2020). Much of the research on the dopamine system has focused on addiction-related disorders, and it has been suggested that sex differences between different dopamine projections underlie sex differences in addiction (Becker, 2016). In rodents, ovariectomized female rats exhibit smaller initial dopamine increases after cocaine treatment than castrated male rats. Estradiol treatment of ovariectomized female rats enhanced stimulated dopamine release in the dorsolateral striatum but not in the vomeronasal nucleus, resulting in sex differences in the balance between these two dopaminergic projections (Becker, 2016). Moreover, it is not clear whether sex differences regarding the balance of the dopaminergic nervous systems are involved in the generation of sex differences in pain and pain-related emotions. It may be an important potential target.

While many of the previous studies have focused on sex differences in the anatomical structure of dopamine neurons and sex differences related to dopamine levels, it has been suggested that how sex differences in microcircuit regulatory mechanisms

mediate sex-differentiated dopamine dynamics is worthy of equal attention (Zachry et al., 2021). Studies suggested that there are local regulatory mechanisms in the ventral tegmental area of the midbrain limbic dopamine system to the striatal circuits that are independent of somatic activity and that these processes can occur through both homogeneous synaptic mechanisms (e.g., presynaptic dopamine self-receptors and dopamine transporter proteins) and heterosynaptic mechanisms (e.g., retrograde signaling of postsynaptic cholinergic and GABAergic systems, etc.) (Zachry et al., 2021), so that the dopamine released by the striatal axonal terminals can be independently and rapidly regulated. In addition, these regulations are potential targets of sex differences in ovarian hormone-dependent and non-dependent dopamine regulation (Zachry et al., 2021). These mechanisms have been shown to be key mediators of multiple psychiatric disorders and involved in the expression of sex-specific behaviors.

3.3. Serotonin

As a monoamine neurotransmitter, serotonin plays a vital role in regulating emotions (Kraus et al., 2017), learning (Grossman et al., 2022), memory (Wu et al., 2021), sleep (Monti, 2011), and appetite (Blundell, 1984), and is closely related to pain and neuropsychiatric disorders such as major depression and anxiety (Zhou et al., 2022). In recent decades, selective serotonin reuptake inhibitor (SSRI) drugs have been the most commonly prescribed medications for depression. Clinical and preclinical studies suggest that amitriptyline, a tricyclic antidepressant used to treat mood disorders, neuropathic pain, and migraine, can increase serotonin levels and restore behavioral responses associated with pain and depression (Zhang et al., 2017). Long-term administration of fluoxetine, an SSRI, was found to prevent anxiety and depression caused by sciatic nerve injury without affecting mechanical allodynia (Barthas et al., 2017). Researchers had found, but controversially, that SSRIs were more effective for females compared to tricyclic antidepressants (Kornstein et al., 2000). Sex differences regarding the serotonergic system had been much reported. In particular, 5-Hydroxy indoleacetic acid (5-HIAA) was reported to be increased in the cerebrospinal fluid of women suffering from depression (Rubinow et al., 1998). Studies have shown increases in 5-HT activity, 5-HT synthesis, and 5-HT metabolites in the brains of female rats compared to male ones (Carlsson and Carlsson, 1988; Haleem et al., 1990). In a clinical study comparing SSRIs with tricyclics, researchers found that menopause significantly affected treatment outcomes and pointed out that this sex-specific difference may be related to the hormonal milieu (Yonkers and Simoni, 2018). Studies conducted with multiple models of depression such as the Chronic Mild Stress Model, the Learned Helplessness Model, the Flinders Sensitive Line rats, and the Lipopolysaccharide-Induced Sickness Behavior in mice have shown that serotonergic neurochemical responses are affected differently in males and females, resulting in sex-dependent behavioral effects (Serova et al., 2002; Dalla et al., 2010).

In previous studies, researchers have noted that sex steroids such as testosterone, progesterone, estrogen, and HPA axis, all have effects on the serotonin pathway (Songtachalert et al., 2018). Activated immune inflammation induces the indoleamine-2,3-dioxygenase (IDO) and tryptophan catabolite (TRYCAT) pathways, thereby enhancing tryptophan degradation and increasing the generation of TRYCATs, including kynurenine and quinolinic acid, exerting an overall anxiogenic effect. The effect of immune activation on IDO is greater in females than in males, therefore, females are more likely to exhibit elevated anxiogenic TRYCAT levels following immune challenge. Moreover, aberrations in the IDO-activated TRYCAT pathway are observed in pregnant females and parturients and are associated with increased levels of postpartum anxiety (Songtachalert et al., 2018).

In addition to the metabolic pathways of serotonin, studies have also found that there are sex differences in serotonin receptors (Zhang et al., 1999; Snoeren et al., 2014; Yamada et al., 2015). There were also differences in 5-HT_{1A} receptor responses between males and females in the repeated stress restraint model in rats. Only males exhibited elevated 5-HT_{1A} receptor G protein coupling responses after repetitive restraint, whereas only females showed increased 5-HT_{1A} receptor responses in the hippocampus following single or repeated exposure (Philippe et al., 2022). In studies exploring sex-related differences in genetics, stress, and the nervous system, female 5-HT_{1B} receptor knockout mice showed significantly lower immobility time and significantly higher baseline hippocampal 5-HT levels than male 5-HT_{1B} receptor knockout mice or male and female wild-type mice in tail suspension and forced swimming tests (Jones and Lucki, 2005). This suggests that female 5-HT_{1B} receptor knockout mice exhibit sex-related disinhibition of 5-HT release, which maintains higher baseline levels of hippocampal 5-HT and behavioral vulnerability to 5-HT depletion (Jones and Lucki, 2005). Moreover, the serotonin transporter protein is also worthy of investigation as a target for many anxiolytic and antidepressant drugs. Using 5-HT transporter (5-HTT) gene-deficient mice as an anxiety animal model, researchers examined cerebral blood flow during resting and amygdala hyperresponsiveness periods using resting-state functional magnetic resonance imaging (rs-fMRI) (Kolter et al., 2021). The results indicated that amygdala reactivity in 5-HTT-deficient mice is regulated by the 5-HTT genotype in males. Whereas, in females it is regulated by the estrous cycle and the predominant influence of gonadotropins may mask genotypic effects (Kolter et al., 2021).

In conclusion, the role of the serotonin system in the sex-differentiated modulation of pain, anxiety, and depression is a matter worthy of investigation.

3.4. Gamma-aminobutyric acid (GABA)

GABA, as one of the important inhibitory neurotransmitters, regulates the encoding of pain and anxiety-depressive mood (Cerne et al., 2022). It has been reported that the anxiolytic effect of GABA depends mainly on its binding to the $GABA_A$ receptors ($GABA_{AR}$). The benzodiazepine anxiolytic $GABA_{AR}$ modulators have been in clinical use for decades (Sollozo-Dupont et al., 2015). $GABA_{AR}$ functions through its subunit composition, the activation of which allows GABA to exert trophic effects in immature neurons.

Recent studies found that GABA-mediated responses were sexually dimorphic even in the absence of gonadal hormone and that there were sex differences in the expression of $GABA_{AR}$ subtypes (Mir et al., 2020). Researchers assessed sex differences in $GABA_{AR}$ function of hypothalamic neurons before brain masculinization

by gonadal hormones by culturing 16-day rat embryonic ventral medial hypothalamus neurons *in vitro*, combined with calcium imaging and electrophysiological recordings (Mir et al., 2020). Optogenetic-specific activation of the dmPFC/vlPAG neural pathway had been reported to produce analgesic and anxiolytic effects in chronic pain-anxiety mice. dmPFC-specific activation of inhibitory neurons in dmPFC was reported to induce nociception and anxiety under normal conditions and chronic pain, and the $GABA_{AR}$ or mGluR1 antagonists can produce analgesic and anxiolytic effects (Yin et al., 2020). However, this study focused only on male mice and it is unknown whether female ones have the same phenotype.

In studies of disorders associated with altered mPFC functions such as schizophrenia, ADHD (Aoki et al., 2013), post-traumatic stress disorder (Lou et al., 2020), depression (Yang L. et al., 2021), and drug addiction (Jasinska et al., 2015), etc., researchers suggested that sex-differentiated manifestations can be partially explained by sex differences in G protein gated inwardly-rectifying K^+ (GIRK)-dependent signaling in mPFC pyramidal neurons. Neuronal GIRK channels are formed by homo- or heteromeric assembly of GIRK1/GIRK2/GIRK3 subunits. They play a key role in regulating excitability throughout the brain and are associated with a variety of neurological disorders as well as sex differences in cellular functions. Sex differences in $GABA_{BR}$-GIRK signaling are attributed to a phosphorylation-dependent transport mechanism (Marron Fernandez De Velasco et al., 2015). There are sex differences in the $GABA_{BR}$-GIRK signaling pathway in these neurons. $GABA_{BR}$-dependent GIRK currents in the anterior limbic region of the mPFC were greater in adolescent male mice than in females, but this sex difference was not observed in pyramidal neurons in layer 5/6 of the adjacent limbic cortex.

Previous studies have revealed sex differences in the expression levels of the GABA signaling components, namely, glutamic acid decarboxylase (GAD), GABA receptor subunit, and GABA transporter (GAT) (Pandya et al., 2019). Analysis of sex-specific changes in the expression of GAD, $GABA_{A/BR}$ subunit, and GAT in the human primary sensory and motor cortex revealed sex-dependent differences in the expression of the $GABA_{AR}$ subunit in the superior cerebral gyrus (STG). There is a significant sex-dependent difference in the expression of the $\alpha 1$ subunit of STG: males present significantly higher levels of expression compared to women across all stages of life in STG. Older females had significantly lower $\alpha 2$, $\alpha 5$, and $\beta 3$ subunit expression in the STG compared to older males. These changes found in the STG may significantly affect GABAergic neurotransmission and lead to sex-specific disease susceptibility and progression (Pandya et al., 2019). There is still a lack of evidence as to whether these baseline differences are involved in the sex-differentiated manifestations of pain and related emotions and behaviors.

In studies on male and female smokers in terms of nicotine dependence, cigarette cravings, and mood or pain sensitivity, researchers used single-photon emission computed tomography (SPECT) to image subjects (Cosgrove et al., 2011). The results showed that females (both female smokers and female non-smokers) had higher $GABA_A$-benzodiazepine receptor ($GABA_A$-BZR) availability than all males. $GABA_A$-BZR availability was negatively correlated with craving and pain sensitivity in female smokers, but not in male smokers. This suggests a sex-specific modulation of $GABA_A$-BZR availability and demonstrates the potential of $GABA_A$-BZRs to mediate smoking cravings and pain symptoms in female and male smokers (Cosgrove et al., 2011).

It is estimated that GABAergic neurons account for more than half of the hypothalamic neuronal population (Searles et al., 2000), and they may explain some of the structural and functional sex differences observed in the mammalian brain. Studies have reported sex differences in GABA turnover rates in discrete hypothalamic structures in adult rats and determined that these differences may be related to differences in GAD65 and/or GAD67 mRNA levels (Sagrillo and Selmanoff, 1997). There is evidence that GAD65 mRNA levels are significantly higher in female rats in the dorsomedial nucleus (DMN), while GAD67 mRNA levels are higher in male rats in the medial amygdala. These data reveal significant sex differences in GABA turnover and GAD mRNA levels in hypothalamic GABAergic neurons of specific populations (Bowman et al., 2013).

Whether the differential manifestations of these GABAergic neurons participate in the sex differences in pain and pain-related affective behaviors remains to be further studied.

3.5. Oxytocin

Oxytocin (Oxt) is a nine-amino-acid peptide hormone that is synthesized and released in the brain primarily by neurons in the paraventricular (PVN) and supraoptic nuclei (SON) of the hypothalamus (Rossoni et al., 2008). Oxt is thought to be associated with pain, and clinically, plasma oxytocin levels are reduced in women with fibromyalgia syndrome (Anderberg and Uvnas-Moberg, 2000). Intranasal administration of Oxt leads to changes in the activity of the bilateral thalamus, left caudate nucleus, and right amygdala, and ameliorates pain in patients with chronic low back pain (Schneider et al., 2020). Epidural oxytocin induces analgesia in patients with severe chronic pain and also improves patients' moods and quality of life.

Oxt has anti-injurious and antinociceptive hormonal effects on neuropathic pain (Xin et al., 2017) induced by nerve injury, which is mediated by its receptor (OTR) and likely occurs due to co-localization of these neurons within OTR-binding sites, such as the spinal dorsal horn (Veronneau-Longueville et al., 1999; Wrobel et al., 2011). Interestingly, in the pain model in rats, Oxt content in the PVN was found to be significantly reduced, but Oxt content in the spinal cord remained unchanged. The researchers also observed that intracerebroventricular injection of Oxt increased the mechanical hypersensitivity response threshold in a dose-dependent manner, whereas intrathecal injection of Oxt did not induce any analgesia. These results indirectly suggest that Oxt in the brain may have an analgesic effect independent of the spinal cord (Zhang et al., 2015). Furthermore, Oxt also plays a crucial role in social behavior, stress, and depression, as verified in animal experiments (Neumann, 2008; Massey et al., 2016). More than one study has suggested that activation of OTR in the VTA is critical for the expression of reward-like properties of social interactions (Song et al., 2016; Borland et al., 2018). However, there are clear sex differences in the embryonic development of Oxt /OTR, which may indicate sex differences in their involvement in pain/behavior (Tamborski et al., 2016; Aulino and Caldwell, 2020). In clinical studies, the expression of Oxt at rs4813625, a single nucleotide polymorphism linked to Oxt was found to correlate more with nociception, anxiety, and wellbeing in

females, while no such correlation was found in males (Love et al., 2012).

Another study showed a correlation between depression severity and methylation of the Oxt promoter region. There was a significant negative correlation between critical life events and the mean methylation status as well as the methylation status of single CpG sites in the Oxt promoter region. Whereas, there was no association between depression severity and Oxt methylation. However, there were significant sex differences in the methylation status of Oxt, with females having higher methylation rates than males, suggesting that in patients with depressive disorders, Oxt activation is lower in female patients compared to male ones (Sanwald et al., 2020). Interestingly, in an animal experiment, 3-nitropropionic acid (3-NP)-induced Huntington's disease model was found to have both anxiety and depressive behaviors. 3-NP also reduced the levels of OTR and mGluR2 in the striatum and increased mGluR5. Oxt pretreatment was performed to ameliorate anxiety and depression and to reverse the abnormal expression of OTR, mGluR2, and mGluR5 under the disease state. These behavioral and molecular alterations act similarly between male and female animals (Khodagholi et al., 2022). Meanwhile, some studies support that Oxt may interact with mGluR2 and influence addictive behavior in rats and that this receptor interaction is similar between females and males (Bernheim et al., 2017). However, some researchers have suggested that sex differences in Oxt -regulated emotions tend to occur in the presence of negative stress, for example, one study found that male rats exposed to the stress of social defeat exhibited reduced social avoidance after receiving Intracerebroventricular (ICV) infusions of Oxt (Lukas et al., 2011). Whereas, ICV infusion of Oxt did not reduce social avoidance in stressed female rats (Lukas and Neumann, 2014). The same dose of intranasal Oxt reversed social avoidance in male mice exposed to social defeat, a phenomenon not observed in female mice (Steinman et al., 2016). Nevertheless, sex differences of Oxt in pain affective reactions remain worthy of further study.

4. Conclusion

In the study of pain-induced emotional disorders, most animal experiments only use male mice. It is generally considered that many neurological and behavioral functions are affected by estrogen, including emotion, cognitive function, and pain (McEwen and Milner, 2017). Sex hormones, particularly estradiol and progesterone, play an important role in pain perception and mood swings (Vincent and Tracey, 2010). It has been reported that there is a strong link between mood swings and sex hormones, particularly endogenous hormones (Hernandez-Hernandez et al., 2019; Frokjaer, 2020). Menstrual (or estrous) cycles in females altered pain perception (Kaur et al., 2018), depression (Kaur et al., 2018; Zhao et al., 2021), and even neuronal activity in certain brain regions (D'Souza and Sadananda, 2017). Researchers often do not use female mice for research based on these complexities. However, there is also a contrary view. Studies have shown that there is no significant difference in social behavior, depression-like, anxiety-like behavior, and pain threshold in female mice with pain during different estrus periods (Zhao et al., 2021). In any case, it has been reported in the literature that women have higher rates of pain, depression, and anxiety, and the extensive use of male animal experiments has slowed the process of developing drugs that are more suitable for women, such as analgesia, antidepressants, and antianxiety. There is a huge contradiction in this. We cannot ignore these differences. In the future, research needs to include females to further clarify the mechanism of pain-induced emotional disorders and the targets of sex-differentiated regulation of related neurotransmitters and modulation, which is believed to provide better background support for individual precision medicine.

Author contributions

All authors listed have made a substantial, direct, and intellectual contribution to the work and approved it for publication.

Funding

This work was supported by Natural Science Foundation of Shandong Province (No. ZR2021QH103), National Natural Science Foundation of China (No. 82174499), Innovative Research Team of High-level Local Universities in Shanghai, Innovation Team and Talents Cultivation Program of National Administration of Traditional Chinese Medicine (No. ZYYCXTD-C-202008), and Shanghai Key Laboratory for Acupuncture Mechanism and Acupoint Function (No. 21DZ2271800).

Conflict of interest

The authors declare that the research was conducted in the absence of any commercial or financial relationships that could be construed as a potential conflict of interest.

Publisher's note

References

Alba-Delgado, C., Llorca-Torralba, M., Horrillo, I., Ortega, J. E., Mico, J. A., Sánchez-Blázquez, P., et al. (2013). Chronic pain leads to concomitant noradrenergic impairment and mood disorders. *Biol. Psychiatry* 73, 54–62. doi: 10.1016/j.biopsych.2012.06.033

Allichon, M. C., Ortiz, V., Pousinha, P., Andrianarivelo, A., Petitbon, A., Heck, N., et al. (2021). Cell-type-specific adaptions in striatal medium-sized spiny neurons and their roles in behavioral responses to drugs of abuse. *Front. Synapt. Neurosci.* 65, 13799274. doi: 10.3389/fnsyn.2021.799274

Anderberg, U. M., and Uvnas-Moberg, K. (2000). Plasma oxytocin levels in female fibromyalgia syndrome patients. *Z. Rheumatol.* 59, 373–379. doi: 10.1007/s003930070045

Aoki, Y., Inokuchi, R., Suwa, H., and Aoki, A. (2013). Age-related change of neurochemical abnormality in attention-deficit hyperactivity disorder: a meta-analysis. *Neurosci. Biobehav. Rev.* 37, 1692–1701. doi: 10.1016/j.neubiorev.2013.04.019

Aulino, E. A., and Caldwell, H. K. (2020). Subtle sex differences in vasopressin mRNA expression in the embryonic mouse brain. *J. Neuroendocrinol.* 32, e12835. doi: 10.1111/jne.12835

Bangasser, D. A., Reyes, B. A., Piel, D., Garachh, V., Zhang, X. Y., Plona, Z. M., et al. (2013). Increased vulnerability of the brain norepinephrine system of females to corticotropin-releasing factor overexpression. *Mol. Psychiatry* 18, 166–173. doi: 10.1038/mp.2012.24

Bangasser, D. A., Wiersielis, K. R., and Khantsis, S. (2015). Sex differences in the locus coeruleus-norepinephrine system and its regulation by stress. *Brain Res.* 1641, 177–188. doi: 10.1016/j.brainres.2015.11.021

Bangasser, D. A., Zhang, X., Garachh, V., Hanhauser, E., and Valentino, R. J. (2011). Sexual dimorphism in locus coeruleus dendritic morphology: a structural basis for sex differences in emotional arousal. *Physiol. Behav.* 103, 342–351. doi: 10.1016/j.physbeh.2011.02.037

Barthas, F., Humo, M., Gilsbach, R., Waltisperger, E., Karatas, M., Leman, S., et al. (2017). Cingulate overexpression of mitogen-activated protein kinase phosphatase-1 as a key factor for depression. *Biol. Psychiatry* 82, 370–379. doi: 10.1016/j.biopsych.2017.01.019

Becker, J. B. (2016). Sex differences in addiction. *Dialog. Clin. Neurosci.* 18, 395–402. doi: 10.31887/DCNS.2016.18.4/jbecker

Bernheim, A., Leong, K., Berini, C., and Reichel, C. M. (2017). Antagonism of mGlu2/3 receptors in the nucleus accumbens prevents oxytocin from reducing cued methamphetamine seeking in male and female rats. *Pharmacol. Biochem. Behav.* 161, 13–21. doi: 10.1016/j.pbb.2017.08.012

Bhattacherjee, A., Djekidel, M. N., Chen, R., Chen, W., Tuesta, L. M., and Zhang, Y. (2019). Cell type-specific transcriptional programs in mouse prefrontal cortex during adolescence and addiction. *Nat. Commun.* 10, 4169–4118. doi: 10.1038/s41467-019-12054-3

Blundell, J. E. (1984). Serotonin and appetite. *Neuropharmacology* 23, 1537–1551.

Borland, J. M., Grantham, K. N., Aiani, L. M., Frantz, K. J., and Albers, H. E. (2018). Role of oxytocin in the ventral tegmental area in social reinforcement. *Psychoneuroendocrinology* 95, 128–137. doi: 10.1016/j.psyneuen.2018.05.028

Bowman, B. R., Kumar, N. N., Hassan, S. F., McMullan, S., and Goodchild, A. K. (2013). Brain sources of inhibitory input to the rat rostral ventrolateral medulla. *J. Compar. Neurol.* 521, 213–232. doi: 10.1002/cne.23175

Bristow, G. C., Bostrom, J. A., Haroutunian, V., and Sodhi, M. S. (2015). Sex differences in GABAergic gene expression occur in the anterior cingulate cortex in schizophrenia. *Schizoph. Res.* 167, 57–63. doi: 10.1016/j.schres.2015.01.025

Busch, C., Bohl, J., and Ohm, T. G. (1997). Spatial, temporal and numeric analysis of Alzheimer changes in the nucleus coeruleus. *Neurobiol. Aging* 18, 401–406.

Bushnell, M. C., Ceko, M., and Low, L. A. (2013). Cognitive and emotional control of pain and its disruption in chronic pain. *Nat. Rev. Neurosci.* 14, 502–511. doi: 10.1038/nrn3516

Campi, K. L., Greenberg, G. D., Kapoor, A., Ziegler, T. E., and Trainor, B. C. (2014). Sex differences in effects of dopamine D1 receptors on social withdrawal. *Neuropharmacology* 77, 208–216. doi: 10.1016/j.neuropharm.2013.09.026

Carlsson, M., and Carlsson, A. (1988). A regional study of sex differences in rat brain serotonin. *Prog. Neuro-Psychopharmacol. Biol. Psychiatry* 12, 53.

Cerne, R., Lippa, A., Poe, M. M., Smith, J. L., Jin, X., Ping, X., et al. (2022). GABAkines: advances in the discovery, development, and commercialization of positive allosteric modulators of GABAA receptors. *Pharmacol. Therapeut.* 234, 108035. doi: 10.1016/j.pharmthera.2021.108035

Chen, Q., Li, X., and Zhuo, M. (2021). NMDA receptors and synaptic plasticity in the anterior cingulate cortex. *Neuropharmacology* 197, 108749. doi: 10.1016/j.neuropharm.2021.108749

Chung, A. S., Miller, S. M., Sun, Y., Xu, X., and Zweifel, L. S. (2017). Sexual congruency in the connectome and translatome of VTA dopamine neurons. *Sci. Rep.* 7, 11120. doi: 10.1038/s41598-017-11478-5

Cosgrove, K. P., Esterlis, I., Mason, G. F., Bois, F., O'Malley, S. S., and Krystal, J. H. (2011). Neuroimaging insights into the role of cortical GABA systems and the influence of nicotine on the recovery from alcohol dependence. *Neuropharmacology* 60, 1318–1325. doi: 10.1016/j.neuropharm.2011.01.020

Dalla, C., Pitychoutis, P. M., Kokras, N., and Papadopoulou-Daifoti, Z. (2010). Sex differences in animal models of depression and antidepressant response. *Basic Clin. Pharmacol. Toxicol.* 106, 226–233. doi: 10.1111/j.1742-7843.2009.00516.x

Dazzi, F., and Scicchitano, C. (2014). Neurotransmitters: gender's differences. *Rivista di Psichiatria* 49, 237. doi: 10.1708/1668.18264

Dentresangle, C., Le Cavorsin, M., Savasta, M., and Leviel, V. (2001). Increased extracellular DA and normal evoked DA release in the rat striatum after a partial lesion of the substantia nigra. *Brain Res.* 893, 178–185. doi: 10.1016/S0006-8993(00)03311-4

Dieb, W., Ouachikh, O., Alves, S., Boucher, Y., Durif, F., and Hafidi, A. (2016). Nigrostriatal dopaminergic depletion increases static orofacial allodynia. *J. Headache Pain* 17, 11. doi: 10.1186/s10194-016-0607-z

Ding, X., Gao, X., Wang, Z., Jiang, X., Lu, S., Xu, J., et al. (2021). Preoperative chronic and acute pain affects postoperative cognitive function mediated by neurotransmitters. *J. Mol. Neurosci.* 71, 515–526. doi: 10.1007/s12031-020-01673-x

Doyle, H. H., Eidson, L. N., Sinkiewicz, D. M., and Murphy, A. Z. (2017). Sex Differences in microglia activity within the periaqueductal gray of the rat: a potential mechanism driving the dimorphic effects of morphine. *J. Neurosci.* 37, 3202–3214. doi: 10.1523/JNEUROSCI.2906-16.2017

Doyle, H. H., and Murphy, A. Z. (2018). Sex-dependent influences of morphine and its metabolites on pain sensitivity in the rat. *Physiol. Behav.* 187, 32–41. doi: 10.1016/j.physbeh.2017.11.030

D'Souza, D., and Sadananda, M. (2017). Estrous cycle phase-dependent changes in anxiety- and depression-like profiles in the late adolescent Wistar-Kyoto rat. *Ann. Neurosci.* 24, 136–145. doi: 10.1159/000477151

Fasano, C., Bourque, M., Lapointe, G., Leo, D., Thibault, D., Haber, M., et al. (2013). Dopamine facilitates dendritic spine formation by cultured striatal medium spiny neurons through both D1 and D2 dopamine receptors. *Neuropharmacology* 67, 432–443. doi: 10.1016/j.neuropharm.2012.11.030

Fava, G. A., Benasi, G., Lucente, M., Offidani, E., Cosci, F., and Guidi, J. (2018). Withdrawal symptoms after serotonin-noradrenaline reuptake inhibitor discontinuation: systematic review. *Psychother. Psychosom.* 87, 195–203. doi: 10.1159/000491524

Frokjaer, V. G. (2020). Pharmacological sex hormone manipulation as a risk model for depression. *J. Neurosci. Res.* 98, 1283–1292. doi: 10.1002/jnr.24632

Gao, S., Shen, L., Wen, H., Zhao, Y., Chen, P., and Ruan, H. (2020). The projections from the anterior cingulate cortex to the nucleus accumbens and ventral tegmental area contribute to neuropathic pain-evoked aversion in rats. *Neurobiol. Dis.* 140, 104862. doi: 10.1016/j.nbd.2020.104862

Grossman, C. D., Bari, B. A., and Cohen, J. Y. (2022). Serotonin neurons modulate learning rate through uncertainty. *Curr. Biol.* 32, 586–599.e7. doi: 10.1016/j.cub.2021.12.006

Guillamón, A., de Blas, M. R., and Segovia, S. (1988). Effects of sex steroids on the development of the locus coeruleus in the rat. *Dev. Brain Res.* 40, 306–310.

Haleem, D. J., Kennett, G. A., and Curzon, G. (1990). Hippocampal 5-hydroxytryptamine synthesis is greater in female rats than in males and more decreased by the 5-HT1A agonist 8-OH-DPAT. *J. Neural Trans.* 79, 93–101.

Han, G. S., and Domaille, D. W. (2022). Connecting the dynamics and reactivity of arylboronic acids to emergent and stimuli-responsive material properties. *J. Mater. Chem. B Mater. Biol. Med.* 1, 6263–6278. doi: 10.1039/D2TB00968D

Hasbi, A., Nguyen, T., Rahal, H., Manduca, J. D., Miksys, S., Tyndale, R. F., et al. (2020). Sex difference in dopamine D1–D2 receptor complex expression and signaling affects depression- and anxiety-like behaviors. *Biol. Sex Differ.* 11, 8. doi: 10.1186/s13293-020-00285-9

Hernandez-Hernandez, O. T., Martinez-Mota, L., Herrera-Perez, J. J., and Jimenez-Rubio, G. (2019). Role of estradiol in the expression of genes involved in serotonin neurotransmission: implications for female depression. *Curr. Neuropharmacol.* 17, 459–471. doi: 10.2174/1570159X16666180628165107

Hipólito, L., Wilson-Poe, A., Campos-Jurado, Y., Zhong, E., Gonzalez-Romero, J., Virag, L., et al. (2015). Inflammatory pain promotes increased opioid self-administration: role of dysregulated ventral tegmental area μ opioid receptors. *J. Neurosci.* 35, 12217–12231. doi: 10.1523/JNEUROSCI.1053-15.2015

Hirschberg, S., Li, Y., Randall, A., Kremer, E. J., and Pickering, A. E. (2017). Functional dichotomy in spinal- vs. prefrontal-projecting locus coeruleus modules splits descending noradrenergic analgesia from ascending aversion and anxiety in rats. *eLife* 6, e29808. doi: 10.7554/eLife.29808

Huang, S., Zhang, Z., Gambeta, E., Xu, S. C., Thomas, C., Godfrey, N., et al. (2020). Dopamine inputs from the ventral tegmental area into the medial prefrontal cortex modulate neuropathic pain-associated behaviors in mice. *Cell Rep.* 31, 107812. doi: 10.1016/j.celrep.2020.107812

Janak, P. H., and Tye, K. M. (2015). From circuits to behaviour in the amygdala. *Nature* 517, 284–292. doi: 10.1038/nature14188

Jasinska, A. J., Chen, B. T., Bonci, A., and Stein, E. A. (2015). Dorsal medial prefrontal cortex (MPFC) circuitry in rodent models of cocaine use: implications for drug addiction therapies. *Addict. Biol.* 20, 215–226. doi: 10.1111/adb.12132

Jones, M. D., and Lucki, I. (2005). Sex differences in the regulation of serotonergic transmission and behavior in 5-HT receptor knockout mice. *Neuropsychopharmacology* 30, 1039–1047. doi: 10.1038/sj.npp.1300664

Joshi, N., and Chandler, D. (2020). "Chapter 10: sex and the noradrenergic system," in *Handbook of Clinical Neurology*, eds R. Lanzenberger, G. S. Kranz, and I. Savic (Amsterdam: Elsevier), 167–176. doi: 10.1016/B978-0-444-64123-6.00012-6

Kaur, S., Benton, W. L., Tongkhuya, S. A., Lopez, C. M. C., Uphouse, L., and Averitt, D. L. (2018). Sex differences and estrous cycle effects of peripheral serotonin-evoked rodent pain behaviors. *Neuroscience* 38, 487–100. doi: 10.1016/j.neuroscience.2018.05.017

Khodagholi, F., Maleki, A., Motamedi, F., Mousavi, M. A., Rafiei, S., and Moslemi, M. (2022). Oxytocin prevents the development of 3-NP-induced anxiety and depression in

male and female rats: possible interaction of OXTR and mGluR2. *Cell Mol. Neurobiol.* 42, 1105–1123. doi: 10.1007/s10571-020-01003-0

Kim, D., Yao, Z., Graybuck, L. T., Kim, T. K., Nguyen, T. N., Smith, K. A., et al. (2019). Multimodal analysis of cell types in a hypothalamic node controlling social behavior. *Cell* 179, 713–728.e17. doi: 10.1016/j.cell.2019.09.020

Kolter, J. F., Hildenbrand, M. F., Popp, S., Nauroth, S., Bankmann, J., Rother, L., et al. (2021). Serotonin transporter genotype modulates resting state and predator stress-induced amygdala perfusion in mice in a sex-dependent manner. *PLoS ONE* 16, e0247311. doi: 10.1371/journal.pone.0247311

Kornstein, S. G., Schatzberg, A. F., Thase, M. E., Yonkers, K. A., McCullough, J. P., Keitner, G. I., et al. (2000). Gender differences in treatment response to sertraline vs. imipramine in chronic depression. *Am. J. Psychiatry* 157, 1445–1452. doi: 10.1176/appi.ajp.157.9.1445

Kraus, C., Castren, E., Kasper, S., and Lanzenberger, R. (2017). Serotonin and neuroplasticity: links between molecular, functional and structural pathophysiology in depression. *Neurosci. Biobehav. Rev.* 77, 317–326. doi: 10.1016/j.neubiorev.2017.03.007

Landau, A. M., Phan, J., Iversen, P., Lillethorup, T. P., Simonsen, M., Wegener, G., et al. (2015). Decreased *in vivo* α2 adrenoceptor binding in the flinders sensitive line rat model of depression. *Neuropharmacology* 91, 97–102. doi: 10.1016/j.neuropharm.2014.12.025

LeGates, T. A., Kvarta, M. D., and Thompson, S. M. (2019). Sex differences in antidepressant efficacy. *Neuropsychopharmacology* 44, 140–154. doi: 10.1038/s41386-018-0156-z

Li, X., Matsuura, T., Xue, M., Chen, Q., Liu, R., Lu, J., et al. (2021). Oxytocin in the anterior cingulate cortex attenuates neuropathic pain and emotional anxiety by inhibiting presynaptic long-term potentiation. *Cell Rep.* 36, 109411–109411. doi: 10.1016/j.celrep.2021.109411

Liu, R., Xue, M., Li, X., and Zhuo, M. (2020). Sex difference in synaptic plasticity in the anterior cingulate cortex of adult mice. *Molecul. Brain* 13, 41–41. doi: 10.1186/s13041-020-00583-8

Llorca-Torralba, M., Borges, G., Neto, F., Mico, J. A., and Berrocoso, E. (2016). Noradrenergic locus coeruleus pathways in pain modulation. *Neuroscience* 338, 93–113. doi: 10.1016/j.neuroscience.2016.05.057

Llorca-Torralba, M., Camarena-Delgado, C., Suárez-Pereira, I., Bravo, L., Mariscal, P., Garcia-Partida, J. A., et al. (2022). Pain and depression comorbidity causes asymmetric plasticity in the locus coeruleus neurons. *Brain* 145, 154–167. doi: 10.1093/brain/awab239

Llorente-Berzal, A., McGowan, F., Gaspar, J. C., Rea, K., Roche, M., and Finn, D. P. (2022). Sexually dimorphic expression of fear-conditioned analgesia in rats and associated alterations in the endocannabinoid system in the periaqueductal grey. *Neuroscience* 480, 117–130. doi: 10.1016/j.neuroscience.2021.11.005

Lou, T., Ma, J., Wang, Z., Terakoshi, Y., Lee, C. Y., Asher, G., et al. (2020). Hyper-activation of mPFC underlies specific traumatic stress-induced sleep-wake EEG disturbances. *Front. Neurosci.* 14, 883. doi: 10.3389/fnins.2020.00883

Love, T. M., Enoch, M., Hodgkinson, C. A., Peciña, M., Mickey, B., Koeppe, R. A., et al. (2012). Oxytocin gene polymorphisms influence human dopaminergic function in a sex-dependent manner. *Biol. Psychiatry* 72, 198–206. doi: 10.1016/j.biopsych.2012.01.033

Lowes, D. C., Chamberlin, L. A., Kretsge, L. N., Holt, E. S., Abbas, A. I., Park, A. J., et al. (2021). Ventral tegmental area GABA neurons mediate stress-induced blunted reward-seeking in mice. *Nat. Commun.* 12, 3539. doi: 10.1038/s41467-021-23906-2

Loyd, D. R., and Murphy, A. Z. (2006). Sex differences in the anatomical and functional organization of the periaqueductal gray-rostral ventromedial medullary pathway in the rat: a potential circuit mediating the sexually dimorphic actions of morphine. *J. Comp. Neurol.* 496, 723–738. doi: 10.1002/cne.20962

Lukas, M., and Neumann, I. D. (2014). Social preference and maternal defeat-induced social avoidance in virgin female rats: sex differences in involvement of brain oxytocin and vasopressin. *J. Neurosci. Methods* 234, 101–107. doi: 10.1016/j.jneumeth.2014.03.013

Lukas, M., Toth, I., Reber, S. O., Slattery, D. A., Veenema, A. H., and Neumann, I. D. (2011). The neuropeptide oxytocin facilitates pro-social behavior and prevents social avoidance in rats and mice. *Neuropsychopharmacology* 36, 2159–2168. doi: 10.1038/npp.2011.95

Madla, C. M., Gavins, F. K. H., Merchant, H. A., Orlu, M., Murdan, S., and Basit, A. W. (2021). Let's talk about sex: differences in drug therapy in males and females. *Adv. Drug Deliv. Rev.* 175, 113804. doi: 10.1016/j.addr.2021.05.014

Manza, P., Shokri-Kojori, E., Wiers, C. E., Kroll, D., Feldman, D., McPherson, K., et al. (2022). Sex differences in methylphenidate-induced dopamine increases in ventral striatum. *Mol. Psychiatry* 27, 939–946. doi: 10.1038/s41380-021-01294-9

Markham, J. A., and Juraska, J. M. (2002). Aging and sex influence the anatomy of the rat anterior cingulate cortex. *Neurobiol. Aging* 23, 579–588. doi: 10.1016/S0197-4580(02)00004-0

Markovic, T., Pedersen, C. E., Massaly, N., Vachez, Y. M., Ruyle, B., Murphy, C. A., et al. (2021). Pain induces adaptations in ventral tegmental area dopamine neurons to drive anhedonia-like behavior. *Nat. Neurosci.* 24, 1601–1613. doi: 10.1038/s41593-021-00924-3

Marron Fernandez De Velasco, E., Hearing, M., Xia, Z., Victoria, N. C., Luján, R., and Wickman, K. (2015). Sex differences in GABA(B)R-GIRK signaling in layer 5/6 pyramidal neurons of the mouse prelimbic cortex. *Neuropharmacology* 95, 353–360. doi: 10.1016/j.neuropharm.2015.03.029

Mason, S. T. (1979). Noradrenaline and behaviour. *Trends Neurosci.* 2, 82–84.

Massey, S. H., Backes, K. A., and Schuette, S. A. (2016). Plasma oxytocin concentration and depressive symptoms: a review of current evidence and directions for future research. *Depress Anxiety* 33, 316–322. doi: 10.1002/da.22467

McEwen, B. S., and Milner, T. A. (2017). Understanding the broad influence of sex hormones and sex differences in the brain. *J. Neurosci. Res.* 95, 24–39. doi: 10.1002/jnr.23809

Mercer Lindsay, N., Chen, C., Gilam, G., Mackey, S., and Scherrer, G. (2021). Brain circuits for pain and its treatment. *Sci. Transl. Med.* 13, eabj7360. doi: 10.1126/scitranslmed.abj7360

Mir, F. R., Wilson, C., Cabrera Zapata, L. E., Aguayo, L. G., and Cambiasso, M. J. (2020). Gonadal hormone-independent sex differences in GABAA receptor activation in rat embryonic hypothalamic neurons. *Br. J. Pharmacol.* 177, 3075–3090. doi: 10.1111/bph.15037

Mogil, J. S. (2020). Qualitative sex differences in pain processing: emerging evidence of a biased literature. *Nat. Rev. Neurosci.* 21, 353–365. doi: 10.1038/s41583-020-0310-6

Monroe, T. B., Fillingim, R. B., Bruehl, S. P., Rogers, B. P., Dietrich, M. S., Gore, J. C., et al. (2018). Sex differences in brain regions modulating pain among older adults: a cross-sectional resting state functional connectivity study. *Pain Med.* 19, 1737–1747. doi: 10.1093/pm/pnx084

Monti, J. M. (2011). Serotonin control of sleep-wake behavior. *Sleep Med. Rev.* 15, 269–281. doi: 10.1016/j.smrv.2010.11.003

Mulvey, B., Bhatti, D. L., Gyawali, S., Lake, A. M., Kriaucionis, S., Ford, C. P., et al. (2018). Molecular and functional sex differences of noradrenergic neurons in the mouse locus coeruleus. *Cell Rep.* 23, 2225–2235. doi: 10.1016/j.celrep.2018.04.054

Neugebauer, V., Mazzitelli, M., Cragg, B., Ji, G., Navratilova, E., and Porreca, F. (2020). Amygdala, neuropeptides, and chronic pain-related affective behaviors. *Neuropharmacology* 170, 108052. doi: 10.1016/j.neuropharm.2020.108052

Neumann, I. D. (2008). Brain oxytocin: a key regulator of emotional and social behaviours in both females and males. *J. Neuroendocrinol.* 20, 858–865. doi: 10.1111/j.1365-2826.2008.01726.x

Osborne, N. R., Cheng, J. C., Rogachov, A., Kim, J. A., Hemington, K. S., Bosma, R. L., et al. (2021). Abnormal subgenual anterior cingulate circuitry is unique to women but not men with chronic pain. *Pain* 162, 97. doi: 10.1097/j.pain.0000000000002016

Pandya, M., Palpagama, T. H., Turner, C., Waldvogel, H. J., Faull, R. L., and Kwakowsky, A. (2019). Sex- and age-related changes in GABA signaling components in the human cortex. *Biol. Sex Differ.* 10, 5. doi: 10.1186/s13293-018-0214-6

Philippe, T. J., Bao, L., Koblanski, M. E., and Viau, V. (2022). Sex differences in serotonin 5-HT 1A receptor responses to repeated restraint stress in adult male and female rats. *Int. J. Neuropsychopharmacol.* 25, 863–876. doi: 10.1093/ijnp/pyac046

Phillips, A. L., Burr, R. L., and Dunner, D. L. (2018). rTMS effects in patients with co-morbid somatic pain and depressive mood disorders. *J. Affect. Disord.* 241, 411–416. doi: 10.1016/j.jad.2018.08.065

Pignatelli, A., and Belluzzi, O. (2017). Dopaminergic neurones in the main olfactory bulb: an overview from an electrophysiological perspective. *Front. Neuroanat.* 11, 7. doi: 10.3389/fnana.2017.00007

Pinos, H., Collado, P., Rodriguez-Zafra, M., Rodriguez, C., Segovia, S., and Guillamón, A. (2001). The development of sex differences in the locus coeruleus of the rat. *Brain Res. Bull.* 56, 73–78. doi: 10.1016/S0361-9230(01)00540-8

Poulin, J., Caronia, G., Hofer, C., Cui, Q., Helm, B., Ramakrishnan, C., et al. (2018). Mapping projections of molecularly defined dopamine neuron subtypes using intersectional genetic approaches. *Nature neuroscience* 21, 1260–1271. doi: 10.1038/s41593-018-0203-4

Presto, P., and Neugebauer, V. (2022). Sex differences in CGRP regulation and function in the amygdala in a rat model of neuropathic pain. *Front. Mol. Neurosci.* 15, 928587. doi: 10.3389/fnmol.2022.928587

Rivera-Garcia, M. T., McCane, A. M., Chowdhury, T. G., Wallin-Miller, K. G., and Moghaddam, B. (2020). Sex and strain differences in dynamic and static properties of the mesolimbic dopamine system. *Neuropsychopharmacology* 45, 2079–2086. doi: 10.1038/s41386-020-0765-1

Rossoni, E., Feng, J., Tirozzi, B., Brown, D., Leng, G., and Moos, F. (2008). Emergent synchronous bursting of oxytocin neuronal network. *PLoS Comput. Biol.* 4, e1000123. doi: 10.1371/journal.pcbi.1000123

Rubinow, D. R., Schmidt, P. J., and Roca, C. A. (1998). Estrogen-serotonin interactions: implications for affective regulation. *Biol. Psychiatry* 44, 839–850.

Sagrillo, C. A., and Selmanoff, M. (1997). Castration decreases single cell levels of mRNA encoding glutamic acid decarboxylase in the diagonal band of broca and the sexually dimorphic nucleus of the preoptic area. *J. Neuroendocrinol.* 9, 699–706.

Sanwald, S., Gahr, M., Widenhorn-Muller, K., Schonfeldt-Lecuona, C., Richter, K., Connemann, B. J., et al. (2020). Relation of promoter methylation of the oxytocin gene to stressful life events and depression severity. *J. Mol. Neurosci.* 70, 201–211. doi: 10.1007/s12031-019-01446-1

Schneider, I., Schmitgen, M. M., Boll, S., Roth, C., Nees, F., Usai, K., et al. (2020). Oxytocin modulates intrinsic neural activity in patients with chronic low back pain. *Eur. J. Pain* 24, 945–955. doi: 10.1002/ejp.1543

Searles, R. V., Yoo, M. J., He, J. R., Shen, W. B., and Selmanoff, M. (2000). Sex differences in GABA turnover and glutamic acid decarboxylase (GAD(65) and GAD(67)) mRNA in the rat hypothalamus. *Brain Res.* 878, 11–19. doi: 10.1016/S0006-8993(00)02648-2

Serafini, R. A., Pryce, K. D., and Zachariou, V. (2020). The mesolimbic dopamine system in chronic pain and associated affective comorbidities. *Biol. Psychiatry* 87, 64–73. doi: 10.1016/j.biopsych.2019.10.018

Serova, L., Rivkin, M., Nakashima, A., and Sabban, E. L. (2002). Estradiol stimulates gene expression of norepinephrine biosynthetic enzymes in rat locus coeruleus. *Neuroendocrinology* 75, 193–200. doi: 10.1159/000048237

Snoeren, E. M. S., Veening, J. G., Olivier, B., and Oosting, R. S. (2014). Serotonin 1A receptors and sexual behavior in female rats: a review. *Pharmacol. Biochem. Behav.* 121, 43–52. doi: 10.1016/j.pbb.2013.11.017

Sollozo-Dupont, I., Estrada-Camarena, E., Carro-Juarez, M., and Lopez-Rubalcava, C. (2015). GABAA/benzodiazepine receptor complex mediates the anxiolytic-like effect of *Montanoa tomentosa*. *J. Ethnopharmacol.* 162, 278–286. doi: 10.1016/j.jep.2014.12.070

Song, Z., Borland, J. M., Larkin, T. E., O., Malley, M., and Albers, H. E. (2016). Activation of oxytocin receptors, but not arginine-vasopressin V1a receptors, in the ventral tegmental area of male Syrian hamsters is essential for the reward-like properties of social interactions. *Psychoneuroendocrinology* 74, 164–172. doi: 10.1016/j.psyneuen.2016.09.001

Songtachalert, T., Roomruangwong, C., Carvalho, A. F., Bourin, M., and Maes, M. (2018). Anxiety disorders: sex differences in serotonin and tryptophan metabolism. *Curr. Top. Med. Chem.* 18, 1704–1715. doi: 10.2174/1568026618666181115093136

Sramek, J. J., Murphy, M. F., and Cutler, N. R. (2016). Sex differences in the psychopharmacological treatment of depression. *Dialog. Clin. Neurosci.* 18, 447–457. doi: 10.31887/DCNS.2016.18.4/ncutler

Stalter, M., Westendorff, S., and Nieder, A. (2020). Dopamine gates visual signals in monkey prefrontal cortex neurons. *Cell Rep.* 30, 164–172.e4. doi: 10.1016/j.celrep.2019.11.082

Steinman, M. Q., Duque-Wilckens, N., Greenberg, G. D., Hao, R., Campi, K. L., Laredo, S. A., et al. (2016). Sex-specific effects of stress on oxytocin neurons correspond with responses to intranasal oxytocin. *Biol. Psychiatry* 80, 406–414. doi: 10.1016/j.biopsych.2015.10.007

Sun, L., Liu, R., Guo, F., Wen, M., Ma, X., Li, K., et al. (2020). Parabrachial nucleus circuit governs neuropathic pain-like behavior. *Nat. Commun.* 11, 5974–5974. doi: 10.1038/s41467-020-19767-w

Tamborski, S., Mintz, E. M., and Caldwell, H. K. (2016). Sex differences in the embryonic development of the central oxytocin system in mice. *J. Neuroendocrinol.* 28, 4. doi: 10.1111/jne.12364

Tobaldini, G., Reis, R. A., Sardi, N. F., Lazzarim, M. K., Tomim, D. H., Lima, M. M. S., et al. (2018). Dopaminergic mechanisms in periaqueductal gray-mediated antinociception. *Behav. Pharmacol.* 29, 225–233. doi: 10.1097/FBP.0000000000000346

Van Bockstaele, E. J., Bajic, D., Proudfit, H., and Valentino, R. J. (2001). Topographic architecture of stress-related pathways targeting the noradrenergic locus coeruleus. *Physiol. Behav.* 73, 273–283. doi: 10.1016/S0031-9384(01)00448-6

Vathy, I., and Etgen, A. M. (1988). Ovarian steroids and hypothalamic norepinephrine release: studies using *in vivo* brain microdialysis. *Life Sci.* 43, 1493–1499.

Veronneau-Longueville, F., Rampin, O., Freund-Mercier, M. J., Tang, Y., Calas, A., Marson, L., et al. (1999). Oxytocinergic innervation of autonomic nuclei controlling penile erection in the rat. *Neuroscience* 93, 1437–1447.

Vincent, K., and Tracey, I. (2010). Sex hormones and pain: the evidence from functional imaging. *Curr. Pain Headache Rep.* 14, 396–403. doi: 10.1007/s11916-010-0139-1

Vos, T., Lim, S. S., Abbafati, C., Abbas, K. M., Abbasi, M., Abbasifard, M., et al. (2020). Global burden of 369 diseases and injuries in 204 countries and territories, 1990–2019: a systematic analysis for the global burden of disease study 2019. *Lancet* 396, 1204–1222. doi: 10.1016/S0140-6736(20)30925-9

Wang, G., Erpelding, N., and Davis, K. D. (2014). Sex differences in connectivity of the subgenual anterior cingulate cortex. *Pain* 155, 755–763. doi: 10.1016/j.pain.2014.01.005

Wang, X., Mokhtari, T., Zeng, Y., Yue, L., Hu, L., Xue-Qiang, W., et al. (2021). The distinct functions of dopaminergic receptors on pain modulation: a narrative review. *J. Neural Transpl. Plast.* 202, 16682275. doi: 10.1155/2021/6682275

Wrobel, L., Schorscher-Petcu, A., Dupre, A., Yoshida, M., Nishimori, K., and Tribollet, E. (2011). Distribution and identity of neurons expressing the oxytocin receptor in the mouse spinal cord. *Neurosci. Lett.* 495, 49–54. doi: 10.1016/j.neulet.2011.03.033

Wu, X., Morishita, W., Beier, K. T., Heifets, B. D., and Malenka, R. C. (2021). 5-HT modulation of a medial septal circuit tunes social memory stability. *Nature* 599, 96–101. doi: 10.1038/s41586-021-03956-8

Xin, Q., Bai, B., and Liu, W. (2017). The analgesic effects of oxytocin in the peripheral and central nervous system. *Neurochem. Int.* 10, 357–364. doi: 10.1016/j.neuint.2016.12.021

Yamada, C., Sadakane, C., Nahata, M., Saegusa, Y., Nakagawa, K., Okubo, N., et al. (2015). Serotonin 2C receptor contributes to gender differences in stress-induced hypophagia in aged mice. *Psychoneuroendocrinology* 55, 81–93. doi: 10.1016/j.psyneuen.2015.02.006

Yang, H., de Jong, J. W., Cerniauskas, I., Peck, J. R., Lim, B. K., Gong, H., et al. (2021). Pain modulates dopamine neurons *via* a spinal-parabrachial-mesencephalic circuit. *Nat. Neurosci.* 24, 1402–1413. doi: 10.1038/s41593-021-00903-8

Yang, L., Liu, C., Li, W., Ma, Y., Huo, S., Ozathaley, A., et al. (2021). Depression-like behavior associated with E/I imbalance of mPFC and amygdala without TRPC channels in mice of knockout IL-10 from microglia. *Brain Behav. Immun.* 97, 68–78. doi: 10.1016/j.bbi.2021.06.015

Yin, J. B., Liang, S. H., Li, F., Zhao, W. J., Bai, Y., Sun, Y., et al. (2020). dmPFC-vlPAG projection neurons contribute to pain threshold maintenance and antianxiety behaviors. *J. Clin. Invest.* 130, 6555–6570. doi: 10.1172/JCI127607

Yonkers, K. A., and Simoni, M. K. (2018). Premenstrual disorders. *Am. J. Obstet. Gynecol.* 218, 68–74. doi: 10.1016/j.ajog.2017.05.045

Yu, W., Pati, D., Pina, M. M., Schmidt, K. T., Boyt, K. M., Hunker, A. C., et al. (2021). Periaqueductal gray/dorsal raphe dopamine neurons contribute to sex differences in pain-related behaviors. *Neuron* 109, 1365–1380.e5. doi: 10.1016/j.neuron.2021.03.001

Zachry, J. E., Nolan, S. O., Brady, L. J., Kelly, S. J., Siciliano, C. A., and Calipari, E. S. (2021). Sex differences in dopamine release regulation in the striatum. *Neuropsychopharmacology* 46, 491–499. doi: 10.1038/s41386-020-00915-1

Zhang, L., Ma, W., Barker, J. L., and Rubinow, D. R. (1999). Sex differences in expression of serotonin receptors (subtypes 1A and 2A) in rat brain: a possible role of testosterone. *Neuroscience* 94, 251–259.

Zhang, L., Wang, J., Niu, C., Zhang, Y., Zhu, T., Huang, D., et al. (2021). Activation of parabrachial nucleus: ventral tegmental area pathway underlies the comorbid depression in chronic neuropathic pain in mice. *Cell Rep.* 37, 109936. doi: 10.1016/j.celrep.2021.109936

Zhang, M., Liu, Y., Zhao, M., Tang, W., Wang, X., Dong, Z., et al. (2017). Depression and anxiety behaviour in a rat model of chronic migraine. *J. Headache Pain* 18, 27–27. doi: 10.1186/s10194-017-0736-z

Zhang, Y., Yang, Y., Dai, R., Wu, H., Li, C., and Guo, Q. (2015). Oxytocin in the paraventricular nucleus attenuates incision-induced mechanical allodynia. *Exp. Ther. Med.* 9, 1351–1356. doi: 10.3892/etm.2015.2285

Zhao, W., Li, Q., Ma, Y., Wang, Z., Fan, B., Zhai, X., et al. (2021). Behaviors related to psychiatric disorders and pain perception in C57BL/6J mice during different phases of estrous cycle. *Front. Neurosci.* 156, 50793. doi: 10.3389/fnins.2021.650793

Zhou, W., Jin, Y., Meng, Q., Zhu, X., Bai, T., Tian, Y., et al. (2019). A neural circuit for comorbid depressive symptoms in chronic pain. *Nat. Neurosci.* 22, 1649–1658. doi: 10.1038/s41593-019-0468-2

Zhou, Y. S., Meng, F. C., Cui, Y., Xiong, Y. L., Li, X. Y., Meng, F. B., et al. (2022). Regular aerobic exercise attenuates pain and anxiety in mice by restoring serotonin-modulated synaptic plasticity in the anterior cingulate cortex. *Med. Sci. Sports Exerc.* 54, 566–581. doi: 10.1249/MSS.0000000000002841

frontiers | Frontiers in Molecular Neuroscience

TYPE Original Research
PUBLISHED 22 February 2023
DOI 10.3389/fnmol.2022.1027063

OPEN ACCESS

EDITED BY
Yize Li,
Tianjin Medical University General Hospital, China

REVIEWED BY
Jingjing Yuan,
First Affiliated Hospital of Zhengzhou University, China
Bao-Chun Jiang,
Zhejiang University, China

*CORRESPONDENCE
Xingrong Song
sxjess@126.com

SPECIALTY SECTION
This article was submitted to Pain Mechanisms and Modulators, a section of the journal Frontiers in Molecular Neuroscience

RECEIVED 24 August 2022
ACCEPTED 16 November 2022
PUBLISHED 22 February 2023

CITATION
Guo X, Zhang G, Cai W, Huang F, Qin J and Song X (2023) Long non-coding RNA rhabdomyosarcoma 2-associated transcript contributes to neuropathic pain by recruiting HuR to stabilize DNA methyltransferase 3 alpha mRNA expression in dorsal root ganglion neuron.
Front. Mol. Neurosci. 15:1027063.
doi: 10.3389/fnmol.2022.1027063

Long non-coding RNA rhabdomyosarcoma 2-associated transcript contributes to neuropathic pain by recruiting HuR to stabilize DNA methyltransferase 3 alpha mRNA expression in dorsal root ganglion neuron

Xinying Guo[1], Gaolong Zhang[1], Weihua Cai[2], Fa Huang[1], Jingwen Qin[1] and Xingrong Song[1]*

[1]Department of Anesthesiology, Guangzhou Women and Children's Medical Center, Guangzhou Medical University, Guangdong Provincial Clinical Research Center for Child Health, Guangzhou, China, [2]Department of Anesthesia, McGill University, Montreal, QC, Canada

Introduction: Long non-coding RNAs (lncRNAs) act as key regulators in multiple human diseases. In particular, the dysfunction of lncRNAs in dorsal root ganglion (DRG) contributes to the pathogenesis of neuropathic pain (NP). Nevertheless, the role and mechanism of most lncRNAs in NP remain unclear.

Methods: Two classic chronic NP models, including L4 spinal nerve ligation (SNL) model and chronic constriction injury (CCI) of the sciatic nerve, were performed. Mechanical allodynia and heat hyperalgesia were used to evaluate neuropathic pain. DRG microinjection was used to deliver agents into DRG. qRT-PCR, immunofluorescence, immunoprecipitation, western blotting, siRNA transfection, AAV transduction were performed to investigate the phenotypes and molecular basis.

Results: Here, we discovered that *Rmst* as a lncRNA was specifically expressed in *Atf3*$^{+}$ injured DRG neurons and significantly upregulated following peripheral nerve damage. *Rmst* overexpression by direct DRG injection of AAV5-*Rmst* causes neuropathic symptoms in the absence of nerve damage. Conversely, blocking *Rmst* expression in injured DRGs alleviated nerve injury-induced pain hypersensitivities and downregulated *Dnmt3a* expression. Furthermore, we found peripheral nerve damage induced *Rmst* increase could interact with RNA-binding protein HuR to stabilize the *Dnmt3a* mRNA.

Conclusion: Our findings reveal a crucial role of *Rmst* in damaged DRG neurons under NP condition and provide a novel target for drug development against NP.

KEYWORDS

neuropathic pain, dorsal root ganglia, *Rmst* lncRNA, HuR, DNA methyltransferase 3 alpha (*DNMT3A*), mRNA stability

Introduction

Chronic pain has been a perplexing problem for decades. Globally, approximately one-fifth of people suffer from chronic pain (Tompkins et al., 2017), and about thirty percent of these patients have gone through the symptoms of neuropathic pain (NP) (van Hecke et al., 2014). Patients with NP have detrimental effects on their quality of life and ability. In addition to personal suffering, chronic pain is a substantial financial burden on society, and lies billions of dollars every year (van Velzen et al., 2020). However, there are limited treatments available for NP. Dorsal root ganglia (DRG) neuron is responsible for conveying the nociception in peripheral nerve injury. Peripheral nerve damage-induced maladaptive alterations at transcriptional and translational levels of pain-associated genes in the primary afferents of DRG neurons contribute to these abnormal spontaneous activities and subclinical behavioral patterns (Li et al., 2020; Pan et al., 2021). Hence, identifying new targets and mechanisms in damaged DRGs could open a novel avenue against NP.

As potent and multifaceted roles of long non-coding RNAs (lncRNAs) in gene regulation, lncRNAs are paid much attention in many human illnesses, including NP (Wu et al., 2016, 2019). However, the function of most lncRNAs in NP is not thoroughly understood. A lncRNA called rhabdomyosarcoma 2-associated transcript (*Rmst*) was essential for neuronal differentiation (Ng et al., 2012) and neurogenesis (Ng et al., 2013). Although previous studies showed that *Rmst* was involved in neurological disorders (Hou and Cheng, 2018; Ma et al., 2021; Zhao et al., 2021; Li et al., 2022), little is known about its role in NP.

DNA methyltransferase 3 alpha gene encodes the *Dnmt3a* protein and is responsible for catalyzing 5-methylcytosine methylation. The aberrant regulation of Dnmt3a is implicated in multiple nervous diseases (Feng et al., 2005; Clemens and Gabel, 2020), especially in NP (Guo et al., 2019). Increased Dnmt3a have been found in injured DRG (Shao et al., 2017; Zhao et al., 2017). What's more, the increased-Dnmt3a was able to mediate the epigenetic inaction of the voltage-dependent potassium channel subunit (Kcna2) *via* DNA hypermethylation of Kcna2 promoter region (Zhao et al., 2017). Depletion of Dnmt3a in the injured DRGs effectively attenuated NP by restoring *Kcna2* expression (Zhao et al., 2017, p. 3). These studies suggested that Dnmt3a plays a pivotal role in regulating DNA methylation of nerve damage related gene alterations. Nevertheless, it is unclear how peripheral nerve damage triggers the activation of Dnmt3a in injured DRG.

Here, we sought to characterize a lncRNA rhabdomyosarcoma 2-associated transcript (*Rmst*) in injured DRG neurons was substantially increased in NP. The nerve damage triggered *Rmst* expression in injured DRGs contributes to regulating Dnmt3a through interaction with RNA binding protein HuR in NP. Thus, the role and mechanism of *Rmst* may provide novel and insightful directions for NP management in clinic.

Materials and methods

Bioinformatics

RNA sequencing dataset for mouse DRG after peripheral nerve injury was obtained from previous research (Wu et al., 2016). The mouse DRG was harvested 7 days after L4 spinal nerve ligation (SNL) model and sequencing was performed on the Illumina HiSeq2500 platform with 2 × 100-bp paired-end reads.

For scRNA-seq dataset for mouse DRG after peripheral nerve injury, we obtained the cell count matrix and metadata from Gene Expression Omnibus (GEO) with the series record GSE155622 (Wang K. et al., 2021). The mouse DRG was harvested for Smart-seq2 as smart-seq2 was better to captured low abundance transcripts as well as more lncRNAs (Wang X. et al., 2021). All metadata was also obtained from GSE155622.

Animals

C57BL/6J adult mice were from SPF Biotechnology Co., Ltd (Beijing, China). A 12-h light-dark cycle environment with unlimited access to food and water was used to house mice. All processes were endorsed by the Animal Care and Use Committee at Guangzhou Medical University.

Chronic neuropathic pain model

Two classic chronic NP models, including L4 SNL model and chronic constriction injury (CCI) of the sciatic nerve, were performed as described previously (Li et al., 2020). SNL model was established by tightly ligating L4 spinal nerve distal to DRG with 7-0 silk suture. L4 spinal nerve was exposed in the matched sham mice, however, the L4 spinal nerve was neither ligated nor transected. CCI model was established by loosely ligated the sciatic nerve at three spots with 1 mm-intervals by 7-0 silk suture. Sham animals did not receive the ligation of the sciatic nerve.

Behavioral tests

As previous described, mechanical allodynia was quantified by measuring paw withdrawal frequency by low (0.07 g) and median (0.4 g) von Frey filaments (Stoelting Co., Wood Dale, IL, USA) (Li et al., 2020). We use two calibrated plastic filaments to stimuli the central of plantar surface of hind paws. A positive response is quick withdrawal of the paw. Mice were totally received 10 applications. The paw withdrawal frequency describes the positive withdrawal responses within 10 applications.

Heat hyperalgesia was quantified by measuring paw withdrawal latencies after heat stimulation as described (Li et al., 2020). All mice before behavior test were left in a glass surface in individual plexiglas cages. A beam of light was applied to the central of hind paw. The performance of a positive response is a swift raise of the hind paw. The Model 336 Analgesia Meter (IITC Inc., Life Science Instruments. Woodland Hills, CA, USA) was automatically records the withdrawal latency from heating source. 4–5 trials on each side were performed at intervals of 5 min.

Dorsal root ganglion microinjection

As described previously, DRG microinjection was carried out (Li et al., 2020). After 3-cm-long skin incision, we firstly exposed the corresponding spinal nerve (L4 and/or L3). After that, we used rongeur to remove the unilateral articular processes for DRG microinjection. The glass micropipette was carefully inserted into the exposed ipsilateral L4 and/or L3 DRGs and 1 μl of either siRNA solution or viral solution was injected into L4 and/or L3 DRG. The injection was performed at a rate of 10 nl/s. After the injection was completed, the pipette was left in place for 10 min before removal to allow the fluid to distribute and the pressure within the DRG to equalize. The skin was sutured with 6-0 silk and mice were kept on a heating pad. All reagent and surgical instruments are sterilized in advance.

Dorsal root ganglion neuronal culture

We performed DRG neuron cultures as described (Li et al., 2020). We first prepared complete neurobasal medium (CNM) including 10% fetal bovine serum, and 1x antibiotics, 2% B-27 supplement, and 1% GluMax supplement. 3–4 weeks mice were used for collecting DRGs. The collected DRGs were incubated with collagenase solution including dispase, collagenase type I in HBSS. All reagents are from Thermofisher Scientific Company (Waltham, MA, USA).

Quantitative real-time RT–PCR

The TRIzol Reagent (Cat. No:15596026, Invitrogen Corporation, Carlsbad, CA, USA) was used for extracting RNA from DRGs, followed by reverse transcription using PrimeScript RT Master Mix (Cat. No: RR036A, Takara Bio Inc, Shiga, Japan). Quantitative PCR were performed using TB Green Premix Ex Taq II (Tli RNaseH Plus) (Cat. No: RR820A, Takara Bio Inc, Shiga, Japan) on a CFX96 Touch Real-Time PCR Detection System (Bio-Rad Laboratories, Inc., Hercules, CA, USA). Finally, relative fold changes of each gene were calculated by ΔCt method ($2^{-\Delta\Delta Ct}$). **Supplementary Table 1** included all primer information.

Ribonucleic acid stability assay

Primary neurons grew in 6-well plate and were treated with actinomycin D (Cat. No:A1410, Sigma-Aldrich, Burlington, MA, USA) for testing the mRNA stability. After that, we collected neurons at 0, 2, 4, 8, and 12 h after actinomycin D treatment for RNA extraction.

Nuclear/cytoplasmic ribonucleic acid fraction isolation

Cytoplasmic and Nuclear RNA purification Kit were purchased from Norgen Biteck Corp. (Cat. No: NGB-21000, Thorold, ON, Canada). After Nuclear and cytoplasmic RNA fraction isolation, various gene expression levels in both nuclear and cytoplasmic fractions of all samples were calculated by RT-PCR as protocol above.

Nuclear/cytoplasmic protein isolation

Nuclear and cytoplasmic protein were separated using the NE-PER nuclear and cytoplasmic extraction reagents (Cat. No: 78833, Thermofisher Scientific Company, Waltham, MA, USA) following the manufacturer's instructions. The collected protein was aliquoted and stored at −80°C.

Plasmids constructs and virus production

The pAAV-CMV-mRmst-:WPRE vector (vector ID: VB220510-1032tdc) and AAV5-Rmst virus packaging was designed and constructed to overexpress the Rmst expression by VectorBuilder Company (Chicago, IL, USA). Briefly, the full-length cDNA of Rmst (NR_028262.1) was amplified by RT-PCR. After that, double enzyme-digested PCR products were ligated into the mammalian ncRNA expression AAV vector as a plasmid. AAV5-Gfp (vector ID: VB150925-10026) is used as negative control. SiRNA for *Rmst* and *Dnmt3a* were designed and produced by Tsingke Biotechnology Co., Ltd. (Beijing, China). All siRNA sequencing used in this work were listed at **Supplementary Table 1**.

Immunohistochemistry staining

Mice were perfused with 4% PFA after deep isoflurane before being analyzed by immunohistochemistry. The DRGs were collected and post-fixed in 4% PFA overnight, followed by dehydrating in 30% sucrose for two nights at 4°C. Finally, the DRGs were sectioned at 15–20 μm and kept them in −80°C refrigerator.

Before primary antibody incubation, the section was blocked in 1X PBS with 10% donkey serum and 0.3% Triton X-100. The sections were then incubated with anti-DNMT3a (Santa Cruz, Dallas, TX, USA) overnight at 4°C followed by incubating secondary antibody conjugated to Cy3 (1:500, Jackson ImmunoResearch, West Grove, PA, USA) for 2 h. Finally, the sections were mounted using Fluoroshield^{TM} with DAPI (Cat. No: F6057, Sigma-Aldrich, Burlington, MA, USA).

Ribonucleic acid-binding protein immunoprecipitation (RIP)

The Magna RIP Kit were purchased from EMD Millipore (Burlington, MA, USA) company for RIP assay. A anti-HuR antibody (Santa Cruz, Dallas, TX, USA) was used in RIP assay. After purification of RNA, RT-PCR was performed following the previous protocol.

Western blotting

The collected protein was firstly separated using SDS-PAGE electrophoresis on the basis of size, followed by moving to PVDF membranes with appropriate size. The blot was then immediately placed in 5% fresh non-fat milk powder for blocking for 1 h. Next, the appropriate primary and secondary antibodies were used to incubate the transferred membrane according to the recommended dilution and time in datasheet. The rabbit anti-DNMT3b (1:500), rabbit anti-DNMT3a (1:500), and rabbit anti-histone H3 (1:1,000) were purchased from Cell Signaling Technology (Danvers, MA, USA). The mouse anti-HuR (1:500) and rabbit anti-GAPDH (1:1,000) were purchased from Santa Cruz company (Dallas, TX, USA). Membranes were visualized by the Clarity Western ECL Substrate (Cat. No: 170-5060, Bio-Rad Laboratories, Inc., Hercules, CA, USA), exposed by ChemiDoc Touch (Bio-Rad Laboratories, Inc., Hercules, CA, USA) and analyzed by Image J.

Statistical analysis

Sample size estimation was based on certain assumptions, including significance level, expected placebo mean, expected treatment mean, standard deviation, power, expected dropout. In our case, expected placebo mean, expected treatment mean, standard deviation, and expected dropout were depended on our pilot studies and previous report in the field (Li et al., 2020; Pan et al., 2021). After that, sample sizes were calculated using nQUERY software, assuming a significance level of 0.05, 90% power and homogeneous variances for the 2 samples to be compared, with the means and SEM for different parameters predicted from pilot study. The data is presented as mean ± SEM and analyzed by GraphPad Prism 8. The Shapiro–Wilk test was used for normal distribution test. If the data passed the normality test, the *t*-test or ANOVA was used in this study by GraphPad Prism 8 software according to experimental design and the detailed statistical method was listed in figure legend. The interaction of factors after ANOVA is provided in result. A *P*-value of less than 0.05 was considered statistical significant.

Results

Increased rhabdomyosarcoma 2-associated transcript in damaged dorsal root ganglions was found in neuropathic pain

As the critical role of lncRNAs during the formation of NP, we extracted the 10 most up-and downregulated lncRNAs in L4 DRGs 7 days after SNL model (**Figure 1A**) from the previous RNA sequencing dataset (Wu et al., 2016). Among them, we found *Rmst*, a previously reported brain specific lncRNA (Ng et al., 2012), was also expressed in damaged DRGs (**Figure 1A**). As previous research has been found that *Rmst* was specific to neuron (Briese et al., 2016), we are wondering the distribution of *Rmst* in the neuron subtype after nerve injury. Thus, we analyzed the scRNA sequencing dataset from DRGs with peripheral nerve damage (Wang K. et al., 2021). As the smart-seq2 technology was better to captured low

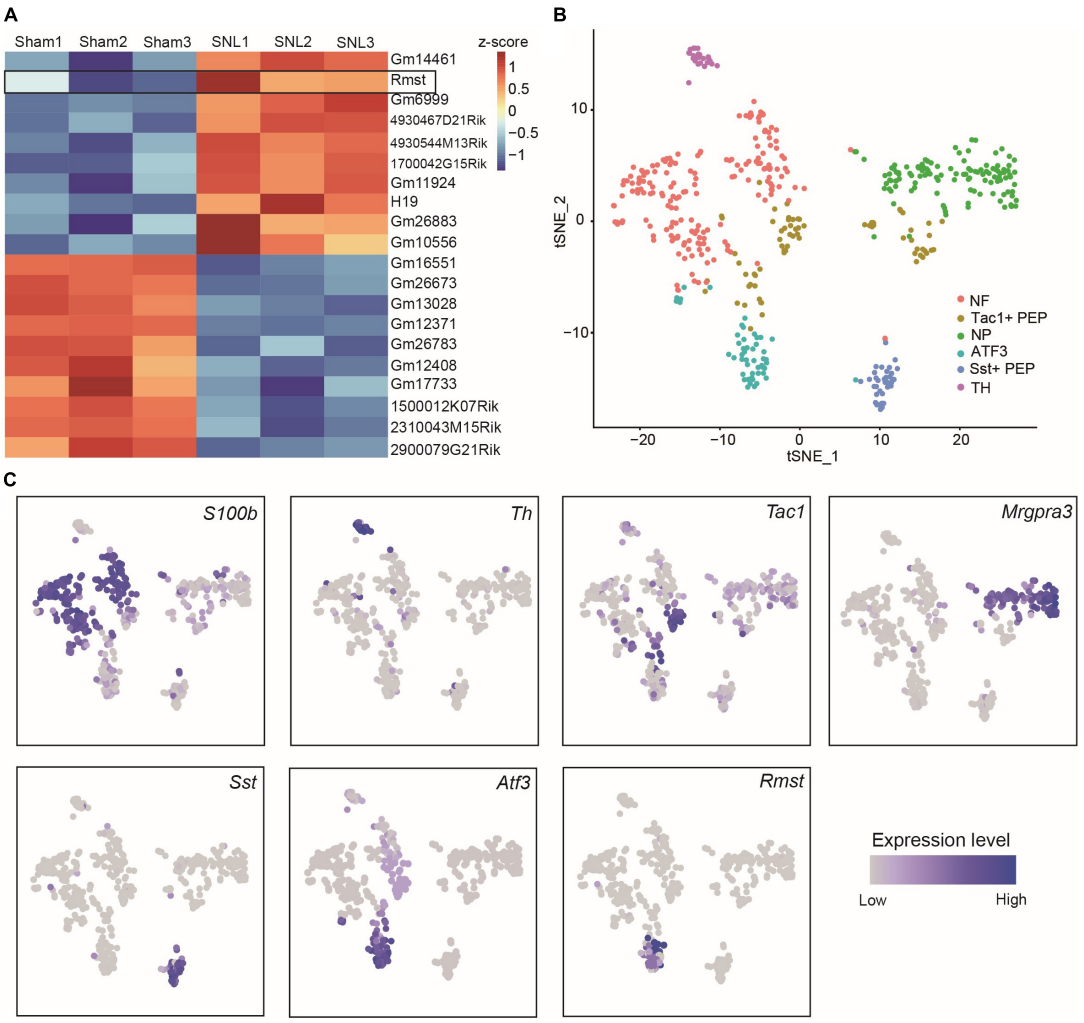

FIGURE 1
Rhabdomyosarcoma 2-associated transcript (*Rmst*) was specifically expressed in *Atf3*$^{+}$ injured neurons. **(A)** The 10 most up- and downregulated lncRNAs in L4 DRGs after SNL model. The heatmap was created using Z-score values obtained from RNA-seq dataset. **(B)** TSNE plot of all cells from DRGs after nerve injury. Each dot was color-coded and annotated by neural subtypes. NF: neurofilament, NP: non-peptidergic neurons, TH: tyrosine hydroxylase, PEP: peptidergic neurons. **(C)** TSNE plots showing scRNA-seq data, colored by gene expression level, showing *S100b, Th, Tac1, Mrgpra3, Sst, Atf3*, and *Rmst* expression.

abundance transcripts as well as more lncRNAs (Wang X. et al., 2021), we focused on the smart-seq2 analysis to explore DRG neuron subtype. In t-distributed stochastic neighbor embedding (tSNE), 6 traditional classification neuronal subtype was found (Figure 1B), including *S100b*$^{+}$ neurofilament (NF), *Mgpra3*$^{+}$ non-peptidergic neurons (NP), *Th*$^{+}$ tyrosine hydroxylase (TH), *Tac1*$^{+}$ and *Sst*$^{+}$ peptidergic neurons (PEP), and *Atf3*$^{+}$ injured neuron (Figures 1B,C). Interestingly, we found *Rmst* was specifically expressed in *Atf3*$^{+}$ injured neuron (Figure 1C), suggesting that *Rmst* may be involved in NP.

To provide the adequate evidence, we performed animal neuropathic pain model to validate the result. We found lncRNA *Rmst* expression was increased early and persistently at least 28 days in damaged DRGs after SNL surgery but not sham surgery (Figure 2A) [$F(5,36) = 5.942$]. To be specific, *Rmst* expression was elevated 1.58-fold on day 3, 2.07-fold on day 7, 2.01-fold on day 14, 1.99-fold on day 21, 1.88-fold on day 28 after SNL but not in the contralateral L4 DRGs and L3 DRGs (Figures 2A–D) [Figure 2B: $F(5,36) = 1.896$; Figure 2C: $F(5,36) = 0.7694$; Figure 2D: $F(5,36) = 2.980$]. A similar phenomenon was observed in another NP mouse model called CCI model (Figures 2E,F) [Figure 2E: $F(5,36) = 3.530$]; [Figure 2F: $F(5,36) = 0.8966$]. The *Rmst* expression in damaged DRGs were elevated 1.97-fold on day 3, 2.23-fold on day 7, 2.23-fold on day 14, 2.46-fold on day 21, 2.3-fold on day 28 after CCI model (Figure 2E). Taken together, our data showed peripheral nerve damage could trigger the elevated *Rmst* expression in the damaged DRGs that maintained at least until 1-month

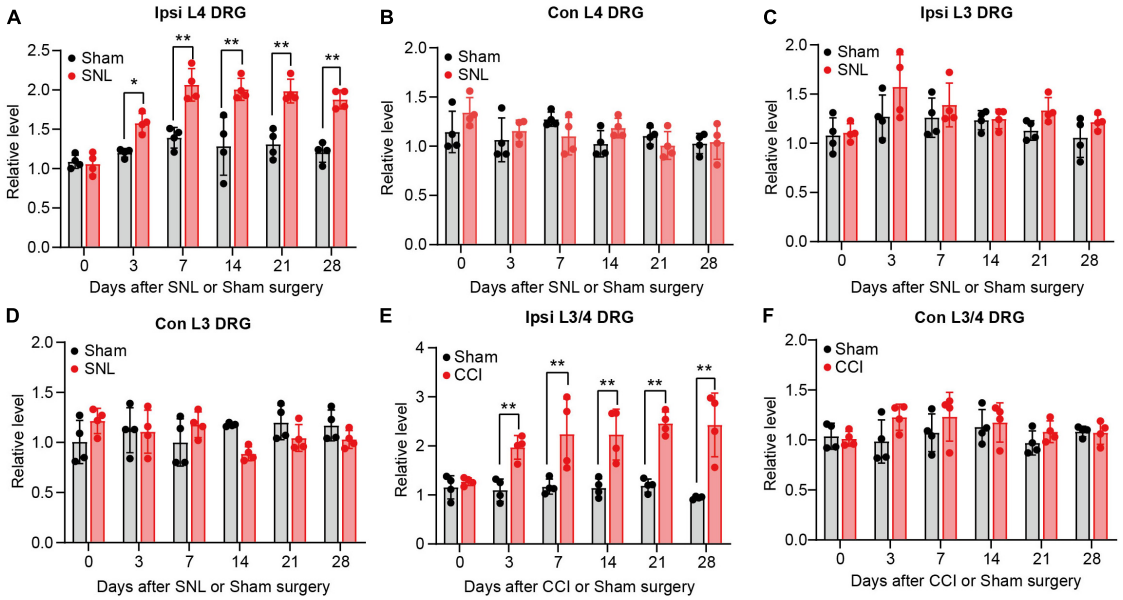

FIGURE 2
Rhabdomyosarcoma 2-associated transcript (*Rmst*) upregulation was found in damaged DRG of mice after SNL or CCI model. **(A–D)** Level of *Rmst* in ipsilateral L4 DRGs **(A)**, contralateral L4 DRGs **(B)**, ipsilateral L3 DRGs **(C)**, and contralateral L3 DRGs **(D)** after SNL or sham surgery $n = 16$. **(E,F)** Levels of *Rmst* in the ipsilateral **(E)** and contralateral **(F)** side L3/4 DRGs after CCI or sham surgery $n = 8$. Two-way ANOVA followed by *post-hoc* Tuckey test. $^*P < 0.05$ and $^{**}P < 0.01$ compared with sham group at each time point.

post-SNL, suggesting that *Rmst* may take part in the nerve damage-induced NP.

Blocking rhabdomyosarcoma 2-associated transcript expression in damaged dorsal root ganglions alleviated neuropathic pain

As the apparent change of *Rmst* in damaged DRGs, we further ask whether blocking *Rmst* expression in injured DRG could alleviate pain hypersensitivity. We first confirmed that DRG microinjection of siRmst, but not Scr, 3 days before SNL could block SNL-induced increased *Rmst* expression (Figure 3A) [$F(3,8) = 65.29$]. Microinjection of siRmst also slightly reduced basal expression of *Rmst* expression (Figure 3A). More importantly, we found pre-microinjection of siRmst could ameliorate SNL-induced nociceptive hypersensitivities, including mechanical allodynia (Figures 3B,C) [Figure 3B: $F(12,80) = 9.633$; Figure 3C: $F(12,80) = 10.15$] and heat hyperalgesia (Figure 3D) [Figure 3D: $F(12,80) = 17.99$]. Neither Scr nor siRmst changed basal paw response to mechanical or heat stimuli while mice received sham surgery (Figures 3B–D). We then ask the role of *Rmst* during the maintenance period after SNL model. We first confirmed that DRG microinjection of siRmst in maintenance period after SNL (Figure 3E) [$F(3,8) = 30.85$]. As expected, siRmst delivery through DRG microinjection on day 7 post-SNL rescued pain hypersensitivity (Figures 3F–H) [Figure 3F: $F(18,112) = 3.614$; Figure 3G: $F(18,112) = 3.312$; Figure 3H: $F(18,112) = 20.60$]. Our data strongly support that nerve damage triggered nociceptive hypersensitivity may be attributed to elevated *Rmst* expression in the damaged DRG.

Dorsal root ganglion long non-coding RNA *Rmst* overexpression produces nociceptive hypersensitivity

Next, we asked if DRG *Rmst* overexpression in neuron is sufficient for NP production. As the previous paper has reported *Rmst* was specifically expressed in the neuron (Briese et al., 2016), we utilized Adeno-associated Virus 5 (AAV5) following the previous papers (Li et al., 2020) to package *Rmst* full-length vector (AAV5-Rmst) and microinjected to the ipsilateral DRG to overexpress the *Rmst* expression. As a proof of concept, we found DRG microinjection of AAV5-Rmst in the ipsilateral side could particularly increase *Rmst* expression in ipsilateral side but neither contralateral side nor AAV5-Gfp (Figure 4A) [$F(3,8) = 84.17$]. More importantly, pain symptoms (Figures 4B–D) [Figure 4B: $F(15,96) = 5.679$; Figure 4C: $F(15,96) = 3.432$; Figure 4D: $F(15,96) = 14.98$] were induced third weeks after *Rmst* overexpression in DRG of naïve mice. It means that, even without nerve damage, DRG *Rmst* overexpression in neuron could result in NP-like symptoms.

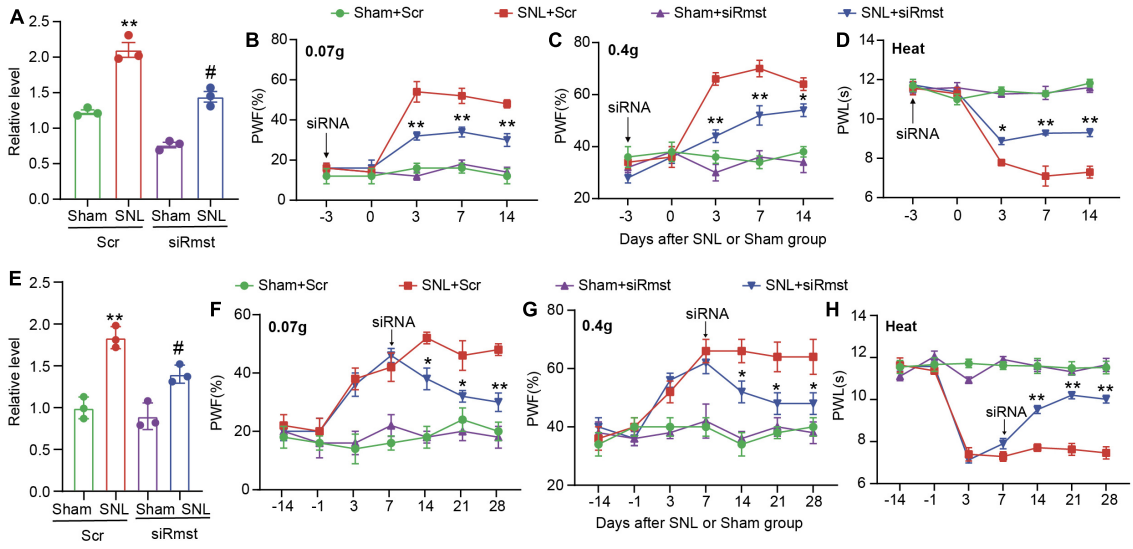

FIGURE 3
Blocking nerve damage triggered rhabdomyosarcoma 2-associated transcript (*Rmst*) expression in DRG mitigated the nerve damaged-induced nociceptive hypersensitivity. **(A)** Level of *Rmst* in the L4 DRGs on day 14 after nerve injury model in presence of siRmst or Scr. $n = 12$ mice, One-way ANOVA followed by *post-hoc* Tukey test, $^{**}P < 0.01$ compared with Sham + Scr group and $^{\#}P < 0.05$ compared with SNL + Scr group. **(B–D)** The PWF to von Frey filament **(B,C)** and the PWL to thermal stimuli **(D)** on the development period of NP. $n = 5$ mice, two-way ANOVA followed by *post-hoc* Tukey test, $^{*}P < 0.05$ and $^{**}P < 0.01$ compared with the SNL + Scr group. **(E)** Level of *Rmst* in the L4 DRGs on day 28 after nerve injury model in presence of siRmst or Scr. $n = 12$ mice, One-way ANOVA followed by *post-hoc* Tukey test, $^{**}P < 0.01$ compared with Sham + Scr group and $^{\#}P < 0.05$ compared with SNL + Scr group. **(F–H)** The PWF to von Frey filament **(F,G)** and the PWL to thermal stimuli **(H)** on the maintenance period of NP. $n = 5$ mice, two-way ANOVA followed by *post-hoc* Tukey test, $^{*}P < 0.05$ and $^{**}P < 0.01$ compared with SNL + Scr group. Paw withdrawal frequency: PWF; Paw withdrawal latency: PWL.

Rhabdomyosarcoma 2-associated transcript participated in the nerve damage induced dorsal root ganglion DNA methyltransferase 3 alpha expression after spinal nerve ligation

Next, the detailed mechanism of *Rmst* involved in NP was investigated. As the subcellular location of lncRNA can provide significant information on its function, we utilized cytoplasmic and nucleus RNA extraction protocol to purify populations of subcellar RNA fractions. Consistent with previously report *in vitro* (Zhao et al., 2021), *Rmst* in naïve mouse DRG was distributed predominantly in the cytoplasm (**Figure 5A**). Cytoplasmic lncRNAs can function in the posttranscriptional gene expression through mRNA stability and translation (Rashid et al., 2016). It has been reported that *Rmst* could upregulate DNA methyltransferase 3 (Dnmt3) by increasing the stability for its mRNA (Peng et al., 2020) in MCF7 cells, a breast cancer related epithelial cell line. We then examined whether overexpression of *Rmst* could also increase the *Dnmt3a* and *Dnmt3b* mRNA in primary DRG neuron. Surprisingly, only *Dnmt3a* mRNA as well as protein level increased but not Dnmt3b was observed in cultured neurons co-transduced with AAV5-Rmst (**Figures 5B–D**). In fact, Dnmt3a in primary afferent neurons was reported to participate in NP by repressing the potassium voltage-gated channel Kv1.2 encoded by *Kcna2* (Zhao et al., 2017). To elucidate whether *Rmst* participated in regulating *Dnmt3a* mRNA stability, actinomycin D was used to inhibit the RNA synthesis. We found that *Rmst* could stabilize *Dnmt3a* mRNA transcripts (**Figure 5E**). The half-life of *Dnmt3a* mRNA was around 8.5 h for *Rmst* overexpressed neurons, as compared to 6.5 h for Gfp control (**Figure 5E**) [$F(4,20) = 2.384$]. Next, we found microinjection of siRmst, but not Scr, could abolish the SNL- induced Dnmt3a increases (**Figure 5F**) [$F(3,8) = 17.11$]. Decreased Dnmt3a protein in damaged DRG with the siRmst microinjection after SNL was observed in the nucleus (**Figures 5G,H**) [$F(3,8) = 45.02$].

To further confirm whether *Rmst* is responsible for stabilizing *Dnmt3a* mRNA in the damaged DRG, we inhibited Dnmt3a expression through delivering Dnmt3a siRNA into the DRG after AAV5-Rmst microinjection. We found blocking *Rmst* overexpression-induced Dnmt3a increase could not lower *Rmst* expression (**Figure 6A**) [$F(2,6) = 19.28$] but lead to a fall of *Dnmt3a* mRNA and protein (**Figures 6B,C**) [**Figure 6B**: $F(2,6) = 62.27$; **Figure 6C**: $F(2,6) = 31.06$]. More importantly, blocking Dnmt3a expression attenuated the *Rmst* induced-nociceptive hypersensitivity (**Figures 6D–F**) [**Figure 6D**: $F(8,60) = 13.12$; **Figure 6E**: $F(8,60) = 3.500$; **Figure 6F**: $F(8,59) = 10.35$]. Collectively, nerve injury induced *Rmst* upregulation participates in NP by stabilizing the *Dnmt3a* mRNA expression.

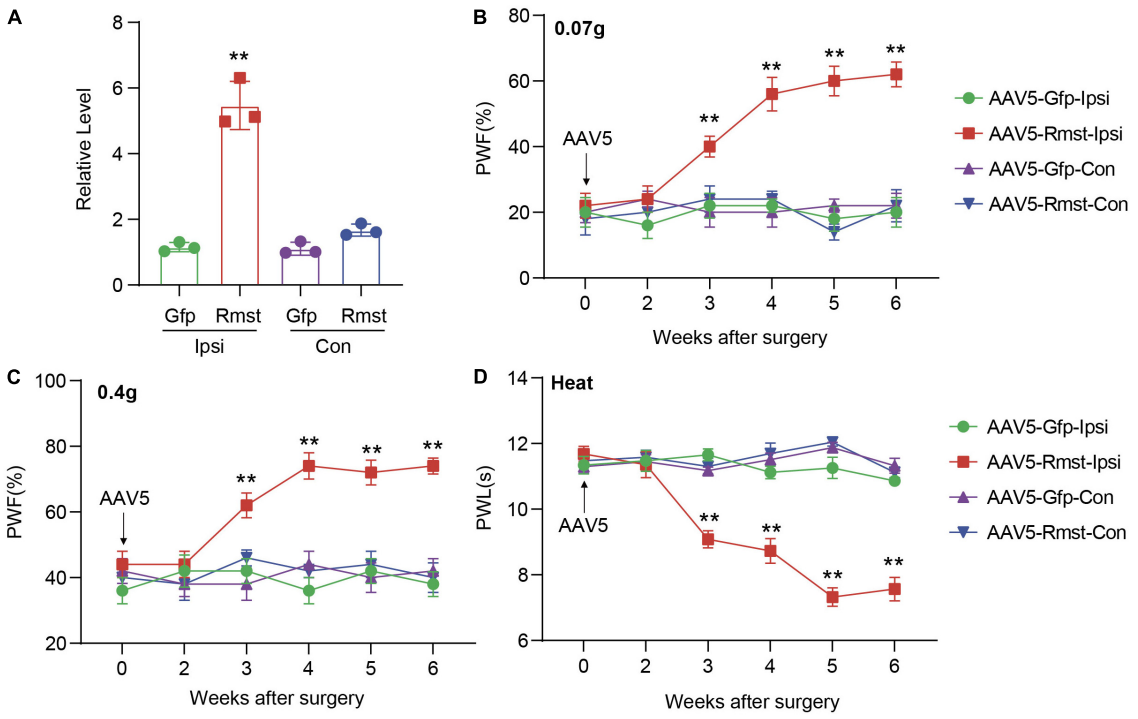

FIGURE 4
Overexpression of DRG rhabdomyosarcoma 2-associated transcript (*Rmst*) produced nociceptive hypersensitivity in naïve mice. **(A)** *Rmst* expression in L3/4 DRGs 6 weeks after receiving AAV5-Rmst or AAV5-Gfp. $n = 6$ mice, two-tailed unpaired Student's *t*-test, $^{**}P < 0.01$ compared with AAV5-Gfp group. **(B–D)** The PWF to von Frey filament **(B,C)** and the PWL to thermal stimuli **(D)** on mice with DRG microinjection of AAV5-Rmst or AAV5-Gfp. $n = 6$, two-way ANOVA followed by *post-hoc* Tukey test, $^{**}P < 0.01$ compared with AAV5-Gfp-Ipsi group.

Rhabdomyosarcoma 2-associated transcript regulates the DNA methyltransferase 3 alpha mRNA stability by interaction with HuR under neuropathic pain condition

Finally, we asked the potential mechanism of *Rmst* induced Dnmt3a upregulation in injured DRG neuron. Given that RNA-binding proteins (RBPs) affect the targeted mRNA stability, we focused on one of well-characterized RBPs, HuR. Notably, HuR was reported as a contributor to nociceptive pain (Kunder et al., 2022) and an anti-HuR could alleviate nerve-injury induced NP (Borgonetti and Galeotti, 2021). In particular, it was HuR reported to stabilize the *Dnmt3* mRNA (Peng et al., 2020). Therefore, under NP condition, we asked whether HuR contributed to *Rmst*-mediated increased Dnmt3a.

We first determined the alteration of HuR in DRGs after SNL or *Rmst* overexpression. Unexpectedly, we found neither SNL nor *Rmst* could regulate the HuR expression in injured DRG (**Figure 7A**). In fact, in many cancerous settings, HuR was increased subcellular localization within the cytoplasm to stabilize various prosurvival mRNA (Schultz et al., 2020). Therefore, we examine whether SNL induced cytoplasmic accumulation of HuR. We found SNL caused a steep increase of HuR protein in the cytoplasm of the damaged DRG while *Rmst* overexpression in DRG was found similar phenomenon (**Figure 7B**). This may suggest that under NP condition, HuR is transported from the nucleus to cytoplasm. Next, RNA immunoprecipitation (RIP) assay revealed that HuR was capable to enrich *Rmst* and *Dnmt3a* in SNL group, approximately 20-fold, and 60-fold, respectively, compared to sham group (**Figure 7C**). Finally, we found overexpression of *Rmst* in primary neuron promoted the binding between *Dnmt3a* mRNA and HuR (**Figure 7D**). Thus, *Rmst* appeared to be the essential regulator that promoted Dnmt3a expression through interacting with HuR in DRG neuron.

Discussion

This is the first study to examine the molecular and cellular function of *Rmst*, a lncRNA in injured DRG neuron that modulates NP. Specifically, the increased *Rmst* was positively regulated Dnmt3a by promoting its mRNA stability and interacting with HuR, which leads to NP. Blocking the elevation of *Rmst* could reverse nerve injury-induced Dnmt3a upregulation and alleviate pain hypersensitivities (**Figure 8**).

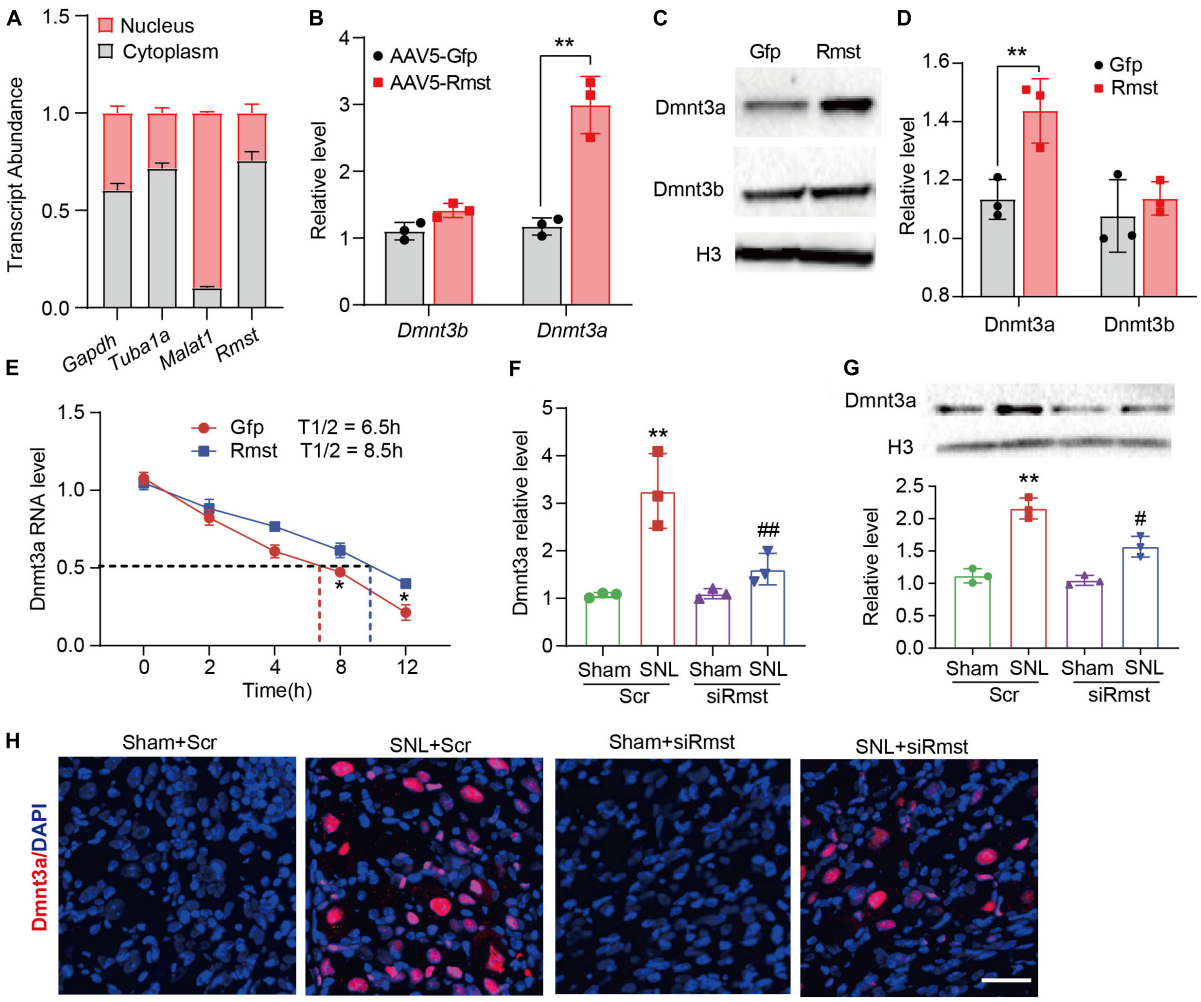

FIGURE 5
Dorsal root ganglion (DRG) rhabdomyosarcoma 2-associated transcript (*Rmst*) participated in the nerve damage induced Dnmt3a expression by stabilizing *Dnmt3a* mRNA. **(A)** Transcript abundance of cytoplasmic and nuclear RNA fractions for *Gapdh* mRNA, *Tuba1a* mRNA, *Malat1* mRNA, and *Rmst* mRNA from mouse DRGs. $n = 3$ mice. **(B)** Level of *Dnmt3a* and *Dnmt3b* mRNA expression in DRG neuron with AAV5-Rmst. *T*-test was used for statistic analysis. $^{**}P < 0.01$ versus AAV5-Gfp group. **(C,D)** Dnmt3a and Dnmt3b protein expression in DRG neuron with AAV5-Rmst. *T*-test was used for statistic analysis. $^{**}P < 0.01$ versus AAV5-Gfp group. **(E)** Primary DRG neurons with the treatment of ActD (5 μg/mL) at multiple time point as shown were treated with AAV5-Rmst or AAV5-Gfp. $n = 3$ biological repeats. $^{*}P < 0.05$ versus AAV5-Rmst group. **(F,G)** Levels of *Dnmt3a* mRNA **(F)** and protein expression **(G)** in ipsilateral L4 DRGs of SNL mice pre-received with siRmst or Scr. $n = 12$, one-way ANOVA followed by *post-hoc* Tukey test, $^{**}P < 0.01$ versus Sham + Scr group and $^{\#}P < 0.05$, $^{\#\#}P < 0.01$ versus SNL + Scr group. **(H)** Immunostaining for the ipsilateral L4 DRGs showed Dnmt3a protein expression in mice post-SNL and pre-delivered with siRmst or Scr. Scale bar = 40 μm.

The present study suggests that *Rmst* in DRGs is likely a key regulator in NP.

In 2013, the first lncRNA involved in NP was reported in detail (Zhao et al., 2013, p. 2). After that, the regulation of lncRNA on NP are popping up over the past few years (Wu et al., 2019). And we are the first to report lncRNA *Rmst* is involved in the NP. In fact, *Rmst* was first identified as non-coding RNA in 2012, and it was essential for neuronal specification in human embryonic stem cells (Ng et al., 2012). Under normal condition, *RMST* in both human and mouse occurs primarily in CNS (Uhde et al., 2010; Ng et al., 2012) and, more importantly, is abundant in neuron (Julian et al., 2013, p. 2; Briese et al., 2016). *RMST* physically interacts with SOX2 and regulates neural fate by regulating neurogenesis related genes (Ng et al., 2013, p. 2). *RMST* deficiency in neural stem cells resulted in glia differentiation (Ng et al., 2013), indicating that *RMST* is important for neural differentiation in particularly during brain development period. However, increased *Rmst* expression was reported in CNS diseases, including stroke (Zhao et al., 2021; Li et al., 2022) and Parkinson's disease (Ma et al., 2021). Blocking *Rmst* expression could protect from neuronal apoptosis and improve neurological function (Ma et al., 2021; Zhao et al., 2021;

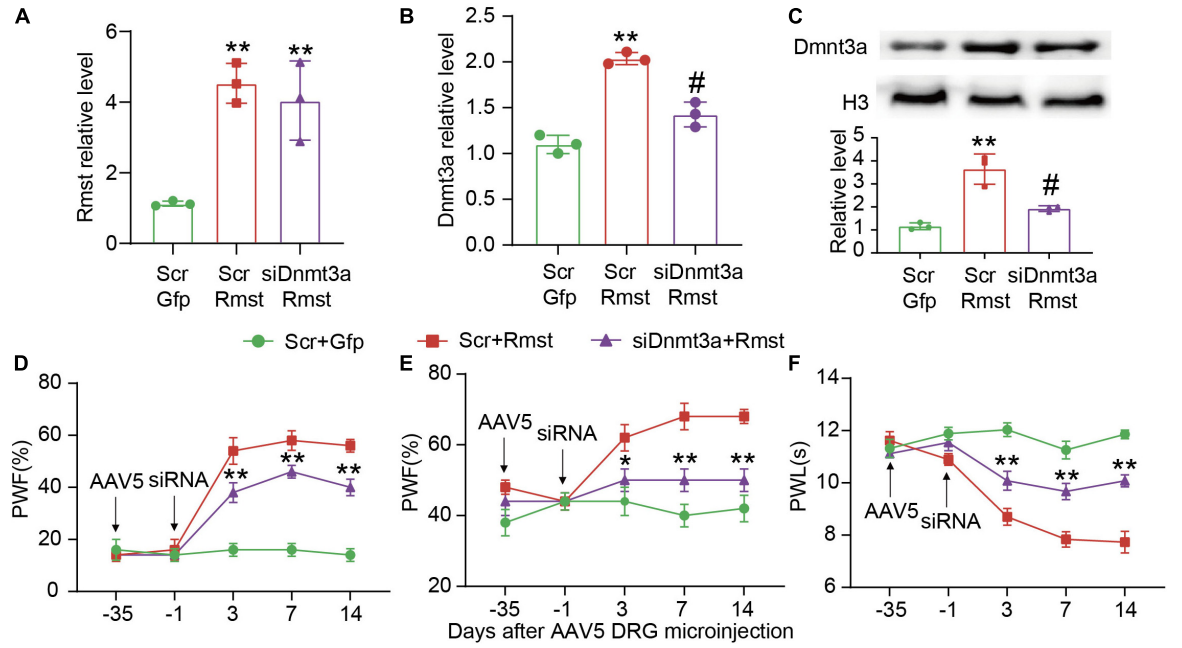

FIGURE 6
Blocking DNA methyltransferase 3 alpha (Dnmt3a) expression mitigated the rhabdomyosarcoma 2-associated transcript (*Rmst*) triggered-mechanical allodynia and heat hyperalgesia. **(A–C)** *Rmst* mRNA **(A)**, *Dnmt3a* mRNA **(B)**, and Dnmt3a protein **(C)** in mice after microinjection with siDnmt3a (Scr as control) and AAV5-Rmst (AAV5-Gfp as control). $^{**}P < 0.01$ versus AAV5-Gfp + Scr group and $^{\#}P < 0.05$ versus AAV5-Rmst + Scr group. **(D–F)** The ipsilateral PWF to von Frey filament **(D,E)** and the PWL to thermal stimuli **(F)** after microinjection of siDnmt3a or Scr in mice pre-received with AAV5-Rmst or AAV5-Gfp. $^{**}P < 0.01$ versus AAV5-Rmst + Scr group.

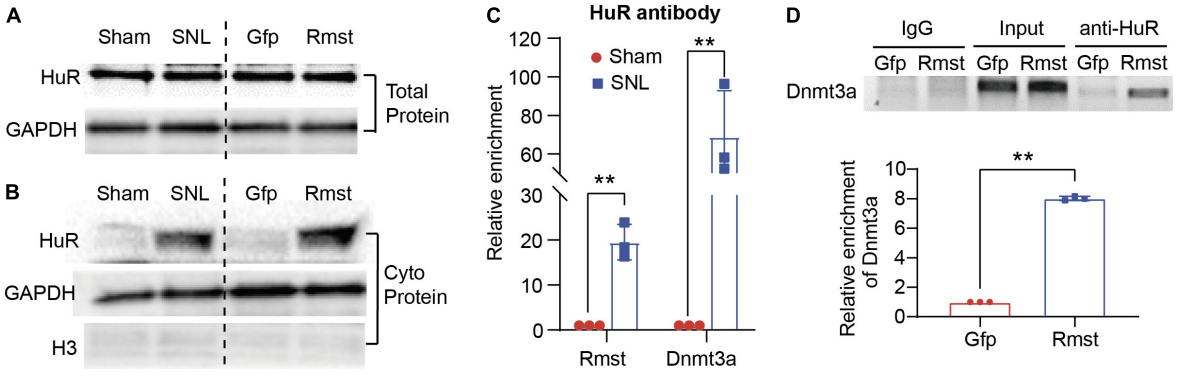

FIGURE 7
Rhabdomyosarcoma 2-associated transcript (*Rmst*) was interaction with HuR to regulate the *Dnmt3a* mRNA Stability Under NP Condition. **(A,B)** Level of HuR expression in total protein **(A)** and cytoplasm protein **(B)** in DRG with SNL model and AAV5-Rmst (AAV5-Gfp as control) DRG microinjection. **(C)** Level of *Rmst* or *Dnmt3a* mRNA immunoprecipitated by anti-HuR on day 7 post-SNL surgery $n = 3$ biological repeats. $^{**}P < 0.01$ versus sham group. **(D)** Level of *Dnmt3a* immunoprecipitated by HuR in DRG neuron with AAV5-Rmst. $n = 3$ biological repeats. $^{**}P < 0.01$ compared with AAV5-Gfp group.

Li et al., 2022), which suggests that excessive *Rmst* expression may cause CNS disease aggravations. Our present study found *Rmst* was also increased expressed in DRG neuron under NP condition. More importantly, blocking *Rmst* expression in injured DRGs could mitigate nerve injury-induced nociceptive hypersensitivity. However, why Rmst siRNA in DRGs did not alter response to mechanical and heat stimuli is unclear, which may be due to low *Rmst* expression in physiological condition. Together, the strong evidence indicates that the dysregulation of *Rmst* in neuron may contribute to NP development.

Evidence has been emerged lncRNAs mediates DNA methylation in various pathological condition (Huang et al., 2022), including schizophrenia (Ni et al., 2021, p. 006), diabetic retinopathy (He et al., 2021, p. 3), colon cancer

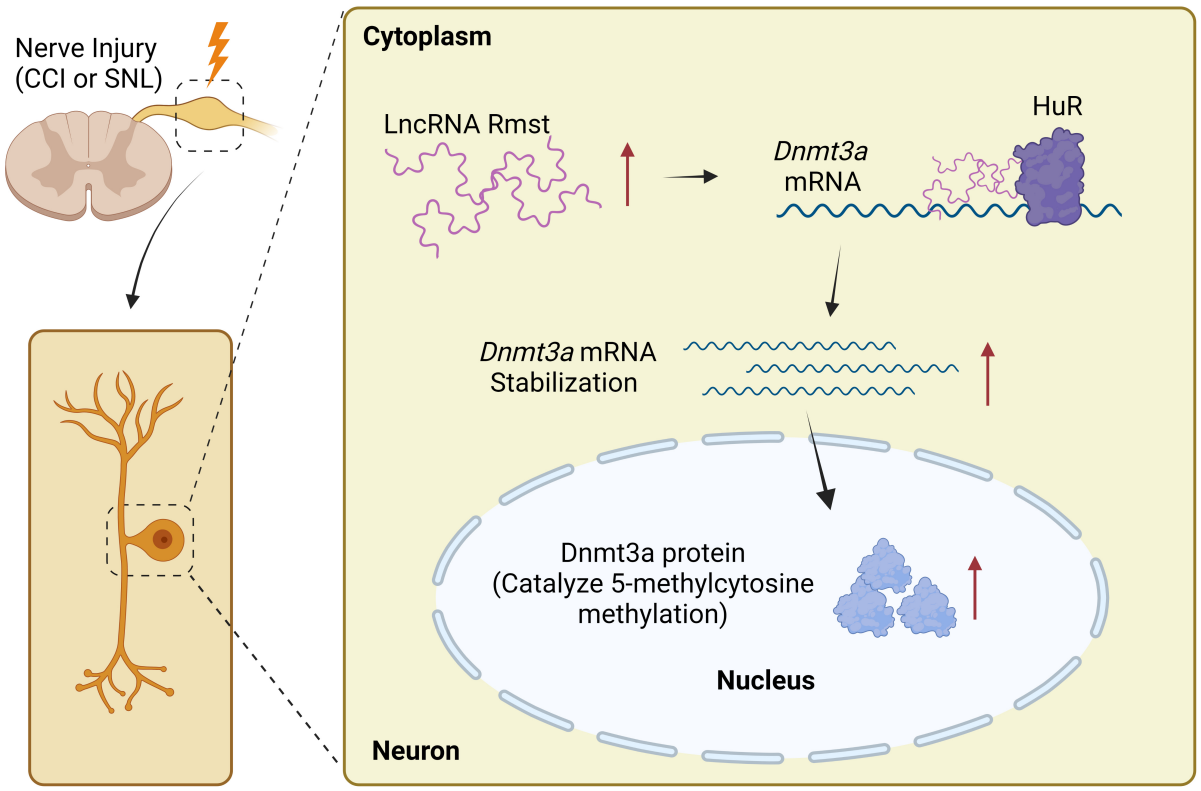

FIGURE 8
Proposed mechanism on rhabdomyosarcoma 2-associated transcript (*Rmst*) in NP. Nerve injury-triggered *Rmst* upregulation interacts with HuR in injured DRGs, resulting in stabilizing *Dnmt3a* mRNA and protein. The latter one has been reported as a critical NP regulator in DRG neurons. In contrast, in normal DRG neuron, *Dnmt3a* mRNA would be degraded without *Rmst*.

(Merry et al., 2015) and so on. In particular, *RMST* was characterized as a positive regulator for DNMT3 but not DNMT1 by increasing *DNMT3* mRNA stability in cancer (Peng et al., 2020). In our study, *Rmst* upregulation may contribute to the nerve damage-triggered Dnmt3a increase by stabilizing its mRNA in NP. Notably, when *Rmst* was overexpressed in DRG neuron, only DNMT3a but not DNMT3b appear to generate, and blocking DRG *Rmst* expression abolished SNL-induced DNMT3a upregulation, which was consistent with previous study (Peng et al., 2020, p. 3). Furthermore, *Rmst* did not directly modulate nociceptive hypersensitivity as in absence of Dnmt3a expression in DRG neuron the overexpression of *Rmst* failed to completely mimic nerve damage-induced nociceptive hypersensitivity. In fact, it has been reported DNMT3a in DRG neurons is involved in the NP (Guo et al., 2019). Knockout DNMT3a in DRG significantly attenuated nociceptive hypersensitivity (Zhao et al., 2017). What's more, in NP, transcriptional factors, such as CREB (Yang et al., 2021) and Oct1 (Zhao et al., 2017), could bind to the promoter region of Dnmt3a to boost Dnmt3a expression. Our study demonstrated that *Rmst* is required for the stability of *Dnmt3a* mRNA, enhancing DNMT3a expression. It should also be noted that *Rmst* also regulates other NP related genes including sex-determining region Y-box2 (*Sox2*) (Ng et al., 2013, p. 2; Zhang et al., 2019, p. 2) and heterogeneous nuclear ribonucleoprotein D (*hnRNPD*) (Liu et al., 2020; Feng et al., 2021). Whether these genes are also regulated by *Rmst* in NP remains to be determined.

Mechanistically, nerve injury-induced elevated *Rmst* could recruit HuR protein, thereby stabilizing the *Dnmt3a* mRNA and reducing the *Dnmt3a* mRNA degradation. HuR, as an RNA-binding protein, is capable to stabilize AU-rich elements (AREs)-containing reporter mRNA in the cytoplasm through binding AREs sequences (Gallouzi et al., 2000). The new finding has pointed out anti-HuR delivery has been proven effective to relieve pain hypersensitivity by inhibiting spinal neuroinflammation (Borgonetti and Galeotti, 2021). Therefore, the effectiveness of analgesics of anti-HuR may also be due to the degradation of *Dnmt3a* mRNA. However, further experiments are needed.

In conclusion, our study indicated that blocking *Rmst* expression in injured DRGs mitigated NP at least in part through enhancing degradation of *Dnmt3a* mRNA. Thus, *Rmst* may become a promising target and provide insightful directions for NP treatment.

Data availability statement

The RNA sequencing dataset for mouse DRG after peripheral nerve injury was obtained from previous research (https://doi.org/10.1177/1744806916629048). The ScRNA-seq dataset for mouse DRG after peripheral nerve injury was from Gene Expression Omnibus (GEO) with the series record GSE155622.

Ethics statement

This animal study was reviewed and approved by Guangzhou Medical University.

Author contributions

XG and XS conceptualized and designed the study. XG and WC contributed to write the manuscript. GZ and FH performed animal model and behavior test. XG and JQ performed molecular experiments. All authors read and approved the final manuscript.

Funding

This work of XS was supported by the National Natural Science Foundation of China (No. 81870823) and Guangzhou Institute of Pediatric/Guangzhou Women and Children's Medical Center Funds (No. GCP-2018-001).

Conflict of interest

The authors declare that the research was conducted in the absence of any commercial or financial relationships that could be construed as a potential conflict of interest.

The reviewer B-CJ declared a past co-authorship with one of the author XG to the handling editor.

Publisher's note

All claims expressed in this article are solely those of the authors and do not necessarily represent those of their affiliated organizations, or those of the publisher, the editors and the reviewers. Any product that may be evaluated in this article, or claim that may be made by its manufacturer, is not guaranteed or endorsed by the publisher.

Supplementary material

The Supplementary Material for this article can be found online at: https://www.frontiersin.org/articles/10.3389/fnmol.2022.1027063/full#supplementary-material

References

Borgonetti, V., and Galeotti, N. (2021). Intranasal delivery of an antisense oligonucleotide to the RNA-binding protein HuR relieves nerve injury-induced neuropathic pain. *Pain* 162, 1500–1510. doi: 10.1097/j.pain.0000000000002154

Briese, M., Saal, L., Appenzeller, S., Moradi, M., Baluapuri, A., Sendtner, M., et al. (2016). Whole transcriptome profiling reveals the RNA content of motor axons. *Nucleic Acids Res.* 44:e33. doi: 10.1093/nar/gkv1027

Clemens, A. W., and Gabel, H. W. (2020). Emerging insights into the distinctive neuronal methylome. *Trends Genet.* 36, 816–832. doi: 10.1016/j.tig.2020.07.009

Feng, J., Chang, H., Li, E., and Fan, G. (2005). Dynamic expression of de novo DNA methyltransferases Dnmt3a and Dnmt3b in the central nervous system. *J. Neurosci. Res.* 79, 734–746. doi: 10.1002/jnr.20404

Feng, X., Niu, L. J., Long, M. T., Luo, K., Huang, X., Chen, M., et al. (2021). Transcranial ultrasound stimulation of the anterior cingulate cortex reduces neuropathic pain in mice. *Evid. Based Complement. Alternat. Med.* 2021:651038. doi: 10.1155/2021/6510383

Gallouzi, I.-E., Brennan, C. M., Stenberg, M. G., Swanson, M. S., Eversole, A., Maizels, N., et al. (2000). HuR binding to cytoplasmic mRNA is perturbed by heat shock. *Proc. Natl. Acad. Sci. U.S.A.* 97, 3073–3078. doi: 10.1073/pnas.97.7.3073

Guo, X., Yao, Y., and Tao, Y.-X. (2019). "Role of DNA methylation in chronic pain," in *Epigenetics of chronic pain*, eds G. Bai and K. Ren (Amsterdam: Elsevier), 99–110. doi: 10.1016/B978-0-12-814070-3.00005-3

He, Y., Dan, Y., Gao, X., Huang, L., Lv, H., Chen, J., et al. (2021). DNMT1-mediated lncRNA MEG3 methylation accelerates endothelial-mesenchymal transition in diabetic retinopathy through the PI3K/Akt/mTOR signaling pathway. *Am. J. Physiol. Endocrinol. Metab.* 320, E598–E608. doi: 10.1152/ajpendo.00089.2020

Hou, X.-X., and Cheng, H. (2018). Long non-coding RNA RMST silencing protects against middle cerebral artery occlusion (MCAO)-induced ischemic stroke. *Biochem. Biophys. Res. Commun.* 495, 2602–2608. doi: 10.1016/j.bbrc.2017.12.087

Huang, W., Li, H., Yu, Q., Xiao, W., and Wang, D. O. (2022). LncRNA-mediated DNA methylation: An emerging mechanism in cancer and beyond. *J. Exp. Clin. Cancer Res.* 41:100. doi: 10.1186/s13046-022-02319-z

Julian, L. M., Vandenbosch, R., Pakenham, C. A., Andrusiak, M. G., Nguyen, A. P., McClellan, K. A., et al. (2013). Opposing regulation of Sox2 by cell-cycle effectors E2f3a and E2f3b in neural stem cells. *Cell Stem Cell* 12, 440–452. doi: 10.1016/j.stem.2013.02.001

Kunder, N., de la Pena, J. B., Lou, T. F., Chase, R., Stanowick, A., Black, B. J., et al. (2022). A conserved RNA-binding protein contributes to nociceptive pain. *J. Pain* 23:14. doi: 10.1016/j.jpain.2022.03.056

Li, J., Wang, N., Nie, H., Wang, S., Jiang, T., Ma, X., et al. (2022). Long non-coding RNA RMST worsens ischemic stroke via microRNA-221-3p/PIK3R1/TGF-β signaling pathway. *Mol. Neurobiol.* 59, 2808–2821. doi: 10.1007/s12035-021-02632-2

Li, Y., Guo, X., Sun, L., Xiao, J., Su, S., Du, S., et al. (2020). N6-methyladenosine demethylase FTO contributes to neuropathic pain by stabilizing G9a expression in primary sensory neurons. *Adv. Sci.* 7:1902402. doi: 10.1002/advs.201902402

Liu, C., Peng, Z., Li, P., Fu, H., Feng, J., Zhang, Y., et al. (2020). lncRNA RMST suppressed GBM cell mitophagy through enhancing FUS SUMOylation. *Mol. Ther. Nucleic Acids* 19, 1198–1208. doi: 10.1016/j.omtn.2020.01.008

Ma, X., Wang, Y., Yin, H., Hua, L., Zhang, X., Xiao, J., et al. (2021). Down-regulated long non-coding RNA RMST ameliorates dopaminergic neuron damage in Parkinson's disease rats via regulation of TLR/NF-κB signaling pathway. *Brain Res. Bull.* 174, 22–30. doi: 10.1016/j.brainresbull.2021.04.026

Merry, C. R., Forrest, M. E., Sabers, J. N., Beard, L., Gao, X. H., Hatzoglou, M., et al. (2015). DNMT1-associated long non-coding RNAs regulate global gene expression and DNA methylation in colon cancer. *Hum. Mol. Genet.* 24, 6240–6253. doi: 10.1093/hmg/ddv343

Ng, S.-Y., Bogu, G. K., Soh, B. S., and Stanton, L. W. (2013). The long noncoding RNA RMST interacts with SOX2 to regulate neurogenesis. *Mol. Cell* 51, 349–359. doi: 10.1016/j.molcel.2013.07.017

Ng, S.-Y., Johnson, R., and Stanton, L. W. (2012). Human long non-coding RNAs promote pluripotency and neuronal differentiation by association with chromatin modifiers and transcription factors: LncRNAs involved in neuronal differentiation. *EMBO J.* 31, 522–533. doi: 10.1038/emboj.2011.459

Ni, C., Jiang, W., Wang, Z., Wang, Z., Zhang, J., Zheng, X., et al. (2021). LncRNA-AC006129.1 reactivates a SOCS3-mediated anti-inflammatory response through DNA methylation-mediated CIC downregulation in schizophrenia. *Mol. Psychiatry* 26, 4511–4528. doi: 10.1038/s41380-020-0662-3

Pan, Z., Du, S., Wang, K., Guo, X., Mao, Q., Feng, X., et al. (2021). Downregulation of a dorsal root ganglion-specifically enriched long noncoding RNA is required for neuropathic pain by negatively regulating RALY-triggered Ehmt2 expression. *Adv. Sci.* 8:e2004515. doi: 10.1002/advs.202004515

Peng, W.-X., Koirala, P., Zhang, W., Ni, C., Wang, Z., Yang, L., et al. (2020). lncRNA RMST enhances DNMT3 expression through interaction with HuR. *Mol. Ther.* 28, 9–18. doi: 10.1016/j.ymthe.2019.09.024

Rashid, F., Shah, A., and Shan, G. (2016). Long non-coding RNAs in the cytoplasm. *Genomics Proteomics Bioinformatics* 14, 73–80. doi: 10.1016/j.gpb.2016.03.005

Schultz, C. W., Preet, R., Dhir, T., Dixon, D. A., and Brody, J. R. (2020). Understanding and targeting the disease-related RNA binding protein human antigen R (HuR). *Wiley Interdiscip. Rev. RNA* 11:e1581. doi: 10.1002/wrna.1581

Shao, C., Gao, Y., Jin, D., Xu, X., Tan, S., Yu, H., et al. (2017). DNMT3a methylation in neuropathic pain. *J. Pain Res.* 10, 2253–2262. doi: 10.2147/JPR.S130654

Tompkins, D. A., Hobelmann, J. G., and Compton, P. (2017). Providing chronic pain management in the "Fifth Vital Sign" era: Historical and treatment perspectives on a modern-day medical dilemma. *Drug Alcohol Depend.* 173, S11–S21. doi: 10.1016/j.drugalcdep.2016.12.002

Uhde, C. W., Vives, J., Jaeger, I., and Li, M. (2010). Rmst is a novel marker for the mouse ventral mesencephalic floor plate and the anterior dorsal midline cells. *PLoS One* 5:e8641. doi: 10.1371/journal.pone.0008641

van Hecke, O., Austin, S. K., Khan, R. A., Smith, B. H., and Torrance, N. (2014). Neuropathic pain in the general population: A systematic review of epidemiological studies. *Pain* 155, 654–662. doi: 10.1016/j.pain.2013.11.013

van Velzen, M., Dahan, A., and Niesters, M. (2020). Neuropathic pain: Challenges and opportunities. *Front. Pain Res.* 1:1. doi: 10.3389/fpain.2020.00001

Wang, K., Wang, S., Chen, Y., Wu, D., Hu, X., Lu, Y., et al. (2021). Single-cell transcriptomic analysis of somatosensory neurons uncovers temporal development of neuropathic pain. *Cell Res.* 31, 904–918. doi: 10.1038/s41422-021-00479-9

Wang, X., He, Y., Zhang, Q., Ren, X., and Zhang, Z. (2021). Direct comparative analyses of 10X genomics chromium and smart-seq2. *Genomics Proteomics Bioinformatics* 19, 253–266. doi: 10.1016/j.gpb.2020.02.005

Wu, S., Bono, J., and Tao, Y.-X. (2019). Long noncoding RNA (lncRNA): A target in neuropathic pain. *Expert Opin. Ther. Targets* 23, 15–20. doi: 10.1080/14728222.2019.1550075

Wu, S., Marie Lutz, B., Miao, X., Liang, L., Mo, K., Chang, Y. J., et al. (2016). Dorsal root ganglion transcriptome analysis following peripheral nerve injury in mice. *Mol. Pain* 12:174480691662904. doi: 10.1177/1744806916629048

Yang, Y., Wen, J., Zheng, B., Wu, S., Mao, Q., Liang, L., et al. (2021). CREB participates in paclitaxel-induced neuropathic pain genesis through transcriptional activation of Dnmt3a in primary sensory neurons. *Neurotherapeutics* 18, 586–600. doi: 10.1007/s13311-020-00931-5

Zhang, L., Xie, R., Yang, J., Zhao, Y., Qi, C., Bian, G., et al. (2019). Chronic pain induces nociceptive neurogenesis in dorsal root ganglia from Sox2-positive satellite cells. *Glia* 67, 1062–1075. doi: 10.1002/glia.23588

Zhao, J.-Y., Liang, L., Gu, X., Li, Z., Wu, S., Sun, L., et al. (2017). DNA methyltransferase DNMT3a contributes to neuropathic pain by repressing Kcna2 in primary afferent neurons. *Nat. Commun.* 8:14712. doi: 10.1038/ncomms14712

Zhao, L., Zhang, M., Yan, F., and Cong, Y. (2021). Knockdown of RMST impedes neuronal apoptosis and oxidative stress in OGD/R-induced ischemic stroke via depending on the miR-377/SEMA3A signal network. *Neurochem. Res.* 46, 584–594. doi: 10.1007/s11064-020-03194-w

Zhao, X., Tang, Z., Zhang, H., Atianjoh, F. E., Zhao, J. Y., Liang, L., et al. (2013). A long noncoding RNA contributes to neuropathic pain by silencing Kcna2 in primary afferent neurons. *Nat. Neurosci.* 16, 1024–1031. doi: 10.1038/nn.3438

frontiers | Frontiers in Molecular Neuroscience

TYPE Brief Research Report
PUBLISHED 23 March 2023
DOI 10.3389/fnmol.2023.1160206

OPEN ACCESS

EDITED BY
Linlin Zhang,
Tianjin Medical University General Hospital,
China

REVIEWED BY
Zhi-Yong Tan,
Hebei University,
China
Qingjian Han,
Fudan University,
China

*CORRESPONDENCE
Yong Chen
✉ yong.chen@duke.edu

SPECIALTY SECTION
This article was submitted to
Pain Mechanisms and Modulators,
a section of the journal
Frontiers in Molecular Neuroscience

RECEIVED 06 February 2023
ACCEPTED 27 February 2023
PUBLISHED 23 March 2023

CITATION
Wang P, Zhang Q, Dias FC, Suttle A, Dong X and Chen Y (2023) TMEM100, a regulator of TRPV1-TRPA1 interaction, contributes to temporomandibular disorder pain.
Front. Mol. Neurosci. 16:1160206.
doi: 10.3389/fnmol.2023.1160206

TMEM100, a regulator of TRPV1-TRPA1 interaction, contributes to temporomandibular disorder pain

Peng Wang[1], Qiaojuan Zhang[1], Fabiana C. Dias[1], Abbie Suttle[1], Xinzhong Dong[2] and Yong Chen[1,3,4]*

[1]Department of Neurology, Duke University, Durham, NC, United States, [2]Solomon H. Snyder Department of Neuroscience, Johns Hopkins University School of Medicine, Baltimore, MD, United States, [3]Center for Translational Pain Medicine, Department of Anesthesiology, Duke University, Durham, NC, United States, [4]Department of Pathology, Duke University, Durham, NC, United States

There is an unmet need to identify new therapeutic targets for temporomandibular disorder (TMD) pain because current treatments are limited and unsatisfactory. TMEM100, a two-transmembrane protein, was recently identified as a regulator to weaken the TRPA1-TRPV1 physical association, resulting in disinhibition of TRPA1 activity in sensory neurons. Recent studies have also shown that *Tmem100*, *Trpa1*, and *Trpv1* mRNAs were upregulated in trigeminal ganglion (TG) after inflammation of the temporomandibular joint (TMJ) associated tissues. These findings raise a critical question regarding whether TMEM100 in TG neurons is involved in TMD pain *via* regulating the TRPA1-TRPV1 functional interaction. Here, using two mouse models of TMD pain induced by TMJ inflammation or masseter muscle injury, we found that global knockout or systemic inhibition of TRPA1 and TRPV1 attenuated pain. In line with their increased genes, mice exhibited significant upregulation of TMEM100, TRPA1, and TRPV1 at the protein levels in TG neurons after TMD pain. Importantly, TMEM100 co-expressed with TRPA1 and TRPV1 in TG neurons-innervating the TMJ and masseter muscle and their co-expression was increased after TMD pain. Moreover, the enhanced activity of TRPA1 in TG neurons evoked by TMJ inflammation or masseter muscle injury was suppressed by inhibition of TMEM100. Selective deletion of *Tmem100* in TG neurons or local administration of TMEM100 inhibitor into the TMJ or masseter muscle attenuated TMD pain. Together, these results suggest that TMEM100 in TG neurons contributes to TMD pain by regulating TRPA1 activity within the TRPA1-TRPV1 complex. TMEM100 therefore represents a potential novel target-of-interest for TMD pain.

KEYWORDS

TMEM100, TRPA1, TRPV1, temporomandibular joint, masseter muscle, bite force, trigeminal ganglion sensory neurons, calcium signal

Introduction

Temporomandibular disorders (TMD) include a group of painful conditions that involve the temporomandibular joint (TMJ), masseter muscles, and connective tissues (Scrivani et al., 2008). Mastication is fundamentally relevant for vertebrate nourishment. In cases of tissue inflammation or injury to the TMJ and masseter muscles, mastication

becomes painful (Svensson et al., 1998; Scrivani et al., 2008; Iodice et al., 2013). Patients experience TMD pain which negatively impacts their overall quality of life. Current pharmacotherapies for TMD pain have limited efficacy and side effects (Andre et al., 2022). A deeper understanding of TMD pain mechanisms and identifying new targets for TMD pain are therefore warranted for developing more effective treatments.

TMD pain critically depends on trigeminal ganglion (TG) sensory neurons that transmit nociceptive signals from the peripheral tissues to the central nervous system. Detection of pain signals by these cells relies on specific transduction machinery. Key components thereof belong to TRP ion channels (Julius, 2013). TRPA1 and TRPV1, two cardinal pain-TRPs, have been critically implicated in both acute and chronic pain and represent possible bona-fide targets for the development of rationally-guided analgesics (Julius, 2013). However, their respective roles in TMD pain remain largely elusive. In addition, previous studies have suggested that TRPA1 and TRPV1 can form a complex of channel heteromers and functionally interact in sensory neurons (Salas et al., 2009; Akopian, 2011; Spahn et al., 2014). Yet, it is undetermined whether the interplay of TRPA1-TRPV1 in sensory neurons of the trigeminal system contributes to TMD pain.

TMEM100, a two-transmembrane protein, was recently identified as an adaptor to regulate the physical and functional interaction of TRPA1-TRPV1 in sensory neurons (Weng et al., 2015). TMEM100 weakens TRPA1-TRPV1 physical association, which results in disinhibition of TRPA1 activity. Conversely, when TMEM100 is absent, TRPV1 forms a tight complex with TRPA1 that greatly suppresses the activity of TRPA1 (Weng et al., 2015). These findings point toward TMEM100 as a potential new target for mitigating pathologic pain, a concept supported by available data on the loss-of-function of TMEM100. For instance, conditional knockout (cKO) of *Tmem100* in dorsal root ganglion (DRG) neurons or subcutaneous injection of TMEM100 inhibitor into the hindpaw blunted mechanical hyperalgesia caused by complete Freund's adjuvant (CFA) in mice (Weng et al., 2015). While these data suggest that disabling TMEM100 may provide a novel strategy to combat DRG-mediated pain, contributions of TMEM100 to TG-mediated TMD pain await experimental clarification. TMD etiologies are attributable to anatomically and functionally unique target tissues (Piette, 1993; Detamore and Athanasiou, 2003). In addition, TMD pain not only has a strikingly different subjective quality when compared to DRG-mediated pain, but also different pharmacological responsiveness (Detamore and Athanasiou, 2003; Cairns, 2010; Andre et al., 2022; Tran et al., 2022).

Here, using two mouse models of chronic TMD pain, TMJ inflammation and masseter muscle injury as we previously described (Chen et al., 2013; Suttle et al., 2022), we sought to investigate whether: (1) genetic knockout or pharmacological inhibition of TRPA1 and TRPV1 attenuates TMD pain; (2) TMEM100 co-expresses with TRPA1 and TRPV1 in TG neurons and their co-expression is increased in TG neurons-innervating the TMJ and masseter muscle; (3) inhibition of TMEM100 suppresses the activity of TRPA1 in TG neurons; and (4) cKO of *Tmem100* in TG neurons or local injection of TMEM100 inhibitor into the TMJ and masseter muscle reduces TMD pain.

Materials and methods

Animals

Trpa1 and *Trpv1* KO mice were from the Jackson Laboratory. *Tmem100* cKO (Advillin-cre^{ER}::Tmem100$^{fl/fl}$) mice were provided by Dr. Xinzhong Dong (Weng et al., 2015). Adv-Cre mice express tamoxifen-inducible Cre recombinase specifically in ~98% of TG/DRG neurons (Hasegawa et al., 2007). Deletion of *Tmem100* was induced *via* daily intraperitoneal (i.p.) injection of tamoxifen (75 mg/kg) for 5 days. Pirt-GCaMP3 mice expressing the genetically-encoded Ca^{2+} indicator GCaMP3 in >96% of DRG/TG neurons (Kim et al., 2014) were used for Ca^{2+}-imaging. Male *KO* and cKO and their respective control mice (background: C57bl/6) were used at 2.5–3.5 months of age. Animals were housed in climate-controlled rooms on a 12/12 h light/dark cycle with water and food available *ad libitum*. Animal protocol was approved by Duke University- Institutional Animal Care and Use Committee (IACUC).

Induction of TMJ inflammation and masseter muscle injury

TMD pain was induced in mice following studies (Guo et al., 2010; Chen et al., 2013; Bai et al., 2019; Suttle et al., 2022). For TMJ inflammation, mice were injected with 10 µl of complete Freund's adjuvant (CFA, 5 mg/mL; Chondrex) into the joint. Controls received incomplete Freund's adjuvant (IFA). For masseter muscle injury, ligation of the tendon of the anterior superficial part of masseter muscle (TASM) was conducted. The TASM was freed from surrounding connective tissues and the tendon was tied with two 6.0-chromic gut ligatures at 1.5 mm-apart during anesthesia with ketamine/xylazine (i.p. 80 mg/8 mg/kg, Sigma-Aldrich). Controls received the same procedure but the tendon was not ligated.

TMD pain behavioral test

Bite force test was used to measure TMD masticatory pain as we previously described (Chen et al., 2013; Suttle et al., 2022). When bite transducer was slowly moved towards the mouse, a bite was invariably elicited. The voltage output during each bite was recorded using Labview 8.0 (National Instruments). The voltage of each bite was determined and converted into force (newton) based on the regression equation derived from calibration. Each animal was tested 3–5 times per time point and the values were averaged. The interval between two trials was >1 min. Mice were randomly assigned to treatment groups. The experimenter was blinded to the treatment conditions and genotypes. Although the baseline values for bite force were not statistically different between groups or genotypes, there were variations (12.84 to 16.13 newtons). To statistically analyze the data in a more objective way, bite force values after treatment were normalized to the baseline for each group and % of bite force changes were compared.

Chemical injections

To determine the effect of systemic inhibition of TRPA1 or TRPV1 on established TMD pain, mice were i.p. administered of

the TRPA1 selective inhibitor HC030031 (Eid et al., 2008) or TRPV1 selective inhibitor SB366791 (Gunthorpe et al., 2004) (Sigma-Aldrich) on day 1 CFA or day 7 TASM, respectively, when TMD pain was the most prominent (see Figure 1). To test the local inhibitory effect of TMEM100, 10 µl of TMEM100 inhibitor T100-Mut (21stCenturyBio) was bilaterally, intraarticularly (i.a.) injected into the TMJs for CFA and intramuscularly (i.m.) injected into the masseter muscle for TASM models, respectively. T100-mut is a Tmem100-mutant-derived peptide which can selectively inhibit TRPA1 activity in TRPA1-TRPV1 complex (Weng et al., 2015). Control animals received 5% DMSO or normal saline.

To track TMJ or masseter muscle innervation by the TG neurons, mice were injected with 2 µl of neural tracer fast blue (FB, 2% aqueous solution; Polysciences) into the TMJ or masseter muscle 15 min before CFA/IFA and TASM/sham.

Immunohistochemistry and quantitative analysis

Mouse TGs were dissected and sectioned at 12 µm. TG sections were blocked with 5% normal donkey serum (Jackson-ImmunoResearch) and incubated overnight with primary antibodies: guinea pig anti-TRPV1 (1:800, Neuromics), rabbit anti-TRPA1 (1:500, Aviva-Systems-Biology), sheep anti-TRPA1 (1:300, LifeSpan-Biosciences), and rabbit anti-TMEM100 (1:600, EMD Millipore). Immunodetection was accomplished with secondary antibodies (AlexaFluor-647, −594 and − 488; 1:600; Invitrogen) and cover-slipped with Vectashield (Vector). Images were acquired using BX61-Olympus upright microscope or Zeiss-780 confocal microscope. 4–6 sections/TG were analyzed. TG neurons were identified by morphology. Using ImageJ software (NIH), the cutoff density threshold was determined by averaging the density of three neurons/section that were judged to be minimally positive. All neurons for which the mean density exceeded the threshold of 25% were counted as positive.

Ca^{2+}-imaging of TG neurons

Following our method (Chen et al., 2021), *ex-vivo* Ca^{2+}-imaging of TG explants was performed to visualize neuronal activity. TGs were dissected from Pirt-GCaMP3 mice and equilibrated in artificial cerebrospinal fluid (ACSF) bubbled with 95% O_2/5% CO_2 at room temperature. After 15 min, explants were placed in a dish with 2 ml of preoxygenated ACSF and imaged using Zeiss-780 upright confocal microscope with 20x water immersion objective at the 488-nm wavelength. TGs were stimulated with TRPA1 agonist JT010 (Takaya et al., 2015) (Sigma-Aldrich) at 100 nM. To examine whether inhibition of TMEM100 attenuates the JT010-induced Ca^{2+} signal, explants were pretreated with T-100 Mut at 200 nM during the 15 min sample equilibration. Ca^{2+} fluorescence intensity of each neuron before (baseline) and after (response) chemical stimulation was determined using ImageJ. The percentage of responding neurons was analyzed.

Statistical analysis

Data were expressed as mean ± SEM. Two-tail *t*-test, one-way ANOVA or two-way ANOVA followed by Dunnett's *post-hoc* test by Graphpad Prism 6 was used for groups comparison. Experimental "N" as used was based on a power analysis of our previous relevant studies involving bite force test, immunohistochemistry, and Ca^{2+}-imaging (Chen et al., 2013, 2021; Suttle et al., 2022). $p < 0.05$ was considered statistically significant.

Results

Knockout or inhibition of Trpa1 and Trpv1 attenuates TMD pain

Whereas TMD has multifactorial etiologies (Ohrbach et al., 2011; Greenspan et al., 2013; Schiffman et al., 2014), a significant subgroup of patients suffer joint inflammation and/or masseter muscle injury (Stohler, 1999; Atsu and Ayhan-Ardic, 2006; Schiffman et al., 2014). To mimic these conditions in mice, we induced TMJ inflammation by injecting CFA into the joint and masseter muscle injury by ligating the TASM following our studies (Chen et al., 2013; Suttle et al., 2022). Bite force measurement, as a clinically relevant read-out, was used to assess masticatory pain of TMD (Chen et al., 2013). Both models resulted in long-lasting masticatory pain, as indicated by a substantial reduction of bite force from day 1 to 11 after CFA and from day 3 to 21 after TASM (Figure 1). KO of *Trpa1* or *Trpv1* significantly suppressed the reduction of bite force in both models (Figures 1A,B,E,F). In line with the results of knockout, systemic blockade of TRPA1 or TRPV1 by i.p. injection of HC030031 and SB366791, respectively, at 3 mg/kg and 10 mg/kg significantly blunted the reduction of bite force (Figures 1C,D,G,H). These data suggest that TRPA1 and TRPV1 are required for TMD pain.

TRPA1 and TRPV1 expressions in TG neurons are increased after TMD pain

We have previously demonstrated that *Trpa1* and *Trpv1* mRNAs in TGs were increased after TMJ inflammation (Chen et al., 2013). Here, we extended this finding and found that the percentage of TRPA1- and TRPV1-immunoreactive TG neurons was elevated after TMJ inflammation, as well as after masseter muscle injury (Figures 1I–L). These data suggest that TG neurons might be the crucial cellular site where TRPA1 and TRPV1 drive TMD pain.

TMEM100 co-expresses with TRPA1 and TRPV1 in TG neurons and their co-expression is increased after TMD pain

Immunostaining demonstrated that TMEM100 co-expressed with TRPA1 and TRPV1 in TG neurons (Figure 2A). Interestingly, their colocalization was substantially increased after CFA or TASM (TMEM100 + TRPA1 + TRPV1/all TG neurons, Figure 2B). Further, their co-expression in TG neurons-innervating the TMJ or masseter muscle was also significantly increased after CFA or TASM

10.3389/fnmol.2023.1160206

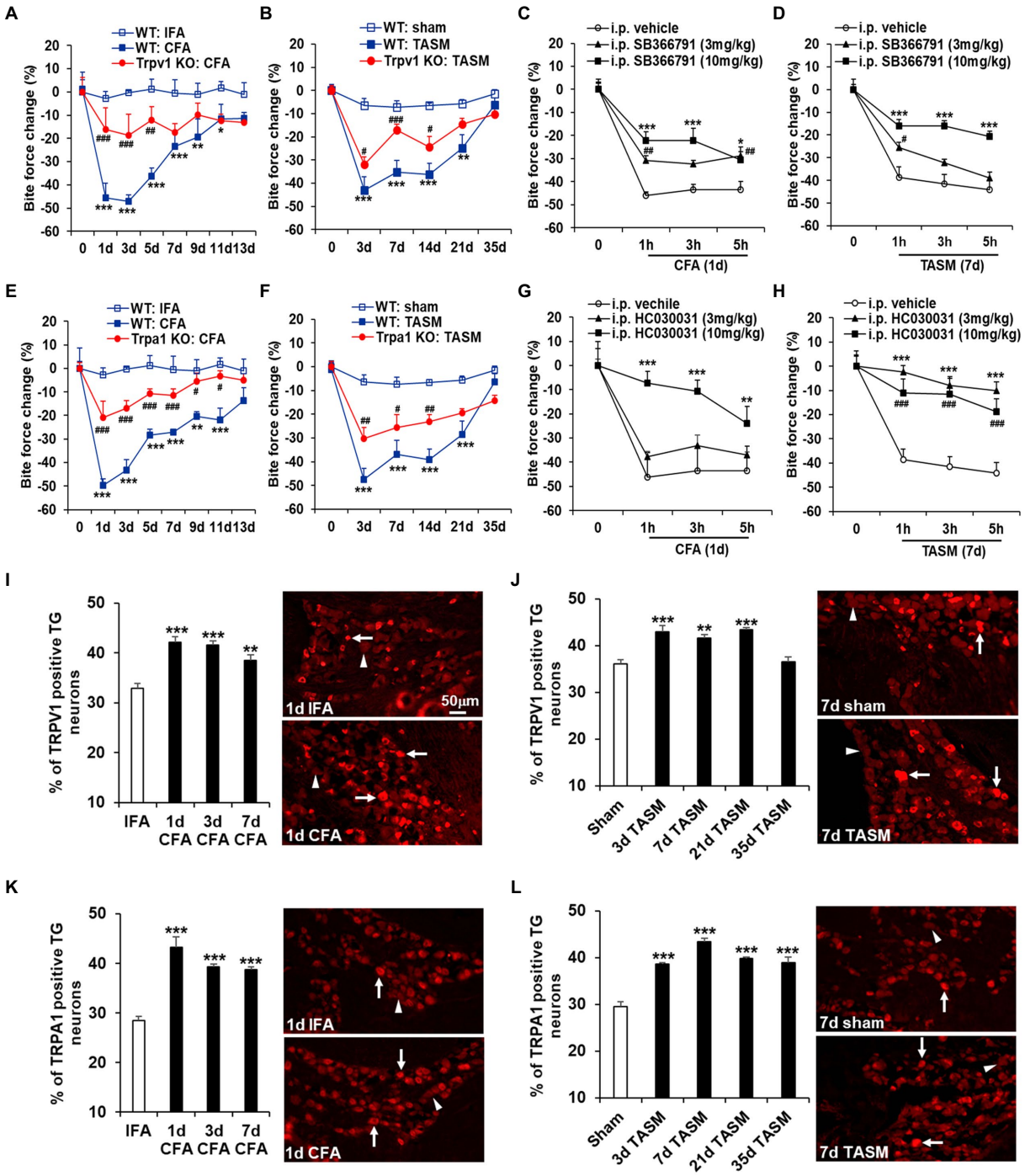

FIGURE 1
Global KO or systemic inhibition of TRPA1 and TRPV1 attenuates TMD pain. **(A,B,E,F)** TMJ inflammation or masseter muscle injury resulted in a long-lasting substantial reduction of bite force, which was attenuated by knocking out *Trpa1* or *Trpv1*. **p* <0.05, ***p* <0.01, and ****p* <0.001 vs. WT: IFA or WT: sham; #*p* <0.05, ##*p* <0.01, and ###*p* <0.001 vs. WT: CFA or WT: TASM. Two-way ANOVA followed by Dunnett's *post-hoc* test. *N* =5–8 mice/group. (**C,D,G,H**) Single i.p. injection of the TRPV1 selective inhibitor SB366791 or TRPA1 selective inhibitor HC030031 at 3mg/kg and 10mg/kg significantly blunted the reduction of bite force caused by TMJ inflammation or masseter muscle injury except that HC030031 at 3mg/kg had no significant impact on bite force reduction in TMJ inflammation model. **p* <0.05, ***p* <0.01, ****p* <0.001, #*p* <0.05, ##*p* <0.01, and ###*p* <0.001 vs. i.p. vehicle (5% DMSO). Two-way ANOVA followed by Dunnett's *post-hoc* test. *N* =4–6 mice/group. Note: '0' on x-axis represents baseline (before CFA or TASM). Exemplary changes of recorded bite force signal for WT: IFA, WT: CFA, and *Trpv1*-KO: CFA groups was shown in Supplementary Figure 1. (**I–L**) Temporal course of upregulation of TRPV1 and TRPA1 in TG neurons after TMJ inflammation or masseter muscle injury. (**I,J**) and (**K,L**) show increased percentage of TRPV1 and TRPA1 immunoreactive TG neurons after TMJ inflammation or masseter muscle injury, respectively. ***p* <0.01 and ****p* <0.001 vs. IFA (1d) or sham (7d). One-way ANOVA followed by Dunnett's *post-hoc* test. *N* =4–5 mice/group. Arrows and arrowheads in images represent immunoreactive positive and negative neurons, respectively. TRPV1 and TRPA1 antibodies' specificity was validated in TG sections from KO mice (Supplementary Figure 2).

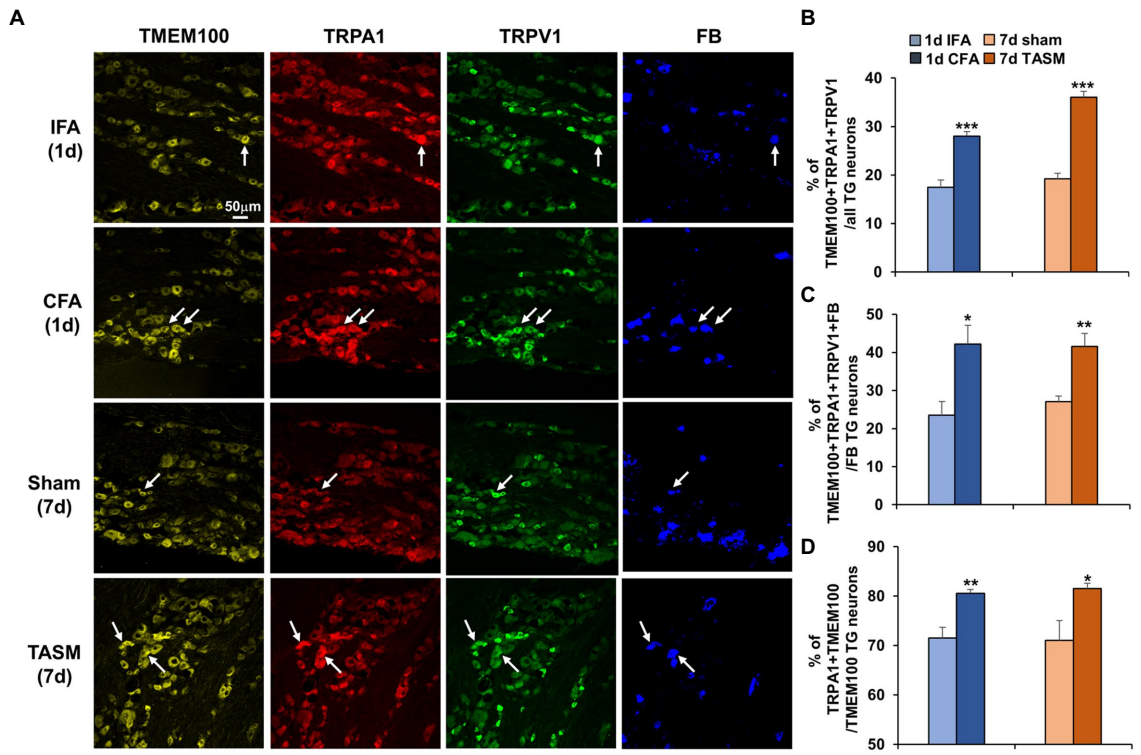

FIGURE 2
Co-expression of TMEM100 with TRPA1 and TRPV1 in TG neurons-innervating the TMJ and masseter muscle is increased after TMJ inflammation or masseter muscle injury. **(A)** Representative images show colocalization of TMEM100, TRPA1, TRPV1, and FB in TG neurons. Arrows in images represent colocalized neurons. **(B–D)** Quantitative analysis shows an increased percentage of TMEM100+TRPA1+TRPV1/total of TG neurons **(B)**, TMEM100+TRPA1+TRPV1+FB/FB-labeled TG neurons **(C)**, and TRPA1+TMEM100/TMEM100 positive neurons **(D)** 1day after CFA or 7days after TASM. *p <0.05, **p <0.01, and ***p <0.001 vs. IFA or sham, two-tail t test. N =4–5 mice/group. TRPV1 and TRPA1 antibodies' specificity was validated in TG sections from KO mice (Supplementary Figure 2) and TMEM100 antibody specificity was previously validated (Yu et al., 2019).

(TMEM100 + TRPA1 + TRPV1 + FB/FB-labeled neurons, Figure 2C). Studies have shown that 45 and 96% of TRPA1 co-express TMEM100 in DRG neurons in mice (Weng et al., 2015) and rats (Yu et al., 2019), respectively, we found that ~71% of TRPA1 co-expressed with TMEM100 in TG neurons of control mice (Figure 2D). These discrepancies might be due to TG vs. DRG and mice vs. rats. Importantly, we found co-expression of TRPA1 with TMEM100 in TG neurons (TRPA1 + TMEM100/TMEM100) was significantly increased after CFA or TASM (Figure 2D).

Inhibition of TMEM100 suppresses the enhanced activity of TRPA1 in TG neurons after TMD pain

Co-localization of TMEM100 with TRPA1 and TRPV1 in TG neurons possibly provides a cellular basis for TMEM100 to regulate TRPA1 activity in TRPV1-TRPA1 complex. We then examined whether TRPA1 activity in TG neurons is enhanced after TMD pain, more importantly, whether this enhancement can be suppressed when inhibiting TMEM100. *Ex vivo* Ca^{2+}-imaging demonstrated an increased percentage of neurons responding to TRPA1 agonist JT010 in organotypic TGs prepared from mice received CFA or TASM (Figure 3). Importantly, this increase was conspicuously reduced by the TMEM100 inhibitor T100-Mut. Of note, T100-Mut did not abolish TRPA1 activity, possibly due to a fraction of TRPA1-expressing neurons which do not contain TMEM100 (Figure 2D). Nevertheless, these data suggest that TMEM100 regulates TRPA1 activity in TG neurons under TMD pain.

cKO of Tmem100 in TG neurons or local administration of T100-Mut into the TMJ or masseter muscle attenuates TMD pain

It was reported that *Tmem100* mRNA in TG was upregulated after inflammation of masseter muscle (Chung et al., 2016). Consistently, we found TMEM100 expression in TG neurons is increased after TMJ inflammation or masseter muscle injury (Figures 4A,B). We next examined whether deletion of *Tmem100* in TG neurons reduces TMD pain. In Adv-Cre::$Tmem100^{fl/fl}$ mice after tamoxifen treatment, we found TMEM100 expression in TG neurons was dramatically reduced (Figure 4C), validating the knockout efficiency. Behavioral assays revealed that cKO of *Tmem100* in TG neurons significantly suppressed the reduction of bite force in both models (Figures 4D,F). Considering co-expression of TMEM100, TRPA1, and TRPV1 in TG neurons-innervating the TMJ and masseter muscle is elevated after TMD pain (Figure 2), we next determined the effect of local inhibition of TMEM100 in these tissues on TMD pain. Interestingly, we observed that i.a. or i.m. injection of T100-Mut at 0.66 mM and 2 mM [10 μl,

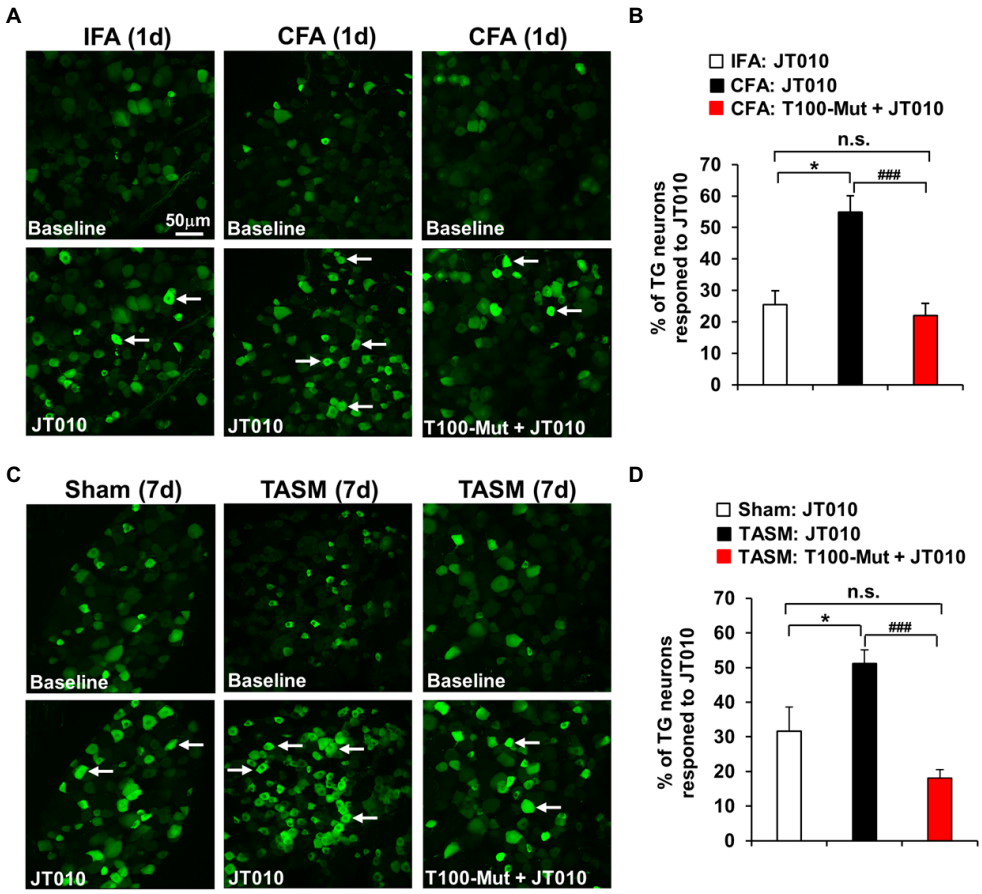

FIGURE 3
Inhibition of TMEM100 suppresses the enhanced neuronal activity of TRPA1 in TG after TMJ inflammation or masseter muscle injury. **(A,C)** Representative Ca^{2+}-imaging of GCaMP3-expressing TG neurons in an *ex-vivo* preparation illustrates the increased Ca^{2+}-signal in response to the TRPA1 selective agonist JT010 (100nM) 1day after CFA (**A**) or 7days after TASM (**C**), which was reduced by pretreatment of the TMEM100 inhibitor T100-Mut (200nM). **(B,D)** Quantitative analysis shows increased percentage of total TG neurons responding to JT010 after CFA **(B)** or TASM **(D)** was reduced by T100-Mut. $^{*}p$ <0.05 and $^{###}p$ <0.001, one-way ANOVA followed by Dunnett's *post-hoc* test. *N* =4–8 mice/group. Arrows in images represent responder neurons.

doses chosen based on Weng et al. (2015)] into the TMJ or masseter muscle for CFA and TASM models, respectively, attenuated the reduction of bite force (Figures 4E,G). These data suggest that sensory neuron-TMEM100 contributes to TMD pain.

Discussion

Although TMEM100 has been demonstrated to modulate pain *via* regulating TRPA1-TRPV1 interaction at the DRG level (Weng et al., 2015), experimental evidence regarding whether TMEM100 controls orofacial pain at the TG level remains lacking. Here, we found that genetic knockout or pharmacological inhibition of TRPA1 and TRPV1 attenuated TG-mediated TMD pain. We further demonstrated that TMEM100 colocalized with TRPA1 and TRPV1 in TG neurons and their co-expression was increased in TG neurons-innervating the TMJ and masseter muscle after TMD pain. Importantly, inhibition of TMEM100 suppressed TRPA1 activity in TG neurons and cKO of *Tmem100* in TG neurons or local injection of TMEM100 inhibitor into the TMJ and masseter muscle attenuated TMD pain. These findings suggest that TMEM100 in TG neurons contributes to TMD pain through regulating TRPA1 activity in TRPA1-TRPV1 complex.

Therapeutic targets for TMD pain are desirable because current pharmacotherapeutics have limited efficacy and side effects (Cairns, 2010; Andre et al., 2022; Tran et al., 2022). TRPA1 and TRPV1 have been implicated in a variety of pain states, including trigeminally-mediated pain (Julius, 2013; Luo et al., 2021). For instance, TRPA1 and TRPV1 might be involved in migraine, headache and dental pain (Benemei et al., 2013; Luo et al., 2021), for which TMD shares significant co-morbidity (Ohrbach et al., 2011). In addition, TRPV1 has been detected in TG neurons-innervating the TMJ, masseter muscle, and synovial lining cells (Sato et al., 2005; Lund et al., 2010; Lindquist et al., 2021). Notably, we and others previously found that inflammation of TMJ-associated tissues upregulates *Trpa1* and *Trpv1* genes in TG (Chen et al., 2013; Chung et al., 2016). These findings raise an important question as to whether TRPA1 and TRPV1 are involved in TMD pain. Here, we found that TMJ inflammation as well as masseter muscle injury led to an upregulation of TRPA1 and TRPV1 in TG neurons at the protein levels. Importantly, bite force reduction was substantially attenuated by global KO or systemic

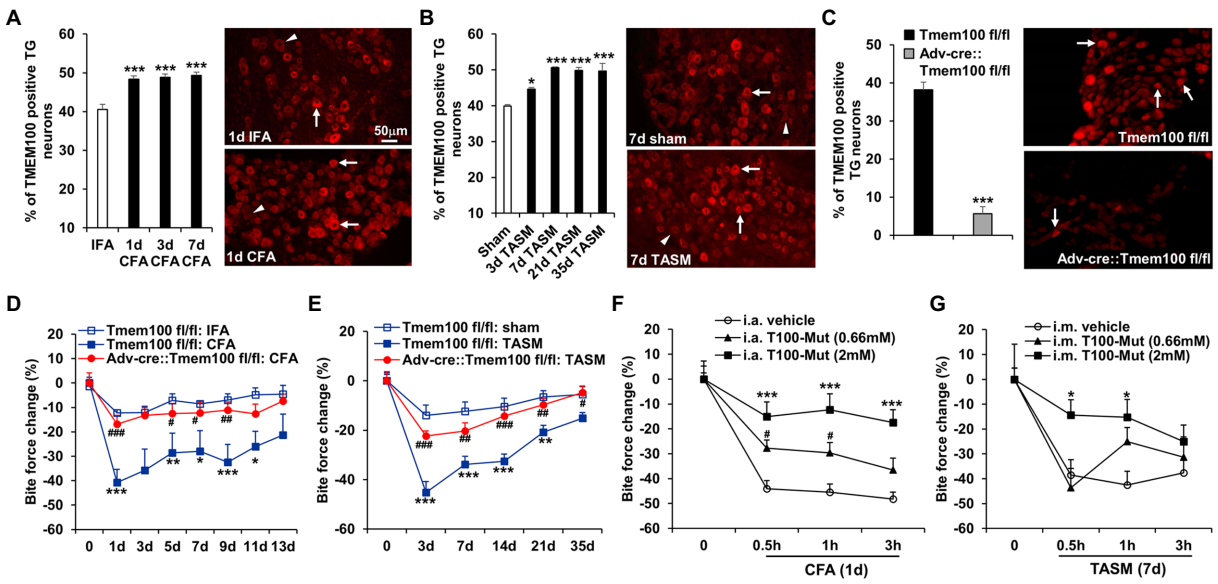

FIGURE 4
Conditional KO of *Tmem100* in TG neurons or local administration of TMEM100 inhibitor attenuates TMD pain. **(A,B)** TMJ inflammation **(A)** or masseter muscle injury **(B)** led to an increased expression of TMEM100 in TG neurons. **p* <0.05 and ****p* <0.001 vs. IFA or sham. One-way ANOVA followed by Dunnett's *post-hoc* test. *N* =4–5 mice/group. Arrows and arrowheads in images represent TMEM100 immunoreactive positive and negative neurons, respectively. **(C)** Depletion of TMEM100 in TG neurons in *Tmem100* cKO mice. Immunostaining shows dramatic reduction of TMEM100-immunoreactive TG neurons in Adv-cre::Tmem100$^{fl/fl}$ mice after tamoxifen treatment. ****p* <0.001, two-tailed *t*-test, *n* =3–4 mice/group. **(D,E)** cKO of *Tmem100* in TG neurons attenuates TMD pain after TMJ inflammation **(D)** or masseter muscle injury **(E)**. **p* <0.05, ***p* <0.01, and ****p* <0.001 vs. Tmem100$^{fl/fl}$: IFA or sham; $^{\#}p$ <0.05, $^{\#\#}p$ <0.01, and $^{\#\#\#}p$ <0.001 vs. Tmem100$^{fl/fl}$: CFA or TASM. Two-way ANOVA followed by Dunnett's *post-hoc* test. *N* =4–9 mice/group. **(F,G)** local injection of the TMEM100 inhibitor T100-Mut into the TMJ (i.a.) or masseter muscle (i.m.) at 0.66mM and 2mM suppressed the reduction of bite force after CFA **(F)** or TASM **(G)** except that T100-Mut had no effect on bite force reduction at 0.66mM in TASM model. **p* <0.05, ****p* <0.001, and $^{\#}p$ <0.05 vs. i.a. or i.m. vehicle (normal saline). Two-way ANOVA followed by Dunnett's *post-hoc* test. *N* =5–7 mice/group. Note: '0' on x-axis represents baseline (before CFA or TASM).

inhibition of these ion channels, providing an important demonstration that TRPV1 and TRPA1 are essential for TMD pain. Interestingly, using bite force test, Wang et al. previously found that TRPV1 has a marginal effect and TRPA1 has no influence on pain induced by CFA injection into the masseter muscle (Wang et al., 2017, 2018). It is worth noting that bite force reduction induced by masseter myositis in these studies was of short duration, i.e., <3 days, which contrasts with pain-behavior duration of TMJ inflammation (>11 days) or masseter muscle injury (>21 days) in our study. Therefore, one possible explanation for these discrepant findings might be due to distinct mouse models.

TRPA1 and TRPV1 in sensory neurons can form a complex and functionally interact to modulate pathological pain (Salas et al., 2009; Akopian, 2011; Spahn et al., 2014; Weng et al., 2015). Interestingly, it was recently discovered that TMEM100 contributes to DRG-mediated pain *via* impairing TRPA1 function in TRPA1-TRPV1 complex (Weng et al., 2015). In the present study, several lines of evidence demonstrate that TMEM100 modulates TG-mediated TMD pain. First, TMEM100 co-expressed with TRPA1 and TRPV1 in TG neurons-innervating the TMJ and masseter muscle and their co-expression was elevated after TMD pain. These data suggest that TG neurons may provide a critical cellular locale whereby TMEM100 mediates TMD pain *via* governing the functional interaction of TRPA1-TRPV1. Second, to gain a mechanistic insight into the role of TMEM100 in TMD pain, our Ca^{2+} imaging assay showed that the percentage of TG neurons responsive to TRPA1 agonist JT010 was increased after TMJ inflammation or masseter muscle injury. Importantly, the enhanced activity of TRPA1 was suppressed when inhibiting TMEM100, suggesting a regulatory role of TMEM100 on TRPA1 function in trigeminal sensory system. Third, selective deletion of *Tmem100* in TG neurons or local injection of TMEM100 inhibitor into TG neurons-innervating TMJ and master muscle tissues significantly blunted TMD pain. These compelling data suggest that TMEM100 might form a multi-protein complex with TRPA1 and TRPV1 in TG neurons and mediate TMD pain through regulating TRPA1 activity within the complex. Although there are some distinct differences in pain processing mechanisms, anatomical specificities, and behavioral phenotypes between spinal and trigeminal systems under pathophysiological states (Luo et al., 2021), our findings support a novel concept that TMEM100 contributes to trigeminally-mediated pain. Future studies are needed to investigate whether TMEM100 is also involved in modulating other types of trigeminal pain, such as dental pain, migraine, and trigeminal neuralgia. Interestingly, a recent study reported that TMEM100 co-expresses with TRPA1 and TRPV1 in human odontoblasts, implicating a potential role of TMEM100 in dental pain (Liu et al., 2021). In addition, based on the data showing that 95 and 74% of TMEM100-positive sensory neurons express CGRP in mice (Weng et al., 2015) and rats (Yu et al., 2019), respectively, and in view of CGRP's crucial role in migraine (Dussor, 2019), it would be interesting to investigate whether TMEM100 contributes to migraine *via* regulating CGRP levels.

There is a critical need for identifying novel targets for TMD pain and better understanding of its underlying mechanisms because TMD pain is inadequately managed. Our study for the first time

demonstrates that TMEM100 contributes to TG-mediated TMD pain *via* a mechanism of action involving the regulatory effect on TRPA1 activity in TRPA1-TRPV1 complex. TRPA1 and TRPV1 are recognized as analgesic targets for development of effective therapies. However, clinical trials based on their inhibitors are delayed or stuck due to off-target thermoregulatory effects and blunting of normal noxious sensation (Moran, 2018). Thus, new modes of regulating the ion channel's activity rather than inhibition of ion channel *per se* in pain transmission pathways represent promising alternative approaches to combat pain. Given that the TMEM100 inhibitor can attenuate TMD pain when it is locally administrated into TMJ or masseter muscle tissues, our study implicates that TMEM100 could serve as a peripheral-topical target for reducing TMD pain while avoiding potential side effects of systemic treatments.

Data availability statement

The original contributions presented in the study are included in the article/supplementary material, further inquiries can be directed to the corresponding author/s.

Author contributions

PW contributed to conception, design, data acquisition, analysis, interpretation, and critically revised the manuscript. QZ, FD, and AS contributed to data acquisition analysis, interpretation, and critically revised the manuscript. XD contributed to conception and critically revised the manuscript. YC contributed to conception, design, data acquisition, analysis, and interpretation, drafted and critically revised the manuscript. All authors gave final approval and agreed to be accountable for all aspects of the work.

Funding

This research was supported by the National Institutes of Health R01DE027454 and R01DE027454-02S2 (YC) and R01GM087369 (XD).

Acknowledgments

We thank Steven Shen's technical support.

Conflict of interest

The authors declare that the research was conducted in the absence of any commercial or financial relationships that could be construed as a potential conflict of interest.

Publisher's note

All claims expressed in this article are solely those of the authors and do not necessarily represent those of their affiliated organizations, or those of the publisher, the editors and the reviewers. Any product that may be evaluated in this article, or claim that may be made by its manufacturer, is not guaranteed or endorsed by the publisher.

Supplementary material

The Supplementary material for this article can be found online at: https://www.frontiersin.org/articles/10.3389/fnmol.2023.1160206/full#supplementary-material

References

Akopian, A. N. (2011). Regulation of nociceptive transmission at the periphery via TRPA1-TRPV1 interactions. *Curr. Pharm. Biotechnol.* 12, 89–94. doi: 10.2174/138920111793937952

Andre, A., Kang, J., and Dym, H. (2022). Pharmacologic treatment for temporomandibular and temporomandibular joint disorders. *Oral Maxillofac. Surg. Clin. North Am.* 34, 49–59. doi: 10.1016/j.coms.2021.08.001

Atsu, S. S., and Ayhan-Ardic, F. (2006). Temporomandibular disorders seen in rheumatology practices: a review. *Rheumatol. Int.* 26, 781–787. doi: 10.1007/s00296-006-0110-y

Bai, Q., Liu, S., Shu, H., Tang, Y., George, S., Dong, T., et al. (2019). TNFα in the trigeminal nociceptive system is critical for temporomandibular joint pain. *Mol. Neurobiol.* 56, 278–291. doi: 10.1007/s12035-018-1076-y

Benemei, S., De Cesaris, F., Fusi, C., Rossi, E., Lupi, C., and Geppetti, P. (2013). TRPA1 and other TRP channels in migraine. *J. Headache Pain* 14:71. doi: 10.1186/1129-2377-14-71

Cairns, B. E. (2010). Pathophysiology of TMD pain--basic mechanisms and their implications for pharmacotherapy. *J. Oral Rehabil.* 37, 391–410. doi: 10.1111/j.1365-2842.2010.02074.x

Chen, Y., Wang, Z. L., Yeo, M., Zhang, Q. J., López-Romero, A. E., Ding, H. P., et al. (2021). Epithelia-sensory neuron cross talk underlies Cholestatic itch induced by Lysophosphatidylcholine. *Gastroenterology* 161, 301–317.e16. doi: 10.1053/j.gastro.2021.03.049

Chen, Y., Williams, S. H., Mcnulty, A. L., Hong, J. H., Lee, S. H., Rothfusz, N. E., et al. (2013). Temporomandibular joint pain: a critical role for Trpv4 in the trigeminal ganglion. *Pain* 154, 1295–1304. doi: 10.1016/j.pain.2013.04.004

Chung, M. K., Park, J., Asgar, J., and Ro, J. Y. (2016). Transcriptome analysis of trigeminal ganglia following masseter muscle inflammation in rats. *Mol. Pain* 12:174480691666852. doi: 10.1177/1744806916668526

Detamore, M. S., and Athanasiou, K. A. (2003). Structure and function of the temporomandibular joint disc: implications for tissue engineering. *J. Oral Maxillofac. Surg.* 61, 494–506. doi: 10.1053/joms.2003.50096

Dussor, G. (2019). New discoveries in migraine mechanisms and therapeutic targets. *Curr. Opin. Physiol.* 11, 116–124. doi: 10.1016/j.cophys.2019.10.013

Eid, S. R., Crown, E. D., Moore, E. L., Liang, H. A., Choong, K. C., Dima, S., et al. (2008). HC-030031, a TRPA1 selective antagonist, attenuates inflammatory- and neuropathy-induced mechanical hypersensitivity. *Mol. Pain* 4:48. doi: 10.1186/1744-8069-4-48

Greenspan, J. D., Slade, G. D., Bair, E., Dubner, R., Fillingim, R. B., Ohrbach, R., et al. (2013). Pain sensitivity and autonomic factors associated with development of TMD: the OPPERA prospective cohort study. *J. Pain* 14:T63-74.e61-66. doi: 10.1016/j.jpain.2013.06.007

Gunthorpe, M. J., Rami, H. K., Jerman, J. C., Smart, D., Gill, C. H., Soffin, E. M., et al. (2004). Identification and characterisation of SB-366791, a potent and selective vanilloid receptor (VR1/TRPV1) antagonist. *Neuropharmacology* 46, 133–149. doi: 10.1016/s0028-3908(03)00305-8

Guo, W., Wang, H., Zou, S., Wei, F., Dubner, R., and Ren, K. (2010). Long lasting pain hypersensitivity following ligation of the tendon of the masseter muscle in rats: a model of myogenic orofacial pain. *Mol. Pain* 6:40. doi: 10.1186/1744-8069-6-40

Hasegawa, H., Abbott, S., Han, B. X., Qi, Y., and Wang, F. (2007). Analyzing somatosensory axon projections with the sensory neuron-specific Advillin gene. *J. Neurosci.* 27, 14404–14414. doi: 10.1523/jneurosci.4908-07.2007

Iodice, G., Danzi, G., Cimino, R., Paduano, S., and Michelotti, A. (2013). Association between posterior crossbite, masticatory muscle pain, and disc displacement: a systematic review. *Eur. J. Orthod.* 35, 737–744. doi: 10.1093/ejo/cjt024

Julius, D. (2013). TRP channels and pain. *Annu. Rev. Cell Dev. Biol.* 29, 355–384. doi: 10.1146/annurev-cellbio-101011-155833

Kim, Y. S., Chu, Y., Han, L., Li, M., Li, Z., Lavinka, P. C., et al. (2014). Central terminal sensitization of TRPV1 by descending serotonergic facilitation modulates chronic pain. *Neuron* 81, 873–887. doi: 10.1016/j.neuron.2013.12.011

Lindquist, K. A., Belugin, S., Hovhannisyan, A. H., Corey, T. M., Salmon, A., and Akopian, A. N. (2021). Identification of trigeminal sensory neuronal types innervating masseter muscle. *eNeuro* 8, ENEURO.0176–ENEU21.2021. doi: 10.1523/eneuro.0176-21.2021

Liu, Y., Wang, Y., Lou, Y., Tian, W., and Que, K. (2021). Functional expression of TRPA1 channel, TRPV1 channel and TMEM100 in human odontoblasts. *J. Mol. Histol.* 52, 1105–1114. doi: 10.1007/s10735-021-10018-w

Lund, J. P., Sadeghi, S., Athanassiadis, T., Caram Salas, N., Auclair, F., Thivierge, B., et al. (2010). Assessment of the potential role of muscle spindle mechanoreceptor afferents in chronic muscle pain in the rat masseter muscle. *PLoS One* 5:e11131. doi: 10.1371/journal.pone.0011131

Luo, Y., Suttle, A., Zhang, Q., Wang, P., and Chen, Y. (2021). Transient receptor potential (TRP) ion channels in orofacial pain. *Mol. Neurobiol.* 58, 2836–2850. doi: 10.1007/s12035-021-02284-2

Moran, M. M. (2018). TRP channels as potential drug targets. *Annu. Rev. Pharmacol. Toxicol.* 58, 309–330. doi: 10.1146/annurev-pharmtox-010617-052832

Ohrbach, R., Fillingim, R. B., Mulkey, F., Gonzalez, Y., Gordon, S., Gremillion, H., et al. (2011). Clinical findings and pain symptoms as potential risk factors for chronic TMD: descriptive data and empirically identified domains from the OPPERA case-control study. *J. Pain* 12, T27–T45. doi: 10.1016/j.jpain.2011.09.001

Piette, E. (1993). Anatomy of the human temporomandibular joint. An updated comprehensive review. *Acta Stomatol. Belg.* 90, 103–127. PMID: 8237635

Salas, M. M., Hargreaves, K. M., and Akopian, A. N. (2009). TRPA1-mediated responses in trigeminal sensory neurons: interaction between TRPA1 and TRPV1. *Eur. J. Neurosci.* 29, 1568–1578. doi: 10.1111/j.1460-9568.2009.06702.x

Sato, J., Segami, N., Yoshitake, Y., Kaneyama, K., Abe, A., Yoshimura, H., et al. (2005). Expression of capsaicin receptor TRPV-1 in synovial tissues of patients with symptomatic internal derangement of the temporomandibular joint and joint pain. *Oral Surg. Oral Med. Oral Pathol. Oral Radiol. Endod.* 100, 674–681. doi: 10.1016/j.tripleo.2005.03.008

Schiffman, E., Ohrbach, R., Truelove, E., Look, J., Anderson, G., Goulet, J. P., et al. (2014). Diagnostic criteria for temporomandibular disorders (DC/TMD) for clinical and research applications: recommendations of the international RDC/TMD consortium network* and orofacial pain special interest groupdagger. *J. Oral Facial Pain Headache* 28, 6–27. doi: 10.11607/jop.1151

Scrivani, S. J., Keith, D. A., and Kaban, L. B. (2008). Temporomandibular disorders. *N. Engl. J. Med.* 359, 2693–2705. doi: 10.1056/NEJMra0802472

Spahn, V., Stein, C., and Zollner, C. (2014). Modulation of transient receptor vanilloid 1 activity by transient receptor potential ankyrin 1. *Mol. Pharmacol.* 85, 335–344. doi: 10.1124/mol.113.088997

Stohler, C. S. (1999). Muscle-related temporomandibular disorders. *J. Orofac. Pain* 13, 273–284. PMID: 10823041

Suttle, A., Wang, P., Dias, F. C., Zhang, Q., Luo, Y., Simmons, L., et al. (2022). Sensory neuron-TRPV4 modulates temporomandibular disorder pain via CGRP in mice. *J. Pain.* doi: 10.1016/j.jpain.2022.12.001. [Epub ahead of print]

Svensson, P., Arendt-Nielsen, L., and Houe, L. (1998). Muscle pain modulates mastication: an experimental study in humans. *J. Orofac. Pain* 12, 7–16. PMID: 9656894

Takaya, J., Mio, K., Shiraishi, T., Kurokawa, T., Otsuka, S., Mori, Y., et al. (2015). A potent and site-selective agonist of TRPA1. *J. Am. Chem. Soc.* 137, 15859–15864. doi: 10.1021/jacs.5b10162

Tran, C., Ghahreman, K., Huppa, C., and Gallagher, J. E. (2022). Management of temporomandibular disorders: a rapid review of systematic reviews and guidelines. *Int. J. Oral Maxillofac. Surg.* 51, 1211–1225. doi: 10.1016/j.ijom.2021.11.009

Wang, S., Brigoli, B., Lim, J., Karley, A., and Chung, M. K. (2018). Roles of TRPV1 and TRPA1 in spontaneous pain from inflamed masseter muscle. *Neuroscience* 384, 290–299. doi: 10.1016/j.neuroscience.2018.05.048

Wang, S., Lim, J., Joseph, J., Wang, S., Wei, F., Ro, J. Y., et al. (2017). Spontaneous and bite-evoked muscle pain are mediated by a common nociceptive pathway with differential contribution by TRPV1. *J. Pain* 18, 1333–1345. doi: 10.1016/j.jpain.2017.06.005

Weng, H. J., Patel, K. N., Jeske, N. A., Bierbower, S. M., Zou, W., Tiwari, V., et al. (2015). Tmem100 is a regulator of TRPA1-TRPV1 complex and contributes to persistent pain. *Neuron* 85, 833–846. doi: 10.1016/j.neuron.2014.12.065

Yu, H., Shin, S. M., Wang, F., Xu, H., Xiang, H., Cai, Y., et al. (2019). Transmembrane protein 100 is expressed in neurons and glia of dorsal root ganglia and is reduced after painful nerve injury. *Pain Rep* 4:e703. doi: 10.1097/pr9.0000000000000703

Frontiers in
Molecular Neuroscience

Leading research into the brain's molecular structure, design and function

Part of the most cited neuroscience series, this journal explores and identifies key molecules underlying the structure, design and function of the brain across all levels.

Discover the latest Research Topics

See more →

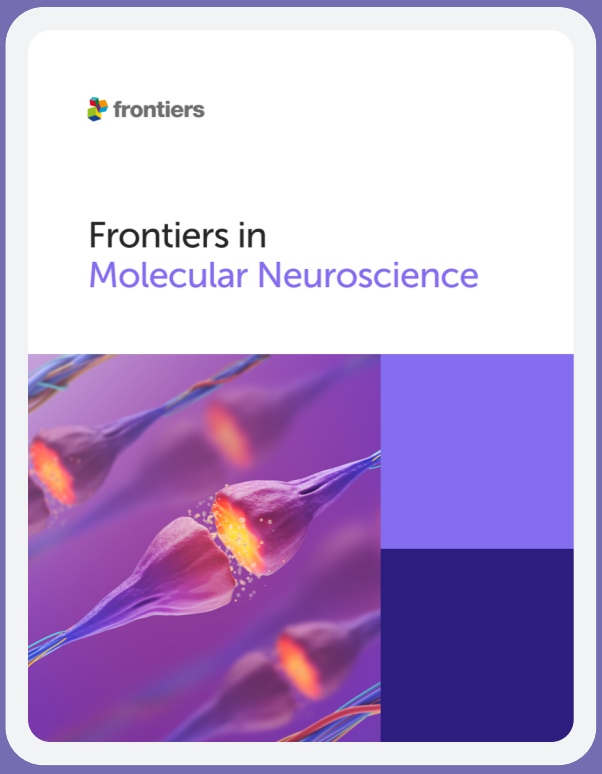

Frontiers

Avenue du Tribunal-Fédéral 34
1005 Lausanne, Switzerland
frontiersin.org

Contact us

+41 (0)21 510 17 00
frontiersin.org/about/contact